EMERGING INFECTIOUS DISEASES®

CDC
CENTERS FOR DISEASE CONTROL AND PREVENTION

40 Years of AIDS

June 2021

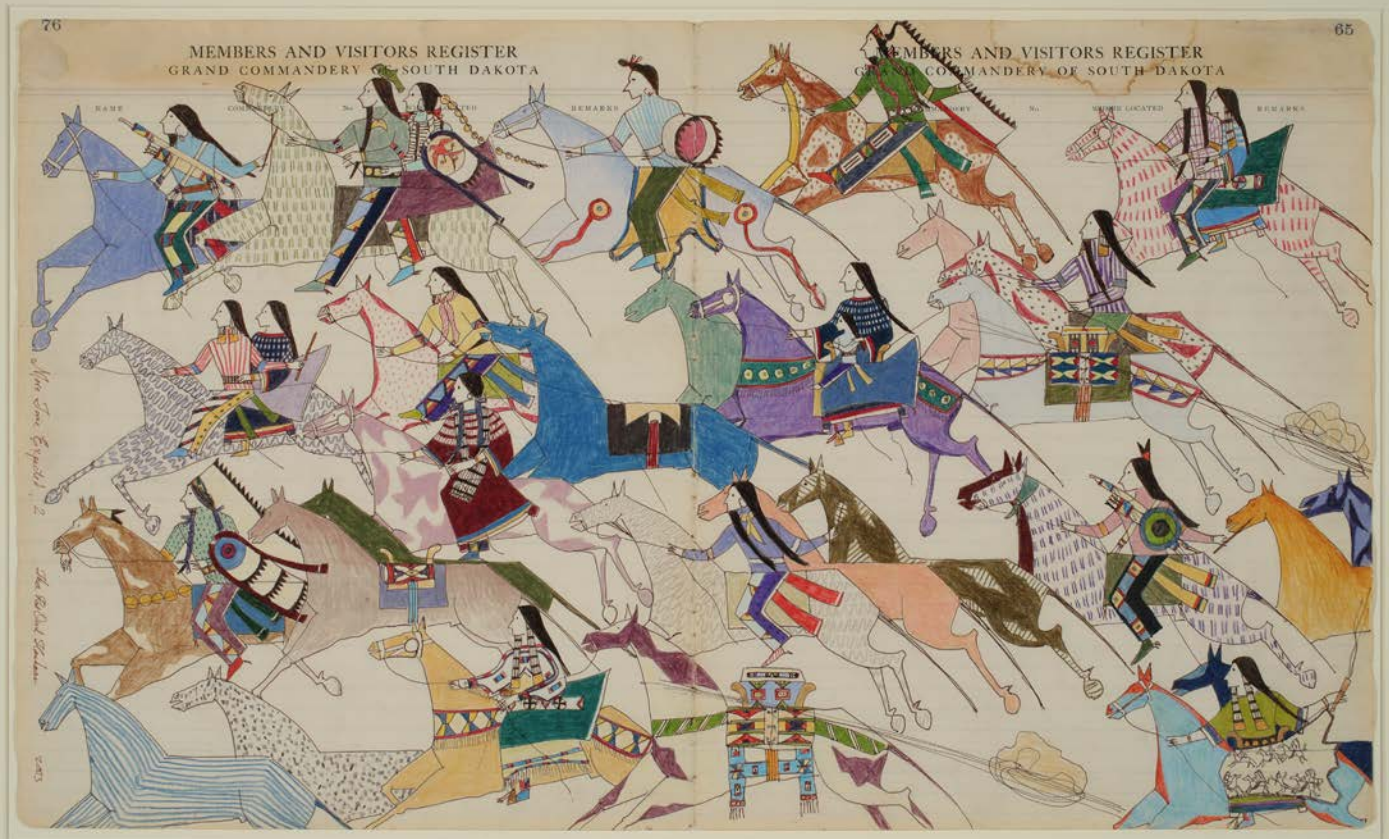

Thomas Red Owl Haukaas (1950–), *More Time Expected*, 2002. Hand-made ink and pencil on antique ledger paper, 16.5 in x 27.5 in/41.9 cm x 69.9 cm. Tacoma Art Museum, 1701 Pacific Avenue. Tacoma, WA 98402, United States. Gift of Greg Kucera and Larry Yocom in honor of Rock Hushka.

EMERGING INFECTIOUS DISEASES®

Emerging Infectious Diseases is published monthly by the Centers for Disease Control and Prevention, 1600 Clifton Rd NE, Mailstop H16-2, Atlanta, GA 30329-4027, USA. Telephone 404-639-1960; email, eideditor@cdc.gov

EMERGING INFECTIOUS DISEASES®

40 Years of AIDS **June 2021**

On the Cover:

Thomas Red Owl Haukaas (1950–), *More Time Expected*, 2002. Hand-made ink and pencil on antique ledger paper, 16.5 in x 27.5 in/41.9 cm x 69.9 cm. Tacoma Art Museum, 1701 Pacific Avenue. Tacoma, WA 98402, United States. Gift of Greg Kucera and Larry Yocom in honor of Rock Hushka.

About the Cover p. 1762

Perspective

Reflections on 40 years of AIDS
K.M. De Cock et al. **1553**

Synopses

Pertactin-Deficient *Bordetella pertussis*, Vaccine-Driven Evolution, and Reemergence of Pertussis
L. Ma et al. **1561**

Medscape EDUCATION ACTIVITY

Rocky Mountain Spotted Fever in a Large Metropolitan Center, Mexico–United States Border, 2009–2019
We found substantial differences in frequency of common clinical characteristics between cases diagnosed by PCR or by immunofluorescence antibody testing.
O.E. Zazueta et al. **1567**

Research

Medscape EDUCATION ACTIVITY

Neurologic Disease after Yellow Fever Vaccination, São Paulo, Brazil, 2017–2018
Disease should be diagnosed by using Brighton Collaboration case definitions and cerebrospinal fluid IgM reactivity.
A.F. Ribeiro et al. **1577**

Macrolide-Resistant *Mycoplasma pneumoniae* Infections in Children, Ohio, USA
M.M. Lanata et al. **1588**

Seroprevalence of Severe Acute Respiratory Syndrome Coronavirus 2 IgG in Juba, South Sudan, 2020
K.E. Wiens et al. **1598**

Medscape EDUCATION ACTIVITY

HIV Infection as Risk Factor for Death among Hospitalized Persons with Candidemia, South Africa, 2012–2017
HIV-seropositive persons with candidemia demonstrated increased adjusted risk for 30-day mortality and should be evaluated for intensive care.
N.P. Govender et al. **1607**

Molecular Epidemiology and Evolutionary Trajectory of Emerging Echovirus 30, Europe
K.S.M. Benschop et al. **1616**

Twenty-Year Public Health Impact of 7- and 13-Valent Pneumococcal Conjugate Vaccines in US Children
M. Wasserman et al. **1627**

Precision Tracing of Household Dengue Spread Using Inter- and Intra-Host Viral Variation Data, Kamphaeng Phet, Thailand
I. Maljkovic Berry et al. **1637**

Association between Birth Region and Time to Tuberculosis Diagnosis among Non–US-Born Persons in the United States
A. Talwar et al. **1645**

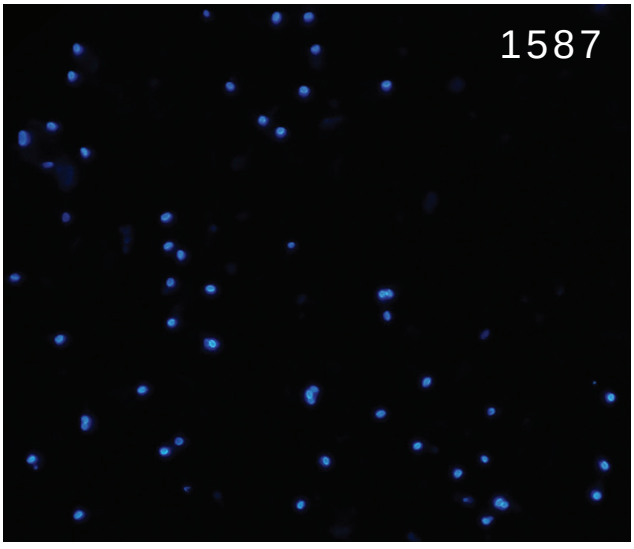

Case–Control Study of Risk Factors for Acquired Hepatitis E Virus Infections in Blood Donors, United Kingdom, 2018–2019
I. Smith et al. **1654**

Increased Incidence of Antimicrobial-Resistant Nontyphoidal *Salmonella* Infections, United States, 2004–2016
F. Medalla et al. **1662**

Dispatches

Rapid Detection of SARS-CoV-2 Variants of Concern, Including B.1.1.28/P.1, British Columbia, Canada
N. Matic et al. **1673**

Epidemiologic Evidence for Airborne Transmission of SARS-CoV-2 during Church Singing, Australia, 2020
A.L. Katelaris et al. **1677**

Ebola Virus IgG Seroprevalence in Southern Mali
S. Bane et al. **1681**

Trends in Viral Respiratory Infections During COVID-19 Pandemic, South Korea
S. Yum et al. **1685**

Serotype-Switch Variant of Multidrug-Resistant *Streptococcus pneumoniae* Sequence Type 271
E.M. Scherer et al. **1689**

Reemergence of Scabies Driven by Adolescents and Young Adults, Germany, 2009–2018
F. Reichert et al. **1693**

Role of *Anopheles stephensi* Mosquitoes in Malaria Outbreak, Djibouti, 2019
V. Pommier de Santi et al. **1697**

Recurrent Swelling and Microfilaremia Caused by *Dirofilaria repens* Infection after Travel to India
L. Huebl et el. **1701**

EMERGING INFECTIOUS DISEASES®
June 2021

Melioidosis in Children, Brazil, 1989–2019
R.X.R. Lima, D.B. Rolim **1705**

Seroepidemiologic Survey of Crimean-Congo Hemorrhagic Fever Virus in Logging Communities, Myanmar
T. Smiley Evans et al. **1709**

Cutaneous Leishmaniasis Caused by an Unknown *Leishmania* Strain, Arizona, USA
M. de Almeida et al. **1714**

Molecular Characterization and Antimicrobial Resistance in *Neisseria gonorrhoeae*, Nunavut Region of Inuit Nunangat, Canada, 2018–2019
A.E. Singh et al. **1718**

Leishmaniases in European Union and Neighboring Countries
E. Berriatua et al. **1723**

Brucellosis Outbreak Traced to Commercially Sold Camel Milk through Whole-Genome Sequencing, Israel
S. Bardenstein et al. **1728**

Research Letters

Highly Pathogenic Avian Influenza A(H5N8) Virus in Swans, China, 2020
X. Li et al. **1732**

Rapid Antigen Test for Postmortem Evaluation of SARS-CoV-2 Carriage
M. Zacharias et al. **1734**

Respiratory Viral Shedding in Healthcare Workers Reinfected with SARS-CoV-2, Brazil, 2020
M.R. Amorim et al. **1737**

EMERGING INFECTIOUS DISEASES®
June 2021

Multisystem Inflammatory Syndrome in Adults after Mild SARS-CoV-2 Infection, Japan
Y. Yamada et al. **1740**

Changing Molecular Epidemiology of Hepatitis A Virus Infection, United States, 1996–2019
S. Ramachandran et al. **1742**

Molecular Typing of *Burkholderia mallei* Isolates from Equids with Glanders, India
H. Singha et al. **1745**

Atypical *Brucella inopinata*–Like Species in 2 Marine Toads
R.A. Glabman et al. **1748**

Incursion of Novel Highly Pathogenic Avian Influenza A(H5N8) Virus, the Netherlands, October 2020
N. Beerens et al. **1750**

Retrospective Identification of Early Autochthonous Case of Crimean-Congo Hemorrhagic Fever, Spain, 2013
A. Negredo et al. **1754**

Evidence of Oropouche Orthobunyavirus Infection, Colombia, 2017
D.E. Gómez-Camargo et al. **1756**

Fecal Excretion of *Mycobacterium leprae*, Burkina Faso
A. Millogo et al. **1758**

Comment Letter

Postvaccination COVID-19 among Healthcare Workers, Israel
Z. Yousaf, K. Mushtaq **1761**

About the Cover

Fluid Motion and Frozen Time
B. Breedlove **1762**

Etymologia

Enterocytozoon bieneusi
M. Moniot et al. **1587**

Online Report

Proposal for Human Respiratory Syncytial Virus Nomenclature below the Species Level
V. Salimi et al.
https://wwwnc.cdc.gov/eid/article/27/6/20-4608_article

Correction

Vol. 26 No. 12
GenBank accession numbers have been added for the sequenced viral sequences from Lymphocytic Choriomeningitis Virus Infections and Seroprevalence, Southern Iraq **1760**

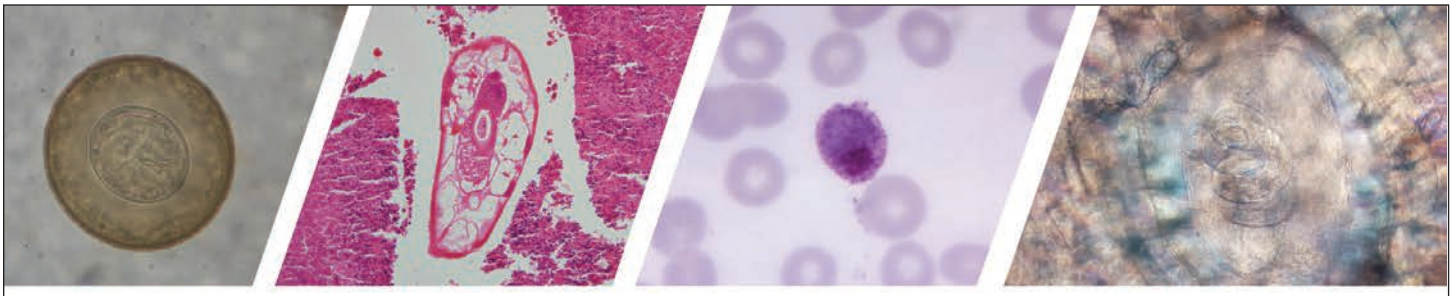

DPDx

Diagnostic Assistance and Training in Laboratory Identification of Parasites

A free service of CDC available to laboratorians, pathologists, and other health professionals in the United States and abroad

- Diagnosis from photographs of worms, histological sections, fecal, blood, and other specimen types
- Expert diagnostic review
- Formal diagnostic laboratory report
- Submission of samples via secure file share

Visit the DPDx website for information on laboratory diagnosis, geographic distribution, clinical features, parasite life cycles, and training via Monthly Case Studies of parasitic diseases.

www.cdc.gov/dpdx
dpdx@cdc.gov

U.S. Department of Health and Human Services
Centers for Disease Control and Prevention

CS272346-DE

Reflections on 40 Years of AIDS

Kevin M. De Cock,[1] Harold W. Jaffe,[1] James W. Curran

"When the history of AIDS and the global response is written, our most precious contribution may well be that, at a time of plague, we did not flee, we did not hide, we did not separate ourselves."

—Jonathan Mann, Founding Director of Project SIDA and the World Health Organization Global Programme on AIDS, 1998

June 2021 marks the 40th anniversary of the first description of AIDS. On the 30th anniversary, we defined priorities as improving use of existing interventions, clarifying optimal use of HIV testing and antiretroviral therapy for prevention and treatment, continuing research, and ensuring sustainability of the response. Despite scientific and programmatic progress, the end of AIDS is not in sight. Other major epidemics over the past decade have included Ebola, arbovirus infections, and coronavirus disease (COVID-19). A benchmark against which to compare other global interventions is the HIV/AIDS response in terms of funding, coordination, and solidarity. Lessons from Ebola and HIV/AIDS are pertinent to the COVID-19 response. The fifth decade of AIDS will have to position HIV/AIDS in the context of enhanced preparedness and capacity to respond to other potential pandemics and transnational health threats.

Forty years ago, on June 5, 1981, the Centers for Disease Control's Morbidity and Mortality Weekly Report described 5 cases of *Pneumocystis* pneumonia in gay men (*1*). That report heralded the HIV/AIDS pandemic, which has resulted in over 75 million HIV infections and 32 million deaths. In 2011, we reviewed 30 years of AIDS and commented that the HIV/AIDS response would be a benchmark against which responses to other health threats would be compared (*2*). After 40 years of AIDS, we present our personal reflections on scientific and global health evolution over the fourth decade of AIDS in a world that has recently suffered other major epidemics. We focus on biomedical advances because these have had the greatest effect on HIV transmission and disease; advances in structural and behavioral interventions are reviewed in the CDC Compendium of Evidence-Based Interventions and Best Practices for HIV Prevention (*3*).

After the initial MMWR report was published, it took 2–3 years for the cause of AIDS, the novel retrovirus designated HIV, to be identified (*4*,*5*), and many more years to uncover its simian origin (*6*). Because of the asymptomatic spread of HIV, the long incubation period before disease, and transmission through sex and blood, millions of persons around the world, including several hundred thousand in the United States, were infected by the time the first AIDS cases were reported. The epidemiology and natural history of HIV infection, combining elements of acute and chronic diseases, ensured a diverse and long-lasting pandemic.

The history of HIV/AIDS and the struggle to contain it have seen the best and worst of human nature. Frequent examples of discrimination and exclusion are contrasted by leadership, illustrated by community activists (*7*), Jonathan Mann molding the first global response (*8*), Kofi Annan rallying the United Nations behind the search for a global fund (*9*), and President George W. Bush committing United States generosity to a war on HIV/AIDS of uncertain duration (*10*). Despite continued instances of injustice, the story has overall been a positive one, providing lessons for how to respond to other epidemic and pandemic threats.

Evolving Epidemiology

The Joint United Nations Programme on HIV/AIDS (UNAIDS) estimates that in 2019, 38 million persons worldwide were living with HIV, 1.7 million became newly infected, and 690,000 died with HIV disease

Author affiliations: Centers for Disease Control and Prevention, Atlanta, Georgia, USA (K.M. De Cock, H.W. Jaffe); Emory University and Emory Center for AIDS Research, Atlanta (J.W. Curran)

DOI: https://doi.org/10.3201/eid2706.210284

[1]Retired.

(*11*). Compared with 2010 estimates, overall HIV incidence in 2019 decreased by 23% and mortality by 37%. However, age stratification shows that new infections have decreased by 52% among children but by only 13% among adults. With reduced mortality rates yet continued HIV incidence and population growth, the overall number of persons living with HIV was 24% greater in 2019 than in 2010.

Global summaries hide regional differences. The epicenter of the pandemic remains in East and southern Africa, which account for 54% of all HIV-infected persons and 43% of incident HIV infections and deaths (*11*). High prevalence of HIV-infected persons with unsuppressed viremia predicts high incidence and maintenance of community infection, an observation that applies to regions and countries, as well as specific populations such as men who have sex with men (MSM).

The next greatest HIV burden is in the Asia and Pacific region, where the population is vastly greater than that of East and southern Africa but there are 3.5 times fewer HIV-infected persons (*11*). Despite overall prevention progress, HIV incidence has not declined equally everywhere; little success has been seen in eastern Europe, the Middle East, and Central Asia.

Ever clearer is the global burden of HIV in key populations: MSM, transgender persons, people who inject drugs, sex workers and their clients, and incarcerated persons. In 2019, an estimated 62% of all new HIV infections were in members of those key populations (*11*). In 7 of the 8 UNAIDS regions, key populations accounted for 60%–99% of incident HIV infections; only in East and southern Africa, where the proportion was 28%, were new infections predominant in general populations (*11*).

Among high-income nations, the most heavily affected country is still the United States. In 2018, a total of 37,881 HIV infections were newly reported, with regional differences (*12*). In the South, the rate of new infections was more than twice that for the Midwest, where the rate was the lowest. Major disparities by race/ethnicity persist; the rate among Black/African American persons is 2 times that among Hispanic and 8 times that among White persons. Also associated with higher rates are factors indicating social deprivation and poverty, even allowing for racial and ethnic disparities. Among new HIV infections, 70% resulted from male-to-male sex. A cause for concern is potential overlap between the HIV/AIDS and opioid epidemics through increased drug injection and needle sharing, which has resulted in explosive HIV outbreaks (*13*).

Evolving Science and Program

In our 2011 commentary (*2*), we considered the following as priorities: improving use of existing interventions, defining how best to use HIV testing and antiretroviral therapy (ART) for prevention as well as treatment, continuing the quest for new knowledge and interventions, and ensuring sustainability of the global response. By and large, progress has been made on all fronts.

After the CAPRISA 004 trial of precoital and postcoital use of tenofovir gel was published in 2010 (*14*), the Ring (*15*) and Aspire (*16*) studies (randomized, placebo-controlled trials in South Africa) examined the protective efficacy of a self-inserted vaginal ring impregnated with slow-release dapivirine, a nonnucleoside reverse transcription inhibitor. The overall efficacy rates for reducing HIV incidence were 31% (Ring) and 27% (Aspire); many questions about overall efficacy, adherence, and differences by age remained. This collective experience provided proof of concept for woman-controlled prevention but did not provide the definitive public health solution to high HIV incidence among young women in Africa.

Four pivotal randomized trials (*17*–*20*) of oral preexposure prophylaxis (PrEP) with Truvada (combination of tenofovir and emtricitabine) were pivotal for international licensing of the compound. The relevant trials studied MSM, transgender women having sex with men, and at-risk heterosexual persons. A review of evidence considered another 9 studies, some of tenofovir alone, in different populations including people who inject drugs (*21*). The pivotal trials showed reduced HIV incidence (44%–86%) with Truvada use. However, a consistent observation has been a strong association between efficacy and adherence; PrEP is effective, but the drugs need to be taken.

Subsequent research focused on differential tissue penetration of drugs to relevant anatomic sites in men and women and on modes of drug delivery. HIV Prevention Trials Network (HPTN) studies compared the prevention efficacy of the long-acting injectable drug cabotegravir with Truvada in men and transgender women who have sex with men (study 083 [*22*]) and in heterosexual women (study 084 [*23*]). Interim results showed that cabotegravir, delivered every 8 weeks by injection, was associated with 66% lower incidence than oral Truvada in study 083 and 89% less in study 084. The long half-life of cabotegravir enables intermittent dosing, but waning drug levels over time may become subtherapeutic, thus requiring additional interventions to prevent infection and preclude development of drug resistance.

In its 2016 guidelines, the World Health Organization (WHO) recommended public health use of PrEP, as have other national and international regulatory or advisory bodies. However, the enthusiasm engendered by PreP science needs to be tempered by consideration of cost, need for rigorous adherence, rising rates of other sexually transmitted infections and thus need for continued condom use, and contraception for women. Long-acting injectables could be a major advance, but accessibility and logistics for their delivery need to be considered.

Mathematical modeling and ecologic studies suggested that greatly increased delivery of ART could reduce HIV transmission at the community level. The definitive study showing that ART provided prevention benefits was the landmark HPTN 052 study (*24*), published in interim form in 2011. This trial among discordant couples found a 96% reduction in HIV transmission among those who started ART early versus those for whom it was deferred. Combined with an influential modeling study (*25*) that suggested that regular HIV testing and immediate use of ART could suppress and perhaps ultimately eliminate HIV transmission, the results of HPTN 052 led to studies in East and southern Africa of the so-called test and treat intervention (*26*–*29*). These studies were community randomized evaluations of widespread HIV testing and immediate ART compared with standard care; the primary endpoint was HIV incidence. These large, expensive implementation science studies yielded rich information but did not lead to local HIV elimination. Of the 4 studies, 2 showed no significant incidence reduction and the other 2 showed 20%–30% reduction.

One of the reasons for the unexpectedly modest differences in HIV incidence between intervention and control communities in the test and treat study was changing global practice with regard to when to start ART. In 2015, results of the START (*30*) and TEMPRANO (*31*) trials showed unequivocally that immediate ART, irrespective of CD4+ lymphocyte count, resulted in reduced HIV-associated disease and death, ending more than 2 decades of argument about when to start treatment. WHO rapidly changed global recommendations to immediately start ART, one result of which was erosion of differences between intervention and control communities in the test and treat trials.

Although test and treat did not reduce HIV incidence to the extent hoped for, the accumulated evidence supports the notion of early, universal ART for extending the lives of HIV-positive persons as well as reducing the prevalence of unsuppressed viremia, the driver of HIV transmission. Large observational studies (*32*) showed that persons with suppressed viremia do not transmit the virus sexually, leading to the slogan "U = U"—undetectable equals untransmittable. This experience provides a much more compelling argument for active HIV case finding through increased HIV testing and partner notification, to enhance individual and public health through early treatment.

Although none of the approaches described provides a unique solution, the combination of widespread HIV testing, early ART for those infected, and PrEP for those at risk offers opportunity for substantially limiting the epidemic. Such approaches have been associated with reductions in new HIV infections among MSM in London, UK (*33*), and in New South Wales, Australia (*34*). In the United States, these advances—testing, case finding including through partner notification, universal treatment, PrEP, and rapid molecular investigation of clusters for service provision—have been incorporated into a revised national strategy for HIV elimination (*35*).

Progress toward an HIV vaccine remains discouraging. The only report of protective efficacy, published in 2009, has been the RV-144 study in Thailand (*36*), which investigated use of a recombinant canarypox vector vaccine (ALVAC-HIV) delivered in 4 monthly priming injections followed by a recombinant glycoprotein 120 subunit vaccine (AIDSVAX B/E) given in 2 additional injections. Reported efficacy was 26%–31%, but statistical and technical interpretation of these results was controversial (*37*). In 2016, the HVTN 702 study was launched in South Africa and used the same product as in the Thailand trial but modified for the dominant subtype C. After interim analysis, the study was halted for futility in early 2020 (*38*). Other efficacy studies of vaccines based on so-called mosaic immunogens from diverse HIV subtypes are in progress.

There has been great interest in broadly neutralizing antibodies to HIV, which some infected persons produce naturally and which might protect against a wide variety of strains. Two international trials of infusions with a broadly neutralizing antibody, VRC01, every 8 weeks showed relative protection against sensitive strains but no significantly reduced HIV incidence overall (*39*).

In 2014, UNAIDS launched its 90:90:90 initiative, aiming for 90% of persons with HIV infection to be diagnosed, 90% of those with an HIV diagnosis to receive ART, and 90% of those receiving treatment to show viral suppression by 2020. Globally, the respective proportions in 2019 were 81%, 82%, and 88%, so that an estimated 59% of persons living with HIV

were showing viral suppression. Initially, 90:90:90 (with a goal of these numbers being 95s by 2030) was an advocacy proposal rather than an evidence-based initiative, but these targets have become adopted as policy promising "epidemic control," itself a concept requiring precise definition (*40*).

ART scale-up, increased male circumcision, and prevention of mother-to-child transmission have all contributed to encouraging advances in the most heavily affected regions of Africa (*11*,*41*,*42*). Successful program implementation and declines in new HIV infections and deaths, combined with scientific progress, have led to a certain complacency that "AIDS is over." Former US Secretary of State Hillary Clinton and staff promoted the idea that current tools could abruptly halt the epidemic. We largely agree with the 2018 judgment of the International AIDS Society–Lancet Commission on AIDS: "The HIV/AIDS community made a serious error by pursuing 'the end of AIDS' message" (*43*). Key populations, hiding in obscurity as well as in plain sight, will probably remain as reservoirs, even with highly performing programs. Experience in East and southern Africa has highlighted the challenge of adequate service provision to youth and men. Stigma and discrimination remain barriers in many parts of the world, and lack of an HIV cure (a priority research area) and vaccine remain scientific obstacles (*44*).

Evolving Global Health

The HIV/AIDS pandemic has evolved in parallel with other global health events that necessarily influence how HIV/AIDS is perceived and prioritized. In a 2012 paper, author K.D.C. suggested that global health trends could best be analyzed through the lenses of development, public health, and health security (*45*). The fourth decade of AIDS started in the aftermath of the global financial crisis and the influenza (H1N1) pandemic and is finishing amid the coronavirus disease (COVID-19) pandemic. Although substantial progress has been made toward reducing maternal deaths, improving child survival rates, and scaling up programs for HIV/AIDS, malaria, and tuberculosis, the past decade has seen major disease outbreaks and a consequent focus on health security. Because of its sociodemographic effects, AIDS was portrayed as a security issue in United Nations discussions early in this century. With massive scale-up of treatment and prevention, HIV/AIDS is now perceived as another public health priority rather than a security emergency.

In 2014, Ebola was reported in Guinea, Liberia, and Sierra Leone, far west of previously recognized outbreaks. The epidemic lasted until mid-2016 and ultimately resulted in 28,646 reported cases and 11,323 deaths (*46*). Infections were exported to 3 other countries in Africa, several countries in Europe, and the United States. This health crisis resulted in widespread fear of possible global spread, unparalleled global mobilization of emergency health assistance including use of armed forces of the different high-income countries, and political involvement at the highest levels of governments and the United Nations. Subsequent outbreaks of Ebola have occurred in Uganda and the Democratic Republic of the Congo (DRC), including a large epidemic in conflict-ridden eastern DRC in 2018–2020 that resulted in 3,481 reported cases and 2,299 deaths (*47*). Underemphasized aspects of these Ebola epidemics were that cases over the past 6 years represent more than 90% of all cases reported cumulatively since recognition of Ebola in 1976; that vast geographic distances were involved; and that these outbreaks were largely urban, sometimes involving capital and other major cities. Ebola epidemiology has changed from that of an exotic, remote infection in Africa to one capable of causing extensive urban outbreaks threatening global health (*48*). Also of note was that field research conducted during the outbreaks under the most difficult conditions showed efficacy of a vaccine and therapeutics, both now considered the standard of care for Ebola (*49*,*50*).

Over the past decade, arboviral epidemic activity has been diverse. The epidemics of yellow fever in Angola and the DRC in 2015–2016 were the world's largest over the past 30 years. A total of 965 cases and 400 deaths were reported, but true numbers were far greater. Over 30 million persons were vaccinated, and shortage of yellow fever vaccine required healthcare providers to resort to the untested practice of fractionating vaccine doses (*51*). Huge epidemics of chikungunya and dengue occurred internationally; virus was transmitted to areas previously considered at low risk, such as Europe (*52*). In 2015, the Zika epidemic raised global concern when infection with this virus was shown to be associated with microcephaly in infants and with Guillain-Barré syndrome and to be sexually transmissible. The outbreak resulted in at least 3,700 cases of birth defects in the Americas (*53*).

In 2005, after the outbreak of severe acute respiratory syndrome (SARS), WHO revised its International Health Regulations (*54*). A key change was authority to declare a Public Health Emergency of International Concern, a health emergency that could result in international spread or required coordinated action. WHO has implemented this authority only 6

times, 5 of them during the fourth decade of AIDS: for polio (2014), Ebola (2014 and 2019), Zika (2015), and COVID-19 (2019).

Related to health security are the interrelated challenges of global warming, demographic change, and migration. Climate change affects social and environmental determinants of health, such as access to clean air, water, shelter, and arable lands, but also exerts direct health effects. The United Nations High Commissioner for Refugees characterized 2010–2019 as "a decade of displacement," during which 100 million persons were forced to flee their homes, many because of conflict such as that in the Middle East. During 2014–2020, some 20,000 migrants crossing the Mediterranean Sea to Europe drowned, and another 12,000 or more were unaccounted for.

Broad themes that have dominated global health discourse include the transition from the era of the Millennium Development Goals (MDGs; 2000–2015) to that of the broader Sustainable Development Goals (SDGs; 2015–2030) (*55*) and the issue of universal health coverage. Other disease-specific programs require continued support, such as the unfinished efforts to eradicate polio and Guinea worm disease. The MDGs had 3 specific health goals relating to child survival; maternal health; and HIV/AIDS, tuberculosis, and malaria. Only 1 of the 17 SDGs is devoted to health, SDG3, which has 13 targets and 28 indicators. Specifically, SDG3 calls for: "By 2030, end the epidemics of AIDS, tuberculosis, malaria and neglected tropical diseases and combat hepatitis, water-borne diseases and other communicable diseases." Another target and WHO priority is provision of universal health coverage, global access to decent healthcare, and protection against penury from out-of-pocket health expenditures. HIV/AIDS exists in a crowded and complex global health space.

Preparing for the Fifth Decade of AIDS

As the world emerged from the financial crisis a decade ago, there was concern that HIV/AIDS funding might be constrained. Development assistance for health reached $40.6 billion in 2019, an increase of 15% over the amount in 2010 (*56*). Approximately half of this assistance goes to HIV/AIDS, especially for treatment, and to newborn, maternal, and child health. Thus, although health security has eclipsed health development and global public health in this fourth decade of AIDS, financial commitments have been largely maintained.

The overall annual spending on HIV/AIDS by low- and middle-income countries is ≈$20.2 billion, of which ≈$9.5 billion represents donor funding. UNAIDS consistently communicates that to meet SDG targets, overall spending on HIV/AIDS needs to increase by ≈40%. Nonetheless, this HIV-specific spending is privileged compared with funding for other high-impact diseases in low-income settings, such as malaria and tuberculosis. AIDS is no longer among the 10 leading causes of death globally and is now widely viewed as a medically manageable disease. HIV/AIDS prioritization and funding may be justified by the youthful groups affected and its lifelong nature, but this view may be increasingly challenged. Expecting the United States to pay indefinitely for most of the world's HIV/AIDS response is unrealistic. The end of the SDG era in 2030 will probably come with reappraisal of global commitments, including those for global health funding, disease-specific focus, and maintenance of single-disease organizations such as UNAIDS. Over the coming years, HIV/AIDS programs need to show good fiscal management and epidemiologic results, and affected countries need to shoulder an increased share of their disease burdens.

Lessons from HIV/AIDS and Other Epidemics

The most dramatic epidemics in recent time (COVID-19 [*57*], Ebola, and HIV/AIDS) involve quite different biological agents and challenges yet also raise common themes and questions. Especially needed are global responses to challenges that transcend national borders. Pathogen emergence is enhanced by globalization, but globalized systems are needed to address an interconnected worldwide emergency. The slogan "no one is safe until everyone is safe" has been heard in relation to COVID-19, but it was said years ago about HIV. And global health needs global funding.

Individual leaders and organizations have performed valiant work on COVID-19, yet countries have isolated themselves in all senses, resulting in global fragmentation. Major powers look inward yet are reluctant to cede space, and the influence of multilateral agencies is limited. WHO was heavily criticized after the Ebola epidemic in West Africa but is constrained by restricted authority, inadequate funding, and unrealistic expectations from member states. Repeated calls for WHO reform are unclear about what is really wanted.

Honesty is required concerning preparedness and surveillance. The Ebola epidemic in West Africa became as severe as it did because the 3 affected countries had been neglected for years and had no functioning surveillance and public health infrastructure. We cannot say that severe acute respiratory syndrome coronavirus 2 (SARS-CoV-2) was completely

unexpected; the literature on pandemic threats is voluminous. SARS in 2002–2003 was severe but not widespread; the 2009 influenza (H1N1) pandemic was widespread but not severe. It is hubristic to assume that pathogen severity and spread would always segregate, yet we were not prepared. Preparedness metrics can give false reassurance, witnessed by the lamentable response to COVID-19 in the United States in 2020. "Never again" was the mood after the Ebola epidemic in West Africa, but preparedness just seems too hard and costly. Perhaps true preparedness exists only in the military, where personnel train continuously for wars they hope will never happen.

As a result of technologic advances such as whole-genome sequencing, scientific progress on COVID-19 has been breathtakingly rapid compared with early laboratory research on HIV. We hope to not see a replay of the early history of ART, with scientific advances relating to COVID-19, and specifically vaccines, not being rapidly or equitably accessible everywhere. "Vaccine nationalism" is a new term raising the specter of lower risk groups in high-income countries receiving vaccine before, for example, frontline healthcare workers in low-income settings. Healthcare workers have been disproportionately affected by Ebola and COVID-19, highlighting the need for much greater investment in infection prevention and control in healthcare settings worldwide. Attention and innovation are required to ensure maintenance of HIV and other essential public health services amid other outbreaks such as COVID-19.

Although initially slow, the HIV/AIDS response over the years has been a beacon in global health for respect for individuals and their rights and for health equity. More reflection is required with regard to what the responses to HIV and Ebola have taught us and how they might be relevant to COVID-19 and other future epidemics.

Conclusions

Although great need remains, the past decade has seen scientific and programmatic successes with regard to the HIV/AIDS priorities we defined after 30 years of AIDS. Existing interventions have been scaled up, and new tools such as PrEP and long-lasting drug preparations have been introduced. The roles of HIV testing and ART for treatment and prevention have been clarified, and the need for immediate ART for all HIV-infected persons has been proven. The global HIV/AIDS response has been sustained, financing has been maintained, and the world has kept focus on the SDGs. Mann's judgment that "we did not separate ourselves" remains justified. We must also accept that political promises of "the end of AIDS" were hyperbole that current epidemiology does not support.

The COVID-19 pandemic has exploited the fault lines of global systems and existing inequalities in a way that HIV did early on. Regrettably, the solidarity that HIV/AIDS engendered has not yet been carried over. In retrospect, the recent epidemics of Ebola in West Africa and DRC were preparation for the COVID-19 pandemic, but follow-through was lacking. The fifth decade of AIDS will take us to the SDG target date and reassessment of global health and development priorities. HIV/AIDS may not be central to global health discourse as it was earlier, but it will remain a yardstick by which to judge commitment and efforts, including, and especially in relation to, health security.

Addendum

On February 7, 2021, the Ministry of Health of DRC reported a laboratory-confirmed case of Ebola in North Kivu Province, the most heavily affected province during the 2018–2020 outbreak in eastern Congo. The case-patient experienced symptom onset on January 25, 2021, and died in Butembo, a city of ≈1 million persons, on February 4, 2021. She was reportedly linked epidemiologically to an Ebola survivor, and genetic sequencing reportedly showed phylogenetic association with the earlier outbreak rather than a new spillover event. As of February 8, 2021, a total of 118 contacts were being investigated (https://www.who.int/emergencies/diseases/ebola/ebola-2021-north-kivu, https://www.who.int/csr/don/10-february-2021-ebola-drc/en).

Separately, on February 14, 2021, the Ministry of Health of the Republic of Guinea reported an outbreak of Ebola in the subprefecture of Gouécké, Nzérékoré Region, the first report of Ebola in Guinea since the 2014–2016 epidemic. The index case-patient, a nurse, experienced symptoms on January 18, 2021, and died on January 28, 2021. A total of 6 secondary Ebola cases were reported, 1 in a traditional practitioner who cared for the index case-patient and 5 in family members attending her subsequent funeral. Of the 7 case-patients, 5 died. As of February 15, 2021, a total of 192 contacts were being investigated, including in the capital city, Conakry (https://www.who.int/emergencies/diseases/ebola/ebola-2021-nzerekore-guinea, https://www.who.int/csr/don/17-february-2021-ebola-gin/en).

About the Author

Dr. De Cock retired from CDC in December 2020. He had previously served as founding director of Projet RETRO-CI, Abidjan, Côte d'Ivoire; director of the CDC Division of HIV/AIDS Prevention, Surveillance and

Epidemiology; director of the WHO Department of HIV/AIDS; founding director of the CDC Center for Global Health; and director, CDC Kenya.

References

1. Centers for Disease Control. Pneumocystis pneumonia—Los Angeles. MMWR Morb Mortal Wkly Rep. 1981;30:1–3. PMID: 6265753
2. De Cock KM, Jaffe HW, Curran JW. Reflections on 30 years of AIDS. Emerg Infect Dis. 2011;17:1044–8. https://doi.org/10.3201/eid/1706.100184
3. Centers for Disease Control and Prevention. Compendium of evidence-based interventions and best practices for HIV prevention [cited 2021 Apr 18]. https://www.cdc.gov/hiv/research/interventionresearch/compendium/index.html
4. Barré-Sinoussi F, Chermann J-C, Rey F, Nugeyre MT, Chamaret S, Gruest J, et al. Isolation of a T-lymphotropic retrovirus from a patient at risk for acquired immune deficiency syndrome (AIDS). Science. 1983;220:868–71. https://doi.org/10.1126/science.6189183
5. Popovic M, Sarngadharan MG, Read E, Gallo RC. Detection, isolation, and continuous production of cytopathic retroviruses (HTLV-III) from patients with AIDS and pre-AIDS. Science. 1984;224:497–500. https://doi.org/10.1126/science.6200935
6. Hahn BH, Shaw GM, De Cock KM, Sharp PM. AIDS as a zoonosis: scientific and public health implications. Science. 2000;287:607–14. https://doi.org/10.1126/science.287.5453.607
7. France D. How to survive a plague: the inside story of how citizens and science tamed AIDS. New York: Alfred Knopf; 2016.
8. Merson M, Inrig S. The AIDS pandemic. Searching for a global response. 2018. Cham (Switzerland); Springer International Publishing; 2018. p. 25–113.
9. Piot P. No time to lose. A life in pursuit of deadly viruses. New York: W.W. Norton & Co.; 2012. p. 316–34.
10. Fauci AS, Eisinger RW. PEPFAR—15 years and counting the lives saved. N Engl J Med. 2018;378:314–6. https://doi.org/10.1056/NEJMp1714773
11. Joint United Nations Programme on HIV/AIDS. UNAIDS data 2020 [cited 2021 Apr 18]. https://www.unaids.org/sites/default/files/media_asset/2020_aids-data-book_en.pdf
12. Centers for Disease Control and Prevention. HIV surveillance report, 2018 (Preliminary); vol. 30 [cited 2021 Mar 14]. http://www.cdc.gov/hiv/library/reports/hiv-surveillance.html
13. Peters PJ, Pontones P, Hoover KW, Patel MR, Galang RR, Shields J, et al.; Indiana HIV Outbreak Investigation Team. HIV infection linked to injection use of oxymorphone in Indiana, 2014–2015. N Engl J Med. 2016;375:229–39. https://doi.org/10.1056/NEJMoa1515195
14. Abdool Karim Q, Abdool Karim SS, Frohlich JA, Grobler AC, Baxter C, Mansoor LE, et al.; CAPRISA 004 Trial Group. Effectiveness and safety of tenofovir gel, an antiretroviral microbicide, for the prevention of HIV infection in women. Science. 2010;329:1168–74. https://doi.org/10.1126/science.1193748
15. Nel A, van Niekerk N, Kapiga S, Bekker L-G, Gama C, Gill K, et al.; Ring Study Team. Safety and efficacy of a dapivirine vaginal ring for HIV prevention in women. N Engl J Med. 2016;375:2133–43. https://doi.org/10.1056/NEJMoa1602046
16. Baeten JM, Palanee-Phillips T, Brown ER, Schwartz K, Soto-Torres LE, Govender V, et al.; MTN-020–ASPIRE Study Team. Use of a vaginal ring containing dapivirine for HIV-1 prevention in women. N Engl J Med. 2016;375:2121–32. https://doi.org/10.1056/NEJMoa1506110
17. Grant RM, Lama JR, Anderson PL, McMahan V, Liu AY, Vargas L, et al.; iPrEx Study Team. Preexposure chemoprophylaxis for HIV prevention in men who have sex with men. N Engl J Med. 2010;363:2587–99. https://doi.org/10.1056/NEJMoa1011205
18. Baeten JM, Donnell D, Ndase P, Mugo NR, Campbell JD, Wangisi J, et al.; Partners PrEP Study Team. Antiretroviral prophylaxis for HIV prevention in heterosexual men and women. N Engl J Med. 2012;367:399–410. https://doi.org/10.1056/NEJMoa1108524
19. McCormack S, Dunn DT, Desai M, Dolling DI, Gafos M, Gilson R, et al. Pre-exposure prophylaxis to prevent the acquisition of HIV-1 infection (PROUD): effectiveness results from the pilot phase of a pragmatic open-label randomised trial. Lancet. 2016;387:53–60.
20. Molina J-M, Capitant C, Spire B, Pialoux G, Cotte L, Charreau I, et al.; ANRS IPERGAY Study Group. On-demand preexposure prophylaxis in men at high risk for HIV-1 infection. N Engl J Med. 2015;373:2237–46. https://doi.org/10.1056/NEJMoa1506273
21. National Institute for Health and Care Excellence. Pre-exposure prophylaxis of HIV in adults at high risk: Truvada (emtricitabine/tenofovir disoproxil). Evidence summary. [ESNM78] [cited 2021 Mar 14]. https://www.nice.org.uk/advice/esnm78/chapter/full-evidence-summary
22. National Institutes of Health. Long-acting injectable form of HIV prevention outperforms daily pill in NIH study [cited 2021 Apr 18]. https://www.nih.gov/news-events/news-releases/long-acting-injectable-form-hiv-prevention-outperforms-daily-pill-nih-study
23. National Institutes of Health. NIH study finds long-acting injectable drug prevents HIV acquisition in cisgender women [cited 2021 Apr 18]. https://www.nih.gov/news-events/news-releases/nih-study-finds-long-acting-injectable-drug-prevents-hiv-acquisition-cisgender-women
24. Cohen MS, Chen YQ, McCauley M, Gamble T, Hosseinipour MC, Kumarasamy N, et al.; HPTN 052 Study Team. Prevention of HIV-1 infection with early antiretroviral therapy. N Engl J Med. 2011;365:493–505. https://doi.org/10.1056/NEJMoa1105243
25. Granich RM, Gilks CF, Dye C, De Cock KM, Williams BG. Universal voluntary HIV testing with immediate antiretroviral therapy as a strategy for elimination of HIV transmission: a mathematical model. Lancet. 2009;373:48–57. https://doi.org/10.1016/S0140-6736(08)61697-9
26. Iwuji CC, Orne-Gliemann J, Larmarange J, Balestre E, Thiebaut R, Tanser F, et al.; ANRS 12249 TasP Study Group. Universal test and treat and the HIV epidemic in rural South Africa: a phase 4, open-label, community cluster randomised trial. Lancet HIV. 2018;5:e116–25. https://doi.org/10.1016/S2352-3018(17)30205-9
27. Havlir DV, Balzer LB, Charlebois ED, Clark TD, Kwarisiima D, Ayieko J, et al. HIV testing and treatment with the use of a community health approach in rural Africa. N Engl J Med. 2019;381:219–29. https://doi.org/10.1056/NEJMoa1809866
28. Makhema J, Wirth KE, Pretorius Holme M, Gaolathe T, Mmalane M, Kadima E, et al. Universal testing, expanded treatment, and incidence of HIV infection in Botswana. N Engl J Med. 2019;381:230–42. https://doi.org/10.1056/NEJMoa1812281

29. Hayes RJ, Donnell D, Floyd S, Mandla N, Bwalya J, Sabapathy K, et al.; HPTN 071 (PopART) Study Team. Effect of universal testing and treatment on HIV incidence—HPTN 071 (PopART). N Engl J Med. 2019;381:207–18. https://doi.org/10.1056/NEJMoa1814556
30. Lundgren JD, Babiker AG, Gordin F, Emery S, Grund B, Sharma S, et al.; INSIGHT START Study Group. Initiation of antiretroviral therapy in early asymptomatic HIV infection. N Engl J Med. 2015;373:795–807. https://doi.org/10.1056/NEJMoa1506816
31. TEMPRANO ANRS 12136 Study Group. A trial of early antiretrovirals and isoniazid preventive therapy in Africa. N Engl J Med. 2015;373:808–22. https://doi.org/10.1056/NEJMoa1507198
32. Rodger AJ, Cambiano V, Bruun T, Vernazza P, Collins S, van Lunzen J, et al.; PARTNER Study Group. Sexual activity without condoms and risk of HIV transmission in serodifferent couples when the HIV-positive partner is using suppressive antiretroviral therapy. JAMA. 2016;316:171–81. https://doi.org/10.1001/jama.2016.5148
33. Nwokolo N, Hill A, McOwan A, Pozniak A. Rapidly declining HIV infection in MSM in central London. Lancet HIV. 2017;4:e482–3.
34. Grulich AE, Guy R, Amin J, Jin F, Selvey C, Holden J, et al.; Expanded PrEP Implementation in Communities in New South Wales (EPIC-NSW) Research Group. Population-level effectiveness of rapid, targeted, high-coverage roll-out of HIV pre-exposure prophylaxis in men who have sex with men: the EPIC-NSW prospective cohort study. Lancet HIV. 2018;5:e629–37.
35. Fauci AS, Redfield RR, Sigounas G, Weahkee MD, Giroir BP. Ending the HIV epidemic: a plan for the United States. JAMA. 2019;321:844–5. https://doi.org/10.1001/jama.2019.1343
36. Rerks-Ngarm S, Pitisuttithum P, Nitayaphan S, Kaewkungwal J, Chiu J, Paris R, et al.; MOPH-TAVEG Investigators. Vaccination with ALVAC and AIDSVAX to prevent HIV-1 infection in Thailand. N Engl J Med. 2009;361:2209–20. https://doi.org/10.1056/NEJMoa0908492
37. Desrosiers RC. Protection against HIV acquisition in the RV144 trial. J Virol. 2017;91:e00905–17. 10.1128/JVI
38. National Institutes of Health. Experimental HIV vaccine regimen ineffective in preventing HIV [cited 2021 Apr 18]. https://www.niaid.nih.gov/news-events/experimental-hiv-vaccine-regimen-ineffective-preventing-hiv
39. National Institutes of Health. Antibody infusions prevent acquisition of some HIV strains, NIH studies find [cited 2021 Apr 18]. https://www.niaid.nih.gov/news-events/antibody-infusions-prevent-acquisition-some-hiv-strains-nih-studies-find
40. Ghys PD, Williams BG, Over M, Hallett TB, Godfrey-Faussett P. Epidemiological metrics and benchmarks for a transition in the HIV epidemic. PLoS Med. 2018; 15:e1002678.
41. Grabowski MK, Serwadda DM, Gray RH, Nakigozi G, Kigozi G, Kagaayi J, et al.; Rakai Health Sciences Program. HIV prevention efforts and incidence of HIV in Uganda. N Engl J Med. 2017;377:2154–66. https://doi.org/10.1056/NEJMoa1702150
42. Borgdorff MW, Kwaro D, Obor D, Otieno G, Kamire V, Odongo F, et al. HIV incidence in western Kenya during scale-up of antiretroviral therapy and voluntary medical male circumcision: a population-based cohort analysis. Lancet HIV. 2018;5:e241–9. https://doi.org/10.1016/S2352-3018(18)30025-0
43. Das P, Horton R. Beyond the silos: integrating HIV and global health. Lancet. 2018;392:260–1.
44. Eisinger RW, Fauci AS. Ending the HIV/AIDS pandemic. Emerg Infect Dis. 2018;24:413–6.
45. De Cock KM, Simone PM, Davison V, Slutsker L. The new global health. Emerg Infect Dis. 2013;19:1192–7. https://doi.org/10.3201/eid1908.130121
46. Lo TQ, Marston BJ, Dahl BA, De Cock KM. Ebola: anatomy of an epidemic. Annu Rev Med. 2017;68:359–70. https://doi.org/10.1146/annurev-med-052915-015604
47. World Health Organization. Ending an Ebola outbreak in a conflict zone [cited 2021 Apr 18]. https://storymaps.arcgis.com/stories/813561c780d44af38c57730418cd96cd
48. Arwady MA, Bawo L, Hunter JC, Massaquoi M, Matanock A, Dahn B, et al. Evolution of Ebola virus disease from exotic infection to global health priority, Liberia, mid-2014. Emerg Infect Dis. 2015;21:578–84. https://doi.org/10.3201/eid2104.141940
49. Mulangu S, Dodd LE, Davey RT Jr, Tshiani Mbaya O, Proschan M, Mukadi D, et al.; PALM Writing Group; PALM Consortium Study Team. A randomized, controlled trial of Ebola virus disease therapeutics. N Engl J Med. 2019;381:2293–303. https://doi.org/10.1056/NEJMoa1910993
50. Henao-Restrepo AM, Camacho A, Longini IM, Watson CH, Edmunds WJ, Egger M, et al. Efficacy and effectiveness of an rVSV-vectored vaccine in preventing Ebola virus disease: final results from the Guinea ring vaccination, open-label, cluster-randomised trial (Ebola Ça Suffit!). Lancet. 2017;389:505–18. https://doi.org/10.1016/S0140-6736(16)32621-6
51. World Health Organization. Yellow fever outbreak Angola, Democratic Republic of the Congo and Uganda 2016–2017 [cited 2021 Mar 14]. https://www.who.int/emergencies/yellow-fever/en
52. Paixão ES, Teixeira MG, Rodrigues LC. Zika, chikungunya and dengue: the causes and threats of new and re-emerging arboviral diseases. BMJ Glob Health. 2018;3(Suppl 1) :e000530.
53. Musso D, Ko AI, Baud D. Zika virus infection—after the pandemic. N Engl J Med. 2019;381:1444–57. https://doi.org/10.1056/NEJMra1808246
54. World Health Organization. International Health Regulations (2005). 2nd ed. Geneva: The Organization; 2008.
55. United Nations. The 17 goals [cited 2021 Apr 18]. https://sdgs.un.org/goals
56. Institute for Health Metrics and Evaluation. Financing global health 2019. Tracking health spending in a time of crisis [cited 2021 Mar 14]. http://www.healthdata.org/policy-report/financing-global-health-2019-tracking-health-spending-time-crisis
57. World Health Organization. Weekly epidemiological update on COVID-19—13 April 2021 [cited 2021 Apr 27]. https://www.who.int/publications/m/item/weekly-epidemiological-update-on-covid-19---13-april-2021

Address for correspondence: Kevin M. De Cock, c/o Miriam McNally, 669 Palmetto Ave, Suites H–I, Chico, CA 95926, USA, and PO Box 25705-00603, Lavington, Nairobi, Kenya; email: kevinmdecock@outlook.com

Pertactin-Deficient *Bordetella pertussis*, Vaccine-Driven Evolution, and Reemergence of Pertussis

Longhuan Ma[1], Amanda Caulfield,[1] Kalyan K. Dewan, Eric T. Harvill

Recent reemergence of pertussis (whooping cough) in highly vaccinated populations and rapid expansion of *Bordetella pertussis* strains lacking pertactin (PRN), a common acellular vaccine antigen, have raised the specter of vaccine-driven evolution and potential return of what was once the major killer of children. The discovery that most circulating *B. pertussis* strains in the United States have acquired new and independent disruptive mutations in PRN is compelling evidence of strong selective pressure. However, the other 4 antigens included in acellular vaccines do not appear to be selected against so rapidly. We consider 3 aspects of PRN that distinguish it from other vaccine antigens, which might, individually or collectively, explain why only this antigen is being precipitously eliminated. An understanding of the increase in PRN-deficient strains should provide useful information for the current search for new protective antigens and provide broader lessons for the design of improved subunit vaccines.

Bordetella pertussis, the causative agent of pertussis (whooping cough), continues to reemerge in countries that have high vaccine coverage, such as the United States, and has accelerated since the switch during the mid-1990s from whole-cell pertussis (wP) formulations comprising many partially characterized bacterial proteins to the less reactogenic 1–5 component acellular pertussis (aP) vaccines (*1*,*2*). These aP vaccines, including DTaP (diphtheria, tetanus, and aP for children) and Tdap (tetanus, diphtheria, and aP for adolescents and adults), protect against disease, but this protection wanes rapidly and does not prevent colonization or transmission of the pathogen (*3*–*5*). In this background of suboptimally performing aP vaccines, many countries have noted the emergence and expansion of strains specifically lacking pertactin (PRN), a membrane bound autotransporter, and 1 of up to 5 *B. pertussis* protein antigens included in the vaccines (*6*–*11*).

Author affiliation: University of Georgia College of Veterinary Medicine, Athens, Georgia, USA

DOI: https://doi.org/10.3201/eid2706.203850

PRN-deficient *B. pertussis* strains have recently been reported in countries using aP vaccines, including the United States, Australia, Sweden, Italy, Norway, the United Kingdom, France, Belgium, Finland, the Netherlands, and Japan. The frequency of PRN-deficient strains has been variable, but these strains have risen to dominance in the United States (85%), Australia (>80%), Sweden (69%), and Italy (55%) (*7*–*11*). Lower frequencies were reported from Japan, which showed a major decrease from a prevalence of 41% during 2008–2010 to 8% during 2014–2016 and correlated with a change to aP vaccine formulations that exclude PRN (*6*,*11*–*12*). Denmark, which uses the monocomponent pertussis toxin (PT) vaccine, had no reports of PRN-deficient isolates before 2012, and the 4 PRN-deficient strains detected since have been associated with human migration from countries with PRN in their vaccines (*6*). Limited data are available from the predominantly developing countries that use wP vaccines to enable a robust comparison between the effects that aP and wP have on the selection of PRN. A sequencing study of the only 2 clinical isolates reported from India, which still uses wP, showed that the isolates still retained the broadly encountered PRN gene allele *prn-1* (*13*). Considered together, these observations provide a strong correlation between the use of aP vaccines containing PRN and the appearance and increase to prominence of PRN-deficient strains.

Lineages of all bacteria are constantly evolving, but increasing to dominance alone is not conclusive evidence of a causal relationship between use of PRN-containing aP vaccines and loss of PRN. A PRN mutation could be carried along with a strain that is increasing in dominance because of 1 or many other mutations. However, the appearance of a wide variety of PRN mutations, each arising from a diversity of *B. pertussis* lineages over time, provides additional strong evidence in favor of vaccine-driven selection

[1]These authors contributed equally to this article.

on PRN in particular. Although insertions of IS481 at multiple genomic locations are the most common PRN mutation, there is a large diversity of disruptions to PRN expression, including deletions within the signal sequence, promoter inversion, transversions resulting in a stop codon, deletions resulting in a stop codon, and full-gene deletion (*2*,*6*,*12*). The variety of genomic lesions that have led to loss of PRN indicates that numerous independent selection and expansion events have occurred in most of the lineages now circulating in many countries using aP vaccines. Providing more direct experimental data, such as murine models aimed at investigating PRN-deficient *B. pertussis* infection, have demonstrated an overall defect in colonization in unvaccinated mice, but advantages in both colonization and competition in assays using aP-vaccinated mice (*14*–*16*).

Together, these observations strongly support the hypothesis that loss of PRN confers a fitness advantage over wildtype *B. pertussis* particular to the aP vaccinated populations in which they are arising. However, there are 4 other antigens included in aP vaccines that are not being disrupted or lost. Why are the other vaccine antigens not being mutated at similar rates? What are the characteristics of PRN that might lead to the loss of this antigen in particular? Understanding multiple possible explanations, and distinguishing between them where possible, will be useful for ongoing efforts to improve vaccines to control *B. pertussis* spread and disease.

Role of PRN

PRN is an autotransporter protein located on the surface of *B. pertussis* (*17*). Similar to all autotransporters found in gram-negative pathogens, PRN has 3 functional domains: the N terminal signal sequence, the passenger domain, and a C-terminal autotransporter domain. The signal sequence guides the passenger and transporter domains into the periplasm, enabling the transporter domain to form a pore in the outer membrane for translocation of the passenger domain to the cell surface. The protein is then cleaved by an outer membrane protease, the passenger domain remaining in contact with the surface by noncovalent interactions (*18*,*19*).

The function of PRN is only partially understood. PRN is considered one of several virulence factors found in *B. pertussis* and has been shown to serve as an adhesin, facilitating attachment to various mammalian epithelial cells (*20*,*21*). The 3-dimensional structure of PRN (PDB no. 1DAB) shows 16 right-handed parallel β-helixes, the largest β-helix structure recorded to date. Two Arg–Gly–Asp tripeptide motifs within the helical structure appear to be potential attachment sites to many mammalian adhesion proteins (*22*–*24*). PRN is reported to be essential for resisting neutrophil-mediated clearance and possesses additional immunomodulatory abilities that aid *B. pertussis* in suppressing the production of proinflammatory cytokines (*25*,*26*). The benefits of functional expression of PRN in pathogenesis are consistent with its conservation in *B. pertussis* and other pathogenic *Bordetella* species. Loss of such a factor would be expected to be costly to the organism, yet PRN-deficient strains appear to be rapidly expanding in aP vaccinated populations, suggesting a recent rebalancing of fitness costs and benefits.

Unique Features of PRN among Vaccine Antigens

PRN is conserved in *B. pertussis*, *B. parapertussis*, and *B. bronchiseptica* under the same *Bordetella* virulence gene regulatory system, suggesting that PRN has a more general role in pathogenesis that is not restricted to the human-specific *B. pertussis*. However, there are 16 other autotransporter genes identified in the genome of *B. pertussis*, 5 of which are disrupted by frameshift mutations (*27*). Park et al. (*28*) observed that autotransporters, as a group, are much more highly mutated or lost than other virulence factors. There appears to be no major loss in in vitro growth or in vivo fitness that prevents the expansion of *B. pertussis* strains lacking PRN, indicating that the functional contributions of PRN in pathogenesis might be redundant or that complementary functions, potentially mediated by other autotransporters, might be compensating for any deficiencies caused its loss. This finding can be contrasted with PT, which requires a complex operon to assemble and another to export, has a central and nonredundant role in the pathogenesis of *B. pertussis*, and has no paralogs in the genome that can replace it. This finding is consistent with the rarity of clinical isolates lacking PT, compared with the abundance of PRN-deficient strains (*29*–*31*). For these and potentially other reasons, it might be that loss of PRN can be tolerated, but loss of PT would result in a more serious fitness defect.

Examination of the location and conformation of the different acellular vaccine components showed that most antibody functions directed against these antigens occur away from the bacterial surface. Both PT and the mature surface-associated filamentous hemagglutinin (FHA) (*32*) are secreted and diffuse away into the surrounding host environment. Therefore, antibodies directed against released FHA and PT would primarily neutralize toxin function by binding to the secreted molecules in the surrounding

milieu, or to molecules in the process of being shed, mitigating potential surface-directed antibody effects. These antibodies do not effectively localize to the bacterial surface and thus do not facilitate complement activation or fragment crystallizable region (FcR)–mediated phagocytosis that would result in direct bacterial killing (Figure 1, panel A) (*33*,*34*). Fimbriae (FIM), although generally anchored to the bacteria, might extend more than a cell length away from the cell surface. Because FIM are composed of repeated structures with many copies of the same antigenic molecule, most FIM antibodies would be bound to parts of the structure extended >1 micron from the bacterial membrane, which is an enormous distance for highly reactive complement components to travel. Antibodies bound to fimbria would not be arrayed on a 2-dimensional surface required to optimally bind and activate complement or FcRs (Figure 1, panel B) (*35*).

However, PRN is the only aP vaccine antigen that remains closely associated with the outer membrane. When cognate antibodies bind PRN, they become arrayed on the bacterial surface in a conformation that is particularly effective in binding and activating complement component C1q. The subsequent complement cascade that is activated rapidly deposits component in the adjacent membrane that opsonizes the cell and assembles into a membrane attack complex to lyse the bacterial membrane (*33*–*36*). The combination of the array of antibodies, bolstered by the complement components cleaved and activated in the immediate vicinity, would effectively opsonize the bacteria for efficient phagocytic killing (Figure 1, panel C).

The model we provide (Figure 1), although largely hypothetical, is consistent with evidence that aP vaccination is effective in preventing severe disease (by binding and neutralizing a key factor that mediate aspects of disease) but is much less effective in preventing nasopharyngeal colonization. Most antibodies, similar to those directed against secreted PT/FHA or distal FIM, do not effectively target and kill the bacteria. This model would also explain why loss of PRN might enable partial evasion of aP-induced immunity, and is also consistent with human surveys that showed that 3-component aP vaccines containing PT, FHA, and PRN were more efficacious than 2-component vaccines lacking PRN (*37*,*38*).

Persistence of PRN Antibodies

Despite the shortcomings of aP vaccines in generating a strong memory response, and the resulting waning immunity of these vaccines against disease (*39*,*40*), aP vaccines induce robust IgG titers against most of its component antigens. However, this strong humoral response, although protecting against symptoms of pertussis, does not prevent the pathogen from colonizing the upper respiratory tract or from transmitting between hosts (*3*). Furthermore, although initially induced at high levels, circulating antibodies decay relatively rapidly across all age groups (*4*,*40*–*43*). Studies evaluating dynamic levels of specific antibodies across time have consistently shown differential rates of decay for the various antigen-specific antibodies, with PT antibody titers decaying more rapidly than antibodies to FHA and PRN (Figure 2). Similarly, FIM2/3 have been reported to poorly stimulate generation of protective antibodies postinfection and postvaccinations (*4*,*43*), although these data conflict with those of other reports that show higher levels of FIM antibodies, even at 10 years postvaccination.

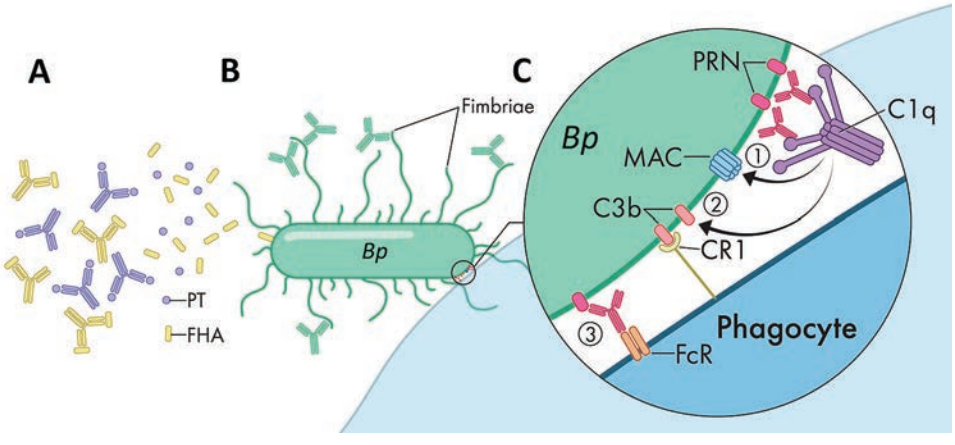

Figure 1. Model for various roles of antibodies against antigens in acellular pertussis vaccine. A) Antibodies against PT and FHA neutralize secreted virulence factors and mitigate disease progression but are not targeted to the bacterial surface. B) Antibodies attaching to fimbriae poorly activate the complement system far from the bacterial membrane. C) Antibody-PRN complex induces strong bactericidal activity via multiple synergistic functions. This complex activates complement to form a MAC, activates complement to deposit components such as C3b that opsonize the bacterial surface, and binds FcRs on phagocytes to activate phagocytosis. PRN labels indicate strains specifically lacking PRN. *Bp*, *Bordetella pertussis*; CR1, complement receptor type 1; FcR, fragment crystallizable region; FHA, filamentous hemagglutinin; MAC, membrane attack complex; PRN, pertactin; PT, pertussis toxin.

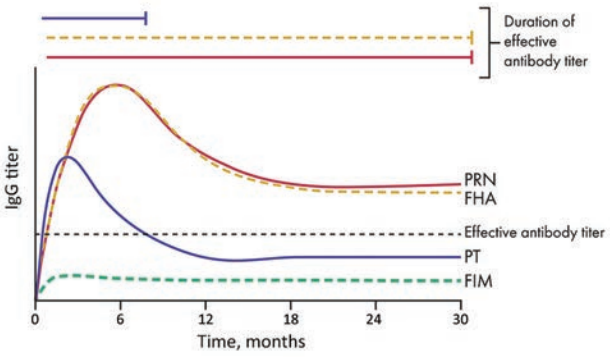

Figure 2. Differential decay of antibodies against acellular pertussis vaccine antigens and their effective capacity for protection. Antibodies against PRN and FHA remain at relatively higher titers for a longer period. However, PT-specific antibodies decrease to low titers rapidly. A consistently low level of antibodies against FIM is induced. Solid lines indicate antibodies that have high protective capacity, and dotted lines indicate antibodies that had low protective capacity. Only PRN antibodies are highly protective and persist at high titers for years. FHA, filamentous hemagglutinin, FIM, fimbriae; PT, pertussis toxin; PRN, pertactin.

However, the higher antibody titers observed in these reports are also noted to decrease sharply and are likely to reach unprotective levels over a relatively short time. This rapid waning immunity against PT and FIM would be expected to narrow the window of selective pressure against these antigens.

In contrast to antibodies against PT, antibodies against PRN and FHA are relatively more persistent (Figure 2) (*38,44,45*), suggesting that there is a longer period after vaccination when there are effective titers of antibodies against FHA and PRN. This finding would be expected to result in strong pressure against PRN and FHA. However, in a search for serologic correlates of immunity to pertussis, Le et al. (*4*) noted that FHA provides relatively little contribution to protection but PRN had a higher protective role.

These observations have recently been validated in studies by Lesne et al., who used human serum bactericidal assays to determine that antibodies to PRN, but no other aP component, are bactericidal in in vitro complement killing assays (*46*). These findings somewhat conflict with those of previous studies and testing methods, which often prioritize PT IgG as an indicator for protection against pertussis (*4,45,47*). However, the short period during which levels of neutralizing antibodies against PT remain elevated, in contrast to bactericidal antibodies against PRN, suggests that PRN antibodies might be a more appropriate measure for pertussis immunity.

The short period during which antibodies to PT remain at elevated levels indicates that there is a longer period when antibodies to PRN remain at high levels, but levels of antibodies to PT have decreased. Le et al. also noted that a much larger proportion of enrolled patients tested before aP vaccination already had high titers of antibodies to PRN, and many had antibodies to PT (*4*). Therefore, in addition to its surface localization and strong opsonizing potential, the persistence of the PRN antibodies is likely to contribute to prolonged selection against this antigen in particular.

Discussion

The rapid reemergence of pertussis noted in the early 2000s brought much initial speculation. Factors such as human migration, increased sensitivity of testing, increased volumes of testing, and reporting through heightened surveillance have been proposed to contribute to the observed resurgence (*1–3*). However, the collective experience in countries switching from wP vaccines to aP vaccines strongly suggests that these safer, but less effective, vaccines have contributed to the resurgence of pertussis. In addition, the way multiple PRN-deficient strains have swept across countries that use aP vaccines presents a strong case in favor of vaccine-driven selection against PRN (*6–12*). What has remained unclear is what will be the consequences of these changes. Will PRN-deficient strains continue to evolve, loosing other vaccine antigens until they escape vaccine effects completely? Or will the loss of these factors result in strains attenuated in virulence such that they become more like commensals than pathogens? Or is PRN really the only antigen that can be lost without serious fitness costs?

The 3 aspects of PRN we have highlighted for selective loss of PRN (i.e., its functional redundancy, the relatively longer functional persistence of antibodies against it, and its close location to the surface membrane for productive complement fixation) are not an exhaustive list of all possibilities and are not mutually exclusive. Sufficient sustained selective pressure against any particular antigen is likely to lead to its loss or change. Efforts to improve the current vaccine should be informed by a careful consideration of the lessons learned from this instance. If PRN is being lost because it is the only surface antigen, then should we replace it with 1 or more new surface antigens? If it is lost because its function is at least partly redundant then should we select some molecule(s) that is less likely to be redundant? In designing new vaccines, it would be prudent to carefully consider the issues that appear to be enabling potential vaccine escape mutants, such as PRN-deficient strains, to rapidly expand and rise to prominence.

This study was supported by the National Science Foundation (grant no. DGE-1545433) and the National Institutes of Health (grant nos. R21DC018496, 1R21AI156293-01, 1R21AI159347-01, and 1R56AI149787-01A1).

About the Authors

Mr. Longhuan and Ms. Caulfield are graduate students in the Department of Infectious Diseases, College of Veterinary Medicine, University of Georgia, Athens, GA. Their primary research interests are host–pathogen interactions and the transmission of *B. pertussis* by using mouse models of infection.

References

1. Jackson DW, Rohani P. Perplexities of pertussis: recent global epidemiological trends and their potential causes. Epidemiol Infect. 2014;142:672–84. https://doi.org/10.1017/S0950268812003093
2. Pawloski LC, Queenan AM, Cassiday PK, Lynch AS, Harrison MJ, Shang W, et al. Prevalence and molecular characterization of pertactin-deficient Bordetella pertussis in the United States. Clin Vaccine Immunol. 2014;21:119–25. https://doi.org/10.1128/CVI.00717-13
3. Warfel JM, Zimmerman LI, Merkel TJ. Acellular pertussis vaccines protect against disease but fail to prevent infection and transmission in a nonhuman primate model. Proc Natl Acad Sci U S A. 2014;111:787–92. https://doi.org/10.1073/pnas.1314688110
4. Le T, Cherry JD, Chang SJ, Knoll MD, Lee ML, Barenkamp S, et al.; APERT Study. Immune responses and antibody decay after immunization of adolescents and adults with an acellular pertussis vaccine: the APERT Study. J Infect Dis. 2004;190:535–44. https://doi.org/10.1086/422035
5. Breakwell L, Kelso P, Finley C, Schoenfeld S, Goode B, Misegades LK, et al. Pertussis vaccine effectiveness in the setting of pertactin-deficient pertussis. Pediatrics. 2016;137:e20153973. https://doi.org/10.1542/peds.2015-3973
6. Barkoff AM, Mertsola J, Pierard D, Dalby T, Hoegh SV, Guillot S, et al. Pertactin-deficient *Bordetella pertussis* isolates: evidence of increased circulation in Europe, 1998 to 2015. Euro Surveill. 2019;24:1700832. https://doi.org/10.2807/1560-7917.ES.2019.24.7.1700832
7. Martin SW, Pawloski L, Williams M, Weening K, DeBolt C, Qin X, et al. Pertactin-negative *Bordetella pertussis* strains: evidence for a possible selective advantage. Clin Infect Dis. 2015;60:223–7. https://doi.org/10.1093/cid/ciu788
8. Byrne S, Slack AT. Analysis of *Bordetella pertussis* pertactin and pertussis toxin types from Queensland, Australia, 1999-2003. BMC Infect Dis. 2006;6:53. https://doi.org/10.1186/1471-2334-6-53
9. Weigand MR, Williams MM, Peng Y, Kania D, Pawloski LC, Tondella ML; CDC Pertussis Working Group. Genomic survey of *Bordetella pertussis* diversity, United States, 2000–2013. Emerg Infect Dis. 2019;25:780–3. https://doi.org/10.3201/eid2504.180812
10. Hiramatsu Y, Miyaji Y, Otsuka N, Arakawa Y, Shibayama K, Kamachi K. Significant decrease in pertactin-deficient *Bordetella pertussis* isolates, Japan. Emerg Infect Dis. 2017;23:699–701. https://doi.org/10.3201/eid2304.161575
11. Zomer A, Otsuka N, Hiramatsu Y, Kamachi K, Nishimura N, Ozaki T, et al. *Bordetella pertussis* population dynamics and phylogeny in Japan after adoption of acellular pertussis vaccines. Microb Genom. 2018;4:e000180. https://doi.org/10.1099/mgen.0.000180
12. Otsuka N, Han HJ, Toyoizumi-Ajisaka H, Nakamura Y, Arakawa Y, Shibayama K, et al. Prevalence and genetic characterization of pertactin-deficient *Bordetella pertussis* in Japan. PLoS One. 2012;7:e31985. https://doi.org/10.1371/journal.pone.0031985
13. Alai S, Ghattargi VC, Gautam M, Patel K, Pawar SP, Dhotre DP, et al. Comparative genomics of whole-cell pertussis vaccine strains from India. BMC Genomics. 2020;21:345. https://doi.org/10.1186/s12864-020-6724-8
14. van Gent M, van Loo IH, Heuvelman KJ, de Neeling AJ, Teunis P, Mooi FR. Studies on Prn variation in the mouse model and comparison with epidemiological data. PLoS One. 2011;6:e18014. https://doi.org/10.1371/journal.pone.0018014
15. Safarchi A, Octavia S, Luu LD, Tay CY, Sintchenko V, Wood N, et al. Pertactin negative *Bordetella pertussis* demonstrates higher fitness under vaccine selection pressure in a mixed infection model. Vaccine. 2015;33:6277–81. https://doi.org/10.1016/j.vaccine.2015.09.064
16. Hegerle N, Dore G, Guiso N. Pertactin deficient *Bordetella pertussis* present a better fitness in mice immunized with an acellular pertussis vaccine. Vaccine. 2014;32:6597–600. https://doi.org/10.1016/j.vaccine.2014.09.068
17. Brennan MJ, Li ZM, Cowell JL, Bisher ME, Steven AC, Novotny P, et al. Identification of a 69-kilodalton nonfimbrial protein as an agglutinogen of *Bordetella pertussis*. Infect Immun. 1988;56:3189–95. https://doi.org/10.1128/IAI.56.12.3189-3195.1988
18. Henderson IR, Navarro-Garcia F, Nataro JP. The great escape: structure and function of the autotransporter proteins. Trends Microbiol. 1998;6:370–8. https://doi.org/10.1016/S0966-842X(98)01318-3
19. Wells TJ, Tree JJ, Ulett GC, Schembri MA. Autotransporter proteins: novel targets at the bacterial cell surface. FEMS Microbiol Lett. 2007;274:163–72. https://doi.org/10.1111/j.1574-6968.2007.00833.x
20. Everest P, Li J, Douce G, Charles I, De Azavedo J, Chatfield S, et al. Role of the *Bordetella pertussis* P.69/pertactin protein and the P.69/pertactin RGD motif in the adherence to and invasion of mammalian cells. Microbiology (Reading). 1996;142:3261–8. https://doi.org/10.1099/13500872-142-11-3261
21. Leininger E, Roberts M, Kenimer JG, Charles IG, Fairweather N, Novotny P, et al. Pertactin, an Arg-Gly-Asp-containing *Bordetella pertussis* surface protein that promotes adherence of mammalian cells. Proc Natl Acad Sci U S A. 1991;88:345–9. https://doi.org/10.1073/pnas.88.2.345
22. Emsley P, McDermott G, Charles IG, Fairweather NF, Isaacs NW. Crystallographic characterization of pertactin, a membrane-associated protein from *Bordetella pertussis*. J Mol Biol. 1994;235:772–3. https://doi.org/10.1006/jmbi.1994.1029
23. Emsley P, Charles IG, Fairweather NF, Isaacs NW. Structure of *Bordetella pertussis* virulence factor P.69 pertactin. Nature. 1996;381:90–2. https://doi.org/10.1038/381090a0
24. Junker M, Schuster CC, McDonnell AV, Sorg KA, Finn MC, Berger B, et al. Pertactin β-helix folding mechanism suggests common themes for the secretion and folding of autotransporter proteins. Proc Natl Acad Sci U S A. 2006;103:4918–23. https://doi.org/10.1073/pnas.0507923103
25. Inatsuka CS, Xu Q, Vujkovic-Cvijin I, Wong S, Stibitz S, Miller JF, et al. Pertactin is required for *Bordetella species* to resist neutrophil-mediated clearance. Infect Immun. 2010;78:2901–9. https://doi.org/10.1128/IAI.00188-10

26. Hovingh ES, Mariman R, Solans L, Hijdra D, Hamstra HJ, Jongerius I, et al. *Bordetella pertussis* pertactin knock-out strains reveal immunomodulatory properties of this virulence factor. Emerg Microbes Infect. 2018;7:39. https://doi.org/10.1038/s41426-018-0039-8
27. Parkhill J, Sebaihia M, Preston A, Murphy LD, Thomson N, Harris DE, et al. Comparative analysis of the genome sequences of *Bordetella pertussis*, *Bordetella parapertussis* and *Bordetella bronchiseptica*. Nat Genet. 2003;35:32–40. https://doi.org/10.1038/ng1227
28. Park J, Zhang Y, Chen C, Dudley EG, Harvill ET. Diversity of secretion systems associated with virulence characteristics of the classical bordetellae. Microbiology (Reading). 2015;161:2328–40. https://doi.org/10.1099/mic.0.000197
29. Linz B, Ivanov YV, Preston A, Brinkac L, Parkhill J, Kim M, et al. Acquisition and loss of virulence-associated factors during genome evolution and speciation in three clades of *Bordetella* species. BMC Genomics. 2016;17:767. https://doi.org/10.1186/s12864-016-3112-5
30. Bouchez V, Hegerle N, Strati F, Njamkepo E, Guiso N. New data on vaccine antigen deficient *Bordetella pertussis* isolates. Vaccines (Basel). 2015;3:751–70. https://doi.org/10.3390/vaccines3030751
31. Bouchez V, Brun D, Cantinelli T, Dore G, Njamkepo E, Guiso N. First report and detailed characterization of *B. pertussis* isolates not expressing pertussis toxin or pertactin. Vaccine. 2009;27:6034–41. https://doi.org/10.1016/j.vaccine.2009.07.074
32. Nash ZM, Cotter PA. *Bordetella* filamentous hemagglutinin, a model for the two-partner secretion pathway. Microbiol Spectr. 2019;7:319–28. https://doi.org/10.1128/microbiolspec.PSIB-0024-2018
33. Hellwig SM, Rodriguez ME, Berbers GA, van de Winkel JG, Mooi FR. Crucial role of antibodies to pertactin in *Bordetella pertussis* immunity. J Infect Dis. 2003;188:738–42. https://doi.org/10.1086/377283
34. Weiss AA, Mobberley PS, Fernandez RC, Mink CM. Characterization of human bactericidal antibodies to *Bordetella pertussis*. Infect Immun. 1999;67:1424–31. https://doi.org/10.1128/IAI.67.3.1424-1431.1999
35. Lambris JD, Ricklin D, Geisbrecht BV. Complement evasion by human pathogens. Nat Rev Microbiol. 2008;6:132–42. https://doi.org/10.1038/nrmicro1824
36. Jongerius I, Schuijt TJ, Mooi FR, Pinelli E. Complement evasion by *Bordetella pertussis*: implications for improving current vaccines. J Mol Med (Berl). 2015;93:395–402. https://doi.org/10.1007/s00109-015-1259-1
37. Greco D, Salmaso S, Mastrantonio P, Giuliano M, Tozzi AE, Anemona A, et al.; Progetto Pertosse Working Group. A controlled trial of two acellular vaccines and one whole-cell vaccine against pertussis. N Engl J Med. 1996;334:341–8. https://doi.org/10.1056/NEJM199602083340601
38. Gustafsson L, Hallander HO, Olin P, Reizenstein E, Storsaeter J. A controlled trial of a two-component acellular, a five-component acellular, and a whole-cell pertussis vaccine. N Engl J Med. 1996;334:349–55. https://doi.org/10.1056/NEJM199602083340602
39. van Twillert I, Han WG, van Els CA. Waning and aging of cellular immunity to *Bordetella pertussis*. Pathog Dis. 2015;73:ftv071. https://doi.org/10.1093/femspd/ftv071
40. Tomovici A, Barreto L, Zickler P, Meekison W, Noya F, Voloshen T, et al. Humoral immunity 10 years after booster immunization with an adolescent and adult formulation combined tetanus, diphtheria, and 5-component acellular pertussis vaccine. Vaccine. 2012;30:2647–53. https://doi.org/10.1016/j.vaccine.2012.02.013
41. Taranger J, Trollfors B, Lagergård T, Sundh V, Bryla DA, Schneerson R, et al. Correlation between pertussis toxin IgG antibodies in postvaccination sera and subsequent protection against pertussis. J Infect Dis. 2000;181:1010–3. https://doi.org/10.1086/315318
42. Munoz FM, Bond NH, Maccato M, Pinell P, Hammill HA, Swamy GK, et al. Safety and immunogenicity of tetanus diphtheria and acellular pertussis (Tdap) immunization during pregnancy in mothers and infants: a randomized clinical trial. JAMA. 2014;311:1760–9. https://doi.org/10.1001/jama.2014.3633
43. Abu Raya B, Srugo I, Kessel A, Peterman M, Vaknin A, Bamberger E. The decline of pertussis-specific antibodies after tetanus, diphtheria, and acellular pertussis immunization in late pregnancy. J Infect Dis. 2015;212:1869–73. https://doi.org/10.1093/infdis/jiv324
44. Heininger U, Cherry JD, Stehr K. Serologic response and antibody-titer decay in adults with pertussis. Clin Infect Dis. 2004;38:591–4. https://doi.org/10.1086/381439
45. Storsaeter J, Hallander HO, Gustafsson L, Olin P. Levels of anti-pertussis antibodies related to protection after household exposure to *Bordetella pertussis*. Vaccine. 1998;16:1907–16. https://doi.org/10.1016/S0264-410X(98)00227-8
46. Lesne E, Cavell BE, Freire-Martin I, Persaud R, Alexander F, Taylor S, et al. Acellular pertussis vaccines induce anti-pertactin bactericidal antibodies which drives the emergence of pertactin-negative strains. Front Microbiol. 2020;11:2108. https://doi.org/10.3389/fmicb.2020.02108
47. Lee AD, Cassiday PK, Pawloski LC, Tatti KM, Martin MD, Briere EC, et al.; Clinical Validation Study Group. Clinical evaluation and validation of laboratory methods for the diagnosis of *Bordetella pertussis* infection: culture, polymerase chain reaction (PCR) and anti-pertussis toxin IgG serology (IgG-PT). PLoS One. 2018;13:e0195979. https://doi.org/10.1371/journal.pone.0195979

Address for correspondence: Kalyan K. Dewan, Department of Infectious Diseases, College of Veterinary Medicine, University of Georgia, Athens, GA 30602, USA; email: kaldew@uga.edu or kkd112014@gmail.com

Rocky Mountain Spotted Fever in a Large Metropolitan Center, Mexico–United States Border, 2009–2019

Oscar E. Zazueta, Paige A. Armstrong, Adriana Márquez-Elguea, Néstor Saúl Hernández Milán, Amy E. Peterson, Diego F. Ovalle-Marroquín, Maria Fierro, Rodolfo Arroyo-Machado, Moises Rodriguez-Lomeli, Guillermo Trejo-Dozal, Christopher D. Paddock

Medscape EDUCATION ACTIVITY

In support of improving patient care, this activity has been planned and implemented by Medscape, LLC and Emerging Infectious Diseases. Medscape, LLC is jointly accredited by the Accreditation Council for Continuing Medical Education (ACCME), the Accreditation Council for Pharmacy Education (ACPE), and the American Nurses Credentialing Center (ANCC), to provide continuing education for the healthcare team.

Medscape, LLC designates this Journal-based CME activity for a maximum of 1.00 ***AMA PRA Category 1 Credit(s)™***. Physicians should claim only the credit commensurate with the extent of their participation in the activity.

Successful completion of this CME activity, which includes participation in the evaluation component, enables the participant to earn up to 1.0 MOC points in the American Board of Internal Medicine's (ABIM) Maintenance of Certification (MOC) program. Participants will earn MOC points equivalent to the amount of CME credits claimed for the activity. It is the CME activity provider's responsibility to submit participant completion information to ACCME for the purpose of granting ABIM MOC credit.

All other clinicians completing this activity will be issued a certificate of participation. To participate in this journal CME activity: (1) review the learning objectives and author disclosures; (2) study the education content; (3) take the post-test with a 75% minimum passing score and complete the evaluation at http://www.medscape.org/journal/eid; and (4) view/print certificate. For CME questions, see page 1765.

Release date: May 12, 2021; Expiration date: May 12, 2022

Learning Objectives

Upon completion of this activity, participants will be able to:

- Analyze symptoms of RMSF in the current study
- Assess the epidemiology of RMSF in the current study
- Evaluate the results of diagnostic testing for RMSF in the current study
- Distinguish the risk of mortality associated with RMSF in the current study

CME Editor

Terie A. Grant, BS, Copyeditor, Emerging Infectious Diseases. *Disclosure: Terie A. Grant, BS, has disclosed no relevant financial relationships.*

CME Author

Charles P. Vega, MD, Health Sciences Clinical Professor of Family Medicine, University of California, Irvine School of Medicine, Irvine, California. *Disclosure: Charles P. Vega, MD, has disclosed the following relevant financial relationships: served as an advisor or consultant for GlaxoSmithKline.*

Authors

Disclosures: ***Oscar E. Zazueta, MD; Paige A. Armstrong, MD, MHS; Adriana Márquez-Elguea, MD; Néstor Saúl Hernández Milán, MD, PhD; Amy E. Peterson, DVM, PhD; Diego F. Ovalle-Marroquín, MD; Maria Fierro, MD, MPH; Rodolfo Arroyo-Machado, RN; Moises Rodriguez-Lomeli, MD; Guillermo Trejo-Dozal, MD;*** *and* ***Christopher D. Paddock, MD, MPHTM,*** *have disclosed no relevant financial relationships.*

Author affiliations: Secretariat of Health of Baja California (Instituto de Servicios de Salud Pública del Estado de Baja California), Mexicali, Mexico (O.E. Zazueta, A. Márquez-Elguea, N.S.H. Milán, D.F. Ovalle-Marroquín, R. Arroyo-Machado, M. Rodriguez-Lomeli, G. Trejo-Dozal); Centers for Disease Control and Prevention, Atlanta, Georgia, USA (P.A. Armstrong, A.E. Peterson, C.D. Paddock); Imperial Country Public Health Department, El Centro, California, USA (M. Fierro)

DOI: https://doi.org/10.3201/eid2706.191662

Epidemic levels of Rocky Mountain spotted fever (RMSF) have persisted in Mexicali, Mexico, since the initial outbreak was first reported in December 2008. We compared clinical and epidemiologic data of cases in Mexicali during 2009–2019 between patients with an IgG titer reactive with *Rickettsia rickettsii* bacteria by indirect immunofluorescence antibody (IFA) assay and those who demonstrated DNA of *R. rickettsii* in a whole blood sample when tested by PCR. We identified 4,290 patients with clinical and epidemiologic features compatible with RMSF; of these, 9.74% tested positive by IFA and 8.41% by PCR. Overall, 140 patients died (11-year case-fatality rate 17.97%). Substantial differences in the frequency of commonly recognized clinical characteristics of RMSF were identified between PCR-positive and IFA-positive cases. The Mexicali epidemic is unique in its size and urban centralization. Cases confirmed by PCR most accurately reflect the clinical profile of RMSF.

Rocky Mountain spotted fever (RMSF), a severe and potentially deadly tickborne disease caused by *Rickettsia rickettsii* bacteria, occurs throughout the Americas. The classic epidemiology of RMSF is characterized by isolated and sporadic cases of disease that occur predominantly in rural or suburban settings (*1*). Occasionally, regional endemic foci of infection are described, which can persist for years, or sometimes decades (*2*). During the early 2000s, investigators identified multiple outbreaks of RMSF among several small communities in Arizona in the United States and in Sonora, Mexico (*3*–*6*). A feature common to each of these outbreaks has been the presence of large populations of stray and free-ranging dogs heavily infested with ticks. In these settings, canine populations can sustain and perpetuate massive numbers of brown dog ticks (*Rhipicephalus sanguineus* sensu lato), which serve as efficient vectors of *R. rickettsii* bacteria.

In December 2008, cases of RMSF were first recognized among residents of a neighborhood in Mexicali, the capital city of Baja California, Mexico (*7*,*8*). During the next few years, cases were identified in adjacent and distant neighborhoods. In contrast to almost all previously described outbreaks of RMSF, this epidemic emerged within a large metropolitan center, continues in the present day, and has affected hundreds of persons throughout the city. Cases of RMSF are now also reported beyond the city limits from several small communities in the Mexicali Valley (*9*,*10*).

The ongoing epidemic of RMSF in Mexicali resembles past and present outbreaks in Arizona and northern Mexico. Cases of disease occur primarily in impoverished neighborhoods, where the presence of large populations of stray dogs infested with infected brown dog ticks greatly increase the human risk for exposure to the pathogen (*10*–*13*). Efforts to document the scope and magnitude of RMSF in Mexicali have been hampered by limited access to sensitive and specific diagnostic techniques, the relatively nonspecific clinical findings observed during the early stages of illness, and incomplete awareness among many residents and local health care providers of the regional risk and scope of the epidemic (*10*). To more accurately characterize the epidemiology of RMSF in Mexicali, we compiled and analyzed data available for all cases with serologic or molecular evidence of infection that were reported to the Secretariat of Health of Baja California (ISESALUD) during 2009–2019.

Methods

Setting

Mexicali is located at the Mexico–United States border, adjacent to the California town of Calexico. According to the National Institute of Statistics and Geography in Mexico, this large urban center extends across 114 km^2 and has a population of ≈700,000 persons. The Mexicali Valley, comprising 13,700 km^2, extends southeast of the city and is inhabited by ≈250,000 persons. Most city residents receive their medical care at hospitals and clinics operated by the Mexican Institute of Social Security (60%), ISESALUD (21%), and the Institute for Social Security and Services for State Workers (13%) (*14*).

Collection of Data

We analyzed clinical and epidemiologic data for all cases of RMSF reported to ISESALUD in the Mexicali metropolitan area and the Mexicali Valley during 2009–2019 by abstracting data retrospectively from the standardized case report used by the Mexicali General Hospital and Ministry of Health clinics across the city (*15*) and all major hospitals in the area. Case definitions are established nationwide by the Directorate General of Epidemiology (DGE) (*15*,*16*). A probable case is defined as fever (>38.5°C) and ≥2 of the following signs or symptoms: headache, myalgia, rash, purpura, meningeal signs, alterations in cerebrospinal fluid, hemorrhage, liver enzyme abnormality, hematologic alterations, hyponatremia, leukocytosis, leukopenia, elevated levels of lactate dehydrogenase, or shock. Cases also require ≥1 of the following epidemiologic criteria during the 2 weeks preceding illness onset: history of tick bite or direct contact with a tick-infested dog, ticks identified in or around the patient's household, or travel to or

residence in a neighborhood where cases of RMSF had been recently identified. Confirmed cases include those in patients with a serum IgG titer ≥64 to *R. rickettsii* antigens, determined by an indirect immunofluorescence antibody (IFA) assay on serum samples, and those for whom PCR evaluation of a whole blood specimen demonstrates DNA of a spotted fever group *Rickettsia* (SFGR). For this investigation, we compared frequencies of clinical and epidemiologic characteristics identified for those patients with a positive PCR result with those identified by a positive IFA result.

Laboratory Testing

During 2009, serum specimens were serially diluted beginning at 1:80; for all subsequent years, 1:64 was used as the first dilution. Antibody titers were expressed as the reciprocal of the last reactive dilution, and titers ≥64 were considered positive. Molecular analyses were performed by using a *Rickettsia* genus–specific real-time assay targeting a 74-bp segment of the citrate synthase gene and primers CS-F and CS-R and probe CS-P, as previously described (*17*). Samples with cycle threshold values <38 were considered positive on the basis of the cutoff for this assay established by the Mexico Secretariat of Health, Institute of Epidemiological Diagnosis and Reference.

Mapping and Statistical Analyses

We transformed physical addresses of PCR-positive case-patients into geographic coordinates by using an automated algorithm developed by Mexico's National Institute of Statistics and Geography. We created maps using Epi Info 7 (Centers for Disease Control and Prevention, https://www.cdc.gov/epiinfo). We described categorical variables as counts and proportions and continuous variables by using mean, median, and range. We used the *t*-test for comparisons of means and Fisher exact test for comparisons of proportions. Because of the large number of cases, we assumed that continuous data followed a normal distribution according to the central limit theorem. We did not report missing data. We used Stata 14 (StataCorp, https://www.stata.com) to perform all statistical analyses. This study was approved by the Institutional Review Board of Tijuana General Hospital (approval no. HGT-2017-000058).

Results

During 2009–2019, a total of 4,290 persons in metropolitan Mexicali and the Mexicali Valley had illnesses meeting the DGE case definition for probable cases of RMSF (Figure 1). Of those, a diagnostic assay was performed on 2,532 patients, and a positive result from either assay was recorded for 921 (36.37%). We excluded 142: those for whom only an IgM titer was available (n = 102) and those for whom an IFA result was reported as positive but without a reported antibody titer (n = 40). Of the total probable cases identified by the surveillance case definition, 779 (18.15%) met DGE criteria for a confirmed case, 418 (53.66%) with a positive test result by IFA and 361 (46.34%) by PCR (Table 1). For 341 confirmed cases, only PCR was performed, for 417 only IFA, and for 21 both tests. Of those tested by PCR and IFA, 20 had positive results with both assays, and 1 was negative by PCR but positive by IFA.

The median time from illness onset until the collection of whole blood for PCR and serum for IFA was 5 days (interquartile range [IQR] 3–8 days). The geometric mean titers of IFA-positive cases were 175 during 2009–2011, 231 during 2012–2015, and 156 during 2016–2019. Approximately two thirds (64.2%) of positive serum samples were collected during the first week of illness.

Nearly half (378, 48.52%) of all positive case-patients resided in the city of Mexicali. The remaining case-patients originated from several neighborhoods adjacent to but beyond the city limits (243 [31.19%]), the region of Puebla (57 [7.32%]), and from the Mexicali Valley (101 [12.97%]). The cumulative 11-year average incidence rate of RMSF during this period, including PCR- and IFA-confirmed cases, was 7.22/100,000 population/year (1.76–29.16/100,000 population/year) (Figure 2).

Among all confirmed case-patients, the mean age was 23.89 years (SD 17.65, IQR 9–36 years), which did not differ significantly between those whose cases were confirmed by IFA or PCR. Most patients (440 [56.48%]) were female. Cases occurred during each month of the year but were more frequent during the summer months (Figure 3). A disproportionately higher number of IFA-confirmed cases were identified during February and March; nonetheless, 156 (37.32%) of all IFA-positive cases were reported during early 2009, shortly after the outbreak was first recognized and before widespread access to confirmatory PCR assays. A total of 410 case-patients were hospitalized, 271 (66.1%) of whom were confirmed by PCR only, 123 (30%) by IFA only, and 16 (3.9%) by both assays. The mean length of stay of hospitalized case-patients was 8.89 days (median 5 days, IQR 1–11 days), a mean of 9.23 days for PCR-confirmed patients and 7.33 days for IFA-confirmed patients (p = 0.20).

Overall, 140 patients died (11-year case-fatality rate 17.97%): 125 (89.28%) whose illness was diagnosed

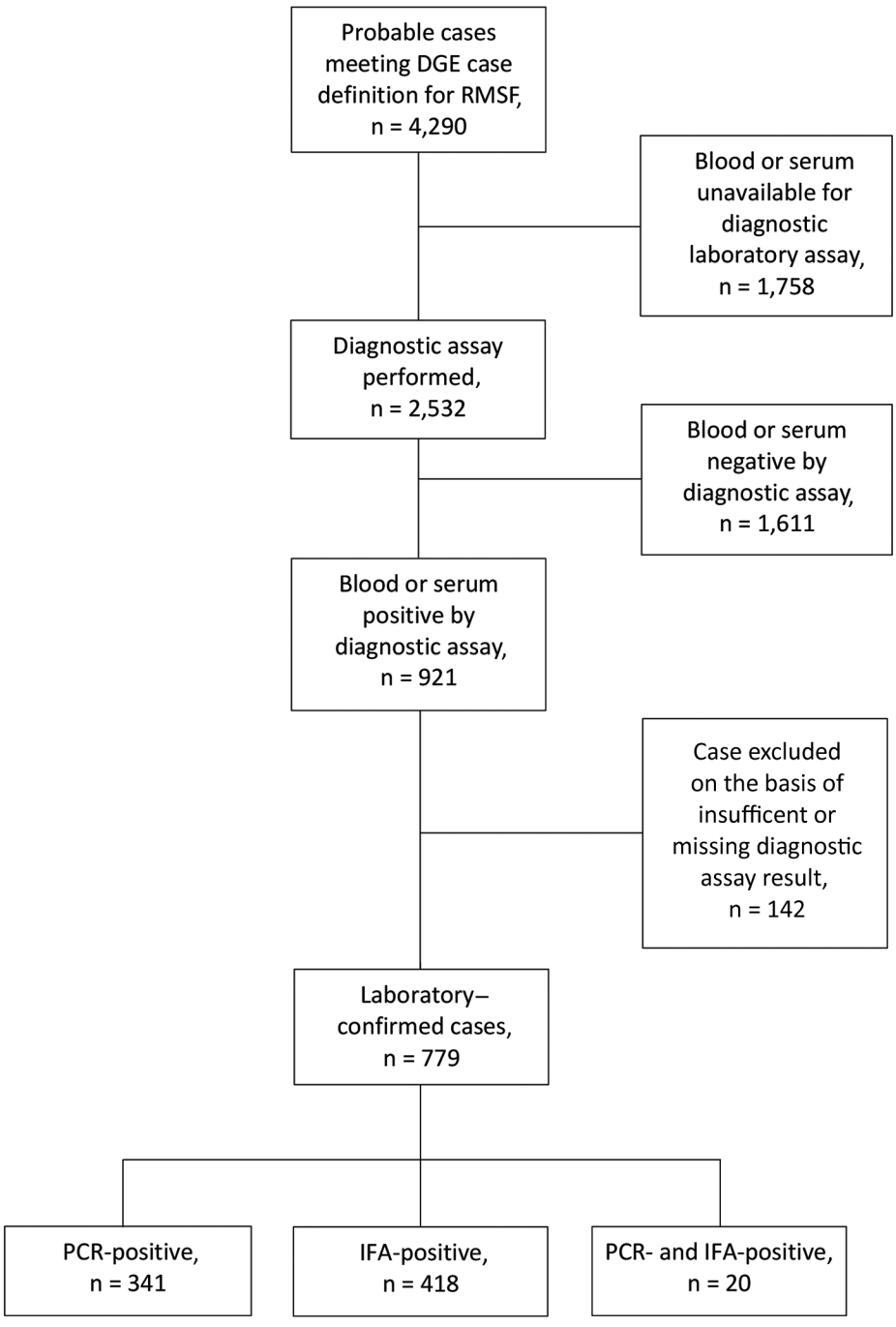

Figure 1. Flowchart used to determine case status of patients in whom Rocky Mountain spotted fever was diagnosed, Mexicali, Mexico, 2009–2019. DGE, Directorate General of Epidemiology; IFA, indirect immunofluorescence antibody assay; RMSF, Rocky Mountain spotted fever.

by PCR only, 11 (7.86%) by IFA only, and 4 (2.86%) by both assays. Approximately one quarter of deaths occurred among children ≤15 years of age (Table 2). The case-fatality rate was 36.66% for PCR-positive and 2.63% for IFA-positive patients ($p<0.001$). PCR-confirmed case-patients were significantly more likely to be admitted to a hospital ($p<0.001$) and die from their infections than were case-patients confirmed by IFA (Table 3).

Among patients with laboratory-confirmed cases, the predominant signs and symptoms were fever (100%), headache (86.43%), myalgia (61.66%), arthralgia (53.10%), nausea (48.22%), abdominal pain (45.45%), and rash (43.27%). However, statistically significant differences were identified in the frequencies of several of these features, and many other clinical findings, when comparing PCR-positive versus IFA-positive patients (Table 3).

Table 1. Frequency of laboratory-confirmed cases of Rocky Mountain spotted fever by assay, Mexicali, Mexico, 2009–2019*

Period	No. (%)			Total no. cases
	PCR-positive	IFA-positive	PCR- and IFA-positive	
2009–2011	73 (20.74)	275 (78.13)	4 (1.14)	352
2012–2015	172 (56.95)	114 (37.75)	16 (5.30)	302
2016–2019	96 (76.80)	29 (23.20)	0 (0)	125
Total	341 (43.77)	418 (53.66)	20 (2.57)	779

*IFA, indirect immunofluorescence antibody assay.

Geospatial analysis of PCR-confirmed cases during the periods 2009–2011, 2012–2015, and 2016–2019 revealed marked expansion of recognized cases across Mexicali. During the first 3 years of the outbreak, cases were concentrated predominantly in the western part of the city from where the index case originated in 2008. During 2012–2015, cases were subsequently identified in the southern portion of the city (Figure 4, panel A) and the region of Puebla in southeastern Mexicali. The Mexicali Valley also experienced progressively more cases during 2016–2019 (Figure 4, panel B). Cases have been identified in almost every neighborhood of Mexicali over the course of the epidemic, often repeatedly in the same areas over time.

Discussion

The epidemiology of RMSF in Mexicali shares many features of epidemic RMSF identified previously among communities in other regions of southwestern North America (*3*–*6*,*13*). During the 1940s, investigators in Mexico were the first to identify and characterize the ecologic, epidemiologic, and social determinants of outbreaks of RMSF that emerged among small and impoverished communities of Sinaloa, Sonora, Durango, and Coahuila. These highly lethal outbreaks, ignited by unchecked canine populations that supported massive peridomestic infestations by brown dog ticks, resulted in high attack rates among women and children and ended in death for most infected patients (*13*,*18*,*19*). Contemporary outbreaks in Sonora and Coahuila also involve predominantly economically vulnerable populations and are particularly devastating among children, for whom mortality rates range from 30% to 57% (*13*,*20*–*22*). The Mexicali epidemic is similarly represented by a large number of pediatric patients and a nearly 37% case-fatality rate among PCR-positive cases. The year-round occurrence of the disease, with notable peaks during the summer and fall months, also reflects the previously described seasonal pattern of RMSF in northern Mexico.

The Mexicali epidemic is unique from all previously described outbreaks of RMSF in terms of its magnitude, urban concentration, and widespread persistence. The timing and origin of the introductory event that precipitated this multiyear outbreak remains unknown. However, the circumstances that propelled its expansion and eventual perpetuation across the city, including high-density, low-income neighborhoods with large numbers of free-roaming and stray dogs and abundant brown dog tick populations, exist within many other metropolitan areas across Mexico and Latin America. In this context, similar urban outbreaks could plausibly originate elsewhere after local introduction of *R. rickettsii*. As we note, during 2009–2019, surveillance activities by ISESALUD identified 779 patients with laboratory-supported diagnoses of RMSF in Mexicali and the

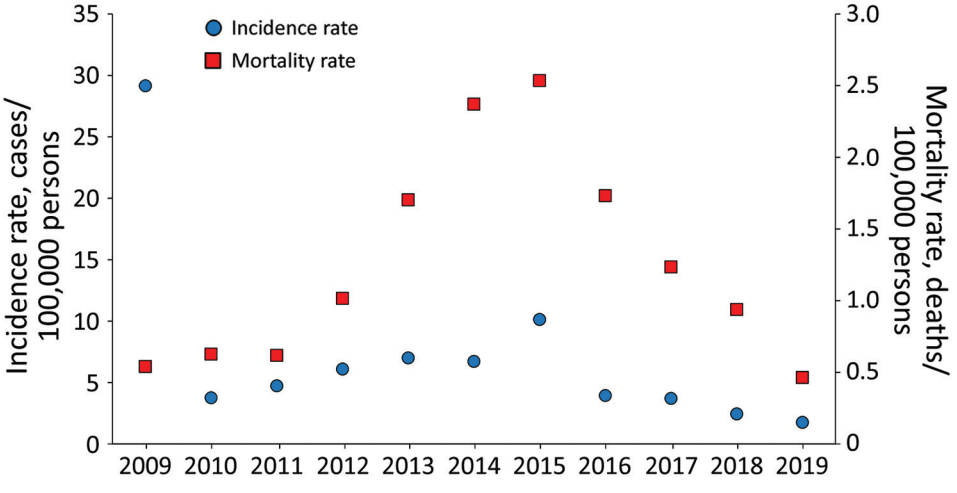

Figure 2. Incidence and mortality rates of laboratory-confirmed Rocky Mountain spotted fever, Mexicali, Mexico, 2009–2019. Scales for the *y*-axes differ substantially to underscore patterns but do not permit direct comparisons.

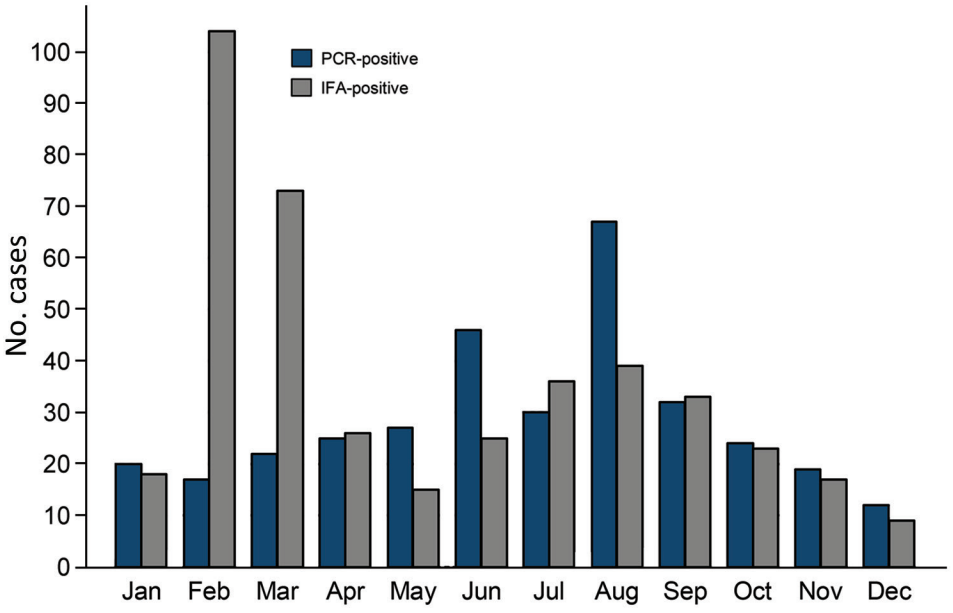

Figure 3. Seasonal distribution of PCR- and IFA-positive cases of Rocky Mountain spotted fever, Mexicali, Mexico, 2009–2019.IFA, indirect immunofluorescence antibody assay.

Mexicali Valley. By comparison, the largest modern outbreak of RMSF in the United States, involving 466 confirmed and probable cases during 2003–2019, has affected predominantly rural tribal communities in Arizona (https://www.azdhs.gov/preparedness/epidemiology-disease-control/index.php#data-stats-past-years). Urban foci of RMSF are described only rarely and sporadically in the United States and other countries of Latin America and are characteristically limited in size and duration (*23*–*26*), so the longevity, remarkably high prevalence, and multifocal distribution of RMSF in a large metropolitan center poses unprecedented public health challenges.

This study is also noteworthy for the large number of PCR-positive cases available for analysis. Various studies indicate that the clinical sensitivities of molecular assays are low early in the illness, but increase as the disease progresses and the patient becomes severely ill (*27*,*28*). PCR-positive patients are more likely to have severe manifestations, which could bias comparisons between groups confirmed by molecular and serologic methods. In addition, the molecular assay used to confirm cases of RMSF in Mexicali is specific only for the genus *Rickettsia* (*17*); because other pathogenic *Rickettsia* species, including *R. massiliae*, *R. parkeri*, and *R. typhi*, are endemic to northern Mexico (*29*–*33*), some PCR-positive patients identified in this series might have represented cases of rickettsial diseases other than RMSF. However, the overall severity of illnesses, coupled with extensive and consistent epidemiologic and environmental evidence implicating brown dog ticks as the principal vector perpetuating this outbreak (*8*–*10*,*12*), suggest strongly that most, if not all, PCR-confirmed cases were indeed infections caused by *R. rickettsii*.

Although IFA methods are used widely for epidemiologic evaluations of RMSF, the use of a single IgG titer can reflect past exposure to an SFGR at an undetermined time and can inaccurately reflect surveillance estimates that define the magnitude and clinical characteristics of RMSF (*29*). Because IgG titers are reflective of the host immune response to *R. rickettsii*, these titers are not expected to be elevated in the first several days of illness, when most patients seek medical attention. In fact, ≈50% of patients with RMSF lack

Table 2. Age distribution of patients with PCR- and IFA-positive cases of fatal Rocky Mountain spotted fever, Mexicali, Mexico, 2009–2019*

Age group, y	No. (%)			
	PCR-positive	IFA-positive	PCR- and IFA-positive	Total
≤15	25 (20)	6 (54.55)	1 (25)	32 (22.86)
16–24	25 (20)	0	0	25 (17.86)
25–44	43 (34.40)	3 (27.27)	2 (50)	48 (34.29)
45–64	28 (22.40)	2 (18.18)	1 (25)	31 (22.14)
≥65	4 (3.20)	0	0	4 (2.86)
Total	129 (100)	11 (100)	4 (100)	140 (100)

*IFA, indirect immunofluorescence antibody assay.

Table 3. Demographic and clinical characteristics of patients with PCR- and IFA-positive cases of Rocky Mountain spotted fever, Mexicali, Mexico, 2009–2019*

Characteristic	Total	PCR-positive	IFA-positive	p value
No. patients	759	341	418	
Sex				
F	433 (57.05)	170 (49.85)	263 (62.92)	<0.001
M	326 (42.95)	171 (50.15)	155 (37.08)	
Age, y (mean ± SD)	23.94 (± 17.67)	24.38 (± 18.89)	23.59 (± 16.62)	0.540
Hospitalized	394 (51.91)	271 (79.47)	123 (29.43)	<0.001
Died	136 (17.92)	125 (36.66)	11 (2.63)	<0.001
Signs and symptoms				
Fever	759 (100)	341 (100)	418 (100)	0.999
Headache	656 (86.43)	288 (84.46)	368 (88.04)	0.166
Myalgia	468 (61.66)	229 (67.16)	239 (57.18)	0.005
Arthralgia	403 (53.10)	197 (57.77)	206 (49.28)	0.023
Retro orbital pain	82 (10.80)	26 (7.04)	58 (13.88)	0.003
Rash	328 (43.27)	181 (53.24)	147 (35.17)	<0.001
Pruritis	139 (18.31)	56 (16.42)	83 (19.86)	0.258
Vomiting	322 (42.42)	188 (55.13)	134 (32.06)	<0.001
Nausea	366 (48.22)	206 (60.41)	160 (38.28)	<0.001
Chills	274 (36.10)	127 (37.24)	147 (35.17)	0.595
Photophobia	78 (10.28)	29 (8.50)	49 (11.72)	0.152
Abdominal pain	345 (45.45)	191 (56.01)	154 (36.84)	<0.001
Diarrhea	188 (24.77)	112 (32.84)	76 (18.18)	<0.001
Conjunctivitis	110 (14.49)	40 (11.73)	70 (16.75)	0.062
Nasal congestion	109 (14.36)	34 (9.97)	75 (17.94)	0.002
Cough	189 (24.93)	72 (21.18)	117 (27.99)	0.035
Pharyngitis	156 (20.58)	69 (20.23)	87 (20.86)	0.857
Rhinitis	106 (13.97)	34 (9.97)	72 (17.22)	0.004
Hepatomegaly	68 (8.96)	44 (12.90)	24 (5.74)	0.001
Splenomegaly	31 (4.08)	21 (6.16)	10 (2.39)	0.010
Adenomegaly	17 (2.24)	7 (2.05)	10 (2.39)	0.810
Jaundice	40 (5.27)	26 (7.62)	14 (3.35)	0.013
Hemorrhage	87 (11.46)	60 (17.60)	27 (6.46)	<0.001
Seizures	32 (4.22)	30 (8.80)	2 (0.48)	<0.001

*Values are no. (%) except as indicated. We excluded from these analyses 20 patients who were positive by both assays.

a diagnostically relevant IFA titer (i.e., >64) during the first week of illness (*34*). In addition, ≥50% of all deaths attributed to *R. rickettsii* occur within 7–9 days after illness, which explains the large percentage of persons who die from RMSF without serologic confirmation (*35*). In this investigation, approximately two thirds of the IFA-confirmed case-patients for whom an illness onset date was recorded had a titer at or above the threshold value for a positive result during the first week of illness. For these reasons, we compared PCR-positive cases to those with only a positive IFA result and identified substantial differences between these groups. The clinical characteristics of PCR-positive case-patients in Mexicali matched closely with those described for well-characterized series from Arizona, USA, and Coahuila and Sonora, Mexico (*3*,*22*,*36*,*37*). In contrast, case-patients with a single IgG titer were less likely to demonstrate many of the classical characteristics of RMSF, including rash, myalgia, abdominal pain, nausea, and vomiting. In addition, the frequencies of hospitalization, jaundice, hemorrhages, seizures, and death were each less common for IFA-positive case-patients. These findings indicate that some or many cases defined by a single positive antibody titer do not accurately reflect the clinical profile of RMSF in Mexico, and that subsequent case definitions for RMSF should require confirmation by molecular methods specific for *R. rickettsii*, or a ≥4-fold rise in IgG titers between paired serum samples.

Because IgG titers reactive with *R. rickettsii* can persist in some persons for >1 year after resolution of the acute infection, some, or perhaps many, of the IFA-positive cases could represent patients exposed to or infected remotely with an SFGR who sought treatment for other febrile, rash-associated diseases endemic to northern Mexico, including dengue, Zika virus infection, or leptospirosis (*13*). Furthermore, we excluded from our analyses ≈1,600 probable case-patients for whom laboratory tests were negative; nonetheless, some, or perhaps many, of these probable cases reflected actual cases of RMSF, particularly those in patients tested early in the course of disease and for whom PCR or IFA methods were unable to detect rickettsial DNA or antibodies reactive with *R. rickettsii*. Collectively, these situations could skew frequencies of clinical characteristics and case-fatality rates, pose limitations to the tabulation of actual cases, and preclude accurate assessment of the incidence of RMSF in Mexicali during the period of study.

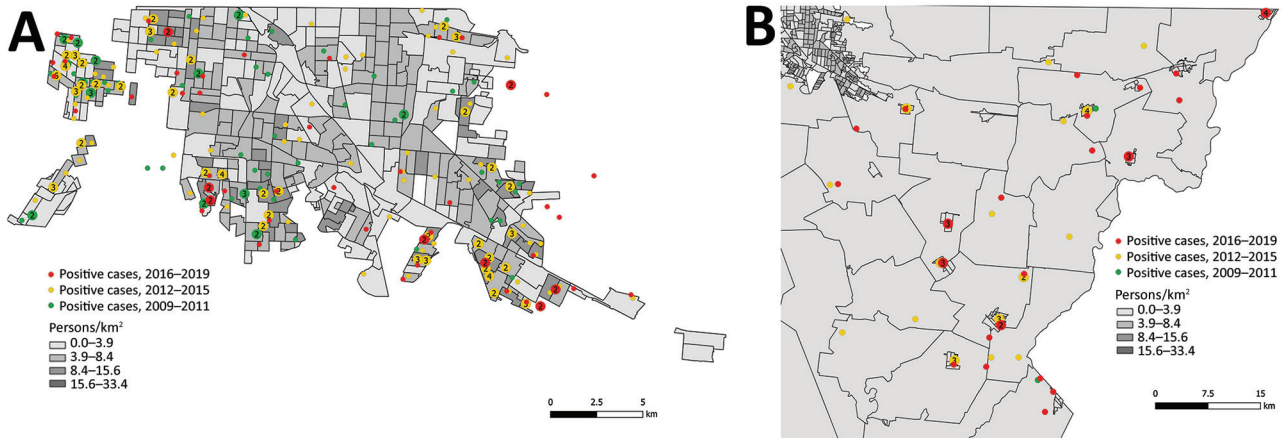

Figure 4. Geographic distribution of all PCR-positive cases of Rocky Mountain spotted fever in Mexicali (A) and the Mexicali Valley (B), Mexico, 2009–2019. Outlined areas represent census-related Basic Geostatistical areas established by the Mexico's National Institute of Statistics and Geography. Numbers in circles represent the number of cases in each location.

During 2009–2019, several hundred foci of RMSF emerged and recurred within multiple neighborhoods across the city of Mexicali, suggesting a transition from epidemic to hyperendemic disease. Similarly concerning is the more recent recognition of RMSF among smaller rural communities of the Mexicali Valley. The longevity and multifocal distribution of RMSF in Mexicali underscore many of the complex challenges faced by public health authorities in this expansive urban setting. Achieving a level of acceptable risk will require coordinated and sustained control and prevention strategies that diminish substantially the numbers of *R. rickettsii*–infected *Rh. sanguineus* s.l. ticks and free-roaming and stray dogs across a densely populated region covering >100 km^2. Because brown dog ticks are predominantly endophilic and spend ≈95% of their life hidden in structural cracks and crevices of human habitations and surrounding structures, this species can be notoriously difficult to control. Surreptitious infestations and high fecundity rates can result in explosive increases in *Rh. sanguineus* s.l. tick populations. Acaricides that contain pyrethoids, including permethrin and cypermethrin, are commonly used in these peridomestic settings because of their relative safety to nontarget species; nonetheless, resistance to these compounds has been identified recently among some brown dog tick populations in Mexico (*38*).

The ecology of RMSF in Mexicali, as in other regions of the southwestern North America with hyperendemic or epidemic levels of disease, is linked inextricably to an overabundance of tick-infested free-ranging and stray dogs in affected communities (*3*,*4*,*10*–*13*,*19*,*39*). Results of a citywide canine serosurvey conducted in Mexicali in 2017 identified antibodies reactive to *R. rickettsii* in 65% of 213 owned dogs, and 55% of all examined animals were infested with brown dog ticks (*10*). Levels of tick infestation and exposure to *R. rickettsii* are likely even greater among stray dogs (*30*,*39*). Movement of free-ranging, tick-infested canines within and among neighborhoods could contribute to multifocal recurrences of RMSF identified in Mexicali during the 11-year study period. Community-based interventions that provide and apply long-acting, acaracide-impregnated collars to large numbers of dogs can bring about rapid and substantial declines in canine and environmental tick populations and cases of RMSF among community inhabitants (*10*,*40*). Nonetheless, the distribution of stray dogs in cities correlates closely with high-density, low-income areas, and sustained interventions are prohibitively expensive for most affected neighborhoods (*40*). In this context, funding from state, national, or international agencies is needed to establish and maintain collaring activities, animal control, and spay and neuter programs that reduce the amplification of brown dog ticks and *R. rickettsii*.

In conclusion, intensified clinical and public education on the regional ecology of RMSF in Mexicali, and the necessity for rapid diagnosis and appropriate treatment, are of paramount importance as the outbreak in this location continues. The emergence and perpetuation of RMSF in Mexicali and in several other states of northern Mexico are not isolated or anomalous outbreaks but rather should be considered harbingers of national or even international concern (*41*). The enormous human and economic costs associated with epidemic RMSF will undoubtedly continue without adoption and use of well-supported and carefully integrated efforts that directly address this public health emergency.

Acknowledgments

We thank Krystal Bejarano from ISESALUD for assistance with data collection.

About the Author

Dr. Zazueta is the state epidemiologist in Baja California, Mexico, and holds an academic appointment at the Autonomous University of Baja California. His research interests include the enhancement of surveillance systems for infectious diseases, with a focus on improving understanding of behavioral, biological, and social determinants of emerging diseases in developing countries.

References

1. Hattwick MA, O'Brien RJ, Hanson BF. Rocky Mountain spotted fever: epidemiology of an increasing problem. Ann Intern Med. 1976;84:732–9. https://doi.org/10.7326/0003-4819-84-6-732
2. Linnemann CC Jr, Jansen P, Schiff GM. Rocky Mountain spotted fever in Clermont County, Ohio: description of an endemic focus. Am J Epidemiol. 1973;97:125–30. https://doi.org/10.1093/oxfordjournals.aje.a121489
3. Demma LJ, Traeger MS, Nicholson WL, Paddock CD, Blau DM, Eremeeva ME, et al. Rocky Mountain spotted fever from an unexpected tick vector in Arizona. N Engl J Med. 2005;353:587–94. https://doi.org/10.1056/NEJMoa050043
4. Drexler N, Miller M, Gerding J, Todd S, Adams L, Dahlgren FS, et al. Community-based control of the brown dog tick in a region with high rates of Rocky Mountain spotted fever, 2012–2013. PLoS One. 2014;9:e112368. https://doi.org/10.1371/journal.pone.0112368
5. Martínez-Medina MA, Alvarez-Hernández G, Padilla-Zamudioa JG, Rojas-Guerra MG. Fiebre manchada de las Montañas Rocosas en niños: consideraciones clínicas y epidemiológicas. Gac Med Mex. 2007;143:137–40.
6. Alvarez-Hernandez G, Murillo-Benitez C, Candia-Plata MC, Moro M. Clinical profile and predictors of fatal Rocky Mountain spotted fever in children from Sonora, Mexico. Pediatr Infect Dis J. 2015;34:125–30. https://doi.org/10.1097/INF.0000000000000496
7. Bustamante-Moreno J, Pon-Mendez A. Actualización en la vigilancia epidemiologica de "Rickettsiosis". Epidemio Bol. 2010;27:14.
8. Eremeeva ME, Zambrano ML, Anaya L, Beati L, Karpathy SE, Santos-Silva MM, et al. *Rickettsia rickettsii* in *Rhipicephalus* ticks, Mexicali, Mexico. J Med Entomol. 2011;48:418–21. https://doi.org/10.1603/ME10181
9. Tinoco-Gracia L, Lomelí MR, Hori-Oshima S, Stephenson N, Foley J. Molecular confirmation of Rocky Mountain spotted fever epidemic agent in Mexicali, Mexico. Emerg Infect Dis. 2018;24:1723–5. https://doi.org/10.3201/eid2409.171523
10. Foley J, Tinoco-Gracia L, Rodriguez-Lomelí M, Estrada-Guzmán J, Fierro M, Mattar-Lopez E, et al. Unbiased assessment of abundance of *Rhipicephalus sanguineus* sensu lato ticks, canine exposure to spotted fever group *Rickettsia*, and risk factors in Mexicali, México. Am J Trop Med Hyg. 2019;101:22–32. https://doi.org/10.4269/ajtmh.18-0878
11. Nicholson WL, Paddock CD, Demma L, Traeger M, Johnson B, Dickson J, et al. Rocky Mountain spotted fever in Arizona: documentation of heavy environmental infestations of *Rhipicephalus sanguineus* at an endemic site. Ann N Y Acad Sci. 2006;1078:338–41. https://doi.org/10.1196/annals.1374.065
12. Tinoco-Gracia L, Quiroz-Romero H, Quintero-Martínez MT, Rentería-Evangelista TB, González-Medina Y, Barreras-Serrano A, et al. Prevalence of *Rhipicephalus sanguineus* ticks on dogs in a region on the Mexico-USA border. Vet Rec. 2009;164:59–61. https://doi.org/10.1136/vr.164.2.59
13. Álvarez-Hernández G, Roldán JFG, Milan NSH, Lash RR, Behravesh CB, Paddock CD. Rocky Mountain spotted fever in Mexico: past, present, and future. Lancet Infect Dis. 2017;17:e189–96. https://doi.org/10.1016/S1473-3099(17)30173-1
14. Instituto Nacional para el Federalismo y el Desarrollo Municipal. Principales datos socioeconomicos por municipio [cited 2021 Jan 15]. http://www.inafed.gob.mx/es/inafed/Principales_Datos_Socioeconomicos_por_Municipio.
15. Secretaría de salud. Subsecretaría de Prevención y Promoción a la Salud. Dirección General de Epidemiología. Manual de procedimientos estandarizados para la vigilancia epidemiológica de las enfermedades transmitidas por vectores (ETV). 2017 [cited 2021 Jan 15]. https://epidemiologia.salud.gob.mx/gobmx/salud/documentos/manuales/36_Manual_ETV
16. Instituto de Diagnóstico y Referencia Epidemiologicos. Guidelines for the laboratory surveillance of rickettsial diseases. Mexico City: Ministry of Health, 2017.
17. Stenos J, Graves SR, Unsworth NB. A highly sensitive and specific real-time PCR assay for the detection of spotted fever and typhus group *Rickettsiae*. Am J Trop Med Hyg. 2005;73:1083–5. https://doi.org/10.4269/ajtmh.2005.73.1083
18. Bustamante ME, Varela G. Una nueva rickettsiosis en México. Existencia de la fiebre manchada americana en los estados de Sinaloa y Sonora. Rev Inst Salubr Enferm Trop. 1943;4:189–211.
19. Bustamante ME, Varela G, Ortiz-Mariotte C. Estudios de fiebre manchada en México. Fiebre manchada en La Laguna. Rev Inst Salubr Enferm Trop. 1946;7:39–49.
20. De Lara Huerta J, Barragán RC. Fiebre manchada de las Montañas Rocosas en pediatría. Revisión clínica de una serie de 115 casos. Rev Enf Inf Ped. 2008;22:4–9.
21. Álvarez-Hernández G, Candia-Plata MC, Delgado-de la Mora J, Acuña-Meléndrez NH, Vargas-Ortega AP, Licona-Enríquez JD. Fiebre maculosa de las Montañas Rocosas en niños y adolescentes mexicanos: cuadro clínico y factores de mortalidad. Salud Publica Mex. 2016;58:385–92. https://doi.org/10.21149/spm.v58i3.7908
22. López-Castillo DC, Vaquera-Aparicio D, González-Soto MA, Martínez-Ramírez R, Rodríguez-Muñoz L, Solórzano-Santos F. Fiebre manchada de montañas rocosas: experiencia en 5 años de vigilancia activa en un hospital pediátrico de segundo nivel en el noreste de México. Bol Med Hosp Infant Mex. 2018;75:303–8.
23. Salgo MP, Telzak EE, Currie B, Perlman DC, Litman N, Levi M, et al. A focus of Rocky Mountain spotted fever within New York City. N Engl J Med. 1988;318:1345–8. https://doi.org/10.1056/NEJM198805263182101
24. Argüello AP, Hun L, Rivera P, Taylor L. A fatal urban case of Rocky Mountain spotted fever presenting an eschar in San Jose, Costa Rica. Am J Trop Med Hyg. 2012;87:345–8. https://doi.org/10.4269/ajtmh.2012.12-0153
25. Nasser JT, Lana RC, Silva CM, Lourenço RW, da Cunha e Silva DC, Donalísio MR. Urbanization of Brazilian spotted fever in a municipality of the southeastern region: epidemiology and spatial distribution. Rev Bras Epidemiol. 2015;18:299–312. https://doi.org/10.1590/1980-5497201500020002

26. Martínez-Caballero A, Moreno B, González C, Martínez G, Adames M, Pachar JV, et al. Descriptions of two new cases of Rocky Mountain spotted fever in Panama, and coincident infection with *Rickettsia rickettsii* in *Rhipicephalus sanguineus* s.l. in an urban locality of Panama City, Panama. Epidemiol Infect. 2018;146:875–8. https://doi.org/10.1017/S0950268818000730
27. Tzianabos T, Anderson BE, McDade JE. Detection of *Rickettsia rickettsii* DNA in clinical specimens by using polymerase chain reaction technology. J Clin Microbiol. 1989;27:2866–8. https://doi.org/10.1128/JCM.27.12.2866-2868.1989
28. Kato C, Chung I, Paddock C. Estimation of *Rickettsia rickettsii* copy number in the blood of patients with Rocky Mountain spotted fever suggests cyclic diurnal trends in bacteraemia. Clin Microbiol Infect. 2016;22:394–6. https://doi.org/10.1016/j.cmi.2015.12.019
29. Straily A, Stuck S, Singleton J Jr, Brennan S, Marcum S, Condit M, et al. Antibody titers reactive with *Rickettsia rickettsii* in blood donors and implications for surveillance of spotted fever rickettsiosis in the United States. J Infect Dis. 2020;221:1371–8. https://doi.org/10.1093/infdis/jiz316
30. Pieracci EG, De La Rosa JDP, Rubio DL, Perales MES, Contreras MV, Drexler NA, et al. Seroprevalence of spotted fever group rickettsiae in canines along the United States–Mexico border. Zoonoses Public Health. 2019;66:918–26. https://doi.org/10.1111/zph.12642
31. López-Pérez AM, Sánchez-Montes S, Foley J, Guzmán-Cornejo C, Colunga-Salas P, Pascoe E, et al. Molecular evidence of *Borrelia burgdorferi* sensu stricto and *Rickettsia massiliae* in ticks collected from a domestic-wild carnivore interface in Chihuahua, Mexico. Ticks Tick Borne Dis. 2019;10:1118–23. https://doi.org/10.1016/j.ttbdis.2019.05.018
32. Delgado-de la Mora J, Sánchez-Montes S, Licona-Enríquez JD, Delgado-de la Mora D, Paddock CD, Beati L, et al. *Rickettsia parkeri* and *Candidatus* Rickettsia andeanae in ticks of the *Amblyomma maculatum* group, Mexico. Emerg Infect Dis. 2019;25:836–8. https://doi.org/10.3201/eid2504.181507
33. Lopéz-Pérez AM, Chaves A, Sánchez-Montes S, Foley P, Uhart M, Barrón-Rodríguez J, et al. Diversity of rickettsiae in domestic, synanthropic, and sylvatic mammals and their ectoparasites in a spotted fever-epidemic region at the western US-Mexico border. Transbound Emerg Dis 2021; Mar 5. PubMed https://doi.org/10.1111/tbed.14027
34. Kleeman KT, Hicks JL, Anacker RL, Philip RN, Casper EA, Hechemy KE, et al. Early detection of antibody to *Rickettsia rickettsii*: a comparison of four serological methods; indirect hemagglutination, indirect fluorescent antibody, latex agglutination, and complement fixation. In: Burgdorfer W, Anacker RL, editors. Rickettsiae and rickettsial diseases. New York: Academic Press, Inc.; 1981. p. 171–8.
35. Paddock CD, Greer PW, Ferebee TL, Singleton J Jr, McKechnie DB, Treadwell TA, et al. Hidden mortality attributable to Rocky Mountain spotted fever: immunohistochemical detection of fatal, serologically unconfirmed disease. J Infect Dis. 1999;179:1469–76. https://doi.org/10.1086/314776
36. Delgado-De la Mora J, Licona-Enríquez JD, Leyva-Gastélum M, Delgado-De la Mora D, Rascón-Alcantar A, Álvarez-Hernández G. Una serie de casos fatales de fiebre manchada de las Montañas Rococsas en Sonora, México. Biomedica. 2018;38:69–76. https://doi.org/10.7705/biomedica.v38i0.3507
37. Alvarez D, Ochoa E, Nichols Heitman K, Binder AM, Alvarez G, Armstrong PA. Epidemiology and clinical features of Rocky Mountain spotted fever from enhanced surveillance, Sonora, Mexico: 2015–2018. Am J Trop Med Hyg. 2020;104:190–7. https://doi.org/10.4269/ajtmh.20-0854
38. Rodriguez-Vivas RI, Ojeda-Chi MM, Trinidad-Martinez I, Bolio-González ME. First report of amitraz and cypermethrin resistance in *Rhipicephalus sanguineus* sensu lato infesting dogs in Mexico. Med Vet Entomol. 2017;31:72–7. https://doi.org/10.1111/mve.12207
39. Ortega-Morales AI, Nava-Reyna E, Ávila-Rodríguez V, González-Álvarez VH, Castillo-Martínez A, Siller-Rodríguez QK, et al. Detection of *Rickettsia* spp. in *Rhipicephalus sanguineus* (sensu lato) collected from free-roaming dogs in Coahuila State, northern Mexico. Parasit Vectors. 2019;12:130. https://doi.org/10.1186/s13071-019-3377-z
40. Alvarez-Hernandez G, Drexler N, Paddock CD, Licona-Enriquez JD, la Mora JD, Straily A, et al. Community-based prevention of epidemic Rocky Mountain spotted fever among minority populations in Sonora, Mexico, using a One Health approach. Trans R Soc Trop Med Hyg. 2020;114:293–300. https://doi.org/10.1093/trstmh/trz114
41. Drexler NA, Yaglom H, Casal M, Fierro M, Kriner P, Murphy B, et al. Fatal Rocky Mountain spotted fever along the United States–Mexico border, 2013–2016. Emerg Infect Dis. 2017;23:1621–6. https://doi.org/10.3201/eid2310.170309

Address for correspondence: Oscar E. Zazueta, Av. Pioneros 1005, Centro Cívico, Mexicali, B.C. 21000, Mexico; email: oez512@mail.harvard.edu

Neurologic Disease after Yellow Fever Vaccination, São Paulo, Brazil, 2017–2018

Ana Freitas Ribeiro,[1] Bruno Fukelmann Guedes,[1] Jamal M.A.H. Sulleiman, Francisco Tomaz Meneses de Oliveira, Izabel Oliva Marcilio de Souza, Juliana Silva Nogueira, Rosa Maria Nascimento Marcusso, Eder Gatti Fernandes, Guilherme Sciascia do Olival, Pedro Henrique Fonseca Moreira de Figueiredo, Ana Paula Rocha Veiga, Flávia Esper Dahy, Natália Nasser Ximenes, Lecio Figueira Pinto, José Ernesto Vidal, Augusto Cesar Penalva de Oliveira

Medscape EDUCATION ACTIVITY

In support of improving patient care, this activity has been planned and implemented by Medscape, LLC and Emerging Infectious Diseases. Medscape, LLC is jointly accredited by the Accreditation Council for Continuing Medical Education (ACCME), the Accreditation Council for Pharmacy Education (ACPE), and the American Nurses Credentialing Center (ANCC), to provide continuing education for the healthcare team.

Medscape, LLC designates this Journal-based CME activity for a maximum of 1.00 ***AMA PRA Category 1 Credit(s)™***. Physicians should claim only the credit commensurate with the extent of their participation in the activity.

Successful completion of this CME activity, which includes participation in the evaluation component, enables the participant to earn up to 1.0 MOC points in the American Board of Internal Medicine's (ABIM) Maintenance of Certification (MOC) program. Participants will earn MOC points equivalent to the amount of CME credits claimed for the activity. It is the CME activity provider's responsibility to submit participant completion information to ACCME for the purpose of granting ABIM MOC credit.

All other clinicians completing this activity will be issued a certificate of participation. To participate in this journal CME activity: (1) review the learning objectives and author disclosures; (2) study the education content; (3) take the post-test with a 75% minimum passing score and complete the evaluation at http://www.medscape.org/journal/eid; and (4) view/print certificate. For CME questions, see page 1766.

Release date: May 18, 2021; Expiration date: May 18, 2022

Learning Objectives

Upon completion of this activity, participants will be able to:

- Compare the Centers for Disease Control and Prevention and Brighton Collaboration criteria for the diagnosis of YEL-AND
- Assess clinical characteristics of patients with YEL-AND
- Distinguish the most common clinical manifestation of YEL-AND in the current study
- Analyze the conclusions of the current study regarding the criteria for diagnosing YEL-AND.

CME Editor

P. Lynne Stockton Taylor, VMD, MS, ELS(D), Technical Writer/Editor, Emerging Infectious Diseases. *Disclosure: P. Lynne Stockton Taylor, VMD, MS, ELS(D), has disclosed no relevant financial relationships.*

CME Author

Charles P. Vega, MD, Health Sciences Clinical Professor of Family Medicine, University of California, Irvine School of Medicine, Irvine, California. *Disclosure: Charles P. Vega, MD, has disclosed the following relevant financial relationships: served as an advisor or consultant for GlaxoSmithKline.*

Authors

Disclosures: ***Ana Freitas Ribeiro, PhD,*** *has disclosed the following relevant financial relationships: served as a speaker or a member of a speakers bureau for Novartis Pharmaceuticals Corporation.* ***Bruno Fukelmann Guedes, MD,*** *has disclosed the following relevant financial relationships: owns stock, stock options, or bonds from Fleury SA.* ***Ana Paula Rocha Veiga, PhD, MD,*** *has disclosed the following relevant financial relationships: served as a speaker or a member of a speakers bureau for Pfizer Inc.; received grants for clinical research from Instituto Butantan.* ***Lecio Figueira Pinto, MD, PhD,*** *has disclosed the following relevant financial relationships: served as an advisor or consultant for UCB Pharma, Inc.; United Medical, LLC; Zodiac Pharmaceuticals; served as a speaker or a member of a speakers bureau for LivaNova, PLC; Prati-Donaduzzi; UCB Pharma, Inc.; United Medical, LLC; Zodiac Pharmaceuticals.* ***José Ernesto Vidal, PhD,*** *has disclosed the following relevant financial relationships: served as an advisor or consultant for Gilead Sciences, Inc.; Janssen-Cilag; Teva Pharmaceutical Industries, Ltd.; United Medical, LLC; served as a speaker or a member of a speakers bureau for GlaxoSmithKline; Janssen-Cilag; Merck Sharp & Dohme GmbH; Roche; Teva Pharmaceutical Industries, Ltd.; United Medical, LLC.* ***Jamal M.A.H. Suleiman, MD; Francisco Tomaz Meneses de Oliveira, MS; Izabel Marcilio, PhD; Juliana Silva Nogueira, MS; Rosa Maria Nascimento Marcusso, MS; Eder Gatti Fernandes, PhD; Guilherme Sciascia do Olival, PhD; Pedro Henrique Fonseca Moreira de Figueiredo, MD; Flávia Esper Dahy, MD; Natália Nasser Ximenes, PhD;*** *and* ***Augusto Cesar Penalva de Oliveira, PhD,*** *have disclosed no relevant financial relationships.*

Author affiliations: Universidade Nove de Julho, São Paulo, Brazil (A.F. Ribeiro); Instituto de Infectologia Emílio Ribas, São Paulo (A.F. Ribeiro, J.M.A.H. Sulleiman, R.M. Nascimento Marcusso, G. Sciascia do Olival, A.P. Rocha Veiga, F. Esper Dahy, J. Ernesto Vidal, A.C. Penalva de Oliveira); Hospital das Clínicas, Universidade de São Paulo, São Paulo (B.F. Guedes, I.O. Marcilio de Souza, P.H.F. Moreira de Figueiredo, N. Nasser Ximenes, L. Figueira Pinto, J. E. Vidal); Irmandade Santa Casa de Misericórdia de São Paulo, São Paulo (F.T. Meneses de Oliveira); Instituto Adolfo Lutz, São Paulo (J. Silva Nogueira); Centro de Vigilância Epidemiológica Prof. Alexandre Vranjac, São Paulo (E. Gatti Fernandes)

DOI: https://doi.org/10.3201/eid2706.204170

[1]These authors contributed equally to this article.

Yellow fever (YF) vaccine can cause neurologic complications. We examined YF vaccine–associated neurologic disease reported from 3 tertiary referral centers in São Paulo, Brazil, during 2017–2018 and compared the performance of criteria established by the Yellow Fever Vaccine Working Group/Centers for Disease Control and Prevention and the Brighton Collaboration. Among 50 patients who met inclusion criteria, 32 had meningoencephalitis (14 with reactive YF IgM in cerebrospinal fluid), 2 died, and 1 may have transmitted infection to an infant through breast milk. Of 7 cases of autoimmune neurologic disease after YF vaccination, 2 were acute disseminated encephalomyelitis, 2 myelitis, and 3 Guillain-Barré syndrome. Neurologic disease can follow fractional vaccine doses, and novel potential vaccine-associated syndromes include autoimmune encephalitis, opsoclonus-myoclonus-ataxia syndrome, optic neuritis, and ataxia. Although the Brighton Collaboration criteria lack direct vaccine causal assessment, they are more inclusive than the Centers for Disease Control and Prevention criteria.

Yellow fever (YF) is an acute febrile illness caused by a mosquito-borne arbovirus of the family *Flaviviridae*. The disease is endemic to the tropical forests of South America and Africa, periodically causing outbreaks and epidemics. The clinical manifestations of YF range from asymptomatic to severe with jaundice and hemorrhage (*1*). The primary preventive strategy is vaccination. The 3 substrains of the 17D vaccine virus currently used for vaccine production (17DD, 17D-204, and 17D-213) have similar safety and immunogenicity profiles (*1*,*2*). The main YF vaccine available in Brazil is 17DD, which is produced by Bio-Manguinhos-Fiocruz (https://www.bio.fiocruz.br). YF vaccine–associated neurologic disease (YEL-AND) is a rare but potentially severe adverse event following immunization (AEFI). The incidence of YEL-AND varies between studies; in the United States and Brazil, the estimated range is 0.2–0.94 cases/100,000 doses (*3*–*6*).

In 2002, the Centers for Disease Control and Prevention (CDC) formed the Yellow Fever Vaccine Safety Working Group, a panel of vaccine safety experts, which proposed a surveillance case definition for YEL-AND. The clinical manifestations included in YEL-AND are meningoencephalitis (neurotropic disease), Guillain-Barré syndrome (GBS), and acute disseminated encephalomyelitis (ADEM) (*7*).

In 2004, the Brighton Collaboration (BC) was commissioned as a vaccine safety research network to develop standardized case definitions for AEFI (*8*). The first BC case definition of aseptic meningitis was issued in 2007 (*9*). Subsequent BC criteria were established for encephalitis, ADEM (*10*), and myelitis (*10*), all distinct from aseptic meningitis (*9*) and each other.

There are fundamental differences between the BC and CDC case definitions. The CDC criteria require that acute brain lesions or dysfunction be evidenced by electroencephalography (EEG) or magnetic resonance imaging (MRI) and exclude causality when the vaccine–symptom interval exceeds 30 days. These criteria render them poorly suited to diagnose YEL-AND in resource-limited settings or during massive vaccination campaigns. The BC criteria encompass a broader range of neurologic syndromes, including aseptic meningitis and myelitis. However, in contrast to the CDC criteria, they lack specific criteria to determine vaccine causality (YF virus IgM in cerebrospinal fluid [CSF]). Both criteria focus on major neurologic syndromes and overlook the rare and atypical ones. Although recent publications used the newer BC criteria (*6*), CDC case definitions are still used routinely by the Brazil Ministry of Health, as seen in the Epidemiologic Surveillance of Post-Vaccination Adverse Events manual (*11*).

During 2017 and 2018, YF virus transmission increased in the southeastern region of Brazil (states of Rio de Janeiro, Espírito Santo, and those parts of São Paulo where the vaccination schedule did not include YF vaccine). In response to this outbreak, the National Immunization Program launched a massive vaccination campaign in the São Paulo metropolitan area. During 2017–2018, a total of 6 million full doses (0.5 mL) and 4 million fractional doses (0.1 mL) of 17DD were administered throughout the São Paulo metropolitan area (E. Gatti Fernandes, unpub. data). We describe suspected YEL-AND cases from tertiary centers in the city of São Paulo during the 2017–2018 vaccination campaign, identify differences between the CDC and BC classification criteria, and describe novel atypical syndromes.

Methods

Our retrospective study included cases from 3 tertiary referral hospitals in the city of São Paulo (Hospital das Clínicas da Faculdade de Medicina da USP, Instituto de Infectologia Emilio Ribas, and Santa Casa de Misericórdia de São Paulo). We included patients who had been vaccinated during the campaign and for whom a case of suspected YEL-AND was reported to the National Post-Vaccination Adverse Events Surveillance System; for patients with nonnotified cases, we included those whose attending physician recognized the case as potential YEL-AND. All cases were included in the

initial analysis, regardless of vaccine–symptom interval. We reviewed the YF vaccination information (first or booster dose, full or fractional dose, alone or in combination with other vaccines); clinical, epidemiologic, and laboratory data from electronic charts; laboratory databases; and (when available) a structured AEFI notification form.

We first classified and analyzed all cases according to the BC criteria for the diagnosis of aseptic meningitis (*9*), encephalitis, myelitis, ADEM (*10*), and GBS (*12*) (Appendix 1, https://wwwnc.cdc.gov/EID/article/27/6/20-4170-App1.pdf). We excluded from final analysis patients with alternative diagnoses or insufficient information. Neurologic autoimmune diseases were not excluded when the YF vaccine was biologically plausible as a trigger. When these atypical clinical syndromes were identified, we assessed causality by using a tool proposed by the World Health Organization (*13*). To compare the performance of the different classification criteria, we also classified cases according to the Brazil Ministry of Health manual (*11*), (Appendix 2, https://wwwnc.cdc.gov/EID/article/27/6/20-4170-App2.pdf), using the same exclusion criteria as the BC criteria. Difficult diagnoses were decided at consensus meetings.

All analyses were performed by using R statistics software version 3.6.3 (https://www.r-project.org). Significance was set at $p<0.05$ for all statistical comparisons.

Results

We identified 50 suspected YEL-AND cases at the 3 tertiary care facilities. Of these, we excluded 8 (16%) cases, 3 because of insufficient information and 5 because of alternative diagnoses (1 each of GBS and Zika virus–reactive IgM in CSF, neurosurgery-associated bacterial meningitis, multiple sclerosis preceding vaccination and postvaccination demyelination, mononucleosis-like syndrome with acute toxoplasmosis, and meningoencephalitis with a positive rapid test result for dengue virus [DENV]).

The final analysis included 42 patients 1–89 years of age; most were male (62%) and White (74%). The median time between vaccination and symptom onset was 15 days (interquartile range [IQR] 5.5–20.0). Cases were associated with the first dose of the YF vaccine for 28 patients and with booster doses for 2 patients; this information was missing for 12 patients. A total of 9 patients received fractional doses and 30 received full doses; this information was missing for 3 patients. For all patients, the YF vaccine was given alone. All patients underwent CSF examination. YF virus IgM immunoreactivity in CSF was performed for 30 patients; reactivity was detected for 15. Reverse transcription PCR for YF virus was performed on CSF for 28 patients; all results were negative. Testing for DENV IgM was also performed on CSF of 28 patients; all results were negative (Tables 1, 2; Appendix 3, https://wwwnc.cdc.gov/EID/article/27/6/20-4170-App3.xlsx).

Table 1. Diagnostic certainty, clinical, epidemiologic, and immunologic investigations for 42 patients with suspected yellow fever vaccine–associated neurologic disease, according to Brighton Collaboration classification criteria, São Paulo, Brazil, 2017–2018*

Characteristic	Aseptic meningitis, n = 24	Encephalitis, n = 8	Guillain-Barré syndrome, n = 3‡	Myelitis, n = 2‡	ADEM, n = 2‡	Unclassified† n = 3‡
Age, y, median (IQR) [range]	36 (23.75–46.75)	40 (30.25–58.25)	59 (43–73)	33 [25–41]	37 [22–52]	28 [25–50]
Sex, no (%)						
F	7 (29)	5 (62)	1 (33)	2 (100)	1 (50)	0
M	17 (71)	3 (38)	2 (67)	0	1 (50)	3 (100)
Vaccine–symptom interval, d, median (IQR) [range]	17 (7.75–20.00)	7 (3.50–17.25)	16 [14–31]	11.5 [0–23]	10 [5–15]	13 [3–29]
No. full/fractional/unknown doses	18/4/2	5/3/0	3/0/0	1/1/0	1/1/0	2/0/1
YF virus IgM in CSF, reactive/total tested	10/17	4/7	0/2	0/1	1/2	0/1
YF virus in CSF detected by PCR, detected/total tested	0/17	0/6	0/2	0/1	0/1	0/1
BC level of diagnostic certainty, no. cases						
Level 1	17	0	1	0	2	NA
Level 2	7	8	2	2	0	NA
Brazil MoH/CDC classification, no. cases	Level 1 NRL: 21; level 2 NRT: 1; definite NRT: 1; suspected NRT: 1	Level 1 NRL: 2; level 2 NRT: 3; definite NRT: 2; suspected NRT: 1	Level 2 PNS: 1; probable PNS:2	Level 1 NRL: 2	Probable CNS: 2	Level 1 NRL: 3

*ADEM, acute disseminated encephalomyelitis; BC, Brighton Collaboration; CDC, Centers for Disease Control and Prevention); CNS, autoimmune neurologic disease with central nervous system involvement; CSF, cerebrospinal fluid; IQR, interquartile range; NA, not applicable; NRL, neurologic disease; NRT, neurotropic disease; MoH, Ministry of Health; PNS, autoimmune neurologic disease with peripheral nervous system involvement; YF, yellow fever.
†Includes 1 case of ataxia, 1 of opsoclonus-myoclonus-ataxia, 1 case of optic neuritis.
‡In groups with <5 cases, range is substituted for IQR.

Table 2. Laboratory, neurophysiologic, and imaging characteristics for 42 patients with suspect YEL-AND, according to classification with the Brighton Collaboration criteria, São Paulo, Brazil, 2017–2018*

Variable	Aseptic meningitis, n = 24	Encephalitis, n = 8	Guillain-Barré syndrome, n = 3‡	Myelitis, n = 2‡	ADEM, n = 2‡	Unclassified,† n = 3‡
CSF parameters§						
Leukocytes >5, no. (%)	24 (100)	7 (87.5)	1 (33)	0	1 (50)	1 (33)
Leukocytes, total/mm^3, median (IQR) [range]	76.50 (53–207.5)	30 (13–70)	1 [0–32]	1 [0–2]	4.5 [2–7]	2 [1–12]
Lymphocytes, median (IQR) [range]	73 (65.5–88.0)	85 (71–93)	51.5 [3 –71]	75 [75–75]	79,5 [79–80]	80 [73–92]
Neutrophils, median (IQR) [range]	10 (3.5–25.0)	3 (0.5–6.0)	23.5 [13–34]	16 [16–16]	19.5 [19–20]	2 [1–3]
Erythrocytes, total/mm^3, median (IQR) [range]	2 (1–12)	5.5 (1–640.50)	302 [249–355]	26 [1–52]	985.5 [131–1,840]	0 [0–3]
Total protein, mg/dL, median (IQR) [range]	53.5 (48–71.5)	60 (47.5–67)	53 [31–66]	27.5 [23–32]	61 [41 – 81]	46 [26–51]
Total glucose, mg/dL, median (IQR) [range]	60 (52.5–64.5)	66 (54.5–92.5)	60.5 [50–71]	72 [66–78]	62.5 [54–71]	
MRI findings, no. cases	Leptomeningeal enhancement, 1; unremarkable, 3	Leptomeningeal enhancement, 1; unremarkable, 5	Facial nerve enhancement, 1; unremarkable, 1	Longitudinally extensive myelitis,1; partial myelitis, 1	White matter abnormalities and extensive myelitis,1; brainstem and cerebellar peduncles abnormalities, 1	Bilateral optic nerve abnormalities,1; unremarkable, 1
EEG/EMG findings, no. cases	EEG: disorganized background, 2; unremarkable, 2	EEG: disorganized background, 6	EMG: AMAN, 1	ND	ND	ND

*ADEM, acute disseminated encephalomyelitis; AMAN, axonal motor polyneuropathy; CSF, cerebrospinal fluid; EEG, electroencephalography; EMG, electromyography; IQR, interquartile range; ND, not done; YF, yellow fever.
†Includes 1 case of ataxia, 1 of opsoclonus-myoclonus-ataxia, and 1 of optic neuritis.
‡In groups with <5 cases, range was substituted for IQR.
§All patients underwent lumbar puncture and CSF analysis.

Aseptic Meningitis

Twenty-four cases were classified as aseptic meningitis (diagnostic certainty level 1 or level 2). These patients had headaches (100%) and fever (92%), which developed a median of 17 days (IQR 7.75–20.0 days) after vaccination. CSF analysis showed a median of 76.5 leukocytes/mm^3. YF virus IgM reactivity in CSF confirmed a vaccine-related disease for 10 patients. Attributing the disease to the YF vaccine was not possible for 14 other patients (nonreactive or unknown YF virus IgM), although for all 24 patients, a structured assessment with a tool proposed by the World Health Organization (*13*) suggested a causal association with vaccination. For IgM-reactive and IgM-nonreactive patients, no differences in CSF cell count or time from vaccination to symptom onset were noted. Except for 1 patient who died, the course of disease for these patients was uncomplicated, and they were discharged a median of 2.5 days after hospital admission (IQR 1.00–5.25 days). One case involved potential transmission through breast-feeding (atypical case).

Encephalitis

Eight patients had encephalitis. Compared with those with aseptic meningitis, these patients had more seizures (50% vs. 0; p = 0.002), more psychosis (37.5% vs. 0; p = 0.011), and longer hospital stays (median 17.5 [IQR 12.00–35.25] vs. 2.5 [IQR 1.00–5.25) days; p = 0.002). One patient died, 4 displayed YF virus IgM reactivity in CSF, and 3 had autoimmune encephalitis.

Autoimmune Disease: ADEM, Myelitis, and GBS

We identified 2 ADEM cases. For 1 patient, paraparesis and somnolence developed 15 days after YF vaccine, and MRI revealed diffuse demyelinating lesions in the brain and cervical spinal cord. This patient was the only one outside of the meningitis and encephalitis groups with CSF positive for YF virus IgM. For the other patient, ataxia developed 5 days after vaccination, and MRI showed T2-weighted and FLAIR signal abnormalities in the dorsal pons and middle cerebellar peduncles. That patient was not tested for YF virus antibodies or RNA.

Two patients experienced spastic quadriparesis, 20 hours and 23 days after vaccination. MRI analysis revealed partial myelitis in the cervical cord (first patient) and longitudinally extensive cervicothoracic myelitis (second patient). Three patients experienced flaccid quadriparesis (14, 16, and 31 days after

vaccination) consistent with GBS. One patient underwent a nerve conduction study, which revealed axonal motor polyneuropathy.

Atypical Cases

We found several cases of neurologic syndromes that are typically autoimmune or occur after infection but that are not traditionally associated with YF vaccination. The encephalitis group included 3 patients with autoimmune encephalitis and antibodies against neural targets. The first patient, a 42-year-old woman, experienced headache and fever 1 day after the first (fractioned) dose of the 17-DD vaccine, followed by psychosis and status epilepticus. She had altered EEG findings and inflammatory CSF; YF virus IgM in CSF was nonreactive. Antineurexin3 IgG was detected in serum and CSF. The second patient, a 14-year-old girl, experienced headache, depression, psychosis, seizures, and EEG slowing 21 days after receiving her first (full) dose of the 17-DD vaccine. A bloody CSF sample (1,142 erythrocytes/mm^3) was reactive for YF virus IgM 3 months after symptom onset, although PCR for YF virus in CSF was negative. That result could be a false positive. The third patient, a 39-year-old woman, experienced fever, vertigo, and psychiatric symptoms 23 days after YF vaccination (full dose, first ever). She was evaluated by a neurologist 45 days after symptom onset. Examination showed opsoclonus-myoclonus-ataxia and encephalopathy, EEG revealed background slowing, and CSF (slightly bloody from a traumatic lumbar puncture) showed 5 leukocytes/mm^3. Immunologic tests for YF virus were not performed in serum or CSF. N-methyl-D-aspartate receptor (NMDA-r) IgG was identified in serum and CSF of the second and third patients. These 3 cases are described in greater detail elsewhere (*14*). All 3 cases met the BC encephalitis case definition and the CDC criteria for level 2 neurotropic disease. However, because the CDC criteria require no evidence of other diagnoses, they were not further classified as suspected or probable YEL-AND.

Three patients exhibited autoimmune syndromes that are unclassifiable per both CDC and BC criteria. The first patient was a 25-year-old man in whom cerebellar ataxia, opsoclonus, and generalized myoclonus, consistent with opsoclonus-myoclonus-ataxia syndrome, developed 29 days after vaccination. MRI and EEG findings were unremarkable, and he recovered over a few months with immunotherapy. He was not investigated for YF virus–specific antibodies or nucleic acid. Information on vaccine (dosing, first, or booster dose) was missing. The second patient was a 50-year-old man in whom dysarthria, imbalance, and mild somnolence developed 13 days after he had received a first (full) dose of the 17-DD vaccine. Physical examination showed global cerebellar ataxia. Neuroimaging and CSF analysis were unremarkable, and the patient improved spontaneously over a few days. PCR and assays to detect YF virus IgM in CSF were not performed. The third patient was a 28-year-old man who reported frontal headache associated with eye movement, followed within 2 weeks by bilateral vision impairment. At admission, he had low visual acuity in the left eye, and MRI showed extensive signal abnormalities in both optic nerves, which was consistent with optic neuritis. CSF was inflammatory but negative for YF virus IgM or by PCR for YF virus. He recovered with immune therapy.

A fourth case occurred after the mother of a 1-year-old boy received her first dose of the YF vaccine (no information on dosing) but continued to breast-feed her child. Seven days after the mother's vaccination, the infant exhibited nasal discharge, headache, fever, anorexia, and malaise. Examination indicated that he was alert and active but dehydrated. Computed tomography (CT) of the brain showed no abnormalities, and CSF analysis indicated 230 leukocytes/mm^3, 12 erythrocytes/mm^3, and 35 mg/dL protein. YF virus IgM and PCRs were not performed for infant or mother. The infant was discharged 9 days after admission.

Fatal Cases

Two patients died. Aseptic meningitis developed in 1 and encephalitis in the other.

A 52-year-old woman with a history of underlying unruptured giant intracranial aneurisms experienced retro-orbital headache, fever, nausea, and vomiting 9 days after receiving a full dose of the YF vaccine. Examination showed nuchal rigidity but was otherwise unremarkable. Brain CT showed giant intracranial aneurysms without bleeding. A lumbar puncture revealed xanthochromic CSF with 3,080 leukocytes/mm^3 (68% neutrophils, 15% lymphocytes), 2 erythrocytes/mm^3, and 163 mg/dL protein. The woman was admitted to the intensive care unit (ICU), where she received treatment for presumed bacterial meningitis. CSF analysis was reactive for YF virus IgM, negative for YF virus by PCR, and negative for DENV IgM. On hospitalization day 14, seizures, left hemiplegia, and coma developed. A second CT showed focal brain edema and a malignant right middle cerebral artery stroke. She died 3 months later. Although the timing of symptoms, fever, the initially benign presentation, and reactive CSF IgM initially indicated

a case of neurotropic disease, the underlying intracranial aneurysms, CSF xanthochromia, and cerebral infarction suggest subarachnoid hemorrhage as a relevant differential diagnosis. The 2 conditions may have occurred concurrently, and for this patient, it would be difficult to determine whether subarachnoid hemorrhage preceded or followed neurotropic disease.

A 19-year-old woman experienced myalgia, vomiting, and progressive headache that started 4 days after receiving a full dose of the 17DD vaccine alone. Mild confusion progressed steadily over the next 12 days. On postvaccination day 16, bilateral convulsive seizures developed; the woman was admitted to the ICU and was comatose at the time of arrival. Brain CT findings were unremarkable. Initial blood chemistry revealed elevated alanine (276U/L) and aspartate (246 U/L) aminotransferase levels (suggesting viscerotropic disease), but results were otherwise unremarkable. A lumbar puncture sample contained 19 leukocytes/mm^3 and 154 mg/dL protein and was negative for YF virus IgM and nucleic acid. Over the next 14 days, sepsis, renal insufficiency, and disseminated intravascular coagulation developed, and the patient died. Autopsy detected centrilobular necrosis and periportal inflammation of the liver and revealed mild perivascular edema and congestion of brain sections. RNA extracted from formalin-fixed paraffin-embedded tissues was positive for YF virus in the lungs and heart but negative in the brain, spleen, and kidney. Because of the low quality of RNA, it was not possible to differentiate between wild type and vaccine strains. This patient experienced multiorgan failure later than usual for viscerotropic disease.

Comparison of BC and CDC (and Brazil Ministry of Health) Classifications

The BC (Figure 1) and CDC (Figure 2) criteria differed in several respects (Figure 3). Of 8 patients in the encephalitis group, 3 were classified as having suspected or definite neurotropic disease according to the CDC criteria. Two cases of encephalitis could not be considered neurotropic disease because EEG and

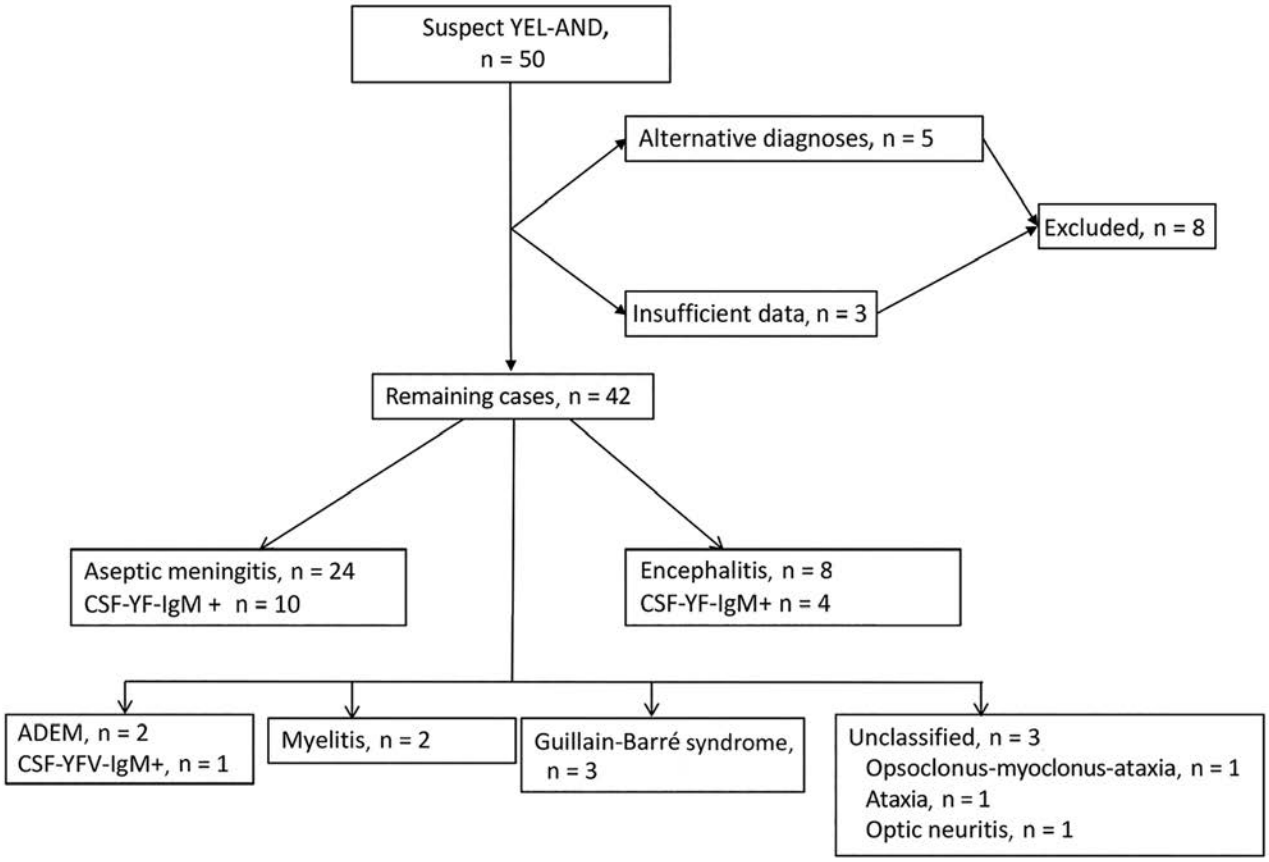

Figure 1. Classification of cases of yellow fever vaccine–associated neurologic disease with Brighton Collaboration criteria, São Paulo, Brazil, 2017–2018. CSF YF IgM, yellow fever virus IgM in cerebrospinal fluid; YEL-AND, yellow fever vaccine-associated neurologic disease; YF, yellow fever; +, positive.

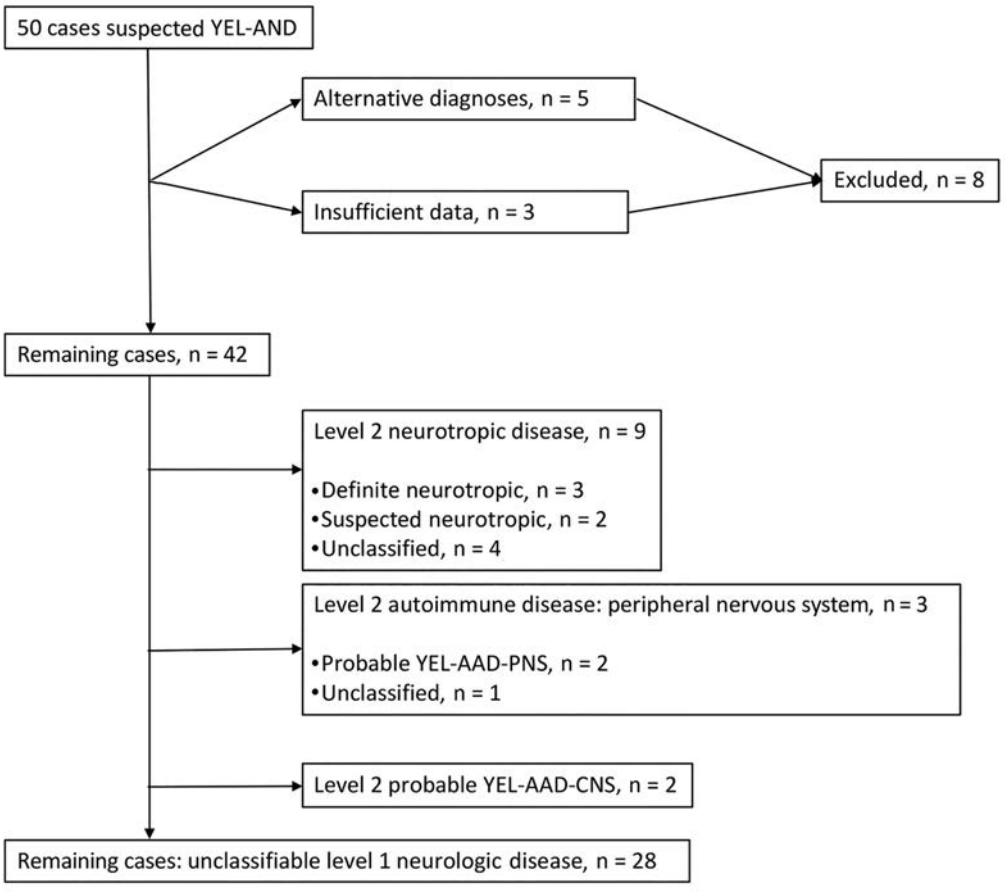

Figure 2. Classification of cases of yellow fever vaccine–associated neurologic disease with Centers for Disease Control and Prevention criteria, São Paulo, Brazil, 2017–2018. YEL-AAD-PNS, autoimmune disease with peripheral nervous system involvement; YEL-AAD-CNS, autoimmune disease with central nervous system involvement; YEL-AND, yellow fever vaccine-associated neurologic disease.

MRI were not performed, and for 3 novel autoimmune encephalitis cases, it was not possible to ascertain causality. The CDC criteria were particularly less inclusive of aseptic meningitis. Of the 24 patients with aseptic meningitis, only 2 were classified as having suspected or definite neurotropic disease (1 patient with meningeal enhancement on MRI, 1 with disorganized backgrounds on EEGs); 21 fell into the level 1 neurologic disease group (including 1 patient whose vaccine–symptom interval was 34 days), either for the absence of a typical MRI (unremarkable, 2 cases; not performed, 19 cases) or EEG findings (unremarkable, 2 cases; not performed, 19 cases). One case was classified as level 2 neurotropic disease but not further classified as suspected or definite neurotropic disease for a 38-day vaccine–symptom interval.

The CDC and BC criteria generally agreed on the classification of ADEM and GBS cases; only 1 GBS case was disregarded as YEL-AND by the CDC criteria because of symptom onset 31 days after vaccination. As expected, myelitis and unclassified cases were also missed by the CDC criteria.

Discussion

Publications on AEFI with YF vaccine are limited mainly to case reports and small case series with varying case definitions. Most published cases do not meet the CDC or BC criteria (*15*). Some retrospective studies used different diagnostic criteria to evaluate incidence of YEL-AND during mass vaccination campaigns (*16*) or long periods of observation in specific regions (*3*,*4*,*6*,*17*). McMahon et al. described 15 cases that had been notified to the Vaccine Adverse Event Reporting System (https://vaers.hhs.gov) in a 15-year period; the criteria used differed slightly from the current CDC criteria: patients with level 1 neurologic disease were classified as having encephalitis, depending on the timing of symptoms or detection of YF IgM in CSF, regardless of MRI or EEG findings (*3*). A group in France used the same criteria but highlighted the differences between encephalitis and meningitis in their report of 4 patients with YEL-AND (*17*). In an active surveillance study during vaccination campaigns in Africa, Breugelmans et al. evaluated 164 suspected cases of severe AEFI, of which only 6 were considered YEL-AND according to the BC case definitions. YF virus IgM in CSF

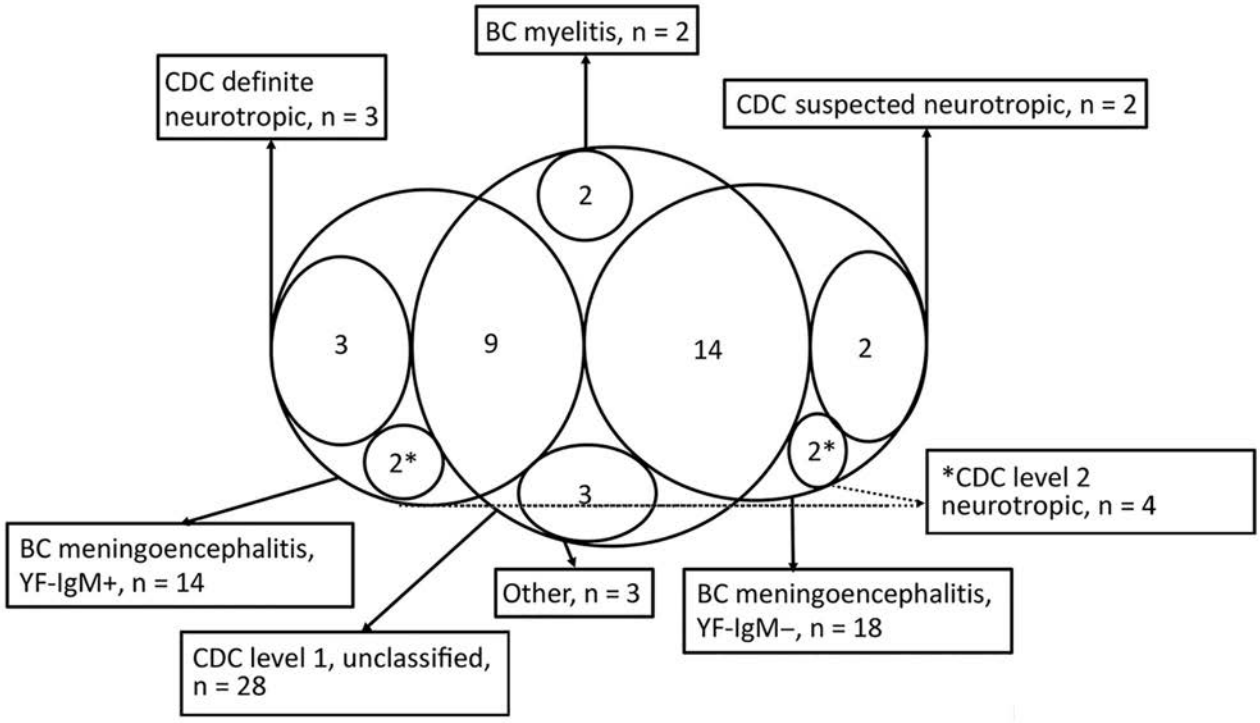

Figure 3. Classification of cases of yellow fever vaccine–associated neurologic disease, São Paulo, Brazil, 2017–2018. Excluded cases, acute disseminated encephalomyelitis cases, and Guillain-Barré syndrome cases not shown. The area with n= 9 represents the intersection between the group "BC meningoencephalitis, YF-IgM+ (reactive CSF-YF-IgM)" and "CDC level 1, unclassified." The area with n = 14 represents the intersection between the group "BC meningoencephalitis, YF-IgM– (nonconfirmed)" and "CDC level 1, unclassified." BC, Brighton Collaboration criteria; CDC, Centers for Disease Control and Prevention criteria; level 1 unclassified, level 1 neurologic disease not classifiable as level 2; level 2 neurotropic, level 2 neurotropic disease not further classified as suspected or definite neurotropic disease; other, includes atypical yellow fever vaccine–associated neurologic disease (optic neuritis, n = 1; ataxia, n = 1; opsoclonus-myoclonus-ataxia syndrome, n = 1); +, positive.

was assessed for only 2 patients, and results for both were negative (*16*). In a series of cases reported to the Vaccine Adverse Event Reporting System during 2007–2013, AEFI cases were classified as YEL-AND if they met the BC case definitions. A total of 17 events were included: 6 GBS, 6 aseptic meningitis, 2 encephalitis, 2 myelitis, and 1 ADEM (*6*). Detecting YF virus RNA in CSF samples is exceedingly rare, which was confirmed in our study.

Cross-reactivity with other flaviviruses was ruled out with DENV immunology. DENV is the main arbovirus in the state of São Paulo; in 2018, infection incidence was 43.4 cases/100,000 inhabitants. The combined incidence of Zika and chikungunya virus infections during the same period was <3 cases/100,000 inhabitants (*18*). All 32 CSF samples tested for DENV IgM were negative, which makes cross-reactivity with flaviviruses unlikely. The patients were evaluated at tertiary referral centers, which enabled a detailed analysis of the clinical characteristics of individual cases. This detailed analysis may be associated with the large proportion of cases with a high or intermediate level of diagnostic certainty according to the BC criteria. On the other hand, hospital-based retrospective studies may be inappropriate for estimating the incidence of events among vaccinees in the general population.

Comparing the case classifications obtained from each criterion revealed major limitations for those from CDC. The definition of neurotropic disease, which requires evidence suggestive of encephalitis on EEG or MRI scans, leads to many meningoencephalitis cases not being properly classified as level 2 neurologic disease, especially for patients with aseptic meningitis. This limitation is relevant for 2 reasons. First, many mass vaccination campaigns take place in countries where YF is endemic, notably low-income and lower-middle-income countries, where access to diagnostic tests is limited. Second, aseptic meningitis may be more common than encephalitis, as observed in our study and previously (*6*) and is typically devoid of parenchymal brain abnormalities that would be evident on an EEG or MRI scans. On the other hand, detection of pathogen-specific IgM-class antibodies in CSF is widely recognized as

indicative of CNS viral invasion and constitutes a relevant indication of causality in the evaluation of suspected YEL-AND. We were able to diagnose meningoencephalitis in more cases by using the BC criteria to ascertain aseptic meningitis and encephalitis with reactive IgM in CSF as evidence of causality (14 cases) than by strictly applying the CDC criteria (3 cases). Increased sensitivity of the BC criteria was also reported by Lindsey et al. Of the 17 cases classified as YEL-AND by using BC-based criteria, only 13 were classified as such by using the CDC case definitions (*6*).

Another limitation of the CDC criteria is exclusion of vaccination as the cause for patients with a vaccine–symptom interval >30-days, which led to exclusion of 3 cases in our study, including 1 patient with reactive IgM in CSF in whom meningoencephalitis developed 38 days after vaccination. Similarly, modifying the CDC criteria enabled Martins et al. to include 2 patients with meningoencephalitis 39 and 36 days after vaccination (*4*).

Our study also expands the range of neurologic complications attributable to YF vaccine. We found 1 case of aseptic meningitis in a breast-feeding infant, which is very rare (only 3 cases with IgM in the CSF of breast-feeding infants have been reported to date [*19*–*21*]), and 3 cases of immune-mediated encephalitides (3 neuronal surface antibody encephalitides and 1 case of antibody-negative opsoclonus-myoclonus-ataxia), which are not traditionally associated with the YF vaccine. However, anti-NMDA-r encephalitis is triggered by infections (*22*), several other vaccines (*23*–*27*), and the YF vaccine (*28*,*29*); as such, anti-NMDA-r encephalitis could represent a novel YEL-AND. Opsoclonus-myoclonus-ataxia is considered a paraneoplastic or parainfectious disease, which is associated with several infections (*30*–*33*), other vaccines (*34*–*39*), and 1 case of YEL-AND described by Martins et al. (*4*).

Last, of the 39 patients with suspected YEL-AND for which information on vaccine dosing was available, 9 had received fractional doses and 30 had received full doses. Although the proportion of cases associated with fractional doses (1:3.3) is smaller than the proportion of fractional doses in the São Paulo region (1:1.5), this finding must be interpreted with caution because the participating centers of our study are tertiary referral centers with statewide catchment areas. AEFI surveillance data from Center for Epidemiologic Surveillance of the State of São Paulo did not show substantially different reporting rates between the 2 doses of the vaccine (E. Gatti Fernandes, unpub. data).

In conclusion, both full and fractional doses of the YF vaccine can cause YEL-AND. Aseptic meningitis is a YEL-AND for which the CDC criteria are particularly exclusive. In contrast to detecting YF virus IgM in CSF, limited value for diagnosing meningoencephalitis has been found for molecular testing, MRI, and EEG. Future studies of YEL-AND should be based on BC case definitions for case ascertainment and on detection of YF virus IgM in CSF for determination of causality for patients with aseptic meningitis and encephalitis. Autoimmune encephalopathies should be included as potential YEL-ANDs.

Acknowledgment

We thank Roosecelis Brasil Martines for her help with the molecular diagnosis in fatal case 2.

About the Author

Dr. Ribeiro is a medical doctor at the Instituto de Infectologia Emilio Ribas in Sao Paulo, Brazil. Her research interests include epidemiologic surveillance, infectious diseases, and immunization.

References

1. Monath TP, Vasconcelos PFC. Yellow fever. J Clin Virol. 2015;64:160–73. https://doi.org/10.1016/j.jcv.2014.08.030
2. Camacho LAB, Freire MS, Leal ML, Aguiar SG, Nascimento JP, Iguchi T, et al.; Collaborative Group for the Study of Yellow Fever Vaccines. Immunogenicity of WHO-17D and Brazilian 17DD yellow fever vaccines: a randomized trial. Rev Saude Publica. 2004;38:671–8. https://doi.org/10.1590/S0034-89102004000500009
3. McMahon AW, Eidex RB, Marfin AA, Russell M, Sejvar JJ, Markoff L, et al.; Yellow Fever Working Group. Neurologic disease associated with 17D-204 yellow fever vaccination: a report of 15 cases. Vaccine. 2007;25:1727–34. https://doi.org/10.1016/j.vaccine.2006.11.027
4. Martins RM, Pavão ALB, de Oliveira PMN, dos Santos PRG, Carvalho SMD, Mohrdieck R, et al. Adverse events following yellow fever immunization: report and analysis of 67 neurological cases in Brazil. Vaccine. 2014;32:6676–82. https://doi.org/10.1016/j.vaccine.2014.05.003
5. Lindsey NP, Schroeder BA, Miller ER, Braun MM, Hinckley AF, Marano N, et al. Adverse event reports following yellow fever vaccination. Vaccine. 2008;26:6077–82. https://doi.org/10.1016/j.vaccine.2008.09.009
6. Lindsey NP, Rabe IB, Miller ER, Fischer M, Staples JE. Adverse event reports following yellow fever vaccination, 2007-13. J Travel Med. 2016;23:taw045. https://doi.org/10.1093/jtm/taw045
7. Staples JE, Gershman M, Fischer M; Centers for Disease Control and Prevention (CDC). Yellow fever vaccine: recommendations of the Advisory Committee on Immunization Practices (ACIP). MMWR Recomm Rep. 2010;59(RR-7):1–27.
8. Bonhoeffer J, Kohl K, Chen R, Duclos P, Heijbel H, Heininger U, et al. Brighton Collaboration. The Brighton Collaboration—enhancing vaccine safety. Vaccine. 2004; 22:2046. https://doi.org/10.1016/j.vaccine.2004.01.016
9. Tapiainen T, Prevots R, Izurieta HS, Abramson J, Bilynsky R, Bonhoeffer J, et al.; Brighton Collaboration Aseptic

Meningitis Working Group. Aseptic meningitis: case definition and guidelines for collection, analysis and presentation of immunization safety data. Vaccine. 2007;25:5793–802. https://doi.org/10.1016/j.vaccine.2007.04.058
10. Sejvar JJ, Kohl KS, Bilynsky R, Blumberg D, Cvetkovich T, Galama J, et al.; Brighton Collaboration Encephalitis Working Group. Encephalitis, myelitis, and acute disseminated encephalomyelitis (ADEM): case definitions and guidelines for collection, analysis, and presentation of immunization safety data. Vaccine. 2007;25:5771–92. https://doi.org/10.1016/j.vaccine.2007.04.060
11. Ministério da Saúde, Secretaria de Vigilância em Saúde. Manual de Vigilância Epidemiológica de Eventos Adversos Pós-Vacinação. 3ª edição. Brasilia, Brazil: Ministério da Saúde; 2014.
12. Sejvar JJ, Kohl KS, Gidudu J, Amato A, Bakshi N, Baxter R, et al.; Brighton Collaboration GBS Working Group. Guillain-Barré syndrome and Fisher syndrome: case definitions and guidelines for collection, analysis, and presentation of immunization safety data. Vaccine. 2011; 29:599–612. https://doi.org/10.1016/j.vaccine.2010.06.003
13. Tozzi AE, Asturias EJ, Balakrishnan MR, Halsey NA, Law B, Zuber PLF. Assessment of causality of individual adverse events following immunization (AEFI): a WHO tool for global use. Vaccine. 2013;31:5041–6. https://doi.org/10.1016/j.vaccine.2013.08.087
14. Guedes BF, Ribeiro AF, Pinto LF, Vidal JE, de Oliveira FG, Sztajnbok J, et al. Potential autoimmune encephalitis following yellow fever vaccination: a report of three cases. J Neuroimmunol. 2021;355:577548. https://doi.org/10.1016/j.jneuroim.2021.577548
15. Thomas RE, Spragins W, Lorenzetti DL. How many published cases of serious adverse events after yellow fever vaccination meet Brighton Collaboration diagnostic criteria? Vaccine. 2013;31:6201–9. https://doi.org/10.1016/j.vaccine.2013.10.050
16. Breugelmans JG, Lewis RF, Agbenu E, Veit O, Jackson D, Domingo C, et al; YF AEFI group. Adverse events following yellow fever preventive vaccination campaigns in eight African countries from 2007 to 2010. Vaccine. 2013;31:1819–29. https://doi.org/10.1016/j.vaccine.2013.01.054
17. Guimard T, Minjolle S, Polard E, Fily F, Zeller H, Michelet C, et al. Short report: incidence of yellow fever vaccine-associated neurotropic disease. Am J Trop Med Hyg. 2009;81:1141–3. https://doi.org/10.4269/ajtmh.2009.09-0295
18. Ministério da Saúde, Secretaria de Vigilância em Saúde. Monitoramento dos casos de dengue, febre de chikungunya e doença aguda pelo vírus Zika até a Semana Epidemiológica 52 de 2018. Boletim epidemiológico. Vol. 50. Jan 2019. Brasilia (Brazil): Ministério da Saúde; 2019.
19. Kuhn S, Twele-Montecinos L, MacDonald J, Webster P, Law B. Case report: probable transmission of vaccine strain of yellow fever virus to an infant via breast milk. CMAJ. 2011;183:E243–5. https://doi.org/10.1503/cmaj.100619
20. Centers for Disease Control and Prevention. Transmission of yellow fever vaccine virus through breast-feeding—Brazil, 2009. MMWR Morb Mortal Wkly Rep. 2010;59:130–2.
21. Traiber C, Coelho-Amaral P, Ritter VRF, Winge A. Infant meningoencephalitis caused by yellow fever vaccine virus transmitted via breastmilk. J Pediatr (Rio J). 2011;87:269–72. https://doi.org/10.2223/JPED.2067
22. Armangue T, Moris G, Cantarín-Extremera V, Conde CE, Rostasy K, Erro ME, et al.; Spanish Prospective Multicentric Study of Autoimmunity in Herpes Simplex Encephalitis. Autoimmune post-herpes simplex encephalitis of adults and teenagers. Neurology. 2015;85:1736–43. https://doi.org/10.1212/WNL.0000000000002125
23. Endres D, Rauer S, Kern W, Venhoff N, Maier SJ, Runge K, et al. Psychiatric presentation of Anti-NMDA receptor encephalitis. Front Neurol. 2019;10:1086. https://doi.org/10.3389/fneur.2019.01086
24. Hofmann C, Baur M-O, Schroten H. Anti-NMDA receptor encephalitis after TdaP-IPV booster vaccination: cause or coincidence? J Neurol. 2011;258:500–1. https://doi.org/10.1007/s00415-010-5757-3
25. Dalmau J, Lancaster E, Martinez-Hernandez E, Rosenfeld MR, Balice-Gordon R. Clinical experience and laboratory investigations in patients with anti-NMDAR encephalitis. Lancet Neurol. 2011;10:63–74. https://doi.org/10.1016/S1474-4422(10)70253-2
26. Blitshteyn S, Brook J. Postural tachycardia syndrome (POTS) with anti-NMDA receptor antibodies after human papillomavirus vaccination. Immunol Res. 2017;65:282–4. https://doi.org/10.1007/s12026-016-8855-1
27. Wang H. Anti-NMDA receptor encephalitis and vaccination. Int J Mol Sci. 2017;18:E193. https://doi.org/10.3390/ijms18010193
28. Spatola M, Petit-Pedrol M, Simabukuro MM, Armangue T, Castro FJ, Barcelo Artigues MI, et al. Investigations in $GABA_A$ receptor antibody-associated encephalitis. Neurology. 2017;88:1012–20. https://doi.org/10.1212/WNL.0000000000003713
29. Hozáková L, Slonková J, Blahutová Š. Anti-NMDAR encephalitis as a serious adverse event probably related to yellow fever vaccination [in Czech]. Klin Mikrobiol Infekc Lek. 2018;24:17–9.
30. Guedes BF, Vieira Filho MAA, Listik C, Carra RB, Pereira CB, Silva ERD, et al. HIV-associated opsoclonus-myoclonus-ataxia syndrome: early infection, immune reconstitution syndrome or secondary to other diseases? Case report and literature review. J Neurovirol. 2018;24:123–7. https://doi.org/10.1007/s13365-017-0603-3
31. Karam E, Giraldo J, Rodriguez F, Hernandez-Pereira CE, Rodriguez-Morales AJ, Blohm GM, et al. Ocular flutter following Zika virus infection. J Neurovirol. 2017;23:932–4. https://doi.org/10.1007/s13365-017-0585-1
32. Gyllenborg J, Milea D. Ocular flutter as the first manifestation of Lyme disease. Neurology. 2009;72:291. https://doi.org/10.1212/01.wnl.0000339491.14474.61
33. Mahale RR, Mehta A, Buddaraju K, Srinivasa R. Parainfectious ocular flutter and truncal ataxia in association with dengue fever. J Pediatr Neurosci. 2017;12:91–2. https://doi.org/10.4103/jpn.JPN_4_16
34. McCarthy JE, Filiano J. Opsoclonus myoclonus after human papilloma virus vaccine in a pediatric patient. Parkinsonism Relat Disord. 2009;15:792–4. https://doi.org/10.1016/j.parkreldis.2009.04.002
35. Huddar A, Bindu PS, Nagappa M, Bharath RD, Sinha S, Mathuranath PS, et al. Pediatric opsoclonus-myoclonus-ataxia syndrome: experience from a tertiary care university hospital. Neurol India. 2018;66:1332–7. https://doi.org/10.4103/0028-3886.241404
36. Stefanowicz J, Izycka-Swieszewska E, Drozyńska E, Pienczk J, Połczyńska K, Czauderna P, et al. Neuroblastoma and opsoclonus-myoclonus-ataxia syndrome—clinical and pathological characteristics. Folia Neuropathol. 2008;46:176–85.
37. Asindi AA, Bell EJ, Browning MJ, Stephenson JB. Vaccine-induced polioencephalomyelitis in Scotland. Scott Med J. 1988;33:306–7. https://doi.org/10.1177/003693308803300409

38. Lapenna F, Lochi L, Iliceto G, Lamberti P, Lamberti P; de Mari M. Post-vaccinic opsoclonus-myoclonus syndrome: a case report. Parkinsonism Relat Disord. 2000;6:241–2. https://doi.org/10.1016/S1353-8020(00)00020-1
39. Bembeeva RT, Petrukhin AS, Bologov AA, Baĭdun LV, Il'ina ES, Samoĭlova MV, et al. Opsoclonus-myoclonus syndrome in children [in Russian]. Zh Nevrol Psikhiatr Im S S Korsakova. 2007;107:4–11.

Address for correspondence: Bruno Fukelmann Guedes, Department of Neurology, Hospital das Clinicas, Faculdade de Medicina da Universidade de São Paulo, Brazil Av Dr. Eneas de Carvalho Aguiar, 255, 5° andar, sala 5084, Cerqueira Cesar 05403-900, São Paulo, SP, Brazil; email: bruno.guedes@hc.fm.usp.br

etymologia

Enterocytoø on bieneusi ['entərə¸saitə'ʒu:ən bıə'nəʊsı]

Maxime Moniot, Philippe Poirier, Céline Nourrisson

From the Greek *en'tĕr-ō-sī'tōn* (intestine), *kútos* (vessel, cell), and *zō'on* (animal), and the surname Bieneus, in memory of the first infected patient whose case was reported in Haiti during 1985. *Enterocytozoon bieneusi*, a member of the wide-ranging phylum Microsporidia, is the only species of this genus known to infect humans. Microsporidia are unicellular intracellular parasites closely related to fungi, although the nature of the relationship is not clear.

E. bieneusi, a spore-forming, obligate intracellular eukaryote, was discovered during the HIV/AIDS pandemic and is the main species responsible for intestinal microsporidiosis, a lethal disease before widespread use of antiretroviral therapies. More than 500 genotypes are described, which are divided into different host-specific or zoonotic groups. This pathogen is an emerging issue in solid organ transplantation, especially in renal transplant recipients.

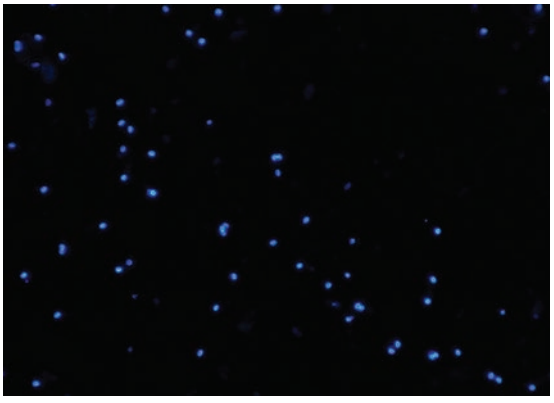

Figure. Spores of *Enterocytozoon bieneusi* in a fecal smear from a patient with intestinal microsporidiosis. Spores are small (≈1.5 μm × 0.5 μm) and egg-shaped (calcofluor-white stain, original magnification ×1,000). Photograph courtesy of Céline Nourrisson.

Sources

1. Desportes I, Le Charpentier Y, Galian A, Bernard F, Cochand-Priollet B, Lavergne A, et al. Occurrence of a new microsporidan: *Enterocytozoon bieneusi* n.g., n. sp., in the enterocytes of a human patient with AIDS. J Protozool. 1985;32:250–4. https://doi.org/10.1111/j.1550-7408.1985.tb03046.x
2. Didier ES, Weiss LM. Microsporidiosis: not just in AIDS patients. Curr Opin Infect Dis. 2011;24:490–5. https://doi.org/10.1097/QCO.0b013e32834aa152
3. Han B, Weiss LM. Microsporidia: obligate intracellular pathogens within the fungal kingdom. Microbiol Spectr. 2017;5:97–113. https://doi.org/10.1128/microbiolspec.FUNK-0018-2016
4. Moniot M, Nourrisson C, Faure C, Delbac F, Favennec L, Dalle F, et al. Assessment of a multiplex PCR for the simultaneous diagnosis of intestinal cryptosporidiosis and microsporidiosis: epidemiologic report from a French prospective study. J Mol Diagn. 2021;23:417–23. https://doi.org/10.1016/j.jmoldx.2020.12.005

Address for correspondence: Maxime Moniot, Laboratoire de Parasitologie Mycologie, Centre Hospitalier Universitaire, 58 Rue Montalembert, Gabriel Montpied 63003, Clermont-Ferrand CEDEX 1, France; email: mmoniot@chu-clermontferrand.fr

Author affiliation: Centre Hospitalier Universitaire, Clermont-Ferrand, France

DOI: https://doi.org/10.3201/eid2706.ET2706

Macrolide-Resistant *Mycoplasma pneumoniae* Infections in Children, Ohio, USA

Mariana M. Lanata,[1] Huanyu Wang, Kathy Everhart, Melisa Moore-Clingenpeel, Octavio Ramilo, Amy Leber

Emergence of macrolide-resistant *Mycoplasma pneumoniae* (MRMp) challenges empiric macrolide therapy. Our goal was to determine MRMp rates and define characteristics of children infected with macrolide-sensitive *M. pneumoniae* (MSMp) versus MRMp in Ohio, USA. We cultured PCR-positive *M. pneumoniae* specimens and sequenced *M. pneumoniae*–positive cultures to detect macrolide resistance mutations. We reviewed medical records to compare characteristics of both groups. We identified 14 (2.8%) MRMp and 485 (97.2%) MSMp samples. Patients in these groups had similar demographics and clinical characteristics, but patients with MRMp had longer hospitalizations, were more likely to have received previous macrolides, and were more likely to have switched to alternative antimicrobial drugs. MRMp-infected patients also had ≈5-fold greater odds of pediatric intensive care unit admission. Rates of MRMp infections in children in central Ohio are low, but clinicians should remain aware of the risk for severe illness caused by these pathogens.

Mycoplasma pneumoniae is a major pathogen that accounts for up to 40% of the total number of community-acquired pneumonias (CAPs) in children and up to 19% of the pediatric CAPs that require hospitalization (*1*,*2*), yet those numbers might not reflect its actual clinical impact because testing for *M. pneumoniae* is not performed routinely. *M. pneumoniae* infection has a wide range of manifestations, from asymptomatic infection to severe pneumonia requiring admission to the intensive care unit (*3*,*4*). Because it lacks a cell wall, *M. pneumoniae* is not susceptible to β-lactam antimicrobial drugs, which are first-line therapy for CAP in children (*5*).

Macrolides are considered the antimicrobial drugs of choice for the treatment of *M. pneumoniae* infections in children (*5*); however, in the past few decades, macrolide-resistant *M. pneumoniae* (MRMp) has emerged. Rates of resistance are highest in Asia, as high as 100%, and reported rates in the United States vary from 3.5% to 13.2% (*3*,*6*–*13*). No published data are available from Ohio, where we conducted our study.

Macrolide resistance is conveyed by single base mutations in the V region of 23S rRNA, which codes for the binding site of macrolides in the *M. pneumoniae* ribosome. The most common mutations include the change of A to C/G/T at location A2063 or at location A2064 (*14*,*15*). These are the 2 mutations associated with macrolide resistance that have been reported in the United States (*3*,*6*).

M. pneumoniae is a slow-growing, fastidious organism, making routine culture and phenotypic antimicrobial drug sensitivity testing impractical for clinical use and limiting the use of these techniques mainly to research purposes. Since molecular assays were developed, diagnosis of *M. pneumoniae* infections has shifted from serology to molecular detection using PCR, resulting in improved sensitivity and specificity. However, even with molecular detection, most clinicians have no information regarding antimicrobial sensitivity of *M. pneumoniae*. Therefore, as in many other settings, we currently have no data on local rates of MRMp, and most children diagnosed with *M. pneumoniae* infection are treated initially with macrolides. If clinical concerns for macrolide resistance occur while children are receiving therapy, clinicians sometimes choose to switch antimicrobial therapy to another agent, although there are no established clinical parameters or guidelines concerning when to consider potential resistance to macrolide antimicrobial drugs.

Studies, emerging mainly from Asia, have reported increased disease severity in adults and children infected with MRMp. More consistently, studies have demonstrated longer duration of fever in

Author affiliation: Nationwide Children's Hospital, Columbus, Ohio, USA

DOI: https://doi.org/10.3201/eid2706.203206

[1]Current affiliation: Marshall University, Huntington, West Virginia, USA.

patients infected with MRMp and longer duration of hospitalization. Other studies have reported more frequent pulmonary complications and the need for changing antimicrobial drug therapy (*16*–*19*). Chen et al. recently published a meta-analysis further consolidating the evidence for longer duration of fever and hospitalization in patients with MRMp, but no differences were reported in clinical presentation, laboratory results, or chest radiograph findings (*20*). Data about MRMp infection in children in the United States remain limited.

The primary objective of this study was to determine the rate of MRMp infections in children in central Ohio, USA. Our second objective was to examine the clinical characteristics, antimicrobial drug treatment, and outcomes in this cohort; to identify potential differences between patients infected with macrolide-sensitive *M. pneumoniae* (MSMp) and those infected with MRMp; and to determine whether infection with MRMp was associated with worse clinical outcomes than infection with MSMp.

Methods

Study Samples

We collected a retrospective convenience sample from standard-of-care clinical samples with orders for *M. pneumoniae* molecular testing performed either using an in-house laboratory-developed PCR for *M. pneumoniae* (*21*) or the PCR for *M. pneumoniae* included as part of a multiplex PCR panel for respiratory pathogens (BioFire FilmArray Respiratory Panel version 1.7; BioFire, https://www.biofiredx.com). We identified samples positive for *M. pneumoniae* and having adequate remnant volume for further analysis using the laboratory database for October 2015–January 2019. The samples consisted of nasopharyngeal or throat swab specimens collected in M4 transport media.

Mycoplasma Culture

We stored samples at 4°C pending PCR results. We cultured the samples that tested positive for *M. pneumoniae* within 48 hours of collection in SP4 glucose broth (Remel, http://www.remel.com) and incubated them at 35°C until isolates grew, or for a maximum of 4 weeks for a negative culture, according to standard procedures (*22*). Culture positivity was identified by color change of the broth and later confirmed by our laboratory-developed *M. pneumoniae* PCR in a subset of patients. We discarded samples displaying bacterial contamination (detected by cloudy or yellow color change).

Sequencing for Macrolide Resistance Detection

We amplified domain V of the 23S-rRNA (nt 1937–2154; reference strain GenBank accession no. X68422) (*23*) from all positive *M. pneumoniae* cultures, where both point mutations that convey macrolide resistance described in the United States are located. We performed Sanger sequencing on the PCR products and compared the sequences with the corresponding region of the wild-type reference strain (ATCC 15322). We sent 2 de-identified samples to a reference laboratory (Mycoplasma Laboratory, University of Alabama at Birmingham, Birmingham, AL, USA) for phenotypic sensitivity testing to assess the effect of a novel mutation (A2065Δ).

Clinical and Treatment Characteristics

We reviewed electronic medical records from all patients with sequenced samples. We collected demographic characteristics, including age, gender, race, patient location, any previous medical encounter during illness, and vaccination status, for each patient. We also collected clinical data such as symptoms at the first medical encounter, including fever, cough, rhinorrhea, rash, and central nervous system manifestations. We recorded all diagnostic testing associated with the medical encounter, including chest radiographs and laboratory testing (blood cultures, complete blood counts, other viral testing) and medical interventions, mainly with regard to antimicrobial drug treatment. This study was approved by the Nationwide Children's Hospital Institutional Review Board (IRB17-01280).

Statistical Analysis

We assessed group comparisons using χ^2 or Fisher exact tests for categorical variables and 2-sample *t*-tests with Satterthwaite corrections for unequal group variance where needed or Wilcoxon rank sum tests for continuous variables. We used multivariable logistic regression to evaluate risk factors for binary outcomes (hospital admission, pediatric intensive care unit [PICU] admission, presence of fever, hypoxemia), with a Firth correction for small sample size when warranted. We used negative binomial regression to evaluate risk factors for continuous outcomes (duration of hospitalization, duration of fever); results have been exponentiated to reflect risk ratios. For all multivariable models, when sample size allowed, we ran separate models for the full cohort as well as for the cohort with viral testing, because of the more limited number of patients who received viral testing; results were similar for both cohorts. We ran separate models for collinear covariates and presented

the model with the best goodness of fit (based on the Akaike Information Criterion). We based variable selection for all multivariable models on backward stepwise selection, with an entry criterion of $p<0.15$; we retained resistance in all models regardless of statistical significance because it was the primary risk factor. We used SAS 9.4 (https://www.sas.com) to conduct all analyses.

Results

Detection of Macrolide Resistance Mutations by Sequencing

During October 2015–January 2019, a total of 744 samples identified as *M. pneumoniae*–positive by PCR were cultured for isolation of *M. pneumoniae*. Among these, 553 (74.3%) yielded a positive *M. pneumoniae* culture (Figure).

We performed sequencing on those 553 culture-positive samples and were successful with 499 (90.2%). The sequences of the V domain of the 23rRNA from a total of 485 (97.2%) samples matched that of the wild-type reference strain. We detected mutations associated with macrolide resistance in 14 samples (2.8%); of those, 11 corresponded to the A2063G and 3 to A2064G mutations (Figure). We also identified 3 samples with a deletion on A2065, a locus adjacent to the mutations described to convey macrolide resistance.

Phenotypic Susceptibility Testing

From the 3 samples with the A2065Δ mutation, we were able to regrow only 2 from frozen aliquots and sent them for phenotypic sensitivity testing. Erythromycin, tetracycline, and levofloxacin were the antimicrobial drugs tested. The *M. pneumoniae* isolates from both samples were sensitive to all 3 drugs according to Clinical and Laboratory Standards Institute guidelines; therefore, this deletion was not found to convey resistance to macrolides (*24*). For purpose of the rest of the analysis, we included these samples in the MSMp group.

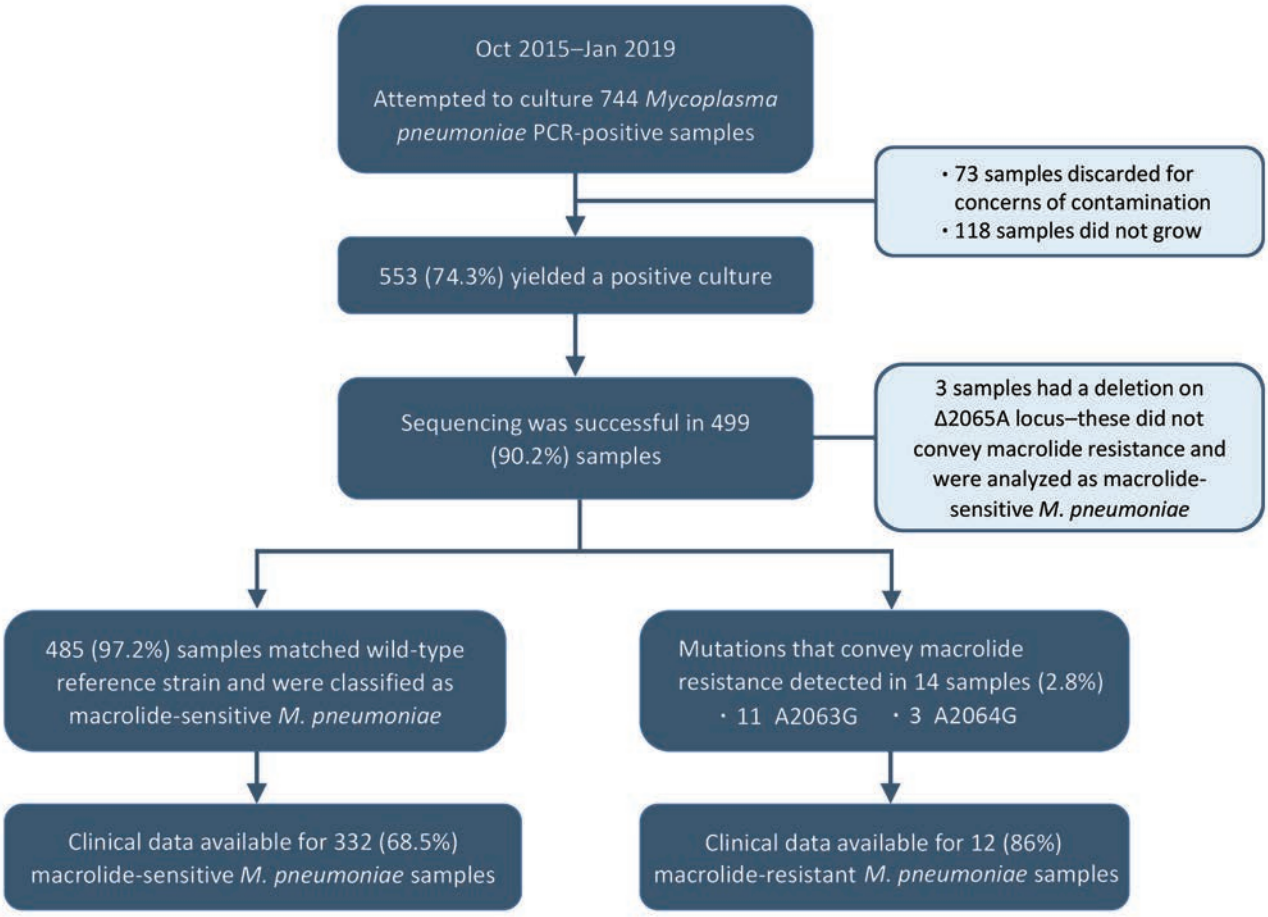

Figure. Flowchart for selection of *Mycoplasma pneumoniae*-positive respiratory samples for macrolide resistance testing and children with available information for analysis of clinical variables in study of children infected with *M. pneumoniae*, Ohio, USA, 2015–2019.

Demographic, Clinical, and Treatment Data

Clinical data were available for 344 (68.9%) of the sequenced samples, including 12/14 (86%) of the MRMp isolates and 332/485 (68.5%) of the MSMp isolates. Both groups of patients had similar demographics, including the presence of concurrent conditions, previous medical encounters, and vaccination status (Table 1). Of the concurrent conditions, asthma was present in 50% of patients. No differences were found in the clinical characteristics at the time of presentation to medical care between both groups, with the exception of maximum temperature among patients who had fever; those in the MRMp group had a lower maximum temperature. Central nervous system manifestations appeared to be more common in the MRMp group; however, this finding was not statistically significant.

Among patients for whom chest radiographs were obtained (12 in the MRMp group and 264 in the MSMp group), most of their radiographs were abnormal (100% of MRMp and 95% of MSMp) (Table 2). Of the 344 patients with clinical data, 91 received their diagnoses by multiplex PCR panel alone, 168 by in-house *M. pneumoniae* PCR alone, and 85 with both. Therefore, viral testing was available in the subset of 176 patients in the cohort tested using the multiplex panel: 10 (83%) patients with MRMp and 166 (50%) patients with MSMp. Viruses identified included rhinovirus/enterovirus, adenovirus, respiratory syncytial virus, coronavirus, influenza B, and parainfluenza types 2 and 3. Although co-detection of viruses was more common in the MSMp group, this difference was not statistically significant. No bacterial co-infections were detected (Table 2).

Macrolide resistance was not significantly associated with duration of fever in univariate (relative risk [RR] 0.99, 95% CI 0.66–1.46) or multivariable (adjusted RR [aRR] 0.93, 95% CI 0.66–1.30) analysis. However,

Table 1. Patient demographics and clinical characteristics of children infected with macrolide-sensitive and macrolide-resistant strains of *Mycoplasma pneumoniae*, Ohio, USA, 2015–2019*

Characteristic	MRMp, n = 12	MSMp, n = 332	p value
Sex			0.9046
M	7 (55)	175 (53)	
F	5 (45)	157 (47)	
Year			0.6508
2015	4 (33)	146 (44)	
2016	1 (8)	51 (15)	
2017	2 (17)	52 (16)	
2018	5 (42)	73 (22)	
2019	0	10 (3)	
Age, y, mean (SD)	9.13 (3.74)	8.73 (4.62)	0.7683
Previous visits			
Any previous visits	8 (67)	188 (57)	0.4901
No. previous visits, median (IQR)	1.5 (1–2)	1 (1–2)	0.3491
Underlying conditions	6 (50)	139 (42)	0.5752
Chronic immunosuppression	1 (8)	5 (2)	0.1392
Up to date in vaccines	12 (100)	316 (97)	>0.9999
Inpatient	6 (50)	130 (39)	0.551
Median duration of hospitalization, d (IQR)	8 (6–10)	2 (1.5–3)	**0.0132**
PICU	3 (25)	21 (6)	**0.0433**
Median duration of PICU stay, d (IQR)	2 (1–8)	2 (1.5–5)	0.8596
Hypoxemia	3 (25)	73 (23)	>0.9999
Median duration of O_2 support, d (IQR)	4 (1–8.5)	1 (0.5–2)	0.1302
Mechanical ventilation	1 (33)	6 (8)	0.2487
Median duration of symptoms, d (IQR)	7 (6.5–13)	7 (5–10)	0.3324
Fever	11 (92)	271 (81)	0.7024
Median duration of fever, d (IQR)	4 (2–7)	4 (2–7)	0.984
Median maximum temperature, °C (IQR)	38.4 (38.1–39.4)	39.1 (38.4–39.7)	**0.0415**
Fatigue	5 (42)	91 (27)	0.3298
Decreased appetite/oral food intake	4 (33)	125 (38)	>0.9999
Decreased urine output	0	22 (7)	>0.9999
Cough	12 (100)	320 (96)	>0.9999
Shortness of breath/respiratory distress	5 (42)	91 (27)	0.3268
Sore throat	0	67 (20)	0.1332
CNS manifestation	2 (17)	10 (3)	0.0607
Nausea/vomiting	1 (8)	55 (17)	0.6987
Diarrhea	1 (8)	30 (9)	>0.9999
Rash	0	25 (7.5)	>0.9999

*Values are no. (%) except as indicated. Bold type indicates statistical significance. CNS, central nervous system; IQR, interquartile range; MRMp, macrolide-resistant *Mycoplasma pneumoniae*; MSMp, macrolide-sensitive *Mycoplasma pneumoniae*; PICU, pediatric intensive care unit.

Table 2. Respiratory examination, chest radiograph findings, and results of viral testing in children infected with *Mycoplasma pneumoniae*, Ohio, USA, 2015–2019*

Test	MRMp, n = 12	MSMp, n = 332	p value
Respiratory examination			
Abnormal	9 (75)	214 (64)	0.5513
Crackles	3 (25)	96 (45)	0.7344
Rales	1 (11)	25 (12)	>0.9999
Rhonchi	1 (11)	23 (11)	>0.999
Decreased breath sounds	5 (56)	104 (49)	0.7441
Wheezing	1 (11)	51 (24)	0.6888
Chest radiograph findings	n = 12	n = 261	>0.9999
Abnormal	12 (100)	243 (93.1)	
Focal consolidation	3 (25)	170 (65.1)	
Multifocal consolidation	4 (33)	41 (15.7)	
Peribronchial thickening	2 (17)	45 (17.2)	
Atelectasis	0	8 (3.1)	
Pleural effusion	1 (11)	39 (14.9)	
Viral testing done by multiplex PCR	10 (83.3)	166 (50)	0.4086
M. pneumoniae alone	9 (90)	118 (71)	
M. pneumoniae + 1 virus	1 (10)	37 (22)	
M. pneumoniae + ≥2 viruses	0	11 (7)	

*Values are no. (%) except as indicated. MRMp, macrolide-resistant *Mycoplasma pneumoniae*; MSMp, macrolide-sensitive *Mycoplasma pneumoniae*.

older age (aRR 1.02 [95% CI 1.0–1.03]) per 1 year increase in age), previous medical visit (aRR = 1.71, 95% CI 1.44–2.04), and previous antimicrobial drug treatment (aRR 1.21, 95% CI 1.03–1.42) were significantly associated with longer duration of fever.

When we evaluated outcomes related to disease severity, MRMp infection was not a risk factor for hospitalization. In multivariable analyses, younger age, presence of concurrent conditions, previous medical encounters, presence of abnormal respiratory examination, and preceding therapy with a nonmacrolide antimicrobial drug were significantly associated with increased odds for hospitalization (Table 3). Among the subset of patients who had viral testing performed, positive viral co-detection was associated with significantly lower odds of hospitalization. We also examined for variables associated with duration of hospitalization and found that, in univariate analysis, patients infected with MRMp strains had significantly longer duration of hospitalization than those infected with MSMp (Table 4); no other study variables were significantly associated with duration of hospitalization.

A total of 24 (7% of the cohort, 17.6% of hospitalizations) patients required PICU admission, the majority (n = 21, 87.5%) because of escalated respiratory support; 5 required invasive ventilation, 1 a Venturi mask, and 13 bilevel positive airway pressure. Two patients were admitted because of concerns of severe sepsis, and 1 because of altered mental status. Macrolide resistance was significantly associated with PICU admission (univariate odds ratio [OR] 5.34, 95% CI 1.39–20.55), as was the presence of concurrent conditions, any previous medical visits, abnormal respiratory exam, and previous therapy with a nonmacrolide antimicrobial drug (Table 5). Although too few patients were admitted to the PICU to enable us to perform a comprehensive multivariable analysis, we found that macrolide resistance remained significantly associated with odds of PICU admission after adjusting one at a time for the presence of concurrent conditions, any previous medical visits, abnormal respiratory examination, and previous therapy with a nonmacrolide antimicrobial drug (adjusted OR [aOR] for macrolide resistance 4.9–5.1; Table 6). Presence of macrolide resistance was not associated with increased risk for hypoxemia when

Table 3. Risk factors for hospital admission in children infected with *Mycoplasma pneumoniae*, Ohio, USA, 2015–2019*

	Univariate analysis		Multivariable analysis	
Risk factor	OR (95% CI)	p value	aOR (95% CI)	p value
Female sex	0.99 (0.64–1.53)	0.9599		
Age, y	0.96 (0.92–1.01)	0.1125	0.928 (0.877–0.982)	0.0096
Underlying condition	3.47 (2.21–5.46)	**<0.0001**	4.234 (2.506–7.155)	<0.0001
Any previous visit	3.6 (2.24–5.78)	**<0.0001**	2.094 (1.131–3.877)	0.0188
Macrolide resistance	1.55 (0.49–4.92)	0.4547	1.171 (0.324–4.231)	0.8094
Abnormal respiratory examination	4.31 (2.55–7.26)	**<0.0001**	4.063 (2.291–7.204)	<0.0001
Previous treatment with antimicrobial drugs	3.03 (1.9–4.83)	**<0.0001**	2.606 (1.377–4.934)	0.0033
Previous nonmacrolide antimicrobial drugs	2.85 (1.78–4.56)	**<0.0001**		
Positive viral test	0.24 (0.08–0.68)	**0.0071**		
MRMp and positive viral test	0.23 (0.04–1.44)	0.1166		

*Bold type indicates statistical significance. aOR, adjusted OR; MRMp: macrolide-resistant *Mycoplasma pneumoniae*; OR, odds ratio.

Table 4. Risk factors for longer duration of hospitalization in children hospitalized with *Mycoplasma pneumoniae* infection, Ohio, USA, 2015–2019*

	Univariate analysis		Multivariable analysis	
Risk factor	RR (95% CI)	p value	aRR (95% CI)	p value
Female sex	0.85 (0.63–1.15)	0.2852		
Age, y	0.98 (0.95–1.01)	0.2213		
Underlying condition	1.25 (0.92–1.71)	0.1592		
Any previous visit	0.83 (0.58–1.16)	0.2734		
Macrolide resistance	2.91 (1.56–5.44)	**0.0008**	2.04 (0.97–4.32)	0.061
Abnormal respiratory examination	1.14 (0.77–1.7)	0.5103		
Previous treatment with antimicrobial drugs	0.94 (0.69–1.27)	0.6882		
Previous nonmacrolide antimicrobial drugs	0.97 (0.71–1.31)	0.8204		
Positive viral test	0.96 (0.69–1.34)	0.8122		
MRMp and positive viral test	1.67 (0.51–5.44)	0.3946		

*Bold type indicates statistical significance. aRR, adjusted RR; MRMp, macrolide-resistant *Mycoplasma pneumoniae*; RR, relative risk.

adjusted for other factors. Only the presence of concurrent conditions (aOR 3.45; p<0.0001) and any previous medical visits (aOR 2.35; p = 0.0151) were significant risks for hypoxemia and oxygen requirement (Table 7).

Antimicrobial Drug Treatment

The number of patients with previous antimicrobial drug prescriptions was similar in both groups (41.7% MRMp, 31.9% MSMp; p = 0.53), with a median duration of 3 days (interquartile range [IQR] 2.5–5.7) for MRMp and 4 days (IQR 2–6) for MSMp (p>0.99). Most (96%) of these were antimicrobial drugs not expected to treat *M. pneumoniae* infection. Median time of prescription was on day 5 of illness (IQR 3–9). Three (25%) patients with MRMp versus 7 (2.1%) with MSMp received therapy with azithromycin before the medical encounter (p = 0.0017). Despite the clinician's lack of knowledge about presence of macrolide resistance, a larger proportion of patients with MRMp infection (25%) than patients with MSMp infection (4.5%) were treated with levofloxacin as the definitive therapy instead of a macrolide (p = 0.0267) (Table 8).

Discussion

Macrolide-resistant *M. pneumoniae* infections are becoming more relevant as pathogen-specific testing is increasing and reports of resistance to macrolides are becoming more widespread throughout the world. Resistance rates vary, but the highest reported resistance rates are from countries in Asia, as high as 100% (*3*,*12*). Lower rates have been reported in Europe and South America; few data are available from the United States (*3*,*13*). In today's globalized world, spread of resistant organisms is common and thus a major concern. Unlike for other bacteria, no cumulative data such as antibiograms are routinely available to help guide empiric therapy for *M. pneumoniae*. Because of *Mycoplasma*'s unique slow growth characteristics and lack of availability of phenotypic susceptibility testing, antimicrobial drug treatment is routinely initiated without any knowledge of macrolide resistance rates.

The ready availability of specific molecular testing for *M. pneumoniae* at Nationwide Children's Hospital, enabled us to generate a large convenience sample of patients infected with *M. pneumoniae* for this study. Our data demonstrated a low rate of MRMp of 2.8%. Although this rate of resistance is lower than those previously described in other studies (*6*–*10*), the difference is likely related to differences in study design. In our study, because of the widespread and routine use of testing for *M. pneumoniae* infections in our institution and affiliated urgent care centers, we were able to include a larger sample size of nonselected patients. The

Table 5. Risk factors for pediatric intensive care unit admission in children infected with *Mycoplasma pneumoniae*, Ohio, USA, 2015–2019*

	Univariate analysis	
Risk factor	OR (95% CI)	p value
Female sex	1.13 (0.5–2.55)	0.7754
Age, y	0.98 (0.9–1.08)	0.7206
Underlying condition	4.32 (1.72–10.88)	**0.0019**
Any previous visit	3.73 (1.31–10.62)	**0.0138**
Macrolide resistance	5.34 (1.39–20.55)	**0.015**
Abnormal respiratory examination	5.34 (1.41–20.21)	**0.0137**
Previous treatment with antimicrobial drugs	3.17 (1.38–7.27)	**0.0066**
Previous nonmacrolide antimicrobial drugs	2.81 (1.23–6.42)	**0.014**
Positive viral test	0.79 (0.31–2.01)	0.6127
MRMp and positive viral test	2.11 (0.27–16.71)	0.4805

*Bold type indicates statistical significance. MRMp, macrolide-resistant *Mycoplasma pneumoniae*; OR, odds ratio.

Table 6. Multivariable models for assessing adjusted risk factors for pediatric intensive care unit admission in children infected with *Mycoplasma pneumoniae*, Ohio, USA, 2015–2019*

Model	aOR (95% CI)	p value
Model 1		
Macrolide resistance	5.111 (1.248–20.926)	**0.0233**
Underlying conditions	4.238 (1.68–10.694)	**0.002**
Model 2		
Macrolide resistance	4.964 (1.247–19.762)	**0.023**
Any previous visits	3.625 (1.273–10.323)	**0.0159**
Model 3		
Macrolide resistance	4.895 (1.227–19.532)	**0.0245**
Abnormal respiratory exam	5.164 (1.37–19.461)	**0.0153**
Model 4		
Macrolide resistance	4.969 (1.241–19.906)	**0.0235**
Any previous antimicrobial drugs	3.076 (1.332–7.101)	**0.0085**
Model 5		
Macrolide resistance	4.911 (1.237–19.499)	**0.0237**
Any previous nonmacrolide antimicrobial drugs	2.717 (1.184–6.234)	**0.0183**

*Bold type indicates statistical significance. aOR, adjusted odds ratio.

resistance mutations detected in our population are similar to others reported worldwide and confirmed that the A2063G mutation was the most commonly found (*8*,*10*,*16*,*25*,*26*). Although it is a novel mutation, a deletion on A2065Δ was detected in 3 isolates, but it did not confer phenotypic resistance to macrolides.

Although children infected with *M. pneumoniae* can have a mild course of disease, some develop severe disease, requiring hospitalization (*1*,*3*,*7*). The presence of mutations associated with macrolide resistance did not affect the need for hospitalization in our study. In the study cohort, 50% of patients infected with MRMp were managed as outpatients. Our findings confirm those of others in different countries (*7*,*18*,*27*,*28*) and a recent surveillance study in the United States (*10*), providing further evidence that children infected with MRMp and MSMp in the United States demonstrated no significant differences in clinical presentation. This finding was also supported in the recent meta-analysis by Chen et al. (*20*). Taken together, these data point to the challenges that clinicians face when treating patients infected with *M. pneumoniae*. Because there is no practical way to identify patients infected with MRMp on the basis of clinical findings, most, if not all, are empirically treated with macrolides and some, albeit a small number, receive ineffective treatment.

Our data indicate that among hospitalized patients infected with MRMp, infections may remain unidentified for days and their conditions may worsen while they receive suboptimal therapy, which likely explains the difference in duration of hospitalizations between both groups. Whereas patients infected with MSMp were hospitalized for a median of 2 days, those infected with MRMp had a median of 8 days of hospitalization. These data confirmed similar findings previously described in other countries (*16*,*27*,*29*) but differ from what was found by Waites et al. in a recent surveillance study, in which they did not find any differences in clinical severity between groups (*10*).

Previous studies have described longer duration of fever in patients infected with MRMp, as well as longer time to defervesce while receiving macrolide therapy, with subsequent quick defervescence when switched to effective therapy (*16*–*18*,*20*,*25*,*29*,*30*). In our pediatric cohort, we found no difference in duration of fever at the first medical encounter. In addition, we found that patients infected with MRMp had

Table 7. Risk factors for hypoxemia in children infected with *Mycoplasma pneumoniae*, Ohio, USA, 2015–2019*

	Univariate analysis		Multivariable analysis	
Characteristic	OR (95% CI)	p value	aOR (95% CI)	p value
Female sex	1.117 (0.68–1.85)	0.6645		
Age, y	0.964 (0.91–1.02)	0.194		
Underlying conditions	3.279 (1.94–5.54)	**<0.0001**	3.46 (2–5.98)	**<0.0001**
Any previous visit	3.202 (1.8–5.69)	**<0.0001**	1.77 (0.94–3.33)	0.0796
Macrolide resistance	1.236 (0.34–4.54)	0.75	0.91 (0.22–3.72)	0.8965
Abnormal respiratory examination	25.288 (6.98–91.64)	**<0.0001**		
Previous treatment with antimicrobial drugs	2.43 (1.45–4.07)	**0.0007**	2.35 (1.18–4.68)	**0.0151**
Previous nonmacrolide antimicrobial drugs	2.129 (1.27–3.58)	**0.0043**		
Positive viral test	0.902 (0.46–1.79)	0.7683		
MRMp and viral positive	0.957 (0.16–5.81)	0.9618		

*Bold type indicates statistical significance. aOR, adjusted odds ratio; MRMp: macrolide-resistant *Mycoplasma pneumoniae*; OR, odds ratio.

Table 8. Antimicrobial drug treatment for children infected with *Mycoplasma pneumoniae*, Ohio, USA, 2015–2019*

Characteristic	MRMp, n = 12	MSMp, n = 332	p value
Patients with previous antimicrobial drug treatment, no. (%)	5 (42)	106 (32)	0.5339
Nonmacrolide	5 (42)	102 (31)	0.5262
Macrolide	3 (25)	7 (2.1)	**0.0017**
Definitive treatment during medical encounter, no. (%)			
Azithromycin	9 (75)	317 (95.5)	**0.0197**
Levofloxacin	3 (25)	15 (4.5)	**0.0267**

*Bold type indicates statistical significance. MRMp, macrolide-resistant *Mycoplasma pneumoniae*; MSMp, macrolide-sensitive *Mycoplasma pneumoniae*.

lower maximum temperatures, which differs from 2 studies from China that described higher fevers in pediatric patients infected with MRMp (*30*,*31*). Because of the retrospective design of our study, we were not able to compare the duration of fever while patients were receiving therapy because most hospitalized patients with MSMp were discharged while still febrile, and a large portion of our cohort was managed as outpatients. Despite this limitation, we documented that patients infected with MRMp were still symptomatic and seeking medical attention while already being treated with macrolides at higher rates when compared with patients infected with MSMp. Likewise, we observed that patients with MRMp infection were more likely to be treated with levofloxacin as an alternative/second-line therapy, which agrees with other reports (*10*,*17*,*18*,*29*). It is crucial to note that several studies mentioned that eventually these patients with MRMp became afebrile, even if they were still receiving macrolide therapy; however, their duration of illness and subsequent hospitalization were longer (*32*). Also, we documented that 196 (57%) patients in our cohort had ≥1 previous medical visit, and 111 (25.6%) received prescriptions for antimicrobial drugs during their visit. Most of those antimicrobial drugs (96%) did not target mycoplasma infections. None of those patients were tested for *M. pneumoniae* infection during this initial encounter, thus contributing to the lack of targeted therapy.

Emerging literature, mainly from Asia, reports that, in addition to longer duration of hospitalization, more severe disease and more complications have been observed in MRMp infected patients. Those studies described more common pleural effusions, worse lung infiltrates, extrapulmonary complications, increased oxygen requirement, and increased need for ICU admission (*16*,*33*,*34*). These findings, however, were not documented in our study, nor in the meta-analysis by Chen et al. (*20*). Even so, in our cohort we observed that patients with MRMp had 4- to 5-fold greater odds for PICU admission, after adjusting for other factors.

The use of a respiratory panel PCR in 176 (51%) patients in the cohort provided additional information for evaluating the interactions between *M. pneumoniae* and viral infections; previous studies on MRMp infections have not analyzed these interactions. The univariate analysis showed that among patients with MRMp infections, viral co-detection was more frequent in those who were not hospitalized. At this point we have no clear explanation for this finding.

Our study's first limitations are that it was performed at a single center and was retrospective. The resistance rates we found were based only on patients who sought medical care, which could lead to a potential bias in our MRMp rate, because not all patients with *M. pneumoniae* infection may need medical attention. From the laboratory perspective, 54 (9.8%) samples that were culture positive were unable to be sequenced. We did not confirm all cultures by *M. pneumoniae* PCR, so it is possible that the culture result was falsely positive. In addition, culture positivity was determined by a color change in the culture medium. Therefore, the presence of any microbial growth could cause color change and be misinterpreted and falsely called *M. pneumoniae* positive, which could be the reason that they failed sequencing. Furthermore, because of the study design, in which we started with the *M. pneumoniae*–positive samples available in the laboratory, no clinical data were available in ≈50% of the samples analyzed. Despite these limitations, we included clinical information from 344 children infected with *M. pneumoniae*, which represents one of the largest contemporary pediatric cohorts published in the United States. Finally, we did not attempt to genotype our isolates of *M. pneumoniae*. Others have reported some association between emerging *p1* gene types and increased macrolide resistance (*35*).

Our study was not designed to address the indications for testing for *M. pneumoniae* in children with CAP, whether detection of *M. pneumoniae* in the upper respiratory tract indicates active infection, or whether antimicrobial drug therapy offers a clear benefit to all patients with *M. pneumoniae* infections. Despite the limitations of the retrospective design, our study showed that lack of specific testing for *M. pneumoniae* frequently led to empiric therapy with noneffective antimicrobial drugs and that children hospitalized

with MRMp infections had a more prolonged clinical course until they were switched to appropriate therapy, suggesting that antimicrobial drug therapy did modify the course of the disease. Large, prospective, multicenter studies are needed to address these key questions to optimize the management of these frequent infections among the pediatric population.

In summary, the rate of MRMp infections in pediatric patients in central Ohio is low (2.8%). Despite this low rate, children hospitalized with MRMp infections had worse clinical outcomes, defined by longer duration of hospitalization and higher odds of PICU admission, than those with infected with MSMp. Although prevalence is low, clinicians should be aware of the possibility of MRMp infection, particularly in patients who do not show clinical improvement while on macrolide therapy.

About the Author

Dr. Lanata is an assistant professor at Marshall University in Huntington, West Virginia. Her main research interest is in antimicrobial stewardship.

References

1. Waites KB, Talkington DF. *Mycoplasma pneumoniae* and its role as a human pathogen. Clin Microbiol Rev. 2004;17:697–728. https://doi.org/10.1128/CMR.17.4.697-728.2004
2. Jain S, Williams DJ, Arnold SR, Ampofo K, Bramley AM, Reed C, et al.; CDC EPIC Study Team. Community-acquired pneumonia requiring hospitalization among U.S. children. N Engl J Med. 2015;372:835–45. https://doi.org/10.1056/NEJMoa1405870
3. Waites KB, Xiao L, Liu Y, Balish MF, Atkinson TP. *Mycoplasma pneumoniae* from the respiratory tract and beyond. Clin Microbiol Rev. 2017;30:747–809. https://doi.org/10.1128/CMR.00114-16
4. Brown RJ, Nguipdop-Djomo P, Zhao H, Stanford E, Spiller OB, Chalker VJ. *Mycoplasma pneumoniae* epidemiology in England and Wales: a national perspective. Front Microbiol. 2016;7:157. https://doi.org/10.3389/fmicb.2016.00157
5. Bradley JS, Byington CL, Shah SS, Alverson B, Carter ER, Harrison C, et al.; Pediatric Infectious Diseases Society and the Infectious Diseases Society of America. The management of community-acquired pneumonia in infants and children older than 3 months of age: clinical practice guidelines by the Pediatric Infectious Diseases Society and the Infectious Diseases Society of America. Clin Infect Dis. 2011;53:e25–76. https://doi.org/10.1093/cid/cir531
6. Pereyre S, Goret J, Bébéar C. *Mycoplasma pneumoniae*: current knowledge on macrolide resistance and treatment. Front Microbiol. 2016;7:974. https://doi.org/10.3389/fmicb.2016.00974
7. Diaz MH, Benitez AJ, Cross KE, Hicks LA, Kutty P, Bramley AM, et al. molecular detection and characterization of *Mycoplasma pneumoniae* among patients hospitalized with community-acquired pneumonia in the United States. Open Forum Infect Dis. 2015;2:ofv106. https://doi.org/10.1093/ofid/ofv106
8. Zheng X, Lee S, Selvarangan R, Qin X, Tang YW, Stiles J, et al. Macrolide-resistant *Mycoplasma pneumoniae*, United States. Emerg Infect Dis. 2015;21:1470–2. https://doi.org/10.3201/eid2108.150273
9. Diaz MH, Benitez AJ, Winchell JM. Investigations of *Mycoplasma pneumoniae* infections in the United States: trends in molecular typing and macrolide resistance from 2006 to 2013. J Clin Microbiol. 2015;53:124–30. https://doi.org/10.1128/JCM.02597-14
10. Waites KB, Ratliff A, Crabb DM, Xiao L, Qin X, Selvarangan R, et al. Macrolide-resistant *Mycoplasma pneumoniae* in the United States as determined from a national surveillance program. J Clin Microbiol. 2019;57:e00968-19. https://doi.org/10.1128/JCM.00968-19
11. Yamada M, Buller R, Bledsoe S, Storch GA. Rising rates of macrolide-resistant *Mycoplasma pneumoniae* in the central United States. Pediatr Infect Dis J. 2012;31:409–11. https://doi.org/10.1097/INF.0b013e318247f3e0
12. Zhou Z, Li X, Chen X, Luo F, Pan C, Zheng X, et al. Macrolide-resistant *Mycoplasma pneumoniae* in adults in Zhejiang, China. Antimicrob Agents Chemother. 2015;59:1048–51. https://doi.org/10.1128/AAC.04308-14
13. Xiao L, Ratliff AE, Crabb DM, Mixon E, Qin X, Selvarangan R, et al. molecular characterization of *Mycoplasma pneumoniae* isolates in the United States from 2012 to 2018. J Clin Microbiol. 2020;58:e00710-20. https://doi.org/10.1128/JCM.00710-20
14. Matsuoka M, Narita M, Okazaki N, Ohya H, Yamazaki T, Ouchi K, et al. Characterization and molecular analysis of macrolide-resistant *Mycoplasma pneumoniae* clinical isolates obtained in Japan. Antimicrob Agents Chemother. 2004;48:4624–30. https://doi.org/10.1128/AAC.48.12.4624-4630.2004
15. Bébéar C, Pereyre S, Peuchant O. *Mycoplasma pneumoniae*: susceptibility and resistance to antibiotics. Future Microbiol. 2011;6:423–31. https://doi.org/10.2217/fmb.11.18
16. Zhou Y, Zhang Y, Sheng Y, Zhang L, Shen Z, Chen Z. More complications occur in macrolide-resistant than in macrolide-sensitive *Mycoplasma pneumoniae* pneumonia. Antimicrob Agents Chemother. 2014;58:1034–8. https://doi.org/10.1128/AAC.01806-13
17. Suzuki S, Yamazaki T, Narita M, Okazaki N, Suzuki I, Andoh T, et al. Clinical evaluation of macrolide-resistant *Mycoplasma pneumoniae*. Antimicrob Agents Chemother. 2006;50:709–12. https://doi.org/10.1128/AAC.50.2.709-712.2006
18. Cardinale F, Chironna M, Chinellato I, Principi N, Esposito S. Clinical relevance of *Mycoplasma pneumoniae* macrolide resistance in children. J Clin Microbiol. 2013;51:723–4. https://doi.org/10.1128/JCM.02840-12
19. Kawai Y, Miyashita N, Kubo M, Akaike H, Kato A, Nishizawa Y, et al. Therapeutic efficacy of macrolides, minocycline, and tosufloxacin against macrolide-resistant *Mycoplasma pneumoniae* pneumonia in pediatric patients. Antimicrob Agents Chemother. 2013;57:2252–8. https://doi.org/10.1128/AAC.00048-13
20. Chen YC, Hsu WY, Chang TH. Macrolide-resistant *Mycoplasma pneumoniae* infections in pediatric community-acquired pneumonia. Emerg Infect Dis. 2020;26:1382–91. https://doi.org/10.3201/eid2607.200017
21. Hardegger D, Nadal D, Bossart W, Altwegg M, Dutly F. Rapid detection of *Mycoplasma pneumoniae* in clinical samples by real-time PCR. J Microbiol Methods. 2000;41:45–51. https://doi.org/10.1016/S0167-7012(00)00135-4
22. Leber AL, editor. Clinical Microbiology Procedures Handbook, 4th ed. Washington (DC): ASM Press; 2016.

23. Wolff BJ, Thacker WL, Schwartz SB, Winchell JM. Detection of macrolide resistance in *Mycoplasma pneumoniae* by real-time PCR and high-resolution melt analysis. Antimicrob Agents Chemother. 2008;52:3542–9. https://doi.org/10.1128/AAC.00582-08
24. Clinical and Laboratory Standards Institute. Methods for antimicrobial susceptibility testing for human mycoplasmas (M43-Al). Annapolis Junction (MD): The Institute; 2011.
25. Lee E, Cho HJ, Hong SJ, Lee J, Sung H, Yu J. Prevalence and clinical manifestations of macrolide resistant *Mycoplasma pneumoniae* pneumonia in Korean children. Korean J Pediatr. 2017;60:151–7. https://doi.org/10.3345/kjp.2017.60.5.151
26. Nakamura Y, Oishi T, Kaneko K, Kenri T, Tanaka T, Wakabayashi S, et al. Recent acute reduction in macrolide-resistant *Mycoplasma pneumoniae* infections among Japanese children. J Infect Chemother. 2021;27:271–6. https://doi.org/10.1016/j.jiac.2020.10.007
27. Wu HM, Wong KS, Huang YC, Lai SH, Tsao KC, Lin YJ, et al. Macrolide-resistant *Mycoplasma pneumoniae* in children in Taiwan. J Infect Chemother. 2013;19:782–6. https://doi.org/10.1007/s10156-012-0523-3
28. Matsubara K, Okada T, Matsushima T, Komiyama O, Iwata S, Morozumi M, et al. A comparative clinical study of macrolide-sensitive and macrolide-resistant *Mycoplasma pneumoniae* infections in pediatric patients. J Infect Chemother. 2009;15:380–3. https://doi.org/10.1007/s10156-009-0715-7
29. Cheong KN, Chiu SS, Chan BW, To KK, Chan EL, Ho PL. Severe macrolide-resistant *Mycoplasma pneumoniae* pneumonia associated with macrolide failure. J Microbiol Immunol Infect. 2016;49:127–30. https://doi.org/10.1016/j.jmii.2014.11.003
30. Chen Y, Tian WM, Chen Q, Zhao HY, Huang P, Lin ZQ, et al. Clinical features and treatment of macrolide-resistant *Mycoplasma pneumoniae* pneumonia in children [in Chinese]. Zhongguo Dang Dai Er Ke Za Zhi. 2018;20:629–34.
31. Ma Z, Zheng Y, Deng J, Ma X, Liu H. Characterization of macrolide resistance of *Mycoplasma pneumoniae* in children in Shenzhen, China. Pediatr Pulmonol. 2014;49:695–700. https://doi.org/10.1002/ppul.22851
32. Kawai Y, Miyashita N, Yamaguchi T, Saitoh A, Kondoh E, Fujimoto H, et al. Clinical efficacy of macrolide antibiotics against genetically determined macrolide-resistant *Mycoplasma pneumoniae* pneumonia in paediatric patients. Respirology. 2012;17:354–62. https://doi.org/10.1111/j.1440-1843.2011.02102.x
33. Zhang Y, Zhou Y, Li S, Yang D, Wu X, Chen Z. The clinical characteristics and predictors of refractory *Mycoplasma pneumoniae* pneumonia in children. PLoS One. 2016;11:e0156465. https://doi.org/10.1371/journal.pone.0156465
34. Kim YJ, Shin KS, Lee KH, Kim YR, Choi JH. Clinical characteristics of macrolide-resistant *Mycoplasma pneumoniae* from children in Jeju. J Korean Med Sci. 2017;32:1642–6. https://doi.org/10.3346/jkms.2017.32.10.1642
35. Kenri T, Suzuki M, Sekizuka T, Ohya H, Oda Y, Yamazaki T, et al. Periodic genotype shifts in clinically prevalent *Mycoplasma pneumoniae* strains in Japan. Front Cell Infect Microbiol. 2020;10:385. https://doi.org/10.3389/fcimb.2020.00385

Address for correspondence: Amy L. Leber, Nationwide Children's Hospital, 700 Children's Dr, Columbus, OH 43205, USA; email: amy.leber@nationwidechildrens.org

Seroprevalence of Severe Acute Respiratory Syndrome Coronavirus 2 IgG in Juba, South Sudan, 2020[1]

Kirsten E. Wiens, Pinyi Nyimol Mawien, John Rumunu, Damien Slater, Forrest K. Jones, Serina Moheed, Andrea Caflisch, Bior K. Bior, Iboyi Amanya Jacob, Richard Lino Lako, Argata Guracha Guyo, Olushayo Oluseun Olu, Sylvester Maleghemi, Andrew Baguma, Juma John Hassen, Sheila K. Baya, Lul Deng, Justin Lessler, Maya N. Demby, Vanessa Sanchez, Rachel Mills, Clare Fraser, Richelle C. Charles,[2] Jason B. Harris,[2] Andrew S. Azman,[3] Joseph F. Wamala[3]

Relatively few coronavirus disease cases and deaths have been reported from sub-Saharan Africa, although the extent of its spread remains unclear. During August 10–September 11, 2020, we recruited 2,214 participants for a representative household-based cross-sectional serosurvey in Juba, South Sudan. We found 22.3% of participants had severe acute respiratory syndrome coronavirus 2 (SARS-CoV-2) receptor binding domain IgG titers above prepandemic levels. After accounting for waning antibody levels, age, and sex, we estimated that 38.3% (95% credible interval 31.8%–46.5%) of the population had been infected with SARS-CoV-2. At this rate, for each PCR–confirmed SARS-CoV-2 infection reported by the Ministry of Health, 103 (95% credible interval 86–126) infections would have been unreported, meaning SARS-CoV-2 has likely spread extensively within Juba. We also found differences in background reactivity in Juba compared with Boston, Massachusetts, USA, where the immunoassay was validated. Our findings underscore the need to validate serologic tests in sub-Saharan Africa populations.

Author affiliations: Johns Hopkins Bloomberg School of Public Health, Baltimore, Maryland, USA (K.E. Wiens, F.K. Jones, J. Lessler, M.N. Demby, A.S. Azman); Republic of South Sudan Ministry of Health, Juba, South Sudan (P.N. Mawien, J. Rumunu, B.K. Bior, I.A. Jacob, R.L. Lako, L. Deng); Massachusetts General Hospital, Boston, Massachusetts, USA (D. Slater, S. Moheed, V. Sanchez, R. Mills, C. Fraser, R.C. Charles, J.B. Harris); International Organization for Migration, Juba (A. Caflisch); World Health Organization, Juba (A.G. Guyo, O.O. Olu, S. Maleghemi, A. Baguma, J.J. Hassen, S.K. Baya, J.F. Wamala); Kabale University School of Medicine, Kabale, Uganda (A. Baguma); Harvard Medical School, Boston (R.C. Charles, J.B. Harris); Médecins Sans Frontières, Geneva, Switzerland (A.S. Azman); Institute of Global Health, Geneva (A.S. Azman)

DOI: https://doi.org/10.3201/eid2706.210568

Globally, >100 million cases and >2.6 million deaths had been attributed to coronavirus disease (COVID-19) as of March 14, 2021 (*1*). Most cases have been reported in Europe and the Americas. In Africa, >2.9 million cases and ≈75,000 deaths have been reported (*1*). Reasons for the lower reported incidence and death associated with COVID-19 in Africa during the first 6–8 months of the pandemic are unclear but may include differences in age distribution, immune history, climate, early mitigation measures, and epidemiologic connectivity between geographic regions (*2*,*3*). However, our understanding of the true spread of severe acute respiratory virus coronavirus 2 (SARS-CoV-2) has been obscured by limited testing capabilities, underreported deaths, and undetected mild or asymptomatic infections (*4*). Population-based serological surveys, hundreds of which have been conducted worldwide, can help shed light on the extent of this underestimation of SARS-CoV-2 infections (*5*,*6*). As of March 18, 2021, only 16 studies published or available in preprint had been conducted in sub-Saharan Africa (*7*–*16*; H. Majiya et al., unpub. data, https://doi.org/10.1101/2020.08.04.20168112; B.N. Alemu et al., unpub. data, https://doi.org/10.1101/2020.10.13.337287; O. Ige et al., unpub. data, https://doi.org/10.1101/2020.11.24.20231324; I.M.O. Adetifa et al., unpub. data, https://doi.org/10.1101/2021.02.09.21251404; R. Lucindeet al.,

[1]A portion of this research was presented at the United States–Japan Cooperative Medical Sciences Program—Virtual Workshop on COVID-19, February 24–26, 2021.

[2]These authors contributed equally to this article.

[3]These authors contributed equally to this article.

unpub. data, https://doi.org/10.1101/2021.02.05.21250735; E.W. Kagucia et al., unpub. data, https://doi.org/10.1101/2021.02.12.21251294; M.J. Peluso et al., unpub. data, https://doi.org/10.1101/2021.03.03.21251639). Only 3 of those reports (from Nigeria, Ethiopia, and Zambia) were population-based representative studies. No serosurveys had been conducted in South Sudan.

South Sudan confirmed its first COVID-19 case in the capital, Juba, on April 4, 2020 (*17*), and saw its first wave of reported cases during May–July 2020 (Figure 1). By August 31, 2020, a total of 1,873 virologically confirmed SARS-CoV-2 infections (≈47/10,000 residents) had been reported from 18,156 reverse transcription PCR (RT-PCR) tests conducted in Juba. RT-PCR testing in South Sudan, including Juba, has remained limited because of scarce reagents, few testing sites, limited willingness to be tested, and logistic challenges. Thus, as in much of sub-Saharan Africa, the true extent of SARS-CoV-2 spread in the population remains unknown.

Understanding SARS-CoV-2 spread is particularly important for guiding COVID-19 mitigation efforts in light of South Sudan's complex humanitarian and public health context. South Sudan has experienced years of conflict, leading to 1.61 million internally displaced persons (IDP). Severe food insecurity affects more than half the population: 6 million people, including 1.3 million malnourished children (*18*,*19*). In Juba, 28.7% of households indicated that they were unable to access health care services when needed in the first 6 months of the pandemic; this number increased to 43.2% among residents in the lowest wealth quintile (*20*). These underlying vulnerabilities may increase risk of SARS-CoV-2 spread and may themselves be compounded by direct and indirect effects of the epidemic.

To estimate the seroprevalence of SARS-CoV-2 antibodies and associated risk factors in Juba, we conducted a representative household-based cross-sectional serosurvey. Here we present the results of this serosurvey and discuss the implications for SARS-CoV-2 surveillance in South Sudan, as well as more broadly for serologic studies conducted in Africa and worldwide.

Methods

Study Design and Participants

We conducted a cross-sectional serosurvey in residential neighborhoods of the city of Juba and Juba County according to protocols from the World Health Organization's Unity Studies (*5*). We determined urban demarcation based on residentially developed areas, local administrative boundaries, and existing transportation networks within the Northern Bari, Munuki, Juba, Kator, Rejaf, and Gondokoro payams (subcounty administrative divisions). Residents of Juba IDP camps I and III, former United Nations Mission in the Republic of South Sudan (UNMISS) civilian protection sites, were not included in the sampling frame.

The survey employed 2-stage cluster sampling. We used enumeration areas (EAs) as clusters and

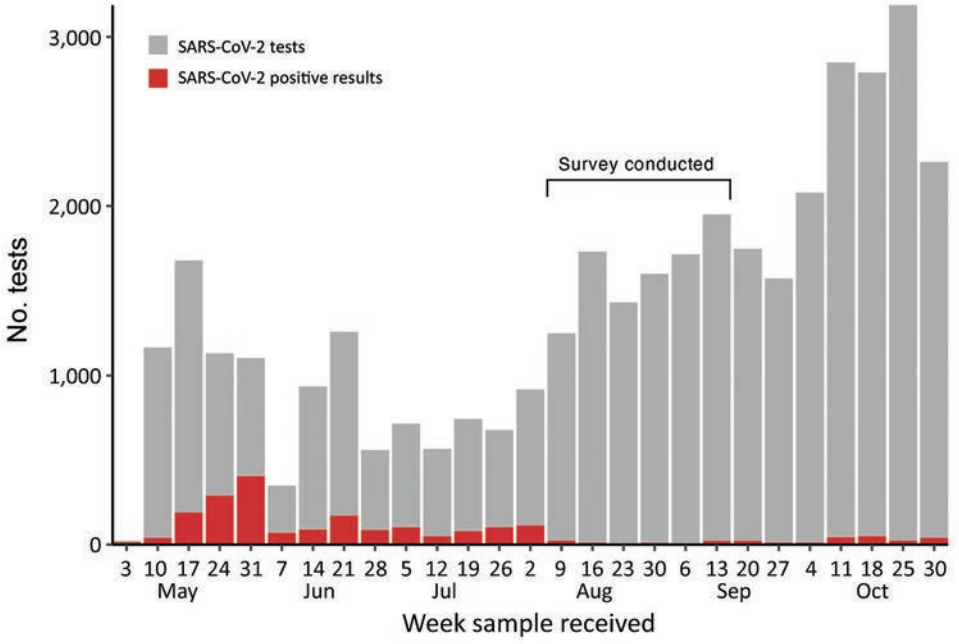

Figure 1. Number of weekly SARS-CoV-2 tests and infections reported in Juba, South Sudan, May 3–October 30, 2020. The survey of seroprevalence of SARS-CoV-2 IgG was conducted August 10–September 11. First coronavirus disease case in South Sudan was identified on April 2 and confirmed on April 4, 2020 (*23*). SARS-CoV-2, severe acute respiratory syndrome coronavirus 2.

selected them using probability proportional to size sampling. We calculated probabilities based on the number of structures in the EA found by satellite imagery; we removed nonresidential areas that were mapped by field teams during a preliminary assessment. Within each sampled EA, we randomly selected 11 residential structures as households to recruit into the study. The target sample size was 2,750 (50 clusters of 55 respondents each), but 11.1% of the original 550 households declined to participate. The main reasons reported were stigma, fear of testing positive, fear that the health worker taking the sample would infect the participant, and concern about samples being taken abroad for analysis. Alternate households were randomly sampled using the same procedure as for the original households. Three initially selected EAs, inhabited by families of military personnel, were inaccessible and therefore we replaced them by randomly sampling new EAs from the same stratum.

We defined a household as a group of persons who slept under the same roof most nights and shared a cooking pot. Regardless of current or past COVID-19 illness, all household members were eligible for inclusion if they or their guardian provided written consent to participate and they were ≥1 year of age and had lived in the area ≥1 week before the survey. For households with ≥10 persons, only first-degree relatives of the head of household were eligible for study inclusion. If multiple households lived in 1 shelter, we blindly drew from labeled papers to randomly select 1 household for inclusion.

We interviewed eligible participants to collect information about sociodemographic characteristics, history of respiratory symptoms, SARS-CoV-2 tests, exposure risks in the previous 2 weeks, and all household deaths. We collected dried blood samples by drawing blood by lancet from a finger, heel, or toe, and applying a few drops onto Whatman 903 (https://www.cytivalifesciences.com) or Ahlstrom grade 226 filter paper (https://www.ahlstrom-munksjo.com). The blood was allowed to thoroughly saturate the paper and air dry overnight at ambient temperature. We stored these dried blood spot (DBS) samples in low gas-permeable plastic bags with desiccant added to reduce humidity and transported the samples at ambient temperature to Massachusetts General Hospital (Boston, MA, USA) according to IATA protocol, where they were stored at 4°C until tested. The South Sudan Ministry of Health Ethics Review Board approved the study protocol.

Laboratory Analysis

DBS were eluted and tested for the presence of SARS-CoV-2 IgG targeting the receptor-binding domain (RBD) of the spike protein of SARS-CoV-2 using a quantitative ELISA previously developed and validated at Massachusetts General Hospital (*21*). The assay quantifies RBD-specific antibody concentrations using IgG-specific RBD monoclonal antibodies; the full protocols used for eluting DBS samples for the ELISA have been described (*22*). Validation of this test was originally based on PCR-positive infections and prepandemic samples from Boston. To determine an appropriate positivity threshold and assess assay specificity, we measured background antibody reactivity using 104 DBS samples collected in Juba in 2015 (*23*). We then selected a seropositivity threshold (0.32 μg/mL) that corresponded to 100% specificity in these prepandemic samples from Juba (i.e., their highest value; Appendix Figure 1, https://wwwnc.cdc.gov/EID/article/27/6/21-0568-App1.pdf) and 99.7% in the prepandemic samples collected from Boston.

Statistical Analysis

To estimate test sensitivity, we used data from a cohort of case-patients in Boston with mild and severe confirmed SARS-COV-2 infections whose antibody concentrations had been characterized at multiple time points after symptom onset (*21*) and supplemented these with recent data collected by DBS samples from nonhospitalized PCR-positive patients in Boston (Appendix Figure 2). On the basis of the trends in positive RT-PCR results in Juba, we assumed that most serosurvey participants, if previously infected, would have been exposed to SARS-CoV-2 at least 30 days before the survey (Figure 1) and restricted the positive-control data to observations >30 days after symptom onset during the follow-up period (Appendix Figure 2). Because infections with mild disease may lead to lower levels of detectable antibodies (M.J. Peluso et al., unpub. data, https://doi.org/10.1101/2021.03.03.21251639), we created synthetic cohorts of positive survey participants so that 80% of the sample had mild infections (defined as not needing hospitalization) and 20% had severe cases (defined as hospitalized, but excluding those that died), a proportion consistent with previous analyses (*24*,*25*) and the predominantly young population in Juba (*26*). From 1,000 resampled participants from positive control cohorts, we estimated an average test sensitivity of 65.5%. To evaluate the impact of our assumptions, we also performed sensitivity analyses testing a range of percentages for assumed mild cases (60%–100%) in the positive control dataset.

To estimate the seroprevalence (proportion of the population previously infected), we followed a

previously published Bayesian approach (*27*) using a regression model that accounted for age and sex of the study population integrated with a binomial model of the sensitivity and specificity of the ELISA. We selected a random sample from the 1,000 synthetic positive control datasets in each iteration of the model. This approach allowed us to adjust the estimates for test performance while propagating uncertainty around test performance in the adjusted estimates. We did not adjust the estimates for clustering within households because of challenges the field team faced in applying the strict household definition described above. We implemented the models in the Stan probabilistic programming language (https://mc-stan.org) (*28*) using the rstan package in R (https://cran.r-project.org). We poststratified our modeled results, accounting for the age distribution of urban populations in South Sudan (*26*) to generate population-representative seroprevalence estimates. Unless otherwise indicated, we reported estimates as the mean of the posterior samples and 95% credible intervals (CrI) as the 2.5th and 97.5th percentiles of this distribution.

In addition, we used the posterior draws for each regression coefficient to calculate by age and sex the relative risk of participants being seropositive. We used a log-binomial regression model to estimate the relative risk of being seropositive among nonworking adults compared with working adults, children, and students. We estimated implied infections by multiplying our estimated seroprevalence percentage by 510,000, Juba's estimated 2020 population size (*29*). We then estimated the ratio of reported to unreported infections by subtracting PCR-confirmed SARS-CoV-2 infections from total implied infections in Juba as of August 31, 2020, allowing for a roughly 2-week delay between infection and a seropositive result (*21*), and divided this estimate of unreported infections by the number of RT-PCR–confirmed SARS-CoV-2 infections. The analysis code we used is available online (https://github.com/HopkinsIDD/juba-sars-cov-2-serosurvey), and additional methods are provided (Appendix).

Results

We recruited a total of 2,214 participants 1–84 years of age from 435 households and provided DBS samples taken during August 10–September 11, 2020. We had complete interview and demographic data for 1,840 (83.2%) but were missing interview data for 374 because of data collection device failures or data entry issues. Of the 1,840 participants, 62.4% were female and 73.5% were 10–49 years of age (Table 1). Both figures were slightly higher than for those same measures from a previous population-representative malaria indicator survey conducted in South Sudan in 2017 (*26*). During April 1–September 11, 2020, a total of 23 deaths (10 male, 13 female) were reported for residents 1–78 years of age within 18 households. None of these deaths were associated with confirmed COVID-19, but 5 patients were reported to have had acute respiratory illness.

We found that 22.3% (494/2214) of samples collected during the survey were above the test positivity threshold, which we selected to have 100% specificity against prepandemic samples from Juba. After adjusting for test sensitivity, we estimated that seroprevalence was 38.3% (95% CrI 31.8%–46.5%) in August 2020. This estimate was based on samples from

Table 1. Characteristics of participants with interview data available (n = 1,840) from survey of seroprevalence of SARS-CoV-2 IgG in Juba, South Sudan*

Characteristic	No. (%)
Sex	
F	1,149 (62.4)
M	691 (37.6)
Age, y	
1–4	68 (3.7)
5–9	224 (12.2)
10–19	448 (24.3)
20–29	459 (24.9)
30–39	307 (16.7)
40–49	139 (7.6)
50–64	120 (6.5)
≥65	75 (4.1)
Payam	
Northern Bari	788 (42.8)
Juba	141 (7.7)
Muniki	397 (21.6)
Kator	229 (12.4)
Rejaf	135 (7.3)
Gondokoro	150 (8.2)
Occupation	
None	408 (22.2)
Child	386 (21.0)
Student	388 (21.1)
Market merchant	89 (4.8)
Healthcare worker	12 (0.7)
Taxi driver	16 (0.9)
Farmer	164 (8.9)
Working with animals	10 (0.5)
Civil servant	120 (6.5)
Health laboratory worker	2 (0.1)
Teacher	20 (1.1)
Traditional healer	1 (0.1)
Religious leader	8 (0.4)
Other	216 (11.7)
Reported test for SARS-CoV-2	
No	1816 (98.7)
Yes	22 (1.2)
Unknown	2 (0.1)
Reported SARS-CoV-2 test results	
Negative	15 (0.8)
Positive	5 (0.3)
Unknown	2 (0.1)

*SARS-CoV-2, severe acute respiratory syndrome coronavirus 2.

participants with matched interview data available. Seroprevalence in the full dataset was nearly indistinguishable from that in the age- and sex-matched dataset (Appendix Table 3), so we used the latter for all subsequent analyses. These results implied that, for each RT-PCR–confirmed SARS-CoV-2 infection tested by the end of August, 103 (95% CrI 86–126) SARS-CoV-2 infections were unreported.

We found no difference in the risk of seropositivity by sex (Table 2). Seroprevalence was highest at 44.9% (95% CrI 36.3%– 56.0%) among participants 10–19 years of age, a 36% higher risk of being seropositive than among participants 20–29 years of age (RR 1.36, 95% CrI 1.11–1.66) (Table 2). However, uncertainty intervals around seroprevalence estimates by age group were large. In addition, nonworking adults had 35% lower risk (RR 0.65, 95% confidence interval 0.50–0.82) of being seropositive compared to working adults, children, and students. Of the seropositive participants, only 5% reported having had a respiratory illness after April 1, 2020 (Appendix Tables 1, 2). We found no notable relationships between seropositivity and other potential SARS-CoV-2 risk factors (Appendix Table 1).

We examined potential sources of uncertainty in our estimates. We found higher background levels of antibody reactivity to the SARS-CoV-2 spike protein RBD in prepandemic samples from Juba compared to prepandemic samples from Boston (Appendix Figure 3) (*21*). Since serological measurements from PCR-confirmed cases in Juba were not available, we could not examine whether there were also differences in postinfection antibody dynamics between the populations. However, we were able to assess the impact that different assumptions about test sensitivity had on the results. If we assumed that 60% of infections in the population were mild, we estimated 35.5% (95% CrI 30.3%–41.4%) seroprevalence (Figure 2, panel A) and that, for each reported case, 96 (95% CrI 82–112) cases were unreported (Figure 2, panel B). In contrast, if we assumed that 100% of infections were mild, we estimated 45.9% (95% CrI 35.9%–61.0%) seroprevalence (Figure 2, panel A) and that, for each reported case, 124 (95% CrI 97–165) were unreported (Figure 2, panel B). Regardless of assumptions, these results indicated that 98%–99% of infections through September 2020 had been unreported.

Discussion

In this study, we estimated that one third of residents of Juba, South Sudan had been infected with SARS-CoV-2 through September 2020. That proportion corresponds to ≈196,000 implied infections, >100 times the number of PCR-confirmed SARS-COV-2 infections over the same time frame. These results reveal that in Juba, similar to in other sub-Saharan Africa populations, although the COVID-19 pandemic has had less apparent health impact than in other parts of the world, the virus has spread extensively.

Adjusting for imperfect immunoassay performance is critical when estimating infection attack rates from serosurveys. Postinfection antibody kinetics vary by infection severity, patient age, and prior exposure, as can test performance. When we tested prepandemic samples from Juba, we found that background SARS-CoV-2 antibody reactivity was higher in Juba than in Boston, which was consistent with findings from studies conducted in other sites in sub-Saharan Africa (*11*,*13*,*30*,*31*). We used these negative controls to estimate test specificity, but we lacked data on the post SARS-CoV-2 infection antibody kinetics and the proportion of infections that were mild or asymptomatic in the Juba population, which led to wide variation in plausible estimates of seroprevalence, as shown in our sensitivity analyses.

Table 2. Crude seropositivity, adjusted seroprevalence, and relative risk of seropositivity by age and sex from survey of seroprevalence of SARS-CoV-2 IgG in Juba, South Sudan.*

Category	No.	No. (%) positive	No. (%) negative	Seroprevalence (95% CrI)	Relative risk (95% CrI)
Overall	1,840	411 (22.3)	1,429 (77.7)	38.3 (31.8–46.5)	
Age, y					
1–4	68	20 (29.4)	48 (70.6)	43 (31.3–56.1)	1.30 (0.96–1.71)
5–9	224	52 (23.2)	172 (76.8)	39.3 (29.5–51.1)	1.19 (0.92–1.51)
10–19	448	124 (27.7)	324 (72.3)	44.9 (36.3–56)	1.36 (1.11–1.66)
20–29	459	89 (19.4)	370 (80.6)	33.3 (25.6–42)	Referent
30–39	307	52 (16.9)	255 (83.1)	30 (21.9–39.3)	0.91 (0.68–1.17)
40–49	139	26 (18.7)	113 (81.3)	33.2 (22.8–45.6)	1.00 (0.71–1.35)
50–64	120	31 (25.8)	89 (74.2)	42.8 (30.6–57.6)	1.29 (0.94–1.73)
65–84	75	17 (22.7)	58 (77.3)	38.8 (25.2–54.8)	1.17 (0.78–1.63)
Sex					
F	1,149	260 (22.6)	889 (77.4)	33.3 (25.6–42)	Referent
M	691	151 (21.9)	540 (78.1)	31.7 (23.6–41.2)	0.95 (0.81–1.12)

SARS-CoV-2, severe acute respiratory syndrome coronavirus 2.

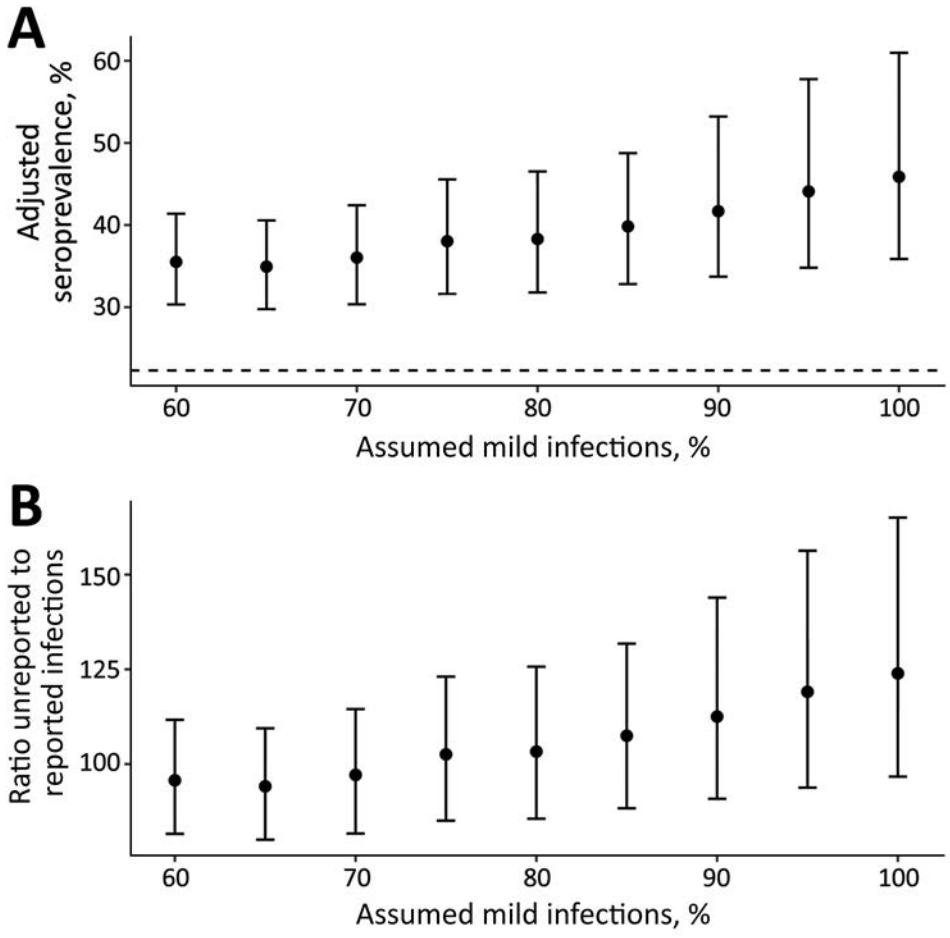

Figure 2. Effects of changing percentage of assumed mild cases in the population on adjusted seroprevalence of severe acute respiratory syndrome coronavirus 2 IgG in Juba, South Sudan. A) Mean adjusted seroprevalence; B) ratio of unreported to reported infections. Error bars represent 95% credible intervals. Dashed line in panel A represents unadjusted seropositivity at 22.3%. Unreported infections in panel B based on 1,873 confirmed coronavirus disease cases in Juba (as of August 31, 2020) and an approximate population of 510,000 in Juba. The *x*-axis in both panels indicates percentage of mild cases included in the synthetic positive control dataset used to estimate assay sensitivity.

Our findings have several implications for SARS-CoV-2 control in South Sudan. At least one third of the population in Juba has been exposed to the virus, and this proportion undoubtedly has increased since the survey was completed in September 2020. The low proportion of seropositive patients reporting respiratory symptoms suggests that the overwhelming majority of these infections were mild or asymptomatic. These estimates will help public health decision makers in South Sudan weigh the costs and benefits of devoting limited resources to COVID-19 mitigation at the cost of other crucial health programs.

One question we were unable to address was whether transmission occurred predominantly within households. However, crowded living conditions among Juba's urban population, including 31.3% of households living in 1- or 2-room shelters and 19.5% of households having ≥4 members sleeping in the same room, support this hypothesis (*20*). Another unanswered question is the extent to which SARS-CoV-2 spread and mitigation measures have exacerbated underlying vulnerabilities, including food insecurity, livelihoods, and co-infections, such as the current measles outbreak in South Sudan (*32*). Follow-up studies would be required to understand the larger impact of the epidemic in Juba as well as in the rest of South Sudan and to better inform public health policy.

These results also have implications for SARS-CoV-2 serosurveillance more broadly. Most serosurveys conducted to date, if they adjust seroprevalence estimates for test performance at all, use sensitivity and specificity estimates provided by assay manufacturers, which may be overly optimistic and based on a narrow range of samples (*6*). In many settings it may not be feasible to collect control data from local populations, but validating different immunoassays in populations in the same region of the world where the assays are being used is critical for appropriate interpretation of study results. Moreover, our findings support previous studies that have called for including mild and asymptomatic SARS-CoV-2 infections in assay validation datasets (*33*). We and others have shown that antibody titers from mild and

asymptomatic infections tend to be lower (*34*–*39*). Thus, validation datasets comprised predominantly of data from severe, hospitalized cases may lead to overestimating assay sensitivity and gross underestimation of SARS-CoV-2 seroprevalence (*33*).

Overall, the SARS-CoV-2 seroprevalence estimates reported in this study are comparable to estimates in Nigeria of 25%–45%, depending on the population sampled (*8*,*10*; H. Majiya et al., unpub. data, https://doi.org/10.1101/2020.08.04.2016811 2). Similarly, seroprevalence was 40% in public sector patients in Cape Town, South Africa (*14*), 12.3% among asymptomatic healthcare workers in Blantyre, Malawi (*12*), and 25.1% among gold mine workers in Côte d'Ivoire (*15*). In Addis Ababa, Ethiopia, seroprevalence among those reporting no close contact with SARS-CoV-2 infected persons was 8.8% in April 2020 (B.N. Alemu et al., unpub. data, https://doi.org/10.1101/2020.10.13.337287). Seroprevalence was lower at 4.3% in blood donors in Kenya in June 2020 (*7*), increasing to 9.1% by September (I.M.O. Adetifa et al., unpub. data, https://doi.org/10.1101/2021.02.09.21251404), and was 10.6% in 6 districts in Zambia in July 2020 (*16*). These lower estimates may be due to differences in SARS-CoV-2 epidemiology, time periods included, or subpopulations measured. Serologic tests may themselves contribute to differences. A study in Kinshasa, Democratic Republic of the Congo, showed that seropositivity in health facility staff was 8%–36% depending on the serological test used (*13*). Nevertheless, findings from these studies taken together indicate that SARS-CoV-2 has spread widely in sub-Saharan Africa (*2*,*3*). This conclusion is supported by a postmortem study in Lusaka, Zambia, which found that among 372 deceased patients, 19.2% were PCR-positive for SARS-CoV-2 (*40*).

One of the limitations of our study is that, as we have described, our positive control datcame from a cohort in Boston. Therefore, despite our efforts to correct for differences between the populations, we do not know how accurate our sensitivity estimates are for Juba or elsewhere in Africa. In addition, we used a single ELISA that measured IgG targeting the RBD of SARS-CoV-2's spike protein. Previous studies have shown variation in sensitivity and specificity of antibody assays that target different antigens (*13*,*41*), suggesting that testing for multiple antigens may provide a better picture of seroprevalence than those targeting a single antigen alone, particularly when validation data are not available from the local population. Although the study had a standard definition for households, the study team faced challenges in following this strict definition; as a result, we were unable to confidently estimate the degree to which SARS-CoV-2 infections clustered within households, nor could we adjust for these variations in the regression model. This difficulty also prevented us from calculating mortality rates based on reported household deaths. Finally, whereas this study was representative of the residential neighborhoods of Juba, the sample did not include an estimated >30,000 IDPs living in 2 camps in Juba (*42*). Nevertheless, 14.3% of households participating in the study self-reported as IDPs, either living in the host community or at another IDP site.

Our study's strengths include that it is one of few population-based seroprevalence studies conducted in and representative of the general population of a city or other geographic region within sub-Saharan Africa. Furthermore, we used specificity estimates based on background antibody levels specific to the local population, adjusted seroprevalence estimates based on test results, and propagated uncertainty around test performance into our final estimates. Because the ELISA we used was quantitative, we reported antibody distributions rather than seropositivity cutoffs alone (Appendix Figure 1). As a result, it would be possible to adjust our estimates further if more accurate sensitivity data become available for this population.

In conclusion, we present evidence that SARS-CoV-2 seroprevalence is much higher in Juba than suggested by confirmed case data alone, which is consistent with findings from other recent serosurveys in sub-Saharan Africa. Future serosurveys in South Sudan will be helpful to confirm these findings and to examine the effect that SARS-CoV-2 spread has had on underlying vulnerabilities. Such seroprevalence studies are needed to understand the impact of the pandemic more broadly in Africa, as well as the ways to most effectively mitigate its effects. For these efforts to be most effective, however, they must be accompanied by efforts to validate serologic tests in local populations.

Acknowledgements

We thank Sebastian Ancavil, Dessalegn Gurmessa, Manahil Qureshi, Susan Atala, Zerihun Zewdie Hurissa, and other colleagues from the Displacement Tracking Matrix unit of the International Organization for Migration (IOM) in South Sudan for their work in support of this study.

This work was supported by the World Health Organization's (WHO) Unity Studies, a global seroepidemiologic standardization initiative, with funding provided to WHO by the COVID-19 Solidarity Response

Fund and the German Federal Ministry of Health COVID-19 Research and Development Fund. This study was also supported by the African Development Bank Fund, in addition to funding from the US National Institutes of Health (R01 AI135115 to A.S.A. and K.E.W.) and the US Centers for Disease Control and Prevention (U01CK000490 to R.C.C. and J.B.H.). IOM's contribution to the study was supported by funding from the European Civil Protection and Humanitarian Aid Operations, the US Office of Foreign Disaster Assistance, the UK Foreign, Commonwealth and Development Office, the German Federal Foreign Office, and Canada's Department of Foreign Affairs, Trade and Development.

About the author

Dr. Wiens is a postdoctoral fellow in the Department of Epidemiology at the Johns Hopkins Bloomberg School of Public Health. Her research interests include seroepidemiology and infectious disease dynamics and control.

References

1. World Health Organization. Weekly epidemiological update: 16 March 2021 [cited 2021 Mar 18]. https://www.who.int/publications/m/item/weekly-epidemiological-update---16-march-2021
2. Rice BL, Annapragada A, Baker RE, Bruijning M, Dotse-Gborgbortsi W, Mensah K, et al. Variation in SARS-CoV-2 outbreaks across sub-Saharan Africa. Nat Med. 2021;27:447–53. https://doi.org/10.1038/s41591-021-01234-8
3. Mbow M, Lell B, Jochems SP, Cisse B, Mboup S, Dewals BG, et al. COVID-19 in Africa: Dampening the storm? Science. 2020;369:624–6. https://doi.org/10.1126/science.abd3902
4. Chitungo I, Dzobo M, Hlongwa M, Dzinamarira T. COVID-19: unpacking the low number of cases in Africa. Public Health in Practice. 2020;1:100038. https://doi.org/10.1016/j.puhip.2020.100038
5. World Health Organization. Population-based age-stratified seroepidemiological investigation protocol for coronavirus 2019 (COVID-19) infection [cited 2021 Feb 11]. https://www.who.int/publications-detail-redirect/WHO-2019-nCoV-Seroepidemiology-2020.2
6. Chen X, Chen Z, Azman AS, Deng X, Sun R, Zhao Z, et al. Serological evidence of human infection with SARS-CoV-2: a systematic review and meta-analysis. Lancet Glob Health. 2021 Mar 8 [Epub ahead of print]. https://doi.org/10.1016/S2214-109X(21)00026-7 PMID: 33705690
7. Uyoga S, Adetifa IMO, Karanja HK, Nyagwange J, Tuju J, Wanjiku P, et al. Seroprevalence of anti-SARS-CoV-2 IgG antibodies in Kenyan blood donors. Science. 2021;371:79–82. https://doi.org/10.1126/science.abe1916
8. Olayanju O, Bamidele O, Edem F, Eseile B, Amoo A, Nwaokenye J, et al. SARS-CoV-2 seropositivity in asymptomatic frontline health workers in Ibadan, Nigeria. Am J Trop Med Hyg. 2021;104:91–4. https://doi.org/10.4269/ajtmh.20-1235
9. Halatoko WA, Konu YR, Gbeasor-Komlanvi FA, Sadio AJ, Tchankoni MK, Komlanvi KS, et al. Prevalence of SARS-CoV-2 among high-risk populations in Lomé (Togo) in 2020. PLoS One. 2020;15:e0242124. https://doi.org/10.1371/journal.pone.0242124
10. Asuquo MI, Effa E, Otu A, Ita O, Udoh U, Umoh V, et al. Prevalence of IgG and IgM antibodies to SARS-CoV-2 among clinic staff and patients. Eur J Immunol. 2020;50:2025–40.
11. Yadouleton A, Sander A-L, Moreira-Soto A, Tchibozo C, Hounkanrin G, Badou Y, et al. Limited specificity of serologic tests for SARS-CoV-2 antibody detection, Benin. Emerg Infect Dis. 2021;27:233–7. https://doi.org/10.3201/eid2701.203281
12. Chibwana MG, Jere KC, Kamn'gona R, Mandolo J, Katunga-Phiri V, Tembo D, et al. High SARS-CoV-2 seroprevalence in health care workers but relatively low numbers of deaths in urban Malawi. Wellcome Open Res. 2020;5:199. https://doi.org/10.12688/wellcomeopenres.16188.2
13. Ndaye AN, Hoxha A, Madinga J, Mariën J, Peeters M, Leendertz FH, et al. Challenges in interpreting SARS-CoV-2 serological results in African countries. Lancet Glob Health. 2021;9:e588–9. https://doi.org/10.1016/S2214-109X(21)00060-7 PMID: 33609481
14. Hsiao M, Davies M-A, Kalk E, Hardie D, Naidoo M, Centner C, et al. SARS-CoV-2 seroprevalence in the Cape Town metropolitan sub-districts after the peak of infections. COVID-19 Special Public Health Surveillance Bulletin. 2020;18(Suppl 5):1–9. Johannesburg (South Africa): National Institute for Communicable Diseases; 2021 [cited 2021 Mar 2]. https://www.nicd.ac.za/wp-content/uploads/2020/09/COVID-19-Special-Public-Health-Surveillance-Bulletin_Issue-5.pdf
15. Milleliri JM, Coulibaly D, Nyobe B, Rey J-L, Lamontagne F, Hocqueloux L, et al. SARS-CoV-2 infection in Ivory Coast: a serosurveillance survey among gold mine workers. Am J Trop Med Hyg. 2021 Mar 18 [Epub ahead of print]. https://doi.org/10.4269/ajtmh.21-0081
16. Mulenga LB, Hines JZ, Fwoloshi S, Chirwa L, Siwingwa M, Yingst S, et al. Prevalence of SARS-CoV-2 in six districts in Zambia in July, 2020: a cross-sectional cluster sample survey. Lancet Glob Health. 2021 Mar 9 [Epub ahead of print]. https://doi.org/10.1016/S2214-109X(21)00053-X
17. World Health Organization. South Sudan. South Sudan confirms first case of COVID-19 [cited 2021 Feb 23]. https://www.afro.who.int/news/south-sudan-confirms-first-case-covid-19
18. Integrated Food Security Phase Classification. South Sudan: IPC results October 2020–July 2021 [cited 2021 Mar 4]. http://www.ipcinfo.org/ipcinfo-website/alerts-archive/issue-31
19. International Organization for Migration Data Tracking Matrix. South Sudan—mobility tracking round 9 initial findings [cited 2021 Mar 4]. https://displacement.iom.int/reports/south-sudan-%E2%80%94-mobility-tracking-round-9-initial-findings
20. International Organization for Migration, World Food Programme. Urban multi-sector needs, vulnerabilities and COVID-19 impact survey (FSNMS+): Juba Town [cited 2021 Mar 4]. https://migration.iom.int/reports/south-sudan-%E2%80%94-urban-multi-sector-needs-vulnerabilities-and-covid-19-impact-survey-fsnms-%E2%80%94
21. Iyer AS, Jones FK, Nodoushani A, Kelly M, Becker M, Slater D, et al. Persistence and decay of human antibody responses to the receptor binding domain of SARS-CoV-2 spike protein in COVID-19 patients. Sci Immunol. 2020;5:eabe0367. https://doi.org/10.1126/sciimmunol.abe0367
22. Slater DM. Preparation of elutions from dried blood spots for ELISAs [cited 2021 Mar 2]. https://www.protocols.io/

view/preparation-of-elutions-from-dried-blood-spots-for-bsrnnd5e
23. Iyer AS, Azman AS, Bouhenia M, Deng LO, Anderson CP, Graves M, et al. Dried blood spots for measuring Vibrio cholerae-specific immune responses. PLoS Negl Trop Dis. 2018;12:e0006196. https://doi.org/10.1371/journal.pntd.0006196
24. Huang C, Wang Y, Li X, Ren L, Zhao J, Hu Y, et al. Clinical features of patients infected with 2019 novel coronavirus in Wuhan, China. Lancet. 2020;395:497–506. https://doi.org/10.1016/S0140-6736(20)30183-5
25. Xu Z, Shi L, Wang Y, Zhang J, Huang L, Zhang C, et al. Pathological findings of COVID-19 associated with acute respiratory distress syndrome. Lancet Respir Med. 2020;8:420–2. https://doi.org/10.1016/S2213-2600(20)30076-X
26. Republic of South Sudan Ministry of Health. Malaria indicator survey 2017: final report. 2019 [cited 2021 Feb 22]. https://www.malariasurveys.org/documents/SSMIS%202017%20final%20report%202019%2005%2020_signed%20(1).pdf
27. Stringhini S, Wisniak A, Piumatti G, Azman AS, Lauer SA, Baysson H, et al. Seroprevalence of anti-SARS-CoV-2 IgG antibodies in Geneva, Switzerland (SEROCoV-POP): a population-based study. Lancet. 2020;396:313–9. https://doi.org/10.1016/S0140-6736(20)31304-0
28. Carpenter B, Gelman A, Hoffman MD, Lee D, Goodrich B, Betancourt M, et al. Stan: a probabilistic programming language. J Stat Softw. 2017;76:1–32. https://doi.org/10.18637/jss.v076.i01
29. United Nations Office for the Coordination of Humanitarian Affairs, Integrated Food Security Phase Classification Technical Working Group, South Sudan National Bureau of Standards. South Sudan total population by county. 2020 [cited 2021 Mar 2]. https://www.humanitarianresponse.info/sites/www.humanitarianresponse.info/files/documents/files/ss_total_population_by_county_map_a4_20201116.pdf
30. Tso FY, Lidenge SJ, Peña PB, Clegg AA, Ngowi JR, Mwaiselage J, et al. High prevalence of pre-existing serological cross-reactivity against severe acute respiratory syndrome coronavirus-2 (SARS-CoV-2) in sub-Saharan Africa. Int J Infect Dis. 2021;102:577–83. https://doi.org/10.1016/j.ijid.2020.10.104
31. Emmerich P, Murawski C, Ehmen C, von Possel R, Pekarek N, Oestereich L, et al. Limited specificity of commercially available SARS-CoV-2 IgG ELISAs in serum samples of African origin. Trop Med Int Health. 2021 Mar 5 [Epub ahead of print]. 10.1111/tmi.13569 https://doi.org/10.1111/tmi.13569
32. World Health Organization. South Sudan. South Sudan launches a nationwide campaign to protect 2.5 million children against measles [cited 2021 Mar 2]. https://www.afro.who.int/news/south-sudan-launches-nationwide-campaign-protect-25-million-children-against-measles
33. Takahashi S, Greenhouse B, Rodríguez-Barraquer I. Are seroprevalence estimates for severe acute respiratory syndrome coronavirus 2 biased? J Infect Dis. 2020;222:1772–5. https://doi.org/10.1093/infdis/jiaa523
34. Kutsuna S, Asai Y, Matsunaga A. Loss of anti–SARS-CoV-2 antibodies in mild COVID-19. N Engl J Med. 2020;383:1695–6.
35. Shirin T, Bhuiyan TR, Charles RC, Amin S, Bhuiyan I, Kawser Z, et al. Antibody responses after COVID-19 infection in patients who are mildly symptomatic or asymptomatic in Bangladesh. Int J Infect Dis. 2020;101:220–5. https://doi.org/10.1016/j.ijid.2020.09.1484
36. Choe PG, Kim K-H, Kang CK, Suh HJ, Kang E, Lee SY, et al. Antibody responses 8 months after asymptomatic or mild SARS-CoV-2 infection. Emerg Infect Dis. 2021;27:928–31. https://doi.org/10.3201/eid2703.204543
37. Cervia C, Nilsson J, Zurbuchen Y, Valaperti A, Schreiner J, Wolfensberger A, et al. Systemic and mucosal antibody responses specific to SARS-CoV-2 during mild versus severe COVID-19. J Allergy Clin Immunol. 2021;147:545–557.e9. https://doi.org/10.1016/j.jaci.2020.10.040
38. Long Q-X, Tang X-J, Shi Q-L, Li Q, Deng H-J, Yuan J, et al. Clinical and immunological assessment of asymptomatic SARS-CoV-2 infections. Nat Med. 2020;26:1200–4. https://doi.org/10.1038/s41591-020-0965-6
39. Lynch KL, Whitman JD, Lacanienta NP, Beckerdite EW, Kastner SA, Shy BR, et al. Magnitude and kinetics of anti-SARS-CoV-2 antibody responses and their relationship to disease severity. Clin Infect Dis. 2020;72:301–8. https://doi.org/10.1093/cid/ciaa979
40. Mwananyanda L, Gill CJ, MacLeod W, Kwenda G, Pieciak R, Mupila Z, et al. Covid-19 deaths in Africa: prospective systematic postmortem surveillance study. BMJ. 2021;372:n334. https://doi.org/10.1136/bmj.n334
41. Oved K, Olmer L, Shemer-Avni Y, Wolf T, Supino-Rosin L, Prajgrod G, et al. Multi-center nationwide comparison of seven serology assays reveals a SARS-CoV-2 non-responding seronegative subpopulation. EClinicalMedicine. 2020;29:100651. https://doi.org/10.1016/j.eclinm.2020.100651
42. International Organization for Migration Data Tracking Matrix. Biometric registration. 2021 [cited 2021 Mar 4]. https://displacement.iom.int/component/biometric-registration

Address for correspondence: Andrew S. Azman, Johns Hopkins Bloomberg School of Public Health–Epidemiology, 615 N Wolfe St, E6003, Baltimore, MD 21205, USA; email: azman@jhu.edu

HIV Infection as Risk Factor for Death among Hospitalized Persons with Candidemia, South Africa, 2012–2017

Nelesh P. Govender, Jim Todd, Jeremy Nel, Mervyn Mer, Alan Karstaedt, Cheryl Cohen, for GERMS-SA[1]

Medscape EDUCATION ACTIVITY

In support of improving patient care, this activity has been planned and implemented by Medscape, LLC and Emerging Infectious Diseases. Medscape, LLC is jointly accredited by the Accreditation Council for Continuing Medical Education (ACCME), the Accreditation Council for Pharmacy Education (ACPE), and the American Nurses Credentialing Center (ANCC), to provide continuing education for the healthcare team.

Medscape, LLC designates this Journal-based CME activity for a maximum of 1.00 ***AMA PRA Category 1 Credit(s)™***. Physicians should claim only the credit commensurate with the extent of their participation in the activity.

Successful completion of this CME activity, which includes participation in the evaluation component, enables the participant to earn up to 1.0 MOC points in the American Board of Internal Medicine's (ABIM) Maintenance of Certification (MOC) program. Participants will earn MOC points equivalent to the amount of CME credits claimed for the activity. It is the CME activity provider's responsibility to submit participant completion information to ACCME for the purpose of granting ABIM MOC credit.

All other clinicians completing this activity will be issued a certificate of participation. To participate in this journal CME activity: (1) review the learning objectives and author disclosures; (2) study the education content; (3) take the post-test with a 75% minimum passing score and complete the evaluation at http://www.medscape.org/journal/eid; and (4) view/print certificate. For CME questions, see page 1767.

Release date: May 19, 2021; Expiration date: May 19, 2022

Learning Objectives

Upon completion of this activity, participants will be able to:

- Describe the effect of HIV infection and other factors on mortality risk from candidemia, according to an analysis of data from a 6-year sentinel surveillance study in South Africa
- Determine the association of intensive care unit admission with mortality risk among adults with HIV infection and candidemia, according to an analysis of data from a 6-year sentinel surveillance study in South Africa
- Identify clinical implications of the effect of HIV infection on mortality risk from candidemia, according to an analysis of data from a 6-year sentinel surveillance study in South Africa

CME Editor

Jill Russell, BA, Copyeditor, Emerging Infectious Diseases. *Disclosure: Jill Russell, BA, has disclosed no relevant financial relationships.*

CME Author

Laurie Barclay, MD, freelance writer and reviewer, Medscape, LLC. *Disclosure: Laurie Barclay, MD, has disclosed no relevant financial relationships.*

Authors

Disclosures: ***Nelesh P. Govender, MBBCh, MMed, MSc Epi, MSc Mycol; Jim Todd, BA, MSc;*** *and* ***Alan Karstaedt, MBBCh,*** *have disclosed no relevant financial relationships.* ***Jeremy Nel, MBChB,*** *has disclosed the following relevant financial relationships: served as an advisor or consultant for Cipla Inc.; Johnson & Johnson Pharmaceuticals Research & Development, L.L.C.; Mylan Laboratories Inc.; served as a speaker or a member of a speakers bureau for AbbVieInc.* ***Mervyn Mer, MD, PhD,*** *has disclosed the following relevant financial relationships: served as a speaker or a member of a speakers bureau for Pfizer Inc.; Sanofi Aventis.* ***Cheryl Cohen, MD, PhD,*** *has disclosed the following relevant financial relationships: received grants for clinical research from Sanofi Pasteur.*

Author affiliations: University of Cape Town, Cape Town, South Africa (N.P. Govender); University of the Witwatersrand, Johannesburg (N.P. Govender, J. Nel, M. Mer, A. Karstaedt, C. Cohen); National Institute for Communicable Diseases,a Division of the National Health Laboratory Service, Johannesburg, South Africa (N.P. Govender, C. Cohen); London School of Hygiene and Tropical Medicine, London, UK (J. Todd)

DOI: https://doi.org/10.3201/eid2706.210128

[1]Members of GERMS-SA are listed at the end of this article.

We determined the effect of HIV infection on deaths among persons ≥18 months of age with culture-confirmed candidemia at 29 sentinel hospitals in South Africa during 2012–2017. Of 1,040 case-patients with documented HIV status and in-hospital survival data, 426 (41%) were HIV-seropositive. The in-hospital case-fatality rate was 54% (228/426) for HIV-seropositive participants and 37% (230/614) for HIV-seronegative participants (crude odds ratio [OR] 1.92, 95% CI 1.50–2.47; p<0.001). After adjusting for relevant confounders (n = 907), mortality rates were 1.89 (95% CI 1.38–2.60) times higher among HIV-seropositive participants than HIV-seronegative participants (p<0.001). Compared with HIV-seronegative persons, the stratum-specific adjusted mortality OR was higher among HIV-seropositive persons not managed in intensive care units (OR 2.27, 95% CI 1.47–3.52; p<0.001) than among persons who were (OR 1.56, 95% CI 1.00–2.43; p = 0.05). Outcomes among HIV-seropositive persons with candidemia might be improved with intensive care.

Candida is a common cause of healthcare-associated bloodstream infections in South Africa; the estimated national incidence risk in 2016–2017 was 84 (95% CI 81–86) cases per 100,000 hospital admissions (*1*). This rate is ≈10-fold higher than that reported in the United States (*2*). The death rate among patients with *Candida* bloodstream infections is high and associated with such factors as confirmed or presumed gastrointestinal source of infection, lack of source control, shorter time to positivity of blood cultures, inappropriate or delayed empiric antifungal treatment, lack of consultation with an infectious disease physician, severe sepsis or septic shock, and severity of underlying conditions (*3*–*5*). The crude mortality rate associated with candidemia was 43% in South Africa in 2016–2017 (*1*). In 2 small case series of HIV-seropositive patients with candidemia (Spain, n = 37; Italy, n = 38), the crude mortality rate was ≈60% (*6*,*7*). HIV infection may be a risk factor for death among persons with culture-confirmed candidemia. In a 2014 population-based surveillance study in Spain, 16 (2%) of 752 patients with candidemia were HIV-seropositive (*8*). Although HIV infection was not associated with death on univariable analysis (OR 0.51, 95% CI 0.07–3.93), the study was underpowered. In contrast, in a United States cohort study of 446 adults with candidemia, 22 (5%) were HIV-seropositive, and HIV infection was associated with a 2-fold increased adjusted hazard of 30-day mortality (hazard ratio 2.02, 95% CI 1.11–3.72) (*9*). This effect of HIV infection on death rates may be mediated by factors related to the host (e.g., neutropenia or neutrophil dysfunction in persons with advanced HIV disease) or the fungal pathogen (infection caused by *Candida* species other than *C. albicans* or by >1 *Candida* spp.) (*6*,*7*,*10*–*12*). Such an association has not been described in a high HIV prevalence setting. By using data from a 6-year sentinel surveillance study at hospitals in South Africa, we examined the effect of HIV infection on the risk for 30-day mortality among persons with candidemia.

Materials and Methods

Study Population

We included persons ≥18 months of age with an episode of culture-confirmed candidemia identified at 29 sentinel hospitals in South Africa during January 1, 2012–December 31, 2017. The HIV prevalence among inpatients is high at these large urban tertiary-academic or regional acute-care hospitals (e.g., 60% at a Cape Town district hospital in 2012–2013) (*13*). A case was defined as illness in a person in whom *Candida* spp. was cultured from blood at a laboratory providing diagnostic pathology services to a sentinel hospital. An episode was defined as a 30-day period from the date of the first positive *Candida* culture. Any positive blood cultures after this period defined a recurrent episode and thus a new case. We excluded children <18 months of age because we did not have HIV PCR results to confirm an HIV diagnosis for a sufficient number of persons.

Surveillance Methods

Cases were reported from public-sector and private-sector pathology laboratories. In general, blood cultures were collected if patients had clinical features of sepsis, including tachycardia, tachypnea, increased or subnormal temperature, a change in sensorium, hypotension, or prostration (*14*). Viable *Candida* isolates were submitted to a reference laboratory for species-level identification and antifungal susceptibility testing, as previously described (*1*). Trained nurses or pharmacists identified culture-confirmed cases in the laboratory and interviewed prospectively enrolled participants or their next of kin or reviewed medical charts or electronic laboratory records. Data were collected through a standardized case report form. The main explanatory variable was the participant's HIV infection status, which was determined during the admission for candidemia. HIV status was self-reported during participant interviews or abstracted from the inpatient chart, a child's outpatient immunization card, or laboratory records. An in-hospital outcome with a date of outcome was determined at the end of admission to the acute-care hospital or if

the participant was transferred to a step-down facility; this outcome was determined at the end of that admission. Outcome was recorded as alive at 30 days for prolonged admissions of >30 days after first positive blood culture. Underlying or immediate cause of death was not recorded. Surveillance officers recorded whether a person had been admitted to the intensive care unit (ICU) at any time during hospitalization, but the specific reason for and dates of ICU admission or discharge were not captured. We calculated a quick Pitt score, an abbreviated version of the Pitt bacteremia score, as the sum of individual scores for body temperature of <35°C (1 point), systolic blood pressure of <90 mm Hg (1 point), cardiac arrest (1 point), mechanical ventilation (1 point), and altered mental status (1 point) on the day of candidemia diagnosis (*15*,*16*).

Data Analysis

We used participant identifiers to remove duplicate records. We described the characteristics of the study participants by using descriptive statistics. To determine risk factors for death, we used classical Mantel-Haenszel methods to calculate crude case fatality ratio, odds ratio (OR), and 95% CI for HIV status and each of the potential confounders (Appendix, https://wwwnc.cdc.gov/EID/article/27/5/21-0128-App1.pdf). We did not assume that individual participant-level outcomes were statistically independent in this sentinel surveillance study. We therefore used a random-effects logistic regression analysis to explicitly model between-cluster variation at sentinel sites and simultaneously adjust for participant-level confounders (*17*) (Appendix). We treated the follow-up period as a fixed 30-day period. We also explored the dose-response effect of HIV on death rates. For this analysis, participants' HIV infection status was recoded as an ordinal variable: HIV-seronegative, HIV-seropositive without advanced immunosuppression (CD4 count ≥200 cells/μL), and HIV-seropositive with advanced immunosuppression (CD4 count <200 cells/μL). Before conducting the analysis, we hypothesized that the effect of HIV infection on death rates would differ among participants with candidemia managed in an ICU and those who were not admitted to an ICU; therefore, we considered ICU admission as an effect modifier a priori. We included participants with recorded dates of positive *Candida* specimen collection and 30-day outcome in a Kaplan-Meier survival analysis. For 67 participants with an outcome date that coincided exactly with the specimen collection date, we recoded their time-to-outcome to 0.5 days. We explored the association between HIV status and ICU admission by classical and multivariable random effects logistic regression analyses as a post-hoc analysis to explore reasons for the main results.

Ethics

For GERMS-SA surveillance, annual ethics approvals were sought and obtained from several university ethics committees in South Africa. We also obtained approval from the London School of Hygiene and Tropical Medicine Research Ethics Committee.

Results

After deduplication, 8,668 cases were detected by GERMS-SA surveillance during the 6-year period. We excluded 3,643 cases diagnosed at non–sentinel sites and 2,462 cases among infants and children <18 months of age. Of 2,563 cases diagnosed at sentinel sites, a case report form had been completed for 1,846 (72%) (Figure 1). Of those, we retained 1,040 cases with both HIV status and outcome data (56%). We noted differences in age, sex, year of diagnosis, province in which the diagnosis was made, and *Candida* species among 717 sentinel-site cases with missing case report forms, 806 cases with completed case report forms but missing HIV status or outcome data, and the 1,040 cases included in the final analysis (Appendix Table 1).

Description of 1,040 Participants Included in the Analysis

Of 1,040 participants, 542 (52%) were men and boys (Table 1, https://wwwnc.cdc.gov/EID/article/27/6/21-0128-T1.htm). The median age of 1,037 participants with recorded age was 37 years (interquartile range [IQR] 23–52 years). Of 1,035 participants with available date of specimen collection, 288 (28%) had a positive *Candida* blood culture within 72 hours of hospital admission. Overall, 50% (514/1,023) participants were managed in the ICU during their hospitalization (data on ICU admission were missing for 17 participants). At the time of diagnosis, most (545/1,011, 54%) had a central venous catheter (CVC) in situ, and 24% (245/1,004) were receiving total parenteral nutrition. Of 1,001 participants for whom data was available, 163 (16%) received previous antifungal treatment. A quick Pitt score was calculated for 652/1,040 participants: 319 (49%) had a 0 score, 184 (28%) had a 1 score, 126 (19%) had a 2 score, 20 (3%) had a 3 score, and 3 (1%) had a 4 score (Appendix). Thus, 149/652 (23%) had a quick Pitt score of ≥2. Of 946 case-patients in which *Candida* species identification was performed at a diagnostic or reference laboratory, 521 (55%) participants were infected with a *Candida* species other than *C. albicans* and

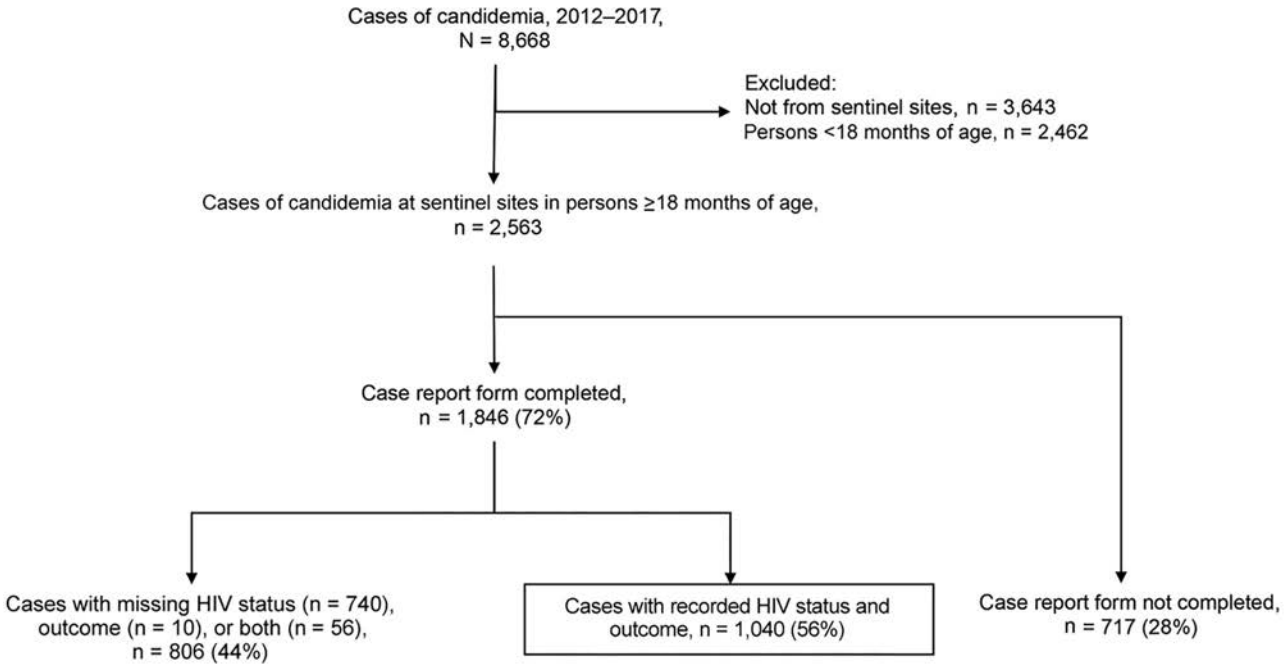

Figure 1. Flowchart demonstrating selection of 1,040 cases of candidemia from a 6-year surveillance period for secondary data analysis, South Africa, 2012–2017.

the remainder with *C. albicans*; 33 (3%) case-patients had a mixed *Candida* infection. Of 1,010 cases, 700 (69%) received systemic antifungal treatment to treat candidemia (participants might have received ≥1 antifungal agent: fluconazole [n = 503], amphotericin B [n = 265], echinocandin [n = 91], or voriconazole [n = 17]). Of 764 cases with a known *Candida* species, available antifungal susceptibility data, and applicable Clinical and Laboratory Standards Institute breakpoints (*18*), 154 (20%) were infected with an antifungal-resistant species. Of these 764, antifungal treatment was recorded for 419, and 9% (38/419) had received inappropriate antifungal treatment. Of 488 cases with recorded information, 361 (74%) had their CVC removed after the candidemia diagnosis. In 4% of patients (45/1,040), evidence of complications of candidemia (deep organ involvement) was indicated in medical charts.

HIV Status and Outcome

Of the 1,040 case-patients, 426 (41%) were HIV-seropositive; we noted several differences in those patients compared with those who were HIV-seronegative (Table 1; Appendix). Among 404 HIV-seropositive persons with available data, 301 (75%) were antiretroviral treatment–experienced. Among 267 participants in whom CD4 count was recorded near the date of the candidemia diagnosis, the median CD4 count was 133 (IQR 42–309) cells/μL; 166/267 (63%) had a CD4 count <200 cells/μL. An additional 35 without a CD4 count had a recorded World Health Organization (WHO) clinical stage of HIV disease. Of these 35 case-patients, illness was WHO stage 3 or 4 in 33 case-patients. Of 141 whose records indicated a recently recorded viral load, 65 (46%) had a viral load of <400 RNA copies/mL. Of the 426 HIV-seropositive persons, 153 (36%) had clinical evidence of HIV-associated wasting. The overall case fatality ratio was 458/1,040 (44%). The case-fatality ratio among HIV-seronegative cases was 37% (230/614) versus 54% (228/426) for HIV-seropositive cases (p<0.001).

Risk Factors for 30-Day Mortality

The crude 30-day case fatality ratio among HIV-seropositive participants was 1.92 (95% CI 1.50–2.47) times higher than among HIV-seronegative participants (p<0.001) (Table 2, https://wwwnc.cdc.gov/EID/article/27/6/21-0128-T2.htm). After adjusting for sentinel hospital, age, sex, year of diagnosis, ICU admission, receipt of systemic antifungal treatment, and *Candida* species, the odds of 30-day mortality were still 1.89 (95% CI 1.38–2.60) times higher among HIV-seropositive participants than among HIV-seronegative participants (Table 3); evidence was strong against the null hypothesis (p<0.001). We noted relatively little confounding of the association between HIV status and 30-day mortality by any available explanatory variable. In the final

model, differences between hospitals accounted for 3% of the variability in deaths (intracluster correlation coefficient = 0.03; p = 0.003). We found evidence of interaction of HIV status and ICU admission. The stratum-specific mortality OR was larger in the group not managed in an ICU (OR 2.27, 95% CI 1.47–3.52; p<0.001) than those who were admitted to the ICU (OR 1.56, 95% CI 1.00–2.43; p = 0.05), although the 95% CIs overlapped (Table 4). In a dose-response analysis, the adjusted odds of 30-day mortality was 1.90 times higher among HIV-seropositive persons with a CD4 count ≥200 cells/μL (95% CI 1.13–3.20; p = 0.02) and 2.18 times higher among persons with a CD4 count <200 cells/μL (95% CI 1.39–3.42; p = 0.001) compared with 30-day mortality among HIV-seronegative persons (Appendix Table 4).

Kaplan-Meier Survival Analysis

An outcome date was available for 1,023 participants. Overall, 44% (452/1,023) died within 30 days. The Kaplan-Meier survival curves diverged for HIV-seropositive and HIV-seronegative persons within 3 days of candidemia diagnosis and then remained roughly parallel until day 30 (Figure 2). Evidence was strong against the hypothesis that survival experience did not differ by HIV status (p<0.001).

Association of HIV Status and ICU Admission

Among 1,023 participants, a lower proportion (175/422, 41%) of HIV-seropositive persons than HIV-seronegative persons (339/601, 56%) were admitted to the ICU (crude OR 0.55, 95% CI 0.42–0.71; p<0.001). After adjustment for sentinel site, age, sex, and quick Pitt score category (n = 583) (Appendix Table 5), HIV-seropositive participants were 60% less likely to be admitted to the ICU than HIV-seronegative participants (OR 0.40, 95% CI 0.25–0.64; p<0.001). Among HIV-seropositive participants, a similar proportion with and without advanced HIV disease were admitted to the ICU (72/166 [43%] vs. 39/99 [39%]; p = 0.53). A similar proportion of HIV-seropositive participants receiving and not receiving antiretroviral treatment were admitted to ICU (116/299 [39%] vs. 50/101 [50%]; p = 0.06).

Discussion

In this surveillance study of hospitalized persons with candidemia in South Africa, the prevalence of HIV infection was 41% (95% CI 38%–44%). The 30-day mortality rate was almost twice as high among HIV-seropositive persons as among HIV-seronegative persons (OR 1.89, 95% CI 1.38–2.60; p<0.001), after adjusting for relevant confounders. The effect of HIV infection on death rates was estimated to be stronger among

Table 3. Random-effects multivariable logistic regression analysis of the effect of HIV on in-hospital death by sentinel site, simultaneously adjusted for potential confounders, among 907 persons with candidemia, South Africa, 2012–2017*

Variable	Summary aOR for death (95% CI)	Wald p value
HIV status		
Seronegative	Referent	
Seropositive	1.89 (1.38–2.60)	<0.001
Age group, y		
<18	Referent	
18–44	2.55 (1.66–3.93)	<0.001
45–64	3.48 (2.21–5.49)	<0.001
≥65	6.47 (3.61–11.61)	<0.001
Sex		
F	Referent	
M	1.27 (0.95–1.70)	0.11
Year		
2012	Referent	
2013	1.26 (0.72–2.19)	0.42
2014	1.34 (0.67–2.68)	0.40
2015	1.17 (0.58–2.33)	0.66
2016	1.08 (0.63–1.86)	0.77
2017	1.53 (0.90–2.61)	0.12
ICU admission		
No	Referent	
Yes	1.70 (1.23–2.36)	0.001
Receipt of systemic antifungal treatment		
No	Referent	
Yes	0.35 (0.25–0.48)	<0.001
Candida species		
C. albicans	Referent	
Other *Candida* spp.	0.66 (0.49–0.89)	0.006

*aOR, adjusted odds ratio; ICU, intensive care unit. Intra-cluster correlation coefficient = 0.03; likelihood ratio test for ρ = 0; p value = 0.003.

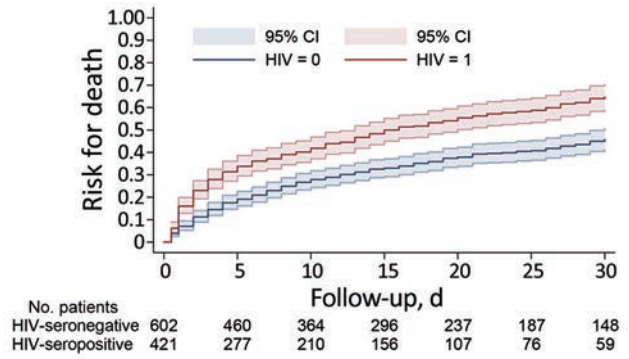

Figure 2. Kaplan-Meier analysis for 1,023 participants with candidemia during a 30-day period after the diagnosis of culture-confirmed candidemia by HIV infection status (outcome date missing for 17 participants), South Africa, 2012–2017. HIV = 0: HIV-seronegative; HIV = 1: HIV-seropositive; p value for log-rank test <0.001.

those not managed in an ICU than those who were, though the 95% CIs overlapped. HIV-seropositive persons also had a substantially lower risk for ICU treatment during their admission than those who were HIV-seronegative.

The overall crude mortality rate associated with candidemia of 44% (95% CI 41%–47%) reported in this study is higher than that reported in resource-rich settings (*19*), possibly owing to differences in our hospitalized cohort. The overall median age was lower, a large proportion were critically ill, and amphotericin B deoxycholate and azoles were the mainstay of treatment, whereas few patients received echinocandins. In our large study, we found a crude mortality rate among HIV-seropositive patients of 54%, which is comparable to the 60% mortality rate reported in 2 case series (*6*,*7*). Our main results are consistent with a United States cohort study that found that HIV infection was associated with a 2-fold increased adjusted hazard of 30-day mortality (*9*). We believe that this association between HIV and death among persons with candidemia is biologically plausible. First, the mechanism for an increased risk for death among HIV-seropositive persons may operate at the individual level. Despite a large proportion having received previous antiretroviral treatment, the median CD4 count among hospitalized HIV-seropositive participants with candidemia in this study was 133 cells/μL, and almost two thirds had advanced HIV disease (defined by the WHO as a CD4 count of <200 cells/μL) (*20*). This finding is consistent with reports of virologic failure and treatment interruption among an increasing proportion of HIV-seropositive patients at acute-care hospitals in South Africa (*21*). Many persons with advanced HIV disease have neutropenia or neutrophil defects (*10*,*11*). This innate immune defect may be a consequence of abnormal progenitor stem cell growth, a deficiency of granulocyte colony-stimulating factor, bone marrow infiltration by opportunistic infectious agents or malignant cells, treatment with particular medicines, or autoimmune phenomena (*10*). The alteration in the innate immune response may then reduce the clearance of *Candida* from the bloodstream, despite appropriate antifungal treatment. People with advanced HIV disease might also have been admitted primarily for management of disseminated tuberculosis, cryptococcal disease, or *Pneumocystis* pneumonia, which are associated with high death rates (*20*). In addition, more than one third of HIV-seropositive participants in this study were recorded to have evidence of HIV-associated wasting. Patients with a poorer nutritional state or loss of lean body mass have worse outcomes (*22*).

Second, an increased risk for death may be a consequence of differential treatment practices at the sentinel hospitals for HIV-seronegative and HIV-seropositive persons. We found that HIV-seropositive persons were 60% less likely to have received intensive care during their hospitalization. Several studies in Italy have documented the large proportion of patients who are managed for candidemia in general medical wards (*23*–*25*). In addition, the adjusted effect of HIV infection on 30-day mortality rates was stronger among participants who were not managed in an ICU during their hospital stay. This finding suggests that intensive care and monitoring of patients

Table 4. Interaction between HIV and intensive care unit admission on in-hospital death among 907 persons with candidemia, adjusted for potential confounders, South Africa, 2012–2017*

Variable	Stratum-specific aOR for death (95% CI)	Wald test p value†
Admitted to ICU		
HIV-seronegative	Referent	
HIV-seropositive	1.56 (1.00–2.43)	0.05
Not admitted to ICU		
HIV-seronegative	Referent	
HIV-seropositive	2.27 (1.47–3.52)	<0.001

*aOR, adjusted odds ratio; ICU, intensive care unit.
†Overall likelihood ratio test for interaction p value = 0.22. Case-fatality ratio for those admitted to an ICU: HIV-seropositive (94/152; 62%), HIV-seronegative (157/301; 52%) versus those not admitted to an ICU: HIV-seropositive (117/224; 52%), HIV-seronegative (76/230; 33%).

with candidemia, including those who are HIV-seropositive, might reduce mortality rates. However, in a resource-limited setting, the number of ICU beds is restricted. The criteria for admission to a public-sector ICU in South Africa includes an assessment of the severity of the acute or underlying illness and whether organ dysfunction can realistically be reversed. These criteria apply equally to those with and without HIV infection, according to a survey of critical care physicians in South Africa, although no data exist on the proportion of HIV-seropositive persons who were eligible for ICU admission but were not referred or were turned down (*26*,*27*). Among HIV-seropositive participants in our study, similar proportions of persons with advanced HIV disease who were receiving antiretroviral treatment were or were not admitted to ICU, suggesting that these factors were not the sole criteria for admission.

We confirmed several well-described risk factors for death among patients with candidemia, including inappropriate or no antifungal treatment, ICU admission, increased age, and a quick Pitt score of ≥2 (*28*). Removal of a CVC following diagnosis of candidemia was protective against death. A limitation of this study is that it was a secondary data analysis and was not specifically designed or powered to answer whether HIV infection was associated with death among patients with candidemia. However, the study was conducted in a high HIV prevalence setting, our sample size was large, and we found strong and consistent evidence against the null hypothesis after adjustment for confounding. Selection bias was a limitation because we excluded 60% of cases diagnosed at sentinel hospitals for whom data for the main exposure and outcome variables were missing. We also found differences among those who were included and excluded from the analysis. For instance, we included a larger proportion of cases among adults 18–44 years of age, cases caused by *C. albicans*, and cases from outside Gauteng Province in the analysis (Appendix). Data were also missing for confounder variables, and we excluded several potentially critical confounders from the main multivariable analysis. However, including these variables in a smaller dataset for multivariable analysis did not change the point estimate for the main exposure effect, although the 95% CI was wider (Appendix Table 3). In ≈20% of cases, HIV status was self-reported by participant or next-of-kin interview if a clear record of HIV status was not in the chart. If HIV-seropositive persons underreported their actual infection status, it might have weakened the association with death demonstrated in this study. Because we were unable to adjust for unmeasured factors, such as the presence or severity of diagnosed or undiagnosed underlying conditions, residual confounding is also possible. We conducted this study in an upper middle-income country, and participants were recruited at urban sentinel hospitals with ICU facilities; therefore, the results might not apply to all hospital populations. Cause of death was not recorded, and we were thus unable to estimate the number of deaths directly attributable to candidemia among either HIV-seropositive or HIV-seronegative participants. We excluded children <18 months of age from this analysis and cannot comment on whether HIV exposure or infection is associated with death in this population.

A key strength of this study was that it was nested within a large active surveillance system; laboratory audits were conducted to ensure that all culture-confirmed cases were captured. The main outcome measure was in-hospital death, a clear endpoint that was unlikely to have been misclassified. Given that most persons with HIV infection live in sub-Saharan Africa and the risk for healthcare-associated infections, including those caused by antimicrobial-resistant fungi, is becoming increasingly critical in this region (*1*,*29*–*31*), our findings might have broader implications than similar studies and are an essential addition to the literature.

In conclusion, we found that the overall crude mortality rate associated with candidemia was high, and HIV-seropositive persons were at ≈2-fold increased adjusted risk for all-cause in-hospital death, compared with their HIV-seronegative counterparts. This effect on mortality rates was weakened among those admitted to the ICU, though HIV-seropositive persons were substantially less likely to have received intensive care. We recommend a high index of suspicion for candidemia among admitted HIV-seropositive persons, regardless of the presence of classical risk factors. We further recommend that HIV-seropositive persons with suspected candidemia rapidly begin appropriate early antifungal treatment, that they be investigated to identify an infection source and control measures instituted, and that they should be considered for intensive care and monitoring to reduce deaths. Where feasible, consultation with an infectious disease specialist would enable this level of care.

Members of GERMS-SA: John Black, Shareef Abrahams, Vanessa Pearce (Eastern Cape Province); Anwar Hoosen, Vicky Kleinhans, Masego Moncho (Free State Province); Alan Karstaedt, Caroline Maluleka, Charl Verwey, Charles Feldman, David Moore, Gary Reubenson, Khine Swe Swe

Han, Jeannette Wadula, Jeremy Nel, Kathy Lindeque, Maphoshane Nchabeleng, Nazlee Samodien, Nicolette du Plessis, Nontombi Mbelle, Nontuthuko Maningi, Norma Bosman, Ranmini Kularatne, Sharona Seetharam, Teena Thomas, Theunis Avenant, Trusha Nana, Vindana Chibabhai (Gauteng Province); Adhil Maharj, Asmeeta Burra, Fathima Naby, Halima Dawood, Jade Mogamberry, Koleka Mlisana, Lisha Sookan, Praksha Ramjathan, Prasha Mahabeer, Romola Naidoo, Sumayya Haffejee, Yacoob Coovadia, Khine Swe Swe Han, Nomonde Dlamini, Surendra Sirkar (KwaZulu-Natal Province); Ken Hamese, Ngoaka Sibiya, Ruth Lekalakala (Limpopo Province); Greta Hoyland, Jacob Lebudi (Mpumalanga Province); Pieter Jooste (Northern Cape Province); Ebrahim Variava, Erna du Plessis (North West Province); Andrew Whitelaw, Kessendri Reddy, Mark Nicol, Preneshni Naicker, Colleen Bamford (Western Cape Province); Adrian Brink, Ebrahim Hoosien, Elizabeth Prentice, Inge Zietsman, Maria Botha, Peter Smith, Terry Marshall, Xoliswa Poswa (Ampath laboratories); Chetna Govind, Juanita Smit, Keshree Pillay, Sharona Seetharam, Suzy Budavari, Victoria Howell (Lancet laboratories); Carel Haumann, Catherine Samuel, Marthinus Senekal (PathCare laboratories); Andries Dreyer, Khatija Ahmed, Louis Marcus, Warren Lowman (Vermaak and Vennote laboratories); Angeliki Messina, Dena van den Bergh, and Karin Swart (Netcare hospital group); Ananta Nanoo, Andries Dreyer, Anne von Gottberg, Anthony Smith, Arvinda Sooka, Cecilia Miller, Charlotte Sriruttan, Cheryl Cohen, Chikwe Ihekweazu, Claire von Mollendorf, Desiree du Plessis, Erika van Schalkwyk, Farzana Ismail, Frans Radebe, Genevie Ntshoe, Gillian Hunt, Hlengani Mathema, Husna Ismail, Jacqueline Weyer, Jackie Kleynhans, Jenny Rossouw, John Frean, Joy Ebonwu, Judith Mwansa-Kambafwile, Karen Keddy, Kerrigan McCarthy, Liliwe Shuping, Linda de Gouveia, Linda Erasmus, Lucille Blumberg, Marshagne Smith, Martha Makgoba, Motshabi Modise, Nazir Ismail, Nelesh Govender, Neo Legare, Nicola Page, Ntsieni Ramalwa, Nuraan Paulse, Phumeza Vazi, Olga Perovic, Penny Crowther-Gibson, Portia Mutevedzi, Riyadh Manesen, Ranmini Kularatne, Ruth Mpembe, Sarona Lengana, Shabir Madhi, Shaheed Vally Omar, Sibongile Walaza, Sonwabo Lindani, Sunnieboy Njikho, Susan Meiring, Thejane Motladiile, Tiisetso Lebaka, Vanessa Quan, Verushka Chetty, Serisha Naicker, Tsidiso Maphanga, Mabatho Mhlanga, Thokozile Gloria Zulu, Ernest Tsotetsi, Phelly Matlapeng, Siphiwe Kutta, Lerato Qoza, Sydney Mogokotleng, Mbali Dube, and Amanda Shilubane (National Institute for Communicable Diseases).

This work was supported in its entirety by the National Institute for Communicable Diseases, a Division of the National Health Laboratory Service, Johannesburg, South Africa.

About the Author

Dr. Govender is a pathologist, medical epidemiologist, and head of the Centre for Healthcare-Associated Infections, Antimicrobial Resistance and Mycoses at the National Institute for Communicable Diseases, South Africa. His research interests include healthcare-associated and AIDS-related mycoses.

References

1. van Schalkwyk E, Mpembe RS, Thomas J, Shuping L, Ismail H, Lowman W, et al.; GERMS-SA. Epidemiologic shift in candidemia driven by *Candida auris*, South Africa, 2016–2017. Emerg Infect Dis. 2019;25:1698–707. https://doi.org/10.3201/eid2509.190040
2. Tsay SV, Mu Y, Williams S, Epson E, Nadle J, Bamberg WM, et al. Burden of candidemia in the United States, 2017. Clin Infect Dis. 2020;71:e449–53. https://doi.org/10.1093/cid/ciaa193
3. Lee RA, Zurko JC, Camins BC, Griffin RL, Rodriguez JM, McCarty TP, et al. Impact of infectious disease consultation on clinical management and mortality in patients with candidemia. Clin Infect Dis. 2019;68:1585–7. https://doi.org/10.1093/cid/ciy849
4. Kim SH, Yoon YK, Kim MJ, Sohn JW. Clinical impact of time to positivity for *Candida* species on mortality in patients with candidaemia. J Antimicrob Chemother. 2013;68:2890–7. https://doi.org/10.1093/jac/dkt256
5. Keighley C, Chen SCA, Marriott D, Pope A, Chapman B, Kennedy K, et al. Candidaemia and a risk predictive model for overall mortality: a prospective multicentre study. BMC Infect Dis. 2019;19:445. https://doi.org/10.1186/s12879-019-4065-5
6. Tumbarello M, Tacconelli E, de Gaetano Donati K, Morace G, Fadda G, Cauda R. Candidemia in HIV-infected subjects. Eur J Clin Microbiol Infect Dis. 1999;18:478–83. https://doi.org/10.1007/s100960050327
7. Bertagnolio S, de Gaetano Donati K, Tacconelli E, Scoppettuolo G, Posteraro B, Fadda G, et al. Hospital-acquired candidemia in HIV-infected patients. Incidence, risk factors and predictors of outcome. J Chemother. 2004;16:172–8. https://doi.org/10.1179/joc.2004.16.2.172
8. Puig-Asensio M, Padilla B, Garnacho-Montero J, Zaragoza O, Aguado JM, Zaragoza R, et al.; CANDIPOP Project; GEIH-GEMICOMED (SEIMC); REIPI. Epidemiology and predictive factors for early and late mortality in *Candida* bloodstream infections: a population-based surveillance in Spain. Clin Microbiol Infect. 2014;20:O245–54. https://doi.org/10.1111/1469-0691.12380
9. Grim SA, Berger K, Teng C, Gupta S, Layden JE, Janda WM, et al. Timing of susceptibility-based antifungal drug administration in patients with *Candida* bloodstream infection: correlation with outcomes. J Antimicrob Chemother. 2012;67:707–14. https://doi.org/10.1093/jac/dkr511
10. Levine AM, Karim R, Mack W, Gravink DJ, Anastos K, Young M, et al. Neutropenia in human immunodeficiency virus infection: data from the women's interagency HIV study. Arch Intern Med. 2006;166:405–10. https://doi.org/10.1001/archinte.166.4.405
11. Kuritzkes DR. Neutropenia, neutrophil dysfunction, and bacterial infection in patients with human immunodeficiency virus disease: the role of granulocyte colony-stimulating factor. Clin Infect Dis. 2000;30:256–70. https://doi.org/10.1086/313642

12. Ramos A, Romero Y, Sánchez-Romero I, Fortún J, Paño JR, Pemán J, et al. Risk factors, clinical presentation and prognosis of mixed candidaemia: a population-based surveillance in Spain. Mycoses. 2016;59:636–43. https://doi.org/10.1111/myc.12516
13. Meintjes G, Kerkhoff AD, Burton R, Schutz C, Boulle A, Van Wyk G, et al. HIV-related medical admissions to a South African district hospital remain frequent despite effective antiretroviral therapy scale-up. Medicine (Baltimore). 2015;94:e2269. https://doi.org/10.1097/MD.0000000000002269
14. Ntusi N, Aubin L, Oliver S, Whitelaw A, Mendelson M. Guideline for the optimal use of blood cultures. S Afr Med J. 2010;100:839–43. https://doi.org/10.7196/SAMJ.4217
15. Vaquero-Herrero MP, Ragozzino S, Castaño-Romero F, Siller-Ruiz M, Sánchez González R, García-Sánchez JE, et al. The Pitt Bacteremia Score, Charlson Comorbidity Index and Chronic Disease Score are useful tools for the prediction of mortality in patients with *Candida* bloodstream infection. Mycoses. 2017;60:676–85. https://doi.org/10.1111/myc.12644
16. Battle SE, Augustine MR, Watson CM, Bookstaver PB, Kohn J, Owens WB, et al. Derivation of a quick Pitt bacteremia score to predict mortality in patients with Gram-negative bloodstream infection. Infection. 2019;47:571–8. https://doi.org/10.1007/s15010-019-01277-7
17. Patterson L, McMullan R, Harrison DA. Individual risk factors and critical care unit effects on Invasive *Candida* infection occurring in critical care units in the UK: a multilevel model. Mycoses. 2019;62:790–5. https://doi.org/10.1111/myc.12956
18. Clinical and Laboratory Standards Institute. Performance standards for antifungal susceptibility testing of yeasts (M60). Wayne (PA): The Institute; 2017.
19. Toda M, Williams SR, Berkow EL, Farley MM, Harrison LH, Bonner L, et al. Population-based active surveillance for culture-confirmed candidemia—four sites, United States, 2012–2016. MMWR Surveill Summ. 2019;68:1–15. https://doi.org/10.15585/mmwr.ss6808a1
20. World Health Organization. Guidelines for managing advanced HIV disease and rapid initiation of antiretroviral therapy [cited 2021 Jan 14]. https://www.who.int/hiv/pub/guidelines/advanced-HIV-disease/en
21. Carmona S, Bor J, Nattey C, Maughan-Brown B, Maskew M, Fox MP, et al. Persistent high burden of advanced HIV disease among patients seeking care in South Africa's national HIV program: data from a nationwide laboratory cohort. Clin Infect Dis. 2018;66(suppl_2):S111–7. https://doi.org/10.1093/cid/ciy045
22. Olsen MF, Abdissa A, Kæstel P, Tesfaye M, Yilma D, Girma T, et al. Effects of nutritional supplementation for HIV patients starting antiretroviral treatment: randomised controlled trial in Ethiopia. BMJ. 2014;348:g3187. https://doi.org/10.1136/bmj.g3187
23. Luzzati R, Merelli M, Ansaldi F, Rosin C, Azzini A, Cavinato S, et al. Nosocomial candidemia in patients admitted to medicine wards compared to other wards: a multicentre study. Infection. 2016;44:747–55. https://doi.org/10.1007/s15010-016-0924-9
24. Scudeller L, Bassetti M, Concia E, Corrao S, Cristini F, De Rosa FG, et al.; MEDICAL group; Società Italiana di Terapia Antinfettiva (SITA); Federazione delle Associazioni dei Dirigenti Ospedalieri Internisti (FADOI). MEDical wards Invasive Candidiasis ALgorithms (MEDICAL): consensus proposal for management. Eur J Intern Med. 2016;34:45–53. https://doi.org/10.1016/j.ejim.2016.07.007
25. Sbrana F, Sozio E, Bassetti M, Ripoli A, Pieralli F, Azzini AM, et al. Independent risk factors for mortality in critically ill patients with candidemia on Italian Internal Medicine Wards. Intern Emerg Med. 2018;13:199–204. https://doi.org/10.1007/s11739-017-1783-9
26. Naidoo K, Singh JA, Lalloo UG. Survey of ethical dilemmas facing intensivists in South Africa in the admission of patients with HIV infection requiring intensive care. South Afr J Crit Care. 2013;29:1–10. https://doi.org/10.7196/sajcc.153
27. Mkoko P, Raine RI. HIV-positive patients in the intensive care unit: a retrospective audit. S Afr Med J. 2017;107:877–81. https://doi.org/10.7196/SAMJ.2017.v107i10.12298
28. Garnacho-Montero J, Díaz-Martín A, García-Cabrera E, Ruiz Pérez de Pipaón M, Hernández-Caballero C, Lepe-Jiménez JA. Impact on hospital mortality of catheter removal and adequate antifungal therapy in *Candida* spp. bloodstream infections. J Antimicrob Chemother. 2013;68:206–13. https://doi.org/10.1093/jac/dks347
29. Lockhart SR, Etienne KA, Vallabhaneni S, Farooqi J, Chowdhary A, Govender NP, et al. Simultaneous emergence of multidrug-resistant *Candida auris* on 3 continents confirmed by whole-genome sequencing and epidemiological analyses. Clin Infect Dis. 2017;64:134–40. https://doi.org/10.1093/cid/ciw691
30. Govender NP, Magobo RE, Mpembe R, Mhlanga M, Matlapeng P, Corcoran C, et al. *Candida auris* in South Africa, 2012–2016. Emerg Infect Dis. 2018;24:2036–40. https://doi.org/10.3201/eid2411.180368
31. Govender NP, Patel J, Magobo RE, Naicker S, Wadula J, Whitelaw A, et al.; TRAC-South Africa group. Emergence of azole-resistant *Candida parapsilosis* causing bloodstream infection: results from laboratory-based sentinel surveillance in South Africa. J Antimicrob Chemother. 2016;71:1994–2004. https://doi.org/10.1093/jac/dkw091

Address for correspondence: Nelesh P. Govender, Centre for Healthcare-Associated Infections, Antimicrobial Resistance and Mycoses, National Institute for Communicable Diseases, Private Bag X4, Sandringham, 2132, South Africa; email: neleshg@nicd.ac.za

Molecular Epidemiology and Evolutionary Trajectory of Emerging Echovirus 30, Europe

Kimberley S.M. Benschop, Eeva K. Broberg, Emma Hodcroft, Dennis Schmitz, Jan Albert, Anda Baicus, Jean-Luc Bailly, Gudrun Baldvinsdottir, Natasa Berginc, Soile Blomqvist, Sindy Böttcher, Mia Brytting, Erika Bujaki, Maria Cabrerizo, Cristina Celma, Ondrej Cinek, Eric C.J. Claas, Jeroen Cremer, Jonathan Dean, Jennifer L. Dembinski, Iryna Demchyshyna, Sabine Diedrich, Susanne Dudman, Jake Dunning, Robert Dyrdak, Mary Emmanouil, Agnes Farkas, Cillian De Gascun, Guillaume Fournier, Irina Georgieva, Ruben Gonzalez-Sanz, Jolanda van Hooydonk-Elving, Anne J. Jääskeläinen, Ruta Jancauskaite, Kathrin Keeren, Thea K. Fischer, Sidsel Krokstad, Lubomira Nikolaeva–Glomb, Ludmila Novakova, Sofie E. Midgley, Audrey Mirand, Richard Molenkamp, Ursula Morley, Joël Mossong, Svajune Muralyte, Jean-Luc Murk, Trung Nguyen, Svein A. Nordbø, Riikka Österback, Suzan Pas, Laura Pellegrinelli, Vassiliki Pogka, Birgit Prochazka, Petra Rainetova, Marc Van Ranst, Lieuwe Roorda, Isabelle Schuffenecker, Rob Schuurman, Asya Stoyanova, Kate Templeton, Jaco J. Verweij, Androniki Voulgari-Kokota, Tytti Vuorinen, Elke Wollants, Katja C. Wolthers, Katherina Zakikhany, Richard Neher, Heli Harvala, Peter Simmonds

Author affiliations: National Institute for Public Health and the Environment, Bilthoven, the Netherlands (K.S.M. Benschop, D. Schmitz, J. Cremer); European Centre for Disease Prevention and Control, Stockholm, Sweden (E.K. Broberg); Biozentrum, University of Basel and Swiss Institute of Bioinformatics, Basel, Switzerland (E. Hodcroft, R. Neher); Karolinska University Hospital and Karolinska Institute, Stockholm (J. Albert, R. Dyrdak); Cantacuzino, Bucharest, Romania (A. Baicus); CHU Clermont-Ferrand, National Reference Centre for Enteroviruses and Parechoviruses, Clermont-Ferrand, France (J. Bailly, A. Mirand); Landspitali-National University Hospital, Reykjavik, Iceland (G. Baldvinsdottir); National laboratory of Health, Environment and Food, Ljubljana, Slovenia (N. Berginc); National Institute for Health and Welfare, Helsinki, Finland (S. Blomqvist); Robert-Koch-Institue, Berlin, Germany (S. Böttcher S. Diedrich, K. Keeren); The Public Health Agency of Sweden, Solna, Sweden (M. Brytting, K. Zakikhany); National Public Health Center, Budapest, Hungary (E. Bujaki, A. Farkas); Instituto de Salud Carlos III, Madrid, Spain (M. Cabrerizo, R. Gonzalez-Sanz); Public Health England, Colindale, UK (C. Celma, J. Dunning); University of Oslo and Oslo University Hospital, Oslo, Norway (S. Dudman); Charles University, Prague, Czech Republic (O. Cinek); Leiden University Medical Center, Leiden, the Netherlands (E.C.J. Claas); University College Dublin, Dublin, Ireland, UK (J. Dean, C. De Gascun, U. Morley); World Health Organization National Polio Entero Reference Laboratory, Norwegian Institute of Public Health, Oslo (J.L. Dembinski, S. Dudman); Public Health Center of the Ministry of Health of Ukraine, Kiev, Ukraine (I. Demchyshyna); Hellenic Pasteur Institute, Athens, Greece (M. Emmanouil, V. Pogka, A. Voulgari-Kokota); Laboratoire National de Santé, Dudelange, Luxembourg (G. Fournier, T. Nguyen, J. Mossong); National Center of Infectious and Parasitic Diseases, Sofia, Bulgaria (I. Georgieva, L. Nikolaeva-Glomb, A. Stoyanova); Microvida, Breda, the Netherlands (J. van Hooydonk-Elving, S. Pas); University of Helsinki and Helsinki University Hospital, Helsinki (A.J. Jääskeläinen); National Public Health Surveillance Laboratory, Vilnius, Lithuania (R. Jancauskaite, S. Muralyte); Nordsjaellands University Hospital, Hilleroed, Denmark (T.K. Fischer); Statens Serum Institute and University of Copenhagen, Copenhagen, Denmark (T.K. Fischer); University Hospital of Trondheim, Norway (S. Krokstad, S.A. Nordbø); National Institute of Public Health, Prague (L. Novakova, P. Rainetova); Danish WHO National Reference Laboratory for Poliovirus, Statens Serum Institut, Copenhagen (S.E. Midgley); Erasmus Medical Center, Rotterdam, the Netherlands (R. Molenkamp); Elisabeth Tweesteden Hospital, Tilburg, the Netherlands (J.-L. Murk, J.J. Verweij); Norwegian University of Science and Technology, Trondheim (S.A. Nordbø); Turku University Hospital, Turku, Finland (R. Österback, T. Vuorinen); University of Milan, Milan, Italy (L. Pellegrinelli); Austrian Agency for Health and Food Safety, Vienna, Austria (B. Prochazka); Rega Institute KU Leuven, Leuven, Belgium (M. Van Ranst, E. Wollants); Maasstad Ziekenhuis, Rotterdam (L. Roorda); Centre de Biologie Est des Hospices Civils de Lyon, Lyon, France (I. Schuffenecker); University Medical Center Utrecht, Utrecht, the Netherlands (R. Schuurman); National Health Services Scotland, Edinburgh, Scotland, UK (K. Templeton); University of Turku, Turku (T. Vuorinen) Amsterdam University Medical Center, Amsterdam, the Netherlands (K.C, Wolthers); University College London, London, UK (H. Harvala); National Health Service, Colindale (H. Harvala); University of Oxford, Oxford, UK (P. Simmonds)

DOI: https://doi.org/10.3201/eid2706.203096

In 2018, an upsurge in echovirus 30 (E30) infections was reported in Europe. We conducted a large-scale epidemiologic and evolutionary study of 1,329 E30 strains collected in 22 countries in Europe during 2016–2018. Most E30 cases affected persons 0–4 years of age (29%) and 25–34 years of age (27%). Sequences were divided into 6 genetic clades (G1–G6). Most (53%) sequences belonged to G1, followed by G6 (23%), G2 (17%), G4 (4%), G3 (0.3%), and G5 (0.2%). Each clade encompassed unique individual recombinant forms; G1 and G4 displayed ≥2 unique recombinant forms. Rapid turnover of new clades and recombinant forms occurred over time. Clades G1 and G6 dominated in 2018, suggesting the E30 upsurge was caused by emergence of 2 distinct clades circulating in Europe. Investigation into the mechanisms behind the rapid turnover of E30 is crucial for clarifying the epidemiology and evolution of these enterovirus infections.

Echovirus 30 (E30) is a common cause of viral meningitis outbreaks and upsurges reported worldwide (*1*–*6*). In 2018, E30 circulation was high, and large-scale E30 meningitis-related upsurges were reported in Denmark, Germany, the Netherlands, Norway, and Sweden, compared with data collected during 2015–2017 (*2*). E30 was detected in 14.5% of all confirmed enterovirus cases (*2*). The virus affected mainly children 0–4 years of age and adults 26–45 years of age, and 75% of cases had central nervous system involvement (*2*).

E30 is classified into the *Enterovirus B* (EV-B) species within the *Picornaviridae* family of human enteroviruses and is divided into 2 genogroups (GG), I and II (*7*). Most currently circulating strains are classified as GGII (*7*,*8*). The genome (positive-sense single-stranded RNA) is ≈7.4 kb long and contains 5′ and 3′ untranslated regions (UTRs) flanking a single open reading frame (ORF), encoding 4 structural proteins (viral protein [VP] 0, VP2, VP3, and VP1) and 7 nonstructural proteins (NSP; 2A, 2B, 2C, 3A, 3B [also known as VPg], 3C, and 3D polymerase [3Dpol]).

E30 outbreaks display a cyclic incidence pattern of 3–5 years (*1*,*7*,*9*–*13*). Typically, outbreaks and upsurges are associated with rapid spread of different, relatively short-lived, strains defined by VP1 capsid gene sequences (*1*,*7*,*8*,*14*–*16*). Novel E30 variants have invariably undergone recombination with other EV-B types before their emergence. Recombination results in the generation of novel recombinant forms (RFs) that are chimaeras of E30-derived structural genes with NSP, 5′ UTR sequences, or both, which are derived from cocirculating E30 strains or other EV-B types, such as E9 and E11 (*10*–*12*,*14*,*17*,*18*). The role of VP1 sequence change, recombination, and other factors driving phenotypic changes in virus transmissibility or pathogenicity, and the contributions of changes in population immunity, are crucial for clarifying the underlying causes of E30 outbreaks and upsurges in cases (*15*,*19*–*22*).

We performed an in-depth analysis of the genetic diversity of E30 strains detected during a large-scale upsurge in cases in Europe during 2018. We collated sequences obtained by participating laboratories in 22 countries and analyzed the epidemiologic and evolutionary profiles in this molecular study.

Methods

Data Collection

An invitation to participate in this study was sent on November 13, 2018, to co-authors of the E30–2018 study (*2*) through the European Centre for Disease Prevention and Control (ECDC) Epidemic Intelligence Information System Vaccine-Preventable Diseases platform (https://www.ecdc.europa.eu/en/publications-data/epidemic-intelligence-information-system-epis), and to members of the European Non-Polio Enterovirus Network (ENPEN; https://www.escv.eu/enpen). We requested pseudonymized data from 2016–2018 with sample identifier, sampling date, specimen type, and sequence in FASTA be sent to ECDC secure file transfer protocol server by January 7, 2019. We also collected optional data, such as patient age, clinical presentation, whether they were hospitalized, and infection outcome. We excluded submissions without virus sequence data (Appendix Figure 1, https://wwwnc.cdc.gov/EID/article/27/6/20-3096-App1.pdf).

Sequence Data Collection

We requested that the FASTA sequence data contain the VP1 gene and collected 1,784 records (Appendix Figure 1). Sequences were obtained from enterovirus-positive samples by using 5′ UTR PCR (*23*) and typed within the VP1 gene by using Sanger sequencing (*2*,*24*). We excluded sequences with indicators of poor sequence quality, such as ≥2 ambiguous or undefined bases, in-frame stop codons, identical to reference E30 strains; sequences of the wrong type, such as E3; or sequences shorter than 200 basepairs or spanning a non-VP1 region. In total, we had 1,407 study sequences that comprised 2 nonoverlapping regions, 1,262 sequences from region 1 (nt positions 2543–2902, according to the prototype E30 strain Bastianni, GenBank accession no. AF311938) and 145 sequences from region 2 (nt positions 2916–3428). Of these, 1,329 sequences were collected during 2016–2018 and 78 during 2010–2015. We used the 2010–2015 sequences

for phylogenetic reconstruction but excluded these from further data analysis (Appendix Figure 1).

For additional analysis of the 3D polymerase (3Dpol) region, we randomly selected records from each clade to ensure fair distribution of sequence data. We asked participants to send either extracted RNA in a QIAGEN (https://www.qiagen.com) spin column at room temperature for next-generation sequencing (NGS) or to conduct 3Dpol sequencing of the 549 nucleotides, as previously described (*17*).

Epidemiologic and Statistical Analyses

We descriptively analyzed clinical symptoms and age. Patients were stratified into the following age groups: <3 months, 3–23 months, 2–5 years, 6–15 years, 16–25 years, 26–45 years, 46–65 years, and >65 years. Crude odds ratios with 95% CI were used to express magnitude of association between continuous or categorical variables in multivariate logistic regression.

Next-Generation Sequencing

Stool suspensions and CSF samples were processed to remove as much nonviral material as possible by using centrifugation, filtration, and endonuclease treatment. RNA was extracted by using the MagNAPure 96 (Roche Diagnostics, https://www.roche.com) automated extraction kit or QIAGEN filters and eluted in 50 μL of elution buffer (Appendix).

Complementary DNA (cDNA) and double stranded DNA (dsDNA) were generated and purified (Appendix). For tagmentation and library preparation, the Nextera XT DNA Library Preparation Kit (Ilumina, https://www.illumina.com) was used according to the manufacturer's instructions. Runs were performed on the Nextseq (Ilumina). Raw data were processed by using Jovian (D. Schmitz et al., unpub. data, https://github.com/DennisSchmitz/Jovian) (Appendix).

Nucleotide Sequences and Phylogenetic Analysis

We conducted VP1 phylogenetic reconstruction with the 1,407 study sequences and 324 sequences extracted from Genbank. We selected region 1 for clade analysis because it is more commonly used for enterovirus typing (*24*). We performed analysis of region 2 sequences based on sequence clustering, in which both region 1 and 2 were available, such as full-length sequences or sequences spanning the entire VP1 gene. Sequencing of the 540 nt 3Dpol gene, positions 5825–6364, also was provided for 12 samples with region 1 sequences (Appendix Figure 1). Sanger sequencing indicated that samples did not display double infection and that VP1 and 3Dpol were from 1 virus. Complete genomes (≈7.3 kb) were generated for 48 sequences by using NGS. To compare 3Dpol groupings within EV species B, we downloaded all sequences available from GenBank as of October 18, 2019, that were >70% complete between positions 5825–6364 with <6 ambiguous base positions and <6 undetermined bases and without stop codons. We aligned the downloaded sequences with complete genomes or 3Dpol sequences from our study.

We aligned data by using sequence editor SSE version 1.3 (http://www.virus-evolution.org). We generated maximum-likelihood and neighbor-joining trees for VP1 and 3Dpol regions by using MEGA version 7 (https://www.megasoftware.net) with the optimal model (general time reversible plus invariant sites plus gamma distribution for rates over sites) and 100 bootstraps (*25*). We analyzed the species B dataset with neighbor-joining and maximum composite likelihood distances.

Nextstrain VP1 Phylodynamic Analysis

The dataset used for Nextstrain phylodynamic analysis comprised 1,285 sequences; 1,215 study sequences (region 1) and 70 complete VP1 sequences extracted from GenBank (Appendix Figure 1). We excluded sequences shorter than 250 bp, sequences from samples collected before 1958, and sequences deemed as outliers during phylogenetic reconstruction. We deemed these outliers recombinants with possible recombination breakpoints within the sequence fragment used made phylogenetic reconstruction impossible.

We aligned sequences by using MAFFT (*26*). We inferred a phylogenetic tree by using IQ-TREE (*27*) and generated time-resolved trees by using TreeTime (*28*) by estimating the mutation rate. When available, we attached to sequences data on country, sample type, E30 clade, age groups, and clinical data, such as whether patients were hospitalized and their symptoms. We provided the resulting Nextstrain build for viewing (https://nextstrain.org/community/enterovirus-phylo/echo30-2019/vp1).

Nextstrain VP1:3Dpol Tanglegram Phylodynamics

We used a dataset of 110 sequences to conduct 3Dpol analysis, including 48 complete genome sequences and 12 3Dpol sequences generated in this study and 50 sequences extracted from GenBank (Appendix Figure 1). We aligned 3Dpol sequences to the E30 reference sequence (GenBank accession no. MK238483) and inferred phylogenetic and time-resolved trees as we did for VP1, but we used a fixed clock rate of 4×10^{-3} substitutions/site/year during the time-

resolved tree reconstruction. We provided the resulting Nextstrain tanglegram build for viewing (https://nextstrain.org/community/enterovirus-phylo/echo30-2019/3D:community/enterovirus-phylo/echo30-2019/vp1) and the codes for both VP1 and 3Dpol analyses (https://github.com/enterovirus-phylo/echo30-2019).

Genbank and ENA Accession Numbers

We deposited VP1 and complete genome sequences in GenBank under accession nos. KC309427–37, KY986976–7033, MK251835–6, MK372854–80, MK507733–7, MK814991–6288, and MK895104–9 and 3Dpol sequences under accession nos. MN395293–303. We deposited NGS fastq reads in European Nucleotide Archive database under accession nos. SAM17101211–58.

Results

Molecular Epidemiology and Demographics

During 2016–2018, a total of 1,329 E30 records representing 1,292 cases that fulfilled the study criteria were submitted from 22 countries (Table 1; Appendix Figure 1). During those 3 years, the total number of E30 cases steadily increased (Table 1). The numbers varied per country per year, and we noted a clear upsurge in 2018 in several, but not all, countries (Table 1; Figure 1). Of the 1,329 records analyzed, 443 (33%) were from the United Kingdom; the Netherlands submitted 198 (15%) and Spain 162 (12%) records. Other countries submitted from 1 (<1%) to 117 (9%) records. Specimen type was reported for 1,312 (98.7%) records. Most (70%; 924/1,312) samples were cerebrospinal fluid specimens, but other specimen types included 269 (21%) from feces specimens, 102 (8%) from respiratory, and 17 (1%) from blood. During the study period, E30 records were submitted more frequently in summer months; 18.4% (n = 244) were submitted in June, 17.6% in July (n = 234), and 11.7% in August (n = 155) (Figure 2).

Age was available for 1,080 (83.6%) cases and ranged from 0 to 73 years with a mean age of 18.7 years. Children <5 years of age (n = 360, 33.3%) and adults 26–45 years of age (n = 409, 37.9%) were most affected (Table 2). Infants ≤3 months of age also were heavily affected (n = 223 cases, 20.6%) (Table 2).

Clinical information was available for 734 (56.8%) E30 cases, of which 380 cases had unknown symptomology. For most (28.7%, n = 211) cases, the recorded signs and symptoms suggested meningitis. Symptoms of acute flaccid paralysis were reported in 1 case, encephalitis in 3 cases, and meningoencephalitis in 8 cases. Fever, either as sole symptom or in combination with other signs and symptoms, was recorded in only 52 (7.1%) cases. Unfortunately, not all records were filled in completely, and clinical data were absent for some samples. Other signs and symptoms mentioned were gastrointestinal symptoms in 6 cases, respiratory symptoms in 6, rash in 2, other neurologic symptoms in 4, or other unspecified in 53 cases; 8 cases had no symptoms. We created an interactive representation of age and clinical features of sequences from E30 cases, which we made available on Nextstrain (https://nextstrain.org/community/enterovirus-phylo/echo30-2019/vp1).

Table 1. Number of echovirus 30 records with curated viral protein 1 sequences by country, 2016–2018*

Country	2016, n = 325	2017, n = 493	2018, n = 511	Total, n = 1,329
Austria	6 (1.8)	3 (0.6)	0	9 (0.7)
Belgium	74 (22.8)	2 (0.4)	15 (2.9)	91 (6.8)
Bulgaria	0	4 (0.8)	4 (0.8)	8 (0.6)
Czech Republic	21 (6.5)	2 (0.4)	3 (0.6)	26 (2.0)
Germany	11 (3.4)	4 (0.8)	12 (2.3)	27 (2.0)
Denmark	7 (2.2)	73 (14.8)	37 (7.2)	117 (8.8)
Spain	86 (26.5)	37 (7.5)	39 (7.6)	162 (12.2)
Finland	1 (0.3)	0	2 (0.4)	3 (0.2)
France	4 (1.2)	2 (0.4)	17 (3.3)	23 (1.7)
Greece	0	3 (0.6)	8 (1.6)	11 (0.8)
Hungary	2 (0.6)	0	0	2 (0.2)
Ireland	13 (4.0)	46 (9.3)	23 (4.5)	82 (6.2)
Iceland	0	0	5 (1.0)	5 (0.4)
Italy	0	0	2 (0.4)	2 (0.2)
Lithuania	0	0	1 (0.2)	1 (0.1)
Luxembourg	0	4 (0.8)	4 (0.8)	8 (0.6)
Netherlands	33 (10.2)	23 (4.7)	142 (27.8)	198 (14.9)
Norway	4 (1.2)	28 (5.7)	34 (6.7)	66 (5.0)
Sweden	0	0	36 (7.0)	36 (2.7)
Slovenia	1 (0.3)	0	3 (0.6)	4 (0.3)
Ukraine	3 (0.9)	2 (0.4)	0	5 (0.4)
United Kingdom	59 (18.2)	260 (52.7)	124 (24.3)	443 (33.3)

*All values expressed as no. (%).

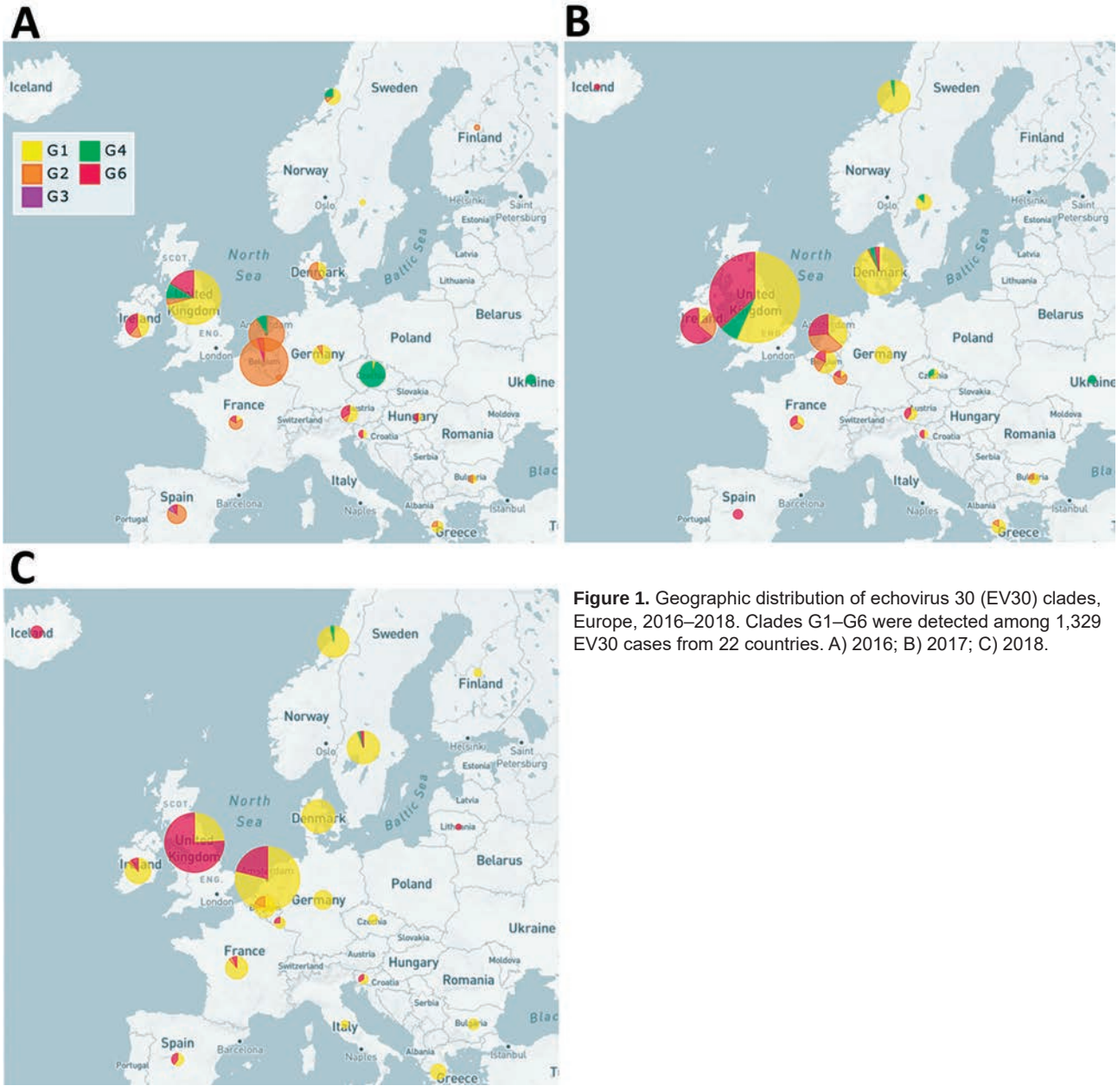

Figure 1. Geographic distribution of echovirus 30 (EV30) clades, Europe, 2016–2018. Clades G1–G6 were detected among 1,329 EV30 cases from 22 countries. A) 2016; B) 2017; C) 2018.

Hospitalization status was available for only 17.6% (n = 228) of cases, only 5 of which had no hospitalization. The low fraction of hospitalization reported limited further analysis. No deaths were reported.

E30 Phylodynamics

Among the 1,329 curated VP1 study sequences, 1,019 (76.7%) could be subdivided into 5 distinct clades, G1–G5, that showed >5% sequence divergence from one another (Figure 3, panel A). The mean divergence between VP1 nucleotide sequences of G1–G5 was 12.4%–15.2%, which translated to 2.8%–3.9% amino acid sequence divergence. Most (704, 53%) sequences belonged to G1, but 229 (17.2%) were in G2, 59 (4.4%) in G4, 4 (0.3%) in G3, and 2 (0.2%) in G5. These sequences all were assigned to GGII, 1 of 2 previously reported genogroups (*7*). The remaining 310 VP1 sequences formed a single clade, G6 (Figure 3), showing 20.6% mean nucleotide differences and 8.5% amino acid differences from the VP1 sequences within G1–G5 clades. G6 was sufficiently divergent from G1–G5 (GGII). The divergence falls within the nucleotide divergence between GGI–GGII (19%–22%) (*7*), and G6 can be considered a third genogroup, GGIII.

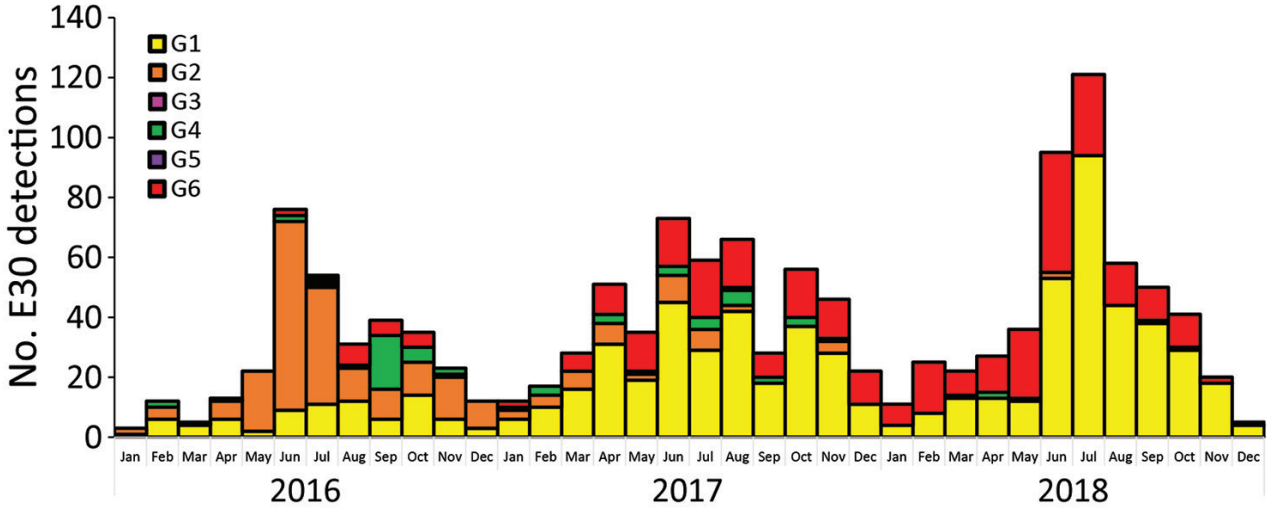

Figure 2. Monthly distribution of echovirus 30 (EV30) clades G1–G6 detected among 1,329 sequences submitted from 22 countries in Europe during 2016–2018.

The phylogeny showed a rapid turnover of E30 clades over the 3 years sampled, shifting from G2 dominating in 2016 to G1 and G6 dominating in 2017 and 2018 (Figure 1). In 2016, 58.5% of strains were G2, and this genotype was identified in 11/22 (50%) countries. G2 was detected in only 8 countries in 2017 and only 4 countries in 2018. Similarly, G4 disappeared during 2016–2018. In 2016, both G1 and G6 were detected, G1 in 24.6% (n = 80) of virus strains in 10 countries and G6 in 6.5% (n = 21) of virus strains in 7 countries. Rates of detection for G1 and G6 steadily increased in 2017; G1 was detected in 59.2% (n = 292) of virus strains in 12 countries and G6 in 26.4% (n = 130) of virus strains in 7 countries (Figure 1). During the 2018 upsurge, 64.6% (330) of sequences reported in 17 countries belonged to G1, and 33.9% (173) in 11 countries belonged to G6 (Figure 1). These data indicate the occurrence of ≥2 distinct viruses dominating the upsurge in 2018 (Figure 1).

We used Nextstrain to create an interactive phylodynamic tree and map to explore relationships of the E30 study VP1 sequences in G1–G6 (https://nextstrain.org/community/enterovirus-phylo/echo30-2019/vp1) (Figure 3, panel B; Appendix Figure 2). We deemed G5 sequences as outliers and did not include these during phylogenetic reconstruction. Molecular clock analysis of the VP1 region revealed an estimated substitution rate of 5.12×10^{-3} substitutions/per site/per year, comparable to rates previously determined for a range of enteroviruses.

Most E30 G1 viruses were detected among infants <3 months of age (135/568, 24%) and in young adults 26–45 years of age (227/568, 40%) (Table 2). G2 (100/145, 68%) and G4 (29/59, 52%) were most frequent among children 3 months–15 years of age. G6 mainly was detected among children 3 months–15 years of age (100/308, 32.5%) and in adults 26–45 years of age (134/308, 43.5%). Only 2 cases of G3 and 1 of G5 were reported with age information (Table 2).

Table 2. Distribution of echovirus 30 cases in Europe by age group and clade*

Clade	Age range								Total no. (%)	Mean age, y (95% CI)	p value
	<3 mo	3–23 mo	2–5 y	6–15 y	16–25 y	26–45 y	46–65 y	>65 y			
G1	124 (55.6)	24 (54.5)	30 (33.3)	58 (43.6)	84 (56.8)	227 (55.9)	18 (0.6)	3 (37.5)	568 (52.6)	19.24 (17.94–20.54)	Referent
G2	41 (18.4)	10 (22.7)	29 (31.2)	23 (17.3)	7 (4.7)	32 (7.9)	2 (6.7)	1 (12.5)	145 (13.4)	12.07 (9.55–14.58)	<0.001
G3	0	0	0	0	0	2 (0.4)	0	0	2 (0.2)	35.5 (29.15–41.85)	0.142
G4	9 (4.0)	0	4 (4.3)	17 (12.8)	11 (7.4)	13 (3.2)	2 (6.7)	0	56 (5.2)	16.82 (13.06–20.57)	0.269
G5	0	0	0	0	0	1 (0.2)	0	0	1 (0.1)	36.84 (NA)	0.260
G6	49 (22.0)	10 (22.7)	30 (32.3)	35 (26.3)	43 (29.0)	134 (33.0)	8 (26.7)	4 (50.0)	308 (28.5)	21.11 (19.34–22.88)	0.090
Total	223	44	93	133	145	449	30	8	1,080	18.73 (17.78–19.68)	0.001

*Values are no. (%) except where otherwise indicated. NA, not applicable.

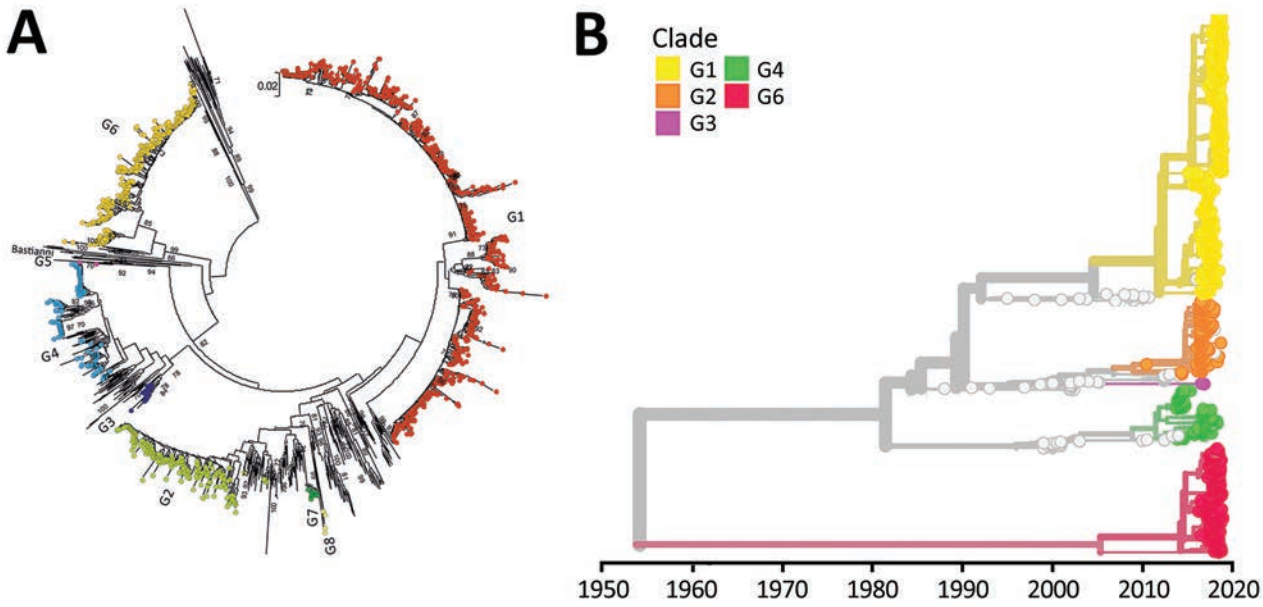

Figure 3. Phylodynamic analysis of region 1 in a curated study of echovirus 30 (E30) viral protein 1 (VP1) sequences from 22 countries in Europe, 2010–2018. We constructed the bootstrapped maximum likelihood neighbor-joining trees using 47 full length sequences and 277 VP1 sequences extracted from GenBank. E30 groups 1–8 are labeled. A) Maximum likelihood trees constructed by using MEGA version 7.0 (https://www.megasoftware.net). Prototype E30 strain Bastianni, (GenBank accession no. AF311938) was used as a reference. Scale bar indicates nucleotide substitutions per site. B) Maximum likelihood trees constructed by using Nextstrain (https://nextstrain.org) from which we dropped several problematic sequences, including group 5.

Amino Acid Diversity

Most E30 VP1 sequences within clades G1, G2, G4, and G6 displayed specific amino acid substitutions. G6 sequences predominantly displayed amino acid changes at position 56 (Y-F), position 84 within the BC loop (V-A), position 87 within the BC loop (E-D), and position 145 (V/I) compared with G1, G2, and G4. Most G1 and G6 sequences had a valine at positions 54 and 120 compared with the G2 and G4 sequences, which had an isoleucine. At position 122, most G4 sequences contained a leucine, whereas G1, G2, and G6 sequences contained a phenylalanine. Interactive data are available on Nextstrain (https://nextstrain.org/community/enterovirus-phylo/echo30-2019/vp1).

Recombination Analysis

We used 110 sequences containing both VP1 and 3Dpol region and complete genome sequences to analyze recombination events between VP1 and the 3′ distal end of the E30 genome (Appendix Figure 1). The E30 3Dpol sequences formed a series of separate clusters interspersed with those of other species B types, indicative of many within-species recombination events during their diversification (Figure 4). We took the entire published sequence dataset and used a nucleotide sequence distance threshold of 8%, based on pairwise sequence comparisons, which divided sequences into distinct groups (Appendix Figure 3), comparable to those derived from a previous analysis of E30 RFs (*17*). Accordingly, species B could be divided into ≈442 RFs, an indication of the frequency and complexity of recombination events occurring during the evolution of this species. We used Nextstrain to generate an interactive tanglegram of VP1 and 3Dpol RFs (https://nextstrain.org/community/enterovirus-phylo/echo30-2019/3D:community/enterovirus-phylo/echo30-2019/vp1) (Figure 5).

We found that 3Dpol sequences of G1–G6 formed 8 recombination groups, which were separated by other published E30 variants and by other species B types (Figure 5). We noted that viruses within most VP1 clades were monophyletic in 3Dpol, but that G1 and G4 each had undergone further recombination (Figure 5; Appendix Figure 4), a split corresponding to the sublineages evident in the VP1-based tree. The split was identified as a time-related phenomenon, with G1 circulating in 2018 representing a different RF from G1 circulating during 2016 and 2017.

Discussion

A large upsurge of E30 infections was reported in several countries in Europe during 2018 (*2*). We

conducted a comprehensive molecular characterization of E30 by using VP1, 3Dpol, and whole genome sequences. Our molecular characterization enabled an analysis of the recombination events occurring during E30 diversification in Europe, which can be conducted only when dealing with a single infection. Our study used a large EV sequence dataset collected worldwide, comprising 1,329 E30 sequences collected from 22 countries in Europe during 2016–2018 and was made possible due to the large-scale collaboration between countries through ENPEN and ECDC.

The data clearly demonstrate that analysis based on phylogenetic clade assignment shows differential dominance of many different clades. The upsurge in 2018 was caused by appearance of several different clades or genogroups of E30 viruses; G1 in GGII (*7*) and G6 in a novel genogroup, GGIII, which we propose in this study. Viruses from both clades had been circulating for ≥2 years. In total, 6 clades were identified during the study period and circulated in a pattern of rapid turnover of newly emerging genetic lineages and RFs and their relatively rapid disappearance over time, a pattern that is typical for other enteroviruses (*1*,*7*,*10*,*12*,*13*,*16*–*18*,*29*). In this study, G2 predominated in 2016 and 2017 in central Europe and were subsequently replaced by the G1 and G6 in 2018 (Figures 1, 2). This genetic turnover and the associated string of recombination events during lineage diversification occurred within the 2- to 5-year cyclical pattern of E30 incidence. As expected, each VP1 group corresponded to a separate RF, but G1 underwent a further recombination event as the virus diversified from a common ancestor dated to around 2011 and G4 underwent a further recombination from an ancestor around 2008. Of note, clade G1 showed a time related split in which G1 sequences circulating in 2018 emerged from those circulating in 2016–2017, coinciding with a recombination generating a novel RF. The absence of G3 and G5 sequences in the study population might reflect a generally lower circulation of these strains or perhaps a period of relative quiescence during the survey period. Long-term

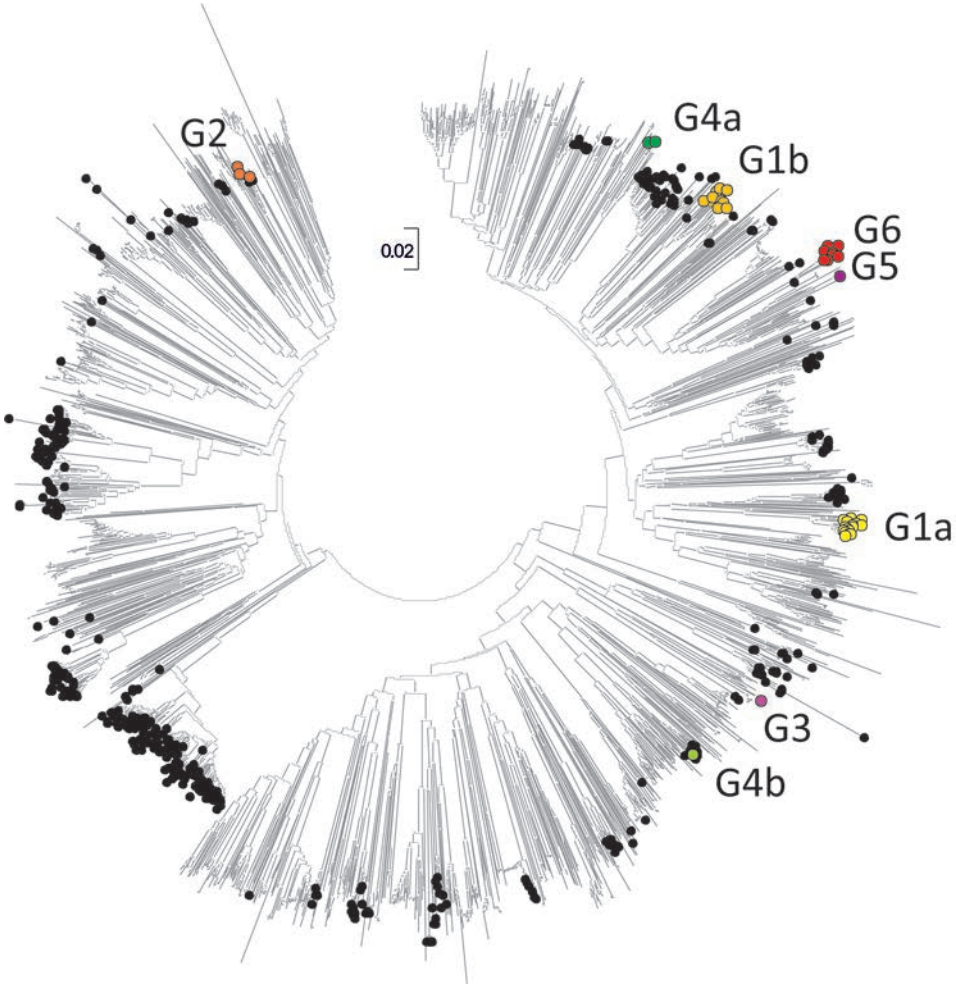

Figure 4. Neighbor-joining tree of 3D polymerase (3Dpol) sequences of echovirus 30 (E30) study samples and sequences from previously described E30 strains. The tree was constructed from Jukes-Cantor corrected nucleotide sequence distances in MEGA version 7.0 (https://www.megasoftware.net). Colored circles represent clades G1–G6 from this study; black circles represent 581 previously described E30 strains; and unlabeled branches represent all other species B types (n = 1,566) available in GenBank as of October 18, 2019. Scale bar indicates nucleotide substitutions per site.

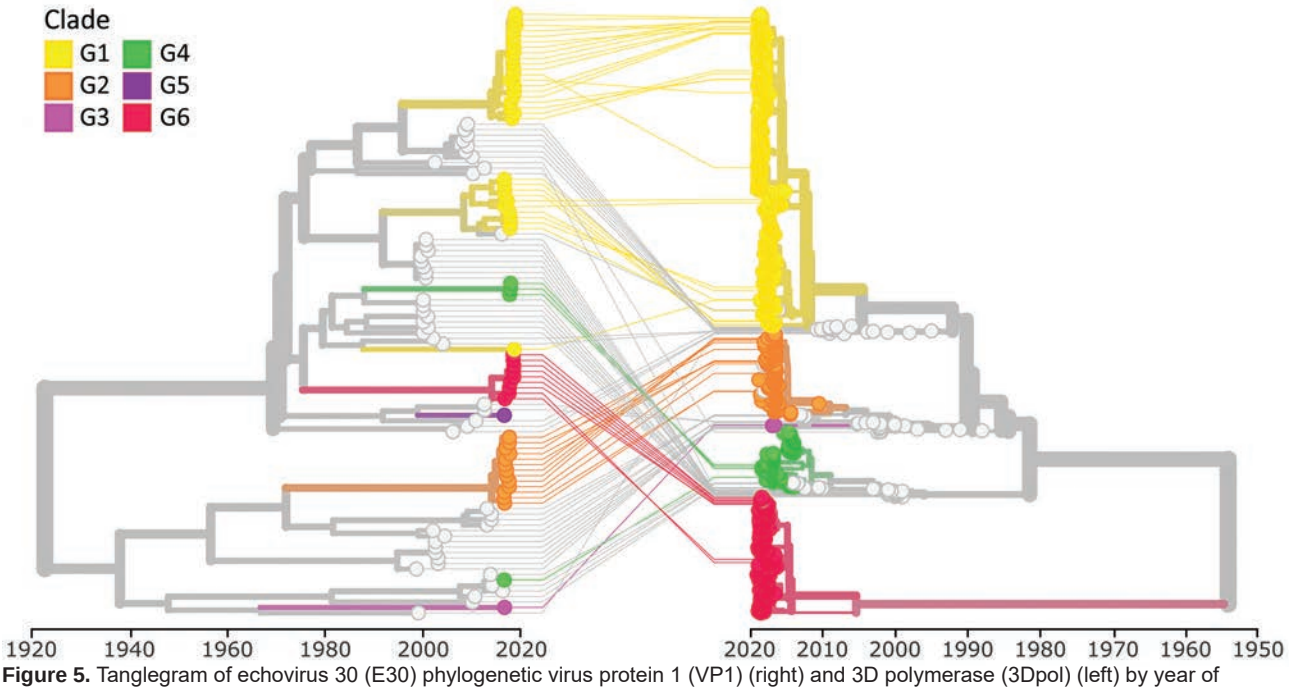

Figure 5. Tanglegram of echovirus 30 (E30) phylogenetic virus protein 1 (VP1) (right) and 3D polymerase (3Dpol) (left) by year of sample collection. We used 110 sequences and rendered the tanglegram by using Nextstrain (https://www.nextstrain.org). Clades G1–G6 are labeled.

surveillance is essential to monitor for potential emergence of these strains in future incidence cycles.

The cocirculation of different E30 clades during the 2018 upsurge and in previous years argues against the idea that the periodic emergence of E30 occurs through the evolution of more pathogenic or transmissible forms of the virus. The cocirculation of several different groups fits better with changes in population susceptibility from birth cohort effects and a breach of a critical immunity level that controls E30 spread within the population (*19*). The high susceptibility is reflected by the high number of infected infants, who would have no immunity, and adults whom we hypothesize have no or waning immunity. However, another possibility is that the appearance of several, potentially convergent, amino acid substitutions in VP1 among different E30 groups represented a form of antigenic selection for escape from existing population immunity. The clustering of sites under selection in the BC loop associated with receptor interactions is consistent with this possibility. Serologic studies are required to explore this hypothesis.

As shown in the original description of the upsurge (*2*), a high percentage of cases showed central nervous system involvement, particularly for infants 0–3 months of age and adults 25–44 years of age, consistent with previous observations (*2*,*30*–*32*). The distribution of E30 clades varied among age groups; most infections in infants <3 months of age were caused by G1 and symptomatology varied from fever to acute flaccid paralysis. However, analysis of the clinical correlates was limited by incomplete reporting; only 30% of reported E30 infections included history of symptoms, which hampered comparisons of clinical presentation between different clades. Another limitation is the retrospective study design and bias toward severe and hospitalized cases.

Using Nextstrain, we visualized the various categories of demographic and clinical data, clades, and RFs. Unfortunately, G5 could not be inferred due to possible recombination events within the fragment. Complete reconstruction of E30 temporal events with geographic spread was hampered by the inevitably uneven sampling and testing in different years by the different contributing countries.

This study underpins the strength of the ENPEN consortium, which brings together virologists, public health experts, infectious disease doctors, and scientists across Europe to enable rapid detection and early warning through standardized surveillance. Previous studies using Nextstrain with 2 EV-D68 datasets have shown the value of combining demographic and phylogenetic analysis, both as retrospective (*33*) and real-time analysis (*34*). The E30 dataset and the 2 EV-D68 datasets (*33*,*34*) available on Nextstrain represent large nonpolio enterovirus datasets that support real-

time tracking of viruses over time and across countries. These data are of considerable value in infection containment and control of nonpolio enteroviruses.

Differences in surveillance systems, case definitions, and sample selection between institutes and countries make standardized data collection difficult, particularly for denominator data. The differences in data collection proved to be a limitation in our study, and the extent of the circulation of the different strains remains unknown. The emergence and disappearance of viruses from different clades across the years suggests that some form of predictive modeling might be undertaken if data were standardized and provided in real-time through networks such as ENPEN.

The mechanisms underlying the complex cyclic pattern of E30 and other enteroviruses and the effects of changing population immunity, antigenic changes, virus diversification, pathogenicity, and recombination need further exploration. The emergence of different enterovirus types, and their associated periodicities and population penetrance, might be driven by multiple mechanisms (*19*), making outbreak and upsurge prediction complex. However, continued structured surveillance can clarify enterovirus circulation and evolution and slowly aid in unraveling the complex nature of enteroviruses.

Acknowledgments

We thank all clinicians and technical staff participating in the European enterovirus/poliovirus surveillance programs in all participating laboratories. We also thank the following for echovirus diagnostics and sequencing: Sanela Numanovic (Norwegian Institute of Public Health Oslo, Norway); Maria Evangelidou (Hellenic Pasteur Institute, Athens, Greece); Maria Takacs (National Public Health Center, Budapest, Hungary); Elenor Hauzenberger and Anna-Lena Hansen (PHAS, Sweden); Elena Pariani and Sandro Binda (University of Milan, Italy); Darja Duh, Nika Volmajer and Katja Soršak (National laboratory of health, environment and food, Centre for medical microbiology, Slovenia).

The study was supported by the Ministry of Health, Welfare and Sport, the Netherlands as part of the EV surveillance program of the National Institute for Public Health and the Environment; the European Union Horizon 2020 research and innovation program (COMPARE grant no. 643476 from Aristotle University of Thessaloniki, Greece); the Wellcome Trust (grant no. ISSF204826/Z/16/Z); the Belgian National Reference Center for Enteroviruses from the RIZIV/INAMI (National Institute for Health and Disability Insurance); and the HONOURs Horizon 2020 Marie Sklodowska-Curie Training Network (grant no. 721367).

About the Author

Dr. Benschop is a molecular virologist. Her primary research interests include molecular epidemiology and evolution of enteroviruses and hepatitis B virus. She also is involved in pathogenesis studies of enteroviruses on organoids.

References

1. Oberste MS, Maher K, Kennett ML, Campbell JJ, Carpenter MS, Schnurr D, et al. Molecular epidemiology and genetic diversity of echovirus type 30 (E30): genotypes correlate with temporal dynamics of E30 isolation. J Clin Microbiol. 1999;37:3928–33. https://doi.org/10.1128/JCM.37.12.3928-3933.1999
2. Broberg EK, Simone B, Jansa J, The EU/EEA Member State C. Upsurge in echovirus 30 detections in five EU/EEA countries, April to September, 2018. Euro Surveill. 2018;23:1800537. PubMed https://doi.org/10.2807/1560-7917.ES.2018.23.44.1800537
3. Likosky WH, Emmons RW, Davis LE, Thompson RSUS. U.S. cases in 1968: epidemiology of echovirus 30 aseptic meningitis. Health Serv Rep. 1972;87:638–42. https://doi.org/10.2307/4594622
4. Trallero G, Casas I, Tenorio A, Echevarria JE, Castellanos A, Lozano A, et al. Enteroviruses in Spain: virological and epidemiological studies over 10 years (1988–97). Epidemiol Infect. 2000;124:497–506. https://doi.org/10.1017/S0950268899003726
5. Trallero G, Avellon A, Otero A, De Miguel T, Perez C, Rabella N, et al. Enteroviruses in Spain over the decade 1998–2007: virological and epidemiological studies. J Clin Virol. 2010;47:170–6. PubMed https://doi.org/10.1016/j.jcv.2009.11.013
6. Milia MG, Cerutti F, Gregori G, Burdino E, Allice T, Ruggiero T, et al. Recent outbreak of aseptic meningitis in Italy due to Echovirus 30 and phylogenetic relationship with other European circulating strains. J Clin Virol. 2013;58:579–83. PubMed https://doi.org/10.1016/j.jcv.2013.08.023
7. Palacios G, Casas I, Cisterna D, Trallero G, Tenorio A, Freire C. Molecular epidemiology of echovirus 30: temporal circulation and prevalence of single lineages. J Virol. 2002;76:4940–9. https://doi.org/10.1128/JVI.76.10.4940-4949.2002
8. Cabrerizo M, Echevarria JE, González I, de Miguel T, Trallero G. Molecular epidemiological study of HEV-B enteroviruses involved in the increase in meningitis cases occurred in Spain during 2006. J Med Virol. 2008;80:1018–24. https://doi.org/10.1002/jmv.21197
9. Bailly JL, Mirand A, Henquell C, Archimbaud C, Chambon M, Charbonne F, et al. Phylogeography of circulating populations of human echovirus 30 over 50 years: nucleotide polymorphism and signature of purifying selection in the VP1 capsid protein gene. Infect Genet Evol. 2009;9:699–708. PubMed https://doi.org10.1016/j.meegid.2008.04.009
10. Lukashev AN, Ivanova OE, Eremeeva TP, Gmyl LV. Analysis of echovirus 30 isolates from Russia and new independent states revealing frequent recombination and reemergence of ancient lineages. J Clin Microbiol. 2008;46:665–70. https://doi.org/10.1128/JCM.02386-06
11. McWilliam Leitch EC, Cabrerizo M, Cardosa J, Harvala H, Ivanova OE, Kroes AC, et al. Evolutionary dynamics and temporal/geographical correlates of recombination in the

human enterovirus echovirus types 9, 11, and 30. J Virol. 2010;84:9292–300. https://doi.org/10.1128/JVI.00783-10
12. Savolainen C, Hovi T, Mulders MN. Molecular epidemiology of echovirus 30 in Europe: succession of dominant sublineages within a single major genotype. Arch Virol. 2001;146:521–37. https://doi.org/10.1007/s007050170160
13. Savolainen-Kopra C, Paananen A, Blomqvist S, Klemola P, Simonen ML, Lappalainen M, et al. A large Finnish echovirus 30 outbreak was preceded by silent circulation of the same genotype. Virus Genes. 2011;42:28–36. https://doi.org/10.1007/s11262-010-0536-x
14. Mirand A, Henquell C, Archimbaud C, Peigue-Lafeuille H, Bailly JL. Emergence of recent echovirus 30 lineages is marked by serial genetic recombination events. J Gen Virol. 2007;88:166–76. https://doi.org/10.1099/vir.0.82146-0
15. Wenner HA, Harmon P, Behbehani AM, Rouhandeh H, Kamitsuka PS. The antigenic heterogeneity of type 30 echoviruses. Am J Epidemiol. 1967;85:240–9. https://doi.org/10.1093/oxfordjournals.aje.a120687
16. Lema C, Torres C, Van der Sanden S, Cisterna D, Freire MC, Gómez RM. Global phylodynamics of echovirus 30 revealed differential behavior among viral lineages. Virology. 2019;531:79–92. https://doi.org/10.1016/j.virol.2019.02.012
17. McWilliam Leitch EC, Bendig J, Cabrerizo M, Cardosa J, Hyypiä T, Ivanova OE, et al. Transmission networks and population turnover of echovirus 30. J Virol. 2009;83:2109–18. https://doi.org/10.1128/JVI.02109-08
18. Bailly JL, Mirand A, Henquell C, Archimbaud C, Chambon M, Regagnon C, et al. Repeated genomic transfers from echovirus 30 to echovirus 6 lineages indicate co-divergence between co-circulating populations of the two human enterovirus serotypes. Infect Genet Evol. 2011;11:276–89. PubMed https://doi.org/10.1016/j.meegid.2010.06.019
19. Pons-Salort M, Grassly NC. Serotype-specific immunity explains the incidence of diseases caused by human enteroviruses. Science. 2018;361:800–3. https://doi.org/10.1126/science.aat6777
20. Huang YP, Lin TL, Lin TH, Wu HS. Antigenic and genetic diversity of human enterovirus 71 from 2009 to 2012, Taiwan. PLoS One. 2013;8:e80942. https://doi.org/10.1371/journal.pone.0080942
21. van der Sanden SM, Koen G, van Eijk H, Koekkoek SM, de Jong MD, Wolthers KC. Prediction of protection against Asian Enterovirus 71 outbreak strains by cross-neutralizing capacity of serum from Dutch donors, The Netherlands. Emerg Infect Dis. 2016;22:1562–9. https://doi.org/10.3201/eid2209.151579
22. Savolainen-Kopra C, Al-Hello H, Paananen A, Blomqvist S, Klemola P, Sobotova Z, et al. Molecular epidemiology and dual serotype specificity detection of echovirus 11 strains in Finland. Virus Res. 2009;139:32–8. https://doi.org/10.1016/j.virusres.2008.10.003
23. Benschop K, Molenkamp R, van der Ham A, Wolthers K, Beld M. Rapid detection of human parechoviruses in clinical samples by real-time PCR. J Clin Virol. 2008;41:69–74. https://doi.org/10.1016/j.jcv.2007.10.004
24. Nix WA, Oberste MS, Pallansch MA. Sensitive, seminested PCR amplification of VP1 sequences for direct identification of all enterovirus serotypes from original clinical specimens. J Clin Microbiol. 2006;44:2698–704. https://doi.org/10.1128/JCM.00542-06
25. Kumar S, Stecher G, Tamura K. MEGA7: Molecular Evolutionary Genetics Analysis version 7.0 for bigger datasets. Mol Biol Evol. 2016;33:1870–4. https://doi.org/10.1093/molbev/msw054
26. Katoh K, Misawa K, Kuma K, Miyata T. MAFFT: a novel method for rapid multiple sequence alignment based on fast Fourier transform. Nucleic Acids Res. 2002;30:3059–66. https://doi.org/10.1093/nar/gkf436
27. Nguyen LT, Schmidt HA, von Haeseler A, Minh BQ. IQ-TREE: a fast and effective stochastic algorithm for estimating maximum-likelihood phylogenies. Mol Biol Evol. 2015;32:268–74. https://doi.org/10.1093/molbev/msu300
28. Sagulenko P, Puller V, Neher RA. TreeTime: Maximum-likelihood phylodynamic analysis. Virus Evol. 2018;4:vex042. https://doi.org/10.1093/ve/vex042
29. Cabrerizo M, Trallero G, Simmonds P. Recombination and evolutionary dynamics of human echovirus 6. J Med Virol. 2014;86:857–64. https://doi.org/10.1002/jmv.23741
30. Helfand RF, Khan AS, Pallansch MA, Alexander JP, Meyers HB, DeSantis RA, et al. Echovirus 30 infection and aseptic meningitis in parents of children attending a child care center. J Infect Dis. 1994;169:1133–7. https://doi.org/10.1093/infdis/169.5.1133
31. Holmes CW, Koo SS, Osman H, Wilson S, Xerry J, Gallimore CI, et al. Predominance of enterovirus B and echovirus 30 as cause of viral meningitis in a UK population. J Med Virol. 2016;81:90–3. https://doi.org/10.1016/j.jcv.2016.06.007
32. Janes VA, Minnaar R, Koen G, van Eijk H, Dijkman-de Haan K, Pajkrt D, et al. Presence of human non-polio enterovirus and parechovirus genotypes in an Amsterdam hospital in 2007 to 2011 compared to national and international published surveillance data: a comprehensive review. Euro Surveill. 2014;19:20964. PubMed https://doi.org/10.2807/1560-7917.es2014.19.46.20964
33. Dyrdak R, Mastafa M, Hodcroft EB, Neher RA, Albert J. Intra- and interpatient evolution of enterovirus D68 analyzed by whole-genome deep sequencing. Virus Evol. 2019;5:vez007. https://doi.org/10.1093/ve/vez007
34. Midgley SE, Benschop K, Dyrdak R, Mirand A, Bailly JL, Bierbaum S, et al. Co-circulation of multiple enterovirus D68 subclades, including a novel B3 cluster, across Europe in a season of expected low prevalence, 2019/20. Euro Surveill. 2020;25:1900749. PubMed https://doi.org/10.2807/1560-7917.ES.2020.25.2.1900749

Corresponding author: Kimberley S.M. Benschop, Centre for Infectious Disease Research, Diagnostics and Laboratory Surveillance, Centre for Infectious Disease Control, National Institute for Public Health and the Environment, PO Box 1, 3720 BA Bilthoven, the Netherlands; email: kim.benschop@rivm.nl

Twenty-Year Public Health Impact of 7- and 13-Valent Pneumococcal Conjugate Vaccines in US Children

Matt Wasserman, Ruth Chapman, Rotem Lapidot, Kelly Sutton, Desmond Dillon-Murphy, Shreeya Patel, Erica Chilson, Vincenza Snow, Raymond Farkouh, Stephen Pelton

Pneumococcal conjugate vaccines (PCVs) have been used in the United States since 2000. To assess the cumulative 20-year effect of PCVs on invasive pneumococcal disease (IPD) incidence among children <5 years of age, we analyzed Active Bacterial Core Surveillance data, conducted a literature review, and modeled expected and observed disease. We found that PCVs have averted >282,000 cases of IPD, including ≈16,000 meningitis, ≈172,000 bacteremia, and ≈55,000 bacteremic pneumonia cases. In addition, vaccination has prevented 97 million healthcare visits for otitis media, 438,914–706,345 hospitalizations for pneumonia, and 2,780 total deaths. IPD cases declined 91%, from 15,707 in 1997 to 1,382 in 2019. Average annual visits for otitis media declined 41%, from 78 visits/100 children before PCV introduction to 46 visits/100 children after PCV13 introduction. Annual pneumonia hospitalizations declined 66%–79%, from 110,000–175,000 in 1997 to 37,000 in 2019. These findings confirm the substantial benefits of PCVs for preventing IPD in children.

Before 2000, children <2 years of age had the highest incidence of invasive pneumococcal diseases (IPDs) such as bacteremia, meningitis, or other infection of a normally sterile site (*1*). Researchers estimated that, in the United States, annual IPD incidence was 165 cases/100,000 children <12 months of age and 203 cases/100,000 children 12–23 months of age (*1*). Until the United States began a universal 7-valent pneumococcal conjugate vaccine (PCV7) immunization program for children in 2000, *Streptococcus pneumoniae* was the leading cause of bacterial meningitis (*1*). *S. pneumoniae* was also the most common bacterial cause of community-acquired pneumonia and otitis media (OM) in young children. Furthermore, in the 1990s, concerns emerged regarding the growing number of pneumococcal isolates with reduced susceptibility to first- and second-line antimicrobial drugs (*1*).

PCV7 was the first pneumococcal conjugate vaccine (PCV) approved for use in children <2 years of age in the United States. Pneumococcal polysaccharide vaccines, which preceded PCVs, are not immunogenic in children <2 years of age (*1*,*2*). PCV7 overcame the challenge of poor immunogenicity among infants and young children through conjugation technology; it was introduced into the US infant immunization schedule in 2000, providing direct protection against several serotypes of invasive and noninvasive pneumococcal disease (*3*,*4*). PCV7 protects against the *S. pneumoniae* serotypes responsible for >80% of IPD cases among children in North America (i.e., serotypes 4, 6B, 9V, 14, 18C, 19F, and 23F) (*1*,*4*). In 2010, PCV13, a vaccine providing protection against 6 additional serotypes (i.e., serotypes 1, 3, 5, 6A, 19A, and 7F), was approved in the United States, partially because of increasing incidence of serotypes not covered by PCV7 (*1*,*4*).

Clinical trial data suggested that PCV7 would be effective against IPD, OM, and according to a post-hoc analysis, pneumonia (*5*). The efficacy of PCV7 (and later PCV13) against all forms of pneumococcal disease was greater than expected, partly because of indirect protection gained through herd immunity (*6*–*8*). The United States was the first country to introduce a PCV program for infants and, during the transition to PCV13, recommended the largest catch-up program for children <5 years of age who had been vaccinated with PCV7 (*9*). After an initially slow uptake limited by constrained supply, the United States has achieved consistently high (>80%) 3-dose

Author affiliations: Pfizer Inc., New York, New York, USA (M. Wasserman, E. Chilson, V. Snow, R. Farkouh); Evidera Market Access Ltd, London, UK (R. Chapman, K. Sutton, D. Dillon-Murphy, S. Patel); Boston University School of Medicine, Boston, Massachusetts, USA (R. Lapidot, S. Pelton)

DOI: https://doi.org/10.3201/eid2706.204238

coverage since 2005 (*10*). It is one of a few countries continuing to use the licensed 4-dose schedule (*10*). A 2020 review demonstrated that PCVs were the only vaccines approved by the US Food and Drug Administration that had no postmarketing safety-related label modifications (*11*).

We quantified the decrease of IPD incidence associated with 20 years of PCV use in the United States. First, we conducted a literature review to inform a decision analytic model. The model estimated the 20-year cumulative effects associated with the PCV program on cases of IPD, OM, and hospitalizations for pneumonia among children <5 years of age in the United States.

Methods

The US Centers for Disease Control and Prevention (CDC) began the Active Bacterial Core Surveillance (ABCs) program to monitor invasive *S. pneumoniae* infections in 1997 (*12*). Although this resource provides invaluable data for assessing IPD, it does not include data on noninvasive syndromes. We conducted a literature review to identify and synthesize published data on all pneumococcal diseases during the past 20 years. We used data from these publications to model the effects of PCVs on childhood pneumococcal disease (*13*).

Literature Review

To estimate the amount of pneumococcal disease averted in the United States, we conducted a systematic literature review in accordance with the Preferred Reporting Items for Systematic Reviews and Meta-Analyses guidelines (*14*). After defining the research questions, data sources, search strategies, and selection criteria (Appendix Tables 1–5, https://wwwnc.cdc.gov/EID/article/27/6/20-4238-App1.pdf), we conducted electronic searches of the PubMed and Embase (https://www.embase.com) databases and manual searches of the gray literature, CDC website (https://www.cdc.gov), and reference lists of 7 published literature reviews (*15*–*21*) (Appendix Figure 1). This study describes only references used for input data or to validate our findings.

Calculations and Outputs

We developed a model using Excel (Microsoft, https://www.microsoft.com) to calculate the national numbers of cases, healthcare visits, hospitalizations, and deaths caused by pneumococcal infection among children <5 years of age during the 20 years after PCV introduction. We used published incidences of each syndrome (i.e., meningitis, bacteremia, bacteremic pneumonia/empyema, sepsis, and other) and relevant population data to calculate the number of cases averted by vaccination. We conducted these calculations for the pre-PCV (i.e., 1997–1999), PCV7 (i.e., 2000–2009), and PCV13 (i.e., 2010–2019) eras (Appendix Figure 2). Although we attributed decreasing illness and deaths to the direct effects of PCVs, policy changes or other interventions also might have contributed to the reduction of disease.

We calculated average incidences for each of the 3 described time periods. Because variance measures were unavailable, we performed all calculations as point estimates. We assumed that without PCVs, disease incidence would have remained constant. We calculated the estimated effect of PCV7 by comparing the difference in reported incidence between the pre-PCV and PCV7 eras; likewise, we considered the effect of PCV13 to be the difference in incidence between the pre-PCV and PCV13 eras. We estimated the incremental effect of including the additional serotypes in PCV13 by comparing incidence between the PCV7 and PCV13 eras. Because factors such as program rollout and uptake delayed the achievement of population-level equilibrium, we excluded the transition years 2000–2001 from the calculation of the effect of PCV7. Similarly, we excluded 2010 from the calculation of the effect of PCV13 (Tables 1, 2; Figures 1, 2). However, we included these years in the analysis of the 20-year aggregate effect of PCV use.

We calculated the number of expected IPD cases without PCV7 as the average incidence during 1997–1999 × population size in each year. We calculated the expected IPD cases if PCV7 vaccination had continued but PCV13 had not been introduced as the average incidence during 2002–2009 × population size in each year. We stratified each calculation by age.

In addition, we calculated total IPD cases averted by PCVs as the difference between the cases expected without vaccination and the cases observed during 2002–2019 (Table 1; Appendix Figure 2). We also calculated the incremental effect of PCV13 versus PCV7 as the difference between cases expected if PCV7 use had continued after 2010 and cases observed during 2011–2019.

To calculate the number of expected IPD deaths without PCVs, we multiplied the observed case-fatality ratio from 1997–2000 (cumulative deaths divided by the cumulative cases in that period) by the expected number of cases from 2000–2019 (*12*). We considered deaths averted by PCVs to be the difference between expected deaths if PCVs had never been introduced and the observed deaths in this period.

Case numbers and incidences were not available for OM and noninvasive pneumonia because they are nonnotifiable diseases. As a result, we calculated the expected ambulatory healthcare visit rates for OM and hospitalization rates for pneumonia without PCVs using the same method as for IPD cases averted.

Model Inputs

We conducted our calculations using population data from the US Census Bureau (*22*) (Appendix Table 6). We considered data on total IPD incidence, distribution of vaccine serotypes, syndrome distribution, healthcare visits for OM, and pneumonia incidence.

We obtained national estimates for IPD cases, rates, and syndromes among children <1, 1–<2, and 2–4 years of age from ABCs reports (*12*) (Appendix Table 7). Because data for 2018 and 2019 were not available, we assumed these years to have the same rates as 2017. We used these data to calculate the average incidence for each of the 2 pre-PCV13 eras (Appendix Table 8).

We also obtained national estimates for overall annual incidence of IPD caused by PCV13 serotypes

Table 1. Invasive pneumococcal disease cases and deaths averted by pneumococcal conjugate vaccines, United States, 1997–2019*

	No. observed, by age, y				No. expected, by age, y				No. averted	
Year	<1	1	2–4	Overall	<1	1	2–4	Overall	Annual	Cumulative
No. cases										
1997	5,360	6,712	3,635	15,707	5,360	6,712	3,635	15,707	NA	NA
1998	6,220	7,630	4,286	18,136	6,220	7,630	4,286	18,136	NA	NA
1999	6,176	7,772	3,837	17,785	6,176	7,772	3,837	17,785	NA	NA
2000	5,699	6,139	3,469	15,306	6,053	7,428	3,883	17,364	2,057	2,057
2001	2,099	2,645	3,143	7,887	6,299	7,539	3,852	17,689	9,802	11,860
2002	1,521	1,261	1,813	4,596	6,202	7,830	3,866	17,899	13,304	25,164
2003	1,642	1,405	1,530	4,577	6,241	7,696	3,936	17,874	13,296	38,460
2004	1,485	1,253	1,454	4,192	6,301	7,730	3,983	18,013	13,821	52,281
2005	1,450	1,419	1,467	4,336	6,286	7,796	4,019	18,101	13,765	66,046
2006	1,366	1,458	1,395	4,219	6,344	7,767	4,019	18,130	13,911	79,956
2007	1,680	1,296	1,560	4,537	6,511	7,826	4,036	18,372	13,835	93,792
2008	1,517	1,284	1,420	4,221	6,487	8,018	4,057	18,562	14,341	108,133
2009	1,485	1,309	1,654	4,449	6,284	7,975	4,099	18,358	13,910	122,043
2010	1,352	1,051	1,611	4,014	6,204	7,726	4,144	18,074	14,060	136,103
2011	832	670	1,012	2,515	6,221	7,755	4,109	18,085	15,571	151,674
2012	616	541	712	1,870	6,163	7,777	4,068	18,009	16,139	167,813
2013	578	595	814	1,988	6,171	7,709	4,036	17,916	15,928	183,741
2014	629	407	754	1,790	6,208	7,721	4,033	17,963	16,173	199,914
2015	733	513	610	1,856	6,253	7,769	4,031	18,053	16,198	216,112
2016	526	212	167	906	6,208	7,828	4,032	18,068	17,163	233,275
2017	452	314	625	1,391	6,112	7,770	4,052	17,934	16,544	249,818
2018	446	309	627	1,382	6,040	7,651	4,061	17,752	16,370	266,188
2019	446	309	627	1,382	6,040	7,651	4,061	17,752	16,370	282,558
No. deaths										
1997	151	34	17	202	151	34	17	202	NA	NA
1998	78	47	NA	126	78	47	NA	126	NA	NA
1999	29	45	60	134	29	45	60	134	NA	NA
2000	130	113	57	301	138	137	64	340	39	39
2001	22	46	57	125	103	66	36	204	79	118
2002	31	NA	32	62	101	68	36	205	143	261
2003	42	21	21	85	102	67	37	206	121	382
2004	39	48	20	107	103	67	37	207	101	483
2005	38	9	38	85	103	68	37	208	123	605
2006	29	9	47	85	104	68	37	209	124	729
2007	37	9	9	56	106	68	37	212	156	885
2008	37	NA	18	55	106	70	38	214	158	1,043
2009	36	9	9	54	103	70	38	210	156	1,199
2010	10	9	9	28	101	67	38	207	179	1,378
2011	38	19	28	85	102	68	38	207	123	1,501
2012	9	9	NA	19	101	68	38	206	187	1,688
2013	9	9	38	57	101	67	37	205	149	1,837
2014	19	NA	9	28	101	67	37	206	178	2,014
2015	10	9	19	38	102	68	37	207	170	2,184
2016	18	4	12	35	101	68	37	207	172	2,356
2017	28	19	38	85	100	68	38	205	120	2,476
2018	16	7	28	51	99	67	38	203	152	2,628
2019	16	7	28	51	99	67	38	203	152	2,780

*Values are rounded to the nearest whole numbers. NA, not applicable.

Table 2. Cases of invasive pneumococcal disease averted by PCV13, United States, 1997–2019*

	No. observed			No. expected			Cumulative cases averted		Difference in
Year	All	PCV13 serotypes	Non-PCV13 serotypes	All	PCV13 serotypes	Non-PCV13 serotypes	All	PCV13 serotypes	non-PCV13 serotype cases†
1997	15,543	14,439	1,104	15,543	14,439	1,104	NA	NA	NA
1998	18,136	16,848	1,288	18,136	16,848	1,288	NA	NA	NA
1999	17,785	16,839	945	17,785	16,839	945	NA	NA	NA
2000	15,306	13,808	1,498	17,364	16,178	1,186	2,057	2,369	−312
2001	7,887	6,561	1,325	17,689	16,481	1,208	11,860	12,289	−429
2002	4,596	3,109	1,487	17,899	16,677	1,223	25,164	25,857	−693
2003	4,577	2,743	1,834	17,874	16,653	1,221	38,460	39,767	−1,307
2004	4,192	2,374	1,818	18,013	16,783	1,230	52,281	54,175	−1,894
2005	4,336	2,589	1,747	18,101	16,864	1,236	66,046	68,450	−2,405
2006	4,219	2,592	1,627	18,130	16,891	1,238	79,956	82,750	−2,793
2007	4,537	3,019	1,518	18,372	17,118	1,255	93,792	96,848	−3,057
2008	4,221	2,635	1,585	18,562	17,294	1,268	108,133	111,507	−3,374
2009	4,449	3,037	1,412	18,358	17,104	1,254	122,043	125,575	−3,532
2010	4,014	2,626	1,388	18,074	16,839	1,235	136,103	139,788	−3,685
2011	2,515	805	1,710	18,085	16,850	1,235	151,674	155,833	−4,160
2012	1,870	400	1,470	18,009	16,779	1,230	167,813	172,213	−4,400
2013	1,988	397	1,591	17,916	16,692	1,224	183,741	188,508	−4,766
2014	1,790	397	1,392	17,963	16,736	1,227	199,914	204,846	−4,932
2015	1,856	398	1,457	18,053	16,820	1,233	216,112	221,268	−5,156
2016	906	398	507	18,068	16,834	1,234	233,275	237,703	−4,429
2017	1,391	398	993	17,934	16,709	1,225	249,818	254,015	−4,197
2018	1,382	396	986	17,752	16,539	1,213	266,188	270,158	−3,970
2019	1,382	396	986	17,752	16,539	1,213	282,558	286,302	−3,744

*Values are rounded to the nearest whole numbers. NA, not applicable; PCV13, 13-valent pneumococcal conjugate vaccine.
†Negative values indicate greater number observed than would be expected.

among children <5 years of age during 1998–2016 (*12*) (Appendix Table 9). We assumed rates during 2017–2019 to be the same as 2016; we weighted these rates by population distribution during those years. We calculated pre-PCV era distribution of PCV13 and non-PCV13 serotypes as the average of 1997–1999 distributions (Appendix Table 10). To ensure serotype incidences were consistent with the observed trends of all IPDs, we imputed PCV13 serotype incidence in 1997 using weighted proportions (i.e., by population size in each age group) and percent change (Appendix Table 9) during 1997–1998. We calculated expected cases caused by PCV13 and non-PCV13 serotypes by multiplying the average pre-PCV era serotype distributions to the total expected number of annual IPD cases. Although the measurement of all averted cases of IPD includes the effects of vaccination and serotype replacement, the measurement of cases averted by PCV13 indicates only the reduction in vaccine type IPDs.

We obtained the proportions of meningitis, bacteremia, bacteremic pneumonia/empyema, sepsis, and other infections among children <2 and 2–4 years of age with IPD from additional unpublished data provided by CDC (*12*; R. Gierke, CDC, pers. comm., 2017 Nov 7) (Appendix Table 11). We assumed the distributions in 1997–1999 to be the same as 2000.

We used the mean rate of ambulatory care visits for OM in children <2, 2–<5, and <5 years of age overall provided by Zhou et al. (*23*; Appendix Table 12, Figure 3). Zhou et al. (*23*) described PCV eras using similar definitions: the pre-PCV period during 1997–1998, the PCV7 period during 2002–2009, and the PCV13 period during 2011–2013 (Appendix Table 13). We assumed the rates in 2014–2019 to be the same as 2013 (Appendix Table 12).

The data sources used various classifications and definitions of pneumonia. The types of data reported also varied widely, including measurements such as ambulatory visits, hospitalizations, index cases in inpatients, and estimates of cases of community-acquired pneumonia. No single data source covered the combined PCV7 and PCV13 periods, nor estimated the incidence of only noninvasive pneumococcal pneumonia. Because hospitalization data represent more severe cases with the largest use of healthcare costs and resources and because no consistent data for ambulatory/outpatient visits for pneumonia during the entire study period were available, we considered only hospitalized cases of pneumonia in this analysis. We used data on hospitalization for pneumonia from multiple sources. We obtained data for the pre-PCV relative to PCV7 eras from Simonsen et al. (*24*), Foote et al. (*25*), and Grijalva et al. (*26*), and for the PCV7 relative to PCV13 period from a 2005–2014 study (*27*) and Tong et al. (*28*). In addition, we used estimates of the difference in hospitalization incidences during the PCV7

period from Grijalva et al. (*23*). We estimated the total number of hospitalizations averted by PCVs using the expected hospitalization data from all sources for 1997–2019 (Appendix Table 14).

Validation

During the literature review, we identified appropriate references against which to validate the consistency of our findings. We did not identify other sources of national multistate data for IPD comparable to the ABCs dataset. Black et al. (*30*) reported Kaiser Permanente data from northern California about the effect of PCV7 on disease epidemiology in children and adults, whereas Yildirim et al. (*31*) reported serotype-specific invasive capacity among children in Massachusetts after PCV introduction (Appendix Figure 4).

We used a large national claims database (*32*), a commercial claims and encounters database (*33*), and Ray et al. (*34*) to validate our OM estimates. We wanted to validate our pneumonia estimates with respect to different types of cases and definitions used by various data sources; however, because of constraints on data availability, we limited our validation to hospitalized cases of all-cause pneumonia. Because of the variation in reporting of pneumonia data, we did not identify any alternate sources for an appropriate validation of our analysis.

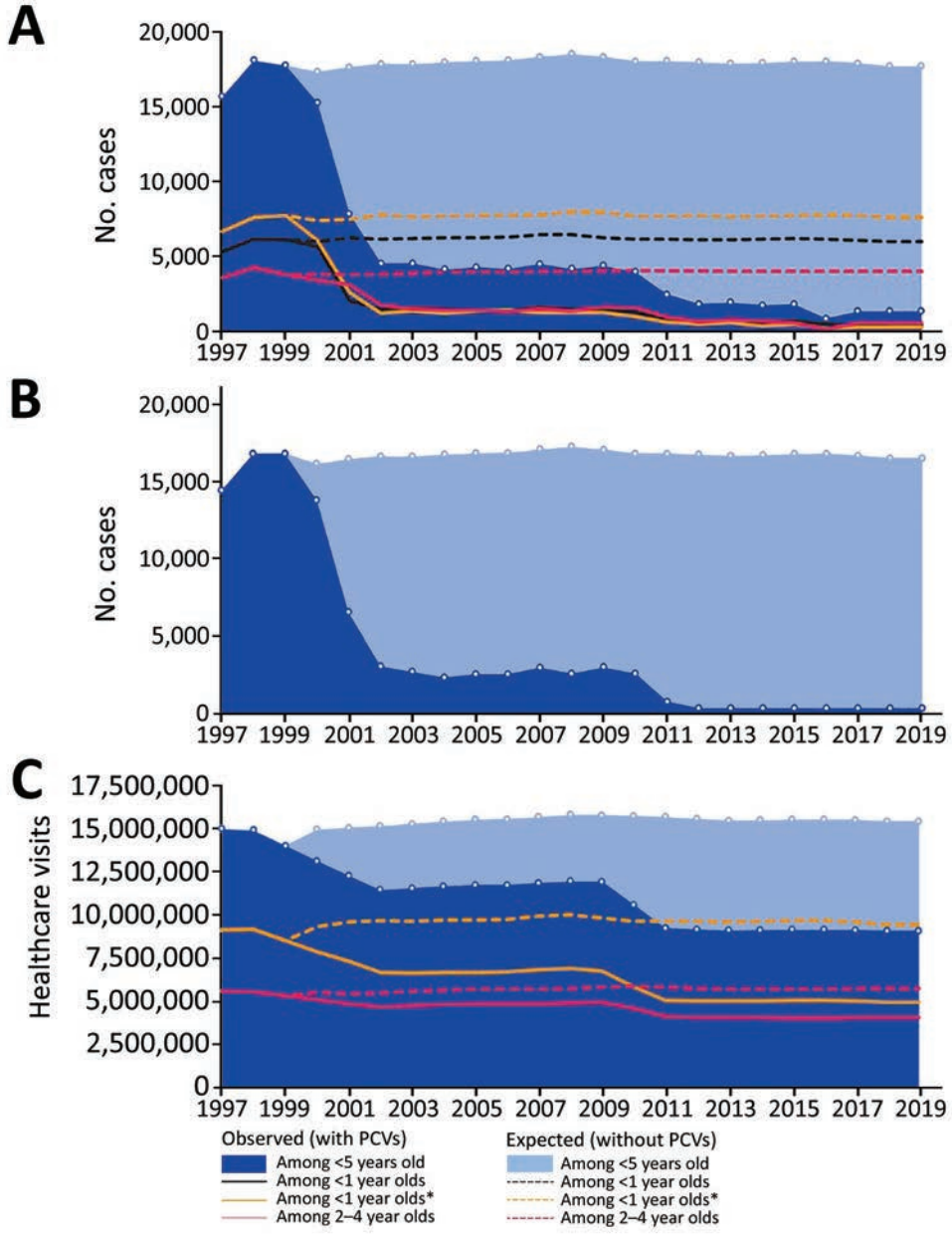

Figure 1. Effects of PCVs on invasive pneumococcal disease (IPD) and otitis media among children <5 years of age, United States, 1997–2019 (*8*,*12*). A) Cases of IPD. B) Cases of IPD caused by 13-valent PCV serotypes. C) Healthcare visits for otitis media. The United States approved 7-valent PCV in 2000 and 13-valent PCV in 2010. Asterisk (*) indicates that for data on healthcare visits for otitis media, age range is 0–2 years. PCV, pneumococcal conjugate vaccine.

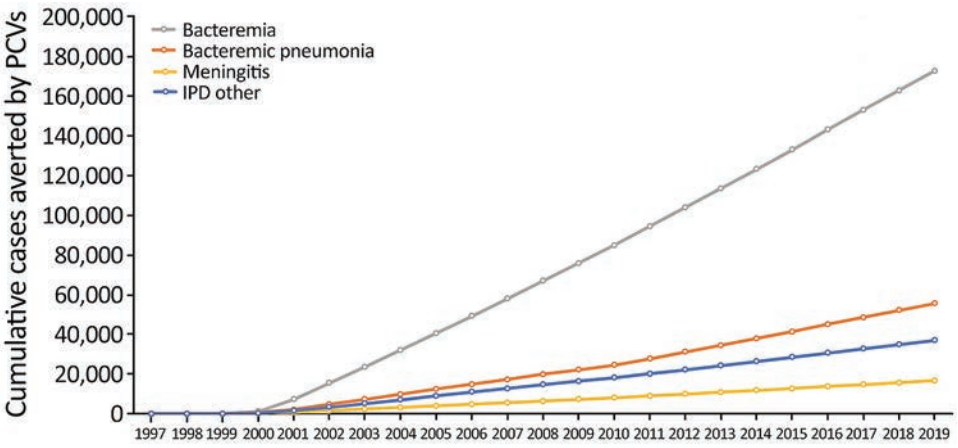

Figure 2. Effects of PCVs on different syndromes of IPD in children <5 years of age, United States, 1997–2019. The United States approved 7-valent PCV in 2000 and 13-valent PCV in 2010. IPD, invasive pneumococcal disease; PCV, pneumococcal conjugate vaccine.

Results

IPD

Among children <5 years of age, the annual number of IPD cases decreased from ≈16,000–18,000 during 1997–1999 to 1,382 in 2019 (Table 1; Figure 1, panel A). We estimated that PCVs averted a cumulative 282,558 cases of IPD during this timeframe. Of those averted cases, we estimated that 146,455 were prevented by PCV13 during 2010–2019. Among children <5 years of age, annual deaths caused by IPD decreased from 126–202 during 1997–1999 (Table 1) to 85 in 2019. We estimated that PCVs prevented a total of 2,780 deaths during this timeframe, including 1,402 deaths prevented by PCV13 during 2010–2019.

The overall IPD incidences in the input ABCs data were generally higher than in the sources used for validation. However, the ABCs and the Kaiser Permanente data (*30*) reflected similar overall trends for the pre-PCV and PCV7 eras; the ABCs and data from Yildrim et al. (*31*) reflected similar overall trends for the PCV7 and PCV13 eras. The differences were probably caused by variations in reporting and patient groups between data sources; the ABCs data are more nationally representative and therefore more generalizable than the population described by Black et al. (*30*).

We observed a decrease in IPD-related deaths after the introduction of PCV7; however, we could not identify whether this trend existed during the pre-PCV period because of limited data (Table 1). Pulido et al. (*35*) described a declining IPD mortality rate during 1990–2005, supporting the ABCs data and indicating that deaths were already decreasing before the introduction of PCVs. Reductions in smoking rates and implementation of laws regarding smoking in public places, shifts from inpatient to outpatient care settings, improved treatments, and varying case definitions might have also contributed to the declining trend.

We estimated that during 2000–2019, PCVs prevented 172,778 cases of bacteremia; 55,532 cases of bacteremic pneumonia and empyema; 16,660 cases of meningitis; and 37,017 cases of other forms of IPD (Figure 2). IPD cases caused by PCV13 serotypes decreased from 14,439 cases in 1997 to 396 in 2019 (Table 2; Figure 1, panel B). During 2000–2019, PCVs are estimated to have averted 286,302 IPD cases caused by vaccine serotypes. During this period, IPD cases caused by non-PCV13 serotypes increased slightly, consistent with modest serotype replacement.

OM Healthcare Visits

The average rate of OM visits among children <5 years of age declined from 78/100 to 46/100 children per year from the pre-PCV (1997–1998) to the PCV13 era (2011–2013). In other words, these visits declined by 39%, from 15,000,483 in 1997 to 9,112,727 in 2019

Table 3. Estimated average incidence of otitis media cases and visits averted by PCVs, United States, 1997–2019*

Measure	1997–1999	2000–2009	2010–2019	Cumulative
Average incidence of visits per 100 children	78	59	46	NA
Expected visits†	NA	154,269,900	155,511,917	309,781,817
Estimated visits	NA	119,429,938	93,025,190	212,455,128
Visits averted‡	NA	34,839,962	62,486,726	97,326,688

*Values are rounded to the nearest whole numbers. PCV7 was approved for use in the United States in 2000; PCV13 was approved for use in the United States in 2010. NA, not applicable; PCV, pneumococcal conjugate vaccine; PCV7, 7-valent PCV; PCV13, 13-valent PCV.
†Visits expected if PCVs had not been introduced.
‡Calculated by subtracting estimated visits from expected visits.

Table 4. Estimated total hospitalized cases of pneumonia averted by PCVs, United States, 1997–2019*

	Estimated hospitalizations					
	Observed, with vaccination		Expected without vaccination		Total hospitalizations averted	
Time period	Minimum	Maximum	Minimum	Maximum	Minimum	Maximum
Pre-PCV era: 1997–1999	NA	NA	339,474	525,675	NA	NA
PCV7 era: 2000–2009†	959,543	1,336,673	597,479	1,822,591	222,611	490,043‡
PCV13 era: 2010–2019§	382,182		598,484		216,303	

*PCV7 was approved for use in the United States in 2000; PCV13 was approved for use in the United States in 2010. NA, not applicable; PCV, pneumococcal conjugate vaccine; PCV7, 7-valent PCV; PCV13, 13-valent PCV.
†Averted hospitalizations during PCV7 era are shown as the difference within the same study with minimum based on Simonson et. al. (*24*) and maximum based on Grijalva et al (*29*) (Appendix Table 14, https;//wwwnc.cdc.gov/EID/article/27/6/20-4238-App1.pdf).
‡Grijalva et al (*29*) reported a change in hospitalization rate; as a result, no observed and expected values were generated.
§Values based on calculations using a single data point.

(Figure 1, panel C). We estimated that PCVs averted a cumulative 97,326,688 OM-related healthcare visits (Table 3).

The overall visit numbers in the input data (*23*) were generally lower than in the sources used for validation (*32*–*34*), but the overall trends for the pre-PCV and PCV7 eras were comparable. The differences might have been caused by varying database populations, because Zhou et al. (*23*) used national data whereas Marom et al. (*32*) and Tong et al. (*33*) mainly considered privately insured patients who might have been more likely to seek care. Therefore, the estimates from Zhou et al. (*23*) are probably more representative on a national level.

Pneumonia Hospitalizations

Annual pneumonia hospitalizations in children <5 years of age declined from 113,116–175,420 in 1997 to 37,882 in 2019. We estimated that PCVs averted a cumulative 438,914–706,345 pneumonia hospitalizations, including 216,303 cases caused by PCV13 serotypes, during the 20 years after PCV introduction in the United States (Table 4).

Discussion

Vaccines, especially PCVs, are lifesaving and cost-effective public health interventions. At the time PCV7 was introduced in the United States, pneumococcal disease caused high rates of death and disease among infants. Despite conservative findings from the clinical trials (*8*), public health officials and healthcare professionals were optimistic about the potential of PCVs to prevent pneumococcal disease. We conducted a literature review and modeling analysis to quantify the effects of PCVs on pneumococcal disease incidence among children <5 years of age, a population at higher risk for IPD and therefore the focus of IPD prevention efforts (*36*). Our analysis demonstrated that PCVs have averted >282,000 cases of IPD and 2,780 associated deaths, with reductions across various IPD syndromes. Since their introduction in 2000, PCVs have averted >430,000 pneumonia hospitalizations and >97,000,000 OM-related healthcare visits.

We could not find data on all OM cases; our analysis instead measured ambulatory care visits using input data from Zhou et al. (*23*). However, because not all children with OM receive treatment through ambulatory care visits, our findings probably underestimate the true effects of PCVs on OM incidence. The annual number of OM visits declined from 78 visits/100 to 46 visits/100 children from the pre-PCV era (1997–1999) to PCV13 era (2010–2019); this 41% decline exceeds the original predictions based on early clinical trial data (*8*). Vaccination is probably the main direct contributor to this reduction; however, vaccination also might have had indirect effects such as changes in the disease definition or clinical coding of OM, as well as changes in prescribing patterns of antimicrobial drugs, which might affect healthcare use. Although not all cases of OM prompt healthcare visits, even mild illnesses might require family members to take time from work to care for their children, further reducing productivity and quality of life in ways not reflected by this metric (*37*).

Because we could not find data on noninvasive pneumonia, we combined multiple data sources to compare pneumonia hospitalizations during the study period. These data are probably underestimates of the true effect of PCVs because most pneumonia cases among children <5 years of age do not require hospitalization.

The overall findings are impressive but nevertheless conservative. We did not consider the direct benefits of reduced sequelae among children >5 years of age nor adults; we also did not consider indirect benefits such as herd immunity, reduced use of antimicrobial drugs and other healthcare resources, increased educational attainment, or improved parental productivity. In addition, we did not analyze data on common but less resource-intensive manifestations of *S. pneumoniae* such as conjunctivitis (*38*,*39*). Finally, this analysis does not reflect PCVs' effects on antimicrobial resistance

(*17*), although preventing infection through vaccination reduces the need for antimicrobial treatment (*40*).

In agreement with other studies (*40*,*41*), we found that IPD cases caused by PCV13 serotypes declined while the number of cases caused by non-PCV13 serotypes slightly increased, reflecting modest serotype replacement. PCVs have been used in the United States longer than in any other country. Because of the large quantity of available data, we conducted a literature review to independently identify appropriate references for model inputs and validation. However, although the available data were extensive, it was not comprehensive. As a result, this research was limited by the lack of a single data source for pneumonia and OM incidences during the entire study period, prompting us to impute values for years when no data were available. In addition, because IPD is a notifiable disease but OM and pneumonia are not, we can only estimate PCVs' true effects on OM and pneumonia incidence using alternative metrics such as ambulatory care visits and hospitalizations. Furthermore, healthcare providers do not usually distinguish the causative bacteria of pneumonia and OM cases, which poses difficulties in analyzing serotype distributions. Finally, we could not find alternative national-level IPD data for the validation analysis, prompting us to compare our results with trends from smaller regions.

CDC and the Advisory Committee on Immunization Practices have recommended the use of PCVs in a national infant immunization program since 2000 (*1*). Our model used available data to quantify the effects of PCV7 and PCV13 on pneumococcal disease burden among children in the United States. Our results demonstrate the effectiveness of PCVs in preventing illness and death among children <5 years of age.

About the Author

Mr. Wasserman is Director of Health Economics and Outcomes Research at Pfizer Inc. His research interests include cost-effectiveness and transmission dynamic modeling of vaccine-preventable diseases.

This work was supported by Pfizer Inc. Pfizer participated in study design; data identification, synthesis, and analysis; manuscript writing; and the decision to submit the article for publication.

E.C., V.S., R.F., and M.W. are employees and stockholders of Pfizer Inc. R.C., K.S., D.D.M., and S.P. are employees of Evidera Market Access Ltd, a healthcare research firm that provides consulting and other research services to pharmaceutical and related organizations. In these salaried positions, they work with a variety of companies and are explicitly precluded from accepting any payment or honoraria directly from them for services rendered. Evidera received payment from Pfizer Inc. for collaboration on this project and article.

S.P. and R.L. received consulting fees from Pfizer, Inc. for their participation in study design and data analysis for this project. S.P. and R.L. are also recipients of investigator-initiated research awards (i.e., Surveillance of Pneumococcal Colonization and Invasive pneumococcal Disease reveals Shift in Prevalent Carriage Serotypes in Massachusetts' Children to Relatively Low Invasiveness [*31*], Evaluation of Serotype 3 Strains collected from Massachusetts' Children 2002–2019) from Pfizer (through Boston Medical Center) relevant to pneumococcal vaccine studies. S.P. has also received honoraria from Merck, Pfizer, and Sanofi for participation in pneumococcal advisory boards and Data and Safety Monitoring Board.

References

1. Advisory Committee on Immunization Practices. Preventing pneumococcal disease among infants and young children. Recommendations of the Advisory Committee on Immunization Practices (ACIP). MMWR Recomm Rep. 2000;49:1–35.
2. Douglas RM, Paton JC, Duncan SJ, Hansman DJ. Antibody response to pneumococcal vaccination in children younger than five years of age. J Infect Dis. 1983;148:131–7. https://doi.org/10.1093/infdis/148.1.131
3. Centers for Disease Control and Prevention. Direct and indirect effects of routine vaccination of children with 7-valent pneumococcal conjugate vaccine on incidence of invasive pneumococcal disease—United States, 1998–2003. MMWR Morb Mortal Wkly Rep. 2005;54:893–7.
4. Kellner JD, Vanderkooi OG, MacDonald J, Church DL, Tyrrell GJ, Scheifele DW. Changing epidemiology of invasive pneumococcal disease in Canada, 1998–2007: update from the Calgary-area *Streptococcus pneumoniae* research (CASPER) study. Clin Infect Dis. 2009;49:205–12. https://doi.org/10.1086/599827
5. Black S, Shinefield H, Fireman B, Lewis E, Ray P, Hansen JR,et al.; Northern California Kaiser Permanente Vaccine Study Center Group. Efficacy, safety and immunogenicity of heptavalent pneumococcal conjugate vaccine in children. Pediatr Infect Dis J. 2000;19:187–95. https://doi.org/10.1097/00006454-200003000-00003
6. Haber M, Barskey A, Baughman W, Barker L, Whitney CG, Shaw KM, et al. Herd immunity and pneumococcal conjugate vaccine: a quantitative model. Vaccine. 2007; 25:5390–8. https://doi.org/10.1016/j.vaccine.2007.04.088
7. Miller E, Andrews NJ, Waight PA, Slack MP, George RC. Herd immunity and serotype replacement 4 years after seven-valent pneumococcal conjugate vaccination in England and Wales: an observational cohort study. Lancet Infect Dis. 2011;11:760–8. https://doi.org/10.1016/S1473-3099(11)70090-1
8. Eskola J. Polysaccharide-based pneumococcal vaccines in the prevention of acute otitis media. Vaccine. 2000;19:S78–82. https://doi.org/10.1016/S0264-410X(00)00283-8

9. Strutton DR, Farkouh RA, Rubin JL, McGarry LJ, Loiacono PM, Klugman KP, et al. Modeling the impact of the 13-valent pneumococcal conjugate vaccine serotype catch-up program using United States claims data. BMC Infect Dis. 2012;12:175. https://doi.org/10.1186/1471-2334-12-175
10. Centers for Disease Control and Prevention. National, state, and urban area vaccination coverage among children aged 19–35 months—United States, 2005. MMWR Morb Mortal Wkly Rep. 2006;55:988–93.
11. Tau N, Yahav D, Shepshelovich D. Postmarketing safety of vaccin es approved by the U.S. Food and Drug Administration: a cohort study. Ann Intern Med. 2020;173:445–9. https://doi.org/10.7326/M20-2726
12. Centers for Disease Control and Prevention. Active Bacterial Core surveillance: surveillance reports. 2020 [cited 2020 Feb 29]. https://www.cdc.gov/abcs/reports-findings/surv-reports.html
13. Chapman R, Sutton K, Dillon-Murphy D, Patel S, Hilton B, Farkouh R, et al. Ten year public health impact of 13-valent pneumococcal conjugate vaccination in infants: a modelling analysis. Vaccine. 2020;38:7138–45. https://doi.org/10.1016/j.vaccine.2020.08.068
14. Moher D, Liberati A, Tetzlaff J, Altman DG; PRISMA Group. Preferred reporting items for systematic reviews and meta-analyses: the PRISMA statement. PLoS Med. 2009; 6:e1000097. https://doi.org/10.1371/journal.pmed.1000097
15. Loo JD, Conklin L, Fleming-Dutra KE, Deloria Knoll M, Park DE, Kirk J, et al. Systematic review of the effect of pneumococcal conjugate vaccine dosing schedules on prevention of pneumonia. Pediatr Infect Dis J. 2014;33:S140–51. https://doi.org/10.1097/INF.0000000000000082
16. Tan TQ. Pediatric invasive pneumococcal disease in the United States in the era of pneumococcal conjugate vaccines. Clin Microbiol Rev. 2012;25:409–19. https://doi.org/10.1128/CMR.00018-12
17. Tin Tin Htar M, van Den Biggelaar AHJ, Sings H, Ferreira G, Moffatt M, Hall-Murray C, et al. The impact of routine childhood immunization with higher-valent pneumococcal conjugate vaccines on antimicrobial-resistant pneumococcal diseases and carriage: a systematic literature review. Expert Rev Vaccines. 2019;18:1069–89. https://doi.org/10.1080/14760584.2019.1676155
18. Myint TTH, Madhava H, Balmer P, Christopoulou D, Attal S, Menegas D, et al. The impact of 7-valent pneumococcal conjugate vaccine on invasive pneumococcal disease: a literature review. Adv Ther. 2013;30:127–51. https://doi.org/10.1007/s12325-013-0007-6
19. Aliberti S, Kaye KS. The changing microbiologic epidemiology of community-acquired pneumonia. Postgrad Med. 2013;125:31–42. https://doi.org/10.3810/pgm.2013.11.2710
20. Arguedas A, Soley C, Abdelnour A. Prevenar experience. Vaccine. 2011;29:C26–34. https://doi.org/10.1016/j.vaccine.2011.06.104
21. Balsells E, Guillot L, Nair H, Kyaw MH. Serotype distribution of *Streptococcus pneumoniae* causing invasive disease in children in the post-PCV era: a systematic review and meta-analysis. PLoS One. 2017;12:e0177113. https://doi.org/10.1371/journal.pone.0177113
22. United States Census Bureau. Population and housing unit estimates tables. 2020 [cited 2020 Mar 1]. https://www.census.gov/programs-surveys/popest/data/tables.html
23. Zhou X, de Luise C, Gaffney M, Burt CW, Scott DA, Gatto N, et al. National impact of 13-valent pneumococcal conjugate vaccine on ambulatory care visits for otitis media in children under 5 years in the United States. Int J Pediatr Otorhinolaryngol. 2019;119:96–102. https://doi.org/10.1016/j.ijporl.2019.01.023
24. Simonsen L, Taylor RJ, Young-Xu Y, Haber M, May L, Klugman KP. Impact of pneumococcal conjugate vaccination of infants on pneumonia and influenza hospitalization and mortality in all age groups in the United States. MBio. 2011;2:e00309–10. https://doi.org/10.1128/mBio.00309-10
25. Foote EM, Singleton RJ, Holman RC, Seeman SM, Steiner CA, Bartholomew M, et al. Lower respiratory tract infection hospitalizations among American Indian/Alaska Native children and the general United States child population. Int J Circumpolar Health. 2015;74:29256. https://doi.org/10.3402/ijch.v74.29256
26. Grijalva CG, Griffin MR, Nuorti JP, Walter ND; Centers for Disease Control and Prevention. Pneumonia hospitalizations among young children before and after introduction of pneumococcal conjugate vaccine—United States, 1997–2006. MMWR Morb Mortal Wkly Rep. 2009;58:1–4.
27. Lessa FC, Spiller MT, Soda E, Weinberger D, Griffin MR, Grijalva CG, et al. Impact of introduction of infant vaccination with 13-valent pneumococcal conjugate vaccine (PCV13) on pneumonia and invasive pneumococcal disease (IPD) hospitalizations in the United States, 2005–2014. Presented at: 11th International Symposium on Pneumococci and Pneumococcal Diseases; 2018 Apr 15–19: Melbourne, Victoria, Australia.
28. Tong S, Amand C, Kieffer A, Kyaw MH. Trends in healthcare utilization and costs associated with pneumonia in the United States during 2008–2014. BMC Health Serv Res. 2018;18:715. https://doi.org/10.1186/s12913-018-3529-4
29. Grijalva CG, Nuorti JP, Arbogast PG, Martin SW, Edwards KM, Griffin MR. Decline in pneumonia admissions after routine childhood immunisation with pneumococcal conjugate vaccine in the USA: a time-series analysis. Lancet. 2007;369:1179–86. https://doi.org/10.1016/S0140-6736(07)60564-9
30. Black S, Shinefield H, Baxter R, Austrian R, Elvin L, Hansen J, et al. Impact of the use of heptavalent pneumococcal conjugate vaccine on disease epidemiology in children and adults. Vaccine. 2006;24:S79–S80. https://doi.org/10.1016/j.vaccine.2005.01.132
31. Yildirim I, Little BA, Finkelstein J, Lee G, Hanage WP, Shea K, et al; the Massachusetts Dept. of Public Health. Surveillance of pneumococcal colonization and invasive pneumococcal disease reveals shift in prevalent carriage serotypes in Massachusetts' children to relatively low invasiveness. Vaccine. 2017;35:4002–9. https://doi.org/10.1016/j.vaccine.2017.05.077
32. Marom T, Tan A, Wilkinson GS, Pierson KS, Freeman JL, Chonmaitree T. Trends in otitis media-related health care use in the United States, 2001–2011. JAMA Pediatr. 2014;168:68–75. https://doi.org/10.1001/jamapediatrics.2013.3924
33. Tong S, Amand C, Kieffer A, Kyaw MH. Trends in healthcare utilization and costs associated with acute otitis media in the United States during 2008–2014. BMC Health Serv Res. 2018;18:318. https://doi.org/10.1186/s12913-018-3139-1
34. Ray GT, Pelton SI, Klugman KP, Strutton DR, Moore MR. Cost-effectiveness of pneumococcal conjugate vaccine: an update after 7 years of use in the United States. Vaccine. 2009;27:6483–94. https://doi.org/10.1016/j.vaccine.2009.08.045
35. Pulido M, Sorvillo F. Declining invasive pneumococcal disease mortality in the United States, 1990–2005. Vaccine.

2010;28:889–92. https://doi.org/10.1016/j.vaccine.2009.10.121
36. World Health Organization. Estimated Hib and pneumococcal deaths for children under 5 years of age, 2000. 2014 [cited 2020 Mar 1]. https://www.who.int/immunization/monitoring_surveillance/burden/estimates/Pneumo_hib/en
37. Shiri T, Khan K, Keaney K, Mukherjee G, McCarthy ND, Petrou S. Pneumococcal disease: a systematic review of health utilities, resource use, costs, and economic evaluations of interventions. Value Health. 2019;22:1329–44. https://doi.org/10.1016/j.jval.2019.06.011
38. Dagan R, Ben-Shimol S, Greenberg D, Givon-Lavi N. A prospective, population-based study to determine the incidence and bacteriology of bacterial conjunctivitis in children <2 years following PCV7/PCV13 sequential implementation. Clin Infect Dis. 2020 Mar 4 [Epub ahead of print]. https://doi.org/10.1093/cid/ciaa197
39. Porat N, Benisty R, Givon-Lavi N, Trefler R, Dagan R. The impact of pneumococcal conjugate vaccines on carriage of and disease caused by *Streptococcus pneumoniae* serotypes 6C and 6D in southern Israel. Vaccine. 2016;34:2806–12. https://doi.org/10.1016/j.vaccine.2016.04.043
40. Jansen KU, Anderson AS. The role of vaccines in fighting antimicrobial resistance (AMR). Hum Vaccin Immunother. 2018;14:2142–9. https://doi.org/10.1080/21645515.2018.1476814
41. Wantuch PL, Avci FY. Current status and future directions of invasive pneumococcal diseases and prophylactic approaches to control them. Hum Vaccin Immunother. 2018;14:2303–9. https://doi.org/10.1080/21645515.2018.1470726

Address for correspondence: Matt Wasserman, Vaccines Outcomes & Evidence, Pfizer Inc., 235 42nd Street, New York, NY 10017, USA; email: matt.wasserman@pfizer.com

Precision Tracing of Household Dengue Spread Using Inter- and Intra-Host Viral Variation Data, Kamphaeng Phet, Thailand

Irina Maljkovic Berry,[1] Melanie C. Melendrez,[1] Simon Pollett, Katherine Figueroa, Darunee Buddhari, Chonticha Klungthong, Ananda Nisalak,[2] Michael Panciera, Butsaya Thaisomboonsuk, Tao Li, Tyghe G. Vallard, Louis Macareo, In-Kyu Yoon, Stephen J. Thomas, Timothy Endy, Richard G. Jarman

Dengue control approaches are best informed by granular spatial epidemiology of these viruses, yet reconstruction of inter- and intra-household transmissions is limited when analyzing case count, serologic, or genomic consensus sequence data. To determine viral spread on a finer spatial scale, we extended phylogenomic discrete trait analyses to reconstructions of house-to-house transmissions within a prospective cluster study in Kamphaeng Phet, Thailand. For additional resolution and transmission confirmation, we mapped dengue intra-host single nucleotide variants on the taxa of these time-scaled phylogenies. This approach confirmed 19 household transmissions and revealed that dengue disperses an average of 70 m per day between households in these communities. We describe an evolutionary biology framework for the resolution of dengue transmissions that cannot be differentiated based on epidemiologic and consensus genome data alone. This framework can be used as a public health tool to inform control approaches and enable precise tracing of dengue transmissions.

Dengue virus (DENV) causes an estimated 390 million infections each year, 96 million of which manifest as clinical disease (*1*). Dengue is endemic in >100 countries. An estimated 3.9 billion persons are at risk for infection, of which 75% reside in the Asia-Pacific region (*2*). DENV control approaches are best informed by granular spatial epidemiology of these viruses, and investigators have long tried to understand the landscape of DENV dynamics and spread. Robust public health surveillance and rigorous academic research have enabled tracking of clinical infections to understand changing demographics, populations at risk, hyperendemicity, transmission, disease severity, and virus dispersal patterns within and across human populations (*3*–*10*). With the advent of sequencing technologies, single-gene and whole-genome DENV analyses have complemented case-based and serologic surveillance and enabled further insights into DENV epidemic dynamics and spread, disease severity, introductions and emergence of novel variants, tracking of DENV transmissions, and monitoring of viral diversity and evolution (*11*–*17*). Investigations of DENV infection dynamics, from the scales of countries and districts down to the city, village, school, and house level, have been performed to describe the patterns and predictors of DENV spread (*7*,*9*,*11*–*13*,*18*–*21*). These studies have enabled many novel insights into DENV transmission and contributed to improved prediction, prevention, and control strategies. Such studies have also emphasized a key limitation of DENV genomic epidemiology: reconstructing transmission chains between households and within households is typically not possible, even though resolving DENV spread at such fine scales would offer major relevance to public health response.

Consensus whole-genome sequences, which are typically used in genomic studies of viral epidemics and spread, typically have insufficient variability to distinguish between infecting strains sampled within 2 weeks of each other, especially if closely sampled in space (*22*). This limitation might lead to unresolved

Author affiliations: Walter Reed Army Institute of Research Viral Diseases Branch, Silver Spring, Maryland, USA (I. Maljkovic Berry, M.C. Melendrez, S. Pollett, K. Figueroa, M. Panciera, T. Li, T.G. Vallard, R.G. Jarman); Armed Forces Research Institute of Medical Sciences, Bangkok, Thailand (D. Buddhari, C. Klungthong, A. Nisalak, B. Thaisomboonsuk, L. Macareo); International Vaccine Institute, Seoul, South Korea (I.-K. Yoon); Upstate Medical University of New York Department of Medicine, Syracuse, New York, USA (S.J. Thomas, T. Endy)

DOI: https://doi.org/10.3201/eid2706.204323

[1]These authors contributed equally to this article.

[2]Deceased.

and low confidence phylogenetic tree topologies, unable to discern the exact relationships between closely related taxa, and thus unable to provide confident insights into the fine scale viral transmission patterns. In the case of DENV, the use of consensus env-gene or whole-genome data has been able to resolve fine-scale clustering of cases within 200 m but has not been able to determine discrete inter-household or within-household transmissions (*12*).

DENV, like other RNA viruses, exists within a host as a population of distinct viral variants. Together, these viral variants are usually assembled into a single viral consensus genome, but separately, they hold additional intra-host variant sequence information that can provide further resolution. Transmission of within-host minor viral variants, existing at low frequencies and therefore often not reflected in the consensus genome, has been reported for several different viral pathogens (*23*–*27*). An increasing number of studies have used this additional genetic information to confirm viral transmissions, and new tools that use both intra- and inter-host genetic variation have been developed for inference of transmission chains and transmission directions (*23*,*26*,*28*,*29*). We designed a study that explicitly measures the patterns of DENV minor variant transmission in a natural epidemic setting, to resolve more spatially explicit viral transmissions.

We investigated the level of transmission reconstruction granularity that can be achieved for DENV by analyzing 410 DENV whole genomes sampled from human and vector specimens in Kamphaeng Phet, Thailand, and sequenced by using next-generation sequencing techniques. A combination of Bayesian analyses and intra-host single nucleotide variant (iSNV) information, along with temporal and spatial epidemiologic data, enabled fine-scale reconstructions of transmission chains and house-to-house spread, as well as genomic confirmation of within-household transmission clusters. This approach could be used in public health to reconstruct fine-scale DENV transmissions and support dengue control and prevention efforts.

Methods

Ethics Statement

The samples used in this study were virus isolates, which originated from samples collected in a study described in Thomas et al. (*30*), per the protocols approved by the institutional review boards (IRBs) of the Thai Ministry of Public Health, Walter Reed Army Institute of Research, and the State University of New York's Upstate Medical University. The IRBs of the University of California, Davis, University of Rhode Island, and University at Buffalo established relying agreements with the Walter Reed Army Institute of Research IRB. All isolates were deidentified, and this study's research team had no access to identification codes.

Prospective Cluster Study and Data Collection

The prospective cluster study method has been described previously (*30*). In brief, the study was conducted in Kamphaeng Phet Province (Kamphaeng Phet), Thailand. A blood sample was obtained from patients admitted to Kamphaeng Phet Hospital with a diagnosis of an acute dengue infection; if positive for DENV by PCR, the virus was isolated with low passage number in C6/36 cell culture or in Toxorhynchites splendens mosquito followed by C6/36 (Appendix Table 1, https://wwwnc.cdc.gov/EID/article/27/6/20-4323-App1.pdf). Patients who were DENV PCR-positive were considered index case-patients for a cluster investigation. The exact house locations of index case-patients was mapped through a geographic information system by using a global positioning system unit. Homes within 100–200 m radius around the index case-patient's house were screened for additional cases in persons with a history of temperature ≥38°C within past 7 days, and a blood sample was collected from those persons who agreed to participate in the study. DENV reverse transcription PCR, viral isolation, and IgM/IgG ELISA were performed on all collected specimens.

Sequencing, Genome Assembly, and Minor Variant Determination

We sequenced all DENV isolates to obtain whole genomes during 2009–2012 by using the Roche 454 FLX system (Roche, https://www.roche.com), the Illumina MiSeq next-generation sequencing system (Illumina, https://www.illumina.com), and, for gap filling, the Applied Biosystems 3130 Sanger sequencing platform (ThermoFisher Scientific, https://www.thermofisher.com). We generated consensus genomes by using the in-house developed ngs_mapper reference mapping pipeline and manually curated to ensure consensus accuracy (*31*). We submitted all consensus genomes to GenBank (accession nos. MN448597–9006). In addition to consensus, we screened all DENV serotype 1 (DENV-1) MiSeq-derived assemblies that had a minimum 1,000× depth of coverage throughout the genome for presence of iSNVs. We excluded DENV serotype 2 (DENV-2) genomes from iSNV analyses because some of the

samples did not have enough coverage, mainly because of being sequenced by using Roche 454. iSNVs were called if they were present at a conservative frequency of ≥1% (minimum Phred of 30) called by Lofreq, a base caller previously shown to confidently call DENV iSNVs at this frequency (*32*,*33*). Additional manual iSNV curation removed variants present because of primer induced error, certain types of sequencing error, and strand bias higher than what was observed in confident iSNVs from each genome. In addition, we manually removed iSNVs that were consistently present at either ends of the reads from the analyses because these iSNVs have previously been shown to be spurious (*33*).

Phylodynamic Analyses

We combined genomes for DENV serotypes 1–4 with GenBank references and aligned by using MUSCLE 3.8 (*34*). We used jModeltest2 to determine the best fit model of nucleotide substitution (*35*) and constructed maximum-likelihood trees for whole-genome sequence data from all 4 serotypes by using PhyML 3.0 with aLRT node support (*36*). Because discrete phylogeographic analyses to infer the household-scale geographic histories of all sampled viruses were computationally unfeasible, we subselected datasets from DENV maximum-likelihood trees that had most taxa sampled from households in the same subdistrict and had sufficient temporal structure (root-tip regression r>0.7) as determined by Temp-Est (*37*). Using these criteria, we selected 2 DENV-1 sublineages and 3 DENV-2 sublineages to infer the inter-household patterns of DENV spread by using BEAST 1.8.4 (*38*). We excluded DENV serotypes 3 and 4 (DENV-3 and DENV-4) from further analyses because of the weak sublineage temporal structure and limited clade sizes by individual subdistricts of Kamphaeng Phet. For each sublineage analysis, we geotagged time-stamped taxa by household as discrete traits. The final Markov Chain Monte Carlo chains had lengths required for statistical convergence, as indicated by effective sample size values >200 for key evolutionary parameters (Appendix Table 2). We constructed and annotated maximum clade credibility (MCC) trees by using TreeAnnotator. We manually inspected the MCC trees to determine probable and possible inter-household transmissions events. We defined probable inter-household transmissions as origin household being directly ancestral to the destination household and both geographic states supported with a probability ≥0.8 and plotted all iSNVs onto the resulting MCC trees. We used this information for confirmation or detection of between-household spread and for detection of within-household connections.

iSNV Distribution Statistical Analyses

We compared the frequency of infected case-patients sharing iSNVs within a transmission cluster with the frequency of samples sharing these iSNVs across the sublineage by using χ^2 test. We defined a transmission cluster as the smallest cluster of genomes in the MCC tree containing all the genomes sharing the same iSNVs. Thus, if shared iSNVs are distributed across the tree in an unrelated manner, the transmission cluster they define will be large and will not differ significantly from the whole sublineage tree. A significant difference from the sublineage tree would thus indicate iSNV clustering not expected by chance. In addition, we compared pairwise p-distances between the genomes sharing iSNVs with 100 replicates of pairwise p-distances between 3 randomly sampled genomes across the 2 DENV-1 sublineages by using an in-house developed script. Using 3 genome pairwise distance in the randomized dataset was determined on the basis of the average size of the significant transmission clusters, as defined by χ^2 test.

Linear Regression Analyses of Transmission-Pair Distance over Sampling Time

We performed crude estimates of the dispersal rate of DENV at an inter-household scale by a univariate linear regression model, which fit the difference in sampling days between confirmed transmission pairs as a single predictor, and distance between confirmed transmission pairs as the outcome variable. We fit this model by using all transmission pairs confirmed by the Bayesian consensus analysis, the iSNV analyses, or both. We used the coefficient of determination (R^2) to determine model fit and the coefficient point estimate and 95% CI to estimate the average rate of DENV spread between households. We performed all regression analyses by using Stata 15.1 (StataCorp, https://www.stata.com).

Results

PCR-confirmed DENV cases in Kamphaeng Phet during 2010–2012 were dominated by DENV-2, with cocirculating DENV-1 and DENV-3. DENV-4 was detected to a small degree in 2011 and 2012 (Appendix Figure 1). A total of 410 DENV whole genomes were sequenced from samples collected during 2009–2012 in Kamphaeng Phet, including 100 DENV-1, 233 DENV-2, 64 DENV-3, and 13 DENV-4 genomes. The unique design of the Kamphaeng Phet cluster study provided an opportunity to investigate fine-scale

DENV spread between households in Kamphaeng Phet. Analyses of DENV serotype 1–4 phylogenetic trees identified 2 DENV-1 and 3 DENV-2 sublineages with adequate temporal structure and sufficient sample size for Bayesian analyses. DENV consensus genomes from DENV-1 and DENV-2 sublineages geotagged by their respective household of sampling were used as discrete traits for Bayesian ancestral state reconstructions. We confirmed between-household direct connections with high probability in 4 DENV-1 cases and 3 DENV-2 cases, in 7 different subdistricts of Kamphaeng Phet (Table 1; Appendix Figures 2, 3).

These analyses also indicated many weakly supported inter-household transmissions (probability of origin or destination household <0.8) (Appendix Table 3). This finding highlighted the limited spatial and temporal resolution that is obtained by consensus genome data only, and prompted an analysis of iSNVs.

We determined iSNVs for each of the DENV-1 genomes and plotted on the sublineage MCC trees of DENV-1. Closely related viruses in the MCC phylogenies often shared the same iSNV spectra, including ≥2 shared iSNVs (Appendix, Appendix Figure 2). In total, this analysis revealed 3 transmission clusters that involved shared iSNVs, revealing direct DENV spread between households that were 20–800 m apart and involved a total of 11 persons (Table 2; Figure). The clusters contained persons from both separate and same households. The transmission confirmed by BEAST in transmission cluster 3 consisted of viruses with very little within-host variation (0 and 1 iSNV) (Appendix Figure 2), indicating that close transmission connections were not always characterized by iSNV sharing. In addition, this transmission cluster showed how iSNVs can be lost in bigger clusters over time, such as the loss of 1853-C/T iSNV in 1 person from household TN18H023 (Appendix Figure 2). Thus, the presence of ≥2 shared iSNVs indicated fine-scale virus transmission connections, whereas absence of ≥2 shared iSNVs did not imply lack of shared connection.

We examined the distribution of sampling times within the 3 iSNV-confirmed transmission clusters to further characterize DENV transmission dynamics at this fine scale. All persons from transmission cluster 3 were sampled within the same day, suggesting that they were inoculated at about the same time (Table 2). The close household proximity and time of infection, together with identical virus consensus sequence and shared minor variants, would indicate infection from a common source and simultaneous minor variant spread to ≥6 different persons. In contrast, persons from transmission cluster 1 were sampled ≈2 weeks apart, a period that exceeds the known DENV incubation period and would have required transmission and preservation of minor variants through several bottlenecks across the invertebrate–vertebrate transmission cycle. By comparison, household transmissions confirmed by BEAST analyses only (no shared iSNVs) were on average 19 days apart (Table 1).

Finally, we used the transmission events confirmed by either Bayesian consensus sequence analysis (Table 1) or iSNV analyses (Table 2) to estimate the rate of DENV spread within subdistricts and between households. We performed a linear regression of transmission-pair distances over sampling time, with a model fit indicating a strikingly linear relationship ($R^2 = 0.91$) and a regression coefficient indicating that DENV disperses an average of 70 m/day (95% CI 54–86 m/day) within subdistricts in this study population (Appendix Figure 4).

Discussion

Dengue control approaches are best informed by granular characterization of the spatial epidemiology of these viruses. Even in active surveillance cohorts, however, resolution of transmissions on a household-scale is hampered by the limited geographic resolution permitted by case count, serologic, or even DENV whole-genome consensus sequence data. Our study

Table 1. Summary of probable household-to-household spread of dengue virus inferred by consensus genomes, Kamphaeng Phet, Thailand, 2009–2012

Serotype and sublineage	Subdistrict	Origin household† (location probability)	Destination household (location probability)	Approximate distance, m	Sampling time difference, d
DENV-1, sublineage 1	LD	LD02H075 (1.0)	LD01H116 (1.0)	1,400	19
DENV-1, sublineage 1	SK	SK06H346 (0.99)	SK06H370 (1.0)	3,000	29
DENV-1, sublineage 7	TN	TN18H021 (0.88)	TN18H014 (1.0)	80	1
DENV-1, sublineage 7	NC	NC06H057 (0.82)	NC06H407 (1.0)	30	0, 14‡
DENV-2, sublineage 2	NB	NB06H055 (0.80)	NB06H084 (1.0)	800	13
DENV-2, sublineage 2	NP	NP08H080 (0.82)	NP08H044 (1.0)	180	0
DENV-2, sublineage 6	SK	SK06H790 (0.99)	SK06H485 (1.0)	3,000	49

*LD, Lan Dokmai; NB, Na Bo Kham; NC, Nakhon Chum; NP, Nong Pling; SK, Sa Kaeo; TN, Thep Nakhon.
†Households are described by their subdistrict, cluster, and house numbers, such that the first 2 letters denote subdistrict, the next 2-digit number denotes cluster, and an H followed by a 3-digit number denotes house number.
‡Two persons from the donor household were dengue virus–positive 2 weeks apart.‡

Table 2. Dengue virus serotype 1 transmission clusters revealed by minor variant sharing, Kamphaeng Phet, Thailand, 2009–2012*

Sublineage	Transmission cluster	Household†	No. persons	Sampling dates	Approximate distance, m
1	1	LD02H056	1	2011 Jun 2	800
		LD10H001	1	2011 Jun 16	
7	2	ST05H002	2	2011 Nov 28–29	0
7	3	TN18H023	3	2012 Oct 10	0–80
		TN18H019	1	2012 Oct 10	
		TN18H021‡	2	2012 Oct 10	
		TN18H014‡	1	2012 Oct 9	

*LD, Lan Dokmai; ST, Song Tham; TN, Thep Nakhon.
†Households are described by their subdistrict, cluster, and house numbers, such that the first 2 letters denote subdistrict, the next 2-digit number denotes cluster, and an H followed by a 3-digit number denotes house number.
‡House or individual involvement with the transmission cluster also confirmed by BEAST analyses (*38*).

leveraged a prospective active surveillance study with dense case sampling over 4 years, 410 whole-genome sequences and a unique combination of within-host and between-host viral genome variability to reconstruct transmission of DENV at unprecedented spatial scales. By using multiple lines of evidence, we tracked the transmission of DENV minor variants to trace DENV transmissions between households. Our findings emphasize the value of deep sequencing in resolving house-to-house transmission patterns, and offer a proof-of-concept approach to use intra-host DENV diversity for fine-scale case linkage as a public health tool. Our approach also resolved 3 transmission chains involving persons residing in the same households, providing direct genomic evidence for peridomestic transmission of DENV. We therefore present an evolutionary biology framework for the resolution of DENV transmissions that cannot be differentiated on the basis of epidemiologic and consensus genome data alone.

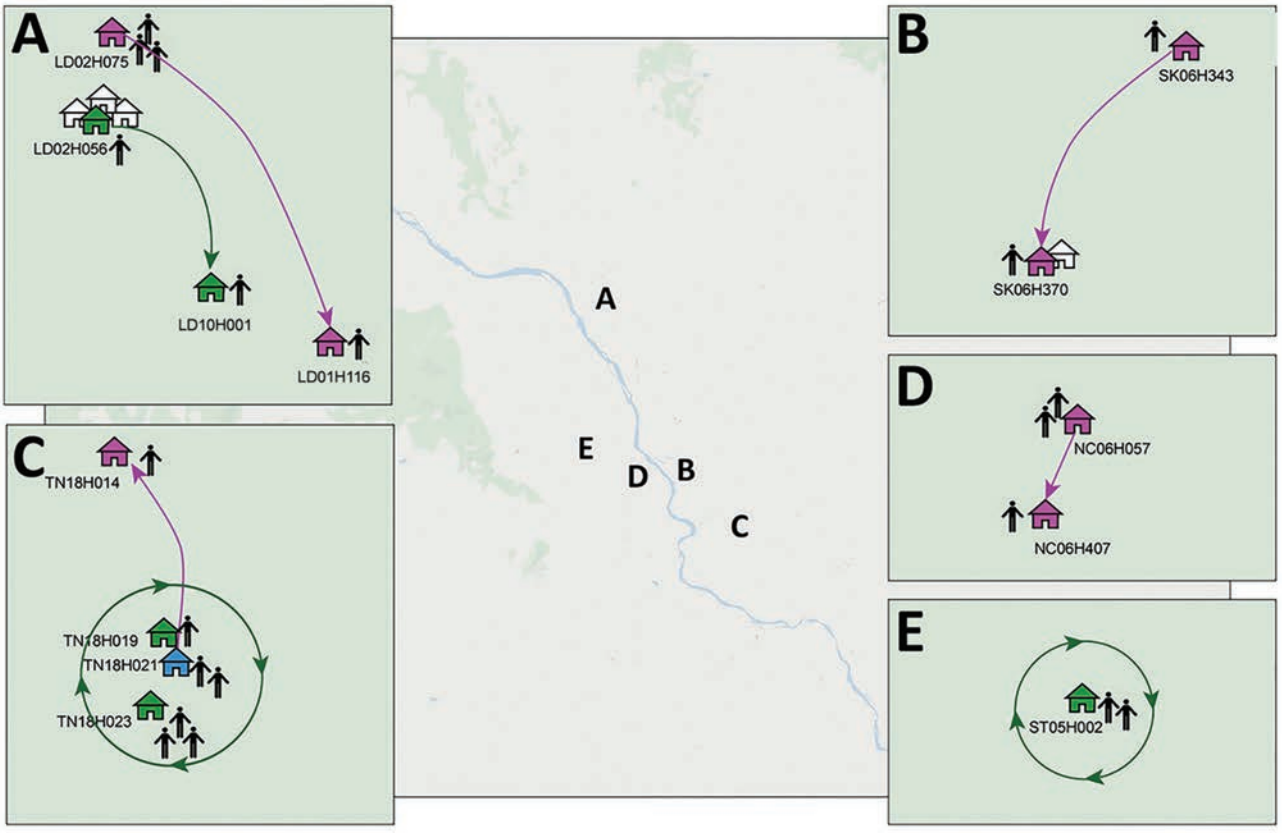

Figure. Approximate locations of dengue virus serotype 1 household transmission clusters and chains, Kamphaeng Phet, Thailand. Chains were confirmed by Bayesian consensus sequence (magenta houses) or minor variant (green houses) analyses or both methods (blue house). Households are described by their subdistrict, cluster, and house numbers, such that the first 2 letters denote subdistrict, the next 2-digit number denotes cluster, and an H followed by a 3-digit number denotes house number. LD, Lan Dokmai; NC, Nakhon Chum; SK, Sa Kaeo; ST, Song Tham; TN, Thep Nakhon.

Our results also show that sharing of iSNV patterns is not guaranteed between epidemiologically linked cases sampled within a 2 week period. iSNVs might be lost because of bottlenecks, genetic drift, or individual immune responses. Therefore, the transmission dynamics of iSNVs are multifactorial, and iSNV-based case-linkage should be performed carefully in the context of complementary epidemiologic and consensus genome data. This point is emphasized by our detection of single iSNVs shared among multiple unrelated cases across entire DENV lineages, suggesting that identical single iSNVs might be stochastically found among unlinked cases. Distinguishing these stochastic iSNVs from transmission-related iSNVs is essential, highlighting the importance of inclusion of closely related background datasets, as done in our study. Only a small proportion of iSNVs in our sequenced cases could be attributed to transmission events, similar to the findings of Sim et al (*39*), and this finding emphasizes the complex evolutionary landscapes of arbovirus iSNVs. Recently, methods have been developed to take into account intra- and inter-host variation for analyses of pathogen spread; however, the limited number of iSNVs in DENV, short sequencing reads, and erroneous or shared iSNVs across unrelated taxa, might be limiting factors influencing the confidence of these tools (*40*–*42*). Our findings also offer a framework to determine functional DENV bottleneck sizes between sampled human dengue cases. Prior studies have shown that bottlenecks within the mosquito vectors themselves range from 5 to 42 genomes and that as many as 11.5% iSNVs are shared between suspected human–human transmission pairs (*39*,*43*). Such bottleneck estimates broadly fit with our observations of constellations of as many as 5 iSNVs shared between human cases sampled 14 days apart. However, long-read sequencing and larger sample sizes, as well as direct samples, from both vector and human populations would be required to definitively determine the number of distinct viral genomes that are passed through human–vector bottlenecks. Even though our genomes were derived from low-passage isolates, we did not observe a significant correlation between the number of passages or passage history and shared iSNVs (Appendix Table 1). Many iSNVs are preserved during low passage of DENV-1 clinical samples; nevertheless, in such instances, care must be taken along with use of appropriate statistics to ensure their accuracy (*44*).

The analyses of our confirmed consensus and minor variant transmission clusters further revealed a strong DENV spatial structure on an inter-household scale. Although household transmission pair distances varied from 0 to 3,000 m, our regression analysis of transmission pair distance over sampling time showed a strong linear relationship, indicating distance is a major determinant of DENV transmission at these ultra-fine spatial scales, and providing pilot estimates of the diffusion speed of DENV spread between households of 70 m/day (95% CI 54–86 m/day). Even though our regression analysis indicated a good model fit (R^2 = 0.91), these coefficient estimates are nevertheless preliminary and are subject to potential nonindependence of transmission pair distance measurements and would benefit from confirmation in greater sample sizes in other study populations. This distance dependent dispersal between households was not noted in a prior Singapore study, which plotted uncorrected consensus genetic distance against geographic distance and sampling times (*21*). This finding highlights the importance of phylogenetic correction for genomic-based DENV tracing. Taken together, these findings support prior research that suggested that DENV transmissions are highly localized on this microspatial scale and might inform vector-control operations (*12*).

Although our findings were derived from an intensive, 4-year active cluster investigation across a very well sampled geographic area, ascertainment bias was a potential weakness in our study. All sequences were either derived from index case-patients accessing care for febrile illness or their contacts who were only sampled in households within 100–200 m of the index case-patient. However, our dense sampling of index cases over a 4-year study period ensured a large number of sequenced specimens across the Kamphaeng Phet region across multiple cluster investigations. Two of the 9 genetically confirmed transmission pairs were detected between persons who were not sampled in the same index case–contact cluster, highlighting the incremental value of genomic data over epidemiologic data alone in DENV transmission tracing. Future improvements in deep sequencing methods (*45*), coupled with more intensive vector and host sampling, could greatly improve our understanding of the invertebrate–vertebrate DENV iSNV bottleneck size and better resolve DENV vector–human transmission dynamics.

In conclusion, we have provided proof-of-concept evidence to support a new evolutionary epidemiologic framework that incorporates both within-host and between-host viral variation to determine fine-scale DENV transmissions. Our framework offers precision tracing of DENV at inter- and intra-household

scales and leverages recent similar applications used for study of influenza and Ebola viruses (*23*,*24*). Our findings warrant larger studies in these and other dengue surveillance cohorts, as well as exploration of how this approach can be used for other arboviruses such as chikungunya and Zika viruses. Ideally, such studies should be coupled with advances in the accuracy of long-read deployable sequencing platforms that could permit near real-time intra-host variant construction (*46*).

Acknowledgments

We thank Henrik Salje and Alan Rothman for their advice.

This work was supported by the National Institute of Allergy and Infectious Diseases (grant no. R01 GM083224), the Military Infectious Diseases Program, and the Armed Forces Health Surveillance Branch and its Global Emerging Infections Surveillance Section.

About the Author

Dr. Maljkovic Berry is the chief of the Viral Genomics section at the Viral Diseases Branch, Walter Reed Army Institute of Research. Her research includes evolution of vectorborne and respiratory viruses as well as viral genomic surveillance.

References

1. Bhatt S, Gething PW, Brady OJ, Messina JP, Farlow AW, Moyes CL, et al. The global distribution and burden of dengue. Nature. 2013;496:504–7. https://doi.org/10.1038/nature12060
2. Brady OJ, Gething PW, Bhatt S, Messina JP, Brownstein JS, Hoen AG, et al. Refining the global spatial limits of dengue virus transmission by evidence-based consensus. PLoS Negl Trop Dis. 2012;6:e1760. https://doi.org/10.1371/journal.pntd.0001760
3. Yoon IK. Focal dengue virus transmission in Kamphaeng Phet, Thailand and implications for management. Southeast Asian J Trop Med Public Health. 2015;46(Suppl 1):17–25.
4. Alera MT, Srikiatkhachorn A, Velasco JM, Tac-An IA, Lago CB, Clapham HE, et al. Incidence of dengue virus infection in adults and children in a prospective longitudinal cohort in the Philippines. PLoS Negl Trop Dis. 2016;10:e0004337. https://doi.org/10.1371/journal.pntd.0004337
5. Nisalak A, Clapham HE, Kalayanarooj S, Klungthong C, Thaisomboonsuk B, Fernandez S, et al. Forty years of dengue surveillance at a tertiary pediatric hospital in Bangkok, Thailand, 1973–2012. Am J Trop Med Hyg. 2016;94:1342–7. https://doi.org/10.4269/ajtmh.15-0337
6. Cucunawangsih, Lugito NPH. Trends of Dengue Disease Epidemiology. Virology (Auckl). 2017;8:1178122X17695836.
7. Messina JP, Brady OJ, Scott TW, Zou C, Pigott DM, Duda KA, et al. Global spread of dengue virus types: mapping the 70 year history. Trends Microbiol. 2014;22:138–46. https://doi.org/10.1016/j.tim.2013.12.011
8. Hoang Quoc C, Henrik S, Isabel RB, In-Kyu Y, Chau NV, Hung NT, et al. Synchrony of dengue incidence in Ho Chi Minh City and Bangkok. PLoS Negl Trop Dis. 2016;10:e0005188. https://doi.org/10.1371/journal.pntd.0005188
9. Bhoomiboonchoo P, Gibbons RV, Huang A, Yoon IK, Buddhari D, Nisalak A, et al. The spatial dynamics of dengue virus in Kamphaeng Phet, Thailand. PLoS Negl Trop Dis. 2014;8:e3138. https://doi.org/10.1371/journal.pntd.0003138
10. Bhoomiboonchoo P, Nisalak A, Chansatiporn N, Yoon IK, Kalayanarooj S, Thipayamongkolgul M, et al. Sequential dengue virus infections detected in active and passive surveillance programs in Thailand, 1994-2010. BMC Public Health. 2015;15:250. https://doi.org/10.1186/s12889-015-1590-z
11. Pollett S, Melendrez MC, Maljkovic Berry I, Duchêne S, Salje H, Cummings DAT, et al. Understanding dengue virus evolution to support epidemic surveillance and countermeasure development. Infect Genet Evol. 2018;62:279–95. https://doi.org/10.1016/j.meegid.2018.04.032
12. Salje H, Lessler J, Maljkovic Berry I, Melendrez MC, Endy T, Kalayanarooj S, et al. Dengue diversity across spatial and temporal scales: Local structure and the effect of host population size. Science. 2017;355:1302–6. https://doi.org/10.1126/science.aaj9384
13. Tian H, Sun Z, Faria NR, Yang J, Cazelles B, Huang S, et al. Increasing airline travel may facilitate co-circulation of multiple dengue virus serotypes in Asia. PLoS Negl Trop Dis. 2017;11:e0005694. https://doi.org/10.1371/journal.pntd.0005694
14. Normile D. Tropical medicine. Surprising new dengue virus throws a spanner in disease control efforts. Science. 2013;342:415. https://doi.org/10.1126/science.342.6157.415
15. Vasilakis N, Cardosa J, Hanley KA, Holmes EC, Weaver SC. Fever from the forest: prospects for the continued emergence of sylvatic dengue virus and its impact on public health. Nat Rev Microbiol. 2011;9:532–41. https://doi.org/10.1038/nrmicro2595
16. Myat Thu H, Lowry K, Jiang L, Hlaing T, Holmes EC, Aaskov J. Lineage extinction and replacement in dengue type 1 virus populations are due to stochastic events rather than to natural selection. Virology. 2005;336:163–72. https://doi.org/10.1016/j.virol.2005.03.018
17. Rico-Hesse R, Harrison LM, Salas RA, Tovar D, Nisalak A, Ramos C, et al. Origins of dengue type 2 viruses associated with increased pathogenicity in the Americas. Virology. 1997;230:244–51. https://doi.org/10.1006/viro.1997.8504
18. Rabaa MA, Klungthong C, Yoon IK, Holmes EC, Chinnawirotpisan P, Thaisomboonsuk B, et al. Frequent in-migration and highly focal transmission of dengue viruses

among children in Kamphaeng Phet, Thailand. PLoS Negl Trop Dis. 2013;7:e1990. https://doi.org/10.1371/journal.pntd.0001990
19. Rabaa MA, Ty Hang VT, Wills B, Farrar J, Simmons CP, Holmes EC. Phylogeography of recently emerged DENV-2 in southern Viet Nam. PLoS Negl Trop Dis. 2010;4:e766. https://doi.org/10.1371/journal.pntd.0000766
20. Jarman RG, Holmes EC, Rodpradit P, Klungthong C, Gibbons RV, Nisalak A, et al. Microevolution of Dengue viruses circulating among primary school children in Kamphaeng Phet, Thailand. J Virol. 2008;82:5494–500. https://doi.org/10.1128/JVI.02728-07
21. Schreiber MJ, Holmes EC, Ong SH, Soh HS, Liu W, Tanner L, et al. Genomic epidemiology of a dengue virus epidemic in urban Singapore. J Virol. 2009;83:4163–73. https://doi.org/10.1128/JVI.02445-08
22. Pybus OG, Tatem AJ, Lemey P. Virus evolution and transmission in an ever more connected world. Proc Biol Sci. 2015;282:20142878. https://doi.org/10.1098/rspb.2014.2878
23. Gire SK, Goba A, Andersen KG, Sealfon RS, Park DJ, Kanneh L, et al. Genomic surveillance elucidates Ebola virus origin and transmission during the 2014 outbreak. Science. 2014;345:1369–72. https://doi.org/10.1126/science.1259657
24. Stack JC, Murcia PR, Grenfell BT, Wood JL, Holmes EC. Inferring the inter-host transmission of influenza A virus using patterns of intra-host genetic variation. Proc Biol Sci. 2013;280:20122173. https://doi.org/10.1098/rspb.2012.2173
25. Zanini F, Brodin J, Thebo L, Lanz C, Bratt G, Albert J, et al. Population genomics of intrapatient HIV-1 evolution. eLife. 2015;4:4. https://doi.org/10.7554/eLife.11282
26. Fischer GE, Schaefer MK, Labus BJ, Sands L, Rowley P, Azzam IA, et al. Hepatitis C virus infections from unsafe injection practices at an endoscopy clinic in Las Vegas, Nevada, 2007-2008. Clin Infect Dis. 2010;51:267–73. https://doi.org/10.1086/653937
27. Worby CJ, Lipsitch M, Hanage WP. Shared genomic variants: identification of transmission routes using pathogen deep-sequence data. Am J Epidemiol. 2017;186:1209–16. https://doi.org/10.1093/aje/kwx182
28. Wymant C, Hall M, Ratmann O, Bonsall D, Golubchik T, de Cesare M, et al. PHYLOSCANNER: inferring transmission from within- and between-host pathogen genetic diversity. Mol Biol Evol. 2017.
29. Skums P, Zelikovsky A, Singh R, Gussler W, Dimitrova Z, Knyazev S, et al. QUENTIN: reconstruction of disease transmissions from viral quasispecies genomic data. Bioinformatics. 2018;34:163–70. https://doi.org/10.1093/bioinformatics/btx402
30. Thomas SJ, Aldstadt J, Jarman RG, Buddhari D, Yoon IK, Richardson JH, et al. Improving dengue virus capture rates in humans and vectors in Kamphaeng Phet Province, Thailand, using an enhanced spatiotemporal surveillance strategy. Am J Trop Med Hyg. 2015;93:24–32. https://doi.org/10.4269/ajtmh.14-0242
31. Vallard T, Melendrez M, Panciera M. ngs_mapper v1.4.2: apipeline for viral and microbial genome construction. 2014 [cited 2016 Mar 25]. https://github.com/VDBWRAIR/ngs_mapper
32. Wilm A, Aw PP, Bertrand D, Yeo GH, Ong SH, Wong CH, et al. LoFreq: a sequence-quality aware, ultra-sensitive variant caller for uncovering cell-population heterogeneity from high-throughput sequencing datasets. Nucleic Acids Res. 2012;40:11189–201. https://doi.org/10.1093/nar/gks918
33. McCrone JT, Lauring AS. Measurements of intrahost viral diversity are extremely sensitive to systematic errors in variant calling. J Virol. 2016;90:6884–95. https://doi.org/10.1128/JVI.00667-16
34. Edgar RC. MUSCLE: a multiple sequence alignment method with reduced time and space complexity. BMC Bioinformatics. 2004;5:113. https://doi.org/10.1186/1471-2105-5-113
35. Darriba D, Taboada GL, Doallo R, Posada D. jModelTest 2: more models, new heuristics and parallel computing. Nat Methods. 2012;9:772. https://doi.org/10.1038/nmeth.2109
36. Guindon S, Delsuc F, Dufayard JF, Gascuel O. Estimating maximum likelihood phylogenies with PhyML. Methods Mol Biol. 2009;537:113–37. https://doi.org/10.1007/978-1-59745-251-9_6
37. Rambaut A, Lam TT, Max Carvalho L, Pybus OG. Exploring the temporal structure of heterochronous sequences using TempEst (formerly Path-O-Gen). Virus Evol. 2016;2:vew007. https://doi.org/10.1093/ve/vew007
38. Drummond AJ, Rambaut A. BEAST: Bayesian evolutionary analysis by sampling trees. BMC Evol Biol. 2007;7:214. https://doi.org/10.1186/1471-2148-7-214
39. Sim S, Aw PP, Wilm A, Teoh G, Hue KD, Nguyen NM, et al. Tracking dengue virus intra-host genetic diversity during human-to-mosquito transmission. PLoS Negl Trop Dis. 2015;9:e0004052. https://doi.org/10.1371/journal.pntd.0004052
40. De Maio N, Worby CJ, Wilson DJ, Stoesser N. Bayesian reconstruction of transmission within outbreaks using genomic variants. PLOS Comput Biol. 2018;14:e1006117. https://doi.org/10.1371/journal.pcbi.1006117
41. Alamil M, Hughes J, Berthier K, Desbiez C, Thébaud G, Soubeyrand S. Inferring epidemiological links from deep sequencing data: a statistical learning approach for human, animal and plant diseases. Philos Trans R Soc Lond B Biol Sci. 2019;374:20180258. https://doi.org/10.1098/rstb.2018.0258
42. Didelot X, Fraser C, Gardy J, Colijn C. Genomic infectious disease epidemiology in partially sampled and ongoing outbreaks. Mol Biol Evol. 2017;34:997–1007. https://doi.org/10.1093/molbev/msw275
43. Lequime S, Fontaine A, Ar Gouilh M, Moltini-Conclois I, Lambrechts L. Genetic drift, purifying selection and vector genotype shape dengue virus intra-host genetic diversity in mosquitoes. PLoS Genet. 2016;12:e1006111. https://doi.org/10.1371/journal.pgen.1006111
44. Fung CK, Li T, Pollett S, Alera MT, Yoon IK, Hang J, et al. Effect of low-passage number on dengue consensus genomes and intra-host variant frequencies. J Gen Virol. 2021;102. https://doi.org/10.1099/jgv.0.001553
45. Grubaugh ND, Gangavarapu K, Quick J, Matteson NL, De Jesus JG, Main BJ, et al. An amplicon-based sequencing framework for accurately measuring intrahost virus diversity using PrimalSeq and iVar. Genome Biol. 2019;20:8. https://doi.org/10.1186/s13059-018-1618-7
46. Karst SM, Ziels RM, Kirkegaard RH, Sørensen EA, McDonald D, Zhu Q, et al. High-accuracy long-read amplicon sequences using unique molecular identifiers with Nanopore or PacBio sequencing. Nat Methods. 2021;18:165–9. https://doi.org/10.1038/s41592-020-01041-y

Address for correspondence: Irina Maljkovic Berry, Walter Reed Army Institute of Research, 503 Robert Grant Ave, Silver Spring, MD 20910, USA; email: irina.maljkovicberry.ctr@mail.mil

Association between Birth Region and Time to Tuberculosis Diagnosis among Non–US-Born Persons in the United States

Amish Talwar, Rongxia Li, Adam J. Langer

Approximately 90% of tuberculosis (TB) cases among non–US-born persons in the United States are attributable to progression of latent TB infection to TB disease. Using survival analysis, we investigated whether birthplace is associated with time to disease progression among non–US-born persons in whom TB disease developed. We derived a Cox regression model comparing differences in time to TB diagnosis after US entry among 19 birth regions, adjusting for sex, birth year, and age at entry. After adjusting for age at entry and birth year, the median time to TB diagnosis was lowest among persons from Middle Africa, 128 months (95% CI 116–146 months) for male persons and 121 months (95% CI 108–136 months) for female persons. We found time to TB diagnosis among non–US-born persons varied by birth region, which represents a prognostic indicator for progression of latent TB infection to TB disease.

Most incident tuberculosis (TB) cases in the United States occur among non–US-born persons (*1*). During 2018, a total of 70.2% of TB disease cases occurred among non–US-born persons, and 46.6% of those cases were diagnosed ≥10 years after those persons arrived in the United States (*1*). TB disease can occur from recent person-to-person transmission but more commonly is the result of progression of latent TB infection (LTBI) to TB disease. LTBI is a form of TB in which a person is infected with *Mycobacterium tuberculosis*, the causative agent of TB, but remains asymptomatic and noncontagious (*2*). Left untreated, LTBI can progress to TB disease among up to 10% of persons with LTBI within their lifetime (*2*). Among non–US-born persons residing in the United States, >85% of TB disease cases are attributed to progression of LTBI to TB disease (*3*,*4*). Consequently, the Centers for Disease Control and Prevention (CDC) recommends that efforts to eliminate TB in the United States, in part, focus on LTBI detection and treatment among non–US-born persons (*5*).

Understanding the factors associated with LTBI progression can help guide detection and treatment efforts by identifying persons with LTBI who are at greatest risk of developing TB disease and concentrating TB prevention resources toward the populations at highest risk. Although persons recently infected with TB and persons with weakened immune systems are at higher risk for progression to TB disease (*6*), the factors affecting the time to develop TB disease remain unclear, particularly for non–US-born persons. Information on time to develop TB disease can help public health officials target interventions for LTBI testing and treatment among at-risk populations before LTBI progresses to TB disease. One study found the risk of developing TB disease among non–US-born persons decreased with increasing time after entering the United States (*7*). However, non–US-born persons are a heterogenous population who differ in health status based on country of origin (*8*), and the effect of birth country on progression from LTBI to TB disease remains unclear. To clarify disease progression among varying population groups, we evaluated the time to develop TB disease according to birthplace among non–US-born persons with reported cases of TB disease in the United States during 2011–2018.

Methods

Using national TB surveillance data, we assessed time from entering the United States to TB disease diagnosis among non–US-born persons in whom TB disease developed during 2011–2018. Because of the

Authors affiliation: Centers for Disease Control and Prevention, Atlanta, Georgia, USA

DOI: https://doi.org/10.3201/eid2706.203663

high number of countries represented among non–US-born persons with TB disease, we categorized birth countries into regions. We assessed time to TB disease diagnosis as time from entry into the United States to time the TB case was reported to a local or state health department. We excluded persons with TB disease attributed to recent transmission (*3*) and focused on persons whose TB disease most likely was caused by progression of LTBI acquired in their birth countries. We compared these times by using bivariate and multivariate survival analysis, and we adjusted for sex, birth year, and age at time of entry into the United States.

Study Population

We derived the study population for this analysis from CDC's National Tuberculosis Surveillance System (NTSS), which has been collecting information on TB disease cases from local and state health departments in the United States since 1953 (*9*,*10*). Case reports include demographic, clinical, and risk factor data. The most recent TB surveillance case definition in NTSS, as of 2009, is available in the 2018 US TB surveillance report (*1*). For this study, we examined cases reported to NTSS during January 2011–December 2018 among non–US-born persons, which included persons born outside the United States or its territories for whom neither parent was a US citizen (Appendix, https://wwwnc.cdc.gov/EID/article/27/6/20-3663-App1.pdf).

We excluded cases reported from US territories or freely associated states (Figure 1). We also excluded cases attributed to recent TB transmission in the United States by using a previously published method that uses NTSS and genotypic data to determine likelihood of recent transmission (*3*). This plausible-source case method attributes cases to recent transmission if ≥1 plausible-source case for the case of interest is identified in NTSS (*3*). With this method, cases either are attributed to recent transmission, not attributed to recent transmission, or receive neither designation if they lack the necessary information to assess for recent transmission, such as missing genotype data. By excluding cases attributed to recent transmission, we were able to analyze cases that were more likely the result of LTBI progression.

We further excluded cases not attributed to recent transmission among persons for whom time from arrival in the United States to TB disease diagnosis was ≤3 months. We excluded this group because TB disease among persons in the country ≤3 months can represent disease that was present at time of US entry rather than LTBI reactivation after

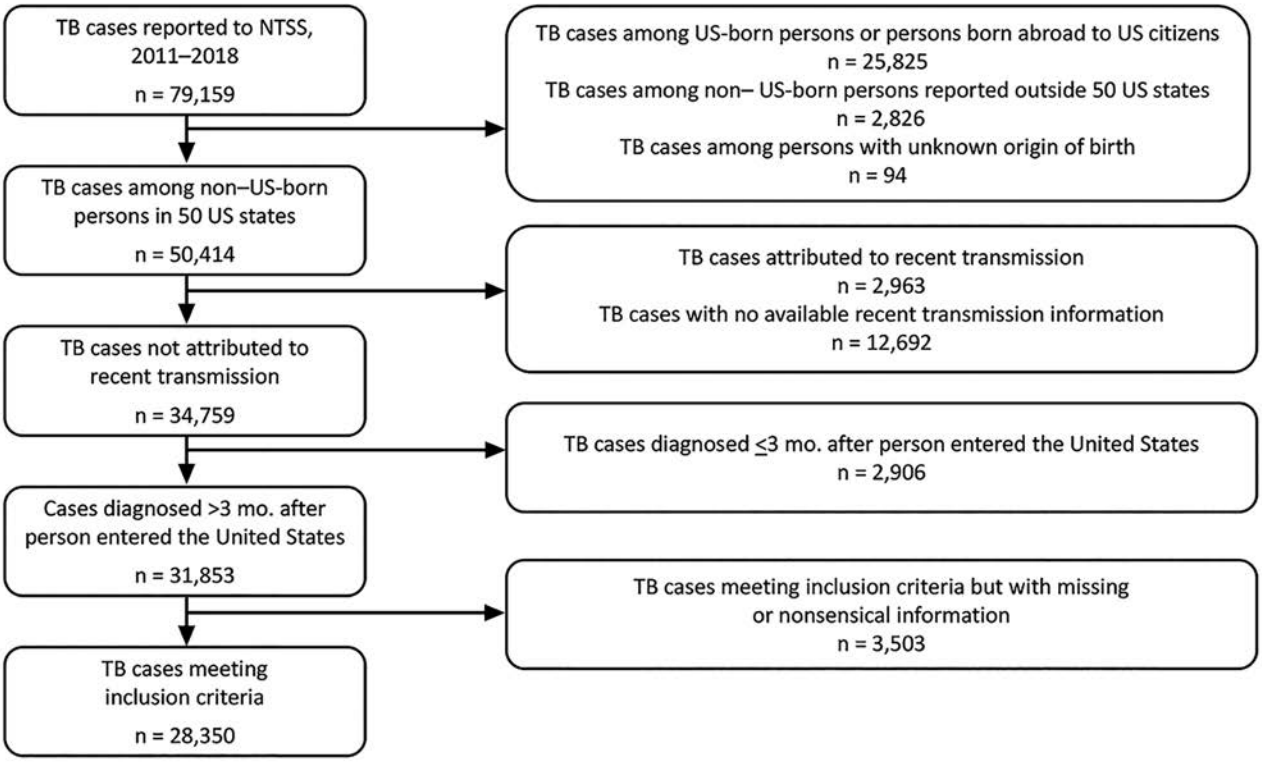

Figure 1. Flowchart of cohort selection process for study evaluating the time to develop TB among non–US-born persons after entering the United States, 2011–2018. NTSS, National Tuberculosis Surveillance System; TB, tuberculosis.

arrival; excluding these cases also helps account for variability in TB disease screening overseas before entry into the United States. We also excluded cases with missing data and observations with nonsensical values for a category, such as <0 months to TB disease diagnosis, <0 years of age at time of entry, and non–US-born persons with United States listed as birth country.

Research Design and Variables

We performed a bivariate analysis and a multivariate analysis examining the association between birth country and time from initial arrival in the United States to TB disease diagnosis, which was our main outcome variable. In addition to birth country, we examined the following case demographic variables as additional covariates for our analyses: sex, age at entry in the United States, and birth year. We performed a bivariate analysis to assess the association between time to TB disease diagnosis and these covariates individually, and we performed the multivariate analysis to account for the effects of these covariates on the association between birth country and time to TB disease diagnosis. For our analyses, we defined time to TB disease diagnosis as the number of months spent in the United States before diagnosis, which we derived by subtracting the NTSS-reported month and year of initial entry into the country from the month and year that the TB disease case was reported. We used the case report date because information regarding the actual disease diagnosis date was unavailable through NTSS; the report date represents the earliest notification to a local public health agency that the patient might have TB disease. Because >200 non-US countries and territories of birth were reported to NTSS during the study timeframe, we used the United Nations (UN) standard country or area codes for statistical use, Series M, No. 49 (M49), which categorizes countries and territories according to geographic location and level of development, to divide these countries and territories into 19 regions for ease of statistical analysis (*11*,*12*) (Appendix). To derive age at US entry, we subtracted NTSS-reported year of initial US entry from the year the TB disease case was reported to NTSS and then subtracted this number from NTSS-reported age at diagnosis. For our analyses, we categorized age into 6 categories. We derived birth year by subtracting age from the year the case was reported, and we categorized birth year into 3 categories; we included birth year in our analysis to adjust for a previously observed birth year cohort effect among non–US-born persons with TB disease reported to NTSS (*13*).

Statistical Analysis

We began by determining the number of patients who had TB disease not attributed to recent transmission and determined the unadjusted median number of months and interquartile range (IQR) that these patients spent in the United States before receiving a TB disease diagnosis. We also determined the unadjusted median number of months according to birth region. We constructed a bivariate Kaplan-Meier survival curve to visually demonstrate the overall distribution of time to TB diagnosis since US entry. We then constructed bivariate Kaplan-Meier curves stratified by each covariate. We tested for statistically significant differences between curves at $p \leq 0.05$ by using the log rank test and reported global p values.

We then used Cox regression to examine the association of time to TB disease diagnosis and birth region, adjusting for the effects of age at US entry, sex, and birth year. We tested the proportional hazards assumption, and our data met this assumption on the basis of an examination of Schoenfeld residual plots (Appendix). Because our data are likely double-truncated, we applied a correction for double-truncation to our sample set (*14*) (Appendix). Using the Cox regression model, we calculated adjusted median times by birth region by fixing age at US entry to 25–44 years (the category with the most observations for 18/19 birth regions) and birth year at 1940–1979 (the category with the most observations for 14/19 birth regions). We reported adjusted median times and 95% CIs separately by sex. Finally, we stratified the observations by the 6 World Health Organization (WHO) regions to more easily demonstrate interregional variations in time to TB diagnosis, and we repeated the Cox regression analysis accordingly (*15*) (Appendix).

Because the time after US entry at which persons with TB disease typically receive a diagnosis is unclear, previous studies have used a range of times to define cases as disease missed on entry as opposed to LTBI reactivation (*16*–*18*). Therefore, we performed a sensitivity analysis to assess the effect of extending the exclusion window from 3 months to 6 months for TB disease missed at time of entry for our Cox regression analysis.

We performed all statistical analyses by using R version 4.0.2 (R Foundation for Statistical Computing, https://www.r-project.org), and we used the R code developed by Rennert and Xie to correct for double truncation (*14*). All data were collected as part of routine disease surveillance and were not part of human subjects research requiring institutional review board approval.

Results

During 2011–2018, a total of 79,159 TB cases were reported to NTSS (Figure 1), of which we excluded 28,745 cases because these were among US-born persons, were not reported from 1 of the 50 states or the District of Columbia, or had no known origin of birth reported. We also excluded 15,655 cases that were either attributed to recent transmission or had no information regarding recent transmission available; 2,906 cases for which the time to TB diagnosis was ≤3 months; and 3,503 cases with missing or nonsensical information for ≥1 of the variables considered. Because only 5% of all datapoints were missing or nonsensical, and <10% of datapoints were missing or nonsensical for any single variable, we performed listwise deletion of cases with any missing or nonsensical data for our analyses. As a result, we included 28,350 cases for our analyses.

Most non–US-born persons who developed TB disease not attributed to recent transmission after arrival to the United States emigrated from Asia (Table 1); the subregion or intermediary region with the highest proportion of non–US-born persons who received a TB diagnosis in the United States not attributed to recent transmission was South-eastern Asia. The unadjusted median number of months that a non–US-born person who developed TB disease spent in the United States before receiving a TB diagnosis not attributed to recent transmission was 143 months (IQR 51–292 months). Persons from Middle Africa had the lowest unadjusted median number of months until TB diagnosis (26 months), and persons from Western Europe had the highest unadjusted median number of months (524 months) (Table 1). We calculated Kaplan-Meier estimates for time to TB diagnosis unstratified by birth region (Figure 2) and stratified by birth region (Figure 3, panel A). We also calculated Kaplan-Meier estimates for the other covariates, including birth region, sex, age at US entry, and birth year (Appendix Figures 1–3). For all 4 covariates we identified statistically significant differences ($p<0.01$) in the survival curves.

We calculated adjusted median times to TB diagnosis by birth region (Table 1) and adjusted times to TB diagnosis by birth region and sex (Figure 3, panels B, C). We noted persons from Middle Africa had the lowest median adjusted time to TB diagnosis, 128 (95% CI 116–146) months for male sex and 121 (95% CI 108–136) months for female. Persons from Northern Europe had the highest median adjusted time to diagnosis, 279 (95% CI 240–343) months for male sex and 265 (95% CI 228–327) months for female.

We also calculated unadjusted and adjusted median times to TB diagnosis by WHO region (Table 2) and the Kaplan-Meier and Cox regression estimates for time to TB diagnosis by WHO region (Figure 4). We found persons from the African Region had the lowest adjusted median time to diagnosis, 169 (95%

Table 1. Median time to diagnosis of tuberculosis disease not attributed to recent transmission for non–US-born persons by region, United States, 2011–2018

Region	No. (%)	Unadjusted median time, mo (IQR)	Adjusted median time, mo (95% CI)*	
			Male sex	Female sex
Africa	2,900 (10.2)			
Eastern Africa	1,618 (5.7)	61 (25–123)	185 (178–193)	175 (167–183)
Middle Africa	286 (1.0)	26 (11–55)	128 (116–146)	121 (108–136)
Northern Africa	125 (0.4)	62 (25–161)	177 (153–206)	166 (143–194)
Southern Africa	56 (0.2)	77 (28–150)	185 (156–229)	175 (146–215)
Western Africa	815 (2.9)	46 (15–124)	162 (152–174)	152 (142–164)
Americas	9,668 (34.1)			
Caribbean	1,238 (4.4)	127 (45–273)	213 (202–225)	201 (190–212)
Central America	7,071 (24.9)	174 (74–338)	246 (242–250)	236 (229–242)
Northern America†	20 (0.1)	353 (176–713)	264 (223–336)	251 (210–321)
South America	1,339 (4.7)	141 (60–244)	230 (218–241)	216 (206–229)
Asia	14,973 (52.8)			
Central Asia	45 (0.2)	60 (33–97)	187 (158–233)	177 (148–219)
Eastern Asia	2,921 (10.3)	210 (88–363)	277 (266–289)	263 (253–275)
Southeastern Asia	7,793 (27.5)	190 (74–325)	245 (241–248)	235 (229–240)
Southern Asia	4,023 (14.2)	76 (27–193)	210 (203–218)	198 (191–206)
Western Asia	191 (0.7)	83 (27–221)	212 (190–240)	200 (180–228)
Europe	660 (2.3)			
Eastern Europe	328 (1.2)	178 (82–274)	236 (218–251)	222 (206–242)
Northern Europe	46 (0.2)	459 (222–619)	279 (240–343)	265 (228–327)
Southern Europe	221 (0.8)	220 (148–485)	245 (205–308)	236 (193–294)
Western Europe	65 (0.2)	524 (200–645)	276 (244–324)	262 (234–309)
Oceania	149 (0.5)	65 (22–164)	213 (179–262)	201 (168–250)

*Age at arrival fixed at 25–44 y, birth year fixed at 1940–1979.
†Excludes United States.

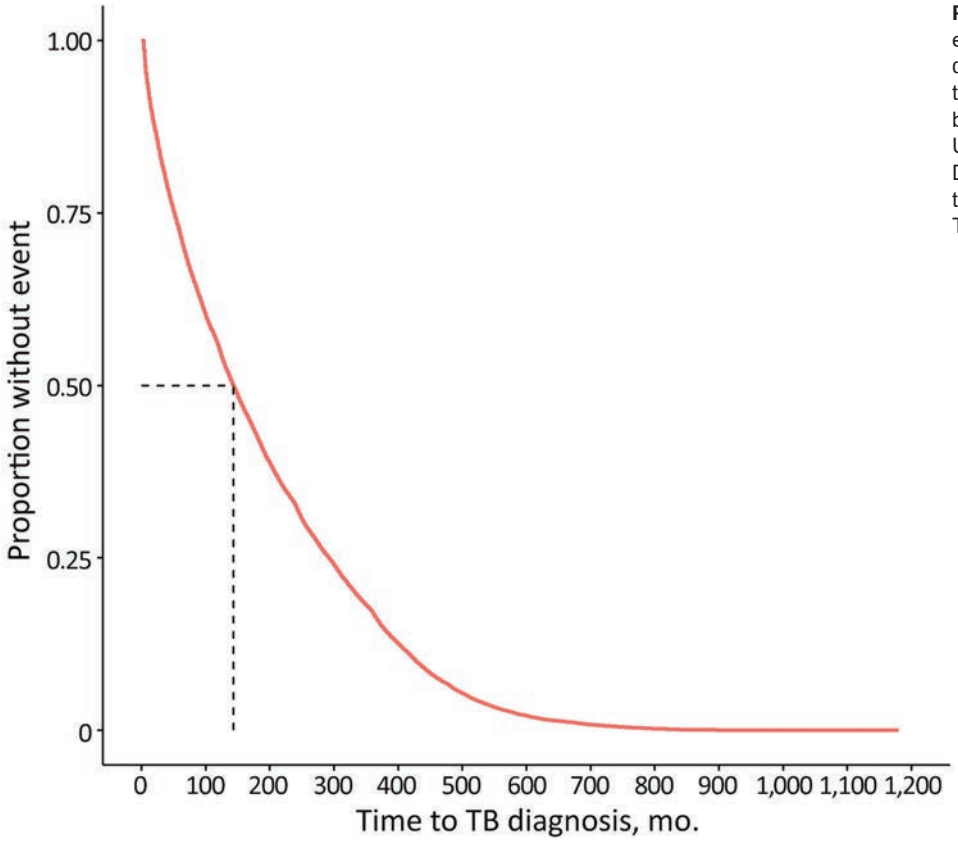

Figure 2. Kaplan-Meier estimate for time to TB disease diagnosis not attributed to recent transmission among non–US-born persons after entering the United States, 2011–2018. Dotted line represents median time for TB disease diagnosis. TB, tuberculosis.

CI 161–176) months for male sex and 157 (95% CI 150–165) months for female. Finally, after performing our sensitivity analyses, we observed that increasing the exclusion window from ≤3 months to ≤6 months changed the adjusted median times for all persons by <10%, regardless of birth region (Appendix Table 4).

Discussion

On the basis of our analysis of NTSS data, the median length of time to TB diagnosis varied according to birth region for non–US-born persons in whom TB disease eventually developed. The lowest adjusted median times to TB disease diagnosis were concentrated among persons originating from Africa. In 2018, 5/10 birth countries associated with the highest TB disease rates in the United States were in Africa, and Africa had the highest TB disease rate globally (*1*,*19*). Whether an actual causal association exists between higher overall TB disease rate in one's birthplace and one's likelihood of developing TB disease earlier is unclear. However, WHO's African Region had the highest proportion of LTBI attributable to recent infection in 2014 (*20*), and persons are most likely to develop TB disease soon after TB infection (*5*). Therefore, shorter time to TB disease diagnosis might be associated with higher annual risk for TB infection. Another possibility is that US healthcare providers might have a higher suspicion for TB disease among certain populations, particularly persons from countries with high TB rates, a known risk factor for developing TB disease because of the higher risk for TB infection in those countries (*5*). Certain host genetic factors have been associated with LTBI progression to TB disease (*21*), so a further possibility is that the differences might reflect genetic differences between persons originating from different regions. Although these potential etiologies are compelling, the differences observed in this study simply could be the consequence of overall poorer health status among persons from different regions because of lower levels of economic development and healthcare access. Of note, 33 of the 47 least-developed countries in the world are located in Africa (*22*), and Africa has the lowest overall healthy life expectancy, which is the number of years that a newborn is expected to live in good health (*23*). In addition, persons with poorer health status, particularly malnutrition (*24*), might be more susceptible to developing TB disease than are healthier persons.

The association between birth region and time to TB diagnosis also might be a consequence of differences in risk factors for progression to TB disease

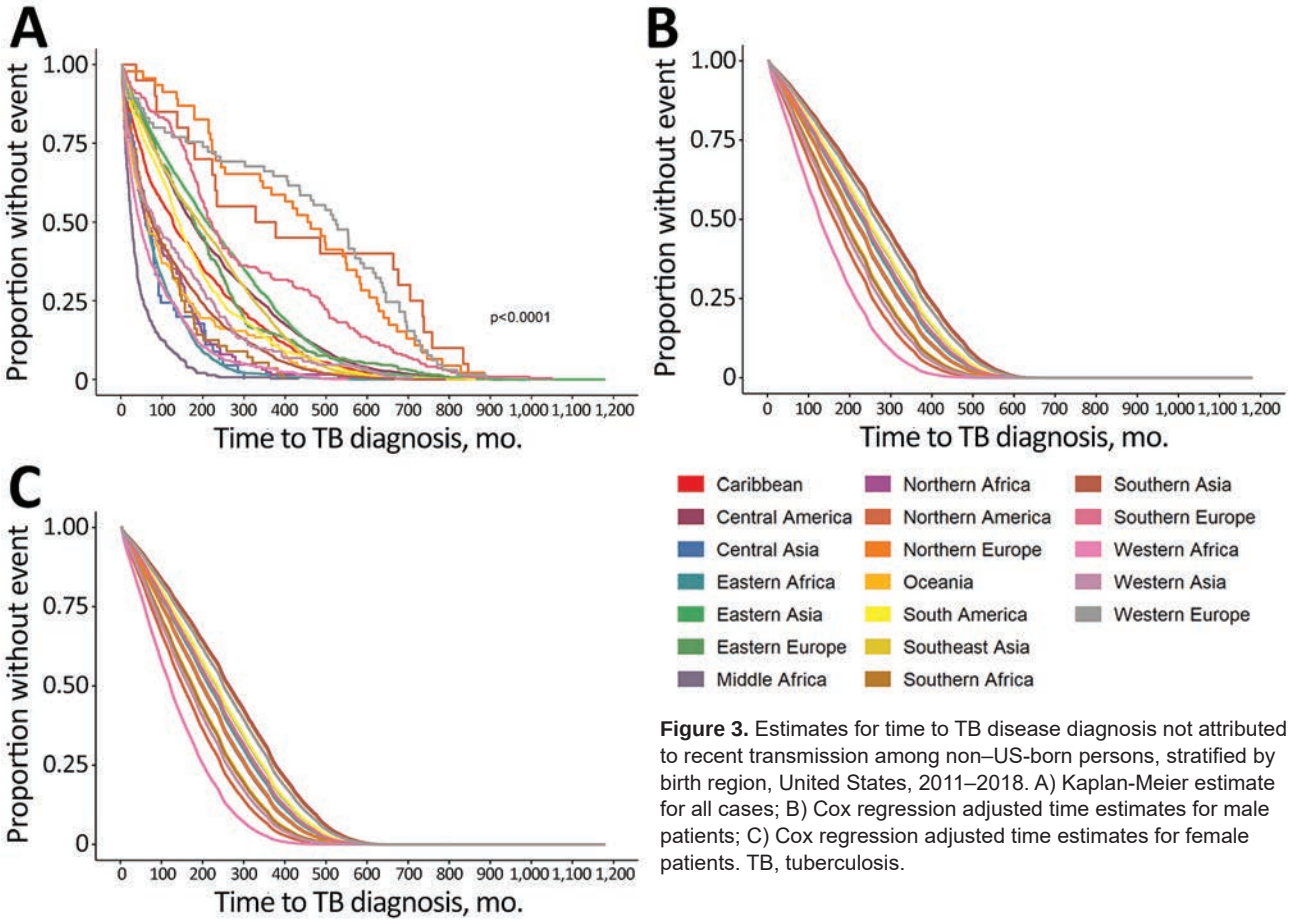

Figure 3. Estimates for time to TB disease diagnosis not attributed to recent transmission among non–US-born persons, stratified by birth region, United States, 2011–2018. A) Kaplan-Meier estimate for all cases; B) Cox regression adjusted time estimates for male patients; C) Cox regression adjusted time estimates for female patients. TB, tuberculosis.

among different regions. Both HIV infection and diabetes mellitus are key risk factors for LTBI reactivation, and HIV infection represents the greatest risk factor for LTBI reactivation (*25*). Worldwide, 9% of incident TB cases in 2018 were among persons living with HIV and 15% of TB cases might be linked to diabetes mellitus (*19*,*26*). In addition, the WHO African Region has the highest prevalence of HIV among incident TB cases (*19*), and the HIV diagnosis rates for Africa-born persons living in the United States are 6 times higher than the rate for the general US population (*27*). Given the possibility of TB and HIV coinfection or TB and diabetes mellitus comorbidity as plausible etiologies for the association between birth region and time to TB disease diagnosis, including HIV status or diabetes mellitus diagnosis as variables in our analysis might appear reasonable. However, even though NTSS offers information on HIV status and diabetes mellitus diagnosis, it does not offer information on the date of testing or diagnosis. Therefore, to use these data, we would have to unjustifiably assume that a person's HIV status or presence of diabetes mellitus were constant throughout the time from US entry to TB disease diagnosis date. This assumption also would be invalid because global HIV incidence was likely low before the 1980s (*28*), and

Table 2. Median time to diagnosis of tuberculosis disease not attributed to recent transmission for non–US-born persons by World Health Organization region, United States, 2011–2018

Region	No. (%)	Unadjusted median time, mo (IQR)	Adjusted median time, mo (95% CI)*	
			Male sex	Female sex
African	2,379 (8.4)	48 (18–111)	169 (161–176)	157 (150–165)
Eastern Mediterranean	1,226 (4.3)	98 (32–215)	211 (202–222)	198 (189–208)
European	779 (2.7)	205 (88–390)	245 (228–266)	234 (214–252)
The Americas†	9,667 (34.1)	161 (67–316)	241 (236–244)	227 (221–234)
Southeast Asian	4,386 (15.5)	71 (26–181)	206 (199–214)	193 (187–201)
Western Pacific	9,913 (35.0)	205 (86–339)	254 (250–260)	244 (240–248)

*Age at arrival fixed at 25–44 y, birth year fixed at 1940–1979.
†Excludes United States.

before 2010, HIV infection could prevent non-US citizens from entering the United States (*29*). In addition, including history of diabetes mellitus as a variable in this study would have resulted in an immortal time bias (*30*). For example, persons who received a diagnosis of diabetes mellitus during the study period, before receiving a diagnosis of TB disease, must have persisted long enough without a TB disease diagnosis to receive a diabetes mellitus diagnosis. For these persons, the period of time from the start of the study period to diabetes mellitus diagnosis is known as immortal time because they might not have developed TB disease during that time interval. However, persons who have never received a diagnosis of diabetes mellitus might have received a TB diagnosis during this immortal time, resulting in a disadvantaged survival time despite not having a diabetes mellitus diagnosis. Therefore, we excluded HIV status and diabetes mellitus diagnosis as variables from this study.

Finally, all refugees entering the United States should undergo a domestic medical examination upon entry, unlike most other persons immigrating to the United States (*31*,*32*). Given that Africa and Asia together account for the highest proportion of refugees coming to the United States since 2010 (*32*), their comparatively low adjusted median times in this study might be a consequence of TB disease diagnosis at the time of their domestic medical evaluation, especially since TB screening is a recommended component of that examination (*33*). However, the domestic medical examination is typically conducted 1–3 months after US entry (*34*), which is within our exclusion window for cases attributable to imported TB disease. In addition, all refugees are screened for TB before US entry, making it less likely that newly diagnosed TB would be detected after entering the country.

The first limitation of our study is that the characteristics of persons who immigrate to the United States might not represent persons who remain in their birth country. One study reported that TB incidence in the birth country was 5.4 times higher than the US TB incidence for persons born in those countries

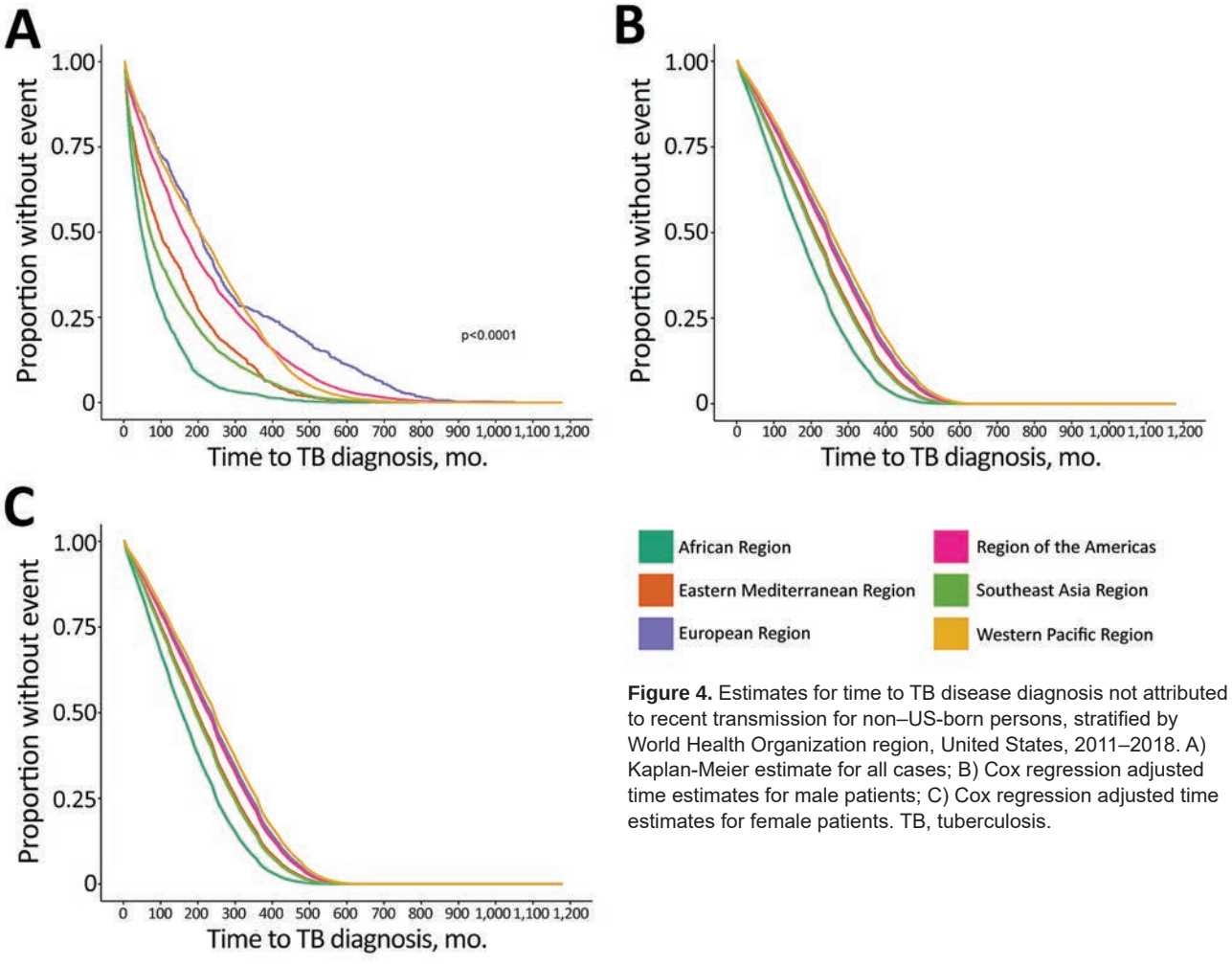

Figure 4. Estimates for time to TB disease diagnosis not attributed to recent transmission for non–US-born persons, stratified by World Health Organization region, United States, 2011–2018. A) Kaplan-Meier estimate for all cases; B) Cox regression adjusted time estimates for male patients; C) Cox regression adjusted time estimates for female patients. TB, tuberculosis.

and who immigrated to the United States (*35*). Another study found that the prevalence by birth country of isoniazid-resistant and multidrug-resistant TB in the United States better correlated with the prevalence by birth country seen in NTSS data than with the prevalence seen in the birth countries themselves (*36*). This finding suggests that non–US-born persons are not representative of the overall birth country population in terms of TB risk. In addition, NTSS does not report country of immediate origin, which can differ from birth country, nor does NTSS account for interceding travel outside the United States after initial US entry, during which TB might have been transmitted. Finally, the health status of immigrants to the United States might be influenced by long-term US residence, causing it to diverge from expected health status on the basis of birth country.

Our study does not account for the number of non–US-born persons emigrating from a particular region nor how those numbers change over time. We also did not account for reason for immigration, such as refugee status, which might affect risk for TB infection. Furthermore, by using regions to categorize countries in this study, we lose the ability to detect differences between those countries. Also, the plausible-source case method NTSS uses has high accuracy compared with field-based assessments of recent transmission that use epidemiologic investigation methods, but this method is not completely accurate and might misclassify certain cases (*3*). In addition, we were unable to assess the effect of HIV status and diabetes mellitus on time to TB disease diagnosis. Finally, our study did not consider the population of non–US-born persons who did not develop TB disease during the study time period.

In conclusion, time to TB disease diagnosis among non–US-born persons in whom TB disease developed in the United States during 2011–2018 varies by birth region, which represents a prognostic indicator for LTBI progressing to TB disease. Targeted LTBI testing and treatment for persons entering the United States who were born in regions with low median times to TB diagnosis might advance progress toward TB elimination in the United States. Additional studies using data sources that include information on risk factors like HIV infection and diabetes mellitus could help determine the potential influence of these conditions on time to LTBI reactivation; such studies also would benefit from accounting for TB rates in birth countries, where feasible. Similar studies in countries with healthcare systems comparable to the United States and diverse immigrant populations also would help determine whether these results are reproducible and could shed light on the etiology underlying regional differences in time to TB disease diagnosis. Nonetheless, our findings can help focus efforts on LTBI detection and treatment among the most vulnerable populations and further advance efforts to eliminate TB disease in the United States.

Acknowledgments

We thank Andrew Hill for his suggestions for data analysis; Carla A. Winston, Thomas R. Navin, Sandy P. Althomsons, Jonathan Wortham, and Kristine M. Schmit for reviewing and providing input for this manuscript; Noah Schwartz, Rebekah Stewart, Peter Cegielski, and Andrew Vernon for providing helpful feedback on the study design; and the National Center for HIV/AIDS, Viral Hepatitis, STD, and TB Prevention, CDC for facilitating the organization of this study.

About the Author

Dr. Talwar is a public health physician in the Office of the Director, Centers for Disease Control and Prevention, Atlanta, Georgia, USA. His primary interests include infectious disease prevention and global health security.

References

1. Centers for Disease Control and Prevention. Reported tuberculosis in the United States, 2018 [cited 2020 Feb 21]. https://www.cdc.gov/tb/statistics/reports/2018/default.htm
2. Centers for Disease Control and Prevention (CDC). Latent tuberculosis infection: a guide for primary health care providers 2013 [cited 2020 Feb 21]. https://www.cdc.gov/tb/publications/ltbi/pdf/targetedltbi.pdf
3. France AM, Grant J, Kammerer JS, Navin TR. A field-validated approach using surveillance and genotyping data to estimate tuberculosis attributable to recent transmission in the United States. Am J Epidemiol. 2015;182:799–807. https://doi.org/10.1093/aje/kwv121
4. Yuen CM, Kammerer JS, Marks K, Navin TR, France AM. Recent transmission of tuberculosis—United States, 2011–2014. PLoS One. 2016;11:e0153728. https://doi.org/10.1371/journal.pone.0153728
5. Talwar A, Tsang CA, Price SF, Pratt RH, Walker WL, Schmit KM, et al. Tuberculosis—United States, 2018. MMWR Morb Mortal Wkly Rep. 2019;68:257–62. https://doi.org/10.15585/mmwr.mm6811a2
6. Centers for Disease Control and Prevention (CDC). TB risk factors [cited 2020 Feb 21]. https://www.cdc.gov/tb/topic/basics/risk.htm
7. Menzies NA, Hill AN, Cohen T, Salomon JA. The impact of migration on tuberculosis in the United States. Int J Tuberc Lung Dis. 2018;22:1392–403. https://doi.org/10.5588/ijtld.17.0185
8. Argeseanu Cunningham S, Ruben JD, Venkat Narayan KM. Health of foreign-born people in the United States: a review. Health Place. 2008;14:623–35. https://doi.org/10.1016/j.healthplace.2007.12.002

9. Yelk Woodruff RS, Pratt RH, Armstrong LR. The US National Tuberculosis Surveillance System: a descriptive assessment of the completeness and consistency of data reported from 2008 to 2012. JMIR Public Health Surveill. 2015;1:e15. https://doi.org/10.2196/publichealth.4991
10. Office of Disease Prevention and Health Promotion (US). National TB Surveillance System [cited 2020 Dec 10]. https://www.healthypeople.gov/2020/data-source/national-tb-surveillance-system
11. United Nations Statistics Division. Standard country or area codes for statistical use, series M, no. 49 (M49) [cited 2020 Mar 2]. https://unstats.un.org/unsd/methodology/m49
12. Committee for the Coordination of Statistical Activities. Note on definition of regions for statistical analysis 2006 [cited 2020 Feb 26]. https://unstats.un.org/unsd/accsub/2006docs-8th/SA-2006-15-Grouping-UNSD.pdf
13. Iqbal SA, Winston CA, Bardenheier BH, Armstrong LR, Navin TR. Age-period-cohort analyses of tuberculosis incidence rates by nativity, United States, 1996–2016. Am J Public Health. 2018;108:S315–20. https://doi.org/10.2105/AJPH.2018.304687
14. Rennert L, Xie SX. Cox regression model with doubly truncated data. Biometrics. 2018;74:725–33. https://doi.org/10.1111/biom.12809
15. World Health Organization. Countries [cited 2020 Dec 10]. https://www.who.int/countries
16. Walter ND, Painter J, Parker M, Lowenthal P, Flood J, Fu Y, et al.; Tuberculosis Epidemiologic Studies Consortium. Persistent latent tuberculosis reactivation risk in United States immigrants. Am J Respir Crit Care Med. 2014;189:88–95.
17. Menzies HJ, Winston CA, Holtz TH, Cain KP, Mac Kenzie WR. Epidemiology of tuberculosis among US- and foreign-born children and adolescents in the United States, 1994–2007. Am J Public Health. 2010;100:1724–9. https://doi.org/10.2105/AJPH.2009.181289
18. Cain KP, Benoit SR, Winston CA, Mac Kenzie WR. Tuberculosis among foreign-born persons in the United States. JAMA. 2008;300:405–12. https://doi.org/10.1001/jama.300.4.405
19. World Health Organization. Global tuberculosis report 2019 [cited 2020 Feb 26]. https://apps.who.int/iris/bitstream/handle/10665/329368/9789241565714-eng.pdf
20. Houben RM, Dodd PJ. The global burden of latent tuberculosis infection: a re-estimation using mathematical modelling. PLoS Med. 2016;13:e1002152. https://doi.org/10.1371/journal.pmed.1002152
21. Abel L, Fellay J, Haas DW, Schurr E, Srikrishna G, Urbanowski M, et al. Genetics of human susceptibility to active and latent tuberculosis: present knowledge and future perspectives. Lancet Infect Dis. 2018;18:e64–75. https://doi.org/10.1016/S1473-3099(17)30623-0
22. United Nations Conference on Trade and Development. Least developed countries (LDCs) [cited 2020 Feb 26]. https://unctad.org/en/Pages/ALDC/Least%20Developed%20Countries/LDCs.aspx
23. World Health Organization. World health statistics 2019: monitoring health for the SDGs [cited 2020 Feb 26]. https://apps.who.int/iris/bitstream/handle/10665/324835/9789241565707-eng.pdf
24. Cegielski JP, McMurray DN. The relationship between malnutrition and tuberculosis: evidence from studies in humans and experimental animals. Int J Tuberc Lung Dis. 2004;8:286–98.
25. Centers for Disease Control and Prevention. Chapter 2: Transmission and pathogenesis of tuberculosis. In: Core curriculum on tuberculosis: what the clinician should know. 6th ed. Atlanta: The Centers; 2013. p. 19–44 [cited 2020 Feb 26]. https://www.cdc.gov/tb/education/corecurr/pdf/corecurr_all.pdf
26. World Health Organization. Tuberculosis & diabetes 2019 [cited 2020 Feb 26]. https://www.who.int/tb/publications/diabetes_tb.pdf
27. Blanas DA, Nichols K, Bekele M, Lugg A, Kerani RP, Horowitz CR. HIV/AIDS among African-born residents in the United States. J Immigr Minor Health. 2013;15:718–24. https://doi.org/10.1007/s10903-012-9691-6
28. Wang H, Wolock TM, Carter A, Nguyen G, Kyu HH, Gakidou E, et al.; GBD 2015 HIV Collaborators. Estimates of global, regional, and national incidence, prevalence, and mortality of HIV, 1980–2015: the Global Burden of Disease Study 2015. Lancet HIV. 2016;3:e361–87. https://doi.org/10.1016/S2352-3018(16)30087-X
29. Centers for Disease Control and Prevention (CDC). Final rule removing HIV infection from U.S. immigration screening 2011 [cited 2020 Apr 20]. https://www.cdc.gov/immigrantrefugeehealth/laws-regs/hiv-ban-removal/final-rule-technical-qa.html
30. Shariff SZ, Cuerden MS, Jain AK, Garg AX. The secret of immortal time bias in epidemiologic studies. J Am Soc Nephrol. 2008;19:841–3. https://doi.org/10.1681/ASN.2007121354
31. Department of Homeland Security. Yearbook of immigration statistics 2019; updated 2020 October 28 [cited 2020 Dec 11]. https://www.dhs.gov/immigration-statistics/yearbook/2019
32. Department of Homeland Security. Refugees and asylees; updated 2020 October 22 [cited 2020 Dec 11]. https://www.dhs.gov/immigration-statistics/refugees-asylees
33. Centers for Disease Control and Prevention. Guidelines for screening for tuberculosis infection and disease during the domestic medical examination for newly arrived refugees; 2019 [cited 2020 Feb 26]. https://www.cdc.gov/immigrantrefugeehealth/guidelines/domestic/tuberculosis-guidelines.html
34. Mitchell T, Weinberg M, Posey DL, Cetron M. Immigrant and refugee health: a Centers for Disease Control and Prevention perspective on protecting the health and health security of individuals and communities during planned migrations. Pediatr Clin North Am. 2019;66:549–60. https://doi.org/10.1016/j.pcl.2019.02.004
35. Tsang CA, Langer AJ, Kammerer JS, Navin TR. US tuberculosis rates among persons born outside the United States compared with rates in their countries of birth, 2012–2016. Emerg Infect Dis. 2020;26:533–40. https://doi.org/10.3201/eid2603.190974
36. Taylor AB, Kurbatova EV, Cegielski JP. Prevalence of anti-tuberculosis drug resistance in foreign-born tuberculosis cases in the U.S. and in their countries of origin. PLoS One. 2012;7:e49355. https://doi.org/10.1371/journal.pone.0049355

Address for correspondence: Amish Talwar, Centers for Disease Control and Prevention, 1600 Clifton Rd NE, Mailstop H21-3, Atlanta, GA 30329-4027, USA; email: atalwar@cdc.gov

Case–Control Study of Risk Factors for Acquired Hepatitis E Virus Infections in Blood Donors, United Kingdom, 2018–2019

Iona Smith, Bengü Said, Aisling Vaughan, Becky Haywood, Samreen Ijaz, Claire Reynolds, Su Brailsford, Katherine Russell, Dilys Morgan

Hepatitis E virus (HEV) is the most common cause of acute viral hepatitis in England. Substantial yearly increases of autochthonous infections were observed during 2003–2016 and again during 2017–2019. Previous studies associated acute HEV cases with consumption of processed pork products, we investigated risk factors for autochthonous HEV infections in the blood donor population in England. Study participants were 117 HEV RNA–positive blood donors and 564 HEV RNA–negative blood donors. No persons with positive results were vegetarian; 97.4% of persons with positive results reported eating pork products. Consuming bacon (OR 3.0, 95% CI 1.7–5.5; p<0.0001), cured pork meats (OR 3.5, 95% CI 2.2–5.4; p<0.0001), and pigs' liver (OR 2.9, 95% CI 1.0–8.3; p = 0.04) were significantly associated with HEV infection. Our findings confirm previous links to pork products and suggest that appropriate animal husbandry is essential to reduce the risk for HEV infection.

A substantial increase in locally acquired cases of hepatitis E virus (HEV) has been observed across Europe; a 10-fold increase of >21,000 cases of HEV was reported in the European Economic Area during 2005–2015 (*1*–*4*). It is difficult to accurately estimate the true burden of HEV due to substantial heterogeneity in available data across member states (*5*).

An increasing trend of acute HEV cases was observed in the United Kingdom, during 2010–2016; peaks were reported in 2015 (1,212 cases), 2016 (1,243 cases), 2018 (1,002 cases), and 2019 (1,202 cases) (*6*). HEV is the most common cause of diagnosed acute viral hepatitis in England (*2*,*7*–*9*). The annual estimate of HEV infections in England is 100,000–150,000 (*9*,*10*), and the actual burden of infection is likely to be higher. In addition to acute symptomatic infection, asymptomatic HEV infection has been reported previously (*11*) and has been observed in blood donors in the United Kingdom. The prevalence of HEV infection is dynamic in England and Wales, as suggested by the fluctuating incidence of acute HEV infections and HEV RNA presence in blood donations (*6*,*12*).

HEV is a RNA virus with 8 genotypes; genotype 1 (G1) and G2 viruses are predominantly found in low- and middle-income countries, whereas G3, G4, and G7 viruses are responsible for infections in high-income countries (*13*). G1 and G2 are transmitted by the fecal–oral route; infection with G3 and G4 viruses is primarily foodborne. HEV is found in many animal species; however, pigs are recognized as the main reservoir (*14*,*15*). A high prevalence of antibodies to HEV in UK swine has been reported (92.8%), along with evidence of current HEV infection in 20.5% (95% CI 17.2%–23.8%) of pigs at the time of slaughter (*16*). These findings were determined using HEV RNA detection in either plasma or cecal samples; HEV was detected in 22/629 (3.5%) of plasma samples and 93/629 (14.9%) of cecal contents (*16*–*18*). The presence of HEV RNA in cecal samples could be caused by environmental contamination; however, multiple other studies in Europe have also observed the presence of HEV RNA at the point of slaughter (*19*–*21*). This presence of viremia at time of slaughter poses a significant risk for HEV-infected products to enter the food chain.

In general, in the United Kingdom, G3 clade 1 (G3 efg) viruses circulate in swine; however, the increase of acute HEV cases in England in 2010 coincided with the emergence of a novel HEV phylotype, G3 clade 2 (G3 abcdhij) viruses (*22*). No evidence has been found of this phylotype in the pig population in England and, although it has been isolated in 1 pig in

Author affiliations: Public Health England, London, UK (I. Smith, B. Said, A. Vaughan, B. Haywood, S. Ijaz, C. Reynolds, S. Brailsford, K. Russell, D. Morgan); National Institute for Health Research Health Protection Research Unit in Emerging and Zoonotic Infections, Liverpool, UK (I. Smith)

DOI: https://doi.org/10.3201/eid2706.203964

Scotland, the isolate fell outside of the dominant human clade (*16*). It is likely, therefore, that the reason the novel phylotype is present is the consumption of pork originating from outside the United Kingdom (*3*,*22*–*24*). Viruses detected in human clinical samples in the United Kingdom, which are closely related to those found in pigs in mainland Europe (*3*,*22*) support this idea; taken together, the evidence suggests a risk for zoonotic transmission from pork products originating from outside of the United Kingdom.

A body of evidence supports the finding that HEV infection can also be acquired from blood products and HEV can be transmitted through transfusion (*25*), and the clinical consequences have been increasingly recognized (*26*,*27*). Therefore, to mitigate the risk for transmission by transfusion, National Health Service Blood and Transplant (NHSBT) introduced HEV-screened components for selected patients in March 2016 following a recommendation from the Advisory Committee on the Safety of Blood, Tissues and Organs (SaBTO). SaBTO subsequently recommended that the UK blood services implement universal screening; beginning April 2017, all blood components have been screened and those used are HEV negative (*28*,*29*).

In addition to mitigating the risk for transmission via transfusion, universal screening of blood donations by NHSBT also provided a new and unique opportunity to understand HEV infection in a population that more closely reflects the general population. The aim of this study was to characterize the clinical features of UK-acquired HEV infection in blood donors in England and investigate the potential risk factors for infection.

Methods

Study Design

We conducted a case–control study April 1, 2018–March 31, 2019, to describe the clinical features of infection and to identify the risk factors for HEV acquisition within the blood donor population in England. As part of the continuing enhanced surveillance, NHSBT contacted all blood donor HEV cases to inform them of their infection. HEV RNA positive samples, detectable by PCR, were sent to the Blood Borne Virus Unit, Public Health England (Colindale, UK) for genotyping (*26*). NHSBT invited donors to take part in the case–control study, which included a link to complete an enhanced surveillance questionnaire designed for this study (*29*). All participants provided consent for their information to be used in the study.

We used case age and donation date to request a sample of eligible controls from NHSBT Donor Insight; they created a dispatch extract of data from their donor database in Excel (Microsoft, https://www.microsoft.com) containing donor's name, postal address, email address, donor number, and donation date. No PII about the controls was shared outside of NHSBT. Controls were age-matched to cases across defined age groups (17–24, 25–44, and ≥45 years) and had donated within the same week as the age-matched case. Controls were not sex-matched to cases; we adjusted for sex in the analysis.

Case Selection

A case was defined as a blood donor, residing in England, who donated blood to NHSBT during the period April 1, 2018–March 31, 2019; who was HEV RNA positive as indicated by a confirmed positive HEV RNA donation testing result; and who had no history of travel outside the United Kingdom in the 9 weeks before donation. NHSBT collected descriptive data for all HEV RNA–positive donors identified within the study period to ensure the cases included in the study were representative of the HEV RNA positive blood donor group.

Control Selection

A control was defined as a blood donor who contemporaneously donated blood to the NHSBT, resides in England, and was confirmed negative for HEV and all other markers of infection during screening. They also had no travel history outside the United Kingdom in the 9 weeks before donation, had not been recently surveyed by NHSBT, and had not opted out of communications from NHSBT.

Data Collection

To characterize the clinical features of indigenously acquired HEV infection and risk factors for HEV infection, we collected the following information from cases and controls: travel history, animal exposures, environmental exposures, alcohol intake, medication, and concurrent conditions. We also asked about the food they consumed and their purchasing preferences; on the basis of published evidence, we included more detailed questions about the consumption of pork products or derivatives. Because of the long incubation period of HEV (2–9 weeks), questions were phrased as, "Are you likely to have eaten the following food items?" We asked cases about the 9-week period before the date of their HEV RNA positive blood donation and asked controls about the 9-week period before their donation.

Study participants who reported a travel history outside the United Kingdom in the 9 weeks (the maximum incubation period for HEV) before donating were excluded from the analysis because they could have contracted HEV through their travel (*30*).

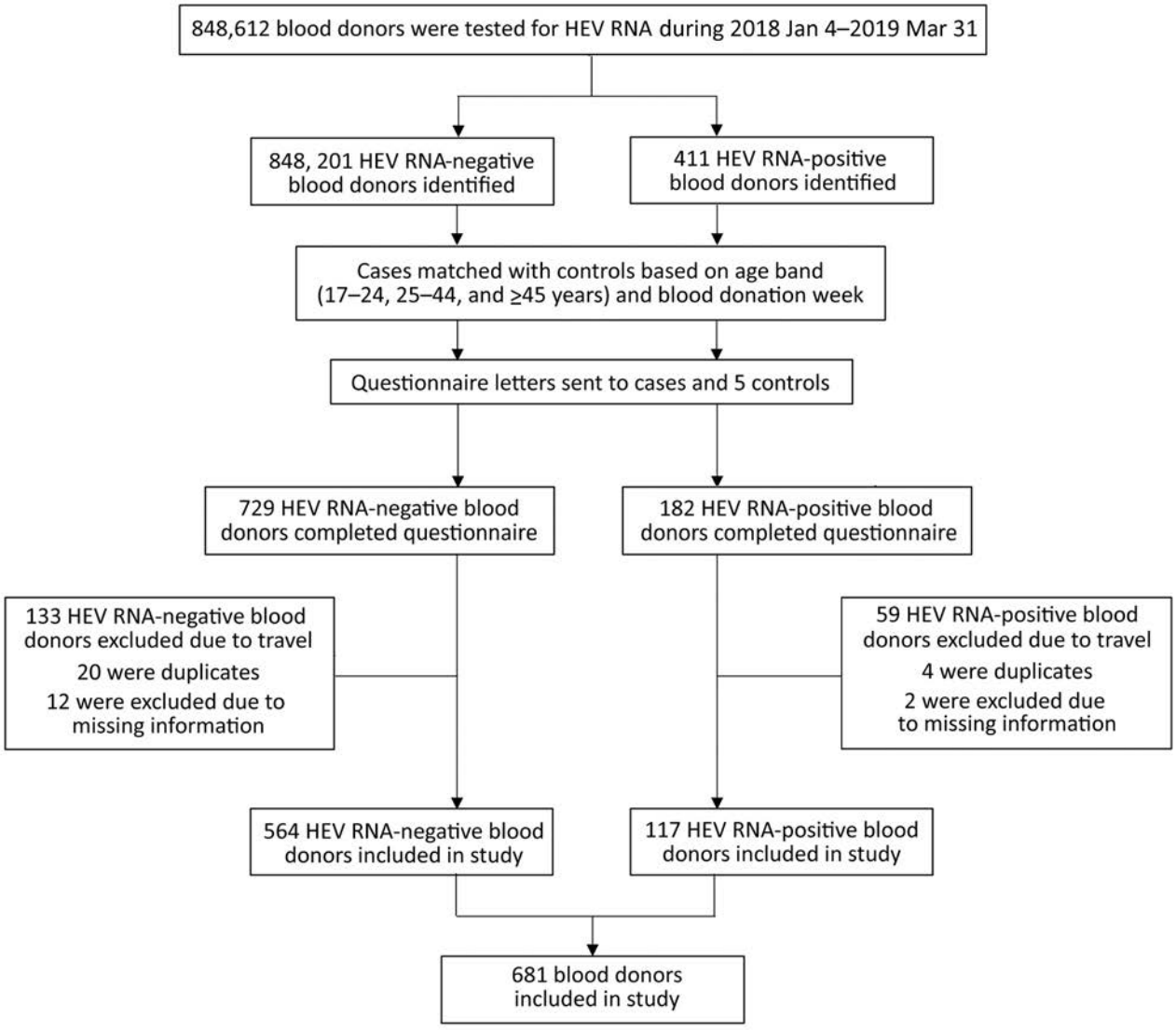

Figure. Recruitment of blood donors to case–control study of hepatitis E virus in blood donors, United Kingdom, 2018–2019.

In terms of patient-identifiable information (PII), controls were not asked to provide any, and their survey data were not linked to their donation record. Cases were requested to provide their name to allow for linkage of questionnaire responses with their laboratory results. Participants were excluded if the questionnaire was incomplete.

Ethics approval was not required because this study used data that were routinely being collected through enhanced surveillance. All participants, however, did consent for their information to be used in the case-control study. PII was removed before analysis, and all data were handled according to Caldicott principles.

Of 411 participants identified as HEV RNA–positive blood donors, 182 (44%) completed the questionnaire. Compared to other studies using online surveys with a blood donor population, which have reported 26% completion of questionnaires, 44% is a strong response rate (*31*). After we excluded duplicate questionnaires, participants who had traveled in the designated period, and those with missing information, 117 HEV RNA–positive blood donors remained in the study.

Data Analysis

To investigate potential risk factors and environmental exposures of HEV, we conducted univariate logistic regression. We included variables with an odds ratio (OR) >1 and $p<0.01$ in a multivariable logistic regression model. In the multivariable analysis, variables with

an adjusted OR <1 or no significant association (p>0.05) with HEV infection were removed from the model in a backward stepwise fashion until all the variables in the model exhibited a degree of association. We adjusted for age and sex at all stages of analysis. We performed all statistical analyses using Stata software version 15 (StataCorp, https://www.stata.com).

Results

Study Demographics

We included a total of 117 HEV RNA–infected blood donors and 564 HEV RNA–negative donors in the case–control study (Figure). The ratio of cases to controls was 1:4.8. The HEV RNA–infected participants corresponded to 28.5% (117/411) of the total infected blood donors identified during the study period (Table 1). As in previous studies (*9*,*26*,*29*), most of the HEV-infected blood donors identified in the study period were male, a similar proportion to the HEV-infected blood donors included in the study. Donors in the age group ≥45 years were the greatest number of all HEV-infected and noninfected blood donors; the predominance of this age group was seen in cases and controls in the study.

HEV Genotype

We conducted sequence and phylogenetic analysis on 24 (20.5%) HEV RNA–positive cases, where viral load was sufficient to do so (*32*,*33*). Phylogenetic analysis showed that all viruses belonged to the HEV G3 phylogroup; 22 (91.7%) of them were HEV G3 clade 2 (abcdhij) viruses and 2 (8.3%) were G3 clade 1 (efg) HEV viruses.

Symptoms

Overall, 41/117 (35%) of cases were symptomatic, and female and male cases experienced symptoms equally. The most commonly reported symptoms were fatigue, joint pain, and headaches; these symptoms were reported by 14%–20% of those with symptoms. Other symptoms experienced by ≈10% of cases included abdominal pain, nausea, change in appetite, and weakness or tingling. All symptoms were experienced significantly more by cases than controls except vomiting, which 1 case and no control reported (p≤0.0001). Overall, 76/117 (65%) of cases and 552/564 (98%) of controls were asymptomatic.

Risk Factors

In the univariate analysis of 19 food items that were likely to have been consumed over the 9-week period before onset of symptoms in the cases and the previous 9-week period to donation in controls, 14 food items were significantly associated with HEV infection (OR >1; p<0.01). Most of these items were animal products (Table 2). No cases and 4 controls were vegetarians. Contact with animals, specifically dogs, was associated with HEV infection (OR 1.7, 95% CI 1.1–2.6; p = 0.01); however, upon inclusion in multivariable analysis, this factor lost significance. The final multivariable model, which was adjusted for age and sex, showed that the only variables of note were bacon, cured pork meats such as sliced salami and cabanos, and pigs' liver (Table 3).

Discussion

The overall prevalence of HEV infection in blood donors detected during this study period is 0.05% (411/848,201). Although we found a higher level of infection than reported previously (*29*), the rate does fluctuate; the study rate shows the continued presence of HEV in the blood donor population, indicating the importance of blood screening. Compared with previous populations used for investigating HEV, the blood donor population is more representative of the general population and has different demographics than the population of acute HEV cases.

We observed a greater presence of HEV in male than female blood donors. This difference between sexes has been a consistent finding in previous studies in England and across Europe (*4*,*11*,*22*,*29*,*34*–*36*). One explanation for the dominance of male cases could be a

Table 1. Age and sex of participants in case–control study of hepatitis E infections in blood donors, 2018–2019*

Characteristic	All HEV RNA–positive samples, n = 411	All HEV RNA–negative samples, n = 848,201	Cases, n = 117	Controls, n = 564
Age group, y				
17–24	24 (5.8)	87,460 (10.3)	5 (4.3)	15 (2.7)
25–44	159 (38.7)	337,240 (39.8)	31 (26.5)	184 (32.6)
>45	228 (55.5)	423,501 (49.9)	81 (69.8)	365 (64.7)
Sex				
F	165 (40.2)	486,388 (57.3)	52 (44.4)	305 (54.1)
Median age, y	45	42	48	50
Age range, y	17–80	17–95	20–78	18–78
M	246 (59.9)	361,813 (42.7)	65 (55.6)	259 (45.9)
Median age, y	49	48	54	52
Age range, y	18–73	17–84	21–72	17–81

*Values are no. (%) participants except as indicated.

Table 2. Univariate analysis of risk factors for hepatitis E infection in study of blood donor–related transmission, 2018–2019*

Risk factor	Cases, n = 117	Controls, n = 564	Univariable analysis	
			OR ((95% CI)	p value
Food consumption				
Bacon‡	102 (87.2)	343 (60.8)	4.6 (2.6–8.2)	<0.0001
Cured pork meat‡	73 (62.4)	158 (28.0)	4.5 (3.0–6.9)	<0.0001
Ham (off-the bone or joint)	42 (35.9)	148 (26.2)	1.6 (1.0–2.4)	0.04
Other pork products	26 (22.2)	79 (14.0)	1.7 (1.0–2.8)	0.04
Other sausages	11 (9.4)	59 (10.5)	0.9 (0.4–1.7)	0.7
Pate‡	35 (29.9)	83 (14.7)	2.5 (1.6–3.9)	<0.0001
Pigs' liver‡	8 (6.8)	10 (1.8)	3.7 (1.4–9.8)	0.01
Pork‡	72 (61.5)	269 (47.7)	1.8 (1.2–2.6)	0.01
Pork pie	40 (34.2)	142 (25.2)	1.5 (0.9–2.2)	0.09
Pork sausages‡	95 (81.2)	340 (60.3)	2.9 (1.7–4.7)	<0.0001
Sliced sandwich ham, prepacked‡	81 (69.2)	307 (54.4)	1.9 (1.3 – 3.0)	0.003
Any pork product‡	114 (97.4)	445 (78.9)	10.5 (3.3–33.6)	<0.0001
Chicken	107 (91.5)	443 (78.6)	3.0 (1.5–5.9)	0.002
Fish	84 (71.8)	395 (70.0)	1.1 (0.7–1.7)	0.7
Game	9 (7.7)	18 (3.2)	2.4 (1.1–5.5)	0.04
Other offal‡	16 (13.7)	34 (6.0)	2.3 (1.2–4.3)	0.01
Shellfish	44 (37.6)	191 (33.9)	1.3 (0.8–1.9)	0.3
Fresh fruit‡	109 (93.2)	472 (83.7)	2.8 (1.3 – 6.0)	0.01
Raw vegetables	81 (69.2)	354 (62.8)	1.5 (1.0–2.3)	0.08
Salad vegetables‡	108 (92.3)	460 (81.6)	3.0 (1.5–6.2)	0.01
Supermarket				
Supermarket A‡	60 (51.3)	202 (35.8)	2.0 (1.3 – 3.0)	0.001
Supermarket B	33 (28.2)	159 (28.2)	1.0 (0.7–1.6)	0.9
Supermarket C	71 (60.7)	312 (55.3)	1.2 (0.8–1.9)	0.3
Supermarket D	15 (12.8)	114 (20.2)	0.6 (0.3–1.0)	0.05
Supermarket E	58 (49.6)	245 (43.4)	1.3 (0.8–1.9)	0.3
Supermarket F	40 (34.2)	150 (26.6)	1.4 (0.9–2.1)	0.1
Supermarket G‡	40 (34.2)	123 (21.8)	1.8 (1.2–2.8)	0.01
Supermarket H	20 (17.1)	112 (19.9)	0.8 (0.5–1.4)	0.5
Supermarket I‡	33 (38.2)	112 (19.9)	1.6 (1.0–2.5)	0.04
Supermarket J	0 (0.0)	2 (0.4)	1 (NA)	NA
Supermarket K	1 (0.9)	14 (2.5)	0.4 (0.1–2.8)	0.3
Local butcher/shop	17 (7.7)	49 (2.3)	3.6 (1.5–8.8)	0.0
Animal contact				
Yes‡	97 (82.9)	389 (69.0)	2.3 (1.4–3.9)	0.0
Cat	48 (41.0)	209 (37.1)	1.2 (0.8–1.8)	0.4
Dog‡	76 (65.0)	297 (52.7)	1.7 (1.1–2.6)	0.01
Rodent	8 (6.8)	24 (4.3)	1.7 (0.8–4.0)	0.2
Pig	5 (4.3)	15 (2.7)	1.6 (0.6–4.5)	0.4
Sheep	2 (1.7)	29 (5.1)	0.3 (0.1–1.4)	0.1
Horse	6 (5.1)	39 (6.9)	0.8 (0.3–1.8)	0.5
Cow	3 (2.6)	20 (3.6)	0.7 (0.2–2.4)	0.6
Alcohol consumption†				
Yes‡	95 (81.2)	395 (70.0)	1.8 (1.1–3.0)	0.02
1–10 units/wk‡	66 (57.4)	279 (49.8)	1.9 (1.1–3.1)	0.02
10–20 units/wk	17 (14.8)	71 (12.7)	1.8 (0.9–3.5)	0.1
≥20 units/wk	10 (8.7)	41 (7.3)	1.6 (0.7–3.7)	0.3
Underlying illnesses				
Medical condition	30 (25.6)	130 (23.1)	1.1 (0.7–1.8)	0.7
Respiratory	4 (3.4)	19 (3.4)	1.1 (0.4–3.2)	0.9
Liver	1 (0.9)	2 (0.4)	1.9 (0.2–21.4)	0.6
Heart	0 (0.0)	1 (0.2)	1 (–)	–
Diabetes	3 (2.6)	5 (0.9)	2.4 (0.6–10.5)	0.2

*Values are no. (%) participants except as indicated. OR, odds ratio. (†Missing information for 2 cases. (‡Significant at univariate analysis.

difference in the consumption of meat (*22*). In the United Kingdom, the National Diet and Nutrition Survey collects information about the diet, nutrient intake, and the nutritional status of the UK population. Their data show that men consistently consume more meat than women (*37*). An alternative explanation for the sex difference is that men may be more clinically susceptible because of sex-driven differences, whereas women are less likely to exhibit acute clinical disease (*30*). However, this study found that symptoms were experienced equally by male and female cases. Ijaz et al. previously noted that men and women have similar levels of IgG for HEV in England (*10*), which suggests a comparable burden of HEV in both sexes. Similar sex differences

have also been observed with other hepatitis viruses (*38*,*39*). The reason why more HEV cases are male remains uncertain and warrants further research.

Previous studies have suggested that the distribution of HEV cases is not uniform and that certain areas in England are at greater risk (*4*,*30*,*40*). The results of our case–control study, however, did not identify geographic clustering of HEV cases among blood donors; this was consistent with the findings of a NHSBT surveillance study of HEV-positive blood donors during March 2016–December 2017 (*29*). As observed in the NHSBT surveillance study, HEV G3 clade 2 was the predominant phylotype detected (*4*,*29*), which suggested that the HEV infections identified in the blood donor population may have resulted from consuming pork products that originated from outside the United Kingdom, because HEV G3 clade 2 is not the predominant phylotype circulating in pigs (*3*,*4*,*16*). Determining the virus's origin is difficult, however, because it is generally accepted that HEV is endemic in swine within the United Kingdom and mainland Europe (*16*,*19*–*21*,*41*,*42*).

Ours is not the first UK case–control study to find that processed pork products and pigs' liver are associated with HEV infection (*30*,*43*,*44*). However, it is one of the first to identify bacon and cured pork meat as risk factors for HEV. The relative contribution of each pork product to the total number of cases should be noted, though; preventing the consumption of pigs' liver would lead to only a modest reduction in HEV cases because relatively few persons eat the liver. Unlike previous studies, this study did not find risk associated with the consumption of pork pies or the consumption of ham and sausages purchased from a specific UK supermarket chain (*30*). Possible causes are changes in the supplier or source of pork for the supermarket chain since the findings of the previous study. Alternatively, there may be differences between the study populations.

Recent studies have investigated the thermal stability of HEV; researchers have not agreed upon the necessary time and temperature for heat inactivation of HEV (*30*,*45*–*47*). Although bacon should be cooked, other cured meats, such as sliced salami and cabanos, may not have been cooked during the curing process, and it is currently unknown whether curing is sufficient to inactivate HEV (*48*). HEV contamination has previously been found in raw meat products (*17*,*18*,*49*); thus, it is biologically feasible that if the curing process was not sufficient to inactivate the HEV then viral transmission could occur from consumption of these products. Further studies are required to understand the parameters required for heat inactivation of HEV and the effect of different treatment procedures such as curing on the virus. Unfortunately, methods for sampling and testing of pork and other food products are not sufficiently robust to provide information about contamination with infectious viruses.

Table 3. Multivariable analysis model of food consumption associated with testing positive for hepatitis E virus, adjusted for age and sex

	Multivariable analysis	
Risk factor	OR (95% CI)	p value
Bacon		<0.0001
No	Referent	
Yes	3.0 (1.7–5.5)	
Cured pork meat		<0.0001
No	Referent	
Yes	3.5 (2.2–5.4)	
Pigs' liver		0.04
No	Referent	
Yes	2.9 (1.0–8.3)	

A limitation of this study is that some blood donors may have previously been infected with HEV and so were not at risk for infection at the time of study. Testing HEV RNA–negative persons for HEV antibodies would have clarified this, but that was not possible in this study.

Of note is the potential effect of recall bias for study participants recounting their potential food and environmental exposures. HEV RNA–positive blood donors were contacted as soon as possible after the donation was confirmed HEV RNA positive. However, the maximum 9-week incubation period of HEV may have led to patients forgetting their food and environmental exposures or recalling them incorrectly. Furthermore, controls would have had a larger time lag due to the time required to identify appropriate controls based on case demographics and to send out the appropriate information. The lag could increase the likelihood of recall bias. In addition, sharing with study participants the information about hepatitis E and its association with pork may have biased the participants' recall response.

Our knowledge of HEV infection in the population was previously limited to a population of acutely infected persons who sought medical care. The introduction of universal screening has led to the availability of an immensely useful cohort of HEV-infected persons different from the cohort of acute HEV cases. HEV-infected blood donors were identified not through medical investigations but through universal screening; thus, they are more representative of the general population compared with the acute HEV population. However, we recommend caution before extrapolating the results of this study to the general population. Because of donor selection guidelines (*50*), the donor population tends to be healthier than the general population; the cutoff of 65 years in new donors and the self-selecting nature of donation suggests that the prevalence of

HEV in the general population is different than that found in the blood donor population.

This study found that HEV infection in blood donors in England was associated with the consumption of 3 pork products; bacon, cured pork meats, and pigs' liver. Bacon and other cured pork meats were not previously identified as risk factors for HEV. The identification of these pork products highlights the importance of accurate information about cooking requirements as well as the role and importance of animal husbandry to prevent HEV infection in pigs. Targeting HEV infection at the source would prevent foodborne transmission to the population.

Acknowledgments

We thank the National Health Service Blood and Transplant Microbiology Services office staff who assisted in contacting donors. We thank all the donors who participated in the study.

About the Author

Ms. Smith is an epidemiologist within the Emerging Infections and Zoonoses team at Public Health England. Key research interests include infectious disease epidemiology and global public health.

References

1. Adlhoch C, Manďáková Z, Ethelberg S, Epštein J, Rimhanen-Finne R, Figoni J, et al. Standardising surveillance of hepatitis E virus infection in the EU/EEA: A review of national practices and suggestions for the way forward. J Clin Virol. 2019;120:63–7. https://doi.org/10.1016/j.jcv.2019.09.005
2. Aspinall EJ, Couturier E, Faber M, Said B, Ijaz S, Tavoschi L, et al.; The Country Experts. Hepatitis E virus infection in Europe: surveillance and descriptive epidemiology of confirmed cases, 2005 to 2015. Euro Surveill. 2017;22:pii=30561. https://doi.org/10.2807/1560-7917.ES.2017.22.26.30561
3. Adlhoch C, Avellon A, Baylis SA, Ciccaglione AR, Couturier E, de Sousa R, et al. Hepatitis E virus: Assessment of the epidemiological situation in humans in Europe, 2014/15. J Clin Virol. 2016;82:9–16. https://doi.org/10.1016/j.jcv.2016.06.010
4. Oeser C, Vaughan A, Said B, Ijaz S, Tedder R, Haywood B, et al. Epidemiology of hepatitis E in England and Wales: a 10-year retrospective surveillance study, 2008–2017. J Infect Dis. 2019;220:802–10. https://doi.org/10.1093/infdis/jiz207
5. Horn J, Hoodgarzadeh M, Klett-Tammen CJ, Mikolajczyk RT, Krause G, Ott JJ. Epidemiologic estimates of hepatitis E virus infection in European countries. J Infect. 2018;77:544–52. https://doi.org/10.1016/j.jinf.2018.09.012
6. Public Health England. Hepatitis E: symptoms, transmission, treatment and prevention. 2019 [cited 2020 May 14]. https://www.gov.uk/government/publications/hepatitis-e-symptoms-transmission-prevention-treatment/hepatitis-e-symptoms-transmission-treatment-and-prevention
7. Izopet J, Tremeaux P, Marion O, Migueres M, Capelli N, Chapuy-Regaud S, et al. Hepatitis E virus infections in Europe. J Clin Virol. 2019;120:20–6. https://doi.org/10.1016/j.jcv.2019.09.004
8. Webb GW, Dalton HR. Hepatitis E: an underestimated emerging threat. Ther Adv Infect Dis. 2019;6:2049936119837162. https://doi.org/10.1177/2049936119837162
9. Tedder RS, Tettmar KI, Brailsford SR, Said B, Ushiro-Lumb I, Kitchen A, et al. Virology, serology, and demography of hepatitis E viremic blood donors in South East England. Transfusion. 2016;56:1529–36. https://doi.org/10.1111/trf.13498
10. Ijaz S, Vyse AJ, Morgan D, Pebody RG, Tedder RS, Brown D. Indigenous hepatitis E virus infection in England: more common than it seems. J Clin Virol. 2009;44:272–6. https://doi.org/10.1016/j.jcv.2009.01.005
11. Said B, Ijaz S, Kafatos G, Booth L, Thomas HL, Walsh A, et al.; Hepatitis E Incident Investigation Team. Hepatitis E outbreak on cruise ship. Emerg Infect Dis. 2009;15:1738–44. https://doi.org/10.3201/eid1511.091094
12. Boland F, Martinez A, Pomeroy L, O'Flaherty N. Blood donor screening for hepatitis E virus in the European Union. Transfus Med Hemother. 2019;46:95–103. https://doi.org/10.1159/000499121
13. Gouilly J, Chen Q, Siewiera J, Cartron G, Levy C, Dubois M, et al. Genotype specific pathogenicity of hepatitis E virus at the human maternal-fetal interface. Nat Commun. 2018;9:4748. https://doi.org/10.1038/s41467-018-07200-2
14. Dalton HR, Stableforth W, Thurairajah P, Hazeldine S, Remnarace R, Usama W, et al. Autochthonous hepatitis E in Southwest England: natural history, complications and seasonal variation, and hepatitis E virus IgG seroprevalence in blood donors, the elderly and patients with chronic liver disease. Eur J Gastroenterol Hepatol. 2008;20:784–90. https://doi.org/10.1097/MEG.0b013e3282f5195a
15. Pavio N, Meng X-J, Renou C. Zoonotic hepatitis E: animal reservoirs and emerging risks. Vet Res. 2010;41:46. https://doi.org/10.1051/vetres/2010018
16. Grierson S, Heaney J, Cheney T, Morgan D, Wyllie S, Powell L, et al. Prevalence of hepatitis E virus infection in pigs at the time of slaughter, United Kingdom, 2013. Emerg Infect Dis. 2015;21:1396–401. https://doi.org/10.3201/eid2108.141995
17. Berto A, Martelli F, Grierson S, Banks M. Hepatitis E virus in pork food chain, United Kingdom, 2009-2010. Emerg Infect Dis. 2012;18:1358–60. https://doi.org/10.3201/eid1808.111647
18. Bouwknegt M, Lodder-Verschoor F, van der Poel WH, Rutjes SA, de Roda Husman AM. Hepatitis E virus RNA in commercial porcine livers in The Netherlands. J Food Prot. 2007;70:2889–95. https://doi.org/10.4315/0362-028X-70.12.2889
19. Rutjes SA, Bouwknegt M, van der Giessen JW, de Roda Husman AM, Reusken CB. Seroprevalence of hepatitis E virus in pigs from different farming systems in The Netherlands. J Food Prot. 2014;77:640–2. https://doi.org/10.4315/0362-028X.JFP-13-302
20. Crossan C, Grierson S, Thomson J, Ward A, Nunez-Garcia J, Banks M, et al. Prevalence of hepatitis E virus in slaughter-age pigs in Scotland. Epidemiol Infect. 2015;143:2237–40. https://doi.org/10.1017/S0950268814003100
21. Burri C, Vial F, Ryser-Degiorgis MP, Schwermer H, Darling K, Reist M, et al. Seroprevalence of hepatitis E virus in domestic pigs and wild boars in Switzerland. Zoonoses Public Health. 2014;61:537–44. https://doi.org/10.1111/zph.12103
22. Said B, Usdin M, Warburton F, Ijaz S, Tedder RS, Morgan D. Pork products associated with human infection caused by an emerging phylotype of hepatitis E virus in England and Wales. Epidemiol Infect. 2017;145:2417–23. https://doi.org/10.1017/S0950268817001388
23. Baechlein C, Schielke A, Johne R, Ulrich RG, Baumgaertner W, Grummer B. Prevalence of Hepatitis E virus-specific antibodies in sera of German domestic pigs estimated by using different assays. Vet Microbiol. 2010;144:187–91. https://doi.org/10.1016/j.vetmic.2009.12.011

24. Rutjes SA, Lodder WJ, Lodder-Verschoor F, van den Berg HH, Vennema H, Duizer E, et al. Sources of hepatitis E virus genotype 3 in The Netherlands. Emerg Infect Dis. 2009;15:381–7. https://doi.org/10.3201/eid1503.071472
25. Colson P, Coze C, Gallian P, Henry M, De Micco P, Tamalet C. Transfusion-associated hepatitis E, France. Emerg Infect Dis. 2007;13:648–9. https://doi.org/10.3201/eid1304.061387
26. Hewitt PE, Ijaz S, Brailsford SR, Brett R, Dicks S, Haywood B, et al. Hepatitis E virus in blood components: a prevalence and transmission study in southeast England. Lancet. 2014;384:1766–73. https://doi.org/10.1016/S0140-6736(14)61034-5
27. Pérez-Gracia MT, García M, Suay B, Mateos-Lindemann ML. Current knowledge on hepatitis E. J Clin Transl Hepatol. 2015;3:117–26.
28. Advisory Committee on the Safety of Blood, Tissues, and Organs. Guidelines from the expert advisory committee on the Safety of Blood, Tissues and Organs (SaBTO) on measures to protect patients from acquiring hepatitis E virus via transfusion or transplantation, 2017 [cited 2019 Mar 20]. https://assets.publishing.service.gov.uk/government/uploads/system/uploads/attachment_data/file/680297/Hepatitis_E_Guidelines.pdf
29. Harvala H, Hewitt PE, Reynolds C, Pearson C, Haywood B, Tettmar KI, et al. Hepatitis E virus in blood donors in England, 2016 to 2017: from selective to universal screening. Euro Surveill. 2019;24:pii=1800386. https://doi.org/10.2807/1560-7917.ES.2019.24.10.1800386
30. Said B, Ijaz S, Chand MA, Kafatos G, Tedder R, Morgan D. Hepatitis E virus in England and Wales: indigenous infection is associated with the consumption of processed pork products. Epidemiol Infect. 2014;142:1467–75. https://doi.org/10.1017/S0950268813002318
31. Sauvage C, Spinardi R, Pelat C, Pouget T, Danic B, Woimant G, et al.; Steering Committee. Noncompliance with blood donor selection criteria - Complidon 2017, France. Transfusion. 2020;60:73–83. https://doi.org/10.1111/trf.15623
32. Ijaz S, Arnold E, Banks M, Bendall RP, Cramp ME, Cunningham R, et al. Non-travel-associated hepatitis E in England and Wales: demographic, clinical, and molecular epidemiological characteristics. J Infect Dis. 2005;192:1166–72. https://doi.org/10.1086/444396
33. Ijaz S, Said B, Boxall E, Smit E, Morgan D, Tedder RS. Indigenous hepatitis E in England and wales from 2003 to 2012: evidence of an emerging novel phylotype of viruses. J Infect Dis. 2014;209:1212–8. https://doi.org/10.1093/infdis/jit652
34. Buti M, Clemente-Casares P, Jardi R, Formiga-Cruz M, Schaper M, Valdes A, et al. Sporadic cases of acute autochthonous hepatitis E in Spain. J Hepatol. 2004;41:126–31. https://doi.org/10.1016/j.jhep.2004.03.013
35. Borgen K, Herremans T, Duizer E, Vennema H, Rutjes S, Bosman A, et al. Non-travel related Hepatitis E virus genotype 3 infections in the Netherlands; a case series 2004 - 2006. BMC Infect Dis. 2008;8:61. https://doi.org/10.1186/1471-2334-8-61
36. Mansuy JM, Abravanel F, Miedouge M, Mengelle C, Merviel C, Dubois M, et al. Acute hepatitis E in south-west France over a 5-year period. J Clin Virol. 2009;44:74–7. https://doi.org/10.1016/j.jcv.2008.09.010
37. Department of Health. National diet and nutrition survey: headline results from years 7 and 8 (combined): data tables (2014/2015–2015/2016) [cited 2019 Mar 12]. https://www.gov.uk/government/statistics/ndns-results-from-years-7-and-8-combined
38. Ruggieri A, Gagliardi MC, Anticoli S. Sex-dependent outcome of hepatitis B and C viruses infections: synergy of sex hormones and immune responses? Front Immunol. 2018;9:2302. https://doi.org/10.3389/fimmu.2018.02302
39. Baig S. Gender disparity in infections of Hepatitis B virus. J Coll Physicians Surg Pak. 2009;19:598–600.
40. Hunter JG, Madden RG, Stone AM, Osborne N, Wheeler B, Vine L, et al. Coastal clustering of HEV; Cornwall, UK. Eur J Gastroenterol Hepatol. 2016;28:323–7. https://doi.org/10.1097/MEG.0000000000000518
41. Kantala T, Heinonen M, Oristo S, von Bonsdorff CH, Maunula L. Hepatitis E virus in young pigs in Finland and characterization of the isolated partial genomic sequences of genotype 3 HEV. Foodborne Pathog Dis. 2015;12:253–60. https://doi.org/10.1089/fpd.2014.1841
42. Walachowski S, Dorenlor V, Lefevre J, Lunazzi A, Eono F, Merbah T, et al. Risk factors associated with the presence of hepatitis E virus in livers and seroprevalence in slaughter-age pigs: a retrospective study of 90 swine farms in France. Epidemiol Infect. 2014;142:1934–44. https://doi.org/10.1017/S0950268813003063
43. Boxman ILA, Jansen CCC, Hägele G, Zwartkruis-Nahuis A, Tijsma ASL, Vennema H. Monitoring of pork liver and meat products on the Dutch market for the presence of HEV RNA. Int J Food Microbiol. 2019;296:58–64. https://doi.org/10.1016/j.ijfoodmicro.2019.02.018
44. Feurer C, Le Roux A, Rossel R, Barnaud E, Dumarest M, Garry P, et al. High load of hepatitis E viral RNA in pork livers but absence in pork muscle at French slaughterhouses. Int J Food Microbiol. 2018;264:25–30. https://doi.org/10.1016/j.ijfoodmicro.2017.10.013
45. Barnaud E, Rogée S, Garry P, Rose N, Pavio N. Thermal inactivation of infectious hepatitis E virus in experimentally contaminated food. Appl Environ Microbiol. 2012;78:5153–9. https://doi.org/10.1128/AEM.00436-12
46. Imagawa T, Sugiyama R, Shiota T, Li TC, Yoshizaki S, Wakita T, et al. Evaluation of heating conditions for inactivation of hepatitis E virus genotypes 3 and 4. J Food Prot. 2018;81:947–52. https://doi.org/10.4315/0362-028X.JFP-17-290
47. Johne R, Trojnar E, Filter M, Hofmann J. Thermal stability of hepatitis E virus as estimated by a cell culture method. Appl Environ Microbiol. 2016;82:4225–31.
48. Montone AMI, De Sabato L, Suffredini E, Alise M, Zaccherini A, Volzone P, et al. Occurrence of HEV-RNA in Italian regional pork and wild boar food products. Food Environ Virol. 2019;11:420–6. https://doi.org/10.1007/s12560-019-09403-2
49. Szabo K, Trojnar E, Anheyer-Behmenburg H, Binder A, Schotte U, Ellerbroek L, et al. Detection of hepatitis E virus RNA in raw sausages and liver sausages from retail in Germany using an optimized method. Int J Food Microbiol. 2015;215:149–56. https://doi.org/10.1016/j.ijfoodmicro.2015.09.013
50. Joint United Kingdom Blood Transfusion and Tissue Transplantation Services Professional Advisory Committee. Guidelines for the blood transfusion services in the UK. 8th edition. 2014 [cited 2020 Jan 20]. https://www.transfusion-guidelines.org/red-book

Address for correspondence: Iona Smith, Public Health England—Tuberculosis, Acute Respiratory, Gastrointestinal, Emerging/Zoonotic Infections and Travel, 61 Colindale Ave, London NW9 5EQ, UK; email: iona.smith@phe.gov.uk or ionacsmith@hotmail.co.uk

Increased Incidence of Antimicrobial-Resistant Nontyphoidal *Salmonella* Infections, United States, 2004–2016

Felicita Medalla, Weidong Gu, Cindy R. Friedman, Michael Judd, Jason Folster, Patricia M. Griffin, Robert M. Hoekstra

Salmonella is a major cause of foodborne illness in the United States, and antimicrobial-resistant strains pose a serious threat to public health. We used Bayesian hierarchical models of culture-confirmed infections during 2004–2016 from 2 Centers for Disease Control and Prevention surveillance systems to estimate changes in the national incidence of resistant nontyphoidal *Salmonella* infections. Extrapolating to the United States population and accounting for unreported infections, we estimated a 40% increase in the annual incidence of infections with clinically important resistance (resistance to ampicillin or ceftriaxone or nonsusceptibility to ciprofloxacin) during 2015–2016 (≈222,000 infections) compared with 2004–2008 (≈159,000 infections). Changes in the incidence of resistance varied by serotype. Serotypes I 4,[5],12:i:- and Enteritidis were responsible for two thirds of the increased incidence of clinically important resistance during 2015–2016. Ciprofloxacin-nonsusceptible infections accounted for more than half of the increase. These estimates can help in setting targets and priorities for prevention.

Nontyphoidal *Salmonella* infections cause an estimated 1.2 million illnesses, 23,000 hospitalizations, and 450 deaths each year in the United States (*1*). Although most infections result in self-limited illness, antimicrobial treatment is recommended for patients with severe infection or at high risk for complications (*2*). Antimicrobial-resistant *Salmonella* infections can cause adverse clinical outcomes, including increased rates of hospitalization, bloodstream infection, other invasive illnesses, and death (*3*–*7*).

Nontyphoidal *Salmonella* infections can be acquired during international travel, from contaminated food and water, through animal contact, and from environmental sources (e.g., wetlands and irrigation water) (*8*–*13*). Antimicrobial-resistant infections have been linked to various food and animal sources (*3*,*14*,*15*). In 2015 and previous years, 5 commonly isolated serotypes (Enteritidis, Typhimurium, Newport, I 4,[5],12:i:- and Heidelberg) accounted for more than half of antimicrobial-resistant *Salmonella* infections in the United States (*16*–*20*). The distribution of antimicrobial-resistant infections caused by some of these common serotypes varied by region (*21*,*22*).

In a previous study, we found that an estimated annual average of 6,200 culture-confirmed infections were resistant to ceftriaxone or ampicillin or nonsusceptible to ciprofloxacin during 2004–2014 (*20*). For the study described in this article, we used the same modeling approach and data sources to estimate changes in incidence. We estimated the contribution of the 5 major serotypes to changes in incidence and describe differences by geographic region. We extrapolated findings to the United States population to provide estimates to help set targets and priorities for reducing antimicrobial resistance among nontyphoidal *Salmonella*.

Methods

Laboratory-Based Enteric Disease Surveillance

Public health laboratories in 50 states and many local health departments receive human *Salmonella* isolates from clinical laboratories and report serotype information to the Centers for Disease Control and Prevention (CDC) through Laboratory-Based Enteric Disease Surveillance (LEDS) (*17*). We excluded serotypes Typhi, Paratyphi A, Paratyphi B (tartrate-negative), and Paratyphi C, which account for <1% of

Author affiliation: Centers for Disease Control and Prevention, Atlanta, Georgia, USA

DOI: https://doi.org/10.3201/eid2706.204486

Salmonella infections in the United States, and whose only known reservoir are humans (*2*,*16*,*17*,*23*). In this article, we use the term *Salmonella* to refer to nontyphoidal *Salmonella*.

National Antimicrobial Resistance Monitoring System

The National Antimicrobial Resistance Monitoring System (NARMS) is a collaboration among CDC, the US Food and Drug Administration, the US Department of Agriculture, and state and local health departments to monitor resistance among enteric bacteria isolated from humans, retail meat, and food animals (*16*,*24*). Public health laboratories in 50 state and 4 local health departments submit every 20th *Salmonella* isolate received from clinical laboratories to CDC for antimicrobial drug susceptibility testing (*16*,*19*,*24*).

During 2004–2016, CDC tested *Salmonella* isolates for susceptibility to agents representing 8–9 antimicrobial classes: aminoglycosides, β-lactam/β-lactamase inhibitors, cephems, macrolides (tested since 2011), penicillins, quinolones, folate pathway inhibitors, phenicols, and tetracyclines (*16*). MICs were determined by broth microdilution with Sensititer (ThermoFisher, https://www.thermofisher.com) and interpreted using criteria from the Clinical and Laboratory Standards Institute (CLSI) when available (*7*,*16*). Using CLSI criteria, we defined ceftriaxone resistance as MIC ≥4 μg/mL, ampicillin resistance as MIC ≥32 μg/mL, and nonsusceptibility to ciprofloxacin as MIC ≥0.12 μg/mL. The ciprofloxacin definition includes both resistant and intermediate CLSI categories because *Salmonella* infections with intermediate susceptibility to ciprofloxacin have been associated with poor treatment outcomes (*6*,*7*,*16*).

Resistance Categories

We defined clinically important resistance as resistance to ceftriaxone, nonsusceptibility to ciprofloxacin, or resistance to ampicillin on the basis of the following criteria: third-generation cephalosporins (e.g., ceftriaxone) and fluoroquinolones (e.g., ciprofloxacin) are used for empiric treatment of severe infections; fluoroquinolones are not recommended for children; and ampicillin is useful for susceptible infections (*2*). We defined and ranked from highest to lowest 3 mutually exclusive categories of clinically important resistance (Appendix Figure 1, https://wwwnc.cdc.gov/EID/article/27/6/20-4486-App1.pdf) (*20*): ceftriaxone/ampicillin resistance (because all ceftriaxone-resistant isolates are ampicillin-resistant); ciprofloxacin nonsusceptibility (nonsusceptible to ciprofloxacin but susceptible to ceftriaxone); and ampicillin-only resistance (ampicillin-resistant but susceptible to ceftriaxone and ciprofloxacin). We included ciprofloxacin-nonsusceptible isolates that were ceftriaxone-resistant in the ceftriaxone/ampicillin category because they are of greatest public health and treatment concern. Many isolates in each category had resistance to other agents. We defined multidrug resistance as resistance to ≥3 classes of antimicrobial agents (*16*,*19*).

Bayesian Hierarchical Model to Estimate Changes

We used 2004–2016 data from LEDS, NARMS, and the US Census Bureau as input in the models (*16*,*17*,*25*). For LEDS, we used the number of culture-confirmed infections by state and year (state-year). We combined serotyped isolates other than Enteritidis, Typhimurium, Newport, I 4,[5],12:i:-, and Heidelberg into an "other" category. We assigned unserotyped and partially serotyped isolates from each state into the 6 serotype categories (Enteritidis, Typhimurium, Newport, I 4,[5],12:i:-, Heidelberg, and other) on the basis of the average proportion of serotyped isolates in each category from 2004–2016. For NARMS, we used resistance proportions among fully serotyped isolates per state-year. We used US Census population data for each state-year to express incidence per 100,000 persons per year (*25*).

A similar Bayesian hierarchical model approach was used from a previous study to estimate the incidence of resistant infections (*20*,*26*). However, we found a Poisson model for LEDS data better captured the uncertainty of *Salmonella* incidence observed at the state-year level instead of the normal distribution used in our previous study (*20*). The model incorporated the random effects of state, year, and state-year interaction to borrow strength from contiguous states and previous years (*20*,*26*–*28*). Alaska and Hawaii were excluded because they are not adjacent to any state; the District of Columbia was also excluded, which began submitting isolates to NARMS in 2008 (*16*,*19*,*20*). We used an approach similar to our previous study to make adjustments for data from Florida, which reported low numbers of isolates compared with its 6 closest states (*17*,*18*,*20*).

We applied the models to generate estimates (referred to as posterior estimates) for *Salmonella* infection incidence rates, resistance proportions, and resistant infection incidence rates (referred to as resistance incidence) by state-year for each of the 6 serotype categories by using Markov chain Monte Carlo simulations (*20*,*26*–*28*). For each serotype category, we estimated resistance incidence for overall

clinically important resistance, the 3 mutually exclusive categories of clinically important resistance, and multidrug resistance. For all *Salmonella*, we calculated overall estimates by summing estimates across the 6 serotype categories. We calculated state-year resistance incidence estimates per 100,000 persons per year as estimated incidence for state-year × estimated resistance proportion for state-year. For estimation of resistance incidence by geographic region, we used the 4 US Census region categories (Midwest, Northeast, South, and West) and aggregated posterior estimates of resistance incidence by year for all states in each region (*25*). For each resistance category, we calculated mean estimates and 95% credible intervals (CrIs) from posterior estimates and mean crude rates by year for the 48 states and those stratified by serotype and region categories (Figure 1; Appendix Figures 2–5) for an overall side-by-side comparison (*20*,*25*,*26*).

To assess changes in resistance incidence, we compared the mean resistance incidence from 2015–2016 with that from two 5-year reference periods during 2004–2016: 2004–2008 and 2010–2014. These reference periods are consistent with those used in NARMS annual reports to assess changes in resistance percentages (*16*). All 50 states have participated in NARMS since 2003; the 2004–2008 period is the early years of nationwide participation and the 2010–2014 period is the recent past. For each resistance and serotype category, we calculated the difference between the posterior estimates of resistance incidence for 2015–2016 and those for each year in the 5-year reference periods for each region to obtain the mean difference and the 95% CrIs. We did not assume homogeneous

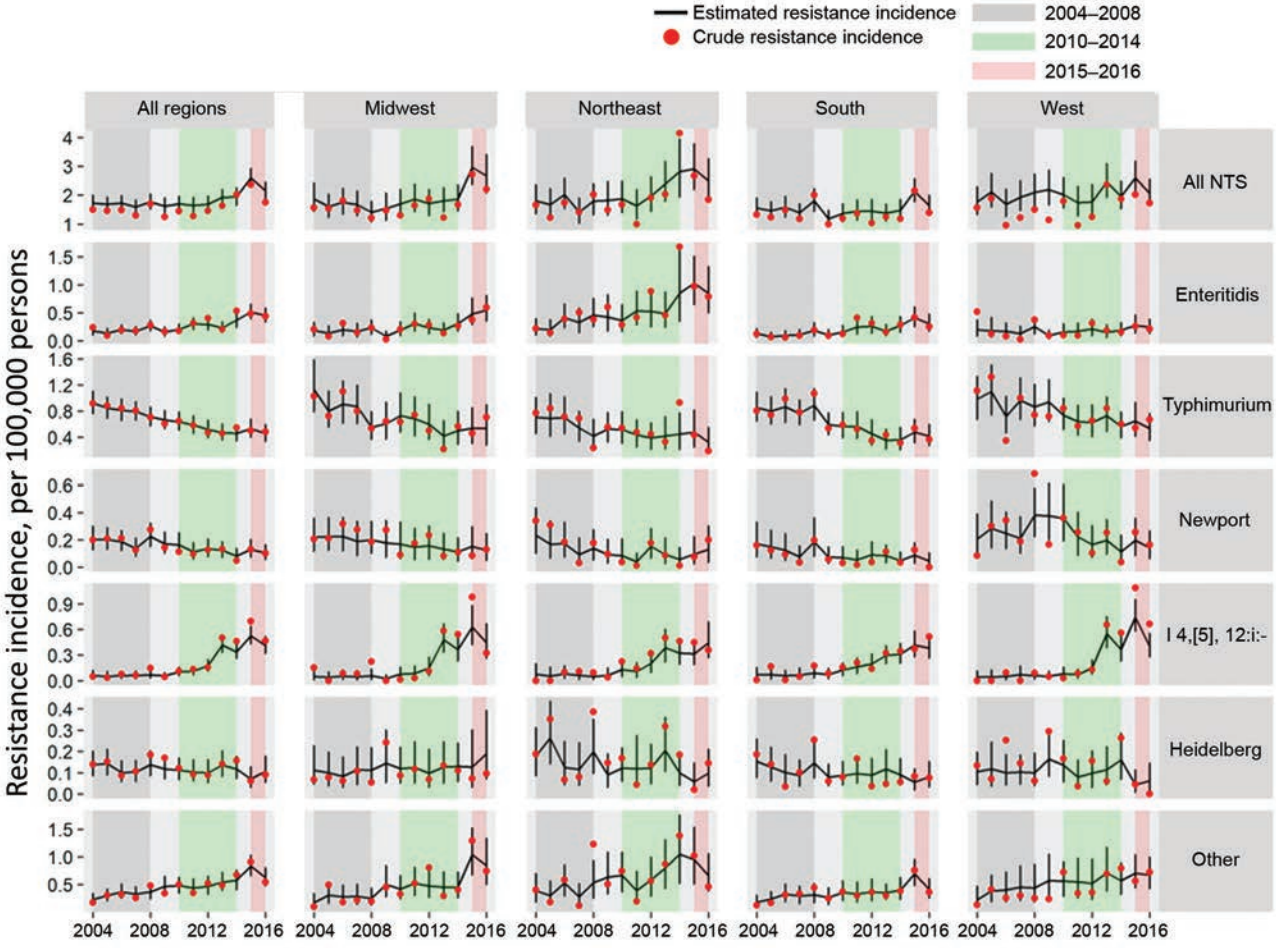

Figure 1. Estimated annual incidence of culture-confirmed nontyphoidal *Salmonella* infections with any clinically important resistance, by serotype and region, United States, 2004–2016. Estimated changes in resistance incidence (mean and 95% credible intervals of the posterior differences per 100,000 persons per year) were derived using Bayesian hierarchical models. Crude resistance incidence rates were derived by multiplying infection incidence and resistance proportion for state-year. Any clinically important resistance was defined as resistant to ceftriaxone, resistant to ampicillin, or ciprofloxacin nonsusceptible. The "other" category comprised serotypes other than Enteritidis, Typhimurium, Newport, I 4,[5],12:i:-, and Heidelberg. US Census regions were used to define 4 geographic regions. NTS, all nontyphoidal *Salmonella* serotypes.

rates across multiple years using this approach. For all *Salmonella*, we calculated the change in resistance incidence, which represents the net change (increase or decrease), for each resistance category, by summing the estimated changes derived for the 6 serotype categories. We describe statistically significant changes (i.e., in which the 95% CrIs do not include 0).

Extrapolating to the US Population

We multiplied the mean estimates of culture-confirmed infections by 29, which is the estimated number of total infections for every culture-confirmed infection in the general population, to estimate the total number of resistant infections for each period and changes in total resistant per 100,000 persons per year during 2015–2016 compared with the reference periods for each resistance category (*1*). We used the average 2015–2016 population estimates for the 50 states (322 million) to extrapolate to the US population (*25*).

Results

During 2004–2016, public health laboratories of state and participating local health departments in the 48 contiguous states reported 539,862 culture-confirmed *Salmonella* infections to LEDS (Appendix Table 1). Among the isolates from these infections, 89% were serotyped; the most common were Enteritidis (20%), Typhimurium (16%), Newport (11%), I 4,[5],12:i:- (4%), and Heidelberg (4%). Public health laboratories in the 48 states submitted 28,265 isolates to NARMS. Of these isolates, 98% were serotyped; the most common were Enteritidis (19%), Typhimurium (16%), Newport (11%), I 4,[5],12:i:- (4%), and Heidelberg (4%).

Clinically Important Resistance and Multidrug Resistance

During 2004–2016, clinically important resistance was detected in 3,546 (12.5%) of 28,265 isolates (Table 1; Appendix Figure 1). Ampicillin-only resistance was detected in 1,857 (6.6%) isolates, ciprofloxacin nonsusceptibility in 854 (3.0%), and ceftriaxone/ampicillin resistance in 835 (3.0%). Only 78 (0.3%) isolates were resistant to ceftriaxone and nonsusceptible to ciprofloxacin; these isolates were included in the 835 categorized as ceftriaxone/ampicillin-resistant. Most (>90%) ciprofloxacin-nonsusceptible isolates had MICs within the intermediate range, 0.12–0.5 (Table 1; Appendix Figure 6).

Of the 28,265 isolates, 2,912 (10.3%) were multidrug resistant (MDR). Of these, 2,633 (90%) had clinically important resistance, which accounted for 74% of the 3,546 isolates with clinically important resistance.

Incidence by Year and Region, 2004–2016

For each resistance category, the trend lines were smoother with model-derived annual estimates of resistance incidence compared with crude rates, particularly when stratified by serotype and region (Figure 1; Appendix Figures 2–5). Crude rates tended to be lower than model-derived estimates because many state-year resistance proportions used in calculating crude rates were 0 because of small sample sizes, whereas the model tended to pull estimates away from 0. Overall, most crude rates were within model-derived 95% CrIs.

Resistance Incidence, 2015–2016

During 2015–2016, the mean annual incidence was 2.38 (95% CrI 1.93–2.86)/100,000 persons for clinically important resistant infections and 1.83 (95%

Table 1. Number and percentage of antimicrobial-resistant nontyphoidal *Salmonella* isolates, by serotype and resistance category, United States, 2004–2016*

	No. (%) isolates							
Resistance category	Enteritidis, n = 5,206	Typhimurium, n = 4,404	Newport, n = 3,140	I 4,[5],12:i:-, n = 1,158	Heidelberg, n = 974	Other fully serotyped, n = 12,878	Not fully serotyped, n = 505	Total nontyphoidal *Salmonella*, N = 28,265
Any clinically important resistance†	548 (10.5)	1,197 (27.2)	284 (9.0)	389 (33.6)	240 (24.6)	843 (6.5)	45 (8.9)	3,546 (12.5)
Multidrug resistance‡	114 (2.2)	1,178 (26.7)	271 (8.6)	382 (33.0)	204 (20.9)	727 (5.6)	36 (7.1)	2,912 (10.3)
Amp-only§	152 (2.9)	897 (20.4)	30 (1.0)	319 (27.5)	120 (12.3)	311 (2.4)	28 (5.5)	1,857 (6.6)
Cef/Amp§¶	15 (0.3)	212 (4.8)	237 (7.5)	39 (3.4)	116 (11.9)	212 (1.6)	4 (0.8)	835 (3.0)
Cipro§#	381 (7.3)	88 (2.0)	17 (0.5)	31 (2.7)	4 (0.4)	320 (2.5)	13 (2.6)	854 (3.0)

*Amp-only, resistant to ampicillin (MIC ≥32 μg/mL) but susceptible to ceftriaxone and ciprofloxacin; Cef/Amp, resistant to ceftriaxone (MIC ≥4 μg/mL) and ampicillin; Cipro, nonsusceptible to ciprofloxacin (MIC ≥0.12 μg/mL) but susceptible to ceftriaxone; NTS, nontyphoidal *Salmonella*, which includes isolates serotyped as Enteritidis, Typhimurium, Newport, I 4,[5],12:i:-, and Heidelberg, isolates serotyped as other than those 5, and those not fully serotyped.
†Includes any of the 3 clinically important resistance patterns (i.e., resistant to ceftriaxone, resistant to ampicillin, or nonsusceptible to ciprofloxacin). Isolates might have resistance to other agents tested.
‡Resistant to ≥3 classes of antimicrobial agents.
§Amp-only, Cef/Amp, and Cipro are mutually exclusive categories of clinically important resistance.
¶Of the 835 isolates with Cef/Amp resistance, 78 (0.3% of all nontyphoidal *Salmonella* isolates) were nonsusceptible to ciprofloxacin. Of the 78 isolates, 71 (91%) had ciprofloxacin MICs within the intermediate range (i.e., 0.12–0.5) (Appendix Figure 6, https://wwwnc.cdc.gov/EID/article/27/6/20-4486-App1.pdf). These 78 isolates were not included in the Cipro category.
#Of the 854 isolates, 785 (92%) had ciprofloxacin MICs within the intermediate range (Appendix Figure 6).

CrI 1.45–2.25)/100,000 persons for MDR infections (Table 2). The 5 major serotypes accounted for 69% of infections with clinically important resistance and 66% with multidrug resistance.

Changes in Resistance Incidence, 2015–2016 versus Reference Periods

The mean annual incidence of infections with any clinically important resistance increased during 2015–2016 compared with 2004–2008; there was no significant change compared with 2010–2014 (Table 2; Figures 2 and 3). Among the resistance categories, the mean annual incidence of ciprofloxacin-nonsusceptible *Salmonella* infections increased during 2015–2016 compared with both reference periods.

Changes in Resistance Incidence, 2015–2016 versus 2004–2008

The mean annual incidence of *Salmonella* infections with clinically important resistance increased by 0.68 (95% CrI 0.13–1.24)/100,000 persons (Table 2). By census region, a significant increase in resistance only occurred in the Midwest (Figure 2). By serotype, I 4,[5],12:i:- had an incidence increase of 0.41(95% CrI 0.27–0.56)/100,000 persons, accounting for 37% of the increase in clinically important resistant *Salmonella* infections (Appendix Table 2). The incidence of resistant I 4,[5],12:i:- infections increased significantly in all 4 regions, with highest increase in the West and Midwest. Enteritidis infections with clinically important resistance increased by 0.29 (95% CrI 0.12–0.47)/100,000 persons, accounting for 26% of the increase in resistant infections. This increase was significant in 3 regions, with highest increase in the Northeast. Infections with clinically important resistance caused by serotypes categorized as other increased by 0.41 (95% CrI 0.12–0.72)/100,000 persons, accounting for 37% of the increase in resistant infections (Figure 2; Appendix Table 2). Typhimurium infections with clinically important resistance decreased (−0.33 [95% CrI –0.58 to −0.07]/100,000 persons).

Although no significant changes were noted in the mean annual incidence of *Salmonella* infections with multidrug or ampicillin-only resistance, some serotypes did change (Figure 2; Appendix Table 2). MDR I 4,[5],12:i:- infections increased (0.40 [95% CrI 0.24–0.56]/100,000 persons); this change was significant in all 4 regions, with highest increase in the West and Midwest. The incidence of MDR Enteritidis infections also increased (0.13 [95% CrI 0.04–0.23]/100,000 persons). We observed a decrease in Typhimurium infections with multidrug resistance (−0.37 [95% CrI –0.59 to −0.14]/100,000 persons) and ampicillin-only resistance (−0.35 [95% CrI –0.61 to −0.10]/100,000 persons). Serotype I 4,[5],12:i:- infections with ampicillin-only resistance increased (0.35 [95% CrI 0.21–0.50]/100,000 persons); this change was significant in all 4 regions, with highest increase in the West and Midwest.

The mean annual incidence of ciprofloxacin-nonsusceptible *Salmonella* infections increased by 0.41

Table 2. Estimated incidence and changes in the incidence of antimicrobial-resistant culture-confirmed nontyphoidal *Salmonella* infections, by resistance category, United States, 2015–2016 versus 2004–2008 and 2010–2014*

	Mean (95% CrI)				
	Resistance incidence, per 100,000 persons per year†			Change in resistance incidence, per 100,000 persons per year‡	
Resistance category	2015–2016	2004–2008	2010–2014	2015–2016 vs. 2004–2008	2015–2016 vs. 2010–2014
Any clinically important resistance§	2.38 (1.93–2.86)	1.70 (1.44–1.98)	1.78 (1.46–2.15)	**0.68 (0.13 to 1.24)‡**	0.60 (−0.002 to 1.20)
Multidrug resistance¶	1.83 (1.45–2.25)	1.51 (1.27–1.79)	1.42 (1.16–1.70)	0.32 (−0.17 to 0.82)	0.41 (−0.07 to 0.92)
Amp-only§	1.19 (0.85–1.56)	1.00 (0.78–1.25)	0.96 (0.73–1.21)	0.19 (−0.25 to 0.63)	0.23 (−0.21 to 0.67)
Cef/Amp§	0.49 (0.37–0.65)	0.43 (0.31–0.58)	0.42 (0.30–0.56)	0.06 (−0.13 to 0.26)	0.08 (−0.11 to 0.26)
Cipro§	0.70 (0.55–0.88)	0.29 (0.19–0.41)	0.41 (0.26–0.64)	**0.41 (0.22 to 0.61)‡**	**0.29 (0.02–0.52)‡**

*Amp-only, resistant to ampicillin (MIC ≥32 μg/mL) but susceptible to ceftriaxone and ciprofloxacin; BHM, Bayesian hierarchical model; Cef/Amp, resistant to ceftriaxone (MIC ≥4 μg/mL) and ampicillin; Cipro, nonsusceptible to ciprofloxacin (MIC ≥0.12 μg/mL) but susceptible to ceftriaxone; CrI, credible interval.

†Mean estimates of resistance incidence and 95% CrIs were derived using BHMs. Serotypes other than Enteritidis, Typhimurium, Newport, I 4,[5],12:i:-, and Heidelberg were combined into the "other" category. For all nontyphoidal *Salmonella*, estimates were derived by summing those for the 6 serotype categories. State-year data were too sparse to use in the BHMs to estimate mean resistance incidence for Cef/Amp among Enteritidis and Cipro among Newport and Heidelberg (4, 5, and 6 Enteritidis isolates, 7, 2, and 8 Newport isolates, and 0, 1, and 3 Heidelberg isolates in 2015–2016, 2004–2008, and 2010–2014, respectively).

‡Resistance incidence in 2015–2016 was compared with that from 2 reference periods, 2004–2008 and 2010–2015 (e.g., increase if 2015–2016 > reference). Mean changes are reported as significant (bold font) if the 95% CrIs (rounded to 2 decimals) do not include 0.

§An overall category of clinically important resistance includes any of 3 resistance patterns (i.e., resistant to ceftriaxone, resistant to ampicillin, or nonsusceptible to ciprofloxacin). Amp-only, Cef/Amp, and Cipro are mutually exclusive categories of clinically important resistance. Isolates with any clinically important resistance might have resistance to other agents tested. Model estimates for overall clinically important resistance were derived separately and might differ from the sum of estimates for the 3 mutually exclusive categories.

¶Resistant to ≥3 classes of antimicrobial agents.

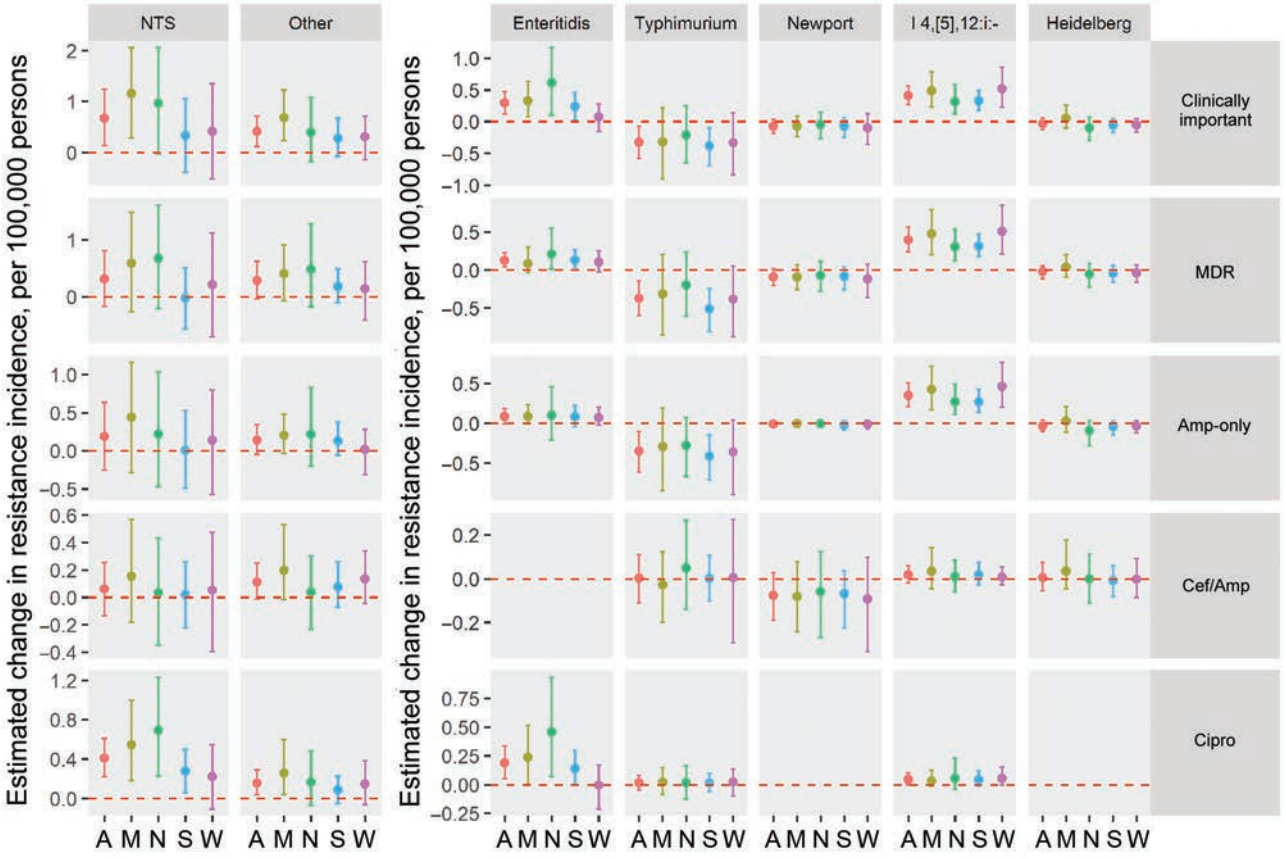

Figure 2. Estimated changes in the incidence of resistant culture-confirmed nontyphoidal *Salmonella* infections, by serotype, resistance category, and geographic region, United States, 2015–2016 versus 2004–2008. Estimated changes in resistance incidence (mean and 95% credible intervals of the posterior differences per 100,000 persons/year) were derived using Bayesian hierarchical models. Amp-only, Cef/Amp, and Cipro are mutually exclusive categories of clinically important resistance: Amp-only, resistant to ampicillin but susceptible to ceftriaxone and ciprofloxacin; Cef/Amp, resistant to ceftriaxone and ampicillin; Cipro, nonsusceptible to ciprofloxacin but susceptible to ceftriaxone. Isolates in each category might have resistance to other agents. Multidrug resistance was defined as resistance to ≥3 classes of antimicrobial agents. The "other" category comprised serotypes other than Enteritidis, Typhimurium, Newport, I 4,[5],12:i:-, and Heidelberg. US Census regions were used to define 4 geographic regions (A, all regions; M, Midwest; N, Northeast; S, South; W, West). MDR, multidrug resistant. NTS, all nontyphoidal *Salmonella* serotypes.

(95% CrI 0.22–0.61)/100,000 persons (Table 2). Ciprofloxacin-nonsusceptible Enteritidis infections increased by 0.19 (95% CrI 0.05–0.34)/100,000 persons, accounting for 47% of the increase in these infections (Appendix Table 2). This increase was significant in 3 regions, most notably in the Northeast (Figure 2). Ciprofloxacin-nonsusceptible infections caused by serotypes categorized as other increased by 0.16 (95% CrI 0.04–0.29)/100,000 persons, accounting for 38% of the increase in ciprofloxacin-nonsusceptible infections (Figure 2; Appendix Table 2).

Changes in Resistance Incidence, 2015–2016 versus 2010–2014

The mean annual incidence of *Salmonella* infections with clinically important resistance did not change compared with the previous 5 years. However, the mean annual incidence of ciprofloxacin-nonsusceptible *Salmonella* infections increased by 0.29 (95% CrI 0.02–0.52)/100,000 persons (Table 2); by region, the increase was significant only in the Midwest (Figure 3). Ciprofloxacin-nonsusceptible Enteritidis infections increased by 0.16 (95% CrI 0.02–0.32)/100,000 persons, accounting for 57% of the increase in ciprofloxacin-nonsusceptible infections (Appendix Table 3).

Extrapolation to the US population

Compared with the number of infections for 2004–2008, an estimated ≈63,000 more *Salmonella* infections with clinically important resistance occurred each year during 2015–2016, from an average of ≈159,000 to ≈222,000; more than half were ciprofloxacin-nonsusceptible (Table 3). Compared with the number of infections for

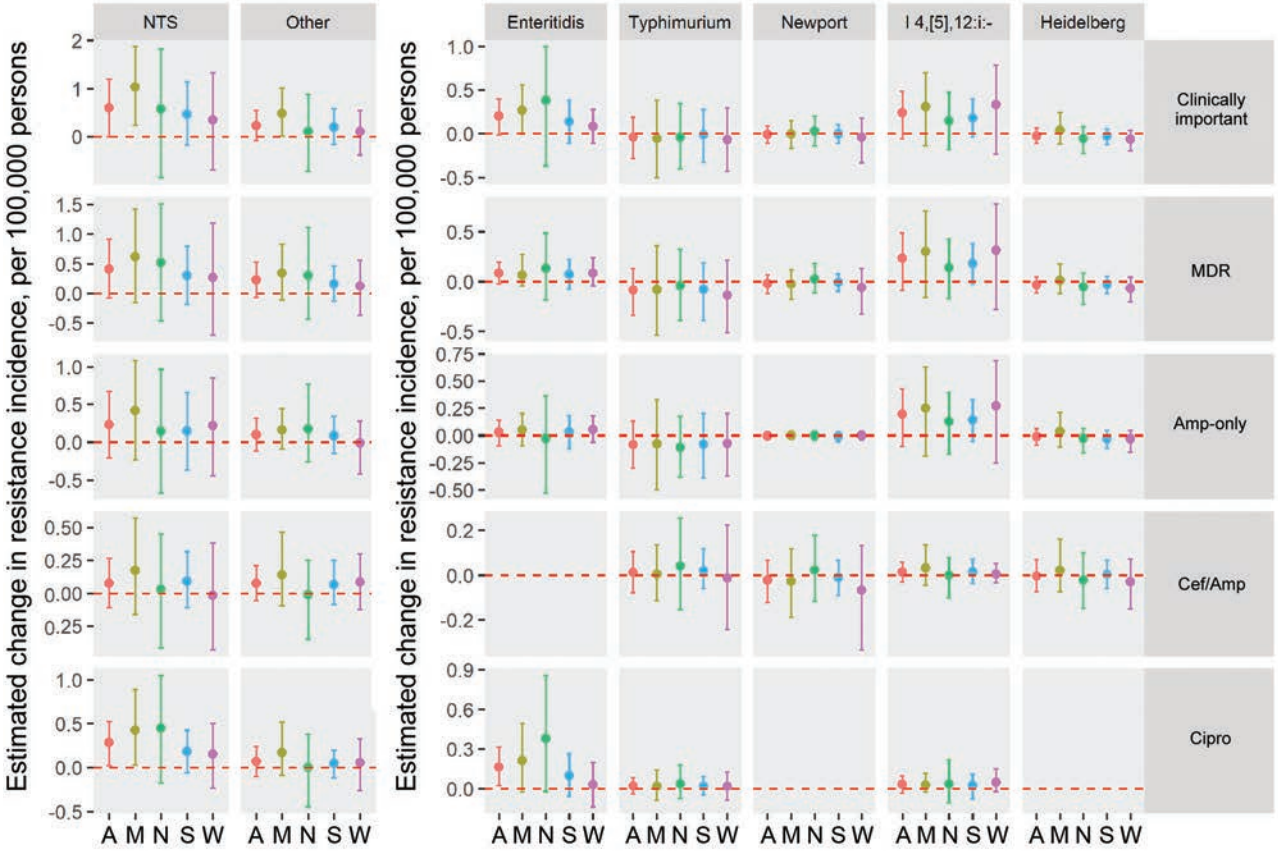

Figure 3. Estimated changes in the incidence of resistant culture-confirmed nontyphoidal *Salmonella* infections, by serotype, resistance category, and geographic region, United States, 2015–2016 versus 2010–2014. Estimated changes in resistance incidence (mean and 95% credible intervals of the posterior differences per 100,000 persons/year) were derived using Bayesian hierarchical models. Amp-only, Cef/Amp, and Cipro are mutually exclusive categories of clinically important resistance: Amp-only, resistant to ampicillin but susceptible to ceftriaxone and ciprofloxacin; Cef/Amp, resistant to ceftriaxone and ampicillin; Cipro, nonsusceptible to ciprofloxacin but susceptible to ceftriaxone. Isolates in each category might have resistance to other agents. Multidrug resistance (MDR) was defined as resistance to ≥3 classes of antimicrobial agents. The "other" category comprised serotypes other than Enteritidis, Typhimurium, Newport, I 4,[5],12:i:-, and Heidelberg. US Census regions were used to define 4 geographic regions (A, all regions; M, Midwest; N, Northeast; S, South; W, West). MDR, multidrug resistant; NTS, all nontyphoidal *Salmonella* serotypes.

the previous 5 years, an estimated ≈56,000 more *Salmonella* infections with clinically important resistance occurred each year during 2015–2016; more than half were ciprofloxacin-nonsusceptible.

Discussion

Our analysis indicates that the incidence of resistant *Salmonella* infections was higher in 2015–2016 than in earlier periods during 2004–2014. The annual incidence of culture-confirmed infections with clinically important resistance increased by 0.68/100,000 persons, a 40% increase in the annual number of infections, during 2015–2016 compared with 2004–2008. Serotypes I 4,[5],12:i:- and Enteritidis were responsible for two thirds of this increase. Ciprofloxacin-nonsusceptible infections accounted for more than half of the increase. Extrapolating to total infections in the US population using a multiplier to account for unreported infections resulted in an estimated ≈63,000 more infections with clinically important resistance per year during 2015–2016 compared with 2004–2008 (from ≈159,000 to ≈222,000 infections).

The increased incidence of ciprofloxacin-nonsusceptible *Salmonella* infections during 2015–2016 compared with incidence for both 2004–2008 and 2010–2014 is a concerning trend. Serotype Enteritidis contributed the most to this increase. Although the incidence of infections with Enteritidis, the most common serotype, has not changed significantly in >10 years, the percentage of ciprofloxacin-nonsusceptible infections has increased almost steadily (*11*,*16*). Chicken and eggs have been the main domestic sources of Enteritidis infections (*29*,*30*). About 20% of Enteritidis infections are linked to international travel, which is an

important source of ciprofloxacin-nonsusceptible Enteritidis infections (*8*,*31*,*32*).

The incidence of infections with clinically important resistance and ciprofloxacin-nonsusceptibility caused by serotypes categorized as other was higher during 2015–2016 than during 2004–2008. Some of these serotypes are emerging or have concerning levels of resistance, including Dublin, Infantis, Kentucky, Hadar, and Agona (*16*,*24*,*33*). Some have been associated with resistance, invasive illness, or both (*11*,*19*,*23*,*33*).

The decrease in resistant Typhimurium infections might be related to the simultaneous increase in I 4,[5],12:i- infections, which some call monophasic Typhimurium (*16*,*18*,*34*). In the 1990s, MDR Typhimurium infections increased markedly in Europe and then in the United States (*35*,*36*). Most isolates from these infections that underwent phage typing were definitive type 104 (*14*,*21*,*35*,*36*). Isolations of this strain have decreased globally; the reasons are not known (*36*)

Changes in resistance incidence by resistance category and serotype varied by geographic region, with significant increases in most regions for serotypes I 4,[5],12:i:- and Enteritidis. An increase in the incidence of I 4,[5],12:i:- infections with multidrug and ampicillin-only resistance occurred in all 4 regions, with highest increase in the West and Midwest. Pork products have been associated with I 4,[5],12:i:- infections with resistance to ampicillin, sulfonamide, streptomycin, and tetracycline in the West (*34*,*37*). The regional pattern of pork consumption has reflected the regional pattern of pork production, which is highest in the Midwest; 8 of the 10 states with the highest production of swine are in the Midwest (*38*,*39*). A study showed that MDR I 4,[5],12:i:- strains from swine in the Midwest during 2014–2016 were typically resistant to ampicillin, sulfonamide, streptomycin, and tetracycline and probably part of a European clade that has spread in the United States and elsewhere; these strains harbored plasmid-mediated resistance genes, which can be transmitted horizontally to other bacteria (*34*). This trend could partly explain the widespread increase in the incidence of MDR I 4,[5],12:i:- infections. International travel could have contributed to an increase in the incidence of ciprofloxacin-nonsusceptible Enteritidis infections, which increased in 3 regions and was highest in the Northeast. International travel has increased since 2014, and residents of northeastern states accounted for more than one third of US travelers during 2015–2016 (*40*). In the United Kingdom, an increase in these infections has been linked to international travel and imported foods (*41*). In the United States, ciprofloxacin-nonsusceptible strains of Enteritidis and other serotypes have been isolated from imported seafood (*42*). Plasmid-mediated quinolone-resistance genes have been detected among ciprofloxacin-nonsusceptible isolates in the United States; these genes might contribute to spread of fluoroquinolone nonsusceptibility (*43*).

Our use of a Bayesian hierarchical model improved the estimates, as shown by the smoothing of resistance incidence and temporal change lines, by addressing issues related to missing and sparse state-year data (*20*,*26*). Our method of calculating the aver-

Table 3. Point estimates of the total number and changes in the total number of resistant nontyphoidal *Salmonella* infections extrapolated to the US population, by resistance category, United States, 2015–2016 versus 2004–2008 and 2010–2014*†

	No. infections/year†			Change in no. infections/year‡	
Resistance category	2015–2016	2004–2008	2010–2014	2015–2016 vs. 2004–2008	2015–2016 vs. 2010–2014
Any clinically important resistance§	222,000	159,000	166,000	**63,000‡**	56,000
Multidrug resistance¶	171,000	141,000	133,000	30,000	38,000
Amp-only§	111,000	93,000	90,000	18,000	21,000
Cef/Amp§	46,000	40,000	39,000	6,000	7,000
Cipro§	65,000	27,000	38,000	**38,000‡**	**27,000‡**

*Amp-only, resistant to ampicillin (MIC ≥32 μg/mL) but susceptible to ceftriaxone and ciprofloxacin; BHM, Bayesian hierarchical model; Cef/Amp, resistant to ceftriaxone (MIC ≥4 μg/mL) and ampicillin; Cipro, nonsusceptible to ciprofloxacin (MIC ≥0.12 μg/mL) but susceptible to ceftriaxone; CrI, credible interval.

†Point estimates extrapolated to the entire US population were calculated by multiplying mean estimates for culture-confirmed infections (derived using BHM) by the multiplier of 29 and the average total U.S. population for 2015–2016 (322 million). The multiplier of 29 is the mean estimate of the total number of infections for every culture-confirmed nontyphoidal *Salmonella* infection. The 95% CrIs were not derived. Extrapolated point estimates were rounded to the nearest thousand.

‡Model-derived mean estimates of changes in resistance incidence (Table 2) used to calculate extrapolated estimates are reported as significant if the 95% CrIs do not include 0; the extrapolated estimates corresponding to these BHM-derived estimates are shown in bold font. Although the 95% CrIs of extrapolated estimates were not derived, they can be assumed to include 0 if the 95% CrIs of BHM-derived estimates include 0.

§An overall category of clinically important resistance includes any of 3 resistance patterns (i.e., resistant to ceftriaxone, resistant to ampicillin, or nonsusceptible to ciprofloxacin). Amp-only, Cef/Amp, and Cipro are mutually exclusive categories of clinically important resistance. Isolates with any clinically important resistance might have resistance to other agents tested. Model estimates for overall clinically important resistance were derived separately and might differ from the sum of BHM estimates for the 3 mutually exclusive categories; thus, extrapolated estimates for the overall category might differ from the sum of mutually exclusive categories.

¶Resistant to ≥3 classes of antimicrobial agents.

age difference in incidence between groups of years is more refined than approaches using a negative binomial model because it does not assume homogeneous resistance incidence rates across multiple years (*11*,*44*). It is therefore less likely to underestimate the variability of estimated changes. However, this analysis is subject to the same limitations described in previous reports, including unmeasured sources of bias and uncertainty derived by combining data from separate unlinked surveillance systems (*20*,*26*). Our estimates of significant changes were limited to comparisons with the reference periods used to assess changes in resistance percentages in NARMS annual reports (*16*). Our choice to compare a recent 2-year period with earlier 5-year periods balanced the need to assess the most current situation with the need for sufficient data to assess significant changes. Because of the low percentage of isolates showing resistance to trimethoprim/sulfamethoxazole (<3%) or decreased susceptibility to azithromycin (<1%), an important agent used to treat serious infections, we did not provide estimates for these agents (*2*,*16*,*18*,*20*). We included infections resistant to ceftriaxone and nonsusceptible to ciprofloxacin in the ceftriaxone/ampicillin-resistance category; they represented only 0.3% of *Salmonella* isolates submitted to NARMS. The fact that some ciprofloxacin nonsusceptible infections were not included in the ciprofloxacin nonsusceptible category further supports our finding that ciprofloxacin-nonsusceptible infections increased during the study period. Increasing use of culture-independent diagnostic tests by clinical laboratories can change the submission of isolates to public health laboratories and reporting of infections (*11*); these changes warrant adjustments in future analyses (*20*).

We multiplied estimates of culture-confirmed infections by 29 to account for undiagnosed infections. However, resistant infections are associated with more severe illness, so they might be more likely to be detected (*3*–*6*). Thus, the appropriate multiplier (the ratio of total infections to culture-confirmed infections) for resistant infections might be <29. To calculate undiagnosed *Salmonella* infections, multipliers of 12 for persons <5 years of age and 23 for persons ≥ 65 years of age have been reported (*45*). Although children <5 years of age have the highest incidence of *Salmonella* infections, older adults might disproportionately account for resistant infections because they are more likely to have serious illness and be hospitalized (*4*,*5*,*44*–*47*); therefore, a multiplier of 23 might be an appropriate choice. However, we chose 29 because it was used in a previous estimate of the total number of *Salmonella* infections in the population (*1*) and because persons 5–64 years of age account for most culture-confirmed infections reported to CDC and most isolates with clinically important resistance submitted to NARMS (*4*,*18*,*44*,*45*). We did not attach uncertainties to the extrapolated total number of resistant infections and changes in that number because uncertainties of the multiplier are not known. Although resistance incidence can vary by demographic subgroup, geographic region, time, and other factors, we did not include additional uncertainties from the extrapolation to the US population using the average 2015–2016 population estimates for the 50 states (*19*,*21*,*22*,*46*,*47*).

Estimates of changes in resistance incidence can help identify trends of greatest concern to set priorities for prevention. Analyses that include the varying distributions of infections by demographic subgroups, season, and recent travel could inform serotype-specific, regional, and source-targeted prevention strategies (*5*,*11*,*21*,*22*,*31*,*44*–*48*). The increasing use of whole-genome sequencing by public health laboratories to characterize *Salmonella* strains will enhance surveillance of antimicrobial-resistant *Salmonella* from human and nonhuman sources (*49*). Antimicrobial agents contribute to resistance wherever they are used, including in food animals and humans (*50*). A One Health approach can help in detecting and controlling antimicrobial resistance, which is a complex and multifaceted problem that affects humans, animals, and the environment (*50*).

Acknowledgments

We thank state and local health departments and their public health laboratories for their contributions to the National Antimicrobial Resistance Monitoring System and Laboratory-Based Enteric Disease Surveillance. We acknowledge Sean Browning for his assistance with Laboratory-Based Enteric Disease Surveillance data.

This work was supported by the Centers for Disease Control and Prevention and the US Food and Drug Administration Center for Veterinary Medicine.

About the Author

Dr. Medalla is an epidemiologist with the National Center for Emerging and Zoonotic Infectious Diseases, Division of Foodborne, Waterborne, and Environmental Diseases, Centers for Disease Control and Prevention. Her research interests include antimicrobial resistance in *Salmonella* and other foodborne and enteric pathogens.

References

1. Scallan E, Hoekstra RM, Angulo FJ, Tauxe RV, Widdowson MA, Roy SL, et al. Foodborne illness acquired in the United States—major pathogens. Emerg Infect Dis. 2011;17:7–15. https://doi.org/10.3201/eid1701.P11101
2. Pegues DA, Miller SI. *Salmonella Species*. In: John E. Bennett, Raphael Dolin, Blaser. MJ, eds. Mandell, Douglas, and Bennett's principles and practice of infectious diseases. Philadelphia: Elsevier Saunders; 2020. p. 2725–36.
3. Varma JK, Greene KD, Ovitt J, Barrett TJ, Medalla F, Angulo FJ. Hospitalization and antimicrobial resistance in *Salmonella* outbreaks, 1984–2002. Emerg Infect Dis. 2005;11:943–6. https://doi.org/10.3201/eid1106.041231
4. Krueger AL, Greene SA, Barzilay EJ, Henao O, Vugia D, Hanna S, et al. Clinical outcomes of nalidixic acid, ceftriaxone, and multidrug-resistant nontyphoidal *Salmonella* infections compared with pansusceptible infections in FoodNet sites, 2006–2008. Foodborne Pathog Dis. 2014;11:335–41. https://doi.org/10.1089/fpd.2013.1642
5. Varma JK, Molbak K, Barrett TJ, Beebe JL, Jones TF, Rabatsky-Ehr T, et al. Antimicrobial-resistant nontyphoidal *Salmonella* is associated with excess bloodstream infections and hospitalizations. J Infect Dis. 2005;191:554–61. https://doi.org/10.1086/427263
6. Crump JA, Barrett TJ, Nelson JT, Angulo FJ. Reevaluating fluoroquinolone breakpoints for *Salmonella enterica* serotype Typhi and for non-Typhi salmonellae. Clin Infect Dis. 2003;37:75–81. https://doi.org/10.1086/375602
7. Clinical and Laboratory Standards Institute. Performance standards for antimicrobial susceptibility testing, 31st edition (M100). Wayne (PA): The Institute; 2021.
8. Johnson LR, Gould LH, Dunn JR, Berkelman R, Mahon BE; FoodNet Travel Working Group. *Salmonella* infections associated with international travel: a Foodborne Diseases Active Surveillance Network (FoodNet) study. Foodborne Pathog Dis. 2011;8:1031–7. https://doi.org/10.1089/fpd.2011.0854
9. Dewey-Mattia D, Manikonda K, Hall AJ, Wise ME, Crowe SJ; Centers for Disease Control and Prevention. Surveillance for foodborne disease outbreaks—United States, 2009–2015. MMWR Surveill Summ. 2018;67:1–11. https://doi.org/10.15585/mmwr.ss6710a1
10. Kozlica J, Claudet AL, Solomon D, Dunn JR, Carpenter LR. Waterborne outbreak of *Salmonella* I 4,[5],12:i:-. Foodborne Pathog Dis. 2010;7:1431–3. https://doi.org/10.1089/fpd.2010.0556
11. Marder Mph EP, Griffin PM, Cieslak PR, Dunn J, Hurd S, Jervis R, et al.; Centers for Disease Control and Prevention. Preliminary incidence and trends of infections with pathogens transmitted commonly through food—Foodborne Diseases Active Surveillance Network, 10 U.S. Sites, 2006–2017. MMWR Morb Mortal Wkly Rep. 2018;67:324–8. https://doi.org/10.15585/mmwr.mm6711a3
12. Centers for Disease Control and Prevention. Multistate outbreaks of *Salmonella* infections linked to contact with live poultry in backyard flocks, 2018 (final update). 2018 Sep 13 [cited 2020 Oct 29]. https://www.cdc.gov/salmonella/backyard-flocks-06-18/index.html
13. Huang JY, Patrick ME, Manners J, Sapkota AR, Scherzinger KJ, Tobin-D'Angelo M, et al. Association between wetland presence and incidence of *Salmonella* enterica serotype Javiana infections in selected US sites, 2005–2011. Epidemiol Infect. 2017;145:2991–7. https://doi.org/10.1017/S0950268817001790
14. Dechet AM, Scallan E, Gensheimer K, Hoekstra R, Gunderman-King J, Lockett J, et al.; Multistate Working Group. Outbreak of multidrug-resistant *Salmonella enterica* serotype Typhimurium definitive type 104 infection linked to commercial ground beef, northeastern United States, 2003–2004. Clin Infect Dis. 2006;42:747–52. https://doi.org/10.1086/500320
15. Varma JK, Marcus R, Stenzel SA, Hanna SS, Gettner S, Anderson BJ, et al. Highly resistant *Salmonella* Newport-MDRAmpC transmitted through the domestic US food supply: a FoodNet case-control study of sporadic *Salmonella* Newport infections, 2002–2003. J Infect Dis. 2006;194:222–30. https://doi.org/10.1086/505084
16. Centers for Disease Control and Prevention. National Antimicrobial Resistance Monitoring System for Enteric Bacteria (NARMS): human isolates final report, 2015. Atlanta: The Centers; 2018.
17. Centers for Disease Control and Prevention. National *Salmonella* Surveillance [cited 2020 Oct 29]. https://www.cdc.gov/nationalsurveillance/salmonella-surveillance.html
18. Centers for Disease Control and Prevention. National Antimicrobial Resistance Monitoring System for Enteric Bacteria [cited 2020 Oct 29]. https://www.cdc.gov/narms/reports/index.html
19. Medalla F, Hoekstra RM, Whichard JM, Barzilay EJ, Chiller TM, Joyce K, et al. Increase in resistance to ceftriaxone and nonsusceptibility to ciprofloxacin and decrease in multidrug resistance among *Salmonella* strains, United States, 1996–2009. Foodborne Pathog Dis. 2013;10:302–9. https://doi.org/10.1089/fpd.2012.1336
20. Medalla F, Gu W, Mahon BE, Judd M, Folster J, Griffin PM, et al. Estimated incidence of antimicrobial drug–resistant nontyphoidal *Salmonella* infections, United States, 2004–2012. Emerg Infect Dis. 2016;23:29–37. https://doi.org/10.3201/eid2301.160771
21. Greene SK, Stuart AM, Medalla FM, Whichard JM, Hoekstra RM, Chiller TM. Distribution of multidrug-resistant human isolates of MDR-ACSSuT *Salmonella* Typhimurium and MDR-AmpC *Salmonella* Newport in the United States, 2003–2005. Foodborne Pathog Dis. 2008;5:669–80. https://doi.org/10.1089/fpd.2008.0111
22. Crim SM, Chai SJ, Karp BE, Judd MC, Reynolds J, Swanson KC, et al. *Salmonella enterica* serotype Newport infections in the United States, 2004–2013: increased incidence investigated through four surveillance systems. Foodborne Pathog Dis. 2018;15:612–20. https://doi.org/10.1089/fpd.2018.2450
23. Jones TF, Ingram LA, Cieslak PR, Vugia DJ, Tobin-D'Angelo M, Hurd S, et al. Salmonellosis outcomes differ substantially by serotype. J Infect Dis. 2008;198:109–14. https://doi.org/10.1086/588823
24. US Food and Drug Administration. 2018 NARMS update: integrated report summary interactive version [cited 2020 Dec 28]. https://www.fda.gov/animal-veterinary/national-antimicrobial-resistance-monitoring-system/2018-narms-update-integrated-report-summary-interactive-version
25. US Census Bureau. Population and housing unit estimates [cited 2020 Oct 29]. http://www.census.gov/popest
26. Gu W, Medalla F, Hoekstra RM. Bayesian hierarchical model of ceftriaxone resistance proportions among *Salmonella* serotype Heidelberg infections. Spat Spatio-Temporal Epidemiol. 2018;24:19–26. https://doi.org/10.1016/j.sste.2017.10.003
27. Lunn DJ, Thomas A, Best N, Spiegelhalter D. WinBUGS—a Bayesian modelling framework: concepts, structure, and extensibility. Stat Comput. 2000;10:325–37. https://doi.org/10.1023/A:1008929526011
28. Lambert PC, Sutton AJ, Burton PR, Abrams KR, Jones DR.

How vague is vague? A simulation study of the impact of the use of vague prior distributions in MCMC using WinBUGS. Stat Med. 2005;24:2401–28. https://doi.org/10.1002/sim.2112
29. Chai SJ, White PL, Lathrop SL, Solghan SM, Medus C, McGlinchey BM, et al. *Salmonella enterica* serotype Enteritidis: increasing incidence of domestically acquired infections. Clin Infect Dis. 2012;54(Suppl 5):S488–97. https://doi.org/10.1093/cid/cis231
30. Marcus R, Varma JK, Medus C, Boothe EJ, Anderson BJ, Crume T, et al.; Emerging Infections Program FoodNet Working Group. Re-assessment of risk factors for sporadic *Salmonella* serotype Enteritidis infections: a case-control study in five FoodNet Sites, 2002–2003. Epidemiol Infect. 2007;135:84–92. https://doi.org/10.1017/S0950268806006558
31. O'Donnell AT, Vieira AR, Huang JY, Whichard J, Cole D, Karp BE. Quinolone-resistant *Salmonella enterica* serotype Enteritidis infections associated with international travel. Clin Infect Dis. 2014;59:e139–41. https://doi.org/10.1093/cid/ciu505
32. Grass JE, Kim S, Huang JY, Morrison SM, McCullough AE, Bennett C, et al. Quinolone nonsusceptibility among enteric pathogens isolated from international travelers—Foodborne Diseases Active Surveillance Network (FoodNet) and National Antimicrobial Monitoring System (NARMS), 10 United States sites, 2004–2014. PLoS One. 2019;14:e0225800. https://doi.org/10.1371/journal.pone.0225800
33. Harvey RR, Friedman CR, Crim SM, Judd M, Barrett KA, Tolar B, et al. Epidemiology of *Salmonella* enterica serotype Dublin infections among humans, United States, 1968–2013. Emerg Infect Dis. 2017;23:1493–501. https://doi.org/10.3201/eid2309.170136
34. Elnekave E, Hong S, Mather AE, Boxrud D, Taylor AJ, Lappi V, et al. *Salmonella enterica* serotype 4,[5],12:i:- in swine in the United States Midwest: an emerging multidrug-resistant clade. Clin Infect Dis. 2018;66:877–85. https://doi.org/10.1093/cid/cix909
35. Rabatsky-Ehr T, Whichard J, Rossiter S, Holland B, Stamey K, Headrick ML, et al.; NARMS Working Group. Multidrug-resistant strains of *Salmonella enterica* Typhimurium, United States, 1997–1998. Emerg Infect Dis. 2004;10:795–801. https://doi.org/10.3201/eid1005.030209
36. Leekitcharoenphon P, Hendriksen RS, Le Hello S, Weill FX, Baggesen DL, Jun SR, et al. Global genomic epidemiology of *Salmonella enterica* Serovar Typhimurium DT104. Appl Environ Microbiol. 2016;82:2516–26. https://doi.org/10.1128/AEM.03821-15
37. Centers for Disease Control and Prevention. Multistate outbreak of multidrug-resistant *Salmonella* I 4,[5],12:i:- and *Salmonella* Infantis infections linked to pork (final update) [cited 2020 Oct 29]. https://www.cdc.gov/salmonella/pork-08-15/index.html
38. US Department of Agriculture, National Agricultural Statistics Service. Quarterly hogs and pigs. 2021 Mar 25 [cited 2021 Apr 19]. https://downloads.usda.library.cornell.edu/usda-esmis/files/rj430453j/7p88db205/mw22w1890/hgpg0321.pdf
39. US Department of Agriculture, Economic Research Service. Factors affecting U.S. pork consumption/LDP-M-130–01. 2005 May [cited 2020 Oct 29]. https://www.ers.usda.gov/webdocs/outlooks/37377/15778_ldpm13001_1_.pdf?v=5280.8
40. US Department of Commerce, National Travel and Tourism Office. U.S. travel and tourism statistics (U.S. resident outbound) [cited 2020 Oct 29]. https://travel.trade.gov/outreachpages/outbound.general_information.outbound_overview.asp
41. Threlfall EJ, Day M, de Pinna E, Charlett A, Goodyear KL. Assessment of factors contributing to changes in the incidence of antimicrobial drug resistance in *Salmonella enterica* serotypes Enteritidis and Typhimurium from humans in England and Wales in 2000, 2002 and 2004. Int J Antimicrob Agents. 2006;28:389–95. https://doi.org/10.1016/j.ijantimicag.2006.07.009
42. Bae D, Kweon O, Khan AA. Isolation and characterization of antimicrobial-resistant nontyphoidal *Salmonella enterica* serovars from imported food products. J Food Prot. 2016;79:1348–54. https://doi.org/10.4315/0362-028X.JFP-15-564
43. Karp BE, Campbell D, Chen JC, Folster JP, Friedman CR. Plasmid-mediated quinolone resistance in human non-typhoidal *Salmonella* infections: an emerging public health problem in the United States. Zoonoses Public Health. 2018;65:838–49. https://doi.org/10.1111/zph.12507
44. Centers for Disease Control and Prevention. Foodborne Diseases Active Surveillance Network (FoodNet): FoodNet 2015 surveillance report (final update). Atlanta: The Centers; 2017.
45. Scallan E, Crim SM, Runkle A, Henao OL, Mahon BE, Hoekstra RM, et al. Bacterial enteric infections among older adults in the United States: Foodborne Diseases Active Surveillance Network, 1996–2012. Foodborne Pathog Dis. 2015;12:492–9. https://doi.org/10.1089/fpd.2014.1915
46. Angelo KM, Reynolds J, Karp BE, Hoekstra RM, Scheel CM, Friedman C. Antimicrobial resistance among nontyphoidal *Salmonella* isolated from blood in the United States, 2003–2013. J Infect Dis. 2016;214:1565–70. https://doi.org/10.1093/infdis/jiw415
47. Crump JA, Medalla FM, Joyce KW, Krueger AL, Hoekstra RM, Whichard JM, et al.; Emerging Infections Program NARMS Working Group. Antimicrobial resistance among invasive nontyphoidal *Salmonella enterica* isolates in the United States: National Antimicrobial Resistance Monitoring System, 1996 to 2007. Antimicrob Agents Chemother. 2011;55:1148–54. https://doi.org/10.1128/AAC.01333-10
48. Boore AL, Hoekstra RM, Iwamoto M, Fields PI, Bishop RD, Swerdlow DL. *Salmonella enterica* infections in the United States and assessment of coefficients of variation: a novel approach to identify epidemiologic characteristics of individual serotypes, 1996–2011. PLoS One. 2015;10:e0145416. https://doi.org/10.1371/journal.pone.0145416
49. McDermott PF, Tyson GH, Kabera C, Chen Y, Li C, Folster JP, et al. Whole-genome sequencing for detecting antimicrobial resistance in nontyphoidal *Salmonella.* Antimicrob Agents Chemother. 2016;60:5515–20. https://doi.org/10.1128/AAC.01030-16
50. Karp BE, Tate H, Plumblee JR, Dessai U, Whichard JM, Thacker EL, et al. National Antimicrobial Resistance Monitoring System: two decades of advancing public health through integrated surveillance of antimicrobial resistance. Foodborne Pathog Dis. 2017;14:545–57. https://doi.org/10.1089/fpd.2017.2283

Address for correspondence: Felicita Medalla, Centers for Disease Control and Prevention, 1600 Clifton Rd NE, Mailstop H24-9, Atlanta, GA 30329-4027, USA; email: fmedalla@cdc.gov

Rapid Detection of SARS-CoV-2 Variants of Concern, Including B.1.1.28/ P.1, British Columbia, Canada

Nancy Matic,[1] Christopher F. Lowe,[1] Gordon Ritchie, Aleksandra Stefanovic, Tanya Lawson, Willson Jang, Matthew Young, Winnie Dong, Zabrina L. Brumme, Chanson J. Brumme, Victor Leung, Marc G. Romney

To screen all severe acute respiratory syndrome coronavirus 2–positive samples in Vancouver, British Columbia, Canada, and determine whether they represented variants of concern, we implemented a real-time reverse transcription PCR–based algorithm. We rapidly identified 77 samples with variants: 57 with B.1.1.7, 7 with B.1.351, and an epidemiologic cluster of 13 with B.1.1.28/P.1.

A robust surveillance system for early identification of severe acute respiratory syndrome coronavirus 2 (SARS-CoV-2) variants of concern (VOCs) is of critical public health value. VOCs have demonstrated in vitro evasion of antibody neutralization (*1*,*2*; W.F. Garcia-Beltran et al., unpub. data, https://www.medrxiv.org/content/10.1101/2021.02.14.21251704v1) and displayed potential for enhanced transmission because of mutations in the spike receptor binding domain (G. Nelson et al., unpub. data, https://www.biorxiv.org/content/10.1101/2021.01.13.426558v1; H. Liu et al., unpub. data, https://www.biorxiv.org/content/10.1101/2021.02.16.431305v1). Surveillance from the United Kingdom demonstrated a rapid increase in cases during September 2020, attributed to the B.1.1.7 variant, which has become predominant in several other countries (*3*). A commercial SARS-CoV-2 real-time reverse transcription PCR (rRT-PCR) demonstrated dropout of the small (S) gene on B.1.1.7 because of a deletion mutation within the spike protein (69/70). Subsequently, the European Centre for Disease Prevention and Control proposed use of a specific commercial assay with 3 targets as a surveillance strategy (*4*).

The B.1.1.28/P.1 variant is an emerging VOC and the predominant strain in certain regions of Brazil. Although uncommon in North America, it has now been detected across several continents. Re-infection of patients with SARS-CoV-2 immunity has raised concerns about resurgence (*5*). Unlike B.1.1.7, the B.1.1.28/P.1 variant does not possess the 69/70 deletion mutation, highlighting the need for a versatile VOC surveillance strategy.

Given the potential for VOCs to enhance transmission, increase deaths, and possibly evade natural or vaccine-induced immune responses, identifying cases of coronavirus disease (COVID-19) caused by VOCs and monitoring their prevalence is critical. We propose a rapid VOC surveillance strategy that uses multiple rRT-PCRs to screen all samples positive for SARS-CoV-2. This study was approved by the Providence Health Care/University of British Columbia and Simon Fraser University Research Ethics Boards (H20–01055).

The Study

During January 26–March 1, 2021, the clinical virology laboratory at St. Paul's Hospital, Vancouver, British Columbia, Canada, conducted VOC testing on nasopharyngeal swab and saliva/mouth rinse samples in which SARS-CoV-2 was detected at any cycle threshold (C_t) value. SARS-CoV-2 detection was performed by using the LightMix SarbecoV E-gene plus EAV control assay (TIB

Author affiliations: St. Paul's Hospital, Vancouver, British Columbia, Canada (N. Matic, C.F. Lowe, G. Ritchie, A. Stefanovic, T. Lawson, W. Jang, M. Young, V. Leung, M.G. Romney); University of British Columbia, Vancouver (N. Matic, C.F. Lowe, G. Ritchie, A. Stefanovic, C.J. Brumme, V. Leung, M.G. Romney); British Columbia Centre for Excellence in HIV/AIDS, Vancouver (W. Dong, Z.L. Brumme, C.J. Brumme); Simon Fraser University, Burnaby, British Columbia, Canada (Z.L. Brumme)

DOI: https://doi.org/10.3201/eid2706.210532

[1]These first authors contributed equally to this article.

Molbiol, https://www.tib-molbiol.de), with the MagNA Pure Compact or MagNA Pure 96 and LightCycler 480 or with the cobas SARS-CoV-2 Test (Roche Molecular Diagnostics, https://diagnostics.roche.com) on the cobas 6800. VOCs were detected with the VirSNiP SARS-CoV-2 Mutation Assays for strain surveillance (TIB Molbiol), targeting specific spike protein variations (N501Y, delHV69/70, K417N, E484K, V1176F). A laboratory-developed test was also developed for N501Y (501F-GCATGTAGAAGTTCAAAAGAAAGT; 501R-TCCTTTACAATCATATGGTTTCCA; 501YProbe FAM-CACT+T+ATGGT GTTGGTTACCA ACCA-IABkFQ; 501NProbe Cy5-CACT+A+ATGG TGTTGGTTACCAACCA-IAbRQSp)anddelHV69/70 (del6970F-TCAACTCAGGACTTGTTCTTAC; del6970R-TGGTAGGACAGGGTTATCAAAC;wtProbe HEX-TGCTAT+ACATG+TCTCTGGGACCA-IABkFQ; delProbe-TEX615-TGCTAT+CTCTG+GGACCAATG-IAbRQSp), in which + denotes locked nucleic acids. Samples were first screened for N501Y, and if detected, we tested subsequent targets to discriminate between the most prevalent VOC within the Vancouver community (B.1.1.7-delHV69/70 and B.1.351-K417N) and newly emerging VOC (B.1.1.28/P.1-V1176F).

For the first presumptive case caused by each VOC, we performed whole-genome sequencing (WGS) in-house on either the MinION (Oxford Nanopore Technologies, https://nanoporetech.com), using the ARTIC nCOV-2019 sequencing protocol V1 (https://www.protocols.io/view/ncov-2019-sequencing-protocol-bbmuik6w) by using V3 primers, or on an Illumina MiSeq (https://www.illumina.com) by using a modified ARTIC nCOV-2019 protocol. Accurate base calling of MinION was performed by using GUPPY 3.1.5 and FASTQ files analyzed with BugSeq (https://BugSeq.com). Illumina data were analyzed with the in-house bioinformatics pipeline MiCall (https://github.com/cfe-lab/MiCall). All presumptive VOCs were subsequently sent to a reference laboratory for confirmatory WGS.

During the study period, 31,833 clinical samples were tested for SARS-CoV-2, and results were positive for 2,618. Of these, 2,430 (92.8%) underwent testing for the 3 major VOC categories (B.1.1.7, B.1.351, B1.1.28/P.1); 1.6% (38/2,430) failed to amplify with the N501Y assay, of which 71.0% (27/38) were reported as indeterminate for SARS-CoV-2, reflecting late C_t values and presumably low viral loads. From the remaining 2,392 samples, 77 VOCs were identified (57-B.1.1.7, 7-B.1.351, and 13-B.1.1.28/P.1). N501Y was not detected in the remaining 2,315 (96.8%) samples, and they were not sent to the reference laboratory for WGS. The VirSNiP and laboratory-developed PCRs were concordant for all detected VOCs.

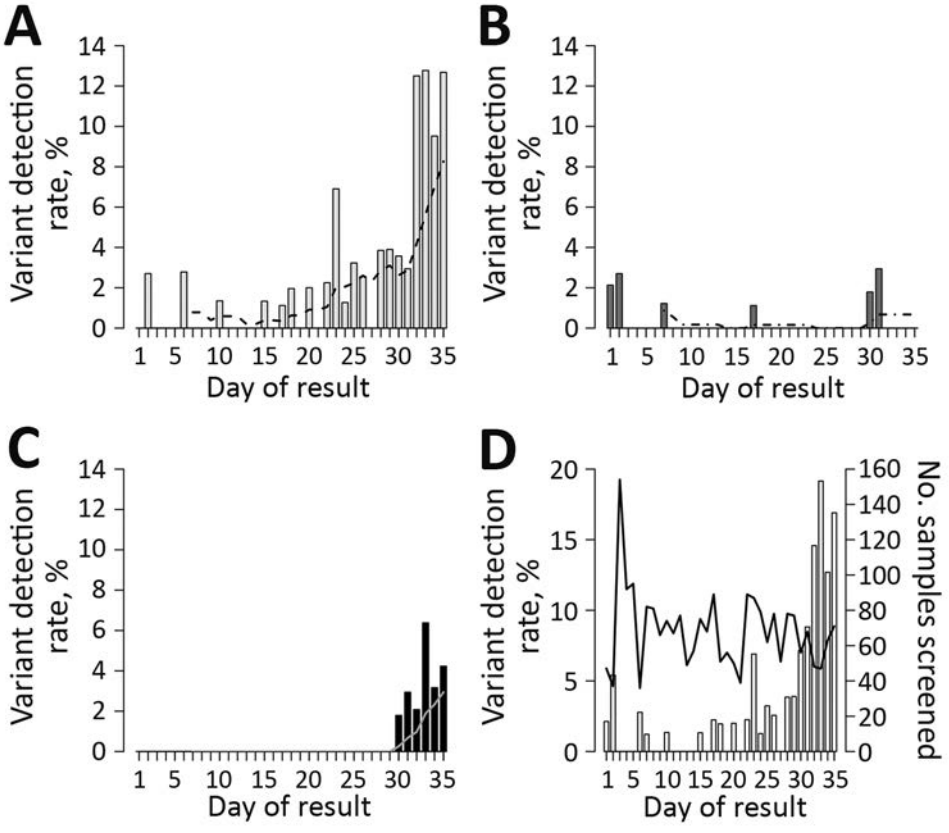

Figure. Rate of detection of severe acute respiratory syndrome coronavirus 2 variants of concern, by day of result, January 26–March 1, 2021, with 7-day moving average. A) B.1.1.7 (UK); dashed line indicates 7-day moving average. B) B.1.351 (South Africa); dashed line indicates 7-day moving average; C) B.1.1.28/P.1 (Brazil),;solid line indicates 7-day moving average; D) all variants of concern; solid line indicates number of samples screened.

During the study period, VOC detection among diagnostic samples rapidly increased (Figure). Of note, identified VOCs included a large cluster of the B.1.1.28/P.1 variant not previously identified in British Columbia. All B.1.1.28/P.1 variants were initially suspected from the K417N assay, for which PCR products were identified at a lower melting temperature than expected. All suspected B.1.1.28/P.1 variants were confirmed when rescreened by using the V1176F target.

The first presumptive B.1.1.28/P.1 variant identified was confirmed by in-house WGS, detecting the following S gene mutations (characteristic of B.1.1.28/P.1): L18F, T20N, P26S, D138Y, R190S, K417T, E484K, N501Y, D614G, H655Y, T1027I, and V1176F. At the time of publication, the reference laboratory had attempted WGS for 54/77 VOCs, of which 7 (12.9%) samples failed WGS, with original C_t values of 24–35. Of the 47 successfully sequenced samples, agreement with PCR was 100% (38-B.1.1.7, 3-B.1.351, and 6-B.1.1.28/P.1).

Conclusions

Implementation of a PCR-based algorithm to detect VOCs has enabled our laboratory to rapidly detect new variants that are in the early stages of community transmission. Our protocol enabled detection of VOCs within 24 hours of COVID-19 diagnosis, a marked advantage over sequencing-based surveillance strategies. VOC positivity rate was 3.2%, but detection rates increased markedly over time, as might be expected with exponential growth observed in other countries.

Although B.1.1.28/P.1 had not been previously reported in our region, presence of this variant was suspected when K417N PCR products with a lower melting temperature than wild-type were observed, suggestive of a non-K417N substitution (e.g., K417T mutation in the B.1.1.28/P.1 variant) (VirSNiP SARS-CoV-2 Spike K417N package insert; TIB Molbiol, Berlin, Germany). Follow-up testing using the V1176F target supported the presumptive identification of B.1.1.28/P.1, which was subsequently confirmed by WGS. Testing all SARS-CoV-2–positive samples for VOCs enabled rapid detection of a discrete new B.1.1.28/P.1 cluster.

Although WGS has been the primary modality for VOC surveillance, universal sequencing of SARS-CoV-2–positive specimens is limited by both laboratory and bioinformatics capacity (*6*). Because of the volume of VOC testing and the limited capacity for high complexity WGS, turnaround times by WGS may be days to weeks. Since the onset of the COVID-19 pandemic, molecular diagnostics (i.e., PCR) have been increasingly adopted by laboratories to promptly identify SARS-CoV-2, and infrastructure has been established for this testing modality. A PCR-based algorithm for the molecular detection of VOCs could be rapidly adopted, providing almost real-time results to inform infection prevention and control and public health measures (*3*,*7*,*8*). PCR may also be more sensitive because WGS is challenging to perform on samples with low viral loads (C_t >30) (*9*). Compared with WGS, PCR screening enhanced sensitivity for VOC detection by >10%.

Although the most prevalent VOCs worldwide harbor N501Y, this mutation is not present in all variants (*10*). A PCR-based algorithm for identifying VOCs that use N501Y as the initial screening target must acknowledge this limitation. Given the rapid emergence of new variants, ongoing surveillance is key, and laboratories considering a PCR-based algorithm would need to adapt the algorithm as VOC prevalence changes. For example, our initial screening PCR targeted N501Y, but because of rising rates of B.1.1.7, we adjusted our laboratory-developed test to include N501Y and delHV69/70 in a duplexed assay.

PCR-based methods for rapid VOC detection should not replace broader VOC surveillance with WGS, which enables identification of non-N501Y VOCs and can characterize emerging mutations in known VOCs. This ability is critical for enabling laboratories to revise their PCR targets in an ongoing manner to keep pace with local VOC circulation.

In summary, our implementation of an rRT-PCR–based algorithm enabled identification of the most common VOCs to date (B.1.1.7, B.1.351, and B.1.1.28/P.1) within 24 hours. This method enables laboratories to perform VOC testing on all SARS-CoV-2–positive samples, enhancing VOC surveillance capacity to support near real-time decision making for interrupting transmission.

This article was preprinted at https://www.medrxiv.org/content/10.1101/2021.03.04.21252928v1.

Acknowledgments

We are grateful to our medical laboratory technologists, who are highly committed to patient care and laboratory quality improvement. We also acknowledge contributions from John Harding and Althea Hayden and the BCCDC Public Health Laboratory (Natalie Prystajecky, Agatha Jassem, Catherine Hogan, Linda Hoang, and Mel Krajden).

This work was supported by COVID-19 rapid response grants from GenomeBC (COV-115 to Z.L.B., C.F.L.; COV-033 to C.J.B.), an Exceptional Opportunities Fund–COVID-19 award from the Canada Foundation for Innovation (C.J.B., C.F.L.), a British Columbia Ministry of Health–Providence Health Care Research Institute COVID-19 Research Priorities Grant (C.J.B., C.F.L.), and Public Health Agency of Canada COVID-19 Immunology Task Force COVID-19 Hot Spots Competition Grant (2021-HQ-000120 to Z.L.B., M.G.R.).

G.R. reports participation as a Roche Diagnostics Sequencing Advisory Panel member. Z.L.B. holds a Scholar Award from the Michael Smith Foundation for Health Research.

About the Author

Dr. Matic is a medical microbiologist at St. Paul's Hospital in Vancouver and a clinical assistant professor at the University of British Columbia. Her primary research interests include virology diagnostics and laboratory quality improvement.

References

1. Liu Y, Liu J, Xia H, Xianwen Z, Fontes-Garfias CR, Swanson KA, et al. Neutralizing activity of BNT162b2-elicited serum—preliminary report. 2021 Feb 28 [cited 2021 Mar 3]. https://www.nejm.org/doi/full/10.1056/NEJMc2102017
2. Xie X, Liu Y, Liu J, Zhang X, Zou J, Fontes-Garfias CR, et al. Neutralization of SARS-CoV-2 spike 69/70 deletion, E484K and N501Y variants by BNT162b2 vaccine-elicited sera [cited 2021 Mar 3]. https://www.nature.com/articles/s41591-021-01270-4
3. Galloway SE, Paul P, MacCannell DR, Johansson MA, Brooks JT, MacNeil A, et al. Emergence of SARS-CoV-2 B.1.1.7 lineage—United States, December 29, 2020–January 12, 2021. MMWR Morb Mortal Wkly Rep. 2021;70:95–9. https://doi.org/10.15585/mmwr.mm7003e2
4. European Centre for Disease Prevention and Control. Rapid increase of a SARS-CoV-2 variant with multiple spike protein mutations observed in the United Kingdom. 2020 Dec 20 [cited 2021 Mar 3]. https://www.ecdc.europa.eu/sites/default/files/documents/SARS-CoV-2-variant-multiple-spike-protein-mutations-United-Kingdom.pdf
5. Sabino EC, Buss LF, Carvalho MPS, Prete CA Jr, Crispim MAE, Fraiji NA, et al. Resurgence of COVID-19 in Manaus, Brazil, despite high seroprevalence. Lancet. 2021; 397:452–5. https://doi.org/10.1016/S0140-6736(21)00183-5
6. World Health Organization. Genomic sequencing of SARS-CoV-2: a guide to implementation for maximum impact on public health. 2021 Jan 8 [cited 2021 Mar 3]. https://www.who.int/publications/i/item/9789240018440
7. Ontario Agency for Health Protection and Promotion (Public Health Ontario), Provincial Infectious Diseases Advisory Committee. Interim guidance for infection prevention and control of SARS-CoV-2 variants of concern for health care settings. 2021 Feb 10 [cited 2021 Mar 3]. https://www.publichealthontario.ca/-/media/documents/ncov/voc/2021/02/pidac-interim-guidance-sars-cov-2-variants.pdf?la=en
8. European Centre for Disease Prevention and Control. Risk assessment: risk related to the spread of new SARS-CoV-2 variants of concern in the EU/EEA-first update. 2021 Jan 21 [cited 2021 Mar 3]. https://www.ecdc.europa.eu/en/publications-data/covid-19-risk-assessment-spread-new-variants-concern-eueea-first-update
9. Charre C, Ginevra C, Sabatier M, Regue H, Destras G, Brun S, et al. Evaluation of NGS-based approaches for SARS-CoV-2 whole genome characterisation. Virus Evol. 2020;6:a075. https://doi.org/10.1093/ve/veaa075
10. Zhang W, Davis B, Chen S, Sincuir Martinez JM, Plummer JT, Vail E. Emergence of a novel SARS-CoV-2 variant in southern California. 2021 Feb 28. [cited 2021 Mar 3]. https://jamanetwork.com/journals/jama/fullarticle/2776543

Address for correspondence: Marc G. Romney, St. Paul's Hospital, Providence Health Care, 1081 Burrard St, Vancouver, BC V6Z 1Y6, Canada; email: mromney@providencehealth.bc.ca

Epidemiologic Evidence for Airborne Transmission of SARS-CoV-2 during Church Singing, Australia, 2020

Anthea L. Katelaris, Jessica Wells, Penelope Clark, Sophie Norton, Rebecca Rockett, Alicia Arnott, Vitali Sintchenko, Stephen Corbett, Shopna K. Bag

An outbreak of severe acute respiratory syndrome coronavirus 2 infection occurred among church attendees after an infectious chorister sang at multiple services. We detected 12 secondary case-patients. Video recordings of the services showed that case-patients were seated in the same section, up to 15 m from the primary case-patient, without close physical contact, suggesting airborne transmission.

The circumstances under which airborne transmission of severe acute respiratory syndrome coronavirus 2 (SARS-CoV-2) might occur are uncertain (*1*,*2*). Previous cluster reports have suggested involvement of airborne transmission (*3*,*4*), but clear epidemiologic evidence is lacking. We investigated a SARS-CoV-2 outbreak in a church in Sydney, New South Wales, Australia, and reviewed the epidemiologic and environmental findings to assess the possibility of airborne transmission of SARS-CoV-2.

The Study

On July 18, 2020, the Western Sydney Public Health Unit was notified of a positive SARS-COV-2 test result for an 18-year-old man (PCR cycle threshold [C_t] values: envelope gene 14.5, nucleocapsid gene 16.8). He had sought testing the day before, after learning of a SARS-COV-2 exposure at a venue he attended on July 11. He reported symptom onset of malaise and headache on July 16 and cough and fever on July 17. He was a church chorist and, during his infectious period (from 48 hours before onset), had sung at four 1-hour services, 1 each on July 15 and 16 and 2 on July 17.

The case-patient had sung from a choir loft, elevated 3.5 m above the congregation, which he entered before and left after the service. He denied touching objects in the church or mixing with the general congregation. Video recordings of the services corroborated this history. We identified close contacts according to the national coronavirus disease (COVID-19) control guidelines at the time (*5*): anyone who had spent >15 min face-to-face or shared a closed space for 2 hours with a case-patient during the infectious period of the case-patient. Initially, 10 other chorists and staff were classified as close contacts and required to quarantine (*5*).

On July 18, the church informed the community about the case-patient, prompting testing among members. On July 20, the Western Sydney Public Health Unit was notified of 2 additional case-patients who reported attendance on July 15 and 16. Neither was known by the primary case-patient.

Because transmission was deemed likely to have occurred at these services, we classified all attendees of the 4 services as close contacts, required to quarantine, and requested to seek baseline SARS-CoV-2 testing regardless of symptoms (in addition to if symptoms developed). Public health staff telephoned attendees (identified by mandatory service sign-in records), released alerts through the church and media, and established a testing clinic on-site. Close contacts were contacted every 2–3 days to inquire about symptoms and advised to retest if symptoms developed.

We identified 508 close contacts across the 4 services (Table), of which 434 (85%) were recorded as having a test within 17 days after exposure. Most contacts were tested 2–7 days after exposure (Appendix Figure 1,

Author affiliations: Western Sydney Local Health District, Sydney, New South Wales, Australia (A. Katelaris, J. Wells, P. Clark, S. Norton, S. Corbett, S.K. Bag); The University of Sydney, Sydney (S. Norton, R. Rockett, A. Arnott, V. Sintchenko, S Corbett, S.K. Bag); New South Wales Health Pathology, Westmead, New South Wales, Australia (R. Rockett, A. Arnott, V. Sintchenko)

DOI: https://doi.org/10.3201/eid2706.210465

Table. Number of SARS-CoV-2 close contacts and case-patients in an outbreak in a church, by service date, Australia, 2020*

Date of service, July	No. contacts†	No. tested‡	Proportion tested, %	No. cases	Secondary attack rate, %
15	215	169	79	5	2.3
16	120	108	90	7§	5.8
17 (2 services)	173	157	91	(1§)	NC
Total	508	434	85	12	2.4

*SARS-CoV-2, severe acute respiratory syndrome coronavirus 2; NC, not calculated.
†Contacts identified through church service sign-in records and staff lists. This procedure might slightly underestimate the number of contacts because some persons might not have signed in and some telephone numbers were illegible or invalid.
‡Contacts were tested within 17 d (14-d incubation period plus 3 d) of the last exposure date. Pathology providers in New South Wales, Australia, routinely report SARS-CoV-2 test results (positive or negative) to public health authorities. This number would not include tests performed under a different name or spelling to that on the sign-in records.
§One case-patient attended 2 services on July 16 and 17. Because of the absence of additional case-patients on July 17, we have attributed exposure of this case-patient to have been on July 16.

https://wwwnc.cdc.gov/EID/article/27/6/21-0465-App1.pdf).

We detected 12 secondary case-patients among 508 service attendees, yielding an overall secondary attack rate (SAR) of 2.4% across the 4 services (Table). Five case-patients attended only the service on July 15 (SAR 5/215, 2.3%), and 7 attended only on July 16 (SAR 7/120, 5.8%). One case-patient who attended on July 16 also attended on July 17; however, no case-patients were identified who attended only a service on July 17. Secondary case-patients showed development of symptoms 2–12 days after exposure (Figure 1). Five of the secondary case-patients were from the same households as earlier cluster case-patients. Thus, these case-patients might have been infected within the household rather than the church. No secondary case-patients reported other SARS-COV-2 exposures outside these services. There were no deaths, although 3 case-patients were hospitalized, including 2 who required intensive care.

SARS-CoV-2 genome sequencing was performed for the primary case-patient and 10 secondary case-patients (*6*). These case-patients formed a single genomic cluster with a maximum of 2 nt changes from the SARS-CoV-2 genome of the primary case-patient (Appendix Figure 2). High C_t values for the remaining 2 case-patients prohibited sequencing.

To further characterize exposures, we determined the seating positions of secondary case-patients within the church. We asked case-patients to describe where they sat, and the video recordings of the services were reviewed, jointly with the case-patients where possible, to confirm locations.

The church was round, and pews were located circumferentially. We were able to locate the exact location of 10 of the 12 secondary case-patients by using the recordings. The remaining 2 case-patients (case-patients 3 and 4) were unable to review the recordings but described the section and row in which they sat. All secondary case-patients sat within a 70° section, below and 1–15 m from the primary case-patient (Figure 2). The primary case-patient faced away from this area, and used a microphone. Cases were not detected in attendees seated in other sections, and the spatial clustering remains if the 5 potentially household-acquired case-patients are excluded (case-patients 7, 8, 10, 12, and 13). None of the other choristers showed symptoms or tested positive for SARS-CoV-2. Use of masks was not in place.

To understand the ventilation, we conducted 2 site visits with the building manager. The church had a high conical roof, and the ventilation system at the apex was not in operating during the services. The doors and windows were largely closed, except

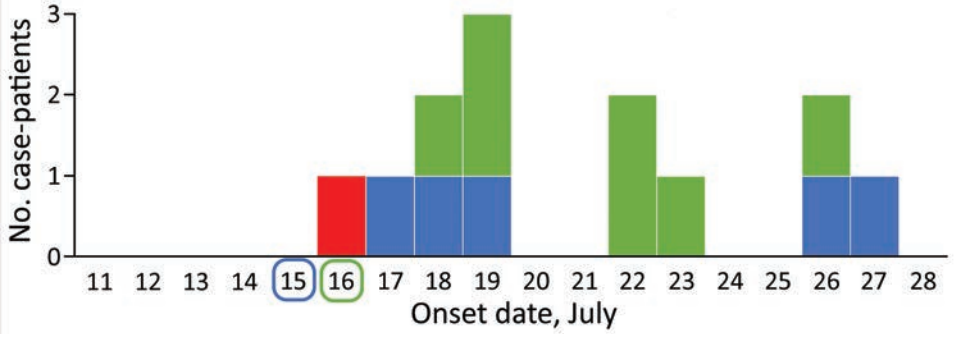

Figure 1. Epidemiologic curve of an outbreak of infection with severe acute respiratory syndrome coronavirus 2 in a church, Australia, 2020. Red indicates symptom onset date for the index case-patient, who sang at 4 services on July 15–17; secondary case-patient symptom onset dates are color coded by date of service attendance as indicated along baseline (1 secondary case-patient attended services on July 16 and 17). The 5 case-patients with onsets of July 22–26 also had exposures to earlier outbreak case-patients in their households.

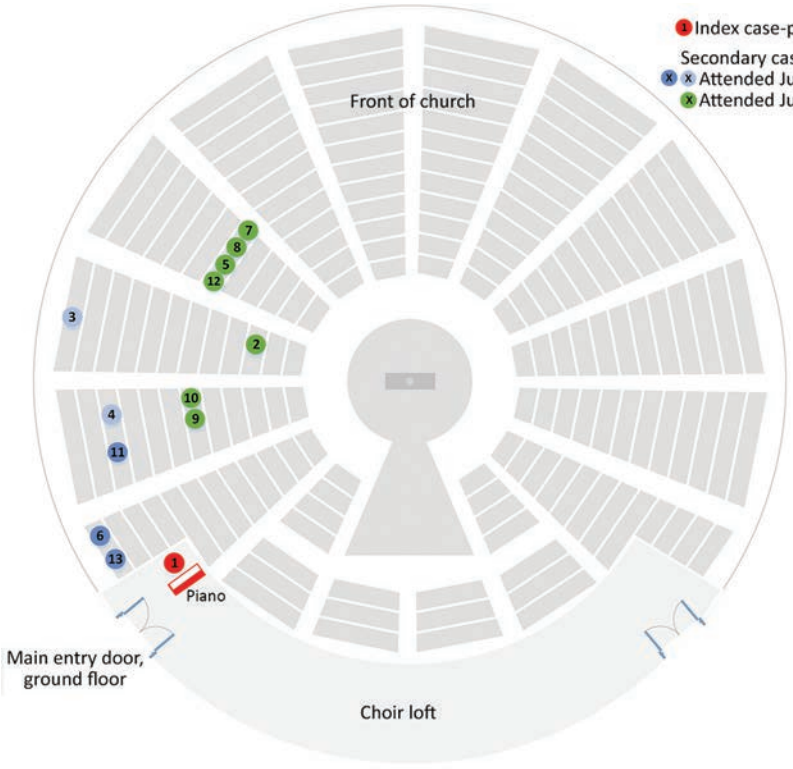

Figure 2. Schematic diagram of church layout showing seating locations of primary and secondary case-patients during an outbreak of infection with severe acute respiratory syndrome coronavirus 2, Australia, 2020. Case numbers are based on order of notification received by the Public Health Unit. Location of case-patients indicated in green and dark blue were confirmed on video recordings; the 2 case-patients indicated in light blue described their locations. The primary case-patient was located in an elevated loft ≈3 m above ground level. He was singing and playing the piano throughout the services and faced toward the piano. Other members of the congregation were seated throughout all sections of the church during the 4 services. Relatively more persons were seated in the front area of the church than in the sides or back.

as persons entered and exited, and the wall fans were off, meaning there was minimal ventilation.

Conclusions

We detected 12 secondary case-patients linked to an infectious case-patient at church services on 2 days. Secondary case-patients were seated in the same area of the church, up to 15 m from the primary case-patient, with whom there was no evidence of close physical contact. We believe that transmission during this outbreak is best explained by airborne spread, potentially the result of 3 factors. First, singing has been demonstrated to generate more respiratory aerosol particles and droplets than talking (*7*). Second, minimal ventilation might have enabled respiratory particles to accumulate in the air, and convection currents might have carried particles toward the pews where secondary case-patients were seated. Third, the primary case-patient was likely near the peak of infectiousness on the basis of low C_t values (*8*) and symptom onset occurring around the exposure dates (*9*). Although we cannot completely exclude fomite transmission, this transmission would not explain the spatial clustering of case-patients within the church over 2 days.

Strengths of our investigation include detailed case and contact follow-up, availability of video recordings of the services to confirm movements and locations of case-patients, high uptake of testing by contacts, and that SARS-CoV-2 genome sequencing provided supportive evidence that case-patients were closely related genomically. In addition, the New South Wales context of low community transmission (*10*) and high estimated case ascertainment (*11*) makes it unlikely that case-patients acquired infection outside this cluster.

A limitation was that most contacts were tested within a week of exposure, which could have been too early to detect some asymptomatic infections. Second, this investigation only provides circumstantial evidence of airborne transmission, and does not help elucidate the exact mechanism of spread. Finally, we are unsure why transmission did not occur at the services on July 17 (except in 1 possible instance); reasons might be related to altered air flow, the primary case-patient being past peak infectiousness, or that cases that did occur went undetected.

This cluster occurred despite adherence to guidelines requiring microphone use and a 3-m cordon around singers. Guidelines for places of worship were tightened after this cluster was detected, including increasing the distance required around a singer to 5 m. However additional mitigation measures might be necessary to prevent airborne infection during church services and singing, including increased natural or artificial ventilation (*12*) or moving activities outdoors.

Acknowledgments

We thank the case-patients, church management, and wider church community for their participation and support during the outbreak management and investigations; Jennifer Paterson, Jennifer Lampard, Stephen Crone, and the Public Health Unit surge team for assistance with case and contact tracing; Kate Ward, Duleepa Jayasundara, and the Institute of Clinical Pathology and Medical Research, New South Wales Health Pathology for their contributions to the study; Aneliese Goodwin, Clement Lee, Carl Banting, Connie Lam, Karen-Ann Gray, Eby Sim, Elena Martinez, Mailie Gall, Jenny Draper, Rosemarie Sadsad, Andrew Ginn, and Qinning Wang for performing genome sequencing and bioinformatic analysis; and the New South Wales Ministry of Health Public Health Response Branch for its participation in the study.

About the Author

Dr. Katelaris is a public health physician and field epidemiologist in the Western Sydney Local Health District Public Health Unit, Sydney, New South Wales, Australia. Her primary research interests include communicable disease control, infectious disease epidemiology, and outbreak investigation.

References

1. Centers for Disease Control and Prevention. Scientific brief: SARS-CoV-2 and potential airborne transmission; 2020 [cited 2020 Dec 19] https://www.cdc.gov/coronavirus/2019-ncov/more/scientific-brief-sars-cov-2.html
2. Wilson N, Corbett S, Tovey E. Airborne transmission of covid-19. BMJ. 2020;370:m3206. https://doi.org/10.1136/bmj.m3206
3. Lu J, Yang Z. COVID-19 outbreak associated with air conditioning in restaurant, Guangzhou, China, 2020. Emerg Infect Dis. 2020;26:2791–3. https://doi.org/10.3201/eid2611.203774
4. Hamner L, Dubbel P, Capron I, Ross A, Jordan A, Lee J, et al. High SARS-CoV-2 attack rate following exposure at a choir practice — Skagit County, Washington, March 2020. MMWR Morb Mortal Wkly Rep. 2020;69:606–10. https://doi.org/10.15585/mmwr.mm6919e6
5. Australian Government Department of Health. Coronavirus disease 2019 (COVID-19) communicable diseases network Australia (CDNA) national guidelines interim advice to public health units, COVID-19, version 3.4. Canberra, 2020 [cited 2021 Mar 30]. https://www1.health.gov.au/internet/main/publishing.nsf/Content/cdna-song-novel-coronavirus.htm
6. Rockett RJ, Arnott A, Lam C, Sadsad R, Timms V, Gray KA, et al. Revealing COVID-19 transmission in Australia by SARS-CoV-2 genome sequencing and agent-based modeling. Nat Med. 2020;26:1398–404. https://doi.org/10.1038/s41591-020-1000-7
7. Alsved M, Matamis A, Bohlin R, Richter M, Bengtsson P, Fraenkel C, et al. Exhaled respiratory particles during singing and talking. Aerosol Sci Technol. 2020;54:1245–8. https://doi.org/10.1080/02786826.2020.1812502
8. Singanayagam A, Patel M, Charlett A, Lopez Bernal J, Saliba V, Ellis J, et al. Duration of infectiousness and correlation with RT-PCR cycle threshold values in cases of COVID-19, England, January to May 2020. Euro Surveill. 2020;25. https://doi.org/10.2807/1560-7917.ES.2020.25.32.2001483
9. Cheng HY, Jian SW, Liu DP, Ng TC, Huang WT, Lin HH; Taiwan COVID-19 Outbreak Investigation Team. Contact tracing assessment of COVID-19 transmission dynamics in Taiwan and risk at different exposure periods before and after symptom onset. JAMA Intern Med. 2020;180:1156–63. https://doi.org/10.1001/jamainternmed.2020.2020
10. Health New South Wales. COVID-19 weekly surveillance in NSW, epidemiological week 29, ending 18 July 2020. NSW Government, 2020 [cited 2021 Mar 29]. https://www.health.nsw.gov.au/Infectious/covid-19/Documents/covid-19-surveillance-180720.pdf
11. Price DJ, Shearer FM, Meehan M, McBryde E, Golding N, McVernon J, et al. Estimating the case detection rate and temporal variation in transmission of COVID-19 in Australia. Technical report, 2020. [cited 2020 Apr 14]. https://www.apprise.org.au/publication/estimating-the-case-detection-rate-and-temporal-variation-in-transmission-of-covid-19-in-australia/
12. Morawska L, Tang JW, Bahnfleth W, Bluyssen PM, Boerstra A, Buonanno G, et al. How can airborne transmission of COVID-19 indoors be minimised? Environ Int. 2020;142:105832. https://doi.org/10.1016/j.envint.2020.105832

Address for correspondence: Anthea L. Katelaris, Centre for Population Health, Locked Bag 7118, Parramatta BC 2124, NSW, Australia; email: anthea.katelaris@health.nsw.gov.au

Ebola Virus IgG Seroprevalence in Southern Mali

Sidy Bane, Kyle Rosenke, Ousmane Maiga, Friederike Feldmann, Kimberly Meade-White, Julie Callison, David Safronetz, Nafomon Sogoba, Heinz Feldmann

Mali had 2 reported introductions of Ebola virus (EBOV) during the 2013–2016 West Africa epidemic. Previously, no evidence for EBOV circulation was reported in Mali. We performed an EBOV serosurvey study in southern Mali. We found low seroprevalence in the population, indicating local exposure to EBOV or closely related Ebola viruses.

The West Africa Ebola virus disease (EVD) epidemic of 2013–2016 mainly affected the countries of Guinea, Sierra Leone, and Liberia; its cause was Ebola virus (EBOV; genus *Ebolavirus*, species *Zaire ebolavirus*) strain Makona (*1*). EBOV was introduced into Senegal and more noticeably into Nigeria; it was also exported into several countries in Europe as well as the United States (*1*). Overall, this outbreak was the largest on record, resulting in ≈30,000 EVD cases and 11,000 deaths (*1*). During this epidemic, EBOV was also introduced twice into Mali from Guinea, both times through the border crossing close to Kouremalé (Figure). One introduction came through a young child who had laboratory-confirmed EVD, which resulted in no transmission despite intimate contact with others (*2*). The second introduction came through an imam who had non–laboratory-confirmed probable EVD, with limited transmission. In total, Mali reported 9 cases and 7 deaths throughout 2014 (*2*). Before those introductions, EBOV or other filovirus infections were not previously reported from Mali. As of April 2021, limited efforts have been made to investigate EBOV prevalence in the country, and a small study did not reveal serologic evidence for human exposure to EBOV (*3*).

Author affiliations: University of Sciences, Techniques, and Technologies of Bamako, Bamako, Mali (S. Bane, O. Maiga, N. Sogoba); National Institutes of Health, Hamilton, Montana, USA (K. Rosenke, F. Feldmann, K. Meade-White, J. Callison, H. Feldmann), Public Health Agency of Canada, Winnipeg, Manitoba, Canada (D. Safronetz)

DOI: https://doi.org/10.3201/eid2706.203510

Southern Mali borders Cote d'Ivoire, Guinea, and Burkina Faso. This region shares 1 ecosystem; therefore, southern Mali is likely to harbor similar arthropod, rodent, and bat species as the neighboring countries, suggesting the possibility that similar zoonotic pathogens may be present (*4*,*5*) (Figure). Therefore, we tested human serum samples originally collected in southern Mali for Lassa fever surveillance (*6*) for the presence of EBOV antibodies.

The Study

We used 600 serum samples from healthy volunteers collected in 2015 in Bamba, Banzana, and Soromba, located in southern Mali, close to the border with Cote d'Ivoire (Figure) (*6*). The human study protocol was originally approved to determine the seroprevalence for Lassa virus and then later addended to also identify the seroprevalence for EBOV (protocol nos. 15-I-N023 and 18-I-N060). We used 2 commercial ELISA kits (Alpha Diagnostic International, https://www.4adi.com) that detect human IgG to Zaire EBOV nucleoprotein (NP) and glycoprotein (GP). We performed the assays according to the manufacturer's instructions by using heat-inactivated serum samples (56°C for 60 min). All tests were run in a biosafety class IIa cabinet by personnel wearing personal protective equipment, including N95 face mask, face shield, laboratory coat, and double gloves.

All serum samples were first screened at a 1:100 dilution using the anti-EBOV GP assay. We observed unexpected high reactivity at this serum dilution (122/600; 20.3%) (Table) that was probably unspecific low-affinity binding or cross-reactivity with other viruses. To reduce unspecific reactivity, we next tested all positive serum samples at 1:400 dilution using the anti-EBOV GP assay, resulting in 3.7% (22/600) positivity, and anti-EBOV NP assay, resulting in 4.0% (24/600) seropositivity (Table). Finally, we tested all samples that were positive at 1:400 dilution at a 1:1,600 serum dilution; anti-EBOV GP assay had 0.2% (1/600) positivity and anti-EBOV NP assay 0.7% (4/600) seropositivity

(Table). Our testing algorithm considered positives at a 1:100 dilution an equivocal test result. A positive reaction at a serum dilution of ≥1:400 was considered a positive test result. Using this algorithm, we detected antibodies to EBOV GP, EBOV NP, or both in 37/600 (6.1%) of the study population. Nine (1.5%) participants had positive IgG responses to both EBOV NP and GP antigens (Table). Our results indicate that the population in southern Mali has had or still has exposure to EBOV or closely related ebolaviruses. The overall seroprevalence range was 1.5% (seropositivity in both) –6.1% (a single assay ≥1:400).

Several scenarios may explain the results of this study. First, EBOV or a related filovirus is endemic and circulating in its reservoir species in southern Mali leading to occasional human exposure. This scenario is supported by a similar geographic environment in the southern neighboring countries that had documented EBOV seroprevalence (*4*,*5*) (Figure). A drawback of this hypothesis is the current failure of finding EBOV or closely related viruses in wildlife species, particularly bats, in most West Africa countries. However, Bombali virus, a new *Ebolavirus* species, was discovered in bats in Sierra Leone and Guinea (*7*,*8*); serologic testing has also indicated circulation in pigs in Sierra Leone and Guinea (*9*,*10*).

A second scenario is that exposure in southern Mali was temporary and occurred through human-to-human contact from cross-border movement during the West Africa EVD outbreak. This scenario may be supported by the sample collection time, February 2015 but remains questionable because no patients with EVD symptoms have been reported in this region. However, this also holds true for Lassa virus; 1 case of Lassa fever has been reported in southern Mali despite high prevalence in the local rodent reservoir (*6*).

Third, all seropositivity is due to cross-reactivity with other viruses or to unspecific, low-affinity antibody binding. Filovirus serology, especially for EBOV, has been controversial over the years. Early reports of sometimes high seropositivity in certain

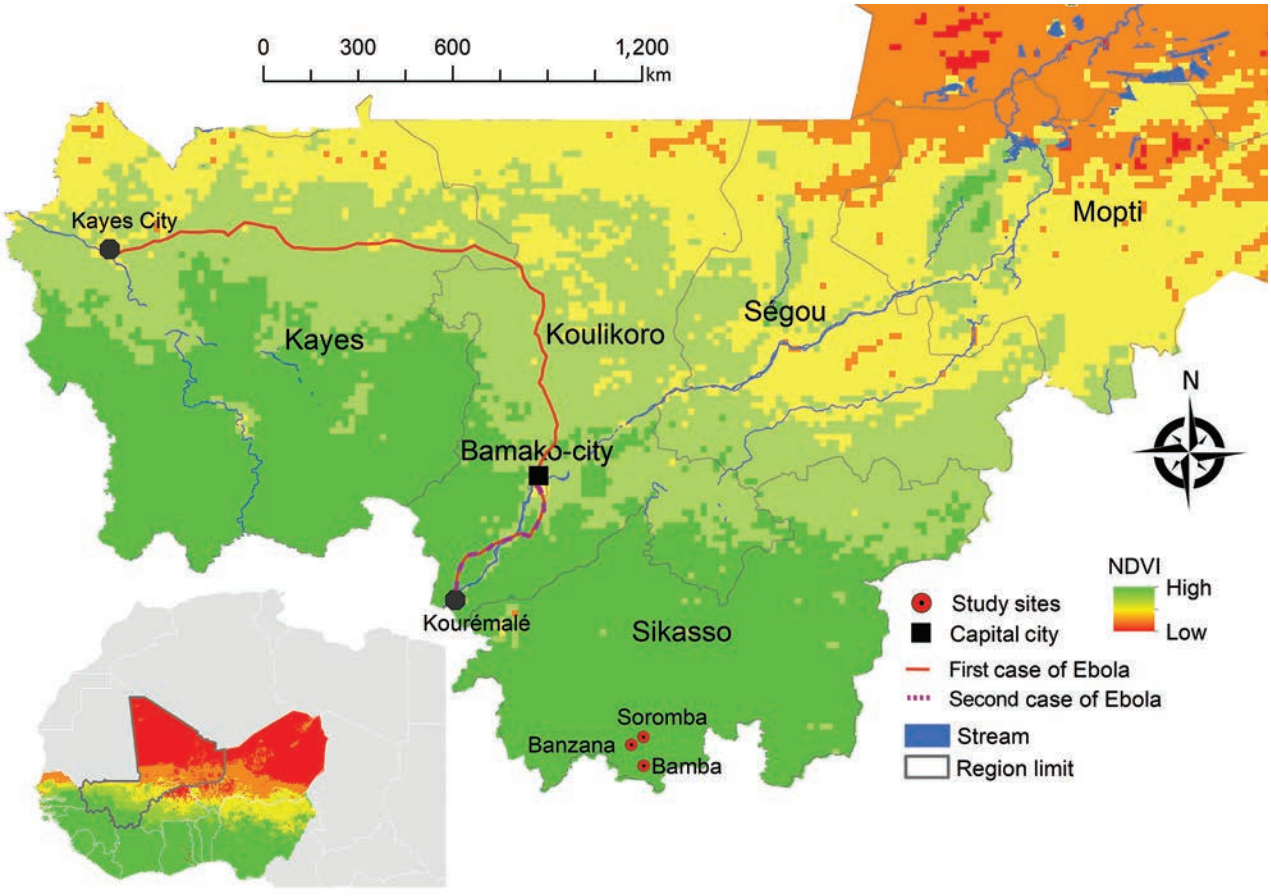

Figure. NDIV map showing 3 study sites, Bamba, Banzana, and Soromba (red circles), for investigation of Ebola virus IgG seroprevalence in southern Mali. Red line indicates first Ebola virus introduction into Mali; purple dashed line indicates the second. Inset map shows NDIVs of countries in West Africa. NDIV, normalized difference vegetation index.

Table. Results of EBOV serology on 600 human samples from southern Mali*

	No. (%) positive								
	EBOV GP IgG			EBOV NP IgG			Both		
Location	1:100	1:400	1:1,600	1:100	1:400	1:1,600	1:100	1:400	1:1,600
Bamba	23 (11.5)	2 (1.0)	0	ND	6 (3.0)	2 (1.0)	NA	1 (0.5)	0
Banzana	39 (19.5)	9 (4.5)	1 (0.5)	ND	5 (2.5)	0	NA	2 (1.0)	0
Soromba	60 (30.0)	11 (5.5)	0	ND	13 (6.5)	2 (1.0)	NA	6 (3.0)	0
Total	122 (20.3)	22 (3.7)	1 (0.2)	ND	24 (4.0)	4 (0.7)	NA	9 (1.5)	0

*A total of 200 samples were tested from each location. EBOV, Ebola virus; GP, glycoprotein. NA, not applicable; ND, not done; NP, nucleoprotein.

regions and populations in Africa were generally thought to be the result of cross-reactivity from the use of assays with low specificity (*11*). However, serologic testing tremendously improved with highly specific and sensitive assays (*12*). Thus, the assumption of false positives as an explanation for the results seems unlikely. The conservation in the NP and GP used as antigens in this study was 67%–75% for NP and 54%–65% for GP among *Ebolavirus* species but does not exclude cross-reactivity among species according to the manufacturer information. In general, GP antibodies are considered more specific due to lower conservation of this protein among ebolavirus species. In our study, the EBOV GP ELISA screening test produced high reactivity at a 1:100 dilution, which probably does not reflect real EBOV seroprevalence as reported from other western and central Africa countries (*13*,*14*). The antigen used in the anti-EBOV GP assay is produced in insect cells; populations may have developed antibodies to insect cell proteins due to exposure through insect consumption (*15*). The NP antigen is produced in *Escherichia coli* bacteria and likely has less protein contaminants than the GP preparation because of more sophisticated antigen purification. However, this concept is speculative; we did not test serum samples in the anti-EBOV NP assay at a 1:100 dilution due to limited sample quantity.

Finally, caution may be necessary when interpreting serologic test results for EBOV and related filoviruses in populations in Africa. Because more reliable, highly specific and sensitive serologic tests are available, more attention should be given to establish proper algorithms for interpretation. Confirmation by independent tests including virus neutralization assays will help. Unfortunately, serum sample volumes in this study were too low to enable such confirmatory testing.

Conclusions

Given the limitations of our study and a conservative approach for interpretation, our results indicate that the population in southern Mali has been and likely still is exposed to EBOV, other *Ebolavirus* species, or related filoviruses at a seroprevalence of 1.5%–6.1%, which is in the range described previously in west and central African countries (*13*,*14*). Additional work is needed to support this finding, including human surveillance in other regions of Mali. Public health preparedness in Mali should include filoviruses. Initial ecologic studies aiming at identifying potential reservoir species of filoviruses seem justified for southern Mali.

Acknowledgments

We thank Rose Perry for assistance with the graphical work. We thank the US National Institute of Allergy and Infectious Disease International Center for Excellence in Research in Mali for their support of field and laboratory work. Research on samples from human subjects was conducted in accordance with the policies and regulations of the NIH and adhered to the principles of the Belmont Report (1979).

This work was funded by the Mali International Center for Excellence in Research, Division of Intramural Research, National Institute of Allergy and Infectious Disease, National Institutes of Health, United States.

About the Author

Dr. Bane is a PhD candidate at the Faculty of Medicine, University of Sciences, Techniques, and Technologies of Bamako, Mali. His research interests are hemorrhagic fever viruses with focus on Ebola virus and Lassa virus.

References

1. Boisen ML, Hartnett JN, Goba A, Vandi MA, Grant DS, Schieffelin JS, et al. Epidemiology and management of the 2013–16 West African Ebola outbreak. Annu Rev Virol. 2016;3:147–71. https://doi.org/10.1146/annurev-virology-110615-040056
2. Diarra B, Safronetz D, Sarro YD, Kone A, Sanogo M, Tounkara S, et al. Laboratory response to 2014 Ebola virus outbreak in Mali. J Infect Dis. 2016;214(suppl 3):S164–8. https://doi.org/10.1093/infdis/jiw200
3. Safronetz D, Sacko M, Sogoba N, Rosenke K, Martellaro C, Traoré S, et al. Vectorborne infections, Mali. Emerg Infect Dis. 2016;22:340–2. https://doi.org/10.3201/eid2202.150688
4. O'Hearn AE, Voorhees MA, Fetterer DP, Wauquier N, Coomber MR, Bangura J, et al. Serosurveillance of viral pathogens circulating in West Africa. Virol J. 2016;13:163. https://doi.org/10.1186/s12985-016-0621-4

5. Pigott DM, Golding N, Mylne A, Huang Z, Henry AJ, Weiss DJ, et al. Mapping the zoonotic niche of Ebola virus disease in Africa. eLife. 2014;3:e04395. https://doi.org/10.7554/eLife.04395
6. Sogoba N, Rosenke K, Adjemian J, Diawara SI, Maiga O, Keita M, et al. Lassa virus seroprevalence in Sibirilia commune, Bougouni district, southern Mali. Emerg Infect Dis. 2016;22:657–63. https://doi.org/10.3201/eid2204.151814
7. Goldstein T, Anthony SJ, Gbakima A, Bird BH, Bangura J, Tremeau-Bravard A, et al. The discovery of Bombali virus adds further support for bats as hosts of ebolaviruses. Nat Microbiol. 2018;3:1084–9. https://doi.org/10.1038/s41564-018-0227-2
8. Karan LS, Makenov MT, Korneev MG, Sacko N, Boumbaly S, Yakovlev SA, et al. Bombali virus in *Mops condylurus* bats, Guinea. Emerg Infect Dis. 2019;25:1774–5. https://doi.org/10.3201/eid2509.190581
9. Fischer K, Jabaty J, Suluku R, Strecker T, Groseth A, Fehling SK, et al. Serological evidence for the circulation of ebolaviruses in pigs from Sierra Leone. J Infect Dis. 2018;218(suppl_5):S305–11. https://doi.org/10.1093/infdis/jiy330
10. Fischer K, Camara A, Troupin C, Fehling SK, Strecker T, Groschup MH, et al. Serological evidence of exposure to ebolaviruses in domestic pigs from Guinea. Transbound Emerg Dis. 2020;67:724–32. https://doi.org/10.1111/tbed.13391
11. Formella M, Gatherer D. The serology of Ebolavirus—a wider geographical range, a wider genus of viruses or a wider range of virulence? J Gen Virol. 2016;97:3120–30. https://doi.org/10.1099/jgv.0.000638
12. Shorten RJ, Brown CS, Jacobs M, Rattenbury S, Simpson AJ, Mepham S. Diagnostics in Ebola virus disease in resource-rich and resource-limited settings. PLoS Negl Trop Dis. 2016;10:e0004948. https://doi.org/10.1371/journal.pntd.0004948
13. Bower H, Glynn JR. A systematic review and meta-analysis of seroprevalence surveys of ebolavirus infection. Sci Data. 2017;4:160133. https://doi.org/10.1038/sdata.2016.133
14. Schoepp RJ, Rossi CA, Khan SH, Goba A, Fair JN. Undiagnosed acute viral febrile illnesses, Sierra Leone. Emerg Infect Dis. 2014;20:1176–82. https://doi.org/10.3201/eid2007.131265
15. Raheem D, Carrascosa C, Oluwole OB, Nieuwland M, Saraiva A, Millán R, et al. Traditional consumption of and rearing edible insects in Africa, Asia and Europe. Crit Rev Food Sci Nutr. 2019;59:2169–88. https://doi.org/10.1080/10408398.2018.1440191

Address for correspondence: Heinz Feldmann, Rocky Mountain Laboratories, 903 S 4th St, Hamilton, MT 59840, USA; email: feldmannh@niaid.nih.gov

Trends in Viral Respiratory Infections During COVID-19 Pandemic, South Korea

Sujin Yum, Kwan Hong, Sangho Sohn, Jeehyun Kim, Byung Chul Chun

We compared weekly positivity rates of 8 respiratory viruses in South Korea during 2010–2019 and 2020. The overall mean positivity rate for these viruses decreased from 54.7% in 2010–2019 to 39.1% in 2020. Pandemic control measures might have reduced the incidence of many, but not all, viral respiratory infections.

The government of South Korea has implemented various measures to respond to the coronavirus disease (COVID-19) pandemic since January 20, 2020, when a case was officially reported in South Korea (*1*). Such interventions can affect the incidence of not only COVID-19 but also other respiratory viruses that are preventable with hygiene practices and social distancing (*2*–*5*). For example, in South Korea the 2019–20 influenza season ended 12 weeks earlier than in 2018–19, possibly because of the adoption of personal hygiene measures and restrictions on international travel (*3*–*5*). However, many viruses can cause acute respiratory infections; it is unknown whether other viruses also might have altered incidence or test positivity rates during the COVID-19 pandemic. We examined how the weekly positivity rates for 8 major respiratory viruses differed during the 2020 COVID-19 pandemic in South Korea compared with rates for 2010–2019.

The Study

We analyzed surveillance data from the Korea Influenza and Respiratory Viruses Surveillance System (KINRESS) established by the Korea Disease Control and Prevention Agency (Cheongju-si, South Korea). This surveillance system documents PCR results for throat and nasal swab samples from outpatients of all ages with symptoms of acute respiratory infections at 52 sentinel medical institutions throughout the country. Samples were identified at 17 regional institutes for environmental health by real-time reverse transcription PCR for 8 viruses: adenovirus, human bocavirus (HBoV), human coronavirus (HCoV), human metapneumovirus (hMPV), human rhinovirus (HRV), influenza virus, human parainfluenza virus (HPIV), and respiratory syncytial virus (RSV) (*6*). We analyzed the weekly positivity rates of all viruses except hMPV during 2010–2019; we analyzed hMPV infections during 2012–2019 because surveillance for this disease began in 2012. We did not consider the changes in testing numerators and denominators because those raw data were not available for 2014–2017. We compared the weekly positivity rates for 2020 with those of weeks 5–52 during 2010–2019 by using a paired *t*-test. We excluded the first 4 weeks of each year to reflect the timing of the identification of COVID-19 in Korea. We reviewed the weekly positivity rates to detect any patterns already existing in the previous 10 years. KINRESS does not include data on severe acute respiratory syndrome coronavirus 2, the causative agent of COVID-19; if a physician sees a patient with suspected COVID-19, he or she refers the patient to designated COVID-19 facilities. We conducted all statistical analyses using SPSS Statistics 24.0 (SPSS Inc., http://www.spss.com).

The overall mean weekly positivity rate for all 8 viruses significantly decreased from 54.7% (SD ±8.3%) during 2010–2019 to 39.1% (SD ±15.3%) in 2020 ($p<0.01$) (Table). The decrease was largest for influenza virus (−9.3%, 95% CI −12.7% to −5.8%), HPIV (−6.1%, 95% CI −7.5% to −4.7%), and RSV (−2.9%, 95% CI −4.4% to −1.4%). However, the positivity rate for HRV increased by 6.6% (95% CI 2.7%–10.4%) and that of HBoV increased by 1.8% (95% CI 0.2%–3.5%) in 2020. The positivity rates for adenoviruses were not significantly different.

In 2020, the total positivity rate for all 8 viruses decreased sharply after week 5, when COVID-19

Author affiliation: Korea University, Seoul, South Korea

DOI: https://doi.org/10.3201/eid2706.210135

Table. Mean weekly positivity rates of respiratory viruses during weeks 5–52, South Korea, 2010–2019 compared with 2020

Virus	Mean positivity (±SD), %		Difference, % (95% CI)
	2010–2019	2020	
All studied viruses	54.7 (±8.3)	39.1 (±15.3)	−15.6 (−21.0 to −10.2)
Adenovirus	7.4 (±2.1)	6.5 (±3.2)	−0.9 (−2.1 to 0.3)
Human bocavirus	2.3 (±2.3)	4.1 (±4.5)	1.8 (0.2 to 3.5)
Human coronavirus	3.4 (±2.4)	1.2 (±2.8)	−2.2 (−3.1 to −1.3)
Human metapneumovirus*	3.1 (±3.4)	0.6 (±1.4)	−2.5 (−3.5 to −1.4)
Human rhinovirus	17.4 (±4.9)	23.9 (±15.0)	6.6 (2.7 to 10.4)
Influenza virus	11.0 (±13.4)	1.7 (±6.7)	−9.3 (−12.7 to −5.8)
Human parainfluenza virus	6.2 (±4.7)	0.1 (±0.3)	−6.1 (−7.5 to −4.7)
Respiratory syncytial virus	3.8 (±4.4)	0.9 (±1.9)	−2.9 (−4.4 to −1.4)

*Surveillance began in 2012.

emerged in South Korea and the government introduced nonpharmaceutical interventions (Figure). The positivity rates of HCoV, hMPV, and influenza virus abruptly decreased after week 5, reaching nearly 0 by the end of 2020. Until mid-2020, the positivity rates of RSV remained unchanged from those of the past 10 years; however, in 2020 the usual late autumn–winter outbreak of RSV did not occur. In contrast, the weekly positivity rate of HBoV increased significantly after the 40th week of 2020 compared with rates for previous years, causing a significantly higher overall HBoV positivity rate in 2020. We did not observe substantial changes in epidemic patterns of AdV and HRV in 2020, although the average positivity rate of HRV was significantly higher than in the previous 10 years.

HRV and adenovirus do not have distinct seasonal trends in South Korea. KINRESS does not include data on the exact serotypes of rhinoviruses

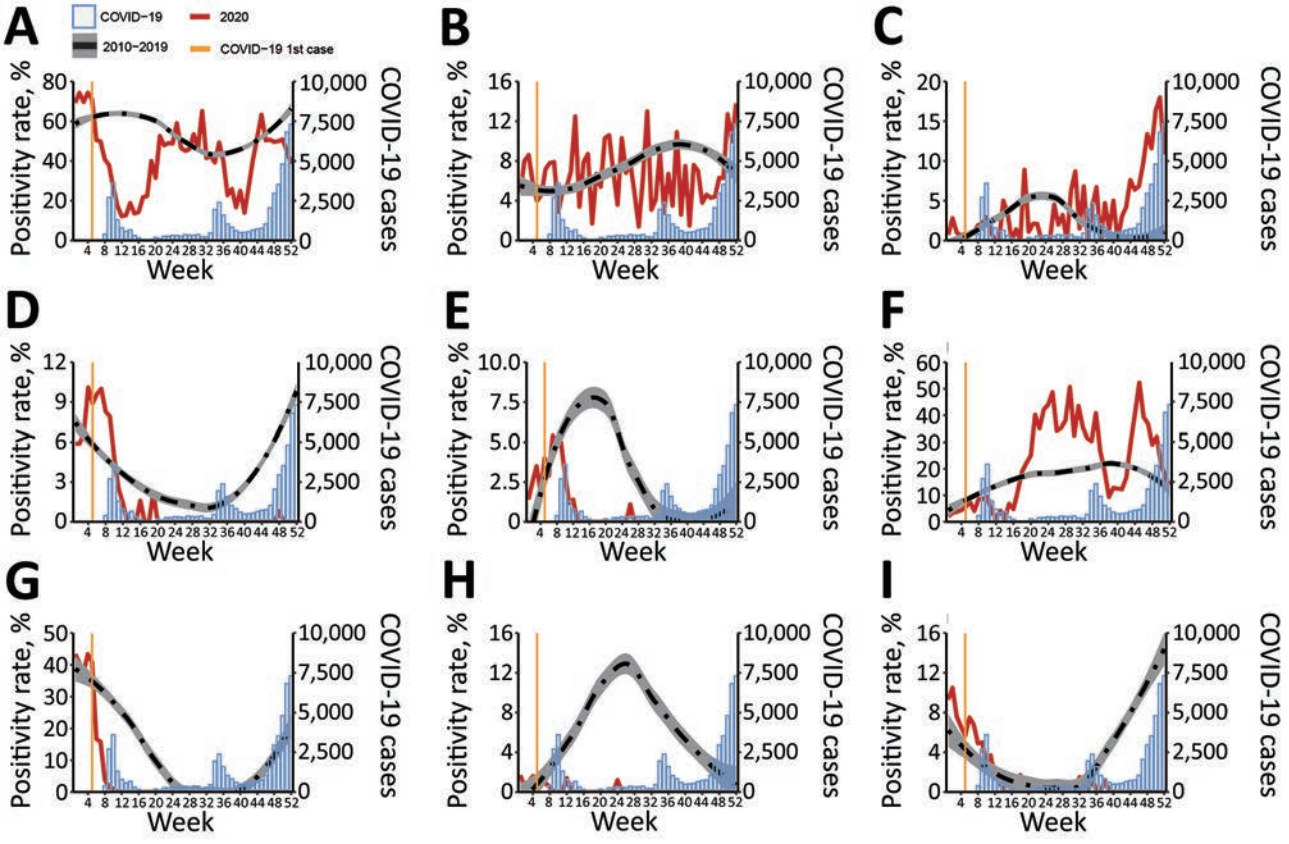

Figure. Mean weekly positivity rates for 8 respiratory viruses, South Korea, 2010–2019 compared with 2020. Vertical yellow line indicates the week of the first COVID-19 case in South Korea (i.e., the 5th week of 2020). Red line indicates weekly viral positivity rate in 2020. Blue bars show reported COVID-19 cases (Korean Ministry of Health and Welfare, http://ncov.mohw.go.kr/en). Dashed line indicates mean weekly positivity rates during 2010–2019 (data smoothed using the Loess method); gray shading indicates 95% CI. A) Total. B) Adenovirus. C) Human bocavirus. D) Human coronavirus. E) Human metapneumovirus. F) Human rhinovirus. G) Influenza virus. H) Human parainfluenza virus. I) Respiratory syncytial virus. COVID-19, coronavirus disease.

and enteroviruses. The other 6 viruses have distinct seasonalities; the timing of the peak is slightly different for each virus and changes slightly each year (*7*). HCoV, influenza virus, and RSV show peak activity in the winter (i.e., December–February); meanwhile, HBoV, hMPV, and HPIV usually show peak activity in the spring to early summer (i.e., March–June) in South Korea (Figure) (*8*). Our results suggest that the positivity rates for seasonal respiratory viruses have significantly decreased in 2020. The exception to this pattern is HBoV, which was highly prevalent in late autumn and winter of 2020, when the third surge of COVID-19 started in South Korea (Figure). The positivity rate of HBoV increased when social distancing measures were strengthened by the government. The average positivity rate of HBoV during weeks 47–52 was 13.3% (SD ±3.3%) in 2020, compared with 0.7% (SD ±0.2%) during the same period in the past 10 years. HBoV is common among children 6–24 months of age in South Korea; this infection requires treatment with oxygen and systemic steroids more frequently than other viral lower respiratory infections in children (*8*).

Conclusions

We found that acute respiratory infections caused by seasonal viruses (except HBoV) had significantly lower positivity rates during the COVID-19 pandemic in South Korea. These overall results agree with other studies on respiratory viruses (*3*–*5*). The positivity rate of HBoV increased in November–December 2020 in proportion to the number of COVID-19 cases. The changes in the positivity rates of HRV and adenovirus, which are not seasonal, showed different patterns; positivity rates of adenovirus did not change and those of HRV significantly increased. Some studies have shown that the detection of HRV has a negative association with influenza A virus and a positive association with adenovirus, HPIV, and RSV (*9*,*10*). Little is known about the interaction of HBoV or severe acute respiratory syndrome coronavirus 2 with other respiratory viruses. Further research on the delayed outbreak of HBoV during the COVID-19 pandemic is needed.

One limitation of this study is that the changes in positivity rates do not necessarily indicate changes in incidence. The number of specimens collected during weeks 5–52 decreased to 4,576 in 2020 from 11,083 in 2019 and 10,734 in 2018. During 2014–2017, KINRESS reported only weekly positivity rates, not raw data on the numbers of specimens. It is possible that in 2020, patients with acute respiratory symptoms might have visited COVID-19 screening centers rather than other facilities. Also, most of the viruses we studied comprise multiple types and species, including many with different circulation patterns. During the study period, case detection and laboratory methods did not change for healthcare centers affiliated with KINRESS.

In conclusion, nonpharmaceutical interventions such as social distancing might have altered trends in seasonal outbreaks of respiratory viruses during the COVID-19 pandemic in South Korea. The effects of these interventions vary for each virus. These results show that respiratory viral activities should be monitored continuously during the pandemic.

This work was supported by the Research Program funded by the Korean Disease Control and Prevention Agency (grant no. 2020-ER5313-00).

About the Author

Dr. Yum is a researcher at Computational Epidemiology Laboratory for Infectious Disease at the Korea University College of Medicine, Seoul, South Korea. Her primary research interests include infectious disease, zoonosis, and spatial epidemiology.

References

1. Ryu S, Chun BC; Korean Society of Epidemiology 2019-nCoV Task Force Team. An interim review of the epidemiological characteristics of 2019 novel coronavirus. Epidemiol Health. 2020;42:e2020006. https://doi.org/10.4178/epih.e2020006
2. Boyce JM, Pittet D; Healthcare Infection Control Practices Advisory Committee; Society for Healthcare Epidemiology of America; Association for Professionals in Infection Control; Infectious Diseases Society of America; Hand Hygiene Task Force. Guideline for hand hygiene in health-care settings: recommendations of the Healthcare Infection Control Practices Advisory Committee and the HICPAC/SHEA/APIC/IDSA Hand Hygiene Task Force. Infect Control Hosp Epidemiol. 2002;23:S3–40. https://doi.org/10.1086/503164
3. Baek S, Lee J, Park K, Lee E, Park S, Lee S, et al. Results of the National Infectious Disease Surveillance, from January to April 2020 [in Korean]. Korean Disease Control and Prevention Agency. 2020 May 5 [cited 2021 Jan 11]. https://www.cdc.go.kr/board/board.es?mid=a20602010000&bid=0034&act=view&list_no=367286
4. Lee H, Lee H, Song K.-H., Kim ES, Park JS, Jung J, et al. Impact of public health interventions on seasonal influenza activity during the SARS-CoV-2 outbreak in Korea. Clin Infect Dis. 2020 May 30 [Epub ahead of print]. https://doi.org/10.1093/cid/ciaa672
5. Hsieh CC, Lin CH, Wang WYC, Pauleen DJ, Chen JV. The outcome and implications of public precautionary measures in Taiwan—declining respiratory disease cases in the COVID-19 pandemic. Int J Environ Res Public Health. 2020;17:4877. https://doi.org/10.3390/ijerph17134877
6. Korea Disease Control and Prevention Agency. Laboratory surveillance service for influenza and respiratory viruses

[in Korean]. 2021 [cited 2021 Jan 10]. http://www.kdca.go.kr/contents.es?mid=a20301090503
7. Moriyama M, Hugentobler WJ, Iwasaki A. Seasonality of respiratory viral infections. Annu Rev Virol. 2020;7:83–101. https://doi.org/10.1146/annurev-virology-012420-022445
8. Kwak KJ, Kim YH, Choi HJ. Clinical characteristics of respiratory viral infection in children during spring/summer: focus on human bocavirus. Allergy Asthma & Respiratory Disease. 2015;3:410–6. https://doi.org/10.4168/aard.2015.3.6.410
9. Tanner H, Boxall E, Osman H. Respiratory viral infections during the 2009–2010 winter season in Central England, UK: incidence and patterns of multiple virus co-infections. Eur J Clin Microbiol Infect Dis. 2012;31:3001–6. https://doi.org/10.1007/s10096-012-1653-3
10. Wu A, Mihaylova VT, Landry ML, Foxman EF. Interference between rhinovirus and influenza A virus: a clinical data analysis and experimental infection study. Lancet Microbe. 2020;1:e254–62. https://doi.org/10.1016/S2666-5247(20)30114-2

Address for correspondence: Byung Chul Chun, Department of Preventive Medicine, Korea University College of Medicine, 73 Goryeodae-ro, Seongbuk-gu, Seoul 02841, South Korea; email: chun@korea.ac.kr

Serotype-Switch Variant of Multidrug-Resistant *Streptococcus pneumoniae* Sequence Type 271

Erin M. Scherer,[1] Bernard Beall, Benjamin Metcalf

We discovered 3 invasive, multidrug-resistant *Streptococcus pneumoniae* isolates of vaccine-refractory capsular serotype 3 that recently arose within the successful sequence type 271 complex through a serotype switch recombination event. Mapping genomic recombination sites within the serotype 3/sequence type 271 progeny revealed a 55.9-kb donated fragment that encompassed *cps3*, *pbp1a*, and additional virulence factors.

Streptococcus pneumoniae (pneumococcus) clonal complex (CC) 271 consists of broadly distributed, antimicrobial drug–resistant pneumococcal strains of serotypes 19F and 19A, first recorded in serotype 19F strains from 1992 (https://pubmlst.org). Two successful multivalent pneumococcal conjugate vaccines (PCV) targeting common invasive pneumococcal disease (IPD) serotypes (*1*,*2*) were introduced in the United States in 2000 (PCV7, targeting serotypes 4, 6B, 9V, 14, 18C, 19F, and 23F) and 2010 (PCV13, targeting PCV7 serotypes plus 1, 3, 5, 6A, 7F, and 19A). Serotype 19A CC271, likely arising through serotype switch with serotype 19F, emerged as the most common cause of IPD in the United States after introduction of PCV7 (*3*). After introduction of PCV13, IPD caused by serogroup 19 CC271 greatly decreased (*2*,*4*).

Three serotype 3 sequence type (ST) 271 pneumococcal isolates from adult invasive pneumonia cases in Connecticut and Maryland, USA, were recovered through the Centers for Disease Control and Prevention Active Bacterial Core surveillance (ABCs) in 2016 (isolate 20155315-S-ABC), 2017 (isolate 20170822-S-ABC), and 2018 (isolate 20182806-S-ABC). These isolates have a common origin; they differ by 6–29 single nucleotide polymorphisms (SNPs) and share identical serotype 3 capsular polysaccharide biosynthetic operons (*cps3*) and penicillin-binding protein (PBP) sequence types (1a-17/2b-16/2x-47). Isolates 20155315-S-ABC and 20170822-S-ABC differed by 6 SNPs and were recovered 16 months apart during 2016–2017 from the same person. These 3 pneumococcal isolates represent a novel recombinant serotype 3 variant of the globally distributed, antimicrobial drug–resistant lineage ST271.

The polysaccharide capsule, of which there are >90 structurally and serologically unique types, is the primary pneumococcal virulence factor (*5*). Serotype 3 is historically associated with higher virulence than other serotypes and currently causes the largest proportion of IPD cases in the United States (>12% of all cases) (*4*). Although serotype 3 is included in PCV13, PCV13 provides poor protection against serotype 3 because of unique qualities of the serotype 3 capsule (*6*,*7*). In keeping with the ST271 heritage, the 3 serotype 3/ST271 isolates share the same antimicrobial-resistance mechanisms, including reduced affinities for β-lactams (mosaic PBPs), dual mechanisms for macrolide resistance (ErmB rRNA methylase and MefA/MsrD macrolide efflux system), clindamycin resistance (ErmB), cotrimoxazole resistance (altered FolA and FolP enzymes), and tetracycline resistance (TetM-mediated ribosome alteration) (Appendix 1, https://wwwnc.cdc.gov/EID/article/27/6/20-3629-App1.xlsx).

To reveal genomic regions within the 3 serotype 3/ST271 progeny resulting from recombination, we first identified likely recipient and donor strains involved in the serotype switch event (Appendix 2, https://wwwnc.cdc.gov/EID/article/27/6/20-3629-App2.pdf). Phylogenetic analysis using publicly available genome sequences revealed single contig ST271 genomes that shared highest relatedness with 3/ST271. Strain A026 (19F/ST271) recovered in China during 2006–2008 was the most highly related putative genetic recipient (Figure, panel A). Two 19F/271

Author affiliation: Centers for Disease Control and Prevention, Atlanta, Georgia, USA

DOI: https://doi.org/10.3201/eid2706.203629

[1]Current affiliation: Emory University, Atlanta, Georgia, USA.

invasive ABCs isolates recovered from infants (6299-05 in Tennessee in 2004 and 2012214924 in California in 2012) had the closest matching PBP type to serotype-switch 3/ST271 isolates, sharing 2 of 3 PBP sequences (PBP2B-16 and PBP2x-47) (Appendix 1). Both ABCs 19F/ST271 isolate genomes shared more relatedness with 3/ST271 than publicly available 19F/271 genomes (Figure, panel A). By using BLAST (https://blast.ncbi.nlm.nih.gov/Blast.cgi) and whole-genome shotgun database (Appendix 2), we identified the likely *cps3* donors (3/ST700 strains B20605 and 73D368810). B20605 and 73D368810 shared sequence identity to the 9522 bp region (*dexB* to *pgm*) encompassing the ≈5,000-bp *cps3* operon of the 3/ST271 isolates. In contrast to serotype 3 strains in the United States that are typically basally

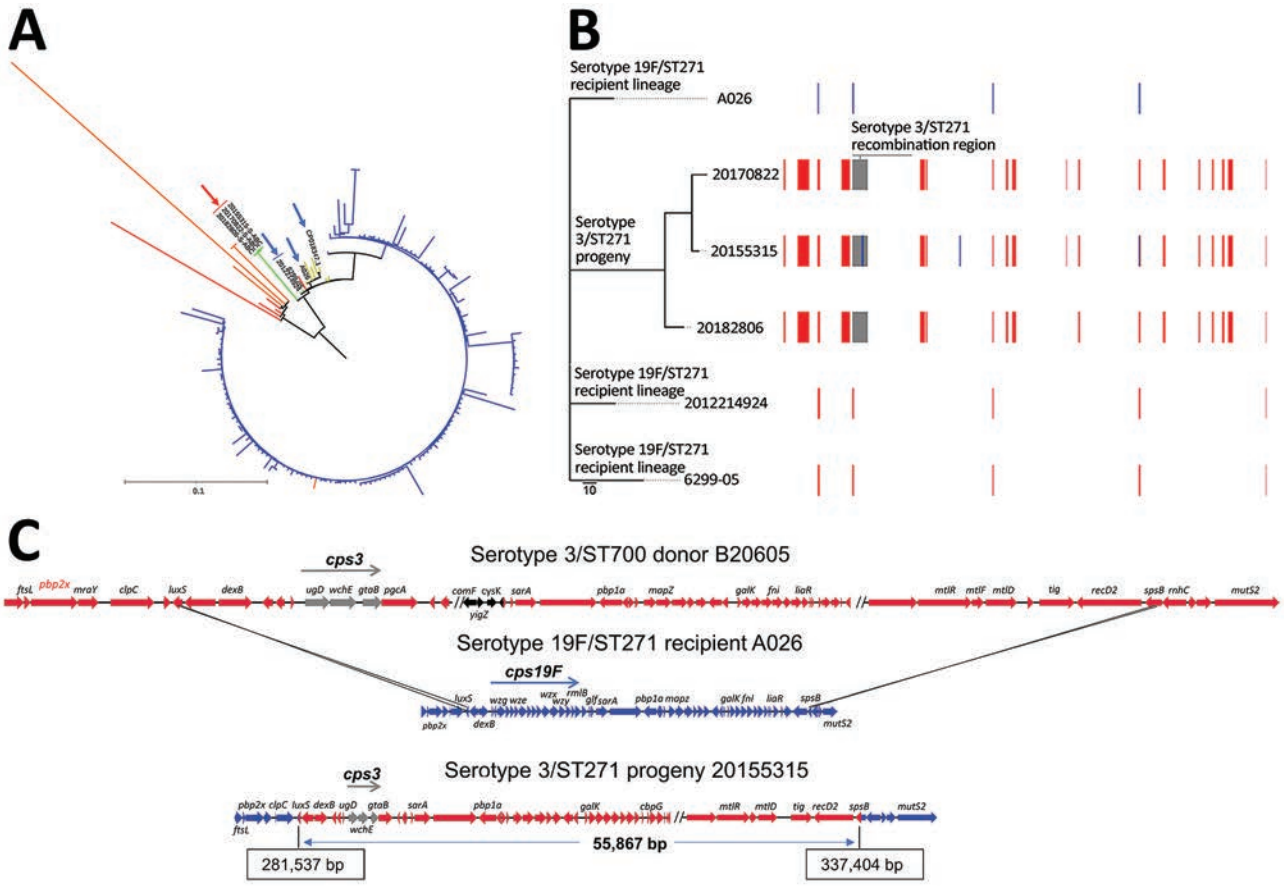

Figure. *Streptococcus pneumoniae* serotype 3/ST271 lineage resulting from a recombination event between a 19F/ST271 recipient and 3/ST700 donor. A) Phylogenetic tree showing progeny serotype 3/ST271 isolates 20155315-S-ABC, 20170822-S-ABC, and 20182806-S-ABC (red arrow) most closely related to the putative recipient 19F/ST271 isolates 6299-05 and 2012214924 (blue arrows). The most closely related ST271 single contig reference is A026 (also indicated with blue arrow). Branch colors: yellow, additional 19F/ST271 Active Bacterial Core surveillance (ABCs) isolates and single contig references; red, single-locus variant single contig references or ABCs isolates; orange, double-locus variant single contig reference or ABCs isolates; blue, ST320 ABCs isolates. Zero-, single-, and double-locus variant, single contig references were identified by using the PubMLST database (https://pubmlst.org). Scale bar corresponds to 1,062 single nucleotide polymorphisms. B) Phylogenetic alignment of the 3 recombinant serotype 3/ST271 isolates and closest known genomic matches of the ST271 recipient lineage and a schematic of recombinant genome fragments, represented by rectangular blocks, that were predicted by Gubbins (*10*). Block locations and sizes are relative to the aligned genomes; red blocks represent sites in common between ≥2 isolates (1 site, <150 bp in length, was not counted among the 17 total shown), blue blocks sites unique to a given isolate, and gray blocks the serotype-switch fragment that replaced the corresponding *cps19F* region within the recipient 19F/ST271 strain. The *cps3* locus was not identified using Gubbins because of its complete divergence from *cps19F* and instead was identified using ProgressiveMauve (*12*) within the encompassed 55.9 kb fragment (panel C). Gray block contains *cps3*, *pbp1a* (PBP1A-17), trigger factor, and choline binding protein G genes. C) Schematic illustrating ancestral recombination event between the 3/ST700 donor (B20605) and 19F/ST271 recipient (A026) to yield the 3/ST271 progeny (20155315-S-ABC). Deduced crossover points, including coordinates in the progeny, are shown. *luxS* and *spsB* genes are shown as blue/red hybrids. The minimum genes of the *cps3* operon required for polysaccharide capsuale biosynthesire shown in gray (*ugd, wchE, gtaB*). Genes with arrows in black differ between B20605 and 73D36881 and are absent in the 3/ST271 isolates. ST, sequence type.

susceptible to antimicrobial drugs (*4*), the likely serotype 3/ST700 donor strain was predicted to have intermediate penicillin resistance attributable to the mosaic *pbp1a* gene (PBP1A-17), which was co-transferred with the donor *cps3* locus to the 19F/ST271 recipient (Appendix 1). Serotype 3/ST700 isolates are documented in several countries in Africa but not in the United States (https://pubmlst.org/spneumoniae).

To identify recombination sites, we mapped sequencing reads from the 3 3/ST271 isolates, 6299-05 (19F/ST271), and 2012214924 (19F/ST271) to A026 (19F/ST271) and then aligned the 6 genomes as described (*8*,*9*) (Appendix 2). The aligned 19F/ST271 and 3/ST271 genome sequences were input into Gubbins (*10*) (Appendix 2), which identified 17 recombinational fragments within 3/ST271 (median size 6,629 bp [range 363–59,159 bp]) (Figure, panel B). BEDTools (*9*) was applied to extract DNA sequences from recombinational fragments, and Prokka (*11*) was used to annotate sequences. Progressive Mauve (*12*) revealed the *cps3* operon in the 3 serotype 3/ST271 isolates on a 55.9-kb fragment that apparently originated from the serotype 3/ST700 donor (Figure, panel C). This region included the *cps3* operon, *pbp1a*, and 2 additional virulence factor genes (trigger factor [*tig*] and choline binding protein G [*cbpG*]). The corresponding region in 3/ST700 isolate B20605 contains genes that differ from serotype 3/ST700 isolate 73D36881 and are absent in the 3/ST271 isolates (Figure, panel C). This difference indicates that additional gene insertions occurred within this potential recombination hotspot in B20605 and 73D36881 and that this region subsequently might have been lost in the serotype 3/ST271 progeny.

When we compared the genes encoded in the serotype-switch region of the recipient with the corresponding region from the progeny and donor, we found they encoded near-identical virulence factors as identified by using the Virulence Factors Database (http://www.mgc.ac.cn/VFs/main.htm). The *tig* and *cbpG* genes have roles in pathogenesis and are cell wall surface–localized, highly conserved among *S. pneumoniae*, and immunogenic (*13*–*15*). Capsular polysaccharides provide the basis of approved *S. pneumoniae* vaccines. The limited efficacy of the serotype 3 component of PCV13 is probably attributable to high-level expression (thickness) of the serotype 3 capsule and its shedding by the bacteria (*6*,*7*). At the nucleotide level, $tig_{20155315\text{-}S\text{-}ABC}$ and tig_{A026} share 99.1% identity (11 SNPs apart); $cbpG_{20155315\text{-}S\text{-}ABC}$ and $cbpG_{A026}$ share 51.0% identity, and *cps3* and *cps19F* operons are highly divergent (*5*). Moreover, the *pbp1a* gene within the 55.9-kb genomic fragment is identical between the 3 3/ST271 isolates and donor 3/ST700 strains and exhibits only 81.7% identity with the putative recipient 19F/ST271 strains. Recombination introduced a distinct virulence factor (replacement of the serotype 19F capsule with a structurally and serologically unique serotype 3 capsule) and introduced diversity in the surface protein virulence factors expressed in the serotype 19F/ST271 lineage.

To understand the effects of recombination, a comparison of fitness and virulence of progeny and parental strains in mouse models might be valuable. Our study highlights the existence of the 3/ST271 strain, because currently no vaccine is available and few antimicrobial drugs are predicted to optimally target this strain should it gain traction. Asymptomatic nasopharyngeal carriage serves as the major reservoir of highly common noninvasive infections and precedes invasive infections. Three nearly isogenic invasive isolates of this clone appearing over an expanse of 3 years in 2 different states is a concerning sign of a successful foothold within the carriage reservoir. All 3 cases were caused by bacteremic pneumonia in middle-aged patients. Of particular interest is the isolation of this strain 16 months apart from blood specimens from the same person (isolates 20155315 and 20170822), which is a rare occurrence and suggests a failure to eradicate the organism and long-term carriage or potentially the reacquisition of the strain from persons in the community. The recovery of still another invasive isolate of this same clone in 2018 further suggests a level of fitness required for long-term survival in the carriage reservoir and potential to cause IPD. Further, after the review process of this manuscript, ABCs has reported recovery of 2 additional closely related 3/ST271 case isolates during 2019 from Minnesota (B. Beall, unpub. data, 2020). This new strain complex has unique features potentially guiding its success, including high antimicrobial resistance, a capsule ineffectively targeted by PCV13, and undefined parameters inherent to the predominant invasive lineage of the post-PCV7 era. These observations emphasize the clear need for a pneumococcal vaccine that effectively targets serotype 3.

Acknowledgments

We thank Zhongya Li, Hollis Walker, Theresa Tran, Sopio Chochua, and Lesley McGee for whole-genome sequencing. We also acknowledge the entire ABCs program for recovery of these novel invasive isolates.

About the Author

Dr. Scherer is an assistant professor in the Division of Infectious Diseases, Department of Medicine, School of Medicine, Emory University, Atlanta, Georgia, USA. Her research interests include understanding what immune responses generate durable immunity against infectious diseases, with a focus on antibody and B cell responses to viral and bacterial pathogens and their vaccines.

References

1. Pilishvili T, Lexau C, Farley MM, Hadler J, Harrison LH, Bennett NM, et al.; Active Bacterial Core Surveillance/ Emerging Infections Program Network. Sustained reductions in invasive pneumococcal disease in the era of conjugate vaccine. J Infect Dis. 2010;201:32–41. https://doi.org/10.1086/648593
2. Moore MR, Link-Gelles R, Schaffner W, Lynfield R, Lexau C, Bennett NM, et al. Effect of use of 13-valent pneumococcal conjugate vaccine in children on invasive pneumococcal disease in children and adults in the USA: analysis of multisite, population-based surveillance. Lancet Infect Dis. 2015;15:301–9. https://doi.org/10.1016/S1473-3099(14)71081-3
3. Beall BW, Gertz RE, Hulkower RL, Whitney CG, Moore MR, Brueggemann AB. Shifting genetic structure of invasive serotype 19A pneumococci in the United States. J Infect Dis. 2011;203:1360–8. https://doi.org/10.1093/infdis/jir052
4. Beall B, Chochua S, Gertz RE Jr, Li Y, Li Z, McGee L, et al. A population-based descriptive atlas of invasive pneumococcal strains recovered within the U.S. during 2015–2016. Front Microbiol. 2018;9:2670. https://doi.org/10.3389/fmicb.2018.02670
5. Bentley SD, Aanensen DM, Mavroidi A, Saunders D, Rabbinowitsch E, Collins M, et al. Genetic analysis of the capsular biosynthetic locus from all 90 pneumococcal serotypes. PLoS Genet. 2006;2:e31. https://doi.org/10.1371/journal.pgen.0020031
6. Poolman J, Kriz P, Feron C, Di-Paolo E, Henckaerts I, Miseur A, et al. Pneumococcal serotype 3 otitis media, limited effect of polysaccharide conjugate immunisation and strain characteristics. Vaccine. 2009;27:3213–22. https://doi.org/10.1016/j.vaccine.2009.03.017
7. Choi EH, Zhang F, Lu YJ, Malley R. Capsular polysaccharide (CPS) release by serotype 3 pneumococcal strains reduces the protective effect of anti-type 3 CPS antibodies. Clin Vaccine Immunol. 2015;23:162–7. https://doi.org/10.1128/CVI.00591-15
8. Langmead B, Salzberg SL. Fast gapped-read alignment with Bowtie 2. Nat Methods. 2012;9:357–9. https://doi.org/10.1038/nmeth.1923
9. Quinlan AR, Hall IM. BEDTools: a flexible suite of utilities for comparing genomic features. Bioinformatics. 2010;26:841–2. https://doi.org/10.1093/bioinformatics/btq033
10. Croucher NJ, Page AJ, Connor TR, Delaney AJ, Keane JA, Bentley SD, et al. Rapid phylogenetic analysis of large samples of recombinant bacterial whole genome sequences using Gubbins. Nucleic Acids Res. 2015;43:e15. https://doi.org/10.1093/nar/gku1196
11. Seemann T. Prokka: rapid prokaryotic genome annotation. Bioinformatics. 2014;30:2068–9. https://doi.org/10.1093/bioinformatics/btu153
12. Darling AE, Mau B, Perna NT. progressiveMauve: multiple genome alignment with gene gain, loss and rearrangement. PLoS One. 2010;5:e11147. https://doi.org/10.1371/journal.pone.0011147
13. Kilian M, Tettelin H. Identification of virulence-associated properties by comparative genome analysis of *Streptococcus pneumoniae*, *S. pseudopneumoniae*, *S. mitis*, three *S. oralis* subspecies, and *S. infantis*. MBio. 2019;10:e01985-19. https://doi.org/10.1128/mBio.01985-19
14. Mann B, Orihuela C, Antikainen J, Gao G, Sublett J, Korhonen TK, et al. Multifunctional role of choline binding protein G in pneumococcal pathogenesis. Infect Immun. 2006;74:821–9. https://doi.org/10.1128/IAI.74.2.821-829.2006
15. Cohen A, Troib S, Dotan S, Najmuldeen H, Yesilkaya H, Kushnir T, et al. *Streptococcus pneumoniae* cell wall-localized trigger factor elicits a protective immune response and contributes to bacterial adhesion to the host. Sci Rep. 2019;9:4295. https://doi.org/10.1038/s41598-019-40779-0

Address for correspondence: Bernard Beall, Centers for Disease Control and Prevention, 1600 Clifton Rd NE, Mailstop C02, Atlanta, GA 30329-4027, USA; email: bbeall@cdc.gov

Reemergence of Scabies Driven by Adolescents and Young Adults, Germany, 2009–2018

Felix Reichert, Maike Schulz, Elke Mertens, Raskit Lachmann, Anton Aebischer

To validate anecdotal evidence on scabies infestations, we analyzed inpatient and outpatient claims data in Germany. Scabies diagnoses increased 9-fold and treatment failure 4-fold during 2009–2018, driven mainly by persons 15–24 years of age. Prevention and control in young adults appear key because of these persons' high mobility and social connectivity.

Anecdotal evidence from clinicians in Germany suggests an increase in scabies; sales of scabicides by pharmacies in Germany have quadrupled during 2012–2017 (*1*,*2*). In addition, clinicians and scientists have raised concerns about resistance to standard treatment (*3*). In Germany, scabies is not reportable, and no recent national incidence estimates exist.

Scabies is diagnosed clinically, but confirmation through skin scrapings or dermatoscopy is not always performed in Germany (*1*). The national guideline recommends a single application of permethrin 5% cream for common scabies (*4*). Ivermectin, licensed in Germany in 2016, is recommended in cases of crusted scabies, immunosuppression, and contraindications for topical treatment (*4*). A second application is recommended after 7–15 days in outbreaks and patients with crusted scabies, immunosuppression, or persistent infestation. We investigated incidence of scabies in Germany for 2009–2018.

The Study

We analyzed claims data of outpatients insured by German statutory health insurance (SHI) funds, which applies to ≈90% of the population of Germany (*5*). Information on all ambulatory consultations and filled prescriptions of SHI-covered patients are gathered and stored up to 10 years for the SHI Physicians' Association by the Central Research Institute of Ambulatory Health Care.

We defined a case as any patient consultation during 2009–2018 marked with code B86, "scabies," from the International Classification of Diseases (ICD), 10th Revision. We counted patients with repeat consultations only once per year. We excluded cases with missing or implausible age or sex information. We extracted, aggregated, and analyzed time of diagnosis, age, sex, and area of residence. We calculated incidence as number of cases per 100,000 SHI members per year. We also analyzed prescribing data for allethrin, benzyl benzoate, crotamiton, ivermectin, lindane, and permethrin linked to cases. We assumed treatment failure and defined repeated prescriptions if a patient received prescriptions for 2 scabicides within a year ≥28 days apart, regardless of substance (*6*). Use of claims data is regulated by the Code of Social Law (Sozialgesetzbuch) in Germany; ethics approval and informed consent are not required.

In 2009, German SHI funds had 70,011,508 members, and scabies was diagnosed 42,585 times in physician practices, out-of-hours services, and hospital emergency departments in the ambulatory setting. In 2018, diagnoses were 382,043 for 72,802,098 members, a 9-fold increase in 9 years (Figure 1) and an overall incidence of 525/100,000 persons.

The highest incidence and a >11-fold increase during 2009–2018 were observed in persons 15–19 and 20–24 years of age (Figure 2). The increase in incidence was more pronounced in boys and men, especially for those 15–19 (23% lower incidence than girls and women in 2009 vs. 7% higher in 2018) and 20–24 years of age (5% lower incidence in 2009

Author affiliations: European Centre for Disease Prevention and Control, Stockholm, Sweden (F. Reichert); Robert Koch Institut, Berlin, Germany (F. Reichert, R. Lachmann, A. Aebischer); Central Research Institute of Ambulatory Health Care in Germany, Berlin, Germany (M. Schulz); Public Health Agency of Lower Saxony, Hanover, Germany (E. Mertens)

DOI: https://doi.org/10.3201/eid2706.203681

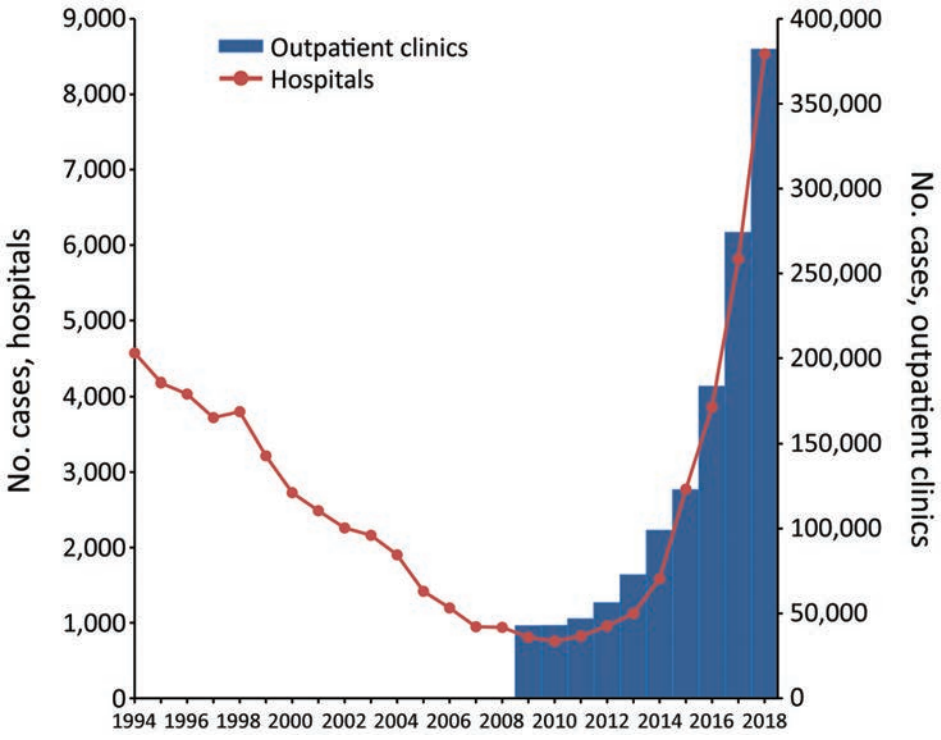

Figure 1. Scabies diagnoses in outpatient clinics among members of statutory health insurance funds and in hospitals, by year, Germany, 1994–2018. Scales for the *y*-axes differ substantially to underscore patterns but do not permit direct comparisons.

vs. 35% higher in 2018). Incidence showed regional differences in 2018; incidence was higher in northern and western federal states (Bremen, Hamburg, North Rhine-Westphalia, and Schleswig-Holstein) than in the other states (Appendix Figure, https://wwwnc.cdc.gov/EID/article/27/6/20-3681-App1.pdf). Reasons for these differences are unknown.

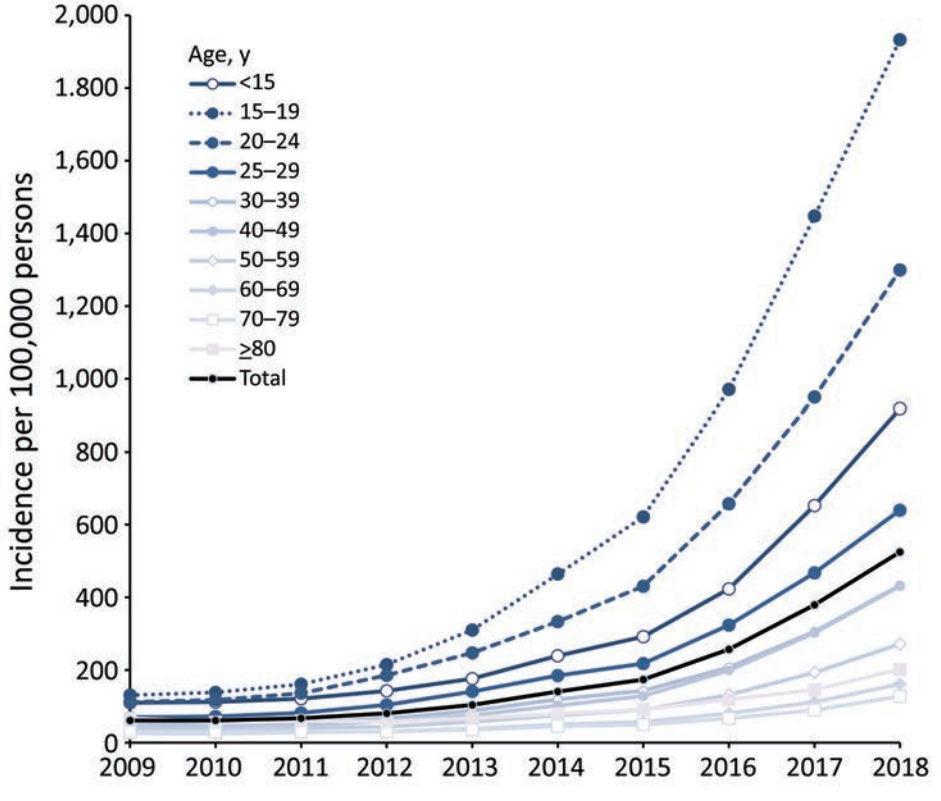

Figure 2. Incidence of scabies diagnoses in outpatient clinics per 100,000 members of statutory health insurance funds, by age group, Germany, 2009–2018.

Filled prescriptions for scabicides increased 14-fold during 2009–2018, from 57,482 to 815,952. Our review of preliminary data through mid-2020 suggests a continued increase. Permethrin was the most commonly used scabicide (90% of prescriptions in 2009; 71% in 2018). Since its licensing in 2016, ivermectin has become the second most prescribed scabicide (27% of prescriptions in 2018). Repeated prescriptions became more common over time (6% of all patients in 2009 vs. 23% in 2018); in 2018, the highest proportion of these was seen in patients 15–19 years of age (Table).

To extend the time period covered, we included diagnostic data from hospitals in Germany available starting in 1994 (most acute care hospitals; n = 1,942 in 2017) (*7*). We extracted the number of hospitalized patients with scabies by age group from publicly available databases (*7*) on the basis of code 133, "acariasis" (1994–1999), from ICD, 9th Revision, and code B86, "scabies" (2000–2018), from ICD, 10th Revision.

As with outpatients, scabies was increasingly diagnosed in inpatients beginning in 2010, indicating the value of these data as a proxy for the time period 1994–2009 (Figure 1). During the period 1994–2018, case numbers decreased for the first 16 years, but the proportion of cases in persons 15–24 years of age persistently increased, from 9% to 20% (Figure 1). The proportion of cases in persons <15 years of age decreased at the same time, from 59% to 46%.

Conclusions

This study, which analyzed claims data, shows a reemergence of scabies in Germany, with a shift in age distribution and an increase in treatment failure. After a decrease in scabies cases from the mid-1990s through 2008, scabies diagnoses increased 9-fold and scabicide prescriptions 14-fold during 2009–2018.

Two main observations may help explain this increase. First, persons 15–24 years of age have been particularly affected by the increase in recent years. In contrast, globally, prevalence is highest in young children, as it was in Germany in the mid-1990s (*8*). A recent report from Norway highlights that this age shift is observed internationally (*9*). Increased incidence was reported from Croatia (*10*), and diagnostic data in the Netherlands since 2012 have shown an incidence increase, including outbreaks not only in care facilities but also among students (E. Fanoy, Public Health Service, Rotterdam-Rijnmond, the Netherlands, pers. comm., May 15, 2020). Adolescents and young adults, particularly male, show the highest social connectivity (*11*). For this generation of young adults, mobility is not limited by country borders, which complicates contact tracing (*12*). The possible contribution of cross-border transmission to the international reemergence of scabies must be investigated in further studies. Moreover, young adults have the highest proportion of new sex partners within the previous year (*13*). Scabies can be seen as a sexually transmitted infection, but unlike other such infections, scabies cannot be prevented by condom use. However, intimate contacts that favor scabies transmission are not limited to sexual intercourse and may be related to other behaviors linked to social connectivity and more common in this age group, such as shared housing and couch surfing.

Second, repeated scabicide prescriptions are especially frequent in adolescents and young adults.

Table. Number of outpatients with repeated scabies treatment prescriptions after >28 d, by age group, Germany, 2009 and 2018

	No. patients with scabicide prescription		No. patients with repeated scabicide prescription		Percentage of patients with repeated prescriptions	
Age group, y	2009	2018	2009	2018	2009	2018
<5	3,844	29,255	248	6,999	6	24
5–9	4,687	33,002	264	7,988	6	24
10–14	3,781	37,693	230	10,298	6	27
15–19	4,900	71,610	314	21,100	6	29
20–24	4,350	57,271	225	14,351	5	25
25–29	3,017	33,830	131	7,072	4	21
30–34	2,235	24,466	106	4,630	5	19
35–39	2,215	23,871	92	4,565	4	19
40–44	3,091	23,327	131	4,689	4	20
45–49	3,062	25,006	133	5,108	4	20
50–54	2,354	24,197	125	4,405	5	18
55–59	1,821	17,485	123	2,941	7	17
60–64	1,274	11,534	87	1,917	7	17
65–69	1,376	8,043	110	1,376	8	17
70–74	1,509	5,778	109	906	7	16
75–79	1,230	6,920	102	1,105	8	16
≥80	3,321	15,998	230	2,228	7	14
Total	48,067	449,286	2,760	101,678	6	23

Failure of first-line treatments is observed in 6%–8% of patients in clinical trials (*14*). Although studies are needed for direct information on treatment failure, repeated prescriptions (as a proxy for treatment failure) occurred in comparable proportion in Germany in 2009 (Table). Alarmingly, since 2009 this proportion has more than doubled in all age groups but has more than quadrupled in adolescents and young adults. Although we cannot exclude reduced drug efficacy, we consider low therapeutic compliance and higher risk of reinfestation resulting from inefficient treatment of contact persons in this group to be the more relevant cause. Young adults show low medication adherence and high social connectivity, in particular within their own peer group (*11*,*15*).

Our analyses of claims data have limitations, including unknown extent of misdiagnosis and incorrect coding, lack of information on patients' compliance and medical history, and retreatment because of persisting symptoms rather than persisting infestation. In addition, recently raised awareness may have led to more diagnosed cases. Furthermore, prescriptions that were not reimbursed by the statutory health insurance but were purchased by the patients themselves in the pharmacy were not included in the database.

In summary, epidemiology of scabies in Germany has changed, and persons 15–24 years of age are the new most-affected age group. This group likely drives a current epidemic with uncurbed dynamics. Treatment failure is particularly high in this age group. Improvements in disease management strategies to address and improve awareness, compliance, risk behavior, and contact identification in peer groups are urgently needed.

Acknowledgments

We thank Cord Sunderkötter for his valuable clinical advice and Ewout Fanoy for sharing his knowledge about scabies in the Netherlands.

About the Author

Dr. Reichert is a fellow of the Postgraduate Training for Applied Epidemiology and European Programme for Intervention Epidemiology Training at Robert Koch Institut, Berlin, Germany. He is a pediatrician by training, with primary research interests in infectious disease epidemiology and parasitic skin diseases.

References

1. Sunderkotter C, Aebischer A, Neufeld M, Loser C, Kreuter A, Bialek R, et al. Increase of scabies in Germany and development of resistant mites? Evidence and consequences. J Dtsch Dermatol Ges. 2019; 17:15–23. https://doi.org/10.1111/ddg.13706
2. Kämmerer E. Skabies: Erfahrungen aus der Praxis. Dtsch Arztebl Int. 2018;115:700–2. https://www.aerzteblatt.de/archiv/197436/Skabies-Erfahrungen-aus-der-Praxis
3. Khalil S, Abbas O, Kibbi AG, Kurban M. Scabies in the age of increasing drug resistance. PLoS Negl Trop Dis. 2017;11:e0005920. https://doi.org/10.1371/journal.pntd.0005920
4. Sunderkötter C, Feldmeier H, Fölster-Holst R, Geisel B, Klinke-Rehbein S, Nast A, et al. S1 guidelines on the diagnosis and treatment of scabies—short version. J Dtsch Dermatol Ges. 2016;14:1155–67. https://doi.org/10.1111/ddg.13130
5. Döring A, Paul F. The German healthcare system. EPMA J. 2010;1:535–47. https://doi.org/10.1007/s13167-010-0060-z
6. Chosidow O. Scabies. N Engl J Med. 2006;354:1718–27. https://doi.org/10.1056/NEJMcp052784
7. Federal Health Monitoring System. Diagnostic data of the hospitals starting from 2000; 2021 [cited 2021 Feb 19]. https://www.gbe-bund.de/gbe/pkg_isgbe5.prc_menu_olap?p_uid=gast&p_aid=59857777&p_sprache=E&p_help=2&p_indnr=544&p_version=6&p_ansnr=64793043
8. Romani L, Steer AC, Whitfeld MJ, Kaldor JM. Prevalence of scabies and impetigo worldwide: a systematic review. Lancet Infect Dis. 2015;15:960–7. https://doi.org/10.1016/S1473-3099(15)00132-2
9. Amato E, Dansie LS, Grøneng GM, Blix HS, Bentele H, Veneti L, et al. Increase of scabies infestations, Norway, 2006 to 2018. Euro Surveill. 2019;24:24.
10. Lugović-Mihić L. The increase in Croatia's scabies incidence: how did refugees and traveling contribute? Travel Med Infect Dis. 2019;29:74. https://doi.org/10.1016/j.tmaid.2019.02.002
11. Bhattacharya K, Ghosh A, Monsivais D, Dunbar RI, Kaski K. Sex differences in social focus across the life cycle in humans. R Soc Open Sci. 2016;3:160097. https://doi.org/10.1098/rsos.160097
12. Expedia Group. Multi-generational travel trends [cited 2020 Apr 23]. https://info.advertising.expedia.com/hubfs/Content_Docs/Rebrand-2018/MultiGen_Travel_Trends_European_Travellers-Small.pdf?hsCtaTracking=c4c56107-f08c-4278-85b7-9fc5832e3b7a%7C3ca9a412-0a25-47c8-82ec-5830ec3b4e85
13. Mercer CH, Tanton C, Prah P, Erens B, Sonnenberg P, Clifton S, et al. Changes in sexual attitudes and lifestyles in Britain through the life course and over time: findings from the National Surveys of Sexual Attitudes and Lifestyles (Natsal). Lancet. 2013;382:1781–94. https://doi.org/10.1016/S0140-6736(13)62035-8
14. Rosumeck S, Nast A, Dressler C. Ivermectin and permethrin for treating scabies. Cochrane Database Syst Rev. 2018;4:CD012994.
15. Glombiewski JA, Nestoriuc Y, Rief W, Glaesmer H, Braehler E. Medication adherence in the general population. PLoS One. 2012;7:e50537. https://doi.org/10.1371/journal.pone.0050537

Address for correspondence: Felix Reichert, Fachgebiet 37, Robert Koch Institut, Seestraße 10, 13353 Berlin, Germany; email: reichertf@rki.de

Role of *Anopheles stephensi* Mosquitoes in Malaria Outbreak, Djibouti, 2019

Vincent Pommier de Santi, Bouh Abdi Khaireh, Thomas Chiniard, Bruno Pradines, Nicolas Taudon, Sébastien Larréché, Abdoulraouf Bourhan Mohamed, Franck de Laval, Franck Berger, Florian Gala, Madjid Mokrane, Nicolas Benoit, Lionel Malan, Abdoulilah Ahmed Abdi, Sébastien Briolant

Anopheles stephensi mosquitoes share urban breeding sites with *Aedes aegypti* and *Culex quinquefasciatus* mosquitoes in the Republic of Djibouti. We present evidence that *A. stephensi* mosquitoes might be responsible for an increase in malaria incidence in this country. We also document resistance of *Plasmodium falciparum* to dihydroartemisinin/piperaquine.

The Republic of Djibouti, bordered by Eritrea, Ethiopia, and Somalia, is a semiarid country in the Horn of Africa. The population comprises <900,000 persons, 70% of whom live in Djibouti, the capital city. Before 2013, malaria was hypoendemic to the country, with low levels of transmission in periruban and rural areas during December–May. Localized outbreaks occurred regularly, possibly caused by migration from surrounding countries. Most cases were caused by infection with *Plasmodium falciparum* (>80%) or *P. vivax*. Before 2013, researchers considered the *Anopheles arabiensis* mosquito to be the primary vector (*1*).

The incidence of malaria had drastically decreased in the country since 2008; by 2012, this transmission level was compatible with preelimination goals (*2*,*3*). In 2013, an autochthonous outbreak of malaria occurred in Djibouti; field entomologic investigations identified *An. stephensi* mosquitoes as a new malaria vector (*4*). This species, a known vector of urban malaria in India and the Arabian Peninsula, has changed the epidemiologic profile of malaria in Djibouti (*5*). In 2018, malaria incidence increased to 25,319 confirmed cases (64% caused by *P. falciparum* and 36% by *P. vivax*) and >100,000 suspected cases (Appendix Figure 1, https://wwwnc.cdc.gov/EID/article/27/6/20-4557-App1.pdf).

The French Armed Forces (FAF) have served in Djibouti for decades. Service members and their families (≈2,700 persons) live in the capital. Despite malaria prevention and treatment measures described elsewhere (*6*), an outbreak among French military personnel occurred in February 2019; failure of early artemisinin combined therapy was documented in 1 patient.

The Study

We collated FAF epidemiologic surveillance data on malaria cases among service members in Djibouti during 1993–2019; the 2019 data included cases among family members. We defined a malaria case as an illness resulting in a positive result on a rapid diagnostic test or thin blood smear.

We conducted the field investigation in the capital during February 28–March 22, 2019. We obtained a dried blood spot on filter paper from each patient and stored the samples in a sealed plastic pouch until processing. We extracted DNA from the samples and

Author affiliations: Aix Marseille University, IRD, AP-HM, SSA, VITROME, Marseille, France (V. Pommier de Santi, B. Pradines, N. Benoit, S. Briolant); IHU-Méditerranée Infection, Marseille (V. Pommier de Santi, B. Pradines, N. Benoit, S. Briolant); French Armed Forces Center for Epidemiology and Public Health, Marseille (V. Pommier de Santi, F. de Laval, F. Berger, M. Mokrane); United Nations Development Program, The Global Fund to Fight AIDS, Tuberculosis and Malaria, Djibouti, Republic of Djibouti (B.A. Khaireh); French Armed Forces Medical Health Service, Djibouti (T. Chiniard, F. Gala, L. Malan); French Armed Forces Biomedical Research Institute, Marseille (B. Pradines, N. Taudon, N. Benoit, S. Briolant); National Center for Malaria, Marseille (B. Pradines, N. Benoit); Bégin Military Teaching Hospital, Paris, France (S. Larréché); Djiboutian Gendarmerie Health Service, Djibouti (A. Bourhan Mohamed); Aix Marseille University, INSERM, IRD, Sciences Economiques & Sociales de la Santé & Traitement de l'Information Médicale, Marseille (F. de Laval, F. Berger); Djiboutian Armed Forces Health Service, Djibouti (A. Ahmed Abdi)

DOI: https://doi.org/10.3201/eid2706.204557

confirmed diagnosis using PCR. We sequenced the antimalarial drug resistance molecular markers *Pfdhfr*, *Pfmdr1*, *Pfcrt*, and the propeller domain of *PfK13* as described elsewhere (*7*). We treated patients with a 3-day regimen of dihydroartemisinin/piperaquine and measured levels of parasitemia on days 0 and 3; this treatment failed in 1 patient with malaria caused by *P. falciparum*. As follow-up for this patient, we collected blood samples from that patient on day 8 to determine piperaquine concentration using liquid chromatographic-tandem mass spectrometry.

We collected adult mosquitoes using human landing catches, CDC light traps, and BG-Sentinel and Suna traps (Biogents, https://www.biogents.com) (Table). We conducted larval prospecting in pools of water in French military camps, Djiboutian military police locations, and the Ambouli Gardens (a public area with a garden market and cattle breeding range). We reared larvae until imago emergence, then identified adult mosquitoes using a morphologic key (Walter Reed Biosystematics Unit, http://vectormap.si.edu/downloads/VHazard Reports/VHR_Anopheles_stephensi_2018.pdf). We extracted DNA from the legs of 103 *An. stephensi* mosquitoes and sequenced the cytochrome oxidase C subunit I gene to confirm morphologic identification. In addition, we conducted a phylogenetic analysis (Appendix Figure 2).

Table. Adult and larval mosquitoes collected by human landing catches and traps, Djibouti, Republic of Djibouti, 2019*

Species and sampling method†	No. (% female)	Resources/time expended
Anopheles stephensi		
HLC	1 (100.0)	2 persons/7 h
BG Sentinel Trap	1 (100.0)	2 traps/120 h
Larval emergence	190 (56.8)	
Subtotal	192 (57.3)	
Aedes aegypti		
HLC	11 (100.0)	2 persons/7 h
BG Sentinel Trap	88 (56.8)	2 traps/120 h
Suna Trap	10 (90.0)	2 traps/96 h
CDC Light Trap	2 (100.0)	2 traps/120 h
Larval emergence	32 (46.9)	
Subtotal	143 (60.8)	
Culex quinquefasciatus		
HLC	113 (100.0)	2 persons/7 h
BG Sentinel Trap	573 (68.2)	2 traps/120 h
Suna Trap	221 (57.5)	2 traps/96 h
CDC Light Trap	408 (66.2)	2 traps/120 h
Larval emergence	26 (92.3)	
Subtotal	1,341 (69.0)	
Other *Culex* sp.		
HLC	43 (100.0)	2 persons/7 h
BG Sentinel Trap	5 (40.0)	2 traps/120 h
Suna Trap	2 (100.0)	2 traps/96 h
CDC Light Trap	10 (100.0)	2 traps/120 h
Larval emergence	99 (71.7)	
Subtotal	159 (80.5)	
Total	1,835 (68.1)	

*HLC, human landing catch.
†Sampling methods were CDC Light traps, BG-Sentinel and Suna traps (Biogents, https://www.biogents.com), as well as HLC and larval emergence in laboratory. Each BG-Sentinel trap was baited with BG-MB5 attractant (Biogents) and a CO_2 production system (>50,000 ppm) based on the fermentation of sugar, yeast, and agar. For larval emergence method, larvae were collected and reared in laboratory until imago emergence.

In the early 2000s, malaria incidence in the FAF was only 1–4 cases per year; during 2011–2013, no cases were documented (Figure 1). Malaria reemerged in 2014 and reached an incidence of 5.9 cases/1,000 persons in 2018 and 8.1 cases/1,000 persons in 2019. In the 2018–19 season, *P. falciparum* and *P. vivax* cocirculated (*P. falciparum* caused 20/38 [53%] cases, *P. vivax* caused 17/38 [45%] cases, and *P. ovale* caused 1 [2%] case). Among the country's population, incidence increased from 25.5 cases/1,000 persons in 2018 to 49.8 cases/1,000 persons in 2019 (Appendix Figure 1) (*8*). In 2019, we documented 1 instance of treatment failure in a FAF service member with *P. falciparum* infection; this patient had a thin blood smear showing a parasitemia level of 2.0%. After 3 days of treatment with dihydroartemisinin/piperaquine, the patient still had a fever and 2.0% parasitemia level. The piperaquine plasma concentration on day 8 was 77.7 ng/mL, above the therapeutic threshold (38.1 ng/mL [95% CI 25.8–59.3] expected on day 7), confirming good regimen adherence and absorption (*9*). This case met the definition for early treatment failure of an artemisinin derivative according to criteria from the World Health Organization (https://apps.who.int/iris/handle/10665/162441). We sequenced molecular markers of resistance to antimalarial drugs for 9 *P. falciparum* isolates (Appendix Table 3). All isolates had molecular markers associated with resistance to mefloquine. In addition, 89% had resistance markers against chloroquine and pyrimethamine or proguanil. We did not observe any mutations in the K13 propeller region (which sometimes contains mutations associated with artemisinin resistance), including the isolate from the patient in whom treatment failed (*10*). In Africa, failures of artemisinin combined therapy potentially caused by K13 mutations observed in Southeast Asia remain rarely described (*11*).

We conducted entomologic investigations during a dry period (i.e., February–March). We collected 1,835 adult mosquitoes and larvae: 1,500 *Culex*, 143 *Aedes aegypti*, and 192 *An. stephensi* (Table). We caught 2 adult *An. stephensi* mosquitoes using the human landing catch and BG-Sentinel trap. We identified 25 breeding sites, 15 of which contained *An. stephensi* larvae. All the *An. stephensi* breeding sites were artificial and located in urban or suburban areas; 9/15 also contained *Ae. aegypti* larvae, *Cx. quinquefasciatus*

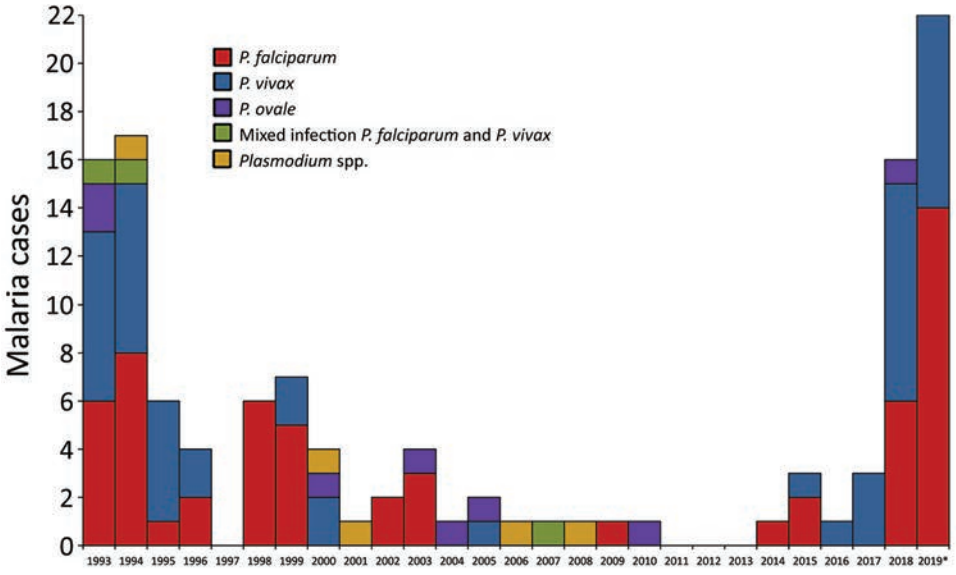

Figure 1. Distribution of 120 malaria cases caused by *Plasmodium* species among French Armed Force members, Djibouti, Republic of Djibouti, 1993–2019. *Data for 2019 include 2 *P. falciparum* infections among service members' families, 1 *P. vivax* relapse, and 3 *P. vivax* infections in France imported from Djibouti.

larvae, or both (Appendix Table 2). Examples of *An. stephensi* breeding sites included manholes, ditches, plastic drums, and water tanks (Figure 2). In military camps, standing water was related to leaks and stagnation caused by faulty maintenance of the water distribution and drainage network. The most productive breeding sites (≈800 water tanks with thousands of *An. stephensi* larvae) were near livestock areas, mainly in the Ambouli Gardens district. We confirmed morphologic identification of adult *An. stephensi* mosquitoes by cytochrome oxidase C subunit I sequencing, which identified 8 haplotypes. Phylogenetic trees did not clearly indicate the origin of *An. stephensi* mosquitoes in Djibouti (Appendix Figure 2).

Conclusions

In the Republic of Djibouti, malaria transmission has increased since 2013. Even populations with strong malaria control programs, such as the FAF, are now affected. In 2018, the country notified the World Health Organization of ≈100,000 suspected cases, mainly among febrile patients with negative results on a rapid diagnostic test (Appendix Figure 1). Considering these suspected cases, we believe the true

Figure 2. *Anopheles stephensi* breeding sites, Djibouti, Republic of Djibouti, 2019. A) Manhole. B) Ditch. C) Plastic drum. D) Water tank.

incidence could be 5 times higher than the 25,319 cases confirmed that year. A recent study (*12*) found a high prevalence (86.5%) of *pf*hrp2 and *pf*hrp3 gene deletion among *P. falciparum* parasites in the city of Djibouti.

We documented an early treatment failure of dihydroartemisinin/piperaquine in an isolate lacking a K13 mutation. This finding could signal the emergence of *P. falciparum* resistance to artemisinin derivatives in Djibouti.

An. stephensi mosquitoes are well-established in Djibouti and have been observed in Sudan and Ethiopia (*13*). Our study shows that this species shares breeding sites with *Ae. aegypti* and *Cx. quinquefasciatus* mosquitoes, highlighting its adaptation to urban areas. Models predict broad expansion of *An. stephensi* mosquito distribution into major cities in Africa, where large malaria outbreaks could occur among growing resident populations susceptible to the disease (*14*). Furthermore, a high level of resistance among mosquitoes to all insecticide families (e.g., organochlorates, pyrethroids, carbamates, and organophosphates) has been described in Djibouti and Ethiopia (*8*,*15*). In semiarid regions such as the Republic of Djibouti, residents often store water in plastic drums that act as breeding sites for *An. stephensi* mosquitoes. To control malaria and limit the spread of this anopheline species, communities and governments should prioritize larval control and access to the water distribution network.

About the Author

Dr. Pommier de Santi is a military physician and specialist in public health and epidemiology at the French Armed Forces Center for Epidemiology and Public Health, Marseille, France. His research interests include vectorborne diseases and other tropical diseases affecting the French Armed Forces and travelers.

References

1. Khaireh BA, Assefa A, Guessod HH, Basco LK, Khaireh MA, Pascual A, et al. Population genetics analysis during the elimination process of *Plasmodium falciparum* in Djibouti. Malar J. 2013;12:201. https://doi.org/10.1186/1475-2875-12-201
2. World Health Organization. World malaria report 2019. 2019 [cited 2020 Oct 21]. https://apps.who.int/iris/rest/bitstreams/1262394/retrieve
3. Ollivier L, Nevin RL, Darar HY, Bougère J, Saleh M, Gidenne S, et al. Malaria in the Republic of Djibouti, 1998–2009. Am J Trop Med Hyg. 2011;85:554–9. https://doi.org/10.4269/ajtmh.2011.11-0122
4. Faulde MK, Rueda LM, Khaireh BA. First record of the Asian malaria vector *Anopheles stephensi* and its possible role in the resurgence of malaria in Djibouti, Horn of Africa. Acta Trop. 2014;139:39–43. https://doi.org/10.1016/j.actatropica.2014.06.016
5. Seyfarth M, Khaireh BA, Abdi AA, Bouh SM, Faulde MK. Five years following first detection of *Anopheles stephensi* (Diptera: Culicidae) in Djibouti, Horn of Africa: populations established—malaria emerging. Parasitol Res. 2019;118:725–32. https://doi.org/10.1007/s00436-019-06213-0
6. Migliani R, Pradines B, Michel R, Aoun O, Dia A, Deparis X, et al. Malaria control strategies in French Armed Forces. Travel Med Infect Dis. 2014;12:307–17. https://doi.org/10.1016/j.tmaid.2014.05.008
7. Voumbo-Matoumona DF, Akiana J, Madamet M, Kouna LC, Lekana-Douki JB, Pradines B. High prevalence of *Plasmodium falciparum* antimalarial drug resistance markers in isolates from asymptomatic patients from the Republic of the Congo between 2010 and 2015. J Glob Antimicrob Resist. 2018;14:277–83. https://doi.org/10.1016/j.jgar.2018.08.003
8. Djibouti Ministry of Health. National strategic plan to fight malaria, 2020–2024 [in French]. 2020 [cited 2020 Oct 22]. https://erc.undp.org/evaluation/managementresponses/keyaction/documents/download/3685
9. Hoglund RM, Workman L, Edstein MD, Thanh NX, Quang NN, Zongo I, et al. Population pharmacokinetic properties of piperaquine in *Falciparum* malaria: an individual participant data meta-analysis. PLoS Med. 2017;14:e1002212. https://doi.org/10.1371/journal.pmed.1002212
10. Ariey F, Witkowski B, Amaratunga C, Beghain J, Langlois AC, Khim N, et al. A molecular marker of artemisinin-resistant *Plasmodium falciparum* malaria. Nature. 2014;505:50–5. https://doi.org/10.1038/nature12876
11. Foguim Tsombeng F, Gendrot M, Robert MG, Madamet M, Pradines B. Are *k13* and *plasmepsin II* genes, involved in *Plasmodium falciparum* resistance to artemisinin derivatives and piperaquine in Southeast Asia, reliable to monitor resistance surveillance in Africa? Malar J. 2019;18:285. https://doi.org/10.1186/s12936-019-2916-6
12. Iriart X, Menard S, Chauvin P, Mohamed HS, Charpentier E, Mohamed MA, et al. Misdiagnosis of imported *falciparum* malaria from African areas due to an increased prevalence of *pfhrp2/pfhrp3* gene deletion: the Djibouti case. Emerg Microbes Infect. 2020;9:1984–7. https://doi.org/10.1080/22221751.2020.1815590
13. Balkew M, Mumba P, Dengela D, Yohannes G, Getachew D, Yared S, et al. Geographical distribution of *Anopheles stephensi* in eastern Ethiopia. Parasit Vectors. 2020;13:35. https://doi.org/10.1186/s13071-020-3904-y
14. Sinka ME, Pironon S, Massey NC, Longbottom J, Hemingway J, Moyes CL, et al. A new malaria vector in Africa: predicting the expansion range of *Anopheles stephensi* and identifying the urban populations at risk. Proc Natl Acad Sci U S A. 2020;117:24900–8. https://doi.org/10.1073/pnas.2003976117
15. Yared S, Gebressielasie A, Damodaran L, Bonnell V, Lopez K, Janies D, et al. Insecticide resistance in *Anopheles stephensi* in Somali Region, eastern Ethiopia. Malar J. 2020;19:180. https://doi.org/10.1186/s12936-020-03252-2

Address for correspondence: Vincent Pommier de Santi, Centre d'épidémiologie et de santé publique des armées, GSBdD Marseille Aubagne—CESPA—BP 40029, Marseille 13568, France; email: v.pommierdesanti@gmail.com

Recurrent Swelling and Microfilaremia Caused by *Dirofilaria repens* Infection after Travel to India

Lena Huebl, Dennis Tappe, Manfred Giese, Sandra Mempel, Egbert Tannich, Benno Kreuels, Michael Ramharter, Luzia Veletzky,[1] Johannes Jochum[1]

Human subcutaneous dirofilariasis is an emerging mosquitoborne zoonosis. A traveler returning to Germany from India experienced *Dirofilaria* infection with concomitant microfilaremia. Molecular analysis indicated *Dirofilaria repens* nematodes of an Asian genotype. Microfilaremia showed no clear periodicity. Presence of *Wolbachia* endosymbionts enabled successful treatment with doxycycline.

Dirofilariasis is a zoonotic filarial infection transmitted through the bite of mosquitoes of various species. Several species of *Dirofilaria* microfilariae, most frequently *D. repens* and *D. immitis*, can infect humans. *D. repens* nematodes cause microfilaremic infection in dogs and other carnivores, which serve as reservoirs. Because humans are aberrant hosts, larvae usually develop into immature, nonfertile worms unable to produce microfilariae (*1*). Patients often report recurrent swelling with subsequent development of subcutaneous nodules, most commonly in the periorbital region (*2*). For most cases, surgical removal and histopathologic examination of the worm leads to diagnosis (*3*). *D. repens* microfilariae circulating in peripheral blood have been detected in humans only rarely (*4*,*5*), and information on periodicity of microfilaremia in aberrant hosts is lacking. One case report describes sampling of *D. repens* microfilariae from morning to midday on a single day and detection of microfilariae in the morning (*5*). Sequencing of the parasite's mitochondrial 12S rDNA has revealed European, African, and Asian genotypes of *D. repens* microfilariae. Successful treatment of *D. repens* infection with doxycycline, which targets the bacterial endosymbiont *Wolbachia*, has been reported (*6*). To our knowledge, *Wolbachia* bacteria have not been detected in *D. repens* microfilariae of the Asian genotype.

The Case

In April 2020, a 38-year-old man visited the outpatient clinic for tropical medicine at the Bernhard Nocht Institute for Tropical Medicine (Hamburg, Germany) 1 week after undergoing endonasal surgery for chronic sinusitis, reporting recurrent facial swelling. Nasal congestion and putrid discharge had started during a 5-week stay in Mysore, South India, his eighth trip in 5 years to the region to attend yoga classes. Two months after returning to Germany, he underwent therapeutic endoscopic septoplasty. Postoperatively, a soft tissue swelling in the right infraorbital and temporal region and general apathy developed, unresponsive to antibacterial therapy. Over 5 weeks, a low-grade eosinophilia of 0.72×10^9/L (10% of total leukocytes) increased to 0.94×10^9/L (14%). The result of an in-house panfilarial IgG-detecting ELISA that used a *D. immitis* extract as antigen was positive. Liver and kidney function test and serologic test results for *Strongyloides*, *Toxocara*, *Fasciola*, *Paragonimus*, *Cysticerca*, and *Gnathostoma* were unremarkable.

Five weeks after his initial visit to our clinic, the patient noticed a painless temporal mass (Figure 1, panel A). Magnetic resonance imaging demonstrated a 10-mm encapsulated lenticular formation

Author affiliations: University Medical Center Hamburg-Eppendorf, Hamburg, Germany (L. Huebl, B. Kreuels, M. Ramharter, L. Veletzky, J. Jochum); Bernhard Nocht Institute for Tropical Medicine, Hamburg (L. Huebl, D. Tappe, E. Tannich, B. Kreuels, M. Ramharter, L. Veletzky, J. Jochum); German Armed Forces Hospital, Hamburg (M. Giese); Radiologische Allianz, Hamburg (S. Mempel); German Center for Infection Research, Partner Site Hamburg-Lübeck-Borstel-Riems, Hamburg (L. Veletzky)

DOI: https://doi.org/10.3201/eid2706.210592

[1]These senior authors contributed equally to this article.

in the deep subcutaneous tissue (Figure 1, panel B). The lesion was surgically removed, and histologic examination showed an adult nematode (Figure 1, panel C). Filtration of 5 mL peripheral blood after hypotonic lysis of blood cells and subsequent Giemsa staining of the filter revealed microfilariae with the morphologic characteristics of *D. repens* (*7*) (Figure 1, panel D; Appendix, https://wwwnc.cdc.gov/EID/article/27/6/21-0592-App1.pdf; Video 1, https://wwwnc.cdc.gov/EID/article/27/6/21-0592-V1.htm; Video 2, https://wwwnc.cdc.gov/EID/article/27/6/21-0592-V2.htm). Sequencing and BLAST analysis (https://blast.ncbi.nlm.nih.gov/Blast.cgi) of a 463-bp fragment of the mitochondrial 12S rDNA (*8*) amplified from the adult worm and the microfilariae revealed 97.9%–99.2% homology with the Asian genotype of *D. repens* isolates from India (GenBank accession nos. GQ292761, KX265050, MT808309), followed by 95.6% homology with *D. repens* isolates from Europe (Greece, accession no. MK192091; Italy accession no., KX265072; Hungary, accession no. KX265070).

To assess possible periodicity of the microfilaremia, we sampled 5 mL of venous blood 4 times daily for 3 consecutive days and counted microfilariae after blood filtration. Blood was collected at fixed times during the day (6:30 AM, 12:00 AM, 6:00 PM, and 10:30 PM). Microfilariae were detectable in varying densities in all blood samples; counts fluctuated between 13 and 35 microfilariae/mL. On 2 days, the microfilaremia was highest in the evening and lowest in the morning samples, whereas on 1 day, the inverse pattern was observed. Thus, although it seems that microfilaremia substantially fluctuates during the day, this short assessment found no clear circadian rhythm of *D. repens* microfilaremia (Figure 2). To test for the presence of endosymbionts, we performed a recently published PCR that detects the FtsZ clade of *Wolbachia* (*9*). PCRs on microfilariae and adult worm samples were positive. With a goal of curative treatment, we administered doxycycline at 200 mg daily for 4 weeks, followed by a 15-mg dose of ivermectin. The patient fully recovered; eosinophil counts returned to reference ranges and microfilaremia disappeared.

Conclusions

The areas where human subcutaneous dirofilariasis is endemic are increasing, probably because of climate change, host mobility, and global travel (*10*). Thus, cases are increasing in areas where this disease is not endemic.

We report a case of microfilaremic *D. repens* infection, which was initially noted as recurrent swelling, in a human. Molecular analysis indicated an Asian genotype of *D. repens* nematodes, which has also

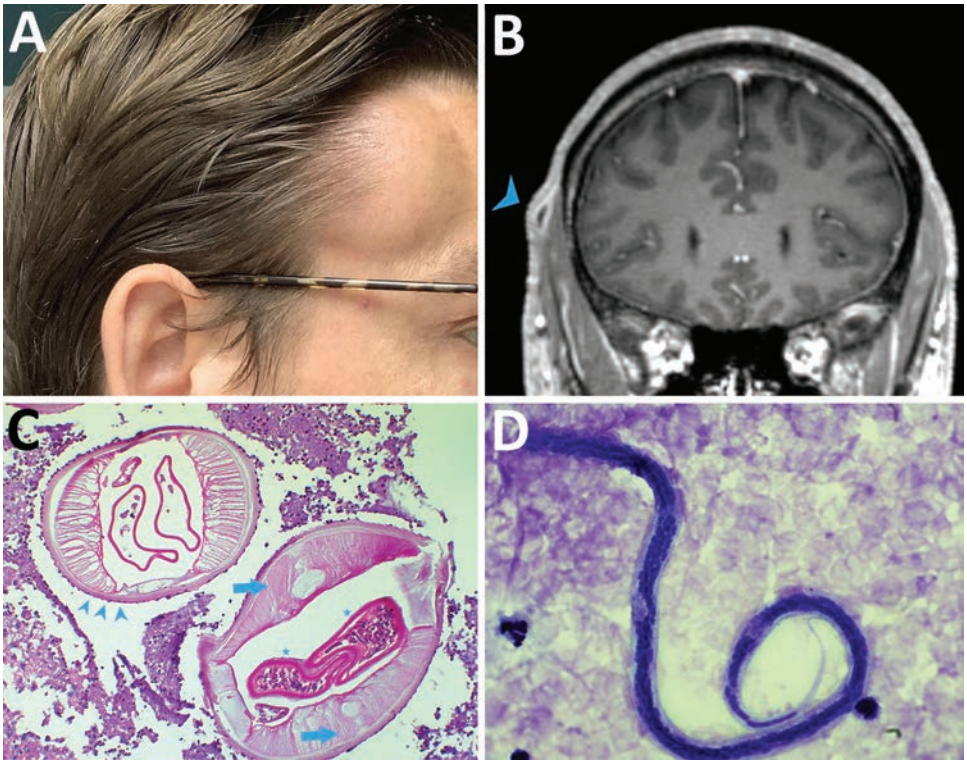

Figure 1. *Dirofilaria repens* infection in man in Germany after travel to India. A) Painless temporal subcutaneous swelling (image taken by the patient at the time of maximal protrusion). B) Contrast-enhanced magnetic resonance image (fat-saturated T1-weighted sequences) demonstrating a subcutaneous 10-mm lesion with central hypointensity and contrast uptake of the surrounding capsule (arrowhead). C) Cross-section through adult *D. repens* worm in subcutaneous tissue, demonstrating the cuticle with external ridges (arrow heads) and internal structures such as smooth muscle fibers (arrows) and gravid uteri (stars). Original magnification ×100; periodic acid-Schiff stain. D) *D. repens* microfilaria of the Asian genotype. Typical features include lack of a sheath, 2–3 separate nuclei in the head space, and absence of nuclei in the tip of the tail. Original magnification ×1,000 with oil; Giemsa stain.

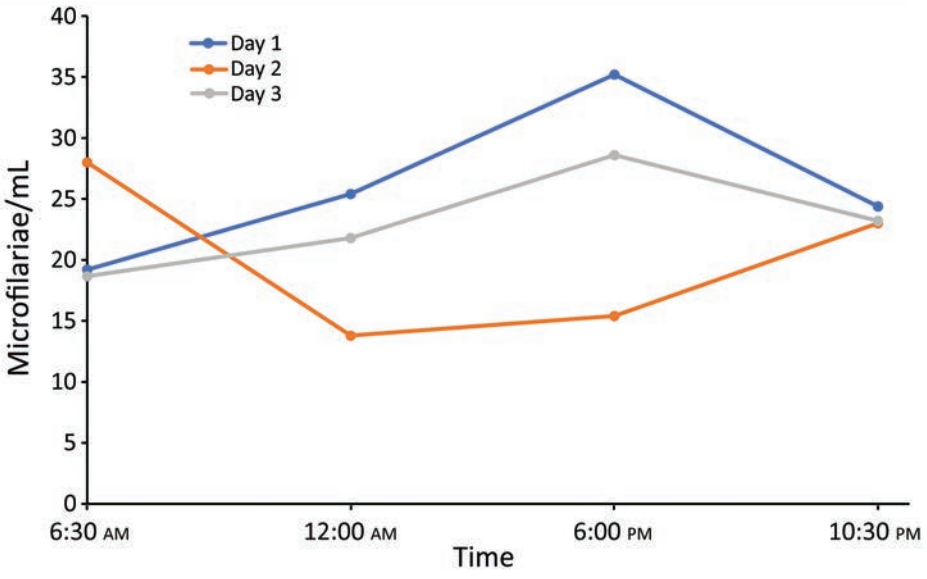

Figure 2. Circulating microfilariae/1 mL blood tested 4 times/day for 3 consecutive days in man in Germany with *Dirofilaria repens* infection after travel to India.

been referred to as Candidatus *Dirofilaria hongkongensis*. Recurrent swellings are often misdiagnosed, not taken seriously, and therefore diagnosed late. Most cases of human dirofilariasis are diagnosed after surgical removal of the adult nematode and subsequent histologic workup (*3*). *D. repens* microfilaremia in humans has been only rarely described (*4*,*5*). Several filarial species result in periodic microfilaremia (*11*), and these fluctuations can be substantial and relevant for diagnosis. Previous studies of dogs have shown that *D. immitis* and *D. repens* microfilaremia fluctuates throughout the day and peaks at night (*12*). Our results showed no clear circadian rhythm, but microfilaremia tended to be higher in the evening, similar to that of canine hosts. However, at time of blood collection, the patient had received the first doses of doxycycline, which might have affected our results.

In our investigation, the adult worm as well as the microfilariae were positive for *Wolbachia*. Doxycycline targeting this bacterial endosymbiont might thus be a treatment option similar to that for infection with other species of filariae (*13*). Molecular analysis of adult worms or microfilariae can reveal new genotypes, thereby increasing our knowledge of parasite biology and ecology (*9*). According to previous reports, *D. repens* of the Asian genotype is distributed on the Indian subcontinent (*14*,*15*). It remains unclear whether some genetic variants differ in their ability to mature and produce microfilaremia in the human host.

Localized subcutaneous swellings, particularly in the periorbital region, are a typical clinical presentation of *D. repens* infection; however, diagnosis might be difficult because of the absence of microfilaremia, eosinophilia, or positive serologic results. However, if microfilariae are detectable, they display specific features that enable microscopic differentiation. In conclusion, paramount for establishing the diagnosis of *D. repens* infection of individual patients are in-depth history taking, a high clinical suspicion, and targeted laboratory evaluation.

Acknowledgments

We thank the patient for providing consent to publish the photograph and clinical data and especially for participating in the periodicity sampling. We also thank Birgit Muntau and Christine Wegner for skillful technical assistance and Jana Held for providing the *Wolbachia* PCR protocol.

About the Author

Dr. Huebl is a resident for tropical medicine at the Department of Tropical Medicine, Bernhard Nocht Institute for Tropical Medicine, and First Department of Medicine, University Medical Center Hamburg-Eppendorf, Hamburg, Germany. She is pursuing a PhD in public health degree at the Medical University of Vienna.

References

1. Simón F, Siles-Lucas M, Morchón R, González-Miguel J, Mellado I, Carretón E, et al. Human and animal dirofilariasis: the emergence of a zoonotic mosaic. Clin Microbiol Rev. 2012;25:507–44. https://doi.org/10.1128/CMR.00012-12
2. Ermakova LA, Nagorny SA, Krivorotova EY, Pshenichnaya NY, Matina ON. *Dirofilaria repens* in the Russian Federation: current epidemiology, diagnosis, and treatment from a federal reference center perspective. Int J Infect Dis. 2014;23:47–52. https://doi.org/10.1016/j.ijid.2014.02.008

3. Pampiglione S, Rivasi F, Angeli G, Boldorini R, Incensati RM, Pastormerlo M, et al. Dirofilariasis due to *Dirofilaria repens* in Italy, an emergent zoonosis: report of 60 new cases. Histopathology. 2001;38:344–54. https://doi.org/10.1046/j.1365-2559.2001.01099.x
4. Potters I, Vanfraechem G, Bottieau E. *Dirofilaria repens* nematode infection with microfilaremia in traveler returning to Belgium from Senegal. Emerg Infect Dis. 2018;24:1761–3. https://doi.org/10.3201/eid2409.180462
5. Kłudkowska M, Pielok Ł, Frąckowiak K, Masny A, Gołąb E, Paul M. *Dirofilaria repens* infection as a cause of intensive peripheral microfilariemia in a Polish patient: process description and cases review. Acta Parasitol. 2018;63:657–63. https://doi.org/10.1515/ap-2018-0077
6. Lechner AM, Gastager H, Kern JM, Wagner B, Tappe D. Case report: successful treatment of a patient with microfilaremic dirofilariasis using doxycycline. Am J Trop Med Hyg. 2020;102:844–6. https://doi.org/10.4269/ajtmh.19-0744
7. Liotta JL, Sandhu GK, Rishniw M, Bowman DD. Differentiation of the microfilariae of *Dirofilaria immitis* and *Dirofilaria repens* in stained blood films. J Parasitol. 2013;99:421–5. https://doi.org/10.1645/12-10.1
8. Casiraghi M, Bain O, Guerrero R, Martin C, Pocacqua V, Gardner SL, et al. Mapping the presence of *Wolbachia pipientis* on the phylogeny of filarial nematodes: evidence for symbiont loss during evolution. Int J Parasitol. 2004;34:191–203. https://doi.org/10.1016/j.ijpara.2003.10.004
9. Sandri TL, Kreidenweiss A, Cavallo S, Weber D, Juhas S, Rodi M, et al. Molecular epidemiology of *Mansonella* species in Gabon. J Infect Dis. 2021;223:287–96. https://doi.org/10.1093/infdis/jiaa670
10. Capelli G, Genchi C, Baneth G, Bourdeau P, Brianti E, Cardoso L, et al. Recent advances on *Dirofilaria repens* in dogs and humans in Europe. Parasit Vectors. 2018;11:663. https://doi.org/10.1186/s13071-018-3205-x
11. Hawking F. The 24-hour periodicity of microfilariae: biological mechanisms responsible for its production and control. Proc R Soc Lond B Biol Sci. 1967;169:59–76. https://doi.org/10.1098/rspb.1967.0079
12. Ionică AM, Matei IA, D'Amico G, Bel LV, Dumitrache MO, Modrý D, et al. *Dirofilaria immitis* and *D. repens* show circadian co-periodicity in naturally co-infected dogs. Parasit Vectors. 2017;10:116. https://doi.org/10.1186/s13071-017-2055-2
13. Taylor MJ, Hoerauf A, Townson S, Slatko BE, Ward SA. Anti-*Wolbachia* drug discovery and development: safe macrofilaricides for onchocerciasis and lymphatic filariasis. Parasitology. 2014;141:119–27. https://doi.org/10.1017/S0031182013001108
14. Winkler S, Pollreisz A, Georgopoulos M, Bagò-Horvath Z, Auer H, To KK, et al. Candidatus *Dirofilaria hongkongensis* as causative agent of human ocular filariosis after travel to India. Emerg Infect Dis. 2017;23:1428–31. https://doi.org/10.3201/eid2308.170423
15. Poppert S, Hodapp M, Krueger A, Hegasy G, Niesen WD, Kern WV, et al. *Dirofilaria repens* infection and concomitant meningoencephalitis. Emerg Infect Dis. 2009;15:1844–6. https://doi.org/10.3201/eid1511.090936

Address for correspondence: Lena Huebl, Department of Tropical Medicine, Bernhard Nocht Institute for Tropical Medicine, and First Department of Medicine, University Medical Center Hamburg-Eppendorf, Martinistraße 52, 20246 Hamburg, Germany; email: l.huebl@uke.de

Melioidosis in Children, Brazil, 1989–2019

Rachel Ximenes Ribeiro Lima,[1] Dionne Bezerra Rolim[1]

We studied 20 confirmed or suspected cases of melioidosis in children in Ceará, Brazil, during 1989–2019. We observed a high death rate, severe signs and symptoms, and substantial environmental exposure. These data suggest that childhood melioidosis might be more severe in Brazil than in other regions.

Melioidosis, an infectious disease caused by the bacterial species *Burkholderia pseudomallei*, is associated with severe symptoms and high death rates (*1*). Although considered an emerging disease, melioidosis has little formal public health recognition (*2*). Researchers initially documented cases in Brazil in 2003 (*3*). As of 2018, Ceará, a coastal state in northeastern Brazil, has the highest incidence in South America; however, sporadic cases have been reported in other states (*4*). Although the disease predominantly affects adults with associated risk factors (*1*), the growing incidence of severe melioidosis among children and adolescents in Ceará highlights the need for clinical and epidemiologic investigations.

The Study

We analyzed all cases of melioidosis in persons <18 years of age documented by the Ceará State Health Department during January 2005–May 2019. This state declared melioidosis a notifiable disease in 2005 (*5*), although the literature records cases from early as 1989 (*6*). We also searched for cases in the SciELO and PubMed databases using the terms "melioidosis" AND "Brazil" OR "children" published during March 2003–May 2019. We also searched the annals of Brazilian Congresses of Pediatric Infectiology from 2003–2018. In total, we identified 16 cases in the health department database (1 case was excluded because of an alternative diagnosis) and 5 in the literature (*3*,*6*). All cases were either suspected or confirmed (Table 1) (*5*,*7*).

We investigated cases using data from patient records and, when possible, from interviews with the patients and their relatives. We analyzed data on age, sex, time of symptom onset, geographic location, occupational or recreational activity involving water or soil during the 2 weeks before symptom onset, underlying conditions, signs and symptoms, laboratory and radiographic findings, clinical evolution, treatment, and clinical outcome. We used the Fisher exact test to assess the correlation between appropriate treatment using carbapenem or ceftazidime during the intensive phase of melioidosis (*8*) and survival. The study protocol was previously approved by the research ethics committees of the University of Fortaleza (Fortaleza, Brazil) (approval no. 3,094,492) and Albert Sabin Children's Hospital (Fortaleza) (approval no. 3,194,070).

We identified 10 confirmed (including 5 before 2005: 4 in 2003, and 1 identified retrospectively in 1989) (*3*,*6*), and 10 suspected cases of melioidosis among children and adolescents. The 10 confirmed cases in persons <18 years of age account for 23.2% of the 43 confirmed cases of melioidosis in the state of Ceará as of May 2019. This proportion is substantially greater than the 5%–15% usually reported for children (*9*).

Most (9/20; 45%) patients were 10–17 years of age. The median age was 11 years for patients with confirmed cases and 9 years for those with suspected cases. For comparison, childhood melioidosis is most prevalent in children <5 years of age in Malaysia (*10*) and in children >10 years of age in Australia (*11*).

As in previous studies (*2*,*12*), most (13/20; 65%) patients in this sample were male. Illnesses occurred most frequently during the rainy season (i.e. February–May), accounting for 65% (13/20) of all cases and 70% (7/10) of confirmed cases. This trend resembles the results of a study in Australia (*11*) and reinforces

Author affiliations: Municipal Department of Health, Fortaleza, Brazil (R.X.R. Lima); University of Fortaleza Medical School (R.X.R. Lima, D.B. Rolim); Ceará State University, Fortaleza (D.B. Rolim)

DOI: https://doi.org/10.3201/eid2706.200154

[1]These authors contributed equally to this article.

Table 1. Clinical definitions in study of melioidosis in children, Brazil, 1989–2019*

Term	Definition
Suspected melioidosis	All patients with suspected melioidosis must have epidemiologic exposure at any time, recent or not, associated with ≥1 of the following criteria: acute febrile illness and respiratory symptoms suggestive of community pneumonia that do not improve with conventional antimicrobial treatment (β-lactam antimicrobial drugs); febrile disease that progresses with systemic inflammatory response syndrome, severe sepsis, or septic shock; prolonged fever of unknown etiology or signs and symptoms similar to tuberculosis that do not respond to tuberculosis treatment; or soft tissue infection (e.g. cutaneous ulcers/abscesses, cellulite, or fasciitis) of chronic evolution (i.e. months) with no response to conventional antimicrobial treatment (e.g. oxacillin, ampicillin associated to sulbactam, or cefalexin).
Confirmed melioidosis	All patients with confirmed melioidosis must meet laboratory (bacteriologic confirmation by microbiological culture or positive PCR) or clinical-epidemiologic criteria (exposure to the same risk situation as patients with laboratory-confirmed melioidosis). Patients with confirmed melioidosis must have signs and symptoms that are compatible with melioidosis and not attributable to a different cause.
Severe disease	Patients with severe melioidosis have clinical signs and symptoms and a high risk for death caused by pneumonia, sepsis, or septic shock.

*These criteria were defined by references (*5*,*7*).

the association between heavy rainfalls and exposure to *B. pseudomallei*. Most (19/20; 95%) patients had environmental exposure during the 14 days before symptom onset (Table 2). Outdoor recreational behavior is common among children in Brazil, especially in the tropics. For example, when intense warm showers interrupt the extended droughts of northeastern Brazil, children often bathe and play in waterfalls, rivers, and dams. This might partially account for the high prevalence of melioidosis among children, especially older children and boys, in this region.

The most frequent clinical manifestations were sepsis (18/20; 90%), pneumonia (18/20; 90%), and septic shock (17/20; 85%) (Table 2). Among confirmed cases, 90% (9/10) of patients had sepsis and pneumonia and 80% (8/10) had septic shock. Among suspected cases, 90% (9/10) of patients had pneumonia, sepsis, and septic shock. Studies in Malaysia have reported similar figures (*10*); however, the main manifestations among children are skin lesions in Australia and infectious parotitis in Cambodia (*13*,*14*). Although the methods used by these studies differ, they suggest that children in Ceará might have more severe clinical manifestations of melioidosis.

Two patients had meningitis, accounting for 20% (2/10) of confirmed cases and 10% (2/20) of total cases; however, a study in Australia observed neuromelioidosis in 3% of pediatric patients (*15*). These findings might indicate either a greater proportion of neurologic involvement or substantial underreporting of less severe manifestations among children with melioidosis in Brazil.

In total, 45% (9/20) of patients died: 60% (6/10) of patients with confirmed cases and 30% (3/10) of those with suspected cases. Childhood melioidosis is associated with a death rate of 35% globally (*9*), although in Australia the rate is reported to be 7% (*13*). In Cambodia, 16.4% of patients die, including up to 71% of patients with bacteremia (*14*). Our findings, which include high prevalence of sepsis and septic shock, 2 cases of severe neurologic involvement, and high death rates, warrant further investigation.

We found that appropriate, timely treatment for melioidosis (*8*) was significantly associated with survival among 20 patients ($p<0.01$). Thus, physicians should consider empirical treatment for suspected melioidosis in patients in areas to which the disease is endemic, especially if the initial treatment was unsuccessful. We did not find a significant association between proper treatment and survival among patients with confirmed ($p = 0.08$) and suspected cases ($p = 0.07$) of melioidosis, possibly because of small sample size.

Conclusion

We describe a high prevalence, death rate, and severity of childhood melioidosis in Brazil. The high death rate and clinical severity might be partially explained by underreporting of mild cases, but the frequent environmental exposures of children in this region warrant further research. These findings emphasize the need for melioidosis awareness among healthcare providers and laboratory professionals. Physicians should consider melioidosis as a differential diagnosis; improved awareness might reduce underreporting and optimize the quality of epidemiologic data. Physicians also should consider empirical treatment in patients who have clinical manifestations compatible with the disease and whose prognosis is compromised by clinical severity.

About the Author

Dr. Lima is a professor at the University of Fortaleza Medical School in Fortaleza, Brazil. Her research interests include clinical pediatrics, neurodevelopment, and infectious disease.

Dr. Rolim is a professor at the University of Fortaleza Medical School in Fortaleza, Brazil. Her research0 interested include infectious disease, melioidosis, and epidemiology.

Table 2. Clinical and epidemiologic characteristics of children with melioidosis, Brazil, 1989–2019*

Pt	Age, y/sex	City	Rainy season†	Potential exposures‡	Pneumonia	Sepsis	Septic shock	Diagnostic results	Timely treatment#	Outcome (time to death)¶
1	0.25/M	Fortaleza	No	Mother lived in rural area during pregnancy§	No	No	No	*Pseudomonas pseudomallei* in cerebrospinal fluid	Yes	Survived
2	15/M	Tejuçuoca	Yes	Swam in river	Yes	Yes	Yes	No test, met clinical epidemiologic criteria	No	Death (40 h)
3	14/F	Tejuçuoca	Yes	Swam in river	Yes	Yes	Yes	*Burkholderia pseudomallei*	No	Death (90 h)
4	10/M	Tejuçuoca	Yes	Swam in river	Yes	Yes	Yes	*B. pseudomallei*	No	Death (6 d)
5	12/F	Tejuçuoca	Yes	Swam in river	Yes	Yes	Yes	*B. pseudomallei*	Yes	Survived
6	17/M	Fortaleza	Yes	Bathed in river/waterfall	Yes	Yes	Yes	*B. pseudomallei*	Yes	Death (10 d)
7	3/M	São João do Jaguaribe	Yes	Swam in river	Yes	Yes	Yes	*B. pseudomallei*	Yes	Death (28 d)
8	13/F	Ipu	No	Bathed in waterfalls	Yes	Yes	Yes	*B. pseudomallei*	No	Death (10 d)
9	3/F	Granja	Yes	Swam in river, bathed in waterfalls	Yes	Yes	No	No test, met clinical epidemiologic criteria	Yes	Survived
10	6/M	Fortaleza	No	Swam in river, bathed in waterfalls	Yes	Yes	Yes	*B. pseudomallei* in bronchoalveolar lavage, met clinical epidemiologic criteria	Yes	Survived
11	6/M	Limoeiro do Norte	No	Swam in river, bathed in waterfalls, fished, drank contaminated water	No	No	No	Negative	Yes	Survived
12	9/F	Pacatuba	No	Swam in river, bathed in waterfalls	Yes	Yes	Yes	Negative	Yes	Death (5 d)
13	13/M	Guaiúba	No	Swam in river, bathed in waterfalls, fished	Yes	Yes	Yes	*B. cepacea* in oropharyngeal swab sample	Yes	Survived
14	1/F	Fortaleza	No	Swam in untreated pool	Yes	Yes	Yes	Negative	Yes	Survived
15	6/M	Canindé	Yes	Swam in river/dams, fished	Yes	Yes	Yes	Negative	No	Death (8 d)
16	3/M	Fortaleza	Yes	Swam in lake/ played with soil	Yes	Yes	Yes	Negative	Yes	Survived
17	9/F	Canindé	Yes	Swam in river/dams, fished	Yes	Yes	Yes	Negative	Yes	Survived
18	11/M	Orós	Yes	Swam in river, fished	Yes	Yes	Yes	Negative	Yes	Survived
19	14/M	Trairí	Yes	Swam in river/dams, fished	Yes	Yes	Yes	Negative	No	Death (4 d)
20	9/M	Trairí	Yes	Swam in river/dams, fished	Yes	Yes	Yes	Negative	Yes	Survived

*Cases 1–10 were confirmed according to diagnostic criteria (5,7); cases 11–20 were suspected. Pt, patient.
†Rainy season in Ceará, Brazil is February–May.
‡During 14 d before symptom onset.
¶From symptom onset.
§Potential vertical transmission.
#As defined in (8).

References

1. Wiersinga WJ, Virk HS, Torres AG, Currie BJ, Peacock SJ, Dance DAB, et al. Melioidosis. Nat Rev Dis Primers. 2018; 4:17107. PubMed https://doi.org/10.1038/nrdp.2017.107
2. Limmathurotsakul D, Golding N, Dance DAB, Messina JP, Pigott DM, Moyes CL, et al. Predicted global distribution of *Burkholderia pseudomallei* and burden of melioidosis. Nat Microbiol. 2016;1:15008. https://doi.org/10.1038/nmicrobiol.2015.8
3. Rolim DB, Vilar DCFL, Sousa AQ, Miralles IS, A lemeida de Oliveira DC, Harnett G, et al. Melioidosis, northeastern Brazil. Emerg Infect Dis. 2005;11:1458–60. https://doi.org/10.3201/eid1109.050493
4. Rolim DB, Lima RXR, Ribeiro AKC, Colares RM, Lima LDQ, Rodríguez-Morales AJ, et al. Melioidosis in South America. Trop Med Infect Dis. 2018;3:60. https://doi.org/10.3390/tropicalmed3020060
5. Governo do Estado do Ceará. Epidemiological surveillance [in Portuguese]. 2014 [cited 2018 May 5]. https://d68d7ba2-f9c4-4028-a03f-3eb98a9b2064.filesusr.com/ugd/6d03c9_6cb4e4208d5a4350a01da5d9a77c5876.pdf
6. XIV congresso brasileiro de infectologia pediatrica. Report of the first case of melioidosis diagnosed in the state of Ceará in 1989 [in Portuguese]. Jornal Paranaense de Pediatria. 2005;6:48–93.
7. Cheng AC, Currie BJ, Dance DAB, Funnell SGP, Limmathurotsakul D, Simpson AJH, et al. Clinical definitions of melioidosis. Am J Trop Med Hyg. 2013;88:411–3. https://doi.org/10.4269/ajtmh.12-0555
8. Dance D. Treatment and prophylaxis of melioidosis. Int J Antimicrob Agents. 2014;43:310–8. https://doi.org/10.1016/j.ijantimicag.2014.01.005
9. Sanderson C, Currie BJ. Melioidosis: a pediatric disease. Pediatr Infect Dis J. 2014;33:770–1. https://doi.org/10.1097/INF.0000000000000358
10. Mohan A, Podin Y, Tai N, Chieng CH, Rigas V, Machunter B, et al. Pediatric melioidosis in Sarawak, Malaysia: epidemiological, clinical and microbiological characteristics. PLoS Negl Trop Dis. 2017;11:e0005650. https://doi.org/10.1371/journal.pntd.0005650
11. Smith S, Stewart JD, Tacon C, Archer N, Hanson J. Children with melioidosis in Far North Queensland are commonly bacteraemic and have a high case fatality rate. Commun Dis Intell Q Rep. 2017;41:E318–21.
12. Currie BJ, Jacups SP. Intensity of rainfall and severity of melioidosis, Australia. Emerg Infect Dis. 2003;9:1538–42. https://doi.org/10.3201/eid0912.020750
13. Mcleod C, Morris PS, Bauert PA, Kilburn CJ, Ward LM, Baird RW, et al. Clinical presentation and medical management of melioidosis in children: a 24-year " prospective study in the Northern Territory of Australia and review of the literature. 2014;60:21–6. https://doi.org/10.1093/cid/ciu733
14. Turner P, Kloprogge S, Miliya T, Soeng S, Tan P, Sar P, et al. A retrospective analysis of melioidosis in Cambodian children, 2009–2013. BMC Infect Dis. 2016;16:688. https://doi.org/10.1186/s12879-016-2034-9
15. Currie BJ, Ward L, Cheng AC. The epidemiology and clinical spectrum of melioidosis: 540 cases from the 20 year Darwin Prospective Study. 2010;4:e900. https://doi.org/10.1371/journal.pntd.0000900

Address for correspondence: Rachel Lima, Ratisbona Street 171, Apt no. 500, Fortaleza, Ceará 60411-220, Brazil; email: rachelx@unifor.br

Seroepidemiologic Survey of Crimean-Congo Hemorrhagic Fever Virus in Logging Communities, Myanmar

Tierra Smiley Evans, Theingi Win Myat, Nang Sarm Hom, Keersten Michelle Ricks, Min Thein Maw, Zaw Min Oo, Aung Than Toe, Nyein Thu Aung, Pyaephyo Aung, Tin Htun Aung, Paul Kuehnert, Kyaw Zin Thant, Ye Tun Win, Wai Zin Thein, Nicole Rae Gardner, Randal Joseph Schoepp, Christine Kreuder Johnson,[1] Hlaing Myat Thu[1]

Crimean-Congo hemorrhagic fever virus (CCHFV) is endemic in Asia, infecting many animal hosts, but CCHFV has not been reported in Myanmar. We conducted a seroepidemiologic survey of logging communities in Myanmar and found CCHFV exposure was common (9.8%) and exposure to wild animal blood and body fluids was associated with seropositivity.

Crimean-Congo hemorrhagic fever (CCHF), caused by Crimean-Congo hemorrhagic fever virus (CCHFV) (*1*), is a widely distributed arboviral disease. Human CCHF cases have been reported in >30 countries in Africa, the Middle East, Asia, and southeastern Europe (*2*). However, clinical cases or seroprevalence studies for CCHFV have not been reported in Myanmar, likely because active surveillance in humans or animals has not been established (*3*).

Hyalomma ticks, 1 of several CCHFV tick family hosts, are considered the primary vector transmitting CCHFV to humans (*4*). *Hyalomma* tick distribution extends into Myanmar (*5*), and CCHF has been reported in the neighboring countries of China and India (*6*,*7*). Expansion of CCHF from countries with known virus circulation to neighboring countries could occur through introduction of infected ticks, human CCHF cases, or movement of animals (*8*). Climate change also is expected to influence the distribution of *Hyalomma* ticks and CCHFV infections (*9*), increasing the likelihood of disease expansion.

Human CCHFV infections can occur through contact with an infected tick or with blood or tissues from infected humans or animals. People living or working closely with livestock or who have heavy exposure to ticks are at increased risk for CCHFV infection (*10*,*11*). Limited investigations have been performed to identify human exposure to CCHFV caused by wild animal contact, despite serologic evidence for exposure to CCHFV in numerous vertebrate species, including birds (Galliformes and Passeriformes), wild hoof stock (Artiodactyla, Cetartiodactyla, and Perissodactyla), carnivores (Carnivora), bats (Chiroptera), hedgehogs (Erinaceomorpha), rabbits and hares (Lagomorpha), elephants (Proboscidea), rodents (Rodentia), and turtles (Testudinata) (*12*).

CCHF has been designated by the World Health Organization as 1 of 10 high-priority emerging infectious diseases (https://www.who.int/emergencies/diseases/2018prioritization-report.pdf). The designation was based on CCHF's epidemic and emergence potential, a high case-fatality rate of up to 80% depending on healthcare infrastructure and CCHFV genotype, and a lack of approved medical countermeasures for CCHF (*14*). Most initial reports of CCHF cases in individual countries have been preceded by epidemiologic surveys that provided evidence of local CCHFV circulation. Our goal was to conduct

Author affiliations: University of California, Davis, Davis, California, USA (T. Smiley Evans, A.T. Toe, N.T. Aung, N.R. Gardner, C.K. Johnson); Department of Medical Research, Yangon, Myanmar (T.W. Myat, N.S. Hom, H.M. Thu); US Army Medical Research Institute of Infectious Diseases, Frederick, Maryland, USA (K.M. Ricks, P. Kuehnert, R.J. Schoepp); Livestock Breeding and Veterinary Department, Yangon (M.T. Maw, Y.T. Win, W.Z. Thein); Myanmar Timber Enterprise, Yangon (Z.M. Oo); Nature Conservation Society Myanmar, Yangon (P. Aung, T.H. Aung); Myanmar Academy of Medical Science, Yangon (K.Z. Thant)

DOI: https://doi.org/10.3201/eid2706.203223

[1]These senior authors contributed equally to this article.

targeted CCHFV surveillance of Myanmar logging communities, which contain an occupational group with expected high exposure to ticks, domestic livestock, and wild animals.

The Study

Myanmar uses a traditional method of elephant logging for timber harvest. Consequently, Myanmar has a large network of communities in which loggers live together in temporary villages with their families and occasionally migrant laborers. We collected data from 102 healthy persons from 5 elephant logging communities in and near the Yenwe Forest Reserve, a protected area in central Myanmar, during June 2016–August 2018. Most (57/102) participants, including persons from forest management, logging crews, and elephant caretakers, worked in the protected area and were exposed to forested areas and vectors associated with CCHFV (Table 1). Participants were 17–67 years of age and the median age was 32.5 years. We collected venous blood samples and quantitative medical and behavioral questionnaires from each participant (Appendix, https://wwwnc.cdc.gov/EID/article/27/6/20-3223-App1.pdf).

We used a bead-based MagPix (Luminex Corporation, https://www.luminexcorp.com) assay platform, developed at the US Army Medical Research Institute of Infectious Diseases, to detect specific IgG reactivity against the nucleoprotein of CCHFV. We used molecular detection of conserved regions of the small, medium, and large segments of bunyavirus to detect CCHFV viremia with conventional PCR (Appendix).

We identified previous CCHFV exposure among study participants, but we did not detect any active infections. Study participants did not exhibit any signs of hemorrhagic fever, and none reported having previously suffered symptoms of hemorrhagic-like illnesses. All participants tested negative for bunyaviruses by consensus PCR. Among study participants, 9.8% (10/102) were seropositive for CCHFV by MagPix IgG assay. Samples categorized as positive ranged from 1,124–8,911 mean fold increase (MFI) and a signal-to-noise ratio (S/N) of 33.8–207.8. Negative samples had an MFI of 44–854 and 1–19.9 S/N. Persons 31–40 years of age were significantly more likely to be seropositive for CCHFV ($p = 0.05$) compared with other age groups. We noted no statistically significant associations between specific occupations and CCHFV exposure (Table 1).

Persons who reported handling live or recently slaughtered primates (age-adjusted odds ratio [$OR_{age\ adjusted}$] = 5.53; $p = 0.020$) or wild carnivores ($OR_{age\ adjusted} = 1.3$; $p = 0.004$) in their lifetimes were more likely to have been exposed to CCHFV (Table 2). Handling primates was significantly correlated with handling carnivores (Pearson's correlation = 0.6; $p<0.001$). Therefore, we used independent multivariable logistic regression models to adjust for age while assessing the association of CCHFV seropositivity for these 2 factors. More male than female persons reported

Table 1. Crimean-Congo hemorrhagic fever virus immunoglobulin G seroprevalence by demographic characteristic and occupation among forest logging camp communities, Myanmar

Characteristic	No. positive	No. negative	Period prevalence (95% CI)
Sex			
M	6	56	0.11 (0.05–0.2)
F	4	36	0.11 (0.04–0.23)
Age group, y			
11–20	0	11	0 (0–0.26)
21–30	3	32	0.09 (0.03–0.22)
31–40	5	19	0.21 (0.09–0.40)
41–50	2	13	0.13 (0.04–0.38)
51–60	0	15	0 (0–0.20)
61–70	0	2	0 (0–0.66)
Primary occupation*			
Extractive industries	0	6	0 (0–0.39)
Crop production	0	2	0 (0–0.66)
Livestock farmer	0	1	0 (0–0.79)
Protected area worker, forest ranger	6	51	0.11 (0.05–0.21)
Housewife	1	2	0.33 (0.06–0.79)
Teacher	0	2	0 (0–0.66)
Migrant laborer	0	5	0 (0–0.43)
Hunter	1	7	0.11 (0.02–0.43)
Dependent	3	27	0.09 (0.03–0.24)
Total	10	92	0.11 (0.05–0.17)

*Persons were asked to report their primary occupations but some engaged in additional activities, outside of their primary occupation. For example, persons who did not identify as being a hunter as their primary occupation may have reported hunting.

Table 2. Distribution of seropositivity to Crimean-Congo hemorrhagic fever virus among persons exposed to wild and domesticated animals in forest logging camp communities, Myanmar*

Risk factor	Exposed no. persons seropositive/no. tested (%)	Unexposed no. persons seropositive/no. tested (%)	Bivariate model		Multivariable model	
			OR	p value	OR	p value
Hunted wildlife						
Ungulate	2/27 (7.4)	8/75 (10.7)	0.67	1.0	NC	NC
Bat	0/1 (0.0)	10/101 (9.9)	2.9†	1.0	NC	NC
Rodent	0/1 (0.0)	10/101 (9.9)	2.9†	1.0	NC	NC
Primate	2/16 (12.5)	8/86 (9.3)	1.39	0.66	NC	NC
Pangolin	2/9 (22.2)	8/93 (8.6)	2.99	0.21	NC	NC
Carnivore	1/9 (11.1)	9/93 (9.7)	1.16	1.0	NC	NC
Any wild animal	4/51 (7.8)	6/51 (11.8)	0.64	0.74	NC	NC
Handled wildlife found dead						
Ungulate	3/32 (9.4)	7/70 (10.0)	0.93	1.0	NC	NC
Bat	1/3 (33.3)	9/99 (9.1)	4.86	0.27	NC	NC
Rodent	1/4 (25.0)	9/98 (9.2)	3.24	0.34	NC	NC
Primate	4/19 (21.1)	6/83 (7.2)	3.37	0.09	NC	NC
Pangolin	1/6 (16.7)	9/96 (9.4)	1.92	0.47	NC	NC
Carnivore	1/10 (10.0)	9/92 (9.8)	1.02	1.0	NC	NC
Any wild animal	8/76 (10.5)	2/26 (7.7)	1.41	1.0	NC	NC
Handled recently slaughtered or live wildlife						
Ungulate	4/26 (15.4)	6/76 (7.9)	2.1	0.27	NC	NC
Bat	1/3 (33.3)	9/99 (9.1	4.86	0.27	NC	NC
Rodent	1/5 (20.0)	9/97 (9.3)	2.42	0.41	NC	NC
Primate	5/23 (21.7)	5/79 (6.3)	4.04	0.04	5.53‡	0.020
Pangolin	2/10 (20.0)	8/92 (8.7)	2.59	0.25	NC	NC
Carnivore	4/12 (33.3)	6/90 (6.7)	6.78	0.02	1.3‡	0.004
Any wild animal	10/88 (11.4)	0/14 (0.0)	3.88†	0.35	NC	NC
Handled live domestic animals						
Goats	0/6 (0.0)	10/96 (10.4)	0.63†	1.0	NC	NC
Pigs	3/23 (13.0)	7/79 (8.9)	1.54	0.69	NC	NC
Poultry	6/57 (10.5)	4/45 (8.9)	1.20	1.0	NC	NC
Cattle	1/8 (12.5)	9/94 (9.6)	1.34	0.58	NC	NC
Elephant	5/43 (11.6)	5/59 (8.5)	1.42	0.74	NC	NC
Any domestic animal	7/60 (11.7)	3/42 (7.1)	1.71	0.52	NC	NC
Slaughtered domestic animals						
Goats	0/0 (0.0)	10/102 (9.8)	NC	NC	NC	NC
Pigs	1/3 (33.3)	9/99 (9.1)	4.86	0.27	NC	NC
Poultry	3/18 (16.7)	7/84 (8.3)	2.18	0.38	NC	NC
Cattle	0/1 (0.0)	10/101 (9.9)	2.9†	1.0	NC	NC
Any domestic animal	9/71 (12.7)	1/31 (3.2)	4.31	0.28	NC	NC

*NC, not calculated; OR, odds ratio.
†Sample odds ratio calculated using unconditional maximum likelihood estimate method.
‡Evaluated in separate multivariable models, adjusting for age.

handling primates (20 male vs. 3 female persons) and carnivores (9 male vs. 3 female persons) and their ages ranged from 19–60 years. Handling primates or carnivores was not statistically significantly associated with any occupational or other behavioral factors.

Among persons who reported handling wildlife, the highest risk species for CCHFV exposure were primates and carnivores. Although sample size for handling some live or recently slaughtered wild animal taxa were low (for instance, <5 persons each reported handling rodents or bats), we found no statistically significant association between combined wildlife taxa evaluated and CCHFV exposure (p = 1.0; Table 2).

A bite from an infected tick was not the likely route of exposure to CCHFV in this community. We evaluated occupations associated with increased forest contact, and thus tick habitat, such as resource extraction, protected area worker (forest ranger), or hunter, as a combined variable, but we found no statistically significant association between occupation and CCHFV exposure.

Contact with domestic animals also was not the likely route of CCHFV exposure in this community. Study participants were not frequently exposed to ruminants, the domestic animal group most reported as associated with CCHFV exposure in endemic countries. Participants were more likely to report contact with pigs or poultry, but these animals have not been identified as amplifying hosts for CCHFV. Contact with live or dead domestic animals of any kind was not associated with CCHFV exposure (Table 2).

Nonhuman primates have not been implicated as natural reservoir hosts or sources of human CCHFV infection. However, rhesus macaques (*Macaca mulatta*) and long-tailed macaques (*M. fascicularis*), which

range throughout Myanmar, have been infected with CCHFV in laboratory settings. Rhesus macaques develop viremia without clinical signs, but long-tailed macaques develop signs of clinical illness and viremia similar to disease progression in humans (*15*). Contact with blood or other bodily fluids, including saliva, urine, or feces, during a period of viremia in macaques could lead to human infection. Similarly, wild carnivores have not been implicated as natural reservoir hosts for CCHFV, but red foxes (*Vulpes vulpes*), which are thought to range in Myanmar, and Pallas's cats (*Otocolobus manul*), which range in central Asia, have demonstrated CCHFV seropositivity and could serve as sources of human infection, particularly through bushmeat hunting, which exposes persons to animal blood and body fluids.

Conclusions

Our findings indicate that CCHFV is circulating in Myanmar with human infections that are either mildly symptomatic or occurring in populations that fall outside of existing surveillance systems. Although exposure to domestic animal amplifying hosts is the most commonly reported exposure type for human CCHFV infections in endemic countries, our findings show that persons with close contact with wild animal reservoir hosts, especially blood and body fluids of nonhuman primates and carnivores, also are at risk for CCHFV infection. Surveillance of at-risk populations in Myanmar should be expanded to better prepare for potential future outbreaks of CCHF.

Acknowledgments

We thank the Department of Medical Research, the Myanmar Timber Enterprise, the Livestock Breeding and Veterinary Department, and the Forest Department of the Republic of the Union of Myanmar for their support and facilitation of this research. We thank Than Toe, Than Swe, Khin Maung Win, Tin Tin Myaing, Cynthie Tin Oo, and Daniel Fishbein for their guidance on working in Myanmar.

Research reported in this publication was supported by the Fogarty International Center of the National Institutes of Health under grant no. K01TW010279. C.J. and N.G. were supported by the United States Agency for International Development (USAID) Emerging Pandemic Threats PREDICT project (cooperative agreement no. GHN-A-OO-09-00010-00). Laboratory work was funded in part by the Global Emerging Infections Surveillance (GEIS) Section of the Armed Forces Health Surveillance Branch (AFHSB) research plans (ProMIS P0141_19_RD and P0129_20_RD) through USAMRIID.

The content is solely the responsibility of the authors and does not necessarily represent the official views of the National Institutes of Health, USAID, or the US Army.

About the Author

Dr. Smiley Evans is a research epidemiologist at the One Health Institute, University of California, Davis, California, USA. Her research focuses on disease transmission dynamics between humans and wildlife and the impact of biodiversity on disease emergence.

References

1. Hoogstraal H. The epidemiology of tick-borne Crimean-Congo hemorrhagic fever in Asia, Europe, and Africa. J Med Entomol. 1979;15:307–417. https://doi.org/10.1093/jmedent/15.4.307
2. Ergönül O. Crimean-Congo haemorrhagic fever. Lancet Infect Dis. 2006;6:203–14. https://doi.org/10.1016/S1473-3099(06)70435-2
3. Al-Abri SS, Abaidani IA, Fazlalipour M, Mostafavi E, Leblebicioglu H, Pshenichnaya N, et al. Current status of Crimean-Congo haemorrhagic fever in the World Health Organization Eastern Mediterranean Region: issues, challenges, and future directions. Int J Infect Dis. 2017;58:82–9. https://doi.org/10.1016/j.ijid.2017.02.018
4. Maltezou HC, Papa A. Crimean-Congo hemorrhagic fever: risk for emergence of new endemic foci in Europe? Travel Med Infect Dis. 2010;8:139–43. https://doi.org/10.1016/j.tmaid.2010.04.008
5. Messina JP, Pigott DM, Golding N, Duda KA, Brownstein JS, Weiss DJ, et al. The global distribution of Crimean-Congo hemorrhagic fever. Trans R Soc Trop Med Hyg. 2015;109:503–13. https://doi.org/10.1093/trstmh/trv050
6. Bente DA, Forrester NL, Watts DM, McAuley AJ, Whitehouse CA, Bray M. Crimean-Congo hemorrhagic fever: history, epidemiology, pathogenesis, clinical syndrome and genetic diversity. Antiviral Res. 2013;100:159–89. https://doi.org/10.1016/j.antiviral.2013.07.006
7. Patel AK, Patel KK, Mehta M, Parikh TM, Toshniwal H, Patel K. First Crimean-Congo hemorrhagic fever outbreak in India. J Assoc Physicians India. 2011;59:585–9.
8. Spengler JR, Bergeron É, Spiropoulou CF. Crimean-Congo hemorrhagic fever and expansion from endemic regions. Curr Opin Virol. 2019;34:70–8. https://doi.org/10.1016/j.coviro.2018.12.002
9. Estrada-Peña A, Sánchez N, Estrada-Sánchez A. An assessment of the distribution and spread of the tick *Hyalomma marginatum* in the western Palearctic under different climate scenarios. Vector Borne Zoonotic Dis. 2012;12:758–68. https://doi.org/10.1089/vbz.2011.0771
10. Vorou R, Pierroutsakos IN, Maltezou HC. Crimean-Congo hemorrhagic fever. Curr Opin Infect Dis. 2007;20:495–500. https://doi.org/10.1097/QCO.0b013e3282a56a0a
11. Deyde VM, Khristova ML, Rollin PE, Ksiazek TG, Nichol ST. Crimean-Congo hemorrhagic fever virus genomics and global diversity. J Virol. 2006;80:8834–42. https://doi.org/10.1128/JVI.00752-06
12. Spengler JR, Bergeron É, Rollin PE. Seroepidemiological studies of Crimean-Congo hemorrhagic fever virus in domestic and wild animals. PLoS Negl Trop Dis.

2016;10:e0004210. https://doi.org/10.1371/journal.pntd.0004210
13. Schwarz TF, Nsanze H, Ameen AM. Clinical features of Crimean-Congo haemorrhagic fever in the United Arab Emirates. Infection. 1997;25:364–7. https://doi.org/10.1007/BF01740819
14. Leblebicioglu H, Ozaras R, Irmak H, Sencan I. Crimean-Congo hemorrhagic fever in Turkey: Current status and future challenges. Antiviral Res. 2016;126:21–34. https://doi.org/10.1016/j.antiviral.2015.12.003
15. Smith DR, Shoemaker CJ, Zeng X, Garrison AR, Golden JW, Schellhase CW, et al. Persistent Crimean-Congo hemorrhagic fever virus infection in the testes and within granulomas of non-human primates with latent tuberculosis. PLoS Pathog. 2019; 15:e1008050. https://doi.org/10.1371/journal.ppat.1008050

Address for Correspondence: Tierra Smiley Evans, 1089 Veterinary Medicine Dr, University of California, Davis, CA 95616, USA; email: tsmevans@ucdavis.edu

Cutaneous Leishmaniasis Caused by an Unknown *Leishmania* Strain, Arizona, USA

Marcos de Almeida, Yueli Zheng, Fernanda S. Nascimento, Henry Bishop, Vitaliano A. Cama, Dhwani Batra, Yvette Unoarumhi, Abaseen K. Afghan, Vivian Y. Shi,[1] Philip E. LeBoit, Eugene W. Liu, Fariba M. Donovan

We investigated an autochthonous case of cutaneous leishmaniasis caused by a genetically different *Leishmania* sp. in a patient in Arizona, USA. This parasite was classified into the subgenus *Leishmania* on the basis of multilocus DNA sequence and phylogenetic analyses of the rRNA locus and 11 reference genes.

Human leishmaniasis is a vectorborne disease occurring mostly in Central and South America, the Europe/Africa Mediterranean area, the Middle East, and the Indian subcontinent. This disease is caused by parasites in the *Leishmania* subgenera *Viannia* and *Leishmania*, affects ≈2.5 million persons, and causes 60,000 deaths yearly worldwide (*1*). The disease has 3 main clinical forms: cutaneous leishmaniasis (CL), the most prevalent form and caused by species in both *Viannia* and *Leishmania* subgenera; mucocutaneous leishmaniasis, caused by species in the subgenus *Viannia*; and visceral leishmaniasis, caused by *L.* (*L.*) *donovani* and *L.* (*L.*) *infantum*. These syndromes might lead to social stigma because of permanent scars, skin disfigurement, and partial/total destruction of oral/nasopharyngeal mucosa and can result in systemic symptoms including splenomegaly, wasting, and even death (*2*).

Species-specific *Leishmania* identification is critical in clinical management and epidemiologic investigations (*2*). Detection and identification of *Leishmania* parasites were traditionally done through microscopic and multilocus enzyme electrophoresis analysis. Currently, PCR-based methods and multilocus DNA sequence analyses (MLSA) combined with next-generation sequencing, have improved phylogenetic resolution and provided insights into parasite identification, classification, genetic polymorphism, virulence, and drug resistance (*3*,*4*).

Leishmania parasites are emerging in previously nonendemic areas (*5*); traditional and exotic *Leishmania* species/strains have been reported in focal areas of the Americas, Europe, Africa, Asia, and the Western Pacific (*6*). In the United States, leishmaniasis is mostly nonreportable and historically considered a travel-associated disease. However, the activity of natural vectors of *Leishmania* and occurrence of autochthonous zoonotic cases of CL and visceral leishmaniasis caused by *L.* (*L.*) *mexicana* or *L.* (*L.*) *infantum* have been reported in several states, including Alabama, Arizona, Arkansas, Delaware, Georgia, Kentucky, Louisiana, Maryland, Mississippi, Ohio, Oklahoma, South Carolina, and Texas (*7*–*10*). Those reports suggest the possibility of local transmission of leishmaniasis, especially in the southwestern US region. We report an autochthonous case of CL from Arizona, USA, caused by an unknown parasite in the subgenus *Leishmania*.

The Study

In December 2017, a 72-year-old woman from Pima County, Arizona, sought medical care for 2 discrete, progressive, edematous, violaceous papular lesions on the low back. The patient had a history of granulomatosis with polyangiitis, chronic sinusitis, chronic kidney disease, and pulmonary coccidioidomycosis. The patient had never traveled internationally and did not have an underlying health condition predisposing her to leishmaniasis.

Author affiliations: Centers for Disease Control and Prevention, Atlanta, Georgia, USA (M. de Almeida, Y. Zheng, F.S. Nascimento, H. Bishop, V.A. Cama, D. Batra, Y. Unoarumhi, E.W. Liu); Eagle Global Scientific, San Antonio, Texas, USA (Y. Zheng); University of Arizona College of Medicine, Tucson, Arizona, USA (A.K. Afghan, V.Y. Shi, F.M. Donovan); University of California, San Francisco, California, USA (P.E. LeBoit)

DOI: https://doi.org/10.3201/eid2706.204198

[1]Current affiliation: University of Arkansas for Medical Sciences, Little Rock, Arkansas, USA.

In January 2018, after a third lesion erupted, we performed skin biopsies. Histologic sections showed nonnecrotizing granulomas in the papillary dermis, and tiny, basophilic, spherical inclusions within histiocyte cytoplasm resembling amastigotes, suggestive of CL. The lesions showed a limited extent and spontaneous improvement; therefore, no specific treatment was prescribed. The patient was followed for almost 2 years, and the 3 skin lesions remained nodular without ulceration, which eventually resolved by December 2019. The patient remained otherwise asymptomatic.

We tested clinical specimens from the patient following the Centers for Disease Control and Prevention (CDC)–approved protocol for using residual specimens from human subjects (use of residual diagnostic specimens from humans for laboratory methods research protocol no. 6756). We used lesion biopsy specimens submitted to CDC for DNA extraction, touch-prep smears, and in vitro culture in Roswell Park Memorial Institute medium (GIBCO-Thermo-Fisher, https://www.thermofisher.com) containing 15% fetal bovine serum at 25°C (*11*). Microscopic analysis of touch-prep smears identified a large number of amastigotes, whereas promastigotes with cellular shape and architecture compatible with species in the subgenus *Leishmania* were observed from culture (Figure 1).

We extracted DNA from biopsy specimens, cultured parasites by using the DNeasy Blood and Tissue Kit (QIAGEN, https://www.qiagen.com), and amplified the internal transcribed spacer 2 (ITS2) locus by using PCR. We then Sanger sequenced amplicons bidirectionally, assembled by using Lasergene Seqman Pro Software (DNASTAR, Inc., https://www.dnastar.com), and compared with sequences in the GenBank database by using BLASTn (https://blast.ncbi.nlm.nih.gov/Blast.cgi) (*11*).

The resulting sequence (380 bp) (GenBank accession no. MT764332) had low similarity with *L.* (*L.*) *donovani* HQ830358 (90.36%), *L.* (*L.*) *infantum* AJ 634370 (89.9%), *Leishmania* sp. FM209179 (89.5%), *L.* (*L.*) *tropica* FJ948457 (89.2%), *L.* (*L.*) *mexicana* FJ948437 (85.1%), and species in the subgenus *Viannia* (≤80.0%). We also tested DNA samples for amplicon melting temperature by using a SYBR green real-time, quantitative PCR protocol, which enables presumptive discrimination of *Leishmania* species (*12*). This analysis showed a melting temperature of 79.5°C, indicating *L.* (*L.*) *infantum* infection. On the basis of PCR analysis, the case-patient was identified as being infected with a *Leishmania* spp., without providing species-level identification.

Figure 1. Cultured *Leishmania* promastigotes of the strain isolated from a patient in Arizona, USA. Morphologic features include a slender elongated body that contains a kinetoplast (K) anterior to the nucleus (N) and flagellum (F). The parasite had a total body length of ≈15 μm. Giemsa-stained; scale bar indicates 10 μm.

We used DNA extracted from cultured parasites by using the MagAttract HMW DNA Kit (QIAGEN) to prepare genomic libraries by using the NEBNext Ultra II DNA Library Prep (New England Biolabs, https://www.neb.com) and subjected them to whole-genome sequencing by using the MiSeq platform (Illumina, https://www.illumina.com). MiSeq sequencing resulted in 22,808,630 *Leishmania* reads that had >100× coverage, 3,464 contigs of 29,491,421 bp, and a GC content of 59.68%.

We conducted MLSA by comparing open reading frames (ORFs) of MiSeq data against GenBank reference sequences at the following loci: β-actin, aspartate aminotransferase, cytosolic glyceraldehyde-3-phosphate dehydrogenase, glucose-6-phosphate dehydrogenase, glucose-6-phosphate isomerase, isocitrate dehydrogenase, cytosolic nicotinamide adenine dinucleotide phosphate, malic enzyme, mannose phosphate isomerase, 6-phosphogluconate dehydrogenase, 6-phosphoglucomutase, heat-shock protein 70, 18SrRNA ITS region and rRNA. We determined similarities between MiSeq and database ORFs, fragment length, and GenBank accession no. (Table, https://wwwnc.cdc.gov/EID/article/27/6/20-4198-T1.htm). Similarities to *Viannia* reference sequences were 99.6% for 18S rRNA and 65.23% for ITS rRNA loci. To visualize the taxonomic location of the isolate from Arizona, we constructed an evolutionary distance tree by using MiSeq 18SrRNA and cytosolic glyceraldehyde-3-phosphate dehydrogenase ORFs, as well as complete reference sequences in the subgenera *Leishmania*, *Viannia*, and *Mundina* (Figure 2).

Conclusions

Leishmania species associated with human clinical cases are typically prevalent in tropical and subtropical foci and classified into 2 subgenera: *Viannia* and *Leishmania*. Nonetheless, environmental changes might contribute to expansion of natural vectors, reservoirs, and emergence of novel *Leishmania* strains and leishmaniasis in nonendemic areas, posing a new and serious challenge to public health (*5*,*6*).

We report an autochthonous case of CL caused by a previously undescribed *Leishmania* parasite in a patient in Arizona. The integrated interpretation of the clinical information, travel history, parasite morphology, CDC species-specific diagnostic test results, and MLSA/phylogenetic analyses suggest that the isolate from Arizona could be a new strain or species within the subgenus *Leishmania*. This isolate is also genetically distinct at the internal transcribed spacer 2 locus from reported isolates for 18 previous cases of leishmaniasis from Arizona, characterized by CDC over the past 10 years, which were detected in travelers returning from disease-endemic areas.

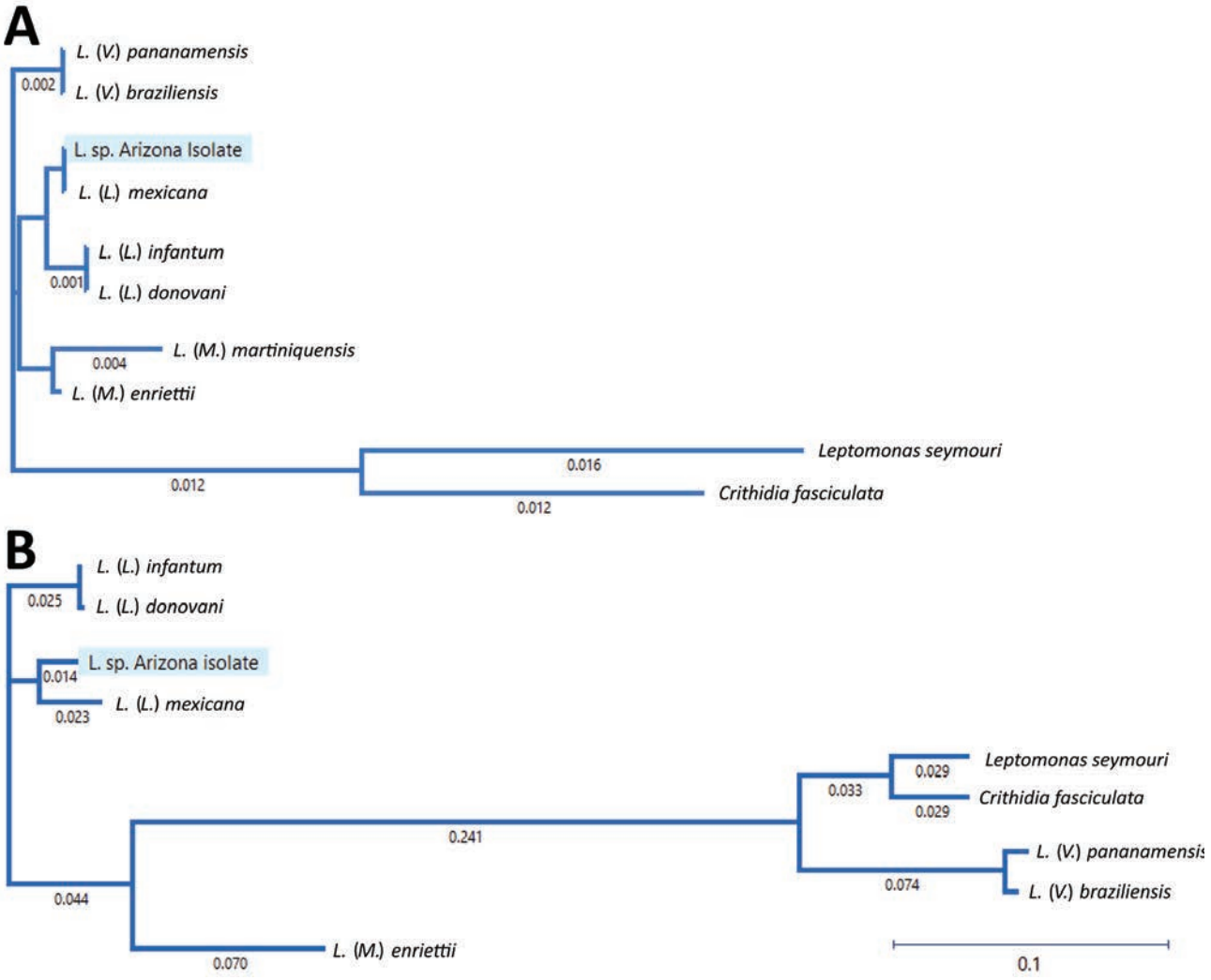

Figure 2. Phylogenetic tree of *Leishmania* subgenus isolates from a patient in Arizona, USA, and reference *Leishmania* species in relationship to species in the subgenera *Leishmania*, *Viannia*, and *Mundina*. A) Phylogenetic tree of *Leishmania* 18S rRNA genes. Sequences of *Crithidia fasciculata* and *Leptomonas seymouri* are included as references. *L*. (*V*.) *panamensis* (GenBank accession no. GQ332362); *L*. (*V*.) *braziliensis* (accession no. GQ332355); *L*. (*L*) *mexinana* (accession no. GQ332260); *L*. (*L*.) *infantum* (accession no. GQ332359); *L*. (*L*.) *donovani* (accession no. GQ332356); *L*. (*M*.) *martiniquensis* (accession no. AF303938); *L*. (*M*.) *enriettii* (accession no. ATAF02000704); *Leptomonas seymore* (accession no. KP717894); and *Crithidia fasciculata* (accession no. Y00055). The 2 non-*Leishmania* trypanosomatids (*Leptomonas seymore* and *Crithidia fasciculata*) were included in the phylogenetic tree because they were previously described as co-infecting parasites in human leishmaniasis cases. B) Phylogenetic tree of glyceraldehyde-3-phosphate dehydrogenase genes. Sequences from *Crithidia fasciculata* and *Leptomonas seymouri* were included as references. Numbers along branches indicate bootstrap values. Scale bars indicate nucleotide substitutions per site.

Despite these findings, we realize that classification of this parasite cannot be conclusively determined based solely on genetic evidence observed in this study. Therefore, further investigations (including multilocus enzyme electrophoresis and whole-genome sequencing with next-generation sequencing long read fragments) will be needed to confirm whether the isolate from Arizona is a new species or a new strain in the subgenus *Leishmania*.

Historically, human leishmaniasis in the United States has been considered an exotic, travel-acquired infection. However, this concept must be reexamined because of the expansion of sylvatic animal reservoirs and natural sand fly vectors of *Leishmania* spp. and reports of human and animal autochthonous cases in several states (*7*–*9*,*13*–*15*). Considering the patient's travel history, the increased reports of zoonotic cases, and the active presence of sand fly vectors/reservoirs in southern areas of the United States, we concluded that the CL reported was probably caused by local parasite transmission. Because there is increasing evidence of likely local transmission, leishmaniasis could be emerging in the southwestern United States.

Acknowledgments

We thank the patient for participating in the study and Sara Sapp and Joel Barret for providing invaluable assistance with illustration preparation and manuscript review.

About the Author

Dr. Marcos de Almeida is a research molecular biologist in the Division of Parasitic Diseases and Malaria, Center for Global Health, Centers for Disease Control and Prevention, Atlanta, GA. His primary research interests are developing diagnostic tests for several parasites of public health concern and leishmaniasis diagnostics.

References

1. Alvar J, Vélez ID, Bern C, Herrero M, Desjeux P, Cano J, et al.; WHO Leishmaniasis Control Team. Leishmaniasis worldwide and global estimates of its incidence. PLoS One. 2012;7:e35671. https://doi.org/10.1371/journal.pone.0035671
2. Herwaldt BL. Leishmaniasis. Lancet. 1999;354:1191–9. https://doi.org/10.1016/S0140-6736(98)10178-2
3. Glaeser SP, Kämpfer P. Multilocus sequence analysis (MLSA) in prokaryotic taxonomy. Syst Appl Microbiol. 2015;38:237–45. https://doi.org/10.1016/j.syapm.2015.03.007
4. Schönian G, Kuhls K, Mauricio IL. Molecular approaches for a better understanding of the epidemiology and population genetics of *Leishmania*. Parasitology. 2011;138:405–25. https://doi.org/10.1017/S0031182010001538
5. González C, Wang O, Strutz SE, González-Salazar C, Sánchez-Cordero V, Sarkar S. Climate change and risk of leishmaniasis in North America: predictions from ecological niche models of vector and reservoir species. PLoS Negl Trop Dis. 2010;4:e585. https://doi.org/10.1371/journal.pntd.0000585
6. Sereno D. *Leishmania* (*Mundinia*) spp.: from description to emergence as new human and animal *Leishmania* pathogens. New Microbes New Infect. 2019;30:100540. https://doi.org/10.1016/j.nmni.2019.100540
7. Douvoyiannis M, Khromachou T, Byers N, Hargreaves J, Murray HW. Cutaneous leishmaniasis in North Dakota. Clin Infect Dis. 2014;59:e73–5. https://doi.org/10.1093/cid/ciu386
8. Kipp EJ, de Almeida M, Marcet PL, Bradbury RS, Benedict TK, Lin W, et al. An atypical case of autochthonous cutaneous leishmaniasis associated with naturally infected phlebotomine sand flies in Texas, United States. Am J Trop Med Hyg. 2020;103:1496–501. https://doi.org/10.4269/ajtmh.20-0107
9. McIlwee BE, Weis SE, Hosler GA. Incidence of endemic human cutaneous leishmaniasis in the United States. JAMA Dermatol. 2018;154:1032–9. https://doi.org/10.1001/jamadermatol.2018.2133
10. de Almeida ME, Spann DR, Bradbury RS. *Leishmania infantum* in US-born dog. Emerg Infect Dis. 2020;26:1882–4. https://doi.org/10.3201/eid2608.200149
11. de Almeida ME, Steurer FJ, Koru O, Herwaldt BL, Pieniazek NJ, da Silva AJ. Identification of *Leishmania* spp. by molecular amplification and DNA sequencing analysis of a fragment of rRNA internal transcribed spacer 2. J Clin Microbiol. 2011;49:3143–9. https://doi.org/10.1128/JCM.01177-11
12. de Almeida ME, Koru O, Steurer F, Herwaldt BL, da Silva AJ. Detection and differentiation of *Leishmania* spp. in clinical specimens by use of a SYBR green-based real-time PCR assay. J Clin Microbiol. 2016;55:281–90. https://doi.org/10.1128/JCM.01764-16
13. Clarke CF, Bradley KK, Wright JH, Glowicz J. Case report: emergence of autochthonous cutaneous leishmaniasis in northeastern Texas and southeastern Oklahoma. Am J Trop Med Hyg. 2013;88:157–61. https://doi.org/10.4269/ajtmh.2012.11-0717
14. Petersen CA, Barr SC. Canine leishmaniasis in North America: emerging or newly recognized? Vet Clin North Am Small Anim Pract. 2009;39:1065–74, vi. https://doi.org/10.1016/j.cvsm.2009.06.008
15. Schaut RG, Robles-Murguia M, Juelsgaard R, Esch KJ, Bartholomay LC, Ramalho-Ortigao M, et al. Vectorborne transmission of *Leishmania infantum* from hounds, United States. Emerg Infect Dis. 2015;21:2209–12. https://doi.org/10.3201/eid2112.141167

Address for correspondence: Marcos de Almeida, Centers for Disease Control and Prevention, 1600 Clifton Rd NE, Mailstop H23-9, Atlanta, GA 30329-4027, USA; email: bnz0@cdc.gov

Molecular Characterization and Antimicrobial Resistance in *Neisseria gonorrhoeae*, Nunavut Region of Inuit Nunangat, Canada, 2018–2019

Ameeta E. Singh, Jasmine Pawa, Kethika Kulleperuma, Errol Prasad, Sonia Marchand, K. Dionne, Maxim Trubnikov, Tom Wong, Michael R. Mulvey, Irene Martin

We assessed antimicrobial resistance (AMR) in *Neisseria gonorrhoeae* in Nunavut, Canada, using remnant gonorrhea nucleic acid amplification test–positive urine specimens. This study confirms the feasibility of conducting *N. gonorrhoeae* AMR surveillance and highlights the diversity of gonococcal sequence types and geographic variation of AMR patterns in the territory.

In 2015, the prevalence of *Neisseria gonorrhoeae* reported in the territory of Nunavut, Canada, 837.6 cases/100,000 residents, was 15 times the national rate in Canada (55.4 cases/100,000 residents) (*1*). Gonorrhea is a notifiable disease in Nunavut, and all positive cases are reported to the department of health. Globally, reports are increasing of *N. gonorrhoeae* with resistance to currently recommended first-line antimicrobial treatment agents (*2*). These resistance rates in some global regions approach or exceed World Health Organization thresholds of 5% to warrant changes to the prescribed gonorrhea treatments (*3*).

The Gonococcal Antimicrobial Surveillance Program of Canada is a culture-based laboratory surveillance system monitoring antimicrobial resistance (AMR) trends and gonococcal sequence types (STs) in *N. gonorrhoeae* (*4*). Traditionally, *N. gonorrhoeae* AMR surveillance has required obtaining cultures from patients for phenotypic testing. In the Canadian Arctic regions, including Nunavut, no information has been available on the prevalence and distribution of *N. gonorrhoeae* AMR patterns because long transport times and conditions preclude transporting cultures; assessment is exclusively done by using nucleic acid amplification tests (NAATs). The National Microbiology Laboratory (Winnipeg, Manitoba, Canada) has addressed this issue by developing molecular assays to predict AMR and molecular STs from remnant NAAT specimens. We sought to assess the prevalence and distribution of AMR *N. gonorrhoeae* STs in Nunavut using NAAT-tested *N. gonorrhoeae*–positive specimens.

Authors Affiliations: University of Alberta, Edmonton, Alberta, Canada. (A.E. Singh); Government of Nunavut, Iqaluit, Nunavut, Canada (J. Pawa, K. Kulleperuma); DynaLIFE Medical Labs, Edmonton (E. Prasad); Qikiqtani General Hospital Laboratory, Iqaluit, Nunavut (S. Marchand, K. Dionne); Indigenous Services Canada, Ottawa, Ontario, Canada (M. Trubnikov, T. Wong); National Microbiology Laboratory, Winnipeg, Manitoba, Canada (M.R. Mulvey, I. Martin)

DOI: https://doi.org/10.3201/eid2706.204407

The Study

Nunavut, at 1,877,787 km^2 the largest territory in Canada, is divided into 3 regions: Qikiqtaaluk (also called Qikiqtani) in the east, Kivalliq in the center, and Kitikmeot in the west. Nunavut's reported 2016 population was 35,994 (*5*), ≈85% of whom identify as Inuit (*6*). Nunavut is one region in Inuit Nunangat, a Canadian Inuktitut term inclusive of the land, water, and ice of the Inuit homeland (*7*).

For this study we used remnant *N. gonorrhoeae* NAAT–positive specimens collected in Nunavut for routine gonococcal diagnostics during January 1, 2018–December 31, 2019. We submitted specimens from the Kitikmeot region to DynaLife Laboratories (https://www.dynalife.ca) and from the Qikiqtaaluk and Kivalliq regions to the Qikiqtani General Hospital Laboratory (Iqaluit, Nunavut, Canada) to the National Microbiology Laboratory for molecular antimicrobial susceptibility prediction using NAATs

and *N. gonorrhoeae* multiantigen sequence typing (NG-MAST). Urine specimens submitted to DynaLife laboratories were tested using the Gen-Probe Aptima Combo 2 test (Hologic, https://www.hologic.com). Testing at the Qikiqtani General Hospital Laboratory was done using the Roche-Cobas test (Roche Molecular Diagnostics, https://diagnostics.roche.com). We did not submit repeat samples or test-of-cure specimens. Ethics approval was obtained from the University of Alberta's Health Research Ethics Board and the Nunavut Research Institute.

We performed NG-MAST as described elsewhere (*8*,*9*). We then tested specimens successfully typed with NG-MAST using single-nucleotide polymorphism (SNP) assays targeting cephalosporin-DS mutations (*ponA*, *mtrR* delA, *porB*, *penA* A311V, *penA* A501, *penA* N513Y, and *penA* G545S), ciprofloxacin-resistance mutations (*gyrA* and *parC*), and azithromycin-resistance mutations (23S rRNA A2059G, C2611T, and *mtrR*) to predict antimicrobial susceptibility. We performed DNA extraction, preparation, real-time PCR, and results analysis as described elsewhere (*9*,*10*). For specimens identified with the same ST, we performed SNP assay testing for a subset of samples and for the remainder of samples within identical ST groups. We inferred AMR profiles based on STs with 4–70 samples if ≥50% of those samples had identical AMR predictions based on SNP results and STs with >70 samples if ≥30 samples were tested with identical AMR predictions. These results are molecular based and have been validated against MIC phenotypes in a previous study (*9*).

All NAAT-tested *N. gonorrhoeae*–positive specimens (n = 1,128) from Nunavut collected between January 1, 2018–December 31, 2019, were included in the study (Table 1). Of these, 106 (9.4%) samples were nontypeable for NG-MAST because of low concentrations of DNA and therefore excluded from further testing. We identified a total of 75 different STs among the remaining 1,022 NAAT-identified isolates from samples submitted from Nunavut (Figure 1). The most prevalent was ST16840 (16.5%), followed by ST5985 (15.3%).

Table 1. Sex and geographic distribution of gonorrhea nucleic acid amplification test positive specimens from Nunavut, Canada, 2018–2019*

Year	Sex	Region			Total by sex	Total
		Kivalliq	Qikiqtaaluk	Kitikmeot		
2018	M	62	112	8	182	432
	F	98	135	17	250	
2019	M	94	166	14	274	696
	F	142	256	22	420	
	Unk	0	0	2	2	
Total		396	669	63		1,128

*Unk, unknown

SNP assay results for predicting AMR were successfully determined for cephalosporin (687 samples), ciprofloxacin (541 samples), and azithromycin (435 samples). We predicted AMR for an additional 289 cephalosporin results, 436 ciprofloxacin results, and 533 azithromycin results on the basis of expected results of prevalent STs tested (Table 2). Within Nunavut, the Qikiqtaaluk region had the highest prevalence of intermediate cephalosporin MICs (51.3%) and resistance to azithromycin (11.3%). The Kivalliq region had the only sample (0.3%) with predicted decreased susceptibility to cephalosporins. We inferred the genetic relationships between the NG-MAST STs by using the maximum-likelihood method and Tamura-Nei model (Figure 2) (*11*,*12*). We predicted most samples in clusters A, B, and D would have elevated

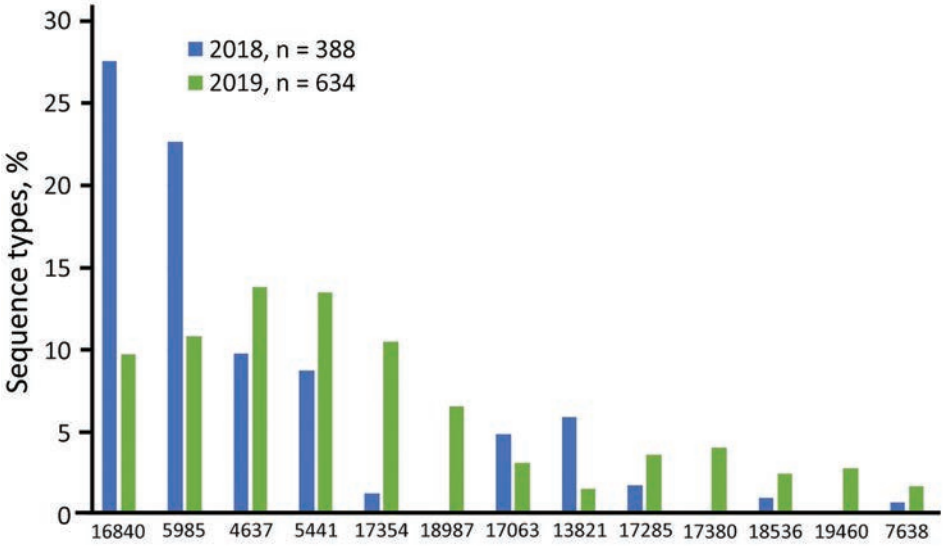

Figure 1. Distribution of prevalent *Neisseria gonorrhoeae* multiantigen sequence typing sequence types of gonorrhea-positive nucleic acid amplification specimens (n = 1,022) from a study of antimicrobial resistance in *N. gonorrhoeae* in the Nunavut region of Inuit Nunangat, Canada, 2018–2019.

Table 2. Predicted AMR of gonorrhea positive nucleic acid amplification specimens from Nunavut, 2018–2019*

Resistance	MICs, mg/L	No. specimens with AMR/no. predicted (%)			
		Qikiqtaaluk	Kivalliq	Kitikmeot	Total
Decreased susceptibility to cephalosporins	≥0.125	0/591 (0)	1/350 (0.3)	0/35 (0)	1/976 (0.1)
Intermediate cephalosporin MICs	0.032–0.063	303/591 (51.3)	49/350 (14.0)	8/35 (22.9)	360/976 (36.9)
Ciprofloxacin resistant	≥1	298/591 (50.4)	50/351 (14.2)	7/35 (20.0)	355/977 (36.3)
Azithromycin resistant	≥2	66/583 (11.3)	2/350 (0.6)	0/35 (0)	68/968 (7.0)

*Denominators indicate predicted number of samples with susceptibility for the given antimicrobial. Not all samples were tested for antimicrobial susceptibilities and not all the samples that were tested gave conclusive results. AMR, antimicrobial resistance.

MICs to cephalosporins but that most samples in cluster C would have azithromycin resistance. We also found that STs were clustered based on geography: in Qikiqtaaluk, we primarily identified STs from clusters A, B and C, but we identified STs from cluster D in all 3 jurisdictions.

Our analysis of routinely collected diagnostic specimens for gonorrhea from Nunavut highlights the usefulness of SNP assays and NG-MAST typing in identifying population-level *N. gonorrhoeae* AMR and delineating transmission patterns (*9*). Current Nunavut treatment guidelines for gonorrhea

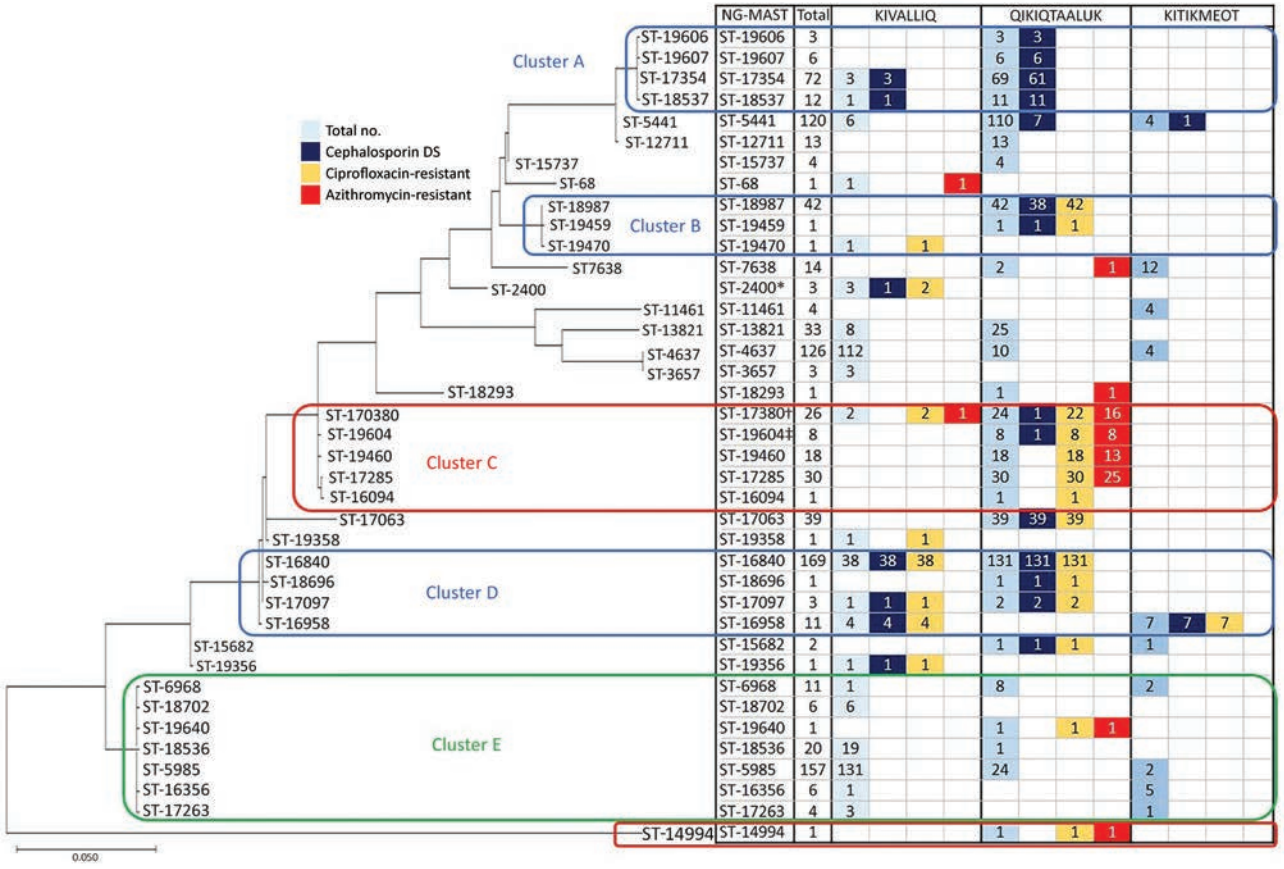

Figure 2. Genetic relationship of *Neisseria gonorrhoeae* multiantigen sequence typing sequence types (STs) of gonorrhea-positive nucleic acid amplification specimens with prevalent and predicted nonsusceptible SNP assay results (n = 975) from a study of antimicrobial resistance in *N. gonorrhoeae* in the Nunavut region of Inuit Nunangat, Canada, 2018–2019. Only prevalent STs or STs whose samples predicted decreased susceptibility to cephalosporins or resistance to ciprofloxacin or azithromycin were included. The evolutionary history was inferred by using the maximum-likelihood method and Tamura-Nei model (*13*). The tree with the highest log likelihood (–4321.41) is shown. Initial trees for the heuristic search were obtained automatically by applying neighbor-joining and BioNJ algorithms to a matrix of pairwise distances estimated using the maximum composite likelihood approach, and then selecting the topology with superior log likelihood value. The tree is drawn to scale, with branch lengths measured in the number of substitutions per site. This analysis involved 39 nucleotide sequences. Codon positions included were 1st+2nd+3rd+Noncoding; a total of 917 positions were in the final dataset. Evolutionary analyses were conducted in MEGA X (*14*). Clusters were identified as STs with ≤5 base pair differences between them. *One of the ST2400 samples was predicted to be cephalosporin decreased susceptibility (not cephalosporin/DS). †The sample that was predicted to be cephalosporin/DS was not azithromycin resistant. ‡The sample that was cephalosporin/DS was also azithromycin resistant. Cephalosporin/DS, cephalosporin intermediate/decreased susceptibility.

recommend dual ceftriaxone/azithromycin therapy (*13*). Although decreased susceptibility to cephalosporins was identified in only 1 sample, the rate of predicted intermediate cephalosporin MICs in Nunavut at 36.9% is >2 times as high as the national rate of 16% in 2018, potentially limiting the long-term use of this agent (*4*). In addition, the 7.0% rate of predicted azithromycin resistance exceeds the World Health Organization threshold of 5% above which a drug is not routinely recommended for treatment (*3*). We also noted substantial geographic variation; the highest prevalence of predicted intermediate cephalosporin MICs (51.3%) and predicted resistance to azithromycin (11.3%) were in the Qikiqtaaluk region. In the adjacent province of Quebec, the reported rate of intermediate cephalosporin MICs was 22% and azithromycin resistance was 11.8% (*4*). NG-MAST typing detected a large number of STs, reflecting the genetic diversity of *N. gonorrhoeae* and suggesting the introduction of multiple strains into the territory.

The first limitation of our study was that no gonococcal cultures were available and cases were compared to national gonococcal cultures, which may not be representative of gonorrhea in all regions. In addition, only urine specimens were collected for gonorrhea in Nunavut. Previous research has highlighted the variability in ST from extragenital sites (*14*,*15*). There are limitations to using culture-independent techniques to predict AMR because specimens often contain low concentrations of DNA, which can limit SNP detection. Gonococcus is also known to mutate easily, which may lead to false-negative results in the SNP assays because of sequence variations in DNA (*9*). A molecular-based approach may overestimate AMR because mutations associated with resistance do not always correlate phenotypically. Finally, we acknowledge the biomedical and technical laboratory approach of this work and the limited partnerships with the Inuit people.

Conclusions

Because research across Inuit Nunangat has historically often been done in an exploitative way that has not respected Inuit self-determination, meaningful partnerships are required to prioritize research activities and develop approaches that add value for and are accepted by communities. Our findings highlight the feasibility of conducting molecular surveillance for *N. gonorrhoeae* AMR using remnant *N. gonorrhoeae*–positive NAAT specimens Data based on these findings can be used to provide Nunavut with up-to-date information about the best choices to treat gonorrhea.

Acknowledgments

We thank Pam Sawatzky, Norman Barairo, and Shelley Peterson for technical assistance.

This project was supported by internal funding from the Public Health Agency of Canada and Indigenous Services Canada.

About the Author

Dr. Singh is a clinical professor with the Division of Infectious Diseases at the University of Alberta in Edmonton. Her primary research interests are clinical and epidemiologic aspects of bacterial STIs, HIV biomedical prevention, and the use of rapid diagnostic tests for diagnosing syphilis and HIV.

References

1. Choudhri Y, Miller J, Sandhu J, Leon A, Aho J. Gonorrhea in Canada, 2010–2015. Can Commun Dis Rep. 2018;44:37–42. https://doi.org/10.14745/ccdr.v44i02a01
2. Unemo M, Seifert HS, Hook III EW, Hawkes S, Ndowa F, et al. Gonorrhoea. Nat Rev Dis Primers. 2019;5:79.
3. World Health Organization, Department of Reproductive Health and Research. Global action plan to control the spread and impact of antimicrobial resistance in *Neisseria gonorrhoeae*. 2012 [cited 2021 Apr 21]. https://www.who.int/reproductivehealth/publications/rtis/9789241503501/en
4. Public Health Agency of Canada, National Microbiology Laboratory. 2020. National surveillance of antimicrobial susceptibilities of *Neisseria gonorrhoeae* annual summary 2018 [cited 2021 Apr 21]. https://www.canada.ca/en/public-health/services/publications/drugs-health-products/national-surveillance-antimicrobial-susceptibilities-neisseria-gonorrhoeae-annual-summary-2018.html
5. Statistics Canada. Population and dwelling count highlight tables, 2016 census [cited 2021 Apr 21]. https://www12.statcan.gc.ca/census-recensement/2016/dp-pd/hlt-fst/pd-pl/Table.cfm?Lang=Eng&T=101&SR=1&S=3&O=D#tPopDwell
6. Nunavut Tunngavik Incorporated. Annual report on the state of Inuit culture and society, 2007–8 [cited 2021 Apr 21]. https://www.tunngavik.com/publications/annual-report-on-the-state-of-inuit-culture-and-society-2007-2008
7. Kanatami IT. National Inuit strategy on research, 2018 [cited 2021 Apr 21]. https://www.itk.ca/wp-content/uploads/2018/04/ITK_NISR-Report_English_low_res.pdf
8. Martin IM, Ison CA, Aanensen DM, Fenton KA, Spratt BG. Rapid sequence-based identification of gonococcal transmission clusters in a large metropolitan area. J Infect Dis. 2004;189:1497–505. PubMed https://doi.org/10.1086/383047
9. Peterson S, Martin I, Demczuk W, Barairo N, Naidu P, Lefebvre B, et al. Multiplex real-time polymerase chain reaction assays for the prediction of cephalosporin, ciprofloxacin, and azithromycin antimicrobial susceptibility of positive *Neisseria gonorrhoeae* nucleic acid amplification test samples. J Antimicrob Chemother. 2020;75:3485–90. https://doi.org/10.1093/jac/dkaa360
10. Trembizki E, Buckley C, Donovan B, Chen M, Guy R, Kaldor J, et al. Direct real-time PCR-based detection of *Neisseria gonorrhoeae* 23S rRNA mutations associated with azithromycin resistance. J Antimicrob Chemother. 2015;70:3244–9.

11. Tamura K, Nei M. Estimation of the number of nucleotide substitutions in the control region of mitochondrial DNA in humans and chimpanzees. Mol Biol Evol. 1993;10:512–26.
12. Kumar S, Stecher G, Li M, Knyaz C, Tamura K. MEGA X: molecular evolutionary genetics analysis across computing platforms. Mol Biol Evol. 2018;35:1547–9. https://doi.org/10.1093/molbev/msy096
13. Gonorrhea public health protocol. Nunavut communicable disease and surveillance manual. Iqaluit (Canada): Nunavut Department of Health. 2018.
14. Didelot X, Dordel J, Whittles LK, Collins C, Bilek N, Bishop CJ, et al. Genomic analysis and comparison of two gonorrhea outbreaks. mBio. 2016;7:e00525–16. https://doi.org/10.1128/mBio.00525-16
15. Ota KV, Fisman DN, Tamari IE, Smieja M, Ng L-K, Jones KE, et al. Incidence and treatment outcomes of pharyngeal *Neisseria gonorrhoeae* and *Chlamydia trachomatis* infections in men who have sex with men: a 13-year retrospective cohort study. Clin Infect Dis. 2009;48:1237–43. https://doi.org/10.1086/597586

Address for correspondence: Ameeta Singh, University of Alberta, Edmonton, 3B20-111 Jasper Ave, Edmonton, AB T5K 0L4, Canada; email: ameeta@ualberta.ca

Leishmaniases in the European Union and Neighboring Countries

Eduardo Berriatua, Carla Maia, Cláudia Conceição, Yusuf Özbel, Seray Töz, Gad Baneth, Pedro Pérez-Cutillas, Maria Ortuño, Clara Muñoz, Zarima Jumakanova, Andre Pereira, Rafael Rocha, Begoña Monge-Maillo, Elkhan Gasimov, Yves Van der Stede, Gregorio Torres, Céline M. Gossner

A questionnaire survey of animal and human health authorities in Europe revealed that leishmaniases are not notifiable in all countries with autochthonous cases. Few countries implement surveillance and control targeting both animal and human infections. Leishmaniases are considered emergent diseases in most countries, and lack of resources is a challenge for control.

Leishmaniases are endemic in humans and animals in part of the European Union (EU) and its neighboring countries. *Leishmania* species in this region are *L. major*, *L. tropica,* and the *L. donovani* complex species (including *L. infantum* and *L. donovani* sensu stricto). All cause cutaneous leishmaniasis (CL); visceral leishmaniasis (VL) is caused mainly by *L. donovani* complex species. There is evidence that the risk for leishmaniases is increasing in some EU and neighboring countries (*1*). We conducted a questionnaire survey to gather information on the epidemiologic situation, surveillance, prevention and control measures, and drivers of emergence of animal and human leishmaniases in this region during 2010–2020.

The Study

The survey included an animal leishmaniasis (AniL) questionnaire referring to *L. infantum* infections in domestic or wildlife hosts and a human leishmaniases (HumL) questionnaire referring to infections by *L. infantum*, *L. major*, *L. tropica* and *L. donovani* s.s. (Appendix, https://wwwnc.cdc.gov/EID/article/27/6/21-0239-App1.pdf). The target audience was the national focal points (national institutes or ministries) of the European Centre for Disease Prevention and Control, the World Health Organization, the European Food Safety Authority, and the World Organisation for Animal Health in countries in which leishmaniases are endemic or those with confirmed or suspected presence of sand fly vectors (*2*). These countries were Albania, Algeria, Armenia, Austria, Azerbaijan, Belgium, Bosnia and Herzegovina, Bulgaria, Croatia, Cyprus, Czechia, Egypt, France, Georgia, Germany, Greece, Hungary, Israel, Italy, Jordan, Kosovo, Lebanon, Libya, Liechtenstein, Luxembourg, Malta, Moldova, Montenegro, Morocco, North Macedonia, Palestine, Portugal, Romania, Serbia, Slovakia, Slovenia, Spain, Tunisia, Turkey, and Ukraine (Figure 1). The questionnaires were administered electronically using the EU survey tool and shared on September 11, 2020 (*3*). Twenty-seven countries (70%) replied to the AniL questionnaire and 24 countries (60%) to the HumL questionnaires; 19 countries (48%) replied to both (Table 1).

We reviewed the countries' epidemiologic status with regards to autochthonous *Leishmania* spp. infections in animals and humans and clinical forms in humans. The mapping of the countries with autochthonous transmission matches previous published information with few discrepancies. For instance, according to the questionnaire, Bosnia and Herzegovina and Hungary do not have autochthonous canine leishmaniasis cases, although such cases have been described (*4*,*5*). Human cases of leishmaniasis due to *L. tropica* were reported in Cyprus and Serbia and due to *L. major* in Georgia; however, none of the literature presents concurring evidence (Table 2).

Animal leishmaniases are notifiable in 17 countries and human leishmaniases in 20 countries (Table 1; Figure 2). In Palestine and Turkey, AniL is not notifiable despite a high prevalence among dogs (*6*,*7*). Similarly,

Author affiliations: Universidad de Murcia, Murcia, Spain (E. Berriatua, P. Pérez-Cutillas, M. Ortuño, C. Muñoz, Z. Jumakanova); Universidade NOVA de Lisboa, Lisbon, Portugal (C. Maia, C. Conceição, A. Pereira, R. Rocha); Ege University, Izmir, Turkey (Y. Özbel, S. Töz); The Hebrew University of Jerusalem, Rehovot, Israel (G. Baneth); Instituto Ramón y Cajal de Investigación Sanitaria, Madrid, Spain (B. Monge-Maillo); World Health Organization Regional Office for Europe, Copenhagen, Denmark. (E. Gasimov); European Food Safety Authority, Parma, Italy (Y. Van der Stede); World Organisation for Animal Health, Paris, France (G. Torres); European Centre for Disease Prevention and Control, Stockholm, Sweden (C.M. Gossner)

DOI: https://doi.org/10.3201/eid2706.210239

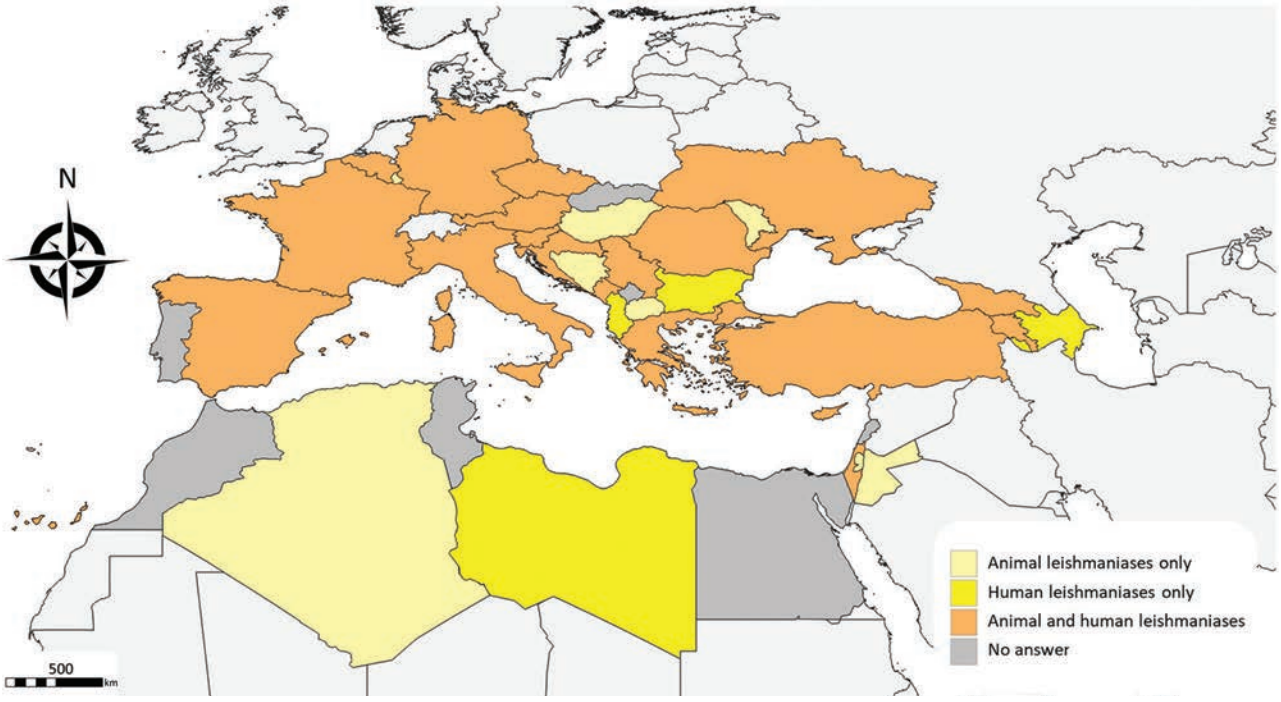

Figure 1. Geographic distribution of countries that responded to survey questionnaires about animal and human leishmaniases in Europe, 2020.

in France, neither AniL nor HumL are notifiable although the diseases are endemic in the south (*8*). Leishmaniases surveillance is not mandatory at the EU level which constitutes a limitation for successful control.

Seven countries conduct AniL surveillance (Table 1), indicative of its low priority among the animal health authorities. The target animal population for surveillance included symptomatic and asymptomatic dogs in Armenia, Cyprus, Italy, Spain, and Ukraine; we also studied wildlife in leishmaniasis foci in Spain. Testing subclinically infected dogs indicated awareness of their role as reservoirs of the parasite (*1*). Similarly, wild lagomorphs were the main reservoir of *L. infantum* in a HumL outbreak in Madrid in Spain (*9*). Surveillance of HumL is conducted in 19 countries, including all of those with autochthonous infections except Serbia (Table 1).

Antibody tests, including the immunofluorescence antibody test, ELISA, and the rapid immunochromatography test, are the main surveillance diagnostic methods used, followed by PCR. Antibody tests play a fundamental role in disease surveillance because they are relatively cheap and easy to use (*10*). However, their sensitivity to detect subclinical infections is lower than that of PCR tests (*10*), and they do not discriminate naturally infected from vaccinated dogs (*11*). PCR tests are ideal for epidemiologic studies to estimate *Leishmania* spp. infection prevalence in healthy hosts, but their diagnostic validity depends on the sample used, the DNA sequence target, and the PCR protocol. Standardization of PCR tests in leishmaniasis diagnosis is needed (*12*).

Of the 7 countries that have ongoing AniL prevention and control programs (Table 1), 5 use topical insecticides for dogs, 5 are diagnosing and treating leishmaniases in dogs, and 2 use canine leishmaniosis vaccines. In all countries, infected dogs may be euthanized on welfare grounds. Lack of funds and treatment costs were considered the most important AniL control challenges. Human leishmaniasis prevention and control activities are implemented in 12 countries (Table 1); for *L. infantum*, actions focused on the use of insecticides on dogs, and for *L. major*, *L. tropica*, and *L. donovani*, the common activity was the use of peridomiciliary and intradomiciliary insecticides. Lack of funds and capacity constraints are considered the main challenges for HumL.

Although zoonotic *L. infantum* strategies are centered on preventing and eliminating infections in dogs, the main parasite reservoir host, we found that insecticides and treatments are not fully effective and are expensive, and so provided to a relatively small proportion of dogs. Leishmaniasis control needs the One Health approach to account for the complexity of its transmission cycle involving humans, domestic animals, wildlife, and sand fly vectors (*13*).

Animal leishmaniases are considered emergent diseases in Cyprus and Jordan and in parts of Algeria,

Table 1. Declared country status of leishmaniases surveillance and control, 2010–2020*

	Autochthonous		Notifiable		Surveillance		Control	
Country	Animal	Human	Animal	Human	Animal	Human	Animal	Human
Albania	NR	VL, CL	NR	Yes	NR	Yes	NR	No
Algeria	Yes	NR	Yes	NR	Yes	NR	Yes	NR
Armenia	Yes	VL	Yes	Yes	Yes	Yes	Yes	Yes
Austria	Not known	No	No	No	No	No	No	No
Azerbaijan	NR	VL, CL	NR	Yes	NR	Yes	NR	Yes
Belgium	No	No	No	No	No	Yes	No	No
Bosnia and Herzegovina	No	NR	Yes	NR	No	NR	No	NR
Bulgaria	NR	VL	NR	Yes	NR	Yes	NR	Yes
Croatia	Yes	VL, CL	Yes	Yes	No	Yes	No	Not known
Cyprus	Yes	VL, CL	Yes	Yes	Yes	Yes	No	No
Czechia	Not known	No	Yes	Yes	No	No	No	No
France	Yes	VL, CL	No	No	No	Yes	No	No
Georgia	Yes	VL	Yes	Yes	No	Yes	No	Yes
Germany	Not known	No	No	No	No	No	No	No
Greece	Yes	VL, CL	Yes	Yes	No	Yes	Yes	Yes
Hungary	Not known	NR	No	NR	No	NR	No	NR
Israel	Yes	VL, CL	Yes	Yes	No	Yes	No	Yes
Italy	Yes	VL, CL	Yes	Yes	Yes	Yes	Yes	Yes
Jordan	Yes	NR	Yes	NR	No	NR	No	NR
Libya	NR	VL, CL	NR	Yes	NR	Yes	NR	Yes
Luxemburg	Not known	NR	No	NR	No	NR	No	NR
Malta	NR	VL, CL	NR	Yes	NR	Yes	NR	Yes
Moldova	No	NR	Yes	NR	No	NR	No	NR
Montenegro	No	VL	Yes	Yes	No	Yes	Yes	No
North Macedonia	Yes	NR	Yes	NR	Yes	NR	Yes	NR
Palestine	Yes	NR	No	NR	No	NR	Yes	NR
Romania	Yes	No	No	Yes	No	No	No	Not known
Serbia	Yes	VL, CL	No	No	No	No	No	Yes
Slovenia	Yes	No	Yes	Yes	No	Yes	No	No
Spain	Yes	VL, CL	Regionally	Yes	Yes	Yes	No	Yes
Turkey	Yes	VL, CL	No	Yes	No	Yes	No	Yes
Ukraine	Yes	VL	Regionally	Yes	Yes	Yes	No	No

*Data source: questionnaires survey on animal and human leishmaniases to national focal points of the European Centre for Disease Prevention and Control, the World Health Organization, the European Food Safety Authority, and the World Organisation for Animal Health; survey conducted in 2020.
CL, cutaneous leishmaniases; NR, no response; VL, visceral leishmaniases.

Armenia, France, Georgia, Jordan, Montenegro, North Macedonia, Romania, Slovenia, Turkey, and Ukraine. The most important AniL emergence risk factor is the lack of control. Human leishmaniases are considered emerging diseases in Cyprus, Libya and Malta and in parts of Albania, Austria, Armenia, Azerbaijan, Georgia, Israel, Italy, Montenegro, and Spain. The main risk factors for HumL emergence are vector expansion for *L. infantum*, and movement of infected persons between countries for *L. major*, *L. tropica*, and *L. donovani*.

In general, the perceived increasing risk for AniL and HumL was in line with the literature. In the EU and its neighborhood, the risks include movement of humans and dogs, increased number of immunosuppressed patients, climate warming, and other environmental changes affecting vector and reservoir host distribution (*1*,*14*). Limitations associated with existing surveillance and control programs, along with the fact that leishmaniases are often regarded as a local problem rather than a transnational problem, are deemed major obstacles to overcome to prevent leishmaniases emergence in the EU and its neighborhood.

Conclusions

Leishmaniases are considered widespread, endemic, or emerging infections in the EU and its neighborhood, yet are neglected and underreported because they are low priority at the country and EU level. Our study revealed a clear need to strengthen leishmaniasis prevention and control programs in the EU and its neighborhood. We recommend analysis of leishmaniasis incidence in the region for an objective assessment of disease emergence, and also improvement of prevention and control programs based on a robust surveillance and following a One Health approach.

Acknowledgments

We thank experts from the public health institutes, animal health institutes, ministries of health, and ministries of agriculture from Albania, Algeria, Armenia, Austria, Azerbaijan, Belgium, Bosnia and Herzegovina, Bulgaria, Croatia, Cyprus, Czechia, France, Georgia, Germany, Greece, Hungary, Israel, Italy, Jordan, Libya, Luxembourg, Malta, Moldova, Montenegro, North Macedonia, Palestine, Romania, Serbia, Slovenia, Spain, Turkey, and Ukraine for

taking the time to answer the questionnaires and providing us the information used to prepare this review on leishmaniasis. In particular, we thank: Silva Bino, Adela Vasili and Teita Myrseli (Albania), Ahmed Chawki El Karim Boughalem (Algeria), Arman Gevoryan, Lusine Paronyan and Narek Hayrapetyan (Armenia), Irene Kászoni-Rückerl and Julia Walochnik (Austria), Yagut Garayeva (Azerbaijan), Javiera Rebolledo (Belgium), Aleksandar Nemet (Bosnia and Herzegovina), Rumen Harizanov (Bulgaria), Tihana Miškić, Ivana Lohman Janković and Eddy Listeš (Croatia), Maria G. Koliou and Vasiliki Christodoulou (Cyprus), Jerome Depaquit, Laurence Lachaud, Christophe Ravel and Patrick Bastien (France), Merab Iosava and Tegniz Chaligava (Georgia),

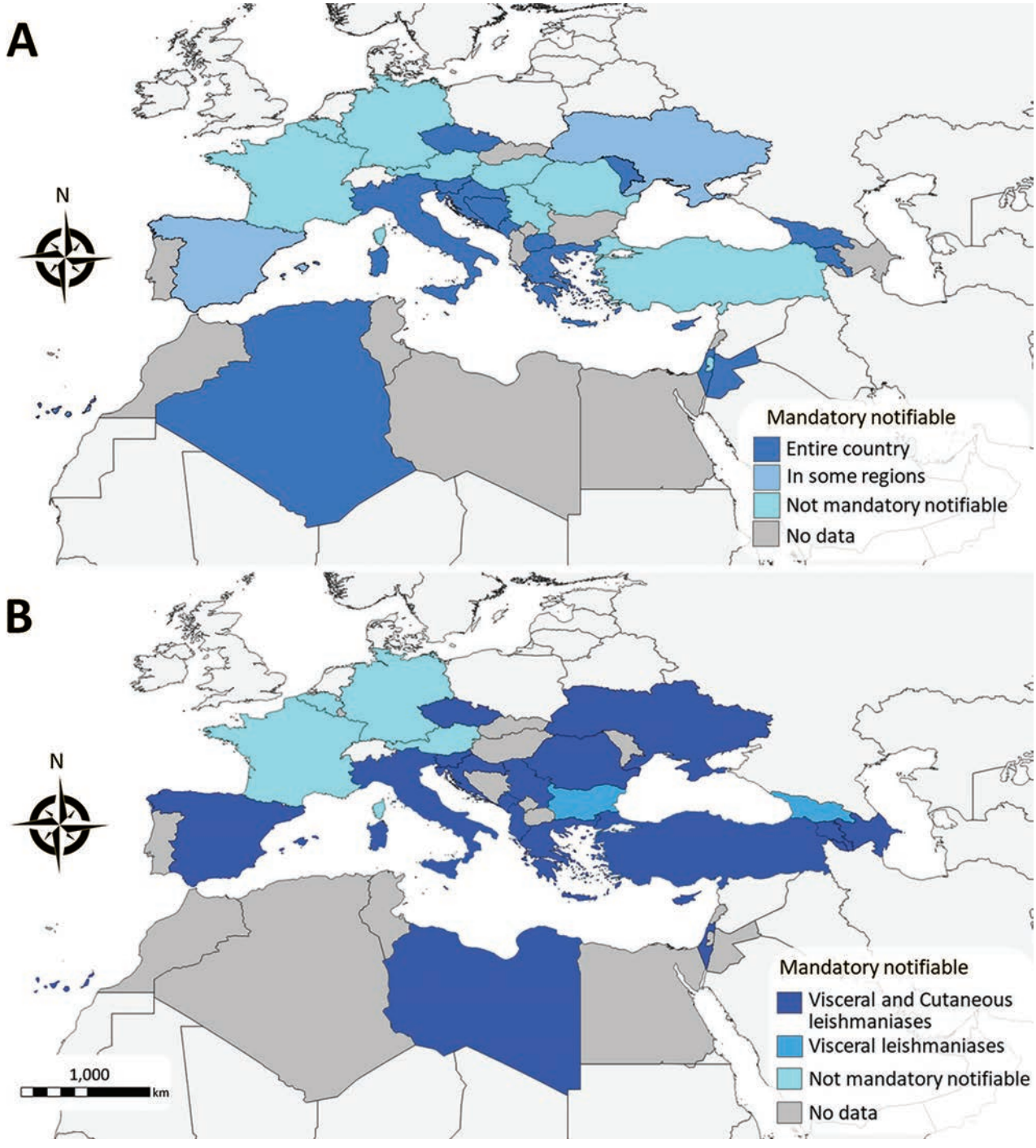

Figure 2. Geographic distribution of mandatory notification status for animal (A) and human (B) leishmaniases, 2020.

Table 2. Declared status of endemicity of *Leishmania* spp. affecting humans, by country

Country	*Leishmania* species			
	L. infantum	*L. major*	*L. tropica*	*L. donovani*
Albania	Yes	No	No	No
Armenia	Yes	No	No	No
Austria	No	No	No	No
Azerbaijan	Yes	Yes	Yes	No
Belgium	No	No	No	No
Bulgaria	Yes	No	No	No
Croatia	Not known	Not known	Not known	Not known
Cyprus	No	No	Yes	Yes
Czechia	No	No	No	No
France	Yes	No	No	No
Georgia	Yes	Yes	No	No
Germany	No	No	No	No
Greece	Yes	No	No	No
Israel	Yes	Yes	Yes	No
Italy	Yes	No	No	No
Libya	Yes	Yes	Yes	Not known
Malta	Yes	No	No	No
Montenegro	Yes	Not known	Not known	No
Romania	No	No	No	No
Serbia	Yes	Not known	Yes	No
Slovenia	No	No	No	No
Spain	Yes	No	No	No
Turkey	Not known	Not known	Yes	Not known
Ukraine	No	No	No	No

Franz J. Conraths (Germany), Danai Pervanidou and Michail Floros (Greece), Tamás Sréter (Hungary), Emilia Anis, Roee Singer, Yael Glazer and Michel Bellaiche (Israel), Alda Natale, Gianluca Rugna, Mose' Alise, Patrizia Parodi, Luigi Gradoni and Pellegrino Daniele (Italy), Mahmoud Alhanatleh (Jordan), Badereddin Annajar (Libya), Maxim Sirbu (Moldova), Mevlida Hrapovic and Nebojša Sekulić (Montenegro), Iyad Adra (Palestine), Alexandru Supeanu and Cristina Daniela Pop (Romania), Mitra Drakulovic and Sasa Ostojic (Serbia), Maja Sočan (Slovenia), Beatriz Fernández Martínez, Francisco Javier Moreno Nuncio, Francisco Javier Nieto Martínez, Soledad Collado Cortés, Jose Luis Sáez Llorente and Alejandro Pérez Riquelme (Spain), Anil Demeli, Ahmet Deniz and Seher Topluoglu (Turkey) and Ihor Kuzin (Ukraine). In addition, we thank Tamás Bakonyi for reviewing and testing the questionnaire.

Y.V.d.S. is employed with the European Food Safety Authority (EFSA) in the ALPHA Unit that provides scientific and administrative support to EFSA's scientific activities in the area of Animal Health and Welfare. The positions and opinions presented in this article are those of the authors alone and are not intended to represent the views or scientific work of EFSA.

About the Author

Dr. Berriatua is a professor of animal health at the University of Murcia in Spain, where he teaches and conducts research on the epidemiology and ecology of parasitic diseases and specifically leishmaniases.

References

1. Gradoni l. the leishmaniases of the Mediterranean region. Curr Trop Med Rep. 2017;4:21–6. https://doi.org/10.1007/s40475-017-0099-1
2. European Centre for Disease Prevention and Control. VectorNet, Phlebotomine sandflies maps. 2021 [cited 2021 Mar 19]. https://www.ecdc.europa.eu/en/disease-vectors/surveillance-and-disease-data/phlebotomine-maps
3. European Commission. EUSurvey, version 1.5. 2021 [cited 2021 Mar 15]. https://ec.europa.eu/eusurvey/home/welcome
4. Colella V, Hodžić A, Iatta R, Baneth G, Alić A, Otranto D. Zoonotic leishmaniasis, Bosnia and Herzegovina. Emerg Infect Dis. 2019;25:385–6. https://doi.org/10.3201/eid2502.181481
5. Tánczos B, Balogh N, Király L, Biksi I, Szeredi L, Gyurkovsky M, et al. First record of autochthonous canine leishmaniasis in Hungary. Vector Borne Zoonotic Dis. 2012;12:588–94. https://doi.org/10.1089/vbz.2011.0906
6. Hamarsheh O, Nasereddin A, Damaj S, Sawalha S, Al-Jawabreh H, Azmi K, et al. Serological and molecular survey of *Leishmania* parasites in apparently healthy dogs in the West Bank, Palestine. Parasit Vectors. 2012;5:183. https://doi.org/10.1186/1756-3305-5-183
7. Ozbel Y, Oskam L, Ozensoy S, Turgay N, Alkan MZ, Jaffe CL, et al. A survey on canine leishmaniasis in western Turkey by parasite, DNA, and antibody detection assays. Acta Trop. 2000;74:1–6. https://doi.org/10.1016/S0001-706X(99)00047-9
8. Lachaud L, Dedet JP, Marty P, Faraut F, Buffet P, Gangneux JP, et al.; Working Group for the Notification of Human Leishmanioses in France. Surveillance of leishmaniases in France, 1999 to 2012. Euro Surveill. 2013;18:20534. https://doi.org/10.2807/1560-7917.ES2013.18.29.20534
9. Carrillo E, Moreno J, Cruz I. What is responsible for a large and unusual outbreak of leishmaniasis in Madrid? Trends Parasitol. 2013;29:579–80. https://doi.org/10.1016/j.pt.2013.10.007
10. Thakur S, Joshi J, Kaur S. Leishmaniasis diagnosis: an update on the use of parasitological, immunological, and molecular methods. J Parasit Dis. 2020 Mar 16;44:1–20.
11. Solano-Gallego L, Cardoso L, Pennisi MG, Petersen C, Bourdeau P, Oliva G, et al. Diagnostic challenges in the era of canine *Leishmania infantum* vaccines. Trends Parasitol. 2017;33:706–17. https://doi.org/10.1016/j.pt.2017.06.004
12. Varani S, Ortalli M, Attard L, Vanino E, Gaibani P, Vocale C, et al. Serological and molecular tools to diagnose visceral leishmaniasis: 2-years' experience of a single center in Northern Italy. PLoS One. 2017;12:e0183699. https://doi.org/10.1371/journal.pone.0183699
13. Palatnik-de-Sousa CB, Day MJ. One Health: the global challenge of epidemic and endemic leishmaniasis. Parasit Vectors. 2011;4:197. https://doi.org/10.1186/1756-3305-4-197
14. Wright I, Jongejan F, Marcondes M, Peregrine A, Baneth G, Bourdeau P, et al. Parasites and vector-borne diseases disseminated by rehomed dogs. Parasit Vectors. 2020;13:546. https://doi.org/10.1186/s13071-020-04407-5

Address for correspondence: Céline M. Gossner, European Centre for Disease Prevention and Control, Gustav III:s Boulevard 40, 168 73 Solna, Sweden; email: celine.gossner@ecdc.europa.eu

Brucellosis Outbreak Traced to Commercially Sold Camel Milk through Whole-Genome Sequencing, Israel

Svetlana Bardenstein, Rachel E. Gibbs, Yael Yagel, Yair Motro, Jacob Moran-Gilad

Brucellosis, a neglected zoonotic disease acquired from contaminated food products, remains a public health concern worldwide. We describe an outbreak in which commercially sold camel milk containing *Brucella melitensis* was distributed across Israel. Whole-genome sequencing linked patients infected with *B. melitensis* to wholesale camel milk and unregulated livestock trade.

Brucellosis, caused by bacteria of the *Brucella* genus, is a neglected zoonotic disease that affects marginalized populations worldwide (*1*). Human transmission occurs mainly through consumption of unpasteurized, contaminated dairy products from infected, domesticated animals. In Israel, brucellosis primarily affects Arab populations, especially the seminomadic Bedouin tribal communities in southern Israel (*2*).

Dromedary camels, which are capable of asymptomatic carriage of *Brucella*, are valuable domesticated animals in Bedouin culture, and unpasteurized camel milk has gained international popularity because of its alleged medicinal properties. Few reported brucellosis outbreak investigations involving camel milk have described families infected by milk from privately owned camels and have used serologic testing to confirm diagnoses (*3*,*4*). The standard tool for molecular typing of *Brucella* has been multilocus variable-number tandem-repeat analysis or multilocus sequence typing (MLST). However, whole-genome sequencing (WGS) is increasingly used for the study of genomic epidemiology of *B. melitensis* (*5*).

Author affiliations: Kimron Veterinary Institute, Ministry of Agriculture and Rural Development, Beit Dagan, Israel (S. Bardenstein); Ben Gurion University of the Negev School of Public Health, Beer Sheva, Israel (R.E. Gibbs, Y. Yagel, Y. Motro, J. Moran-Gilad)

DOI: https://doi.org/10.3201/eid2706.204902

We report an outbreak of human brucellosis with unique epidemiologic characteristics, which originated from commercial, single-brand, unpasteurized camel milk; infection was diagnosed in 19 patients with a common exposure history over 4 months. We demonstrate the utility of WGS for brucellosis outbreak investigations.

The Study

From July–November 2016, the Israeli Ministry of Health noted an increase in brucellosis cases in non-Arab patients in central and northern Israel, raising suspicion of a common source (Figure 1). An epidemiologic investigation noted patients were exposed to the same brand of camel milk. A total of 20 isolates were obtained from 19 patients across Israel (nos. 1–20; Table). Patients from shared households included 2 pairs of siblings and 1 married couple. We studied 2 isolates (nos. 1, 2) from an infant from whom *B. melitensis* was isolated from blood and cerebrospinal fluid. We also included 1 person (isolate no. 12) who consumed camel milk of an unknown brand.

The suspected vendor obtained milk from a Bedouin camel farm in southern Israel (Figure 1). Field investigation of the farm revealed 32 female and 2 male camels. A total of 4 female camels had positive serologic test results for *Brucella*, but none were available for further testing. We sampled 6 bottles of camel milk obtained from a natural food store carrying the suspected brand and recovered a few colonies of *B. melitensis* from 3 of the bottles.

Clinical isolates were submitted to the National Brucellosis Reference Laboratory (Kimron Veterinary Institute, Beit Dagan, Israel) for confirmation, and milk samples were cultured at the same laboratory. In total, 10 *B. melitensis* human isolates from the outbreak and 3 camel milk isolates (nos. 21–23) from the implicated source were available for sequencing. An additional 4

epidemiologically unrelated isolates were sequenced and used as outliers, including 1 isolate from camel milk (no. 24), 2 isolates from patients with *B. melitensis* with no camel milk exposure (nos. 26, 27), and 1 isolate from an unrelated patient with *B. melitensis* acquired after consuming camel milk (no. 25). Finally, we used a *B. melitensis* reference genome sequence from the National Center for Biotechnology Information Sequence Read Archive database (no. 28).

DNA was extracted from *Brucella* isolates by heat killing (80 C°, 10 min) and by using the DNeasy Blood & Tissue kit (QIAGEN, https://www.qiagen.com). Genomic libraries were prepared with a Nextera Flex kit (Illumina, https://www.illumina.com) and subjected to paired-end sequencing by using the Illumina Miseq or Nextseq platforms. Sequences have been deposited in the European Nucleotide Archive (BioProject PRJEB43660).

Figure 1. Geographic distribution of cases of *Brucella melitensis* traced to consumption of commercialized camel milk in Israel, 2016. Shown are the location of the camel farm in southern Israel from which raw milk was obtained), the vendor in central Israel that distributed the milk through direct online sales or other retail stores, and the places of residence of individual case-patients linked to the outbreak.

We used WGS to analyze a total of 18 isolates: 10 human isolates, 3 camel milk isolates, 4 outlier isolates, and 1 reference sequence. Raw sequences underwent quality control using fastQC version 0.11.8 (*6*). We assembled sequence reads that passed QC by the pipeline shovill version 1.0.4 with Trimmomatic version 0.39, SPAdes version 3.13.1, and Pilon version 1.23 with the parameters "–trim –opts –sc" (*7*). We implemented in silico MLST with MLST version 2.10 per the pubMLST *Brucella* spp. Scheme (*8*,*9*). We conducted core genome single-nucleotide polymorphism (SNP) analysis of the WGS assemblies by using ekidna version 0.3.2 (*10*). The sequence from isolate 2 was selected for reference with complete assembly of 3,297,563 bases (Appendix Table 1, https://wwwnc.cdc.gov/EID/article/27/6/20-4902-App1.pdf). We masked resulting core genome SNPs for recombination events using Gubbins version 2.3.4 (*11*) and visualized the final SNP alignment as a minimum-spanning tree created by PHYLOViZ2 (*12*).

We assigned all isolates to sequence type 8 by using in silico MLST. Core genome SNP analysis found 2,443 SNP sites with the sequence from isolate 2 for reference. The phylogenetic tree demonstrated 1 main cluster including 8 human outbreak isolates and all 3 isolates from camel milk (Figure 2). Two human outbreak isolates (nos. 4, 9) did not belong to the main cluster, suggesting ≥1 clone might have caused the outbreak. Isolate 12 clustered with outbreak isolates, confirming that the case-patient who consumed an unknown brand of camel milk was part of the outbreak. Outlier sequences (nos. 25, 27, 28) were genetically distinct from outbreak isolates, expectedly. However, outliers (nos. 26, 24) clustered with outbreak isolates, suggesting an unrecognized epidemiologic link between Bedouin camel farming and outbreak source.

Conclusions

We describe an outbreak of brucellosis unique in its patient population, source of infection, chain of transmission, and use of WGS. Prior outbreak investigations of brucellosis have seldom used WGS to link the outbreak with samples from the implicated source. Here, WGS exposed genetic linkage between bottled camel milk and 8 isolates from 7 patients, providing conclusive evidence of this common source. Isolates obtained from the same person (nos. 1, 2) and that person's sibling (no. 3) clustered tightly, providing internal validity to the discriminative power of WGS. WGS also associated isolate no. 12 (unknown camel milk brand) with the outbreak.

Two isolates (nos. 4, 9) from cases clustered apart from the outbreak strains. Because 4 female camels at the

Table. *Brucella melitensis* isolates included in the study of brucellosis outbreak traced to commercially sold camel milk through whole-genome sequencing, Israel*

Isolate no.	Sequenced	Origin	Age	Location	Relationship	Date of culture confirmation	Source
1	Yes	Human	Child	Jerusalem	Siblings	2016 Aug 30	Blood
2	Yes					2016 Aug 30	CSF
3	Yes	Human	Child	Jerusalem		2016 Oct 15	Blood
4	Yes	Human	Adult	Gan Haim	Married	2016 Jul 20	Blood
5	No	Human	Adult	Gan Haim		2016 Jul 20	Blood
6	Yes	Human	Child	Even Yehuda	Siblings	2016 Oct 7	Blood
7	No	Human	Child	Even Yehuda		2016 Jul 20	Blood
8	Yes	Human	Adult	Tel Aviv	None	2016 Aug 30	Blood
9	Yes	Human	Adult	Jerusalem	None	2016 Aug 14	Blood
10	Yes	Human	Adult	Herzeliya	None	2016 Oct 26	Blood
11	Yes	Human	Child	Elad	None	2016 Aug 3	Blood
12	Yes	Human	Adult	Tirat HaKarmel	None	2016 Nov 20	Blood
13	No	Human	Adult	Kochav Yair	None	2016 Aug 20	Blood
14	No	Human	Adult	Kochav Yair	None	2016 Aug 9	Blood
15	No	Human	Child	Ramat Yishai	None	2016 Sep 23	Blood
16	No	Human	Adult	Kochav Yair	None	2016 Jul 7	Blood
17	No	Human	Adult	Tzalfon	None	2016 Jul 15	Blood
18	No	Human	Adult	Carmiel	None	2016 Aug 8	Blood
19	No	Human	Adult	Haifa	None	2016 Aug 20	Blood
20	No	Human	Adult	Hadera	None	2016 Aug 10	Blood
21	Yes	Camel milk	NA	Food store	None	2017 Jan 15	Milk
22	Yes	Camel milk	NA	Food store	None	2017 Jan 15	Milk
23	Yes	Camel milk	NA	Food store	None	2017 Jan 15	Milk
24	Yes	Camel milk outlier	NA	Rahat	NA	2016 Jul 6	Milk
25	Yes	Human outlier case	NA	Taibe	NA	2016 Jul 11	Blood
26	Yes	Human outlier case	NA	Hebron	NA	2017	Blood
27	Yes	Human outlier case	NA	Haifa	NA	2017	Blood
28	Yes	Reference sequence (SRR4038984†)	NA	NA	NA	NA	NA

*CSF, cerebrospinal fluid; NA, not applicable.
†National Center for Biotechnology Information Sequence Read Archive database.

implicated farm had positive *Brucella* serologic test results, they might have harbored several different strains of *B. melitensis*, which could explain these results. We acquired all bottles of camel milk sampled during a single day, representing just 1 batch, and other batches were not tested. Therefore, the presence of additional clones implicated in this outbreak could not be ascertained.

Surprisingly, isolates 24 and 26 clustered with the outbreak strains, suggesting an unrecognized epidemiologic chain of transmission. This finding could reflect patterns of unregulated animal trade in Israel in which domesticated animals, including camels, are trafficked from Hebron (origin of isolate 26) throughout the Negev region to Bedouin communities (in this case Rahat [origin of isolate 24], the largest Bedouin city). Clustering of these outliers suggests that the outbreak might have been more widespread than documented.

In contrast with traditional patterns of brucellosis cases and case clusters, which occur mainly in small communities where residents consume locally produced unpasteurized dairy products, this outbreak resulted from web-based commercial sales of an unregulated food product. This sales channel enabled the spread of *B. melitensis* throughout Israel, similar to a recent United States report on commercially sold contaminated raw cow milk (*13*). Therefore, modern consumer trends in small agriculture and food production may result in new food safety risks.

The advantages of WGS in this outbreak investigation included the capacity to analyze both related and outlier isolates. This capability enabled us to resolve complex linkages between cases, suggesting unequivocal, temporal relationships that depict outbreak directionality and can aid future preventative measures.

In conclusion, we describe a unique *B. melitensis* outbreak linking human cases with commercially sold, unregulated camel milk. These results demonstrate that WGS can be a powerful tool for investigating transmission of brucellosis, a neglected zoonotic disease, in a world of modernized commercialism.

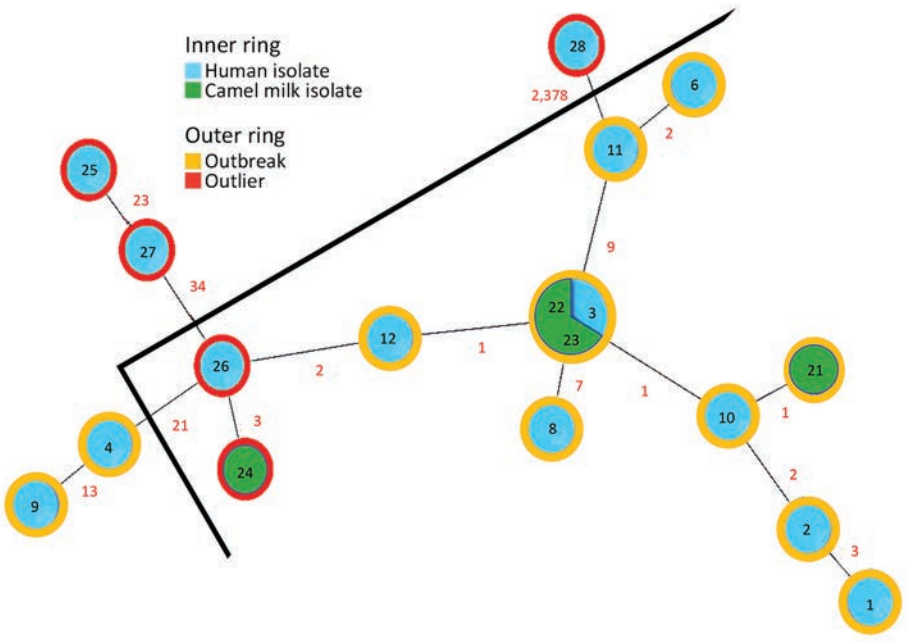

Figure 2. Minimum-spanning tree of core genome single-nucleotide polymorphisms analysis of *Brucella melitensis* outbreak traced to commercially sold camel milk, Israel, 2016. The phylogenetic tree includes human isolates, camel milk isolates, and both human and camel milk outlier sequences; numbers within circles correspond to isolate number given in the article text and numbers in red denote number of differing single-nucleotide polymorphisms between isolates. The nodes are colored according to the epidemiologic link (outbreak isolate or outlier), and outer rings are colored according to the sample source (clinical sample or camel milk).

Acknowledgments

We would like to thank all personnel of the Ministry of Health and Ministry of Agriculture and Rural Development who contributed to the investigation of the outbreak and incident management.

This work was supported by a grant from the Ministry of Agriculture and Rural Development (#33-08-0009).

About the Author

Dr. Svetlana Bardenstein is a veterinary doctor specializing in clinical microbiology and currently heading the World Organisation for Animal Health/Food and Agriculture Organization of the United Nations Brucella Reference Laboratory in Israel. Her main interest is the epidemiology of brucellosis in Israel.

References

1. Pappas G, Papadimitriou P, Akritidis N, Christou L, Tsianos EV. The new global map of human brucellosis. Lancet Infect Dis. 2006;6:91–9. https://doi.org/10.1016/S1473-3099(06)70382-6
2. Anis E, Leventhal A, Grotto I, Gandacu D, Warshavsky B, Shimshony A, et al. Recent trends in human brucellosis in Israel. Isr Med Assoc J. 2011;13:359–62.
3. Shimol SB, Dukhan L, Belmaker I, Bardenstein S, Sibirsky D, Barrett C, et al. Human brucellosis outbreak acquired through camel milk ingestion in southern Israel. Isr Med Assoc J. 2012;14:475–8.
4. Garcell HG, Garcia EG, Pueyo PV, Martín IR, Arias AV, Alfonso Serrano RN. Outbreaks of brucellosis related to the consumption of unpasteurized camel milk. J Infect Public Health. 2016;9:523–7. https://doi.org/10.1016/j.jiph.2015.12.006
5. Tan K-K, Tan Y-C, Chang L-Y, Lee KW, Nore SS, Yee W-Y, et al. Full genome SNP-based phylogenetic analysis reveals the origin and global spread of Brucella melitensis. BMC Genomics. 2015;16:93. https://doi.org/10.1186/s12864-015-1294-x
6. Andrews S. FastQC: a quality control tool for high throughput sequence data. 2018 [cited 2021 Apr 4]. https://www.bioinformatics.babraham.ac.uk/projects/fastqc/
7. Seeman T, Kwong J, Gladman S, Goncalves da Silva A. Shovil. Faster SPAdes assembly of Illumina reads. [cited 2021 Apr 4]. https://github.com/tseemann/shovill
8. Jolley KA, Bray JE, Maiden MCJ. Open-access bacterial population genomics: BIGSdb software, the PubMLST.org website and their applications. Wellcome Open Res. 2018;3:124. https://doi.org/10.12688/wellcomeopenres.14826.1
9. Seeman T. mlst Github [cited 2021 Apr 4]. https://github.com/tseemann/mlst
10. Seeman T. Ekidna [cited 2021 Apr 4]. https://github.com/tseemann/ekidna
11. Croucher NJ, Page AJ, Connor TR, Delaney AJ, Keane JA, Bentley SD, et al. Rapid phylogenetic analysis of large samples of recombinant bacterial whole genome sequences using Gubbins. Nucleic Acids Res. 2015;43:e15–15. https://doi.org/10.1093/nar/gku1196
12. Nascimento M, Sousa A, Ramirez M, Francisco AP, Carriço JA, Vaz C. PHYLOViZ 2.0: providing scalable data integration and visualization for multiple phylogenetic inference methods. Bioinformatics. 2017;33:128–9. https://doi.org/10.1093/bioinformatics/btw582
13. Gruber JF, Newman A, Egan C, Campbell C, Garafalo K, Wolfgang DR, et al. Notes from the field: Brucella abortus RB51 infections associated with consumption of raw milk from Pennsylvania—2017 and 2018. MMWR Morb Mortal Wkly Rep. 2020;69:482–3. https://doi.org/10.15585/mmwr.mm6915a4

Address for correspondence: Jacob Moran-Gilad, Dept. of Health Systems Management, Faculty of Health Sciences, Ben Gurion University of the Negev, POB 653, Beer Sheva 8410501, Israel; email: giladko@post.bgu.ac.il

Highly Pathogenic Avian Influenza A(H5N8) Virus in Swans, China, 2020

Xiang Li,[1] Xinru Lv,[1] Yi Li,[1] Peng Peng, Ruifang Zhou, Siyuan Qin, Enda Ma, Wenqiang Liu, Tian Fu, Peiran Ma, Qing An, Yiran Li, Yuping Hua, Yulong Wang, Chengliang Lei, Dong Chu, Heting Sun, Yanbing Li, Yuwei Gao, Hongliang Chai

Author affiliations: Northeast Forestry University College of Wildlife and Protected Area, Harbin, China (X. Li, X. Lv, Y. Li, T. Fu, P. Ma, Q. An, Yiran Li, Y. Hua, Y. Wang, H. Chai); General Station for Surveillance of Wildlife Disease and Wildlife Borne Diseases, National Forestry and Grassland Administration, Shenyang, China (P. Peng, S. Qin, D. Chu, H. Sun); Bayannur Desert Comprehensive Management Center, Bayannur Forestry Scientific Research Institute, Bayannur, China (R. Zhou); Wildlife and Wetland Conservation Center, Bayannur Forestry and Grassland Administration, Bayannur (E. Ma, W. Liu); State Key Laboratory of Veterinary Biotechnology, Harbin Veterinary Research Institute, Harbin (Yanbing Li); National Forestry and Grassland Administration Department of Wildlife Protection, Beijing, China (C. Lei); Military Veterinary Research Institute of Academy of Military Medical Sciences, Changchun, China (Y. Gao)

DOI: https://doi.org/10.3201/eid2706.204727

In October 2020, highly pathogenic avian influenza A(H5N8) viruses were detected in 2 dead swans in Inner Mongolia, China. Genetic analysis showed that the H5N8 isolates belong to clade 2.3.4.4b and that the isolates cluster with the H5N8 viruses isolated in Eurasia in the fall of 2020.

Since 2008, highly pathogenic avian influenza (HPAI) H5 clade 2.3.4 viruses with various neuraminidase combinations have been identified, and these subtypes have subsequently evolved into different subclades, including clade 2.3.4.4 (*1*–*3*). In contrast to the 2014–2015 H5N8 clade 2.3.4.4 viruses, which spread worldwide through wild migratory birds (*4*), the intercontinental spread of clade 2.3.4.4b viruses began in fall 2016 (*5*). Moreover, clade 2.3.4.4b viruses have had a sustained prevalence in Europe, Africa, and the Middle East in recent years (https://www.oie.int/en/animal-health-in-the-world). In January 2020, clade 2.3.4.4h of HPAI A(H5N6) virus was detected in whooper swans (*Cygnus cygnus*) and mute swans (*C. olor*) in Xinjiang (*6*); however, no outbreaks of H5N8 in mainland China have been reported since 2017. We report the reemergence of HPAI H5N8 viruses from wild aquatic birds in mainland China.

On October 17, 2020, we collected multiple organs (brains, larynx, liver, lung, pancreas, kidney, spleen, and rectum) from 2 dead swans, a whooper swan and a mute swan, in Wuliangsuhai Lake in Bayannur City, Inner Mongolia, China (40.95138889°N, 108.9266667°E) (Figure). We sequenced the H5N8 genomes directly from organs. We isolated 2 H5N8 influenza viruses, A/whooper swan/Inner Mongolia/W1-1/2020(H5N8) and A/mute swan/Inner Mongolia/W2-1/2020(H5N8).

We sequenced the full-length genomes and confirmed that the 2 isolates were HPAI viruses on the basis of the amino acid sequence REKRRKR↓GLFGAI at the hemagglutinin cleavage site. The sequences of these 2 Inner Mongolia H5N8 isolates (IM-H5N8) were deposited into the GISAID database (http://www.gisaid.org; accession nos. EPI1811641–56). The receptor-binding site at the 222–224 (H5 numbering) motif (QRG) suggested avian-like (α 2–3-SA) receptors, and the substitutions D94N, S123P, and S133A (H5 numbering), which are associated with increased binding to human-like (α 2–6-SA) receptors, were identified. The residues Q591, E627, and D701 in the polymerase basic 2 protein suggest that these viruses have not yet adapted to mammalian hosts.

Sequence comparisons showed high nucleotide identity across all 8 gene segments between the 2 IM-H5N8 isolates (99.8%–100%). A BLAST search (https://blast.ncbi.nlm.nih.gov/Blast.cgi) performed in the GISAID database suggested that IM-H5N8 shares the highest nucleotide identity (>99%) with the H5N8 viruses isolated in Eurasia in fall 2020 (EA-H5N8) (Appendix Table 1, https://wwwnc.cdc.gov/EID/article/27/6/20-4727-App1.pdf). These results indicate that IM-H5N8 and EA-H5N8 are descendants of a common ancestral virus. Phylogenetic analysis further confirmed that the 8 segments had a common evolutionary source, clustering with EA-H5N8 and belonging to clade 2.3.4.4b (Appendix Figure).

Clade 2.3.4.4b H5N8 viruses were detected mainly in poultry in Europe in early 2020 but were not related to IM-H5N8 (Appendix Figure) (*7*). On May 12 2020, IM-H5N8 like virus was first detected in poultry in Iraq (*7*). It might be the source of IM-H5N8–like viruses. Soon after, similar viruses were reported in southern central Russia in late July 2020, and they jumped into wild birds in September in Russia and Kazakhstan (Appendix Table 1). Migratory birds moving within several flyways in Eurasia have overlapping breeding areas (*8*), and breeding origin

[1]These first authors contributed equally to this article.

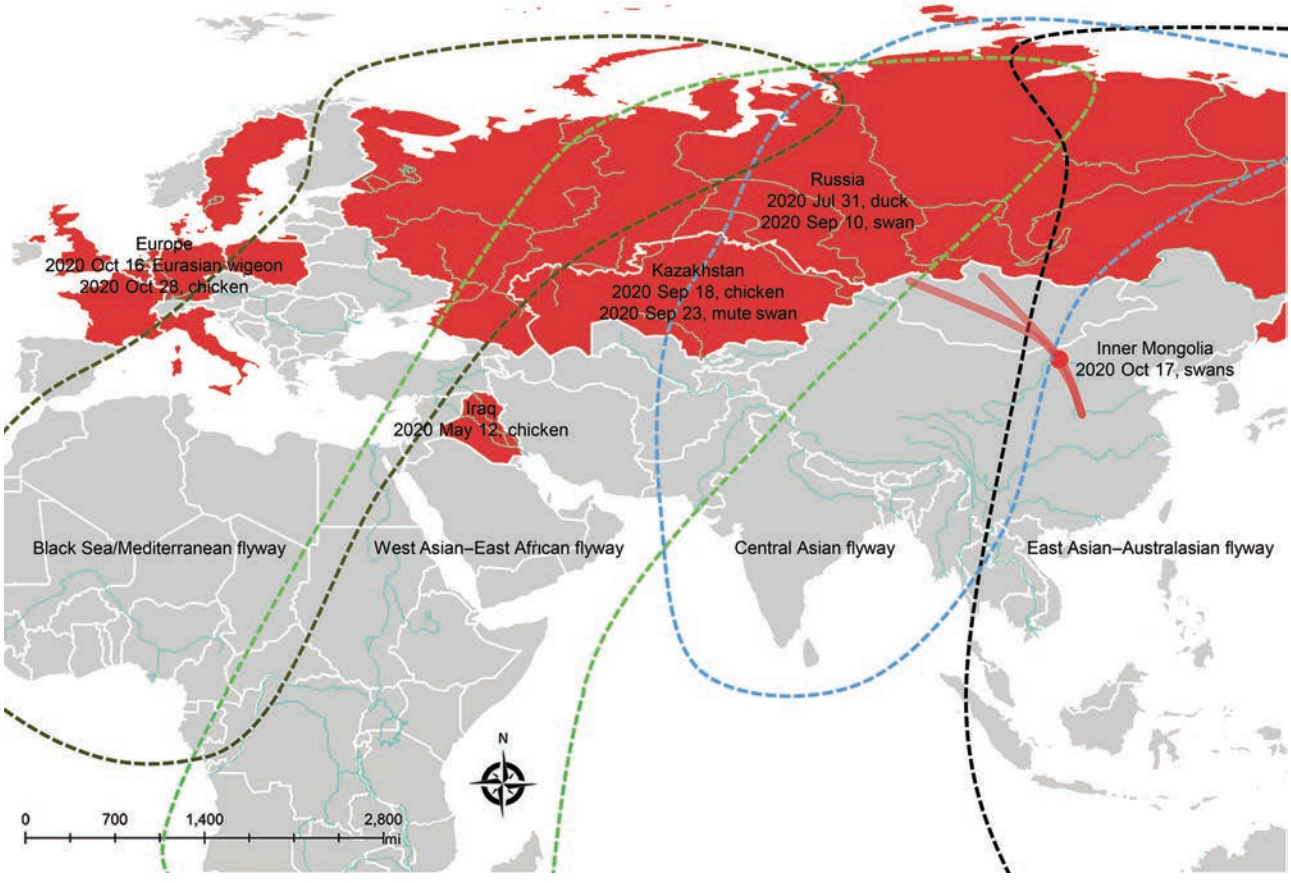

Figure. Global distribution of the influenza A(H5N8) viruses related to 2 H5N8 isolates detected in whooper swans (*Cygnus cygnus*) and mute swans (*C. olor*) in Inner Mongolia, China, 2020. Red dot indicates sampling site in Inner Mongolia; red solid lines indicate whooper swan migratory routes in central China. Dates refer to the day of initial H5N8 virus isolated in poultry and wild birds in each country in 2020.

assignments suggest that migration distances vary by a maximum of ≈3,500 km (*9*). Such a unique ecosystem could be implicated as a pathway for the cross-regional spread of HPAI viruses during the autumn migration of waterfowl. Birds breeding in Russia that migrate along different routes might be responsible for the widespread transmission of H5N8 viruses in both Europe and China in fall 2020.

The migration routes of whooper swans along the Central Asian flyway have been identified (*10*); the widely distributed lakes in western and northern Mongolia (including the lakes in Russia near Mongolia) are important breeding areas, and Inner Mongolia (including Bayannur City, Baotou City, and Ordos City) and Shaanxi (including Yulin City) are the key stopover sites during the migration of whooper swans in China. Whooper swans usually winter along the Yellow River (e.g., in Henan [Sanmenxia Reservoir area] and Shanxi [Shengtian Lake]), and whooper swans also wander between different wintering grounds. Despite no reported outbreak of HPAI A(H5N8) virus in Mongolia, Russia reported a similar swan outbreak of HPAI A(H5N8) virus on August 28, 2020 (https://www.oie.int/wahis_2/temp/reports/en_fup_0000035737_20200915_110259.pdf), which could be the source of the infections in these swans in Bayannur City in Inner Mongolia through swan migration.

In conclusion, we detected HPAI A(H5N8) during the autumn migration of whooper swans through Inner Mongolia. This finding warrants strengthening the monitoring of HPAI A(H5N8) in swans and other migratory waterfowl in the main stopover sites and wintering grounds, especially in the Sanmenxia Reservoir area in Henan Province.

Acknowledgments

We thank the authors and submitting laboratories of the sequences from the GISAID EpiFlu Database.

This study was funded by the National Natural Science Foundation of China (grant no. 31970501) and by the

Surveillance of Wildlife Diseases from the National Forestry and Grassland Administration.

About the Author

Mr. Li is a graduate student at the College of Wildlife and Protected Area at Northeast Forestry University in Heilongjiang, China. His primary research interest is the epidemiology of influenza viruses.

References

1. Gu M, Liu W, Cao Y, Peng D, Wang X, Wan H, et al. Novel reassortant highly pathogenic avian influenza (H5N5) viruses in domestic ducks, China. Emerg Infect Dis. 2011;17:1060–3. https://doi.org/10.3201/eid/1706.101406
2. Wu H, Peng X, Xu L, Jin C, Cheng L, Lu X, et al. Novel reassortant influenza A(H5N8) viruses in domestic ducks, eastern China. Emerg Infect Dis. 2014;20:1315–8. https://doi.org/10.3201/eid2008.140339
3. Cui Y, Li Y, Li M, Zhao L, Wang D, Tian J, et al. Evolution and extensive reassortment of H5 influenza viruses isolated from wild birds in China over the past decade. Emerg Microbes Infect. 2020;9:1793–803. https://doi.org/10.1080/22221751.2020.1797542
4. Global Consortium for H5N8 and Related Influenza Viruses. Role for migratory wild birds in the global spread of avian influenza H5N8. Science. 2016;354:213–7. https://doi.org/10.1126/science.aaf8852
5. Li M, Liu H, Bi Y, Sun J, Wong G, Liu D, et al. Highly pathogenic avian influenza A(H5N8) virus in wild migratory birds, Qinghai Lake, China. Emerg Infect Dis. 2017;23:637–41. https://doi.org/10.3201/eid2304.161866
6. Li Y, Li M, Li Y, Tian J, Bai X, Yang C, et al. Outbreaks of highly pathogenic avian influenza (H5N6) virus subclade 2.3.4.4h in swans, Xinjiang, western China, 2020. Emerg Infect Dis. 2020;26:2956–60. https://doi.org/10.3201/eid2612.201201
7. Lewis NS, Banyard AC, Whittard E, Karibayev T, Al Kafagi T, Chvala I, et al. Emergence and spread of novel H5N8, H5N5 and H5N1 clade 2.3.4.4 highly pathogenic avian influenza in 2020. Emerg Microbes Infect. 2021;10:148–51. https://doi.org/10.1080/22221751.2021.1872355
8. Saito T, Tanikawa T, Uchida Y, Takemae N, Kanehira K, Tsunekuni R. Intracontinental and intercontinental dissemination of Asian H5 highly pathogenic avian influenza virus (clade 2.3.4.4) in the winter of 2014–2015. Rev Med Virol. 2015;25:388–405. https://doi.org/10.1002/rmv.1857
9. Sorensen MC, Dixit T, Kardynal KJ, Newton J, Hobson KA, Bensch S, et al. Migration distance does not predict blood parasitism in a migratory songbird. Ecol Evol. 2019;9:8294–304. https://doi.org/10.1002/ece3.5404
10. Li S, Meng W, Liu D, Yang Q, Chen L, Dai Q, et al. Migratory whooper swans *Cygnus cygnus* transmit H5N1 virus between China and Mongolia: combination evidence from satellite tracking and phylogenetics analysis. Sci Rep. 2018;8:7049. https://doi.org/10.1038/s41598-018-25291-1

Address for correspondence: Hongliang Chai, College of Wildlife and Protected Area, Northeast Forestry University, No. 26 Hexing Rd, Xiangfang District, Harbin 150040, Heilongjiang, China; email: hongliang_chai@hotmail.com

Rapid Antigen Test for Postmortem Evaluation of SARS-CoV-2 Carriage

Martin Zacharias, Verena Stangl, Andrea Thüringer, Martina Loibner, Philipp Wurm, Stella Wolfgruber, Kurt Zatloukal, Karl Kashofer, Gregor Gorkiewicz

Author affiliation: Medical University of Graz, Graz, Austria

DOI: https://doi.org/10.3201/eid2706.210226

Detecting severe acute respiratory syndrome coronavirus 2 in deceased patients is key when considering appropriate safety measures to prevent infection during postmortem examinations. A prospective cohort study comparing a rapid antigen test with quantitative reverse transcription PCR showed the rapid test's usability as a tool to guide autopsy practice.

Rapid detection of severe acute respiratory syndrome coronavirus 2 (SARS-CoV-2) is essential to prevent viral dissemination. Rapid antigen tests (RATs) have recently been approved and are now widely used in the current coronavirus disease (COVID-19) pandemic (1). Although the performance of RATs has been evaluated extensively in clinics (2–4), data on postmortem testing are still lacking (5).

We performed a prospective cohort study in which we evaluated the performance of the Roche/SD Biosensor SARS-CoV-2 RAT (https://www.roche.com) in 30 consecutive deceased COVID-19 patients at the University Hospital, Medical University of Graz (Graz, Austria), during November 28–December 23, 2020. We tested each corpse with nasopharyngeal swabs for RAT (using the manufacturer's kit) and eSwabs (https://www.copanusa.com) for quantitative reverse transcription PCR (qRT-PCR) targeted to the viral envelope (E) and nucleocapsid (N) genes of SARS-CoV-2. Furthermore, we used virus isolation from lung tissue swabs from an additional cohort of deceased COVID-19 patients (n = 11) to compare molecular detection and virus cultivability (Appendix, https://wwwnc.cdc.gov/EID/article/27/6/21-0226-App1.pdf).

All patients were Caucasian, median age was 78 years (range 62–93 years), and 51.2% were female. The median disease duration (interval between the first positive SARS-CoV-2 PCR and death) was 11 days (range 1–43 days). The median postmortem interval (time between death and specimen sampling) was 23 hours (range 8–124 hours; Table; Appendix).

PCR is the current standard for SARS-CoV-2 detection (*1*,*2*). In our cohort, qRT-PCR targeted to the E gene showed a higher sensitivity than qRT-PCR for

Table. Patient characteristics and postmortem data for investigation of rapid antigen test for postmortem evaluation of SARS-CoV-2 carriage, Graz, Austria*

Characteristic	RAT cohort, n = 30	Culture cohort, n = 11
Age, y, median (range)	78 (62–93)	79 (65–93)
Sex, no. (%)		
M	14 (47.7)	6 (56)
F	16 (53.3)	5 (45.4)
Disease duration,† d, median (range)	12 (1–43)	9 (3–34)
Postmortem interval‡, h, median (range)	22 (8–124)	25 (14–68)
qRT-PCR positive, no. (%)	24 (80)	11 (100)
C_t value, median (range)		
E gene	22.8 (14.1–37.3)	19.9 (13.7–36.0)
N gene	26.9 (18.0–34.6)	24.6 (17.3–33.7)
Cultivation positive, no. (%)	NA	7 (63.6)
RAT positive, no. (%)	17 (56.7%)	NA
Total RAT specificity (95% CI§), n = 30	100% (61%–100%)	NA
RAT sensitivity (95% CI§), n = 30	70.8% (50.8%–85.1%)	NA
Total, n = 30		
C_t ≤35,¶ n = 23	73.9% (53.5%–87.5%)	NA
C_t ≤30,¶ n = 18	94.4% (74.2%–99.7%)	NA
C_t ≤25,¶ n = 16	100% (80.6%–100%)	NA

*C_t, cycle threshold; E, envelope; N, nucleocapsid; NA, not applicable; qRT-PCR, quantitative reverse transcription PCR: RAT, rapid antigen test; SARS-CoV-2, severe acute respiratory syndrome coronavirus 2.
†Interval from first positive (antemortem) SARS-CoV-2 PCR to death.
‡Interval from death to specimen sampling.
§Determined via the hybrid Wilson/Brown method (*10*).
¶Determined via E gene qRT-PCR.

the N gene (Appendix Figure 1). Consequently, we used E gene qRT-PCR as the reference in subsequent evaluations. Results showed that 80% (24/30) of cases were qRT-PCR positive, whereas 56.7% (17/30) were RAT positive (Figure, panel A). RAT had an overall specificity of 100% (95% CI 61%–100%) and an overall sensitivity of 70.8% (95% CI 50.8%–85.1%) when using E gene qRT-PCR as the reference. RAT negative cases showed significantly higher C_t values in qRT-PCR compared with RAT positive cases (mean 38.24 [SD 7.01] vs 20.74 [SD 3.46]; Figure, panel B). Correspondingly, RAT sensitivity increased when cases were stratified according to C_t values (C_t ≤35, sensitivity 73.9% [95% CI 53.5%–87.5%]; C_t ≤30, sensitivity 94.4% [95% CI 74.2%–99.7%]; C_t ≤25, sensitivity 100% [95% CI 80.6%–100%]; (Table; Appendix Table 1). Furthermore, when we compared qRT-PCR results from nasopharyngeal swabs of patients in which viral culture was performed (from corresponding lung tissue swabs of an additional cohort), cultivability was restricted to cases with C_t values ≤23.7, which is below the threshold of false-negative RAT cases (C_t values ≥25.8; Figure, panels B, C). These results are in line with most clinical RAT studies that also used virus culture (*2*–*4*,*6*), in which cultivability is exceedingly rare in cases with low viral loads determined with qRT-PCR. We used cultivation from lung tissue swab specimens for this analysis because the lung often shows increased SARS-CoV-2 loads in deceased patients (*7*; Appendix Table 2) and therefore represents a major infection source during autopsy.

Furthermore, we determined parameters that influenced test performance. We noted a significant positive correlation between disease duration and C_t values (Figure, panel D). Such correlation was also evident in RATs; all cases with disease courses >17 days were RAT negative (Figure, panel E). Postmortem intervals did not correlate with C_t values or RAT results (Figure, panels G, H). Thus, a long disease duration rather than a long postmortem interval seems to be the main factor for increased C_t values and negative RATs. RAT and cultivation results closely mirrored each other with respect to viral load (Figure, panels B, C), disease duration (Figure, panels E, F), and postmortem interval (Figure, panels H, I).

Although RAT had an overall lower sensitivity than qRT-PCR in this study, our data suggest that viral loads of false-negative RAT cases are probably below the threshold of cultivability. Because culture is regarded as a measure of virus viability and infectivity (*8*), these cases likely pose only minimal risks of SARS-CoV-2 transmission during postmortem examinations. However, each corpse having a postmortem evaluation must be treated as potentially infectious. Even a PCR-negative nasopharyngeal swab specimen does not exclude the presence of viable virus in other body sites, as shown in COVID-19 (*7*), thus emphasizing the general application of appropriate autopsy safety measures.

In conclusion, RAT should not be seen as a potential replacement for but rather as an addition to of current postmortem testing strategies. Especially

when qRT-PCR is not readily available, RAT might be useful in selecting the most hazardous corpses that should be examined under special conditions (e.g., Biosafety Level 3 [*9*]). RAT could therefore be a valuable adjunct tool in guiding autopsy practice.

About the Author

Dr. Zacharias is a physician-scientist at the Diagnostic and Research Institute of Pathology, Medical University of Graz, Graz, Austria. His main research interests include pulmonary and infectious disease pathology.

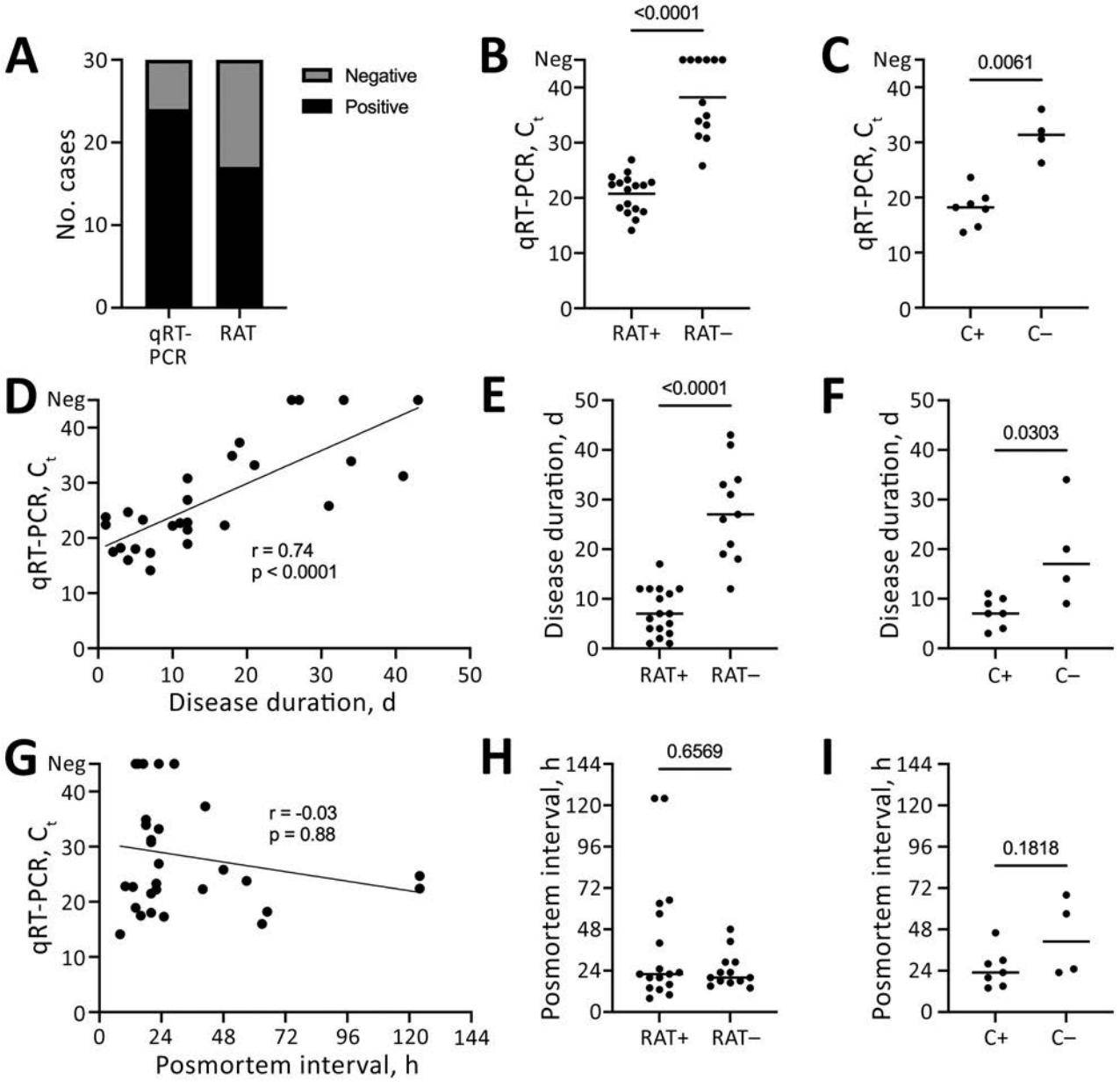

Figure. Postmortem detection and cultivation of SARS-CoV-2 for investigation of RAT for postmortem evaluation of SARS-CoV-2 carriage, Graz, Austria. A) Among 30 deceased SARS-CoV-2 patients, RAT detected fewer positive cases than did qRT-PCR. B) RAT-negative cases show significantly higher C_t values in qRT-PCR compared with RAT-positive cases (Mann-Whitney test). C) Cultivation negative and positive cases mirror C_t values of RAT results (Mann-Whitney test). D–F) Longer disease durations are significantly correlated with higher C_t values (Spearman correlation test; D), negative RAT results (Mann-Whitney test; E), and negative cultivation results (Mann-Whitney test; F). G–I) No significant correlation was found between postmortem intervals and C_t values (Spearman correlation test; G), RAT results (Mann-Whitney test; H), or cultivation results (Mann-Whitney test; I). C, cultivation; C_t, cycle threshold; neg, negative; qRT-PCR, quantitative reverse transcription PCR; RAT, rapid antigen test; SARS-CoV-2, severe acute respiratory syndrome coronavirus 2; +, positive; –, negative.

References

1. Centers for Disease Control and Prevention. Interim guidance for antigen testing for SARS-CoV-2 [cited 2021 Mar 27]. https://www.cdc.gov/coronavirus/2019-ncov/lab/resources/antigen-tests-guidelines.html
2. Dinnes J, Deeks JJ, Berhane S, Taylor M, Adriano A, Davenport C, et al.; Cochrane COVID-19 Diagnostic Test Accuracy Group. Rapid, point-of-care antigen and molecular-based tests for diagnosis of SARS-CoV-2 infection. Cochrane Database Syst Rev. 2021;3:CD013705.
3. Albert E, Torres I, Bueno F, Huntley D, Molla E, Fernández-Fuentes MÁ, et al. Field evaluation of a rapid antigen test (Panbio™ COVID-19 Ag Rapid Test Device) for COVID-19 diagnosis in primary healthcare centres. Clin Microbiol Infect. 2021;27:472.e7–10. https://doi.org/10.1016/j.cmi.2020.11.004
4. Iglòi Z, Velzing J, van Beek J, van de Vijver D, Aron G, Ensing R, et al. Clinical evaluation of Roche SD Biosensor rapid antigen test for SARS-CoV-2 in municipal health service testing site, the Netherlands. Emerg Infect Dis. 2021 Mar 16 [Epub ahead of print]. https://doi.org/10.3201/eid2705.204688
5. Centers for Disease Control and Prevention. Collection and submission of postmortem specimens from deceased persons with confirmed or suspected COVID-19: postmortem guidance [cited 2021 Mar 27]. https://www.cdc.gov/coronavirus/2019-ncov/hcp/guidance-postmortem-specimens.html
6. Singanayagam A, Patel M, Charlett A, Lopez Bernal J, Saliba V, Ellis J, et al. Duration of infectiousness and correlation with RT-PCR cycle threshold values in cases of COVID-19, England, January to May 2020. Euro Surveill. 2020;25:2001483. https://doi.org/10.2807/1560-7917.ES.2020.25.32.2001483
7. Puelles VG, Lütgehetmann M, Lindenmeyer MT, Sperhake JP, Wong MN, Allweiss L, et al. Multiorgan and renal tropism of SARS-CoV-2. N Engl J Med. 2020;383:590–2. https://doi.org/10.1056/NEJMc2011400
8. Jefferson T, Spencer EA, Brassey J, Heneghan C. Viral cultures for COVID-19 infectious potential assessment—a systematic review. Clin Infect Dis. 2020 Dec 20 [Epub ahead of print]. https://doi.org/10.1093/cid/ciaa1764
9. Loibner M, Langner C, Regitnig P, Gorkiewicz G, Zatloukal K. Biosafety requirements for autopsies of patients with COVID-19: example of a BSL-3 autopsy facility designed for highly pathogenic agents. Pathobiology. 2021;88:37–45. https://doi.org/10.1159/000513438
10. Brown LD, Cai TT, DasGupta A. Interval estimation for a binomial proportion. Stat Sci. 2001;16:101–33. https://doi.org/10.1214/ss/1009213286

Address for correspondence: Martin Zacharias, Diagnostic and Research Institute of Pathology, Medical University of Graz, Neue Stiftingtalstraße 6, 8010 Graz, Austria; email: martin.zacharias@medunigraz.at

Respiratory Viral Shedding in Healthcare Workers Reinfected with SARS-CoV-2, Brazil, 2020

Mariene R. Amorim,[1] William M. Souza,[1] Antonio C.G. Barros Jr., Daniel A. Toledo-Teixeira, Karina Bispo-dos-Santos, Camila L. Simeoni, Pierina L. Parise, Aline Vieira, Julia Forato, Ingra M. Claro, Luciana S. Mofatto, Priscila P. Barbosa, Natalia S. Brunetti, Emerson S.S. França, Gisele A. Pedroso, Barbara F.N. Carvalho, Tania R. Zaccariotto, Kamila C.S. Krywacz, André S. Vieira, Marcelo A. Mori, Alessandro S. Farias, Maria H.P. Pavan, Luís Felipe Bachur, Luís G.O. Cardoso, Fernando R. Spilki, Ester C. Sabino, Nuno R. Faria, Magnun N.N. Santos, Rodrigo Angerami, Patricia A.F. Leme, Angelica Schreiber, Maria L. Moretti, Fabiana Granja, José Luiz Proenca-Modena

Author affiliations: University of Campinas, Campinas, Brazil (M.R. Amorim, A.C.G. Barros Jr., D.A. Toledo-Teixeira, K. Bispo-dos-Santos, C.L. Simeoni, P.L. Parise, A. Vieira, J. Forato, L.S. Mofatto, P.P. Barbosa, N.S. Brunetti, E.S.S. França, G.A. Pedroso, B.F.N. Carvalho, T.R. Zaccariotto, K.C.S. Krywacz, A.S. Vieira, M.A. Mori, A.S. Farias, M.H.P. Pavan, L.F. Bachur, L.G.O. Cardoso, M.N.N. Santos, R. Angerami, P.A.F. Leme, A. Schreiber, M.L. Moretti, F. Granja, J.L. Proenca-Modena); University of São Paulo, São Paulo, Brazil (W.M. Souza, I.M. Claro, E.C. Sabino, N.R. Faria); Feevale University, Novo Hamburgo, Brazil (F.R. Spilki); University of Oxford, Oxford, UK (N.R. Faria); Imperial College London, London, UK (N.R. Faria); Campinas Department of Public Health Surveillance, Campinas (R. Angerami); Federal University of Roraima, Boa Vista, Brazil (F. Granja)

DOI: https://doi.org/10.3201/eid2706.210558

We documented 4 cases of severe acute respiratory syndrome coronavirus 2 reinfection by non–variant of concern strains among healthcare workers in Campinas, Brazil. We isolated infectious particles from nasopharyngeal secretions during both infection episodes. Improved and continued protection measures are necessary to mitigate the risk for reinfection among healthcare workers.

Coronavirus disease (COVID-19) is caused by severe acute respiratory syndrome coronavirus 2 (SARS-CoV-2), which emerged in Wuhan, China,

[1]These authors contributed equally to this article.

in late 2019. As of April 8, 2021, COVID-19 has affected >132 million persons and caused >2.87 million deaths around the world (https://covid19.who.int). Whether the immune response elicited by an initial infection protects against reinfection is uncertain. The Pan American Health Organization provisionally defines reinfection as a positive SARS-CoV-2 test result ≥45 days after initial infection, given that other infections and prolonged shedding of SARS-CoV-2 or viral RNA have been ruled out (*1*). Healthcare workers (HCWs) are consistently exposed to SARS-CoV-2 and are therefore susceptible to reinfection.

We investigated 4 cases of SARS-CoV-2 reinfection among HCWs at the Hospital das Clínicas da Unicamp, a tertiary public hospital at the University of Campinas (Campinas, Brazil). This study was approved by the Research Ethical Committee of the University of Campinas (approval no. CAAE-31170720.3.0000.5404). The 4 HCWs, consisting of 3 nurses and 1 staff member, were women with an average age of 44 years (range 40–61 years) (Figure 1, panel A). For the initial infections, symptom onset ranged from April 5–May 10, 2020, and lasted 10–23 days. We identified SARS-CoV-2 RNA in nasopharyngeal swab samples using real-time quantitative reverse transcription PCR (qRT-PCR) 2–4 days after symptom onset (*2*). All 4 HCWs had mild COVID-19 signs and symptoms and recovered (Table). After signs and symptoms resolved, the HCWs tested negative by qRT-PCR, Elecsys Anti-SARS-CoV-2 (Roche Diagnostics, https://diagnostics.roche.com), or both. Reinfection, confirmed by a nucleic acid amplification test using the GeneFinder COVID-19 Plus RealAmp Kit (*3*), developed 55–170 days after symptom onset of the first infection. Signs and symptoms of reinfection lasted 9–23 days. Only 1 HCW had a concurrent condition (chronic bronchitis), and none were immunosuppressed. None required hospitalization during the initial or reinfection episodes (Table). After recovering from their initial infections, all HWCs continued to use the same types of personal protective equipment (i.e., disposable surgical masks, gloves, gowns, and goggles) in accordance with recommendations from the Ministry of Health of Brazil (https://coronavirus.saude.gov.br/saude-e-seguranca-do-trabalhador-epi).

To assess whether infectious SARS-CoV-2 particles were shed in nasopharyngeal secretions during both COVID-19 episodes, we conducted viral isolation in Vero cells (ATCC no. CCL-81) (W.M. de Souza, unpub. data, http://dx.doi.org/10.2139/ssrn.3793486) (Appendix). We inoculated Vero cells with isolated SARS-CoV-2 virions from nasopharyngeal swab samples collected during the first and second infections; we observed a cytopathic effect 3–4 days after inoculation. On day 4, we obtained cell culture supernatant by centrifugation and conducted qRT-PCR selective for the envelope gene to confirm the presence of SARS-CoV-2 RNA; we found the supernatants had 2.8×10^2–1.4×10^{10} RNA copies/mL (*2*).

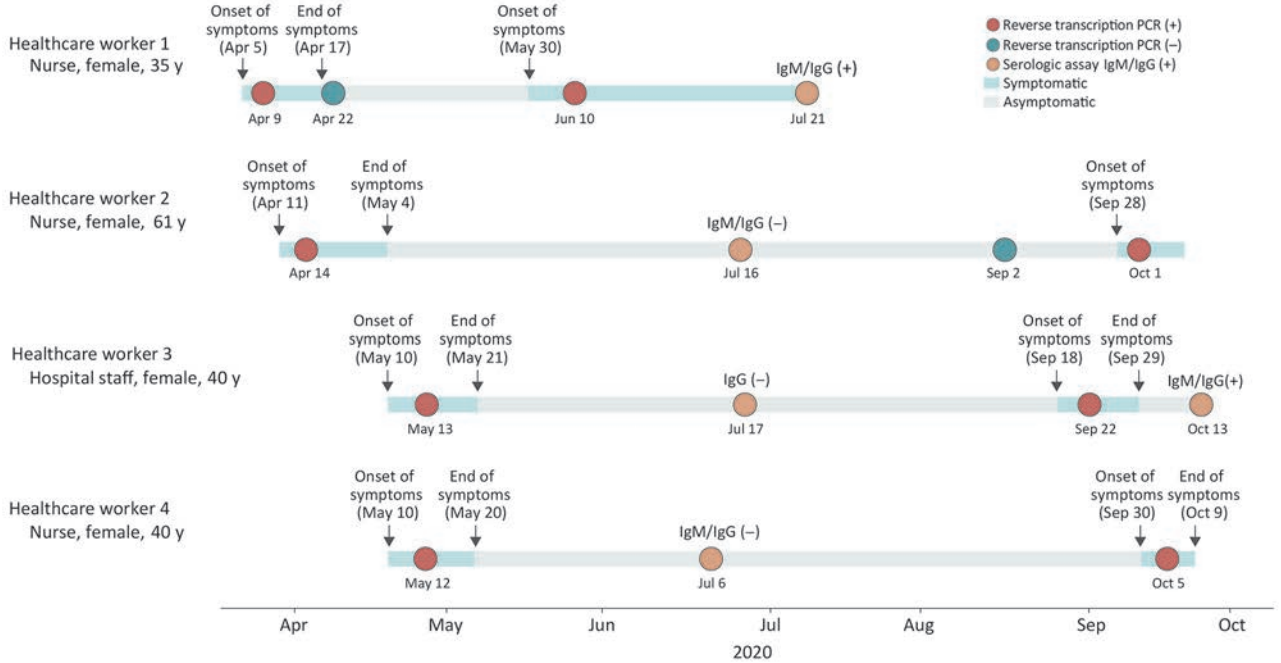

Figure. Timeline of severe acute respiratory syndrome coronavirus 2 reinfections (SARS-CoV-2) among healthcare workers, Brazil, 2020. (+), positive; (–), negative.

Table. Characteristics of healthcare workers with severe acute respiratory syndrome coronavirus 2 reinfections, Brazil, 2020*

Characteristic	Healthcare worker			
	1	2	3	4
Underlying conditions	None	Chronic bronchitis	None	None
Hospitalized	No	No	No	No
Symptoms				
First infection	Fever, headache, chills, sneezing, coryza, and myalgia	Headache, cough, myalgia, odynophagy, coryza, diarrhea, and ageusia	Nasal congestion, coryza, cough, ageusia	Fever, headache, myalgia, coryza, dry cough, vomiting, and malaise
Second infection	Headache, nasal congestion, odynophagia, ageusia, and anosmia	Cough, myalgia, odynophagia, anosmia, and diarrhea	Odynophagia, sneezing, coryza, diarrhea, ageusia, and anosmia	Odynophagia, dry cough, myalgia, malaise, coryza, and headache
Cycle threshold values				
First infection†	E gene: 35.24; N gene: 40.12	E gene: 31.8	E gene: 35.15	E gene: 34.80; RdRp gene: 39.86
Second infection‡	E gene: 31.14; N gene: 31.3; RdRp gene: 32.58	E gene: 20.45; N gene: 20.52; RdRp gene: 22.65	E gene: 26.04; N gene: 26.88; RdRp gene: 28.40	E gene: 23.72; N gene: 23.48; RdRp gene: 25.67
Time between symptom onsets, d	55	170	131	148

*E gene, envelope gene; N gene, nucleoprotein gene; RdRp gene, RNA dependent RNA polymerase gene.
†Real-time quantitative reverse transcription PCR selective for the envelope gene (*2*).
‡Nucleic acid amplification test using the GeneFinder COVID-19 Plus RealAmp Kit (OSANG Healthcare Co. Ltd., http://www.osanghc.com) (*3*).

We confirmed viral isolation by the increased number of RNA copies per milliliter and the decreased cycle threshold values after passage into Vero cells. The isolation of SARS-CoV-2 shows that nasopharyngeal swab samples contained infectious particles during both COVID-19 episodes.

SARS-CoV-2 variants of concern (VOCs; i.e., lineages B.1.1.7, B.1.351, and P.1.), and particularly their mutations in the spike protein, have been associated with reinfection (*4*,*5*). To investigate this association, we sequenced SARS-CoV-2 genomes from samples or isolates in this study using the ARTIC version 3 protocol (https://artic.network/ncov-2019) with MinION sequencing (Oxford Nanopore Technologies, https://nanoporetech.com). We obtained sequences with 66%–99% genome coverage (mean depth >20-fold) for 3 of 4 HCWs (Appendix Figure, https://wwwnc.cdc.gov/EID/article/27/6/21-0558-App1.pdf). We submitted the sequences to GISAID (https://www.gisaid.org; accession nos. EPI_ISL_1511399, EPI_ISL_1511603, EPI_ISL_1511641, and EPI_ISL_1511644). We used the Pangolin COVID-19 Lineage Assigner tool (*6*) to classify samples as members of lineages B.1.1.28 (n = 3) and B.1.1.33 (n = 1); 3 of these samples were taken during the reinfection episodes of HCWs 1, 2, and 4 and 1 during the first episode of HCW 1 (Appendix Figure). These lineages have circulated in Brazil since early March 2020 (*7*) and have not been associated with reinfection or long-term infection. In addition, we found the D614G mutation in the spike protein in samples from both episodes of HCW 1 and the second episode of HCW 2. The D614G mutation has been associated with enhanced viral replication in the upper respiratory tract and increased susceptibility of the virus to neutralization by antibodies (*8*). In addition, we found the V1176F mutation in the spike protein in samples from both episodes of HCW 1 and the second episode of HCW 4; however, the effects of this mutation remain unclear. None of the genomes had the mutations in spike proteins described in 3 recent VOCs (https://cov-lineages.org). Other cases of SARS-CoV-2 reinfection by strains without mutations in the spike protein were documented in India; those infections were associated with lineages B.1.1.8 and B.1.1.29 (*9*). Our results provide additional evidence of SARS-CoV-2 reinfection by non-VOC strains.

In conclusion, we report cases of SARS-CoV-2 reinfection among HCWs. We observed the shedding of infectious viral particles during both infection episodes of each HCW. Hence, the continuation of protective measures, as well as efforts to monitor, track exposures, and identify areas at high risk for infection, are critical to reducing SARS-CoV-2 reinfection, especially among HCWs.

Acknowledgments

We thank Thermo Fisher Scientific, which kindly provided an EVOS inverted microscope for the Biosafety Level 3 facility at Laboratório de Estudos de Vírus Emergentes. We also thank the UNICAMP Task Force Against COVID-19, which facilitated this study. We thank Ministry of Science, Technology and Innovation of Brazil (MCTI) and all members of the Corona-ômica network for financial support. We thank Lucy Matkin for proofreading the text.

This study was supported by grants from São Paulo Research Foundation (FAPESP; grant nos. 2016/00194-8 and 2020/04558-0) and Fundo de apoio ao ensino, pesquisa e extensão da UNICAMP (grant no. 2266/20). This study was also supported by MCTI through the Rede Corona-ômica Brazil/MCTI (funded by the Financier of Studies and Projects [FINEP] grant no. 01.20.0003.00), RedeVírus/MCTI (FINEP grant no. 01.20.0029.000462/20), and the Brazilian National Council for Scientific and Technological Development, CNPq, grant no. 404096/2020-4). This project was supported by the Medical Research Council and FAPESP–Brazil–UK Centre for (Arbo)virus Discovery, Diagnosis, Genomics and Epidemiology partnership award (grant nos. MR/S0195/1 and FAPESP 2018/14389-0). W.M.S. is supported by FAPESP (grant nos. 2017/13981-0 and 2019/24251-9) and CNPq (grant no. 408338/2018-0). N.R.F. is supported by a Wellcome Trust and Royal Society Sir Henry Dale Fellowship (grant no. 204311/Z/16/Z). K.B.S., CLS., and P.L.P were supported by FAPESP fellowships (grant nos. 2020/02159-0, 2020/02448-2, and 2017/26908-0). M.R.A. was supported by Coordination for the Improvement of Higher Education Personnel fellowships. D.A.T.T. and L.S.M. were supported by CNPq fellowships (grant nos. 141844/2019-1 and 382206/2020-7).

About the Author

Ms. Amorim is a doctoral candidate at the Department of Genetics, Evolution, Microbiology and Immunology at the University of Campinas, Brazil. Her research interests include genomic sequencing and epidemiologic surveillance of emerging viruses in Brazil.

References

1. Pan American Health Organization/World Health Organization. Interim guidelines for detecting cases of reinfection by SARS-CoV-2. Washington (DC): The Organizations; 2020.
2. Corman VM, Landt O, Kaiser M, Molenkamp R, Meijer A, Chu DK, et al. Detection of 2019 novel coronavirus (2019-nCoV) by real-time RT-PCR [Erratum in: Euro Surveill. 2020;25: 20200409c; 2020;25:2007303]. Euro Surveill. 2020;25:2000045. https://doi.org/10.2807/1560-7917.ES.2020.25.3.2000045
3. Ong DSY, Claas ECJ, Breijer S, Vaessen N. Comparison of the GeneFinder COVID-19 Plus RealAmp Kit on the sample-to-result Platform ELITe InGenius to the national reference method: an added value of N gene target detection? J Clin Virol. 2020;132:104632. https://doi.org/10.1016/j.jcv.2020.104632
4. Harrington D, Kele B, Pereira S, Couto-Parada X, Riddell A, Forbes S, et al. Confirmed reinfection with SARS-CoV-2 variant VOC-202012/01. Clin Infect Dis. 2021 Jan 9 [Epub ahead of print]. https://doi.org/10.1093/cid/ciab014
5. Nonaka CKV, Franco MM, Gräf T, de Lorenzo Barcia CA, de Ávila Mendonça RN, de Sousa KAF, et al. Genomic evidence of SARS-CoV-2 reinfection involving E484K spike mutation, Brazil. Emerg Infect Dis. 2021;27:27. https://doi.org/10.3201/eid2705.210191
6. Rambaut A, Holmes EC, O'Toole Á, Hill V, McCrone JT, Ruis C, et al. A dynamic nomenclature proposal for SARS-CoV-2 lineages to assist genomic epidemiology. Nat Microbiol. 2020;5:1403–7. https://doi.org/10.1038/s41564-020-0770-5
7. Candido DS, Claro IM, de Jesus JG, Souza WM, Moreira FRR, Dellicour S, et al.; Brazil–UK Centre for Arbovirus Discovery, Diagnosis, Genomics and Epidemiology Genomic Network. Evolution and epidemic spread of SARS-CoV-2 in Brazil. Science. 2020;369:1255–60. https://doi.org/10.1126/science.abd2161
8. Plante JA, Liu Y, Liu J, Xia H, Johnson BA, Lokugamage KG, et al. Spike mutation D614G alters SARS-CoV-2 fitness. Nature. 2021;592:116–21. https://doi.org/10.1038/s41586-020-2895-3
9. Kulkarni O, Narreddy S, Zaveri L, Kalal IG, Tallapaka KB, Sowpati DT. Evidence of SARS-CoV-2 reinfection without mutations in spike protein. Clin Infect Dis. 2021 Feb 16 [Epub ahead of print]. https://doi.org/10.1093/cid/ciab136

Address for correspondence: Jose Luiz Proenca-Modena, Universidade Estadual de Campinas—Genetics, Microbiology and Immunology Rua Monteiro Lobato, 255—Cidade Universitária Campinas Sao Paulo 13083-862, Brazil; email: jlmodena@unicamp.br; Fabiana Granja, Universidade Federal de Roraima, Boa Vista, Roraima, Brazil; email: fabiana.granja@ufrr.br

Multisystem Inflammatory Syndrome in Adults after Mild SARS-CoV-2 Infection, Japan

Yasuhiro Yamada,[1] Kaoru Fujinami,[1] Tadashi Eguchi, Hiroshi Takefuji, Nobuaki Mori

Author affiliations: National Hospital Organization Tokyo Medical Center, Tokyo, Japan (Y. Yamada, K. Fujinami, T. Eguchi, H. Takefuji, N. Mori); University College London, London, UK (K. Fujinami)

DOI: https://doi.org/10.3201/eid2706.210728

In Japan, a 51-year-old man had minimally symptomatic severe acute respiratory syndrome coronavirus 2 infection. Multisystem inflammatory syndrome was diagnosed ≈5 weeks later; characteristics included severe inflammation, cardiac dysfunction, and IgG positivity. Clinicians should obtain detailed history and examine IgG levels for cases of inflammatory disease with unexplained cardiac decompensation.

[1]These authors contributed equally to this article.

Over the course of the coronavirus disease pandemic, severe inflammatory syndromes have been reported in children (*1*–*3*). Since June 2020, the same syndrome has also been reported in adults. The Centers for Disease Control and Prevention has been collecting case reports of multisystem inflammatory syndrome in adults (MIS-A) and published a case series of MIS-A reported from the United Kingdom and United States in November 2020 (*4*).

A healthy 51-year-old man in Japan tested positive for severe acute respiratory syndrome coronavirus 2 (SARS-CoV-2) by PCR on a saliva sample after his wife was infected with SARS-CoV-2. The positive result was obtained 37 days before hospital admission. During the course of his SARS-CoV-2 infection, his only symptom was olfactory disturbance; he had no respiratory symptoms or fever. He became aware of swelling in the right side of his neck and fatigue 3 days before admission. He visited an internal medicine clinic 2 days before admission for sore throat and fever in the range of 38°C and was prescribed levofloxacin for pharyngitis.

He initially came to the emergency department of National Hospital Organization Tokyo Medical Center because of fever and sore throat, which did not improve. On examination, we noted enlargement of the right cervical lymph nodes, and cervical contrast-enhanced computed tomography revealed lymph nodes swollen to 20 mm localized in the right side of the neck and swelling of the posterior wall of the middle pharynx. The patient was admitted with a diagnosis of lymphadenitis, and we initiated ampicillin/sulbactam.

Table. Laboratory studies performed at intensive care unit admission of patient with multisystem inflammatory syndrome after mild severe acute respiratory syndrome coronavirus 2 infection, Japan

Laboratory test	Result	Reference range
C-reactive protein, mg/dL	36.77	<0.14
Procalcitonin, ng/mL	3.67	<0.05
Interleukin 6, pg/dL	565	<4
Leukocyte count, × 10^9 cells/L	22.4	3.0–8.6
Neutrophil count, × 10^9 cells/L	21.0	1.5–5.8
Lymphocyte count, × 10^9 cells/L	1.0	1.0–3.0
Hemoglobin, g/dL	13.2	13.7–16.8
Platelets, × 10^9/L	180	158–348
Serum creatinine, mg/dL	2.54	0.65–1.07
Albumin, g/dL	2.5	4.1–5.1
Aspartate aminotransferase, U/L	19	13–30
Alanine aminotransferase, U/L	37	10–42
Ferritin, ng/mL	1563	17.9–464
Fibrinogen, mg/dL	>900	200–400
D-dimer, ng/mL	5.7	<1
Creatine phosphokinase, U/L	37	59–248
Troponin T, ng/mL	0.861	<0.014
B-type natriuretic peptide, pg/mL	>2000	<18.4

The patient became acutely hypotensive with blood pressure of 73/45 mm Hg 2 days after admission. He was treated with noradrenaline and dobutamine, but blood pressure did not increase despite crystalloid fluid infusion. We changed antibiotics to meropenem and vancomycin, and 100 mg hydrocortisone was administered empirically to treat septic shock. An electrocardiogram showed a negative T wave and sinus tachycardia. Echocardiography showed ejection fraction of 42% and overall decreased left ventricular contraction. No pericardial effusion was observed. Systemic computed tomography showed enlarged lymph nodes only in the right side of the neck and no pneumonia in the lung fields. The patient was admitted to the intensive care unit (ICU) (Table).

The patient's circulation stabilized, and the swollen cervical lymph nodes improved a few days after ICU admission. During his stay in the ICU, we observed generalized edema. However, as inflammation improved, his urine volume increased, and the edema improved. We observed conjunctivitis 8 days after admission. No skin rash or desquamation was observed. Echocardiography performed 11 days after admission showed improvement in cardiac contraction to 64%, and the duration of fever >38°C was 8 days.

Cultures of blood collected at admission yielded negative results. Coronary computed tomography angiography showed no aneurysms or other abnormalities in the coronary arteries.

The case definition of MIS-A in the Centers for Disease Control and Prevention report (*4*) lists the following 5 criteria: 1) severe illness requiring hospitalization in a person ≥21 years of age; 2) a positive test result for current or previous SARS-CoV-2 infection (nucleic acid, antigen, or antibody) during admission or in the previous 12 weeks; 3) severe dysfunction of >1 extrapulmonary organ systems (e.g., hypotension or shock, cardiac dysfunction, arterial or venous thrombosis or thromboembolism, or acute liver injury); 4) laboratory evidence of severe inflammation (e.g., elevated C-reactive protein, ferritin, D-dimer, or interleukin-6); and 5) absence of severe respiratory illness (to exclude patients in which inflammation and organ dysfunction might be attributable simply to tissue hypoxia). This case meets all of these criteria.

Whether MIS-A is associated with acute SARS-CoV-2 infection or is a reaction after acute infection is unclear. In this case, the case-patient's positive SARS-CoV-2 test result occurred 37 days before the onset of MIS-A, and IgG levels were already elevated at the time of admission. This fact supports the notion that

MIS-A can occur after the acute phase of SARS-CoV-2 infection. The only symptom at the time of infection was olfactory disturbance, which is similar to other case reports of MIS-A occurring in asymptomatic or minimally symptomatic patients (*5*).

It has been reported that MIS-A can cause symptoms similar to those of Kawasaki disease (*6*). This case did not meet the American College of Cardiology criteria for Kawasaki disease (*7*) but did meet the definition of incomplete Kawasaki disease. Conjunctivitis persisted for 4 weeks after the onset of MIS-A and gradually improved.

In February 2021, a case definition was proposed for reporting cases of multisystem inflammatory syndrome in adults and children after vaccination (*8*). Considering the possibility that the disease develops after asymptomatic SARS-CoV-2 infection and that increased IgG levels can be involved, MIS-A is rare, but the disease concept of MIS-A should be widely acknowledged. Clinicians should consider obtaining detailed history and examining SARS-CoV-2 IgG levels for cases of severe inflammatory disease with unexplained cardiac decompensation.

Acknowledgments

We thank Shinichi Kimura and Yurie Yamazaki for intensive care, and we thank the clinical staff at National Hospital Organization Tokyo Medical Center for their dedicated clinical practice and patient care.

About the Author

Dr. Yasuhiro Yamada is a physician at National Hospital Organization Tokyo Medical Center, Tokyo, Japan. His research interests include general internal medicine and health economics.

References

1. Godfred-Cato S, Bryant B, Leung J, Oster ME, Conklin L, Abrams J, et al.; California MIS-C Response Team. COVID-19-associated multisystem inflammatory syndrome in children—United States, March–July 2020. MMWR Morb Mortal Wkly Rep. 2020;69:1074–80. https://doi.org/10.15585/mmwr.mm6932e2
2. Belot A, Antona D, Renolleau S, Javouhey E, Hentgen V, Angoulvant F, et al. SARS-CoV-2-related paediatric inflammatory multisystem syndrome, an epidemiological study, France, 1 March to 17 May 2020. Euro Surveill. 2020;25:2001010. https://doi.org/10.2807/1560-7917.ES.2020.25.22.2001010
3. Whittaker E, Bamford A, Kenny J, Kaforou M, Jones CE, Shah P, et al.; PIMS-TS Study Group and EUCLIDS and PERFORM Consortia. Clinical characteristics of 58 children with a pediatric inflammatory multisystem syndrome temporally associated with SARS-CoV-2. JAMA. 2020;324:259–69. https://doi.org/10.1001/jama.2020.10369
4. Morris SB, Schwartz NG, Patel P, Abbo L, Beauchamps L, Balan S, et al. Case series of multisystem inflammatory syndrome in adults associated with SARS-CoV-2 infection—United Kingdom and United States, March–August 2020. MMWR Morb Mortal Wkly Rep. 2020;69:1450–6. https://doi.org/10.15585/mmwr.mm6940e1
5. Hékimian G, Kerneis M, Zeitouni M, Cohen-Aubart F, Chommeloux J, Bréchot N, et al. Coronavirus disease 2019 acute myocarditis and multisystem inflammatory syndrome in adult intensive and cardiac care units. Chest. 2021; 159:657–62. https://doi.org/10.1016/j.chest.2020.08.2099
6. Shaigany S, Gnirke M, Guttmann A, Chong H, Meehan S, Raabe V, et al. An adult with Kawasaki-like multisystem inflammatory syndrome associated with COVID-19. Lancet. 2020;396:e8–10. https://doi.org/10.1016/S0140-6736(20)31526-9
7. McCrindle BW, Rowley AH, Newburger JW, Burns JC, Bolger AF, Gewitz M, et al.; American Heart Association Rheumatic Fever, Endocarditis, and Kawasaki Disease Committee of the Council on Cardiovascular Disease in the Young; Council on Cardiovascular and Stroke Nursing; Council on Cardiovascular Surgery and Anesthesia; and Council on Epidemiology and Prevention. Diagnosis, treatment, and long-term management of Kawasaki disease: a scientific statement for health professionals from the American Heart Association. Circulation. 2017;135:e927–99. https://doi.org/10.1161/CIR.0000000000000484
8. Vogel TP, Top KA, Karatzios C, Hilmers DC, Tapia LI, Moceri P, et al. Multisystem inflammatory syndrome in children and adults (MIS-C/A): case definition & guidelines for data collection, analysis, and presentation of immunization safety data. Vaccine. 2021 Feb 25 [Epub ahead of print].

Address for correspondence: Yasuhiro Yamada, Department of General Internal Medicine, National Hospital Organization Tokyo Medical Center, Tokyo, 152-8902, Japan; email: yayamada0113@gmail.com

Changing Molecular Epidemiology of Hepatitis A Virus Infection, United States, 1996–2019

Sumathi Ramachandran, Guo-Liang Xia, Zoya Dimitrova, Yulin Lin, Martha Montgomery, Ryan Augustine, Saleem Kamili, Yury Khudyakov

Author affiliation: Centers for Disease Control and Prevention, Atlanta, Georgia, USA

DOI: https://doi.org/10.3201/eid2706.203036

Hepatitis A virus (HAV) genotype IA was most common among strains tested in US outbreak investigations and surveillance during 1996–2015. However, HAV genotype IB gained prominence during 2016–2019 person-to-person multistate outbreaks. Detection of previously uncommon strains highlights the changing molecular epidemiology of HAV infection in the United States.

Hepatitis A virus (HAV) is transmitted primarily through person-to-person contact or exposure to contaminated food or water. After the introduction of hepatitis A vaccine recommendations in the United States in 1996, reports of hepatitis A cases decreased progressively from 1999 to 2011 by a total of ≈95% (*1*,*2*). However, we recently showed that hepatitis A cases increased 294% during 2016–2018 compared with 2013–2015 among persons who use drugs (injection or noninjection), persons experiencing homelessness, or men who have sex with men (*3*,*4*).

HAV strains infecting humans are genetically classified into genotypes I, II, and III. Genotype I is further divided into subtypes A, B, and C, and genotypes II and III are divided into subtypes A and B. In this study, we investigated HAV genotype and strain distributions in the United States during 1996–2019.

Genetic testing was performed by using DNA sequencing, and we included HAV sequences obtained from 9,203 specimens collected during outbreak investigations and surveillance activities conducted by the Centers for Disease Control and Prevention (CDC) or state health departments during 1996–2019 (Appendix Table, https://wwwnc.cdc.gov/EID/article/27/6/20-3036-App1.pdf). We performed phylogenetic analysis of a 315 base-pair fragment of the HAV viral protein 1–amino terminus of 2B genomic region amplified from serum specimens (Appendix Figure 1).

We found that during 1996–2015, HAV genotype IA was most common among specimens collected through surveillance (93%; 1,587/1,706) and outbreak investigations (84.4%; 706/836;); genotype IB was detected among only 6.4% (110/1,706) of surveillance and 15.2% (127/836) of outbreak specimens. Genotype IIIA was detected in ≤0.5% of both collections (Table). During 2016–2019, a total 6,661 outbreak specimens were collected from many states across the country (Appendix Figure 2). Sequences from these outbreaks represented ≈19% of all HAV cases reported to CDC through the National Notifiable Diseases Surveillance System (*4*), ≈3 times more specimens than were collected during 1996–2015. Among the 6,661 specimens collected during 2016–2019, genotype IA was identified in 15.7% of specimens, IB in 82.8%, and IIIA in 1.5% (Table).

Among all 9,203 tested specimens, we identified 1,055 HAV strains that we defined as having unique genetic variants; 352 (33.4%) HAV strains were identified from specimens collected during 2016–2019 (Figure). Genetic analyses demonstrate that 63.4% (n = 102) of genotype IB strains and 40% (n = 6) of genotype IIIA strains identified during 2016–2019 belonged to 2 large genetic clusters or groups of closely related HAV strains (Figure), but genotype IA strains were distributed among many small genetic clusters.

The CDC-developed Global Hepatitis Outbreak and Surveillance Technology (GHOST) system improved molecular testing capabilities of state and local health departments during the 2016–2019 multistate outbreaks. Molecular epidemiologic methods have helped clarify HAV transmissions within networks of persons with similar risk factors (*5*). By using genetic testing, CDC has assisted in 25 outbreak investigations associated with a common source transmission by contaminated food (*6*,*7*) and person-to-person transmissions (*8*,*9*).

For 20 years (1996–2016), during the national decrease in HAV cases attributed to increased vaccination, genotype IA was the most detected genotype. However, genotype IB cases associated with

Table. Genotype distribution of HAV specimens collected through surveillance programs and outbreak investigations, United States, 1996–2019*

	No. (%) HAV surveillance specimens †				No. (%) HAV outbreak specimens‡				No. (%) HAV specimens			
Year	Total	IA	IB	IIIA	Total	IA	IB	IIIA	Total	IA	IB	IIIA
1996–2015	1,706	1,587 (93.0)	110 (6.4)	9 (0.5)	836	706 (84.4)	127 (15.2)	3 (0.4)	2,542	2,293 (90.2)	237 (9.3)	12 (0.5)
2016–2019		ND			6,661	1,046 (15.7)	5,518 (82.8)	97 (1.5)	6,661	1,046 (15.7)	5,518 (82.8)	97 (1.5)

*Since 2014, the United States has not had established HAV surveillance programs in place to provide specimens for molecular testing of surveillance cases. Specimens collected as part of outbreak investigations during 2016–2019, might include some sporadic cases. During 1996–2015, ≈130 HAV specimens/year were tested; During 2016–2019, 1,660 specimens/year were tested. HAV, hepatitis A virus; ND, no data.
†Surveillance specimens tested by the Centers for Disease Control and Prevention (CDC) during 1996–2013 included sentinel county surveillance (n = 1,234) during 1996–2006; the Emerging Infectious Disease Program (n = 418) during 2007–2013; and the Border Infectious Disease Surveillance (n = 54) system during 2007–2013.
‡Outbreak specimens sequenced during 1996–2015 (n = 836) were tested by CDC. Outbreak specimens sequenced during 2016–2019 (n = 6,661) included data from CDC testing (n = 5,068) and data captured through technical assistance offered to sites, which included data from Sanger sequences reported to CDC for technical assistance and analysis from state and local public health laboratories (n = 341) and the Food and Drug Administration (n = 3); data from ultradeep sequencing and submission to the Global Hepatitis Outbreak and Surveillance Technology portal by state and local public health laboratories (n = 1,249).

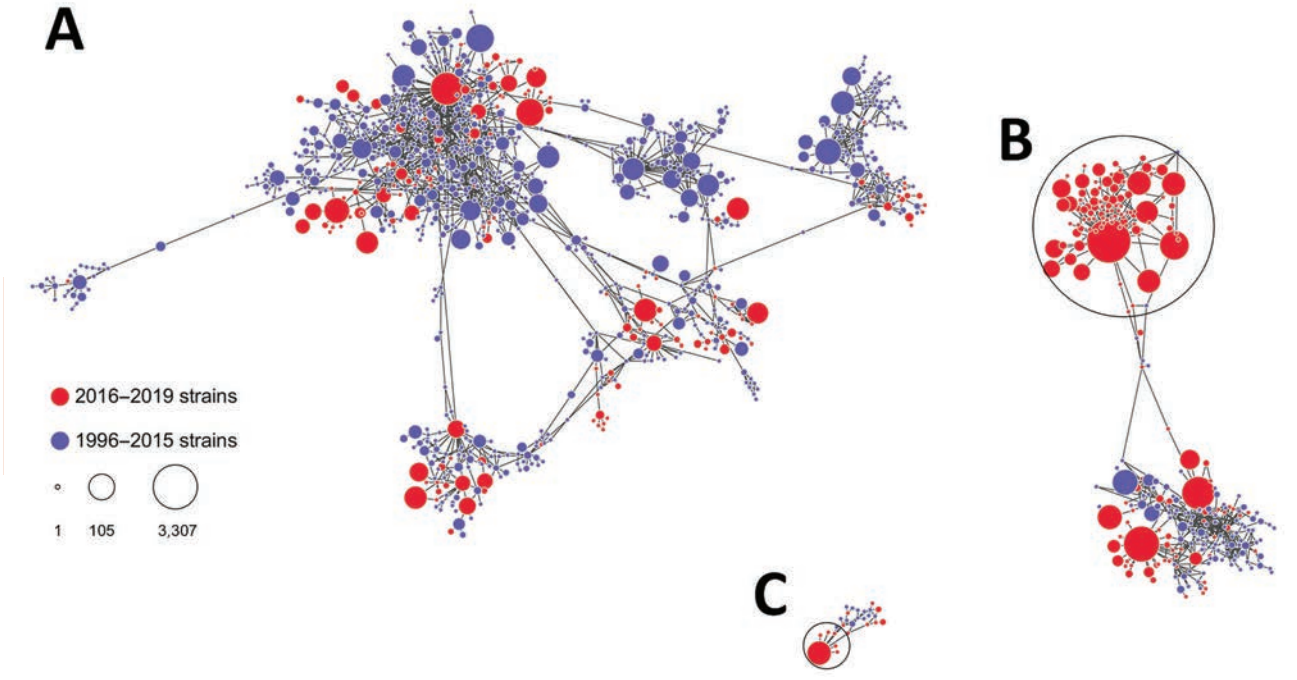

Figure. Genetic relatedness among hepatitis (HAV) strains, United States, 1996–2019. A) IA strains; B) IB strains; C) IIIA strains. Nodes represent HAV strains, and the size of node is proportional to the frequency of the strain; larger nodes denote more frequent detection. Distance between nodes approximates genetic closeness of HAV strains. Genetic clusters of closely related HAV strains encompassing a large fraction of all strains in HAV genotypes IB and IIIA are circled. Visualization created by using Gephi software (https://gephi.org).

outbreaks in multiple states increased during 2016–2019. During that time, IB became the most common genotype, detected in 83% of specimens collected across many states (Appendix Figure 2).

Findings from the National Health and Nutrition Examination Surveys during 1999–2012 revealed that despite the overall increase in HAV antibody among children, prevalence of HAV antibody among US-born adults was low (24%), indicating decreasing immunity to HAV (*10*). However, our molecular data indicate that the increase in number of HAV cases observed in outbreaks during 2016–2019 might not be attributable solely to the decline in the population's HAV immunity. Because HAV genotype IA was dominant in the United States for years, the large person-to-person outbreaks during 2016–2019 reasonably could be expected to be caused by genotype IA strains widely circulating in the country, but our genetic analysis shows predominance of the previously rare HAV genotype IB strains. Identification of 1 large cluster and several small genetic clusters suggests ≥1 introduction of genotype IB to the affected population in multiple states during 2016–2019. On the basis of these findings, we hypothesize that genotype IB was introduced from regions of the world where these strains are endemic and could be responsible for initiation of the outbreaks among vulnerable populations (Appendix Figure 3). GHOST was instrumental in identifying changes in molecular epidemiology of HAV infections and is an example of novel emerging technologies that can be used for national viral hepatitis molecular surveillance program.

Our observations are hallmarks of a change in HAV molecular epidemiology in the United States. GHOST technology is improving hepatitis detection at the state and local level. Our findings emphasize the need for systematic HAV surveillance for strain characterization, timely detection of transmission clusters, and assistance in guiding public health interventions and vaccination efforts.

Acknowledgments

We thank members of the CDC National Center for HIV/AIDS, Viral Hepatitis, STD, and TB Prevention, Division of Viral Hepatitis, Laboratory Branch; the Global Hepatitis Outbreak and Surveillance Technology (GHOST) Team; HAV Outbreak Incident Management Team; US Food and Drug Administration CORE Signals Teams; state and local public health laboratories participating as GHOST ultradeep sequencing testing sites, including the following: Brett Austin, Syreeta Steele, Tracy Basler, and Jovan Shepherd (San Diego County Public Health Laboratory, San Diego,

California, USA); Courtney Edwards, Teresa R. Fields, Matthew Johnson, and Vaneet Arora (Kentucky Department for Public Health); Erica Reaves, Jeannette P. Dill, Katie Nixon, Linda S. Thomas, Victoria N. Stone, and Xiaorong Qian (Tennessee Department of Health); Joseph Yglesias and Ian Stryker (Florida Department of Health, Bureau of Public Health Laboratories); Andrea Leapley (Florida Department of Health, Bureau of Epidemiology); Daryl Lamson, Patrick Bryant, and Kirsten St. George (New York State Department of Health); Sharmila Talekar, Oxana Mazurova, Kim Kilgour, and Elizabeth Franko (Georgia Department of Public Health Laboratory); and state departments of health reporting Sanger sequences as part of technical assistance, including Will Probert, Carlos Gonzalez, and Jill K Hacker (California Department of Public Health [CDPH]) and the CDPH Hepatitis A Epidemiology Team; Michigan State Department of Health; Elizabeth Cebelinski (Minnesota Department of Health); and Jacquelina Woods (US Food and Drug Administration).

About the Author

Dr. Ramachandran is a senior scientist in the National Center for HIV, Viral Hepatitis, STD, and TB Prevention, Centers for Disease Control and Prevention, Atlanta, Georgia, USA. Her research interests include hepatitis surveillance, outbreak response, public health technical assistance, and strategic partnerships.

References

1. Centers for Disease Control and Prevention. Viral hepatitis surveillance, United States, 2011. Atlanta: The Centers; 2012 [cited 2021 Apr 1]. https://www.cdc.gov/hepatitis/statistics/2011surveillance/pdfs/2011HepSurveillanceRpt.pdf
2. Ly KN, Klevens RM. Trends in disease and complications of hepatitis A virus infection in the United States, 1999-2011: a new concern for adults. J Infect Dis. 2015;212:176–82. https://doi.org/10.1093/infdis/jiu834
3. Foster MA, Hofmeister MG, Kupronis BA, Lin Y, Xia GL, Yin S, et al. Increase in hepatitis A virus infections—United States, 2013–2018. MMWR Morb Mortal Wkly Rep. 2019;68:413–5. https://doi.org/10.15585/mmwr.mm6818a2
4. Centers for Disease Control and Prevention. Widespread outbreaks of hepatitis A across the United States [cited 2021 Apr 1]. https://www.cdc.gov/hepatitis/outbreaks/2017March-HepatitisA.htm
5. Nainan OV, Armstrong GL, Han XH, Williams I, Bell BP, Margolis HS. Hepatitis a molecular epidemiology in the United States, 1996-1997: sources of infection and implications of vaccination policy. J Infect Dis. 2005;191:957–63. https://doi.org/10.1086/427992
6. Collier MG, Khudyakov YE, Selvage D, Adams-Cameron M, Epson E, Cronquist A, et al.; Hepatitis A Outbreak Investigation Team. Outbreak of hepatitis A in the USA associated with frozen pomegranate arils imported from Turkey: an epidemiological case study. Lancet Infect Dis. 2014;14:976–81. https://doi.org/10.1016/S1473-3099(14)70883-7
7. Food and Drug Administration. FDA investigates outbreak of hepatitis A illnesses linked to frozen strawberries. Silver Spring (MD): FDA; 2016 [cited 2021 Apr 1]. https://www.fda.gov/food/recallsoutbreaksemergencies/outbreaks/ucm518775.html
8. Peak CM, Stous SS, Healy JM, Hofmeister MG, Lin Y, Ramachandran S, et al. Homelessness and Hepatitis A-San Diego County, 2016-2018. Clin Infect Dis. 2020;71:14–21. https://doi.org/10.1093/cid/ciz788
9. Foster M, Ramachandran S, Myatt K, Donovan D, Bohm S, Fiedler J, et al. Hepatitis A virus outbreaks associated with drug use and homelessness—California, Kentucky, Michigan, and Utah, 2017. MMWR Morb Mortal Wkly Rep. 2018;67:1208–10. https://doi.org/10.15585/mmwr.mm6743a3
10. Klevens RM, Denniston MM, Jiles-Chapman RB, Murphy TV. Decreasing immunity to hepatitis A virus infection among US adults: Findings from the National Health and Nutrition Examination Survey (NHANES), 1999-2012. Vaccine. 2015;33:6192–8. https://doi.org/10.1016/j.vaccine.2015.10.009

Address for correspondence: Sumathi Ramachandran, Centers for Disease Control and Prevention, 1600 Clifton Rd NE, Mailstop A33, Atlanta, GA 30329-4027, USA; email: dcq6@cdc.gov

Molecular Typing of *Burkholderia mallei* Isolates from Equids with Glanders, India

Harisankar Singha,[1] Mandy C. Elschner,[1] Praveen Malik, Sheetal Saini, Bhupendra N. Tripathi, Katja Mertens-Scholz, Hanka Brangsch, Falk Melzer, Raj K. Singh, Heinrich Neubauer

Author affiliations: Indian Council of Agricultural Research—National Research Centre on Equines, Haryana, India (H. Singha, S. Saini); Friedrich-Loeffler-Institut Federal Research Institute for Animal Health, Institute for Bacterial Infections and Zoonoses, Jena, Germany (M.C. Elschner, K. Mertens-Scholz, H. Brangsch, F. Melzer, H. Neubauer); Ministry of Fisheries, Animal Husbandry & Dairying, Government of India, New Delhi, India (P. Malik); Indian Council of Agricultural Research, Krishi Bhawan, New Delhi (B.N. Tripathi); Indian Council of Agricultural Research—Indian Veterinary Research Institute, Izatnagar, India (R.K. Singh)

DOI: https://doi.org/10.3201/eid2706.203232

[1]These first authors contributed equally to this work.

We collected 10 *Burkholderia mallei* isolates from equids in 9 districts in India during glanders outbreaks in 2013–2016. Multilocus variable-number tandem-repeat analysis showed 7 outbreak area–related genotypes. The study highlights the utility of this analysis for epidemiologically tracing of specific *B. mallei* isolates during outbreaks.

Burkholderia mallei is the etiologic agent of the contagious and fatal infection in equids known as glanders. It is one of the most ancient diseases and is distributed worldwide. *B. mallei* infections are frequently reported in South America, the Middle East, South Asia, and some countries in Africa. Equine glanders is a notifiable zoonotic disease; surveillance measures are enforced by the World Organisation for Animal Health (*1*).

Since 2006, equine glanders has been reported in India with consistently higher numbers from the Uttar Pradesh state (*2*,*3*). Regular glanders surveillance programs revealed presence of the disease in 14 states and, during 2015–2018, fresh *B. mallei* infections were reported in 6 states: Jammu and Kashmir, Gujarat, Rajasthan, Delhi, Madhya Pradesh, and Tamil Nadu (*4*). Epidemiologic investigations indicated that trading of equids from Uttar Pradesh to other states played a major role in spreading glanders (*2*). However, *B. mallei* isolates were not genotyped, which is necessary for understanding the epidemiologic association between glanders outbreaks across India.

Our study describes molecular typing of 10 *B. mallei* isolates recovered from horses (n = 4) and mules (n = 6) during 2013–2016 (Table; Appendix 1 Figure, https://wwwnc.cdc.gov/EID/article/27/6/20-3232-App1.pdf). All the affected equids were used for cart pulling and kept in small household stables. Five isolates (3324, 3478, 3701, 3711, and 3712), originating from 3 horses and 2 mules, were from adjoining districts of Uttar Pradesh state, which is regarded as a glanders hotspot zone (*2*). Three isolates (3076, 3081, 3595) from mules were located in 2 districts of Himachal Pradesh. Available information from the equine keeper suggested that these animals were traded from Uttar Pradesh and were responsible for the reported glanders incidence in this state. One isolate was recovered from a mule (3880) in Gujarat and 1 from a horse (3897) in Haryana state; both animals had no recent travel history.

The isolates were recovered from different types of biologic samples (Table) as described previously (*3*) and identified as *B. mallei* by real-time PCR (*1*). Genomic DNA was extracted by using the PureLink genomic DNA isolation kit (Invitrogen, https://www.thermofisher.com) and used for PCR-based multilocus sequence typing (MLST) and multilocus variable-number tandem-repeat (VNTR) analysis (MLVA). We typed all 10 *B. mallei* isolates as sequence type (ST) 40 by the *B. pseudomallei* MLST scheme and ST734 by the *B. cepacia* MLST scheme (*5*–*6*); Appendix 2 Tables 1, 2, https://wwwnc.cdc.gov/EID/article/27/6/20-3232-App2.xlsx).

We conducted MLVA by PCR amplification and sequencing of 23 loci using previously described primers (*7*). We determined sequence length and repeat number for each locus using Geneious software version 6.1.8 (https://www.geneious.com). A distance matrix giving the number of VNTR loci differing between isolates was used for analysis applying the minimum-evolution method implemented in MEGA X software version 10.0.5 (https://www.megasoftware.net).

MLVA assigned the 10 isolates to 7 genotypes, indicating considerable variability among *B. mallei* isolates in India (Figure, panel A). Identical MLVA patterns were observed for isolates 3076 and 3081 from Himachal Pradesh and isolate 3324 from Uttar

Table. Location, host, and isolation year of 10 *Burkholderia mallei* isolates included for molecular typing, India

B. mallei isolate	Place of origin (district, state)	Year isolated	Host species	Salient clinical signs	Sample type
India3076	Solan, Himachal Pradesh	2013	Mule	Blood tinged nasal discharge, respiratory distress	Nasal swab
India3081	Solan,Himachal Pradesh	2013	Mule	Respiratory distress, nasal discharge, cutaneous nodules	Nasal swab
India3324	Hardoi,Uttar Pradesh	2014	Horse	Nasal discharge, hind limb ulcer, liver abscess	Liver abscess
India3478	Agra, Uttar Pradesh	2014	Horse	Hind limb ulceration, lacrimation	Lesion swab
India3595	Mandi, Himachal Pradesh	2015	Mule	Labored breathing, nasal discharge	Nasal swab
India3701	Kasganj,Uttar Pradesh	2015	Mule	Nasal discharge, cutaneous nodules	Lesion swab
India3711	Etah, Uttar Pradesh	2015	Mule	Respiratory distress, cutaneous nodules	Nasal swab
India3712	Ghaziabad, Uttar Pradesh	2015	Horse	Ulcerous nodules on body surface	Nasal swab
India3880	Banaskantha, Gujarat	2016	Mule	Mucopurulent nasal discharge	Nasal swab
India3897	Yamunanagar, Haryana	2016	Horse	Ulcerous nodules on hind limb and forelimb, purulent nasal discharge	Lesion swab

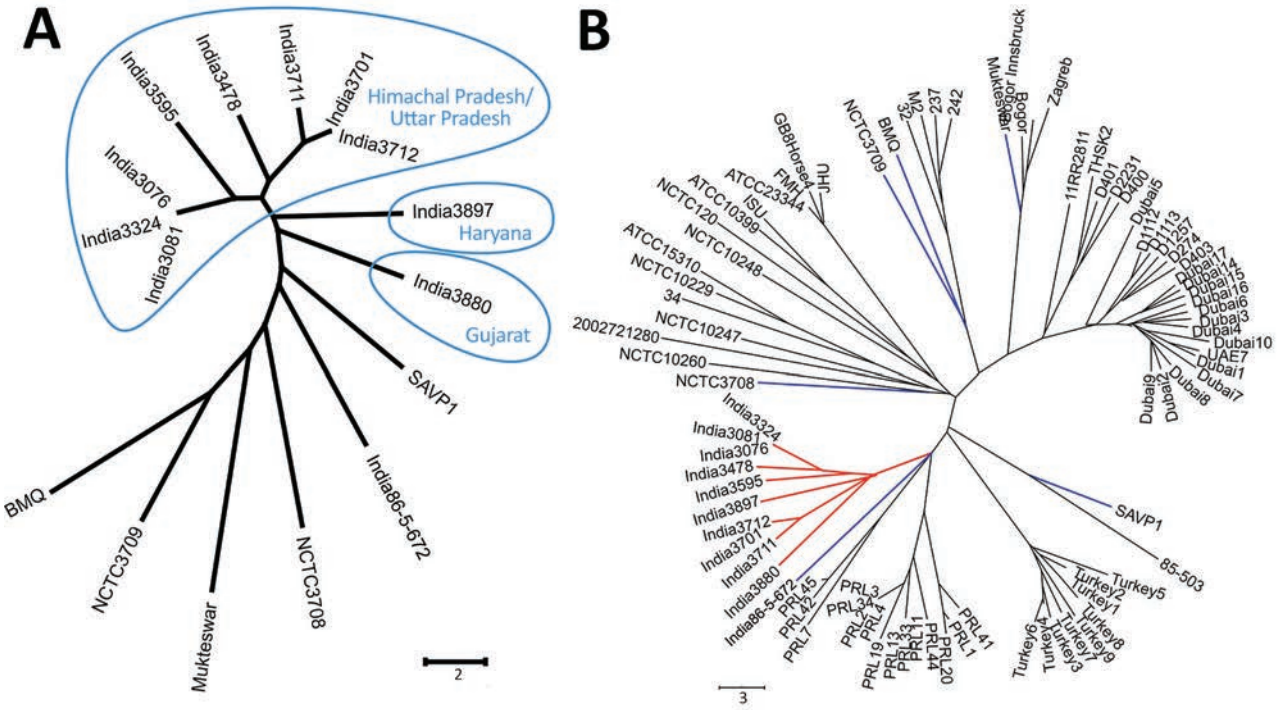

Figure. Minimum evolution trees based on 23 VNTR loci of 10 *Burkholderia mallei* isolates from Himachal Pradesh, Uttar Pradesh, Gujarat, and Haryana states, India, compared with reference sequences. A) Comparison of Himachal Pradesh–Uttar Pradesh cluster isolates (blue circles) with 6 older *B. mallei* isolates from India. B) Comparison of Himachal Pradesh–Uttar Pradesh cluster isolates (red branches) with 77 previously published *B. mallei* isolates, including the 6 others from India (blue branches). Scale bars indicate allelic differences.

Pradesh. These findings correlate with epidemiologic investigations regarding the spread of a particular strain of *B. mallei* by equine movement, emphasizing the need to control equine trade between states. An identical pattern was also observed for *B. mallei* 3701 and 3712, which were isolated from Kasganj and Ghaziabad districts, 190 km apart in Uttar Pradesh state.

The isolates 3897 and 3880 from Haryana and Gujarat differ clearly from the isolates from Himachal Pradesh–Uttar Pradesh cluster (Figure, panel A). However, isolates 3712, 3880, and 3897 were previously grouped into the L2B2sB2 branch by HRM-PCR analysis (*8*), which indicates superiority of MLVA for better epidemiologic resolution of glanders outbreaks.

Comparative MLVA between old and recent isolates from India revealed that most of the earlier isolates Mukteswar, BMQ, NCTC3708, NCTC3709, and India 86–567–2 are distantly related, whereas the isolate SAVP1 showed the highest similarity to the new isolates (Figure, panel A; Appendix 2 Table 3).

Further analysis of these *B. mallei* isolates plus 77 from other countries revealed that the 10 recent isolates of our study form a cluster that is most similar to isolates from Pakistan, followed by isolates from Turkey (Figure, panel B). This finding suggests that *B. mallei* strains prevalent in geographically close countries might have originated from an ancestral clone and gradually disseminated to different areas. Of interest, adoption of a strict regulatory movement policy at the beginning of the 19th century for control and eradication of glanders might have resulted in establishing specific *B. mallei* lineages at different ecologic settings. Our finding confirms previous observations regarding circulation of different *B. mallei* MLVA types in the Middle East (*9*,*10*).

In summary, MLVA proved useful as a genetic tool for classifying *B. mallei* isolates and tracing possible infection chains of glanders outbreaks in equids. VNTR information from more *B. mallei* isolates from India and other countries would be helpful to draw an epidemiologic conclusion between outbreaks.

Acknowledgments

We thank the staff of the involved field veterinary hospitals for their cooperation during field investigation and sample collection. We thank Sita Ram and Gurudutt Sharma for assistance with the collection and processing of clinical samples.

The World Organisation for Animal Health, Paris, provided funding under the Laboratories Twinning Programme.

About the Authors

Dr. Singha is in charge of the National Reference Laboratory for Glanders at the Indian Council of Agricultural Research—National Research Centre on Equines, Hisar, Haryana, India. His primary research interests are diagnosis of glanders, host–pathogen interaction, and molecular typing of *Burkholderia mallei*. Dr. Elschner is in charge of the National Reference Laboratory for Glanders at the Friedrich-Loeffler-Institute, Federal Research Institute of Animal Health, Institute for Bacterial Infections and Zoonoses, Jena, Germany. She also works for the OIE Reference Laboratory for Glanders. Her primary research interest is diagnosis of glanders.

References

1. World Organisation for Animal Health. Glanders and melioidosis. In: Manual of diagnostic tests and vaccines for terrestrial animals. Paris: The Organisation; 2018. p. 1350–62 [cited 2021 May 5]. https://www.oie.int/fileadmin/Home/eng/Health_standards/tahm/3.05.11_GLANDERS.pdf
2. Malik P, Singha H, Khurana SK, Kumar R, Kumar S, Raut AA, et al. Emergence and re-emergence of glanders in India: a description of outbreaks from 2006 to 2011. Vet Ital. 2012;48:167–78.
3. Malik P, Singha H, Goyal SK, Khurana SK, Tripathi BN, Dutt A, et al. Incidence of *Burkholderia mallei* infection among indigenous equines in India. Vet Rec Open. 2015;2:e000129. https://doi.org/10.1136/vetreco-2015-000129
4. Singha H, Shanmugasundaram K, Tripathi BN, Saini S, Khurana SK, Kanani A, et al. Serological surveillance and clinical investigation of glanders among indigenous equines in India from 2015 to 2018. Transbound Emerg Dis. 2020;67:1336–48. https://doi.org/10.1111/tbed.13475
5. Godoy D, Randle G, Simpson AJ, Aanensen DM, Pitt TL, Kinoshita R, et al. Multilocus sequence typing and evolutionary relationships among the causative agents of melioidosis and glanders, *Burkholderia pseudomallei* and *Burkholderia mallei*. J Clin Microbiol. 2003;41:2068–79. https://doi.org/10.1128/JCM.41.5.2068-2079.2003
6. Aanensen DM, Spratt BG. The multilocus sequence typing network: mlst.net. Nucleic Acids Res. 2005;33:W728–33. https://doi.org/10.1093/nar/gki415
7. Hornstra H, Pearson T, Georgia S, Liguori A, Dale J, Price E, et al. Molecular epidemiology of glanders, Pakistan. Emerg Infect Dis. 2009;15:2036–9. https://doi.org/10.3201/eid1512.090738
8. Girault G, Wattiau P, Saqib M, Martin B, Vorimore F, Singha H, et al. High-resolution melting PCR analysis for rapid genotyping of *Burkholderia mallei*. Infect Genet Evol. 2018;63:1–4. https://doi.org/10.1016/j.meegid.2018.05.004
9. Wernery U, Wernery R, Joseph M, Al-Salloom F, Johnson B, Kinne J, et al. Natural *Burkholderia mallei* infection in Dromedary, Bahrain. Emerg Infect Dis. 2011;17:1277–9. https://doi.org/10.3201/eid1707.110222
10. Scholz HC, Pearson T, Hornstra H, Projahn M, Terzioglu R, Wernery R, et al. Genotyping of *Burkholderia mallei* from an outbreak of glanders in Bahrain suggests multiple introduction events. PLoS Negl Trop Dis. 2014;8:e3195. https://doi.org/10.1371/journal.pntd.0003195

Address for correspondence: Mandy C. Elschner, Friedrich Loeffler Institute—Institute of Bacterial Infections and Zoonoses, Naumburger Str. 96a, Jena 07743, Germany; email: mandy.elschner@fli.de; Harisankar Singha, National Research Centre on Equines, Sirsa Rd, Hisar 125001, India; email: hsssankarbty@gmail.com

Atypical *Brucella inopinata*–Like Species in 2 Marine Toads

Raisa A. Glabman, Kimberly A. Thompson, Rinosh Mani, Ryan Colburn, Dalen W. Agnew

Author affiliations: National Institutes of Health, Bethesda, Maryland, USA (R.A. Glabman); Michigan State University, East Lansing, Michigan, USA (R.A. Glabman, K.A. Thompson, R. Mani, R. Colburn, D.W. Agnew; Binder Park Zoo, Battle Creek, Michigan, USA (K.A. Thompson); John Ball Zoo, Grand Rapids, Michigan, USA (R. Colburn)

DOI: https://doi.org/10.3201/eid2706.204001

We describe the isolation of atypical *Brucella inopinata*–like species and unique clinicopathologic findings in 2 adult marine toads (*Rhinella marina*), including oophoritis in 1 toad. These findings represent a novel emerging disease in toads and a possible zoonotic pathogen.

Brucellosis is a worldwide zoonosis caused by gram-negative, intracellular *Brucella* coccobacilli. Expanding from 6 species classically associated with abortion in mammals (*B. melitensis*, *B. suis*, *B. abortus*, *B. ovis*, *B. canis*, and *B. neotomae*), the genus now includes novel strains from marine mammals (*B. ceti*, *B. pinnipedialis*), baboons (*B. papionis*), and foxes (*B. vulpis*). Two of these (*B. ceti*, *B. pinnipedialis*) are also considered atypical *Brucella* species similar to *B. microti* and *B. inopinata* (*1*). Atypical *Brucella* lesions in humans, wild mammals, amphibians, and fish range from localized manifestations to systemic infection with high death rates (*2*–*8*); however, reproductive lesions more

typical of mammalian brucellosis are rare in amphibians. Previous reports of *Brucella* in amphibians have also included asymptomatic infections, suggesting that *Brucella* may be a commensal microorganism or opportunistic pathogen (*9*). The precise epidemiology, pathogenesis, and zoonotic potential of *Brucella* in amphibians remains largely unknown. We report atypical *Brucella* infection in 2 marine toads.

Cases 1 and 2 originated from the same captive breeding marine toad (*Rhinella marina*) colony; the 2 toads cohabited before toad 1's transfer to a different zoological institution, resulting in a 4-year period with no contact before death. Case 1 was in an adult female marine toad with a 1.5-cm subcutaneous mass near the parotid gland. A second mass was palpated within the coelom, and ultrasound suggested ovarian origin. The toad was anesthetized for exploratory celiotomy, and both masses were excised and submitted for histopathology and culture. The coelomic mass was encapsulated within the left ovary, measured 3 × 2 × 2 cm, and contained purulent material (Figure). Histologically, the masses contained multifocal regions of necrosis and amorphous eosinophilic material with sheets of macrophages containing numerous intracytoplasmic, gram-negative, non–acid-fast coccobacilli (Appendix Figure, https://wwwnc.cdc.gov/EID/article/27/6/20-4001-App1.pdf). Diagnosis led to euthanasia; postmortem findings included mild coelomic effusion, lymphohistiocytic pericarditis, and fibrinous peritonitis. Case 2 was in an adult male marine toad, which was submitted for necropsy after being found dead in its enclosure. The toad was in poor body condition with no other lesions found on gross and histologic examination.

We used fresh ovarian tissue from the female toad and pooled fresh tissues (liver, kidney, and spleen) from the male toad for bacterial culture. We incubated duplicate culture plates at 37°C with 5% CO_2 and in ambient conditions (21 + 2°C, no CO_2). After 24 hours of ovarian mass culture incubation, we observed numerous pure bacterial colonies on blood and MacConkey agar at both 37°C and ambient conditions (colony size was smaller at ambient temperature). The pooled samples from the male toad contained mixed bacterial cultures after 24 hours of incubation. We identified the bacterial colony from the female toad with matrix-assisted laser desorption ionization-time of flight mass spectrometry (Microflex LT; Bruker Daltonics, https://www.bruker.com) as *Brucella* sp. (isolate no. 3278), whereas we identified bacterial colonies from the male toad as *Brucella* sp. (isolate no. 5043). Both *Brucella* isolates grew on MacConkey, Thayer-Martin, and blood agar at both 37°C and ambient conditions.

Figure. Celiotomy to remove ovarian mass in a marine toad (case 1). The mass was later diagnosed as *Brucella inopinata*–like oophoritis.

The isolates were positive for catalase, oxidase, urease (<5 min), and hydrogen sulfide production and negative on gel formation test (Appendix). We used the DNA from isolates 3278 and 5043 for the *Brucella* Laboratory Response Network real-time PCR; the DNA tested positive for all 3 targets. We performed partial 16S rDNA PCR assays on isolates 3278 and 5048 and partial recA PCR on isolate 3278. For both isolates, the 16s rDNA sequences had 100% sequence similarity to an atypical *Brucella* sp. isolated from a big-eyed tree frog in Germany (GenBank accession no. HE608873) (*5*). The sequences from both isolates had only 95% coverage and 99.8% sequence similarity to *B. inopinata* strain BO1 (GenBank accession no. NR116161) (*10*). The recA sequence of isolate 3278 had 100% sequence similarity to the *Brucella* sp. isolated from a big-eyed tree frog (GenBank accession no. HE608874). The recA sequence had only 64% coverage and 98.71% sequence similarity to *B. inopinata* strain BO1 (GenBank accession no. FM177719). We submitted the DNA sequences from isolates 3278 and 5043 to GenBank (accession nos. MT471347, MT471348, and MT482342).

We isolated atypical *Brucella inopinata*–like sp. from 2 adult marine toads, one an asymptomatic carrier and the second with oophoritis, a classic lesion described in mammalian *Brucella* infections. Our results suggest that marine toads are another amphibian species susceptible to atypical *Brucella* bacteria and that infection can result in long-term asymptomatic carriers as well as more typical reproductive lesions. Furthermore, this organism was isolated in 2 toads from different zoological institutions but with identical origin, suggesting that infection originated from a common source at least 4 years previously. After leaving the breeding colony, all toads were housed only with conspecifics

and, for a short period of time, with one other species group. Skin swab specimens from all other contacted amphibians at the zoos tested negative for *Brucella*. Diet consisted of a variety of insect species, making 2 separate introductions of *Brucella* from an outside source possible but unlikely. These findings highlight the need for additional testing of atypical *Brucella* spp., a potential emerging disease in amphibians, and warrants precautions when handling amphibians because of the potential for zoonoses.

Acknowledgments

We thank the staff at the Binder Park and John Ball Zoo and Amy Hill, Victoria Watson, and Michelle Magagna.

About the Author

Dr. Glabman is a veterinary anatomic pathologist and PhD candidate at the National Cancer Institute, Center for Cancer Research, at the National Institutes of Health in Bethesda, Maryland, in partnership with Michigan State University. Her primary research interests include comparative and investigative pathology of human and animal models of disease.

References

1. Al Dahouk S, Köhler S, Occhialini A, Jiménez de Bagüés MP, Hammerl JA, Eisenberg T, et al. *Brucella* spp. of amphibians comprise genomically diverse motile strains competent for replication in macrophages and survival in mammalian hosts. Sci Rep. 2017;7:44420. https://doi.org/10.1038/srep44420
2. Fischer D, Lorenz N, Heuser W, Kämpfer P, Scholz HC, Lierz M. Abscesses associated with a *Brucella inopinata*–like bacterium in a big-eyed tree frog (*Leptopelis vermiculatus*). J Zoo Wildl Med. 2012;43:625–8. https://doi.org/10.1638/2011-0005R2.1
3. Eisenberg T, Hamann HP, Kaim U, Schlez K, Seeger H, Schauerte N, et al. Isolation of potentially novel *Brucella* spp. from frogs. Appl Environ Microbiol. 2012;78:3753–5. https://doi.org/10.1128/AEM.07509-11
4. Whatmore AM, Dale E, Stubberfield E, Muchowski J, Koylass M, Dawson C, et al. Isolation of *Brucella* from a White's tree frog (*Litoria caerulea*). JMM Case Rep. 2015;2:1–5. https://doi.org/10.1099/jmmcr.0.000017
5. Soler-Lloréns PF, Quance CR, Lawhon SD, Stuber TP, Edwards JF, Ficht TA, et al. A *Brucella* spp. isolate from a Pac-Man frog (*Ceratophrys ornata*) reveals characteristics departing from classical Brucellae. Front Cell Infect Microbiol. 2016;6:116. https://doi.org/10.3389/fcimb.2016.00116
6. Scholz HC, Mühldorfer K, Shilton C, Benedict S, Whatmore AM, Blom J, et al. The change of a medically important genus: worldwide occurrence of genetically diverse novel *Brucella* species in exotic frogs. PLoS One. 2016;11:e0168872. https://doi.org/10.1371/journal.pone.0168872
7. Shilton CM, Brown GP, Benedict S, Shine R. Spinal arthropathy associated with *Ochrobactrum anthropi* in free-ranging cane toads (*Chaunus* [*Bufo*] *marinus*) in Australia. Vet Pathol. 2008;45:85–94. https://doi.org/10.1354/vp.45-1-85
8. Helmick KE, Garner MM, Rhyan J, Bradway D. Clinicopathologic features of infection with novel *Brucella* organisms in captive waxy tree frogs (*Phyllomeduca sauvagii*) and Colorado river toads (*Incilius alvarius*). J Zoo Wildl Med. 2018;49:153–61. https://doi.org/10.1638/2017-0026R1.1
9. Mühldorfer K, Wibbelt G, Szentiks CA, Fischer D, Scholz HC, Zschöck M, et al. The role of 'atypical' *Brucella* in amphibians: are we facing novel emerging pathogens? J Appl Microbiol. 2017;122:40–53. https://doi.org/10.1111/jam.13326
10. De BK, Stauffer L, Koylass MS, Sharp SE, Gee JE, Helsel LO, et al. Novel *Brucella* strain (BO1) associated with a prosthetic breast implant infection. J Clin Microbiol. 2008;46:43–9. https://doi.org/10.1128/JCM.01494-07

Address for correspondence: Dalen Agnew, Michigan State University Veterinary Diagnostic Laboratory, 4125 Beaumont Road, Lansing, MI 48910; email: agnewd@msu.edu

Incursion of Novel Highly Pathogenic Avian Influenza A(H5N8) Virus, the Netherlands, October 2020

Nancy Beerens, Rene Heutink, Frank Harders, Marit Roose, Sylvia B.E. Pritz-Verschuren, Evelien A. Germeraad, Marc Engelsma

Author affiliation: Wageningen Bioveterinary Research, Lelystad, the Netherlands

DOI: https://doi.org/10.3201/eid2706.204464

Highly pathogenic avian influenza A(H5N8) virus was detected in mute swans in the Netherlands during October 2020. The virus shares a common ancestor with clade 2.3.4.4b viruses detected in Egypt during 2018–2019 and has similar genetic composition. The virus is not directly related to H5N8 viruses from Europe detected in the first half of 2020.

Introduction of highly pathogenic avian influenza (HPAI) H5 clade 2.3.4.4 viruses in Europe caused substantial losses to the poultry industry during 2014–2020. Migratory waterfowl are impli-

cated in the distribution of HPAI H5 viruses along flyways from breeding grounds in northern Russia to wintering sites in Europe (*1*–*3*). During 2016, clade 2.3.4.4b HPAI H5N8 viruses were introduced in Europe (*4*,*5*) and the Netherlands (*6*,*7*). More recent introductions of these viruses were detected in eastern Europe, Germany, and Bulgaria in the first half of 2020 (*8*,*9*).

On October 17, 2020, two mute swans (*Cygnus olor*) were found dead in the province of Utrecht, the Netherlands. The swans were diagnostically tested as part of the wild bird surveillance program for avian influenza virus. Swab samples from the trachea and cloaca were PCR-positive for avian influenza virus. The virus was subtyped as HPAI H5N8 and contained the hemagglutinin (HA) cleavage site sequence PLREKRRKR*GLF.

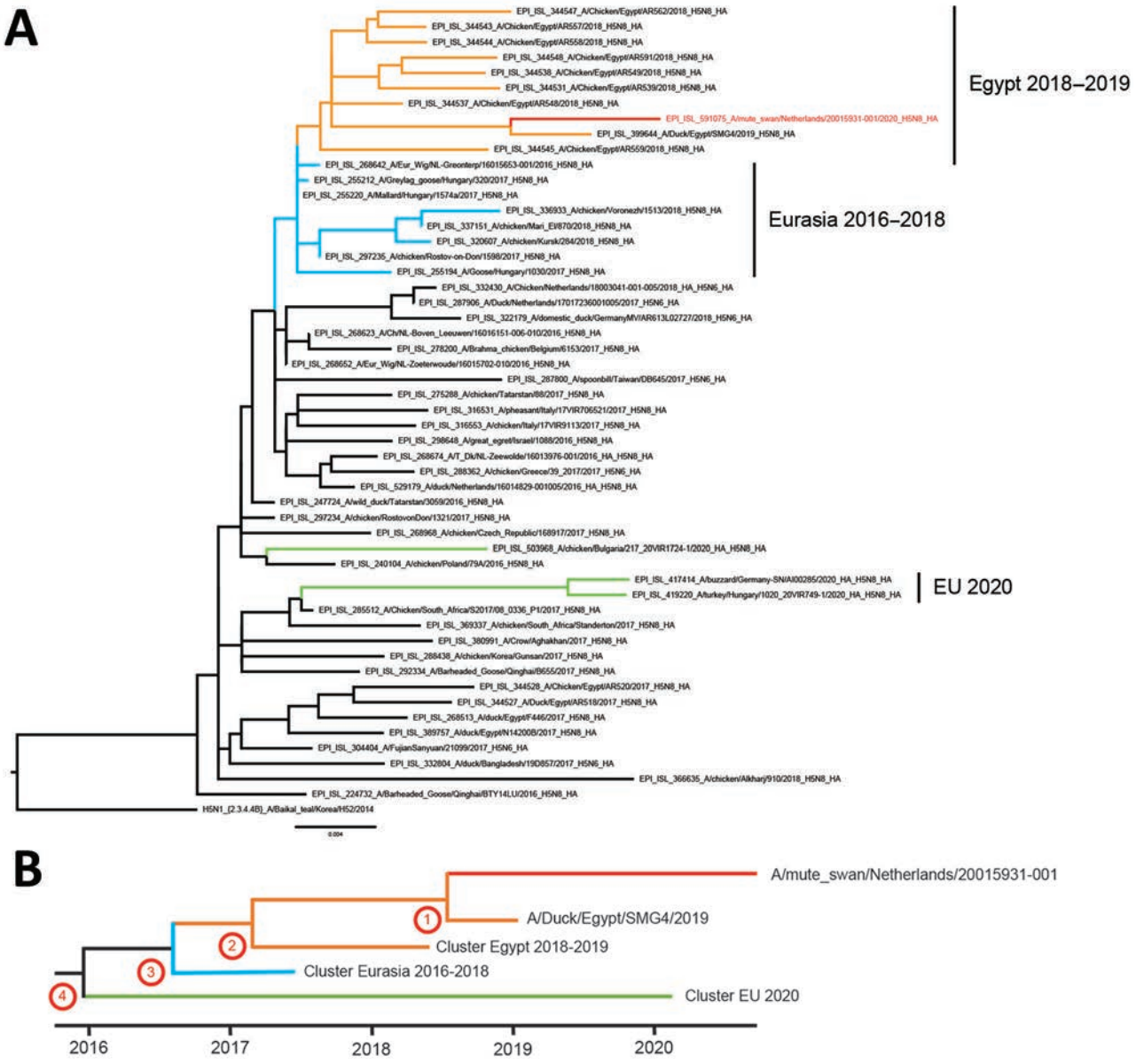

Figure. Phylogenetic analysis of the hemagglutinin (HA) segment of highly pathogenic avian influenza A(H5N8) virus, the Netherlands, October 2020. A) Optimal phylogenetic tree was generated by using the maximum-likelihood method (RAxML version 8.2.12; https://racm-ng.vital) with 100 bootstrap replicates and is shown and drawn to scale. GISAID (https://www.gisaid.org) accession numbers of the viruses are shown in the trees. Scale bar indicates nucleotide substitutions per site. B) Schematic representation of molecular dating of the HA gene segment. The Bayesian coalescent method was used to estimate the time to the most recent common ancestor of the novel H5N8 virus (numbers corresponding to nodes in the Table). Red branches indicate H5N8 virus isolated in the Netherlands in 2020;, green, H5N8 viruses isolated in eastern Europe, Germany, and Bulgaria in 2020; orange, viruses detected in Egypt during 2018–2019; and blue, viruses found in Eurasia during 2016–2018. EU, European Union.

Table. Calculated tMRCA with 95% HPD and posterior value for highly pathogenic avian influenza A(H5N8) virus, the Netherlands, October 2020*

Segment	Node†	tMRCA		Height 95% HPD	Posterior value
		Year	Date		
PB2	1	ND	ND	ND	ND
	2	2016.67	Sep 2016	2016.43–2016.88	0.61
	3	2016.47	Jun 2016	2016.20–2016.68	0.97
	4	2012.70	Sep 2012	2010.50–2014.43	0.96
PB1	1	ND	ND	ND	ND
	2	2017.00	Jan 2017	2016.79–2017.14	0.95
	3	2016.56	Jul 2016	2016.35–2016.76	0.94
	4	2011.21	Mar 2011	2007.91–2013.81	1.00
PA	1	ND	ND	ND	ND
	2	2016.67	Sep 2016	2016.442016.88	0.01
	3	2016.48	Jun 2016	2016.30–2016.67	1.00
	4	2008.70	Sep 2008	2005.77–2011.20	1.00
HA	1	2018.58	Jul 2018	2018.15–2018.91	1.00
	2	2017.18	Mar 2017	2016.88–2017.44	1.00
	3	2016.62	Aug 2016	2016.46–2016.78	1.00
	4	2015.97	Dec 2015	2015.68–2016.23	0.97
NP	1	ND	ND	ND	ND
	2	2016.89	Nov 2016	2016.52–2017.13	0.87
	3	2016.43	Jun 2016	2016.08–2016.69	1.00
	4	2014.71	Sep 2014	2013.32–2015.77	0.95
NA	1	2018.42	Jun 2018	2017.87–2018.88	1.00
	2	2016.98	Dec 2016	2016.80–2017.12	0.99
	3	2016.71	Sep 2016	2016.51–2016.86	1.00
	4	2016.15	Feb 2016	2015.77–2016.40	1.00
M	A	2016.39	May 2016	2015.84–2016.63	0.19
NS	1	ND	ND	ND	ND
	2	2016.92	Dec 2016	2016.70–2017.03	0.01
	3	2016.48	Jun 2016	2016.00–2016.79	0.96
	4	2015.77	Oct 2015	2014.74–2016.40	1.00

*HA, hemagglutinin; HPD, highest posterior density interval; M, matrix protein; NA, neuraminidase; ND, not determined; NP, nucleoprotein; NS, nonstructural protein; PA, polymerase acidic, PB1, polymerase basic 1; PB2, polymerase basic 2; tMRCA, median time of the most recent common ancestor.
†Nodes of the time-scaled phylogenetic tree.

We performed full-genome sequencing as described (*6*) and classified the virus genetically as H5 clade 2.3.4.4b. We performed detailed phylogenetic analyses to study the origin of the novel H5N8 virus (A/mute_swan/Netherlands/20015931–001/2020, GISAID accession no. EPI591075; https://www.gisaid.org). For HA (Figure) and neuraminidase (NA) (Appendix 1 Figure 1, https://wwwnc.cdc.gov/EID/article/27/6/20-4464-App1.pdf), the closest genetic relative was isolated from a duck in Egypt during January 2019 (EPI399644; only HA/NA sequences are available). The virus also shares a common ancestor with other viruses detected in Egypt during 2018–2019 and with viruses detected in the Netherlands and Eurasia during 2016–2018. The HA and NA gene segments of the novel H5N8 virus do not cluster with the H5N8 viruses that caused widespread outbreaks in eastern Europe and Germany earlier in 2020 or with viruses detected in Bulgaria during 2020.

For the other gene segments of the novel H5N8 virus, except for the matrix (M) protein segment, clustering was also observed with H5N8 viruses that circulated in Egypt during 2018–2019 and in Eurasia during 2016–2018 (Appendix 1 Figure 1). However, the M segment clusters with HPAI H5N8 viruses isolated in Asia and Egypt in 2016–2018 but also with the viruses found in eastern Europe and Germany during 2020, which suggests that reassortment with those viruses probably occurred for the M segment. No reassortments with low pathogenicity avian influenza viruses were observed for any of the segments. The genetic distance between the novel H5N8 virus and related viruses detected in Egypt and Eurasia appears relatively large, as demonstrated by the long branch lengths in phylogenetic trees (Appendix 1 Figure 1). This finding suggests long-term, undetected circulation of the virus or that intermediate virus sequences were not available in public databases.

We performed molecular dating by using BEAST (*10*) to estimate the time to the most recent common ancestor (Table; Appendix 1 Figure 2). For the H5 segment, a common ancestor of the novel H5N8 virus and the Egypt 2019 virus (accession no. EPI399644) was dated to July 2018 (node 1; Appendix 1 Figure 2) and with the cluster of viruses from Egypt to approximately March 2017 (node 2; Appendix 1 Figure 2). The common ancestor for the viruses from Eurasia detected during

2016–2018 was dated to August 2016 (node 3; Appendix 1 Figure 2) and with the viruses from eastern Europe and Germany detected in 2020 to approximately December 2015 (node 4; Appendix 1 Figure 2). Similar dating of ancestral viruses was observed for other gene segments, except for M (Appendix 1 Figure 2), for which the common ancestor for the viruses from eastern Europe and Germany detected during 2020 was dated to approximately May 2016 (node A; Appendix 1 Figure 2).

Molecular dating analysis suggests that the ancestor of the novel H5N8 virus detected in the Netherlands during October 2020 has circulated in this genetic form since March 2017 and caused influenza outbreaks in Egypt during 2018–2019. The novel virus incursion is not related to viruses detected in eastern Europe, Germany, and Bulgaria earlier in 2020 but was probably associated with fall migration of wild birds to wintering sites in the Netherlands. Although no HPAI viruses or deaths were observed at wild bird breeding sites in northern Russia, HPAI H5N8 viruses were reported in southern Russia and northern Kazakhstan in September 2020. Some waterfowl species, such as Eurasian wigeon (*Anas penelope*), tufted duck (*Aythya fuligula*), and white-fronted goose (*Anser albifrons*), are known to migrate from these regions to the Netherlands (Dutch Centre For Field Ornithology, https://vogeltrekatlas.nl/soortzoek2.html).

The novel virus was first detected in 2 mute swans that do not migrate over long distances. However, a few days later, virus was also detected in a dead Eurasian wigeon, suggesting that this bird species might have been involved in the incursion of the virus into the Netherlands. Because sequences of the viruses detected in Russia and Kazakhstan are unknown, the relationship between these viruses and the virus detected in the Netherlands remains to be determined. During October, wild bird migration is ongoing, and millions of wild birds will reach their wintering sites in Europe in the coming months. This early detection of HPAI H5N8 virus in the Netherlands predicted a high risk for the poultry industry in Europe during the 2020–2021 winter season.

Acknowledgments

We thank Alex Bossers for providing excellent next-generation sequencing facilities at Wageningen Bioveterinary Research and the authors and submitting laboratories for providing sequences from the GISAID EpiFlu Database (Appendix 2, https://wwwnc.cdc.gov/EID/article/27/6/20-4464-App2.xlsx).

This study was supported by the Dutch Ministry of Agriculture, Nature and Food Quality (projects WOT-01-003-087 and KB-37-003-015).

About the Author

Dr Beerens is a virologist and head of the National Reference Laboratory for Avian Influenza and Newcastle Disease, Lelystad, the Netherlands. Her primary research interests are molecular virology, genetics, and virus evolution.

References

1. Gilbert M, Xiao X, Domenech J, Lubroth J, Martin V, Slingenbergh J. Anatidae migration in the western Palearctic and spread of highly pathogenic avian influenza H5NI virus. Emerg Infect Dis. 2006;12:1650–6. https://doi.org/10.3201/eid1211.060223
2. The Global Consortium for H5N8 and Related Influenza Viruses. Role for migratory wild birds in the global spread of avian influenza H5N8. Science. 2016;354:213–7. https://doi.org/10.1126/science.aaf8852
3. Lee DH, Sharshov K, Swayne DE, Kurskaya O, Sobolev I, Kabilov M, et al. Novel reassortant clade 2.3.4.4 avian influenza A(H5N8) virus in wild aquatic birds, Russia, 2016. Emerg Infect Dis. 2017;23:359–60. https://doi.org/10.3201/eid2302.161252
4. Napp S, Majó N, Sánchez-Gónzalez R, Vergara-Alert J. Emergence and spread of highly pathogenic avian influenza A(H5N8) in Europe in 2016–2017. Transbound Emerg Dis. 2018;65:1217–26. https://doi.org/10.1111/tbed.12861
5. Lycett SJ, Pohlmann A, Staubach C, Caliendo V, Woolhouse M, Beer M, et al.; Global Consortium for H5N8 and Related Influenza Viruses. Genesis and spread of multiple reassortants during the 2016/2017 H5 avian influenza epidemic in Eurasia. Proc Natl Acad Sci U S A. 2020;117:20814–25. https://doi.org/10.1073/pnas.2001813117
6. Beerens N, Heutink R, Bergervoet SA, Harders F, Bossers A, Koch G. Multiple reassorted ruses as cause of highly pathogenic avian influenza A(H5N8) virus epidemic, the Netherlands, 2016. Emerg Infect Dis. 2017;23:1974–81. https://doi.org/10.3201/eid2312.171062
7. Bergervoet SA, Ho CK, Heutink R, Bossers A, Beerens N. Spread of highly pathogenic avian influenza (HPAI) H5N5 viruses in Europe in 2016–2017 appears related to the timing of reassortment events. Viruses. 2019;11:E501. https://doi.org/10.3390/v11060501
8. King J, Schulze C, Engelhardt A, Hlinak A, Lennermann SL, Rigbers K, et al. Novel HPAIV H5N8 reassortant (clade 2.3.4.4b) detected in Germany. Viruses. 2020;12:E281. https://doi.org/10.3390/v12030281
9. Adlhoch C, Fusaro A, Kuiken T, Niqueux E, Staubach C, Terregino C, et al.; European Food Safety Authority; European Centre for Disease Prevention and Control and European Union Reference Laboratory for Avian Influenza. Avian influenza overview February–May 2020. EFSA J. 2020;18:e06194.
10. Suchard MA, Lemey P, Baele G, Ayres DL, Drummond AJ, Rambaut A. Bayesian phylogenetic and phylodynamic data integration using BEAST 1.10. Virus Evol. 2018;4:vey016. https://doi.org/10.1093/ve/vey016

Address for correspondence: Nancy Beerens, Wageningen Bioveterinary Research, Division of Virology, PO Box 65, 8200 AB, Lelystad, the Netherlands; email: nancy.beerens@wur.nl

Retrospective Identification of Early Autochthonous Case of Crimean-Congo Hemorrhagic Fever, Spain, 2013

Ana Negredo,[1] María Sánchez-Ledesma,[1] Francisco Llorente, Mayte Pérez-Olmeda, Moncef Belhassen-García, David González-Calle, María Paz Sánchez-Seco,[2] Miguel Ángel Jiménez-Clavero[2]

Author affiliations: Instituto de Salud Carlos III, Madrid, Spain (A. Negredo, M.P. Sánchez-Seco, M. Pérez-Olmeda); Hospital Universitario de Salamanca, Salamanca, Spain (M. Sánchez-Ledesma, M. Belhassen-García, D. González-Calle); Animal Health Research Center, INIA-CISA, Valdeolmos, Spain (F. Llorente, M.A. Jiménez-Clavero); Centro de Investigación Biomédica en Red de Epidemiologia y Salud Pública, Madrid (M.A. Jiménez-Clavero)

DOI: https://doi.org/10.3201/eid2706.204643

Before this report, 7 autochthonous human cases of Crimean-Congo hemorrhagic fever had been reported in Spain, all occurring since 2016. We describe the retrospective identification of an eighth case dating back to 2013. This study highlights that the earliest cases of an emerging disease are often difficult to recognize.

Crimean-Congo hemorrhagic fever (CCHF) is a widely distributed tickborne disease in humans, emerging in different parts of the world (*1*). In Western Europe, the first and currently only country affected by this disease is Spain, where the etiologic agent, Crimean-Congo hemorrhagic fever virus (CCHFV) (family *Nairoviridae*, genus *Orthonairovirus*), was first identified in ticks in 2010 (*2*). Of note, the first autochthonous cases of CCHF were reported in 2016. In this hitherto first incidence, the index case-patient presumably acquired the infection from a tick bite, whereas a nurse (secondary case-patient) became infected while caring for the index patient (*3*). Since then, 5 more CCHF cases have been reported (Table): 2 in 2018 (1 of them retrospectively diagnosed in 2019) and 3 more in 2020 (*4*,*5*). All these cases (except the nosocomial case in 2016) arose in summer in rural areas of west-central Spain; 5 occurred in the southernmost part of the autonomous community of Castile and León. Field studies have confirmed that these areas are at risk for CCHF occurrence because of the abundance of *Hyalomma lusitanicum* tick vectors; CCHFV has been verified in specimens collected there, and high seroprevalences have been observed in wild and domestic animals (*4*).

Table. Human cases of Crimean-Congo hemorrhagic fever reported to date, in chronological order, Spain

Year	No. cases	Autonomous community/province	Reference
2013	1	Castile and León/Ávila	This study
2016	2	Castile and León/Ávila (index case); community of Madrid/Madrid (secondary case)	(*3*)
2018	2	Extremadura/Badajoz; Castile and León/Salamanca	(*4*)
2020	3	Castile and León/Salamanca	(*5*)

In August 2020, we were contacted by a person who recovered from a severe disease in May 2013, described as "caused by a tick bite," that occurred in the high-risk region referenced previously, and the etiology remained unknown. The patient's occupation did not expose her to animals, and she stated that she had not noticed any tick bites since then. The case was suggestive enough to warrant review of the patient's medical history: 3 days after being bitten by a tick during a walk through the mountains (40°18′26.8″N, 5°40′40.7″W), the patient (then a 32-year-old previously healthy woman) sought medical care after experiencing fever and chills. The patient's general condition worsened the next day (arthromyalgia, nausea, vomiting, and diarrhea), and she was admitted to a local hospital. Physical examination revealed erythema (Figure, panels A, B) and a necrotic lesion on the patient's back in the area of the tick bite (Figure, panel C). Platelet count dropped from 136,000/μL to 17,000/μL in 3 days, accompanied by remarkable leukopenia and neutropenia. Her general condition deteriorated rapidly and she experienced anasarca, gum bleeding, petechiae, and melena; she was transferred to a tertiary hospital.

Laboratory findings included pancytopenia, hypoalbuminemia, and hyperbilirubinemia with elevated transaminases (aspartate aminotransferase [AST] ≤4,000 U/L [reference range 0–33U/L] and alanine aminotransferase [ALT] ≤1,000 U/L [reference range 0–32 U/L]). Intracytoplasmic inclusions (morulae) were described in buffy coat examination.

Despite treatment, septic shock occurred, and supportive treatment was started in the intensive care unit. After 10 days of hospitalization, the patient recovered and was discharged.

Final laboratory diagnostic tests ruled out infection by most common tickborne illnesses (i.e., *Rickettsia*

[1]These first authors contributed equally to this article.

[2]These senior authors contributed equally to this article.

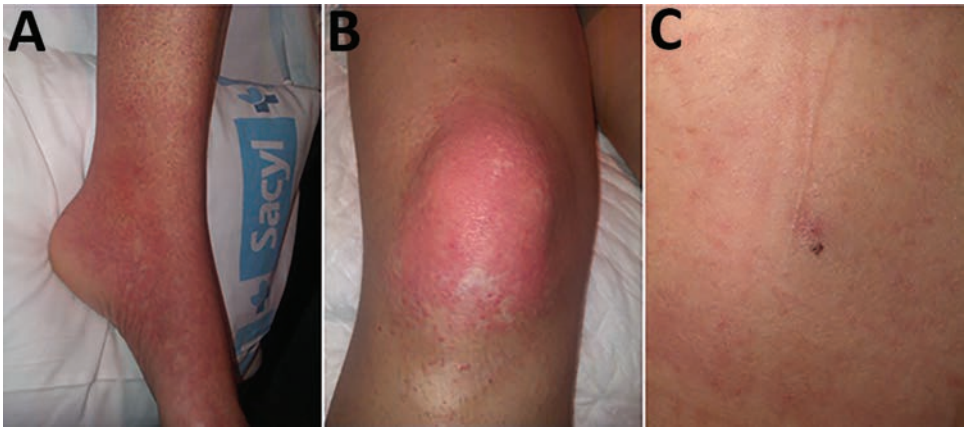

Figure. Retrospectively identified early autochthonous case of Crimean-Congo hemorrhagic fever in a woman in Spain, 2013. A, B) Erythema in the patient's ankle (A) and knee (B) 3 days after a tick bite during a leisure walk. C) Necrotic lesion on patient's back at site of tick bite.

spp., *Borrelia burgdorferi*, *Anaplasma* spp., and *Ehrlichia* spp.) and other suspected etiologies (i.e., cytomegalovirus, *Coxiella* spp., hepatitis C virus, hepatitis B virus, HIV). Stool and blood cultures were negative.

At the time of discharge CCHF was not suspected, probably because this disease had never occurred in Spain or other nearby countries, and buffy coat examination suggested ehrlichiosis. Evidence indicates CCHFV was present in 2010 in ticks ≈150 km from the location where the patient was bitten (*2*), but this finding was not deemed medically relevant at that time. However, examined retrospectively, and with the perspective of 7 CCHF cases in 4 years in Spain, 5 of them in the same area, the case strongly suggested CCHFV infection. In agreement with the patient, a new serum sample was collected and tested by the ID Screen CCHF Double Antigen Multi-species ELISA (ID-Vet, https://www.id-vet.com). The serum sample tested positive for antibodies to CCHFV, further confirmed by Crimean-Congo fever virus Mosaic 2 indirect immunofluorescence test for CCHFV-GPC and CCHFV-N, yielding positive results to both GPC and N antigens (EUROIMMUN, https://www.euroimmun.com). Meanwhile, we located and analyzed whole blood and serum samples that were collected 10 days after symptom onset and subsequently stored. CCHFV genome was detected in blood by nested PCR (*3*) and real-time reverse transcription PCR (*6*), whereas CCHFV-N–specific IgG and IgM were found in serum by indirect immunofluorescence test as described previously. Thus, the most likely cause of the disease suffered by the patient in 2013 was CCHF.

This study demonstrates that the occurrence of CCHF cases in Spain started ≥3 years before the previously reported first known case (Table). This case is the second to be identified retrospectively (*4*), so it would be possible that additional CCHF cases dating even earlier might be diagnosed in the future, since antibodies seem to be long-lasting (>7 years). CCHF should be included in the differential diagnosis after tick bites in areas in which it is endemic. Furthermore, awareness of CCHF is key to prevent nosocomial infections among exposed healthcare workers.

Acknowledgments

We are indebted to the patient without whose initiative and kind collaboration this work would not have been possible. We thank Giovanni Fedele and Raquel Escudero for their valuable help providing stored samples from the patient.

This study has been supported in part from ISCIII, Project RD16CIII/0003/0003, "Red de Enfermedades Tropicales," Subprogram RETICS Plan Estatal de I+D+I 2013-2016, and cofunded by FEDER "Una manera de hacer Europa."

About the Author

Dr. Negredo is a senior researcher at the Arbovirus and Imported Viral Diseases Laboratory, National Center of Microbiology, Madrid, Spain. Her primary research interests are viral hemorrhagic fevers and detection of emerging viruses that circulate in Spain.

References

1. Sorvillo TE, Rodriguez SE, Hudson P, Carey M, Rodriguez LL, Spiropoulou CF, et al. Towards a sustainable One Health approach to Crimean-Congo hemorrhagic fever prevention: focus areas and gaps in knowledge. Trop Med Infect Dis. 2020;5:113. https://doi.org/10.3390/tropicalmed5030113
2. Estrada-Peña A, Palomar AM, Santibáñez P, Sánchez N, Habela MA, Portillo A, et al. Crimean-Congo hemorrhagic fever virus in ticks, Southwestern Europe, 2010. Emerg Infect Dis. 2012;18:179–80. https://doi.org/10.3201/eid1801.111040
3. Negredo A, de la Calle-Prieto F, Palencia-Herrejón E, Mora-Rillo M, Astray-Mochales J, Sánchez-Seco MP, et al.; Crimean Congo Hemorrhagic Fever@Madrid Working Group. Autochthonous Crimean-Congo

hemorrhagic fever in Spain. N Engl J Med. 2017;377:154–61. https://doi.org/10.1056/NEJMoa1615162
4. Coordination Centre for Health Alerts and Emergencies. Ministry of Health. 2020: Report on the situation and risk assessment of transmission of Crimean-Congo hemorrhagic fever (CCHF) virus in Spain [in Spanish] [cited 2020 Nov 11]. https://www.mscbs.gob.es/profesionales/saludPublica/ccayes/analisisituacion/doc/ER_FHCC.pdf
5. Coordination Centre for Health Alerts and Emergencies. Ministry of Health. 2020: Rapid risk assessment. Detection of Crimean-Congo hemorrhagic fever in Salamanca [in Spanish] [cited 2020 Nov 11]. https://www.mscbs.gob.es/fr/profesionales/saludPublica/ccayes/alertasActual/Crimea_Congo/docs/20200827_ERR_Crimea_Congo_Salamanca.pdf
6. Monsalve Arteaga L, Muñoz Bellido JL, Negredo AI, García Criado J, Vieira Lista MC, Sánchez Serrano JÁ, et al. New circulation of genotype V of Crimean-Congo haemorrhagic fever virus in humans from Spain. PLoS Negl Trop Dis. 2021;15:e0009197. https://doi.org/10.1371/journal.pntd.0009197

Address for correspondence: Miguel Ángel Jiménez-Clavero, Animal Health Research Centre, National Institute for Agricultural and Food Research and Technology (INIA-CISA), Ctra Algete- El Casar, s/n, 28130, Valdeolmos (Madrid), Spain; email: majimenez@inia.es

Evidence of Oropouche Orthobunyavirus Infection, Colombia, 2017

Doris E. Gómez-Camargo, Jorge A. Egurrola-Pedraza, Cristopher D. Cruz, Dina Popuche, Margarita M. Ochoa-Díaz, Carolina Guevara, Maria Silva, Eugenio J. Abente, Julia S. Ampuero

Author affiliations: Universidad de Cartagena, Cartagena, Colombia (D.E. Gómez-Camargo, J.A. Egurrola-Pedraza, M.M. Ochoa-Díaz); US Naval Medical Research Unit No. 6, Lima, Peru (C.D. Cruz, D. Popuche, C. Guevara, M. Silva, E.J. Abente, J.S. Ampuero)

DOI: https://doi.org/10.3201/eid2706.204405

We describe an Oropouche orthobunyavirus infection in a women 28 years of age in Colombia. We confirmed the diagnosis by viral isolation, quantitative reverse transcription PCR, and phylogenetic analysis of the small, medium, and large genomic segments. The virus is related to a strain isolated in Ecuador in 2016.

Oropouche fever is an emerging zoonotic disease caused by Oropouche orthobunyavirus (OROV; family *Peribunyaviridae*, genus *Orthobunyavirus*). The disease was initially reported in Trinidad and Tobago in 1955; since then, researchers have documented >30 outbreaks in Brazil and Peru and isolated cases in Panama and Ecuador (*1*,*2*). OROV infection is characterized by acute febrile illness with symptoms such as headache, myalgia, arthralgia, chills, photophobia, nausea, vomiting, and dizziness. Patients with severe cases might have hemorrhaging and aseptic meningitis (*1*).

The OROV virion is enveloped and composed of a tripartite (segment lengths: 958 nt for small, 4,385 nt for medium, and 6,852 nt for large), negative-sense, single-stranded RNA genome (*1*,*3*,*4*). In 1964, Groot (*5*) described antibodies against OROV in serum samples from primates studied in Magdalena Medio and La Lizama (Colombia) in 1957. Since 2009, researchers have identified competent vectors such as *Aedes serratus*, *Coquillettidia venezuelensis*, and *Culex quinquefasciatus* mosquitoes on the Caribbean coast of Colombia (*6*,*7*). We describe an OROV infection in a woman in this region. We confirmed the diagnosis by viral isolation and reverse transcription PCR (RT-PCR).

A woman 28 years of age who did domestic work arrived at the emergency department of the E.S.E. Local Hospital of Turbaco (Turbaco, Colombia) on September 9, 2017. She had a 1-day history of fever, malaise, chills, myalgia, headache, retroocular pain, photophobia, dizziness, sore throat, anorexia, dysgeusia, and nausea. She had conjunctival injection and an axillary temperature of 38.6°C; she had no other pathologic abnormalities and tested negative on a tourniquet test. After receiving informed consent, we collected 12 mL of blood and stored the sample at −80°C.

One aliquot of serum was sent to the laboratory of the US Naval Medical Research Unit No. 6 (Lima, Peru) as part of an ongoing collaborative pathogen surveillance effort with the University of Cartagena (Cartagena, Colombia). This study protocol was approved by the Institutional Ethics Committee in Scientific Research of the University of Cartagena and the US Naval Medical Research Unit No. 6 Institutional Review Board (protocol no. NMRCD.2010.0010) in compliance with all applicable federal regulations governing the protection of human participants.

We extracted RNA from the sample; it tested negative for dengue, Zika, and chikungunya viruses by real-time RT-PCR. We inoculated the sample into Vero 76 cells using a previously described technique

(*8*) and observed a cytopathic effect in 50%–75% of the cells at 4 days after inoculation. We conducted an indirect immunofluorescence assay with pooled polyclonal antisera against flaviviruses (yellow fever virus and dengue virus serotype 3), alphaviruses (Venezuelan equine encephalitis virus, Eastern equine encephalitis virus, and Mayaro virus), hantavirus (Sin Nombre virus), arenaviruses (Allpahuayo virus and Tacaribe virus), cardiovirus (encephalomyocarditis virus), and bunyaviruses (Guaroa virus [GROV], caraparu virus, and OROV); we detected a positive signal with the bunyavirus antisera pool. We conducted another indirect immunofluorescence assay with individual polyclonal antisera against GROV, caraparu virus, and OROV; we detected a positive signal with the OROV polyclonal antisera. The serum sample tested negative for IgM against OROV, GROV, Mayaro virus, and Tacaribe virus by ELISA with whole virus antigen produced in-house. The original clinical samples tested positive by OROV-specific RT-PCR at independent laboratories in Peru and Colombia (*9*).

To characterize the virus at the molecular level, we used supernatant from the viral isolation to extract, amplify, and sequence the viral genome. We amplified the complete genome of the virus using a modified protocol of sequence-independent single primer amplification (*10*). We used the Nextera XT DNA Library Preparation Kit (Illumina, https://www.illumina.com) to prepare a library and sequenced the samples with MiSeq Reagent kit version 3 (600-cycle) (Illumina) according to the manufacturer's instructions.

The phylogenetic analyses of the small, medium, and large segments (GenBank accession nos. MK643115–7) showed that the strain is closely related to a strain isolated in Ecuador in 2016; it also forms a clade with a strain isolated in Peru in 2008 (Figure). We cannot posit transmission dynamics across country borders without additional sequence data. The patient did not travel outside the municipality during the 15 days before symptom onset, suggesting that OROV transmission occurred in Turbaco. *Aedes serratus* and *Culex quinquefasciatus* mosquitoes, which are OROV-competent vectors, have been identified in Turbaco (E. Cano-Perez, pers. comm.).

Our findings support the diagnostic use of OROV-specific RT-PCR for patients with acute febrile illness in this region. The increased use of this diagnostic tool will help clarify levels of circulation of OROV, informing decisions about Force Health Protection of US service members. In conclusion, local transmission of Oropouche orthobunyavirus infection may be occurring in this region.

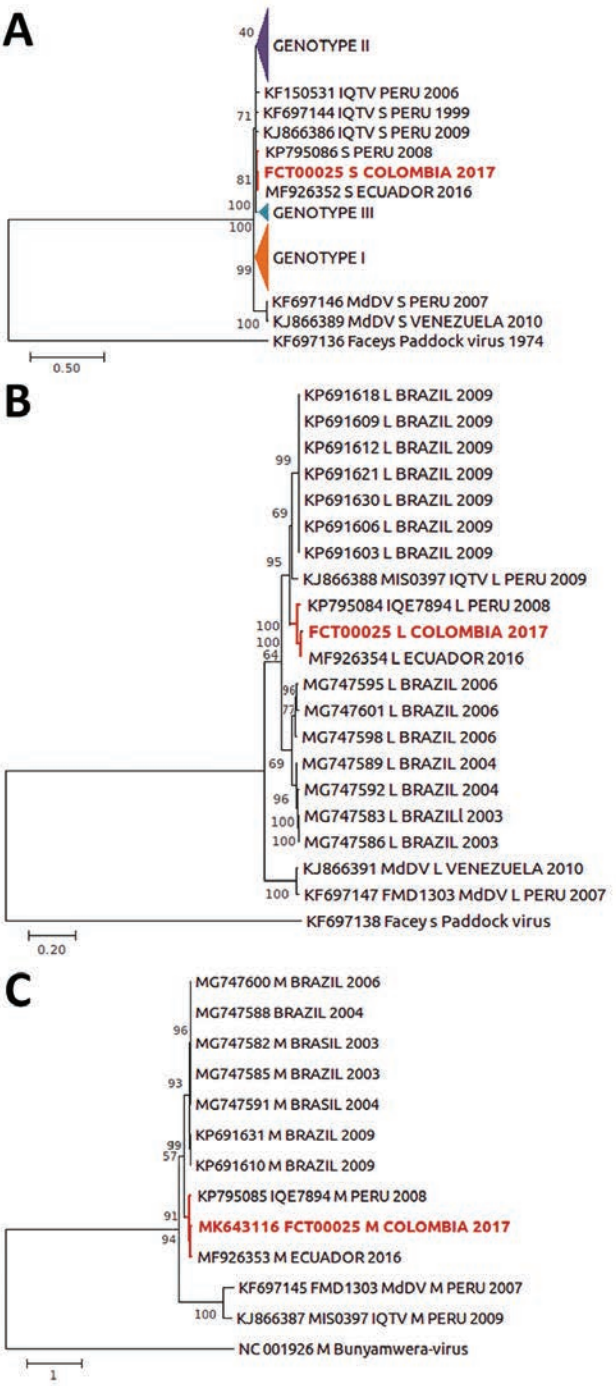

Figure. Maximum-likelihood phylogenetic tree based on the small (A), large (B), and medium (C) segments of Oropouche orthobunyavirus from a patient in Colombia, 2017 (red text), and reference sequences. Numbers to the left of nodes indicate bootstrap values based on 1,000 replicates. GenBank accession numbers are given for representative strains used for comparison. Triangles indicate phylogenetic branches compressed for size (*4*,*9*). Faceys Paddock and Bunyamwera viruses were used as outgroups. Scale corresponds to phylogenetic distance units estimated by likelihood function model. IQTV, Iquitos virus; MdDV, Madre de Dios virus.

Acknowledgments

We thank Ivan Diaz and Omaira Rodriguez for their support of the fieldwork and Juan Camilo Roncallo for his laboratory support.

This study was supported by funding from US Department of Defense Health Agency, Armed Forces Health Surveillance Division, Global Emerging Infections Surveillance Branch (work unit no. 800000.82000.25GB.B0016; ProMIS ID: 20160390211).

About the Author

Dr. Gómez-Camargo is the director of Tropical Medicine Doctoral Program and the UNIMOL Laboratory at the Universidad de Cartagena in Cartagena, Colombia. Her primary research interest is the molecular biology of infectious diseases.

References

1. Romero-Alvarez D, Escobar LE. Oropouche fever, an emergent disease from the Americas. Microbes Infect. 2018;20:135–46. https://doi.org/10.1016/j.micinf.2017.11.013
2. Wise EL, Pullan ST, Márquez S, Paz V, Mosquera JD, Zapata S, et al. Isolation of Oropouche virus from febrile patient, Ecuador. Emerg Infect Dis. 2018;24:935–7. https://doi.org/10.3201/eid2405.171569
3. Sakkas H, Bozidis P, Franks A, Papadopoulou C. Oropouche fever: a review. Viruses. 2018;10:175. https://doi.org/10.3390/v10040175
4. Travassos da Rosa JF, de Souza WM, Pinheiro FP, Figueiredo ML, Cardoso JF, Acrani GO, et al. Oropouche virus: clinical, epidemiological, and molecular aspects of a neglected Orthobunyavirus. Am J Trop Med Hyg. 2017;96:1019–30.
5. Groot Liévano H. Studies on arthropod-transmitted viruses in Colombia [in Spanish]. Revista de la Academia Colombiana de Ciencas Exactas, Físicas y Naturales. 2017;4:12–33.
6. Hoyos-López R, Suaza-Vasco J, Rúa-Uribe G, Uribe S, Gallego-Gómez JC. Molecular detection of flaviviruses and alphaviruses in mosquitoes (Diptera: Culicidae) from coastal ecosystems in the Colombian Caribbean. Mem Inst Oswaldo Cruz. 2016;111:625–34. https://doi.org/10.1590/0074-02760160096
7. Parra-Henao G, Suárez L. Mosquitoes (Diptera: Culiciadae) as potential vectors of arboviruses in the Urabá region, Northwest of Colombia [in Spanish]. Biomedica. 2012;32:252–62. https://doi.org/10.7705/biomedica.v32i2.667
8. Forshey BM, Guevara C, Laguna-Torres VA, Cespedes M, Vargas J, Gianella A, et al.; NMRCD Febrile Surveillance Working Group. Arboviral etiologies of acute febrile illnesses in Western South America, 2000–2007. PLoS Negl Trop Dis. 2010;4:e787. https://doi.org/10.1371/journal.pntd.0000787
9. Saeed MF, Wang H, Nunes M, Vasconcelos PFC, Weaver SC, Shope RE, et al. Nucleotide sequences and phylogeny of the nucleocapsid gene of Oropouche virus. J Gen Virol. 2000;81:743–8. https://doi.org/10.1099/0022-1317-81-3-743
10. Djikeng A, Halpin R, Kuzmickas R, Depasse J, Feldblyum J, Sengamalay N, et al. Viral genome sequencing by random priming methods. BMC Genomics. 2008;9:5. https://doi.org/10.1186/1471-2164-9-5

Address for correspondence: Doris E. Gómez-Camargo, calle 29 #50-50, Laboratorio UNIMOL, Universidad de Cartagena, Campus de la Salud, Cartagena, Colombia; email: dmtropical@unicartagena.edu.co

Fecal Excretion of *Mycobacterium leprae*, Burkina Faso

Anselme Millogo, Ahmed Loukil, Coralie L'Ollivier, Diakourga Arthur Djibougou, Sylvain Godreuil, Michel Drancourt

Author affiliations: Centre Hospitalier Universitaire Souro Sanou, Bobo-Dioulasso, Burkina Faso (A. Millogo); Aix-Marseille-Université, Institut de recherche pour le développement, Institut Hospitalo-Universitaire Méditerranée Infection, Marseille, France (A. Millogo, A. Loukil, M. Drancourt); Université de Montpellier, Institut de Recherche pour le développement, Montpellier, France (A. Millogo, S. Godreuil); Aix-Marseille-Université, IRD, Assistance Publique-Hopitaux de Marseille, Service de Santé des Arméés, Marseille (C. L'Ollivier); Institut de Recherche en sciences de la Santé, Bobo-Dioulasso (D.A. Djibougou); Centre MURAZ, Bobo-Dioulasso (D.A. Djibougou)

DOI: https://doi.org/10.3201/eid2706.200748

Mycobacterium leprae was detected by optical microscopy, fluorescent in situ hybridization, and molecular detection in feces collected for the diagnosis of *Entamoeba coli* enteritis in a leprosy patient in Burkina Faso. This observation raises questions about the role of fecal excretion of *M. leprae* in the natural history and diagnosis of leprosy.

Leprosy caused by *Mycobacterium leprae* remains endemic in Burkina Faso, a West Africa country with a level of disability 2 of 31.2% among new patient cases (*1*). Laboratory diagnosis of leprosy is determined by observation of acid-fast bacilli after microscopic examination of a Ziehl-Neelsen–stained nasal smears and cutaneous lesions (*1*). Recently, fluorescence in situ hybridization (FISH) was introduced as a complementary approach to increase the specificity of microscopic observations (*1*,*2*). We report on the specific microscopic detection of *M. leprae* in the stool specimen of a patient in Burkina Faso.

A 20-year-old man originating from the village of Bama in Burkina Faso sought care at the dermatology department at the Centre Hospitalier Universitaire Souro Sanou (Bobo-Dioulasso, Burkina Faso) for multiple infiltrated papules and nodules on his face and ear pavilions. These symptoms were accompanied by rhinitis and nosebleeds, which had been evolving for >2 months. Clinical examination further showed nasal enlargement (papulonodular), ulcerative-crusted lesions on the limbs, ulnar nerve hypertrophy, and a sausage-like appearance of the fingers, all of which suggested a lepromatous form of leprosy. A nasal smear and skin biopsy were performed on an infiltrative lesion (right arm), and 3 swab specimens were collected from a skin wound (left forearm), crusted lesions (elbow of right arm), and ulcerative papules (left arm). All samples were microscopically examined after Ziehl-Neelsen staining and revealed acid-fast bacilli in all 5 samples. Acid-fast bacilli were further identified as *M. leprae* by partial PCR amplification sequencing of the *rpoB* gene using a validated protocol (*1*).

The patient also had abdominal pain, and stool samples were collected to check for parasites. Microscopic examination (at 400× magnification) of fresh stool specimens mixed with Lugol's solution revealed cysts containing >6 nuclei, suggesting cysts of *Entamoeba coli*. Microscopic examination of the stool specimens filtrate after Ziehl-Neelsen staining (at 60× magnification) revealed 2 acid-fast bacilli per 300 microscopic fields (Figure).

Identification of the pathogens was confirmed by a PCR-based method and FISH for *M. leprae* (Appendix, https://wwwnc.cdc.gov/EID/article/27/6/20-0748-App1.pdf). Because *M. leprae* has been identified as an intra-amoebal pathogen (*3*), we tested the intracystic location of *M. leprae* by FISH in clarified stool specimens using sucrose-density gradients. In brief, the cyst wall was permeabilized by incubating stool specimen in 1 mL of cellulase (Sigma Aldrich, https://www.sigmaaldrich.com) for 48 hours at 45°C (*4*). After cellulase activity was stopped by washing with physiologic water and 5 minutes of centrifugation at 3,000 g, the pellet was incorporated into 4′,6-diamidino-2-phenylindole-FISH staining. Observation of 8 *Escherichia coli* cysts disclosed nuclei stained with 4′,6-diamidino-2-phenylindole and an absence of any detectable *M. leprae* by FISH (Figure). Dynamic, dormant, and dead staining to identify the viability of mycobacteria (*5*) revealed dead mycobacteria in the skin biopsy, the 3 cutaneous swab specimens, and stool specimens, whereas 8 bacilli out of a total of 22 observed in a series of 6 microscopic fields in the nasal smear were dynamic (Appendix Figure).

Previous reports relied only on Ziehl-Neelsen staining to assess the presence of acid-fast bacilli in stool specimens collected from patients in whom leprosy was diagnosed, without any further formal identification (*6*,*7*). In the patient we report, stool-borne acid-fast bacilli were identified as *M. leprae* by 2 independent methods in the presence of negative controls. These *M. leprae* organisms were possibly swallowed by the patient along with blood or upper respiratory secretions during leprosy rhinitis and epistaxis (*7*). This observation correlates with

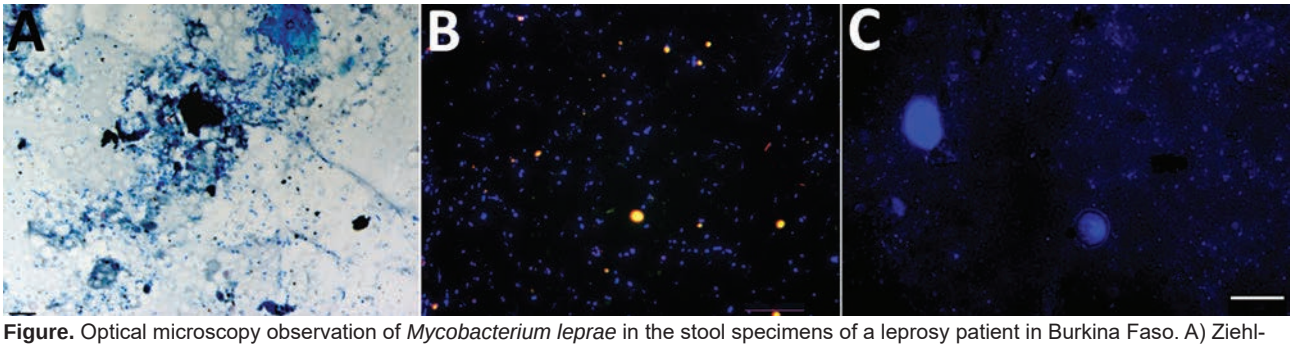

Figure. Optical microscopy observation of *Mycobacterium leprae* in the stool specimens of a leprosy patient in Burkina Faso. A) Ziehl-Neelsen staining; B) fluorescence in situ hybridization. No mycobacteria were observed inside the *Entamoeba coli* cysts (C). Scale bars represent 10 (A), 20 (B), and 20 (C) microns.

a study in armadillos, an *M. leprae* host in some leprosy-endemic regions, in which experimental infection results in the extensive involvement of the intestine and the presence of *M. leprae* in stools (*8*). In the stool specimens of the patient described in this study, only dead *M. leprae* cultures were observed using dynamic, dormant, dead staining, whereas dynamic mycobacteria were detected in the nasal smear (*9*).

On the basis of this research, further studies are required to confirm the prevalence of fecal excretion of *M. leprae* in various leprosy populations. Because stools are a noninvasive specimen, they could be collected for the positive diagnosis of leprosy using appropriate laboratory methods, as reported for the positive diagnosis of pulmonary tuberculosis (*10*). This diagnostic approach is easy to implement, including in children, in contrast to the current biopsy procedure, which requires a qualified staff and post-surgical management.

This work was supported by the government of France under the Investments for the Future Program managed by France's National Research Agency (reference: Méditerranée Infection [project no. 10-IAHU-03]). This work also was supported by the Région Le Sud, Provence Alpes Côte d'Azur, and European 95 funding (grant no. FEDER PA 0000320 PRIMMI).

About the Author

Mr. Millogo is a biology doctoral student at the University of Montpellier, France, and Institut Hospitalo-Universitaire Méditerranée Infection, Marseille, France, and a biologist at the Souro Sanou University Hospital in Bobo-Dioulasso, Burkina Faso. His primary research interests include cutaneous mycobacterioses.

References

1. Millogo A, Loukil A, Fellag M, Diallo B, Ouedraogo AS, Godreuil S, et al. Fluorescent hybridization of *Mycobacterium leprae* in skin samples collected in Burkina Faso. J Clin Microbiol. 2020;58:e02130–19. https://doi.org/10.1128/JCM.02130-19
2. Musso D, Rovery C, Loukil A, Vialette V, Nguyen NL. Leprosy in French Polynesia. New Microbes New Infect. 2019;29:100514. https://doi.org/10.1016/j.nmni.2018.10.010
3. Lahiri R, Krahenbuhl JL. The role of free-living pathogenic amoeba in the transmission of leprosy: a proof of principle. Lepr Rev. 2008;79:401–9. https://doi.org/10.47276/lr.79.4.401
4. Brahim Belhaouari D, Baudoin JP, Gnankou F, Di Pinto F, Colson P, Aherfi S, et al. Evidence of a cellulosic layer in *Pandoravirus massiliensis* tegument and the mystery of the genetic support of its biosynthesis. Front Microbiol. 2019;10:2932. https://doi.org/10.3389/fmicb.2019.02932
5. Loukil A, Darriet-Giudicelli F, Eldin C, Drancourt M. Pulmonary tuberculosis conversion documented by microscopic staining for detection of dynamic, dormant, and dead mycobacteria (DDD staining). J Clin Microbiol. 2018;56:e01108–18. https://doi.org/10.1128/JCM.01108-18
6. Manzullo A, Manzi RO, Lefevre A, Oteiza ML. Investigation of acid-fast bacilli in the digestive tract of leprosy patients. Leprologia. 1965;10:14–6.
7. Koshy A, Karat ABA. A study of acid-fast bacilli in the urine, gastric juice and feces of patients with lepromatous leprosy. Lepr India. 1971;43:3–7.
8. Kirchheimer WF, Storrs EE, Binford CH. Attempts to establish the armadillo (*Dasypus novemcinctus* linn.) as a model for the study of leprosy. II. Histopathologic and bacteriologic post-mortem findings in lepromatoid leprosy in the armadillo. Int J Lepr Other Mycobact Dis. 1972;40:229–42.
9. Palomino JC, Falconi E, Marin D, Guerra H. Assessing the viability of *Mycobacterium leprae* by the fluorescein diacetate/ethidium bromide staining technique. Indian J Lepr. 1991;63:203–8.
10. Drancourt M. Culturing stools to detect *Mycobacterium tuberculosis*. J Clin Microbiol. 2018;56:e02033–17. https://doi.org/10.1128/JCM.02033-17

Address for correspondence: Michel Drancourt, Aix-Marseille-Université, IRD, MEPHI, IHU Méditerranée Infection, 19-21 Boulevard Jean Moulin, 13005 Marseille, France; email: michel.drancourt@univ-amu.fr

Correction: Vol. 26, No. 12

GenBank accession numbers have been added for the sequenced viral sequences from Lymphocytic Choriomeningitis Virus Infections and Seroprevalence, Southern Iraq (H. Alburkatet al.). The article has been corrected online (https://wwwnc.cdc.gov/eid/article/26/12/20-1792_article).

Postvaccination COVID-19 among Healthcare Workers, Israel

Zohaib Yousaf, Kamran Mushtaq

Author affiliations: Hamad Medical Corporation, Doha, Qatar; Dresden International University, Dresden, Germany

DOI: https://doi.org/10.3201/eid2706.210410

To the Editor: We read with interest the article by Amit et al. (*1*), in which the authors discuss postvaccination symptoms as harbinger for severe acute respiratory syndrome coronavirus 2 (SARS-CoV-2) infection in healthcare workers (HCWs). The authors conclude that in HCWs, SARS-CoV-2infection can overlap with postvaccination symptoms caused by high risk for exposure. We agree with the authors regarding the dilemma posed by physical symptoms after vaccination. However, we emphasize that this situation extends beyond HCWs.

We report a 60-year-old previously healthy man who had isolated, progressively worsening fatigue starting 1 day after receiving a second dose of mRNA-based vaccine (Pfizer/BioNTech, https://www.pfizer.com). Reverse transcription PCR of a nasopharyngeal swab sample after fatigue persisted beyond 1 week of vaccination showed a positive result for SARS-CoV-2. The patient later showed development of severe coronavirus disease (COVID-19) pneumonia, requiring admission to an intensive care unit.

HCWs are at a higher risk for exposure and more likely to get tested if symptoms develop after vaccination, as in the study by Amit et al. (*1*). Fatigue is a common symptom after receiving the Pfizer/BioNTech vaccine (*2*). The dilemma associated with persistent postvaccination symptoms is magnified in non-HCWs because of perceived low overall exposure risk. A watch-and-wait strategy with false reassurances caused by postvaccination status in these patients might delay PCR testing, leading to further spread of the virus in the community (D.A. Swan et al., Fred Hutchinson Cancer Research Center, pers. comm., 2021 Mar 5). Thus, knowing when and whom to test postvaccination has major public health repercussions.

COVID-19 vaccines are efficacious in reducing transmission of symptomatic COVID-19 (*2*). Reduction in transmissibility of SARS-CoV-2 postvaccination is unclear (*3*). Vaccinated persons can still transmit the disease even if they are asymptomatic. (*4*). Testing everyone before and after vaccination for SARS-CoV-2 is not a cost-effective strategy. Being socially responsible is the key to contain the pandemic. Thus, preventive measures such as hand hygiene, use of facemasks, and avoiding social gatherings should be continued irrespective of vaccination status.

About the Authors

Dr. Yousaf is a chief clinical fellow in Internal Medicine at Hamad Medical Corporation, Doha, Qatar. His primary research interests are medical education, quality improvement, and clinical research.

Dr. Mushtaq is an internist and chief clinical fellow in gastroenterology and hepatology at Hamad Medical Corporation, Doha, Qatar. His primary research interests are medical education and clinical research.

References

1. Amit S, Beni SA, Biber A, Grinberg A, Leshem E, Regev-Yochay G. Postvaccination COVID-19 among healthcare workers, Israel. Emerg Infect Dis. 2021;27:1219–21. https://doi.org/10.3201/eid2704.210016
2. Polack FP, Thomas SJ, Kitchin N, Absalon J, Gurtman A, Lockhart S, et al.; C4591001 Clinical Trial Group. Safety and efficacy of the BNT162b2 mRNA COVID-19 vaccine. N Engl J Med. 2020;383:2603–15. https://doi.org/10.1056/NEJMoa2034577
3. He X, Lau EH, Wu P, Deng X, Wang J, Hao X, et al. Temporal dynamics in viral shedding and transmissibility of COVID-19. Nat Med. 2020;26:672–5. https://doi.org/10.1038/s41591-020-0869-5
4. Bleier BS, Ramanathan M Jr, Lane AP. COVID-19 vaccines may not prevent nasal SARS-CoV-2 infection and asymptomatic transmission. Otolaryngol Head Neck Surg. 2021;164:305–7. https://doi.org/10.1177/0194599820982633

Address for correspondence: Zohaib Yousaf, Department of Internal Medicine, Hamad General Hospital, Hamad Medical Corporation, PO Box 3050, Doha, Qatar; email: zohaib.yousaf@gmail.com

Thomas Red Owl Haukaas (1950−), *More Time Expected*, 2002. Hand-made ink and pencil on antique ledger paper, 16.5 in × 27.5 in/41.9 cm × 69.9 cm. Tacoma Art Museum, 1701 Pacific Avenue, Tacoma, WA 98402, United States. Gift of Greg Kucera and Larry Yocoreem in honor of Rock Hushka.

Fluid Motion and Frozen Time

Byron Breedlove

In June 1981, five cases of *Pneumocystis* pneumonia in gay men were described in CDC's *Morbidity and Mortality Weekly Report*. Those cases signaled the start of the AIDS pandemic, which now enters its fifth decade and has to date resulted in more than 75 million HIV infections and 32 million deaths worldwide. UNAIDS estimates that in 2019, 38 million persons were living with HIV, 1.7 million became newly infected, and 690,000 died with HIV disease.

Since the beginning of the HIV/AIDS pandemic, artists—some involved in AIDS activist organizations and others working independently—have applied their talents and skills to create, share, and deliver works that depict messages calling for political action and scientific research, documenting the impact of AIDS among various and diverse communities and groups, and celebrating medical breakthroughs and advances in treating AIDS. In 2016, a traveling exhibition entitled *Art AIDS America* examined the ongoing influence and impact of the AIDS pandemic on American art.

Among the more than 125 works featured in that traveling exhibition was *More Time Expected* by Lakota artist Thomas Red Owl Haukaas, displayed on this month's cover. Haukaas conveys both a sense of fluid motion and frozen time in this image, a modern example of Native American ledger art (a genre of

Author affiliation: Centers for Disease Control and Prevention, Atlanta, Georgia, USA

DOI: https://doi.org/10.3201/eid2706.AC2706

narrative drawing or painting on paper or cloth) that developed during the Indian Wars era and continued in the forced relocations of Plains tribes to government reservations from the 1860s through the 1920s. Widespread hunting had depleted buffalo and other game animals that provided hides the tribes traditionally used as canvases for recording events, ceremonies, and exploits. As a result, Native Americans began using paper taken from ledgers and other sources and employing ink, pencils, and watercolors rather than bone or wooden implements dipped in mineral and other natural pigments.

In this work, Haukaas shows a group of Native Americans and horses sweeping from right to left across the paper. The figures and horses are crowded, flattened, and overlapping each other. Riders and horses are looking straight ahead and moving in unison toward a destination beyond the edge of the image. The artist carefully depicts his figures of Native Americans dressed in traditional garb and wearing an array of bright colors and patterns. The horses are also stylized and individualized: many are boldly colored, and others are sketched with repeating patterns and rows of stripes. Half of the horses carry either a single rider or a pair of riders, but the other half are riderless, including the cobalt blue horse that draws attention to the center of the image.

Michelle Reynolds, Associate Director of Marketing and Communications at the Tacoma Art Museum, which organized *Art AIDS America* in partnership with the Bronx Museum of the Arts, explains how this work is related to HIV/AIDS: "The imagery, specifically the riderless horse, explores the complicated issues of stigma surrounding HIV/AIDS and the Native American experience with the disease. Historically, instances of HIV on the reservation are virtually unmentioned, a silence that only worsens an already high rate of infection. The horse with no rider, often used as a symbol for a warrior who fell in battle, represents individuals on the reservation who have died of AIDS-related causes. By focusing on absence within a group, Haukaas plays to the importance of community and families within these settings."

In a 2018 interview, Haukaas told writer and editor Emily Withnall, "My pieces are meant for dialogue, for discussion, for thinking about." Despite the fluidity and motion of his work, the underlying message carried by his portrayal of these riderless horses is the palpable sense of what has been lost. Haukaas, whose works are featured in many museum collections and have been part of numerous exhibitions, does not have formal training in art, and he credits his family and friends for teaching him traditional skills and practices. Known for his talents as a ledger, beadwork, and doll artist, he trained as a psychiatrist.

Through this image, Haukaas reconnects with the traditional ledger art form and uses it as a platform to engender thought and discussion about the ongoing medical and social effects of HIV within reservation communities, throughout other marginalized racial and ethnic communities around the world, and in those regions most affected by this ongoing pandemic. As De Cock, Jaffe, and Curran state in their EID article Reflections on 40 Years of AIDS, "Although initially slow, the HIV/AIDS response over the years has been a beacon in global health for respect for individuals and their rights and for health equity. More reflection is required with regard to what the responses to HIV and Ebola have taught us and how they might be relevant to COVID-19 and other future epidemics."

Bibliography

1. Bronx Museum of Art. Art AIDS America [cited 2021 Apr 14]. http://www.bronxmuseum.org/exhibitions/art-aids-america
2. Centers for Disease Control (CDC). *Pneumocystis* pneumonia—Los Angeles. MMWR Morb Mortal Wkly Rep. 1981;30:250–2.
3. Crimp D. Introduction. AIDS: cultural analysis/cultural activism. JSTOR. 1987;43:3–16. https://doi.org/10.2307/3397562
4. De Cock KM, Jaffe HW, Curran JW. Reflections on 40 years of AIDS. Emerg Infect Dis. 2021;27:1553–60. https://www.cdc.gov/eid/article/27/6/21-0284_article
5. Department of Ethnic Studies, University of California San Diego. Plains Indian ledger art: ledger art history[cited 2021 Apr 23]. https://plainsledgerart.org/history
6. Milwaukee Public Museum. The ledger art collection [cited 2021 Apr 23]. https://www.mpm.edu/research-collections/anthropology/online-collections-research/ledger-art-collection
7. Reynolds M. Object of the Week—"More Time Expected" [cited 2021 Apr 14]. https://www.tacomaartmuseum.org/tamblog-object-of-the-week-more-time-expected
8. Smithsonian Institution, National Museum of American History, Albert H. Small Documents Gallery. Keeping history: Plains Indian ledger drawings [cited 2021 May 11]. https://americanhistory.si.edu/documentsgallery/exhibitions/ledger_drawing_2.html
9. The Joint United Nations Programme on HIV/AIDS. UNAIDS data. 2020 [cited 2021 Apr 20]. https://www.unaids.org/sites/default/files/media_asset/2020_aids-data-book_en.pdf
10. Withnall E. Dance of the monarch [cited 2021 Apr 20]. https://www.elpalacio.org/2018/09/dance-of-the-monarch

Address for correspondence: Byron Breedlove, EID Journal, Centers for Disease Control and Prevention, 1600 Clifton Rd NE, Mailstop H16-2, Atlanta, GA 30329-4027, USA; email: wbb1@cdc.gov

EMERGING INFECTIOUS DISEASES®

Upcoming Issue
Zoonotic Infections

- Industry Sectors Highly Affected by Worksite Outbreaks of Coronavirus Disease, Los Angeles County, California, USA, March 19–September 30, 2020
- Risks and Preventive Strategies for *Clostridioides difficile* Transmission to Household or Community Contacts during Transition in Healthcare Settings
- Severe Acute Respiratory Syndrome Coronavirus 2 P.2 Lineage Associated with Reinfection Case, Brazil, June–October 2020
- Novel Morbillivirus as a Putative Cause of Fetal Death and Encephalitis among Swine
- Seroprevalence of SARS-CoV-2 among Blood Donors and Changes after Introduction of Public Health and Social Measures, London, England
- Whole Genome Analysis of *Streptococcus pneumoniae* Serotype 4 Causing an Outbreak of Invasive Pneumococcal Disease, Alberta, Canada
- Triclabendazole Treatment Failure for *Fasciola hepatica* Infection among Preschool and School-Age Children, Cusco, Peru
- *Plasmodium falciparum* Kelch 13 Mutations, 9 Countries in Africa, 2014–2018
- Susceptibility to SARS-CoV-2 of Well-Differentiated Airway Epithelial Cell Cultures from Domestic and Wild Animals
- Effects of Coronavirus Disease Pandemic on Tuberculosis Notifications, Malawi
- COVID-19 Outbreak on a Passenger Ship and Assessment of Response Measures, Greece, 2020
- Polymicrobial Infections Among Patients with Vascular Q Fever, France, 2014–2020
- *Anthrenus* sp. and an Uncommon Cluster of Dermatitis
- Assessing Community Vulnerability over 3 Waves of COVID-19 Pandemic, Hong Kong, China
- Pneumococcal Disease Outbreak at State Prison, Alabama, USA, September 1–October 10, 2018
- Cluster of Oseltamivir-Resistant and HA Antigenically Drifted Influenza A(H1N1)pdm09 Viruses, Texas, USA, January 2020
- Cross-Sectional Serosurvey of Companion Animals Housed with SARS-CoV-2–Infected Owners, Italy
- Prevalence of Middle East Respiratory Coronavirus in Dromedary Camels, Tunisia
- Possible Human-to-Dog Transmission of SARS-CoV-2, Italy, 2020
- Outbreak of Rabbit Hemorrhagic Disease Virus 2, Ghana
- Confirmed Cases of Ophidiomycosis in Museum Specimens from as Early as 1945, United States
- Murine Piroplasm Parasite *Anthemosoma garnhami* Causing Recrudescing Infection in an HIV-Infected Man from Zimbabwe in South Africa
- Prolonged SARS-CoV-2 RNA Shedding from Therapy Cat after Cluster Outbreak in Retirement Home

Complete list of articles in the July issue at http://www.cdc.gov/eid/upcoming.htm

Earning CME Credit

To obtain credit, you should first read the journal article. After reading the article, you should be able to answer the following, related, multiple-choice questions. To complete the questions (with a minimum 75% passing score) and earn continuing medical education (CME) credit, please go to http://www.medscape.org/journal/eid. Credit cannot be obtained for tests completed on paper, although you may use the worksheet below to keep a record of your answers.

You must be a registered user on http://www.medscape.org. If you are not registered on http://www.medscape.org, please click on the "Register" link on the right hand side of the website.

Only one answer is correct for each question. Once you successfully answer all post-test questions, you will be able to view and/or print your certificate. For questions regarding this activity, contact the accredited provider, CME@medscape.net. For technical assistance, contact CME@medscape.net. American Medical Association's Physician's Recognition Award (AMA PRA) credits are accepted in the US as evidence of participation in CME activities. For further information on this award, please go to https://www.ama-assn.org. The AMA has determined that physicians not licensed in the US who participate in this CME activity are eligible for AMA PRA Category 1 Credits™. Through agreements that the AMA has made with agencies in some countries, AMA PRA credit may be acceptable as evidence of participation in CME activities. If you are not licensed in the US, please complete the questions online, print the AMA PRA CME credit certificate, and present it to your national medical association for review.

Article Title

Rocky Mountain Spotted Fever in a Large Metropolitan Center, Mexico–United States Border, 2009–2019

CME Questions

1. You are seeing a 14-year-old girl who reports a 4-day history of fever and fatigue. You are aware of multiple case reports of Rocky Mountain spotted fever (RMSF) in your community over the past several months. In the current study by Zazueta and colleagues, which of the following symptoms associated with RMSF was most common?

A. Myalgia
B. Fever
C. Headache
D. Rash

2. What should you consider regarding the epidemiology of RMSF in the current study?

A. Only 10% of cases were diagnosed in the city of Mexicali
B. The 11-year incidence rate of RMSF was 230 cases/100,000 population
C. The mean age of cases was 9 years
D. Most cases occurred during summer months

3. You order diagnostic testing for RMSF. What did the current study find regarding such testing?

A. Most diagnostic assays in cases suspected for RMSF were positive
B. Rates of positive indirect fluorescent antibody (IFA) testing were more than double that of positive polymerase chain reaction (PCR) testing
C. Most patients who were hospitalized had a positive PCR test only
D. IFA and PCR tests were nearly never both positive when ordered together

4. What was the approximate mortality rate associated with RMSF in the current study?

A. 0.2%
B. 3%
C. 7%
D. 18%

Earning CME Credit

To obtain credit, you should first read the journal article. After reading the article, you should be able to answer the following, related, multiple-choice questions. To complete the questions (with a minimum 75% passing score) and earn continuing medical education (CME) credit, please go to http://www.medscape.org/journal/eid. Credit cannot be obtained for tests completed on paper, although you may use the worksheet below to keep a record of your answers.

You must be a registered user on http://www.medscape.org. If you are not registered on http://www.medscape.org, please click on the "Register" link on the right hand side of the website.

Only one answer is correct for each question. Once you successfully answer all post-test questions, you will be able to view and/or print your certificate. For questions regarding this activity, contact the accredited provider, CME@medscape.net. For technical assistance, contact CME@medscape.net. American Medical Association's Physician's Recognition Award (AMA PRA) credits are accepted in the US as evidence of participation in CME activities. For further information on this award, please go to https://www.ama-assn.org. The AMA has determined that physicians not licensed in the US who participate in this CME activity are eligible for AMA PRA Category 1 Credits™. Through agreements that the AMA has made with agencies in some countries, AMA PRA credit may be acceptable as evidence of participation in CME activities. If you are not licensed in the US, please complete the questions online, print the AMA PRA CME credit certificate, and present it to your national medical association for review.

Article Title

Neurologic Disease after Yellow Fever Vaccination, São Paulo, Brazil, 2017–2018

CME Questions

1. Which of the following disease states are included in the Brighton Collaboration (BC) criteria for yellow fever vaccine-associated neurologic disease (YEL-AND) but not the Centers for Disease Control and Prevention (CDC) criteria?

A. Aseptic meningitis
B. Meningoencephalitis
C. Encephalomyelitis
D. Guillain-Barré syndrome

2. Which of the following statements regarding clinical characteristics of patients with YEL-AND in the current study is most accurate?

A. The median time between vaccination and symptom onset was 4 days
B. Most cases occurred with the booster dose of the vaccine
C. Half of the cases had a positive cerebrospinal fluid (CSF) immunoglobulin (Ig)M titer against yellow fever (YF)
D. One-third of cases had a positive CSF polymerase chain reaction (PCR) test for YF

3. What was the most common manifestation of YEL-AND in the current study?

A. Aseptic meningitis
B. Encephalitis
C. ADEM
D. Guillain-Barré syndrome

4. What did the current study conclude regarding the use of the CDC and BC criteria for the diagnosis of YEL-AND?

A. Either criteria is sufficient in identifying YEL-AND
B. The BC criteria are more inclusive and require less advanced diagnostic methods
C. The CDC criteria will better identify a broad range of cases consistent with YEL-AND
D. Both criteria should be replaced by local diagnostic criteria

Earning CME Credit

To obtain credit, you should first read the journal article. After reading the article, you should be able to answer the following, related, multiple-choice questions. To complete the questions (with a minimum 75% passing score) and earn continuing medical education (CME) credit, please go to http://www.medscape.org/journal/eid. Credit cannot be obtained for tests completed on paper, although you may use the worksheet below to keep a record of your answers.

You must be a registered user on http://www.medscape.org. If you are not registered on http://www.medscape.org, please click on the "Register" link on the right hand side of the website.

Only one answer is correct for each question. Once you successfully answer all post-test questions, you will be able to view and/or print your certificate. For questions regarding this activity, contact the accredited provider, CME@medscape.net. For technical assistance, contact CME@medscape.net. American Medical Association's Physician's Recognition Award (AMA PRA) credits are accepted in the US as evidence of participation in CME activities. For further information on this award, please go to https://www.ama-assn.org. The AMA has determined that physicians not licensed in the US who participate in this CME activity are eligible for AMA PRA Category 1 Credits™. Through agreements that the AMA has made with agencies in some countries, AMA PRA credit may be acceptable as evidence of participation in CME activities. If you are not licensed in the US, please complete the questions online, print the AMA PRA CME credit certificate, and present it to your national medical association for review.

Article Title

HIV Infection as Risk Factor for Death among Hospitalized Persons with Candidemia, South Africa, 2012–2017

CME Questions

1. Your patient is a 47-year-old man with HIV infection and candidemia. According to the 6-year sentinel surveillance study in South Africa by Govender and colleagues, which of the following statements about the effect of HIV infection and other factors on mortality risk from candidemia is correct?

A. Case-fatality was 37% among HIV-seronegative cases vs 54% for HIV-seropositive cases ($P < .001$)
B. After adjustment for intensive care unit (ICU) care, receipt of systemic antifungal treatment, Candida species, and other factors, 30-day mortality was not significantly different in HIV-positive vs HIV-negative patients
C. Adjusted odds of 30-day mortality in HIV-positive patients was not significantly different according to cluster of differentiation (CD)4 count
D. Survival curves for HIV-seropositive and HIV-seronegative patients did not diverge until 2 weeks after candidemia diagnosis

2. According to the 6-year sentinel surveillance study in South Africa by Govender and colleagues, which of the following statements about the effect of ICU admission on mortality risk among adults with HIV infection and candidemia is correct?

A. Regarding mortality, there was no evidence of interaction of HIV positivity with ICU admission
B. HIV-seropositive patients were significantly more likely than HIV-seronegative patients to be admitted to the ICU
C. Among HIV-seropositive patients, significantly more patients with vs without advanced HIV disease were admitted to the ICU
D. The effect of HIV seropositivity on mortality was weakened among persons admitted to the ICU, but HIV-seropositive patients were substantially less likely to have received ICU care

3. According to the 6-year sentinel surveillance study in South Africa by Govender and colleagues, which of the following statements about clinical implications of the effect of HIV infection on mortality risk from candidemia is correct?

A. A high index of suspicion for candidemia among admitted HIV-seropositive patients is needed only for persons with classical risk factors
B. HIV-seropositive patients with suspected candidemia should be treated with watchful waiting to see if and how symptoms develop
C. HIV-seropositive patients with suspected candidemia should be considered for more intensive care and monitoring to lower mortality
D. Antiretroviral and appropriate early antifungal therapy eliminates increased mortality risk in HIV-seropositive patients with candidemia

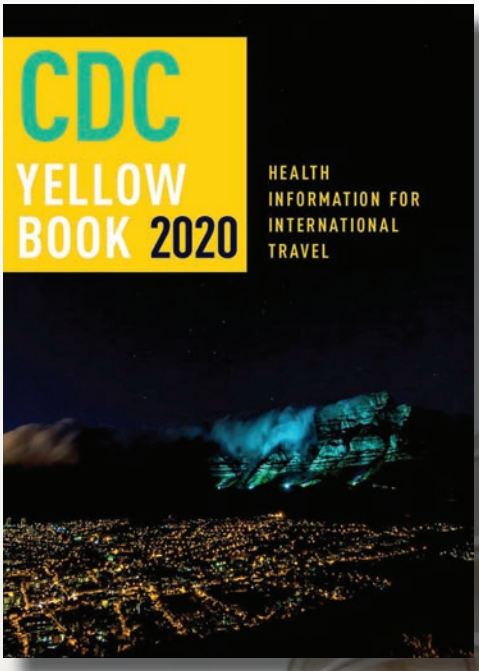

Available Now
Yellow Book 2020

The fully revised and updated CDC Yellow Book 2020: Health Information for International Travel codifies the US government's most current health guidelines and information for clinicians advising international travelers, including pretravel vaccine recommendations, destination-specific health advice, and easy-to-reference maps, tables, and charts.

ISBN: 978-0-19-006597-3 | $115.00 | May 2019 | Hardback | 720 pages

ISBN: 978-0-19-092893-3 | $55.00 | May 2019 | Paperback | 687 pages

Yellow Book 2020 includes important travel medicine updates

- **The latest information on emerging infectious disease threats, such as Zika, Ebola, and henipaviruses**
- **Considerations for treating infectious diseases in the face of increasing antimicrobial resistance**
- **Legal issues facing clinicians who provide travel health care**
- **Special considerations for unique types of travel, such as wilderness expeditions, work-related travel, and study abroad**

OXFORD
UNIVERSITY PRESS

Order your copy at:
www.oup.com/academic